

# University of Southampton Research Repository

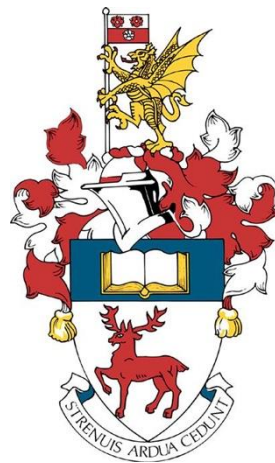
Copyright © and Moral Rights for this thesis and, where applicable, any accompanying data are retained by the author and/or other copyright owners. A copy can be downloaded for personal non-commercial research or study, without prior permission or charge. This thesis and the accompanying data cannot be reproduced or quoted extensively from without first obtaining permission in writing from the copyright holder/s. The content of the thesis and accompanying research data (where applicable) must not be changed in any way or sold commercially in any format or medium without the formal permission of the copyright holder/s.

When referring to this thesis and any accompanying data, full bibliographic details must be given, e.g.

Thesis: Author (Year of Submission) "Full thesis title", University of Southampton, name of the University Faculty or School or Department, PhD Thesis, pagination.

Data: Author (Year) Title. URI [dataset]





# **University of Southampton**

Faculty of Environmental Life Sciences

School of Ocean and Earth Science

**Ecological Consequences of Climatic Forcing in the Arctic Marine Benthos**

by

**Thomas Joshua Williams MSci**

ORCID ID [0000-0002-6616-955X](https://orcid.org/0000-0002-6616-955X)

Thesis for the degree of Doctor of Philosophy

September 2023



# University of Southampton

## Abstract

Faculty of Environmental Life Sciences

School of Ocean and Earth Sciences

Doctor of Philosophy

Ecological Consequences of Climatic Forcing in the Arctic Marine Benthos

by

Thomas Joshua Williams

Climate change is causing unprecedented changes in high-latitude environments, which have widespread implications for the underlying ecology and global climate and ocean systems. Of particular concern is the Arctic seafloor, an integral component of sympagic-pelagic-benthic food-webs, biogeochemical cycling and a variety of ecosystem services.

Arctic climate change studies often overlook changes in the physiological, behavioural, and life-history traits of organisms, instead focusing on observable, macro-level responses such as range shifts and biomass turnovers. However, alterations of trait expression are crucial in determining an organism's capacity to adapt and influence the environment, preceding population and community-level responses. Substantial variability of trait expression is already observed across different spatiotemporal scales, between co-existing species and within conspecifics. As a result of these complexities, accurately assessing the impact of climate change on Arctic benthic biodiversity and ecosystem functioning is challenging.

Here, I use laboratory-based mesocosm experiments, geochemical tracer analyses and simulative ecological extinction scenarios of Arctic benthic model systems to evaluate the consequences of organism responses to climate-driven environmental changes for benthic ecosystem functioning. Overall, my results demonstrate that organism responses are not generic, and can fundamentally alter their ability to persist and mediate aspects of ecosystem functioning. Specifically, I find that the capacity of species to endure climate-induced environmental change does not always equate to sustained contributions towards functional processes such as nutrient cycling and incurs inter- and intra-specific shifts in behaviour and physiological costs within metabolic pathways. Diverse responses to climate change are also reflected in the paleorecords, where intra-specific variability within long-lived cold-water corals influences their reliability in reconstructing deep-water temperature and seawater barium concentrations.

Upscaling from organism responses to species turnover and community-level ecosystem functioning requires an appropriate acknowledgement of species interactions. By factoring in species co-dependencies during the “borealisation” of benthic assemblages, I demonstrate that co-extinctions can intensify the loss of community functioning, while concurrently observing a larger compensation effect from local and surrounding species pools. As such, I provide evidence that incorporating connections between taxa into predictions of biodiversity change enables more realistic assessments of systemic responses to climate-driven environmental change.

Collectively, my findings highlight the influence of context on biodiversity responses and their repercussions on ecosystem functioning. In particular, I show that both individual organisms and

entire assemblages from south of the Polar Front exhibit different responses to climatic forcing compared to north of the Polar Front and at its transition. In doing so, I draw attention to the importance of incorporating gradients of environmental variability into climate change assessments.

I conclude that both environmental and biological variability shape the responses of Arctic benthic invertebrates to climatic forcing and the repercussions on ecosystem functioning. Rather than continuing to generalise responses at the macro-level, climate assessments should move towards incorporating the environmental context, interactions between organisms as well as intra- and inter-specific trait variability to accurately assess cascading effects on ecosystems. Integrating these components enhances our understanding of ecological responses to environmental change and improves predictions of future ecosystem dynamics. This knowledge is crucial for informing the most effective policy and management decisions aimed at mitigating stressor impacts.

# Content List

<b>Content List .....</b>	<b>i</b>
<b>List of Tables.....</b>	<b>vii</b>
<b>List of Figures.....</b>	<b>ix</b>
<b>List of Equations .....</b>	<b>xv</b>
<b>Research Thesis: Declaration of Authorship .....</b>	<b>xvii</b>
<b>Acknowledgements .....</b>	<b>xix</b>
<b>Definitions and Abbreviations.....</b>	<b>xxiii</b>
<b>Chapter 1 Introduction .....</b>	<b>1</b>
1.1 Aims and Objectives .....	8
<b>Chapter 2 Intra- and inter-specific differences in invertebrate behavioural trait expression moderate present and future benthic biogeochemical functioning in regions of rapid climatic transition.....</b>	<b>11</b>
2.1 Abstract .....	12
2.2 Introduction.....	12
2.3 Materials and methods .....	14
2.3.1 Fauna and sediment collection .....	14
2.3.2 Experimental design and set-up.....	15
2.3.3 Seawater carbonate chemistry, temperature and salinity .....	16
2.3.4 Behavioural response of individuals .....	16
2.3.5 Effects on ecosystem process and functioning .....	16
2.3.6 Statistical analysis.....	17
2.4 Results .....	18
2.4.1 Effects on individual behaviour.....	19
2.4.2 Effects on ecosystem process .....	20
2.4.3 Effects on ecosystem functioning .....	23
2.5 Discussion.....	26
<b>Chapter 3 Intra-specific variability in physiological responses underpin acclimation capacities in high-latitude marine invertebrates .....</b>	<b>31</b>

## Content List

3.1 Abstract.....	32
3.2 Introduction .....	32
3.3 Materials and methods.....	34
3.3.1 Fauna and sediment collection.....	34
3.3.2 Experimental design and set-up .....	35
3.3.3 Carbonate chemistry.....	36
3.3.4 Effects on growth and body condition .....	36
3.3.5 Effects on respiration and excretion.....	36
3.3.6 Effects on biochemical status .....	37
3.3.7 Data analysis .....	38
3.4 Results and Discussion.....	39
3.4.1 Effects on growth and body condition .....	39
3.4.2 Effects on respiration and excretion.....	41
3.4.3 Effects on biochemical status .....	43
3.4.4 Acclimation variability in polar invertebrates .....	44

## Chapter 4 **Inter- and intra-colony elemental systematics of a cold-water bamboo coral mediate deep-sea temperature and nutrient proxies**

.....	49
4.1 Abstract.....	50
4.2 Introduction .....	50
4.3 Materials and methods.....	53
4.3.1 Sample collection.....	53
4.3.2 Sample processing .....	53
4.3.3 Hydrographic data .....	53
4.3.4 Analytical procedures .....	56
4.3.4.1 Micro CT scanning .....	56
4.3.4.2 Geochemical analysis .....	56
4.3.4.2.1 Sample preparation.....	56
4.3.4.2.2 Laser ablation Quadrupole ICP-MS .....	56
4.3.4.2.3 Elemental mapping .....	57
4.3.5 Paleo-environmental reconstructions .....	58

4.3.5.1 Age model.....	58
4.3.5.2 Intra-individual covariance and reproducibility .....	59
4.3.5.3 Multi-element, multi-species paleoenvironment calibrations .....	59
4.3.5.4 Inter-individual reproducibility in reconstructed environmental conditions .....	60
4.3.5.5 Statistical analysis.....	61
4.4 Results .....	62
4.4.1 Patterns in coral elements .....	62
4.4.2 Intra-individual E/Ca variability and reproducibility .....	67
4.4.3 Inter-individual E/Ca variability and reproducibility .....	67
4.4.4 Multi-element, multi-species paleoenvironment calibrations .....	73
4.4.5 Paleo-environment reconstructions .....	79
4.4.5.1 Temperature.....	79
4.4.5.2 $[Ba]_{SW}$ .....	84
4.5 Discussion.....	85
4.5.1 Multi-taxa element analysis .....	85
4.5.1.1 Mg/Ca .....	85
4.5.1.2 Ba/Ca .....	85
4.5.2 Microscale trace element discrepancies.....	86
4.5.2.1 Variation within and among individuals.....	87
4.5.2.2 Sr/Ca, U/Ca, Sr/U and Li/Mg in high-Mg calcitic Octocorallia.....	88
4.5.3 Prospect for a E/Ca paleothermometer in <i>Keratoisis</i> sp.....	88
4.5.4 Prospect for a nutrient tracer in <i>Keratoisis</i> sp. .....	90
4.6 Conclusions and Outlook.....	91
<b>Chapter 5 Species co-dependency and vulnerability moderate ecological consequences of species loss.....</b>	<b>95</b>
5.1 Abstract .....	96
5.2 Introduction.....	96
5.3 Material and methods.....	98
5.3.1 Study location and environmental gradient .....	98

5.3.1.1 Modelling tool.....	98
5.3.1.1.1 Correlations, Co-extinctions and Co-compensations.....	100
5.3.2 Statistical analyses .....	101
5.4 Results.....	102
5.4.1 Projected ecosystem futures .....	102
5.4.2 Functional contributions of surviving taxa .....	107
5.4.3 Climate vulnerability vs order of extinctions.....	107
5.5 Discussion.....	110
<b>Chapter 6 Synthesis .....</b>	<b>113</b>
6.1 Future directions.....	119
<b>Appendix A Appendix for Chapter 2.....</b>	<b>123</b>
A.1 References .....	175
<b>Appendix B Appendix for Chapter 3.....</b>	<b>177</b>
B.1 References .....	211
<b>Appendix C Appendix for Chapter 4.....</b>	<b>213</b>
C.1 References .....	260
<b>Appendix D Appendix 1 for Chapter 5.....</b>	<b>261</b>
D.1 References .....	286
<b>Appendix E Appendix 2 for Chapter 5.....</b>	<b>287</b>
E.1 Supplementary code .....	287
E.1.1 Loading of packages.....	287
E.1.2 Initial load of data and data wrangling .....	288
E.1.3 Code S1: Vulnerability of species.....	290
E.1.4 Code S2: Calculating the median abundance above and below the ecotone Polar Front .....	293
E.1.5 Code S3: Calculating correlations for species co-extinctions and co- compensations .....	295

E.1.6	Code S4: Code for deciding co extinctions .....	297
E.1.7	Code S5: Recalculating species probability to compensate based on negative correlations .....	299
E.1.8	Code S6: Calculating co-compensations if there is still biomass left over from the extinctions.....	299
E.1.9	Code S7: Generalised Additive Models (GAMs) of each simulated biodiversity-function relationship. ....	302
E.1.10	Code S8: Model output figures .....	308
<b>Glossary of Terms .....</b>		<b>345</b>
<b>List of References.....</b>		<b>349</b>



## List of Tables

Table 4.1   Geographic coordinates and depths of the coral colonies analysed in this study alongside hydrographic data, carbonate system parameters, estimated age (yr) and uncertainty. Temperature (T), salinity (S) and dissolved oxygen (O <sub>2</sub> ) from conductivity-temperature-depth (CTD) casts taken nearby the coral sample sites are provided. For ageing estimation and uncertainty methodology, refer to Section 4.3.5.1. ....	55
Table 4.2   Selected average JCp-1 elemental ratios normalised to NIST612 as determined over two sessions in May 2022. * refers to the deviation the average element ratios compared with GeoRem preferred compositions <sup>a</sup> Hathorne et al. 2013. Isotopes measured: <sup>7</sup> Li, <sup>26</sup> Mg, <sup>43</sup> Ca, <sup>88</sup> Sr, <sup>138</sup> Ba, <sup>238</sup> U. ....	58
Table 4.3   Summary table of mean element ratios ( $\pm$ 2 standard deviations) measured in each internode across all <i>Keratoisis</i> sp. colonies. Coefficient of variation (CV) and range of values are also presented. Significance of OLS regression: *, p<0.05; **, p<0.01; ***, p<0.001 ....	70
Table 4.4   Correlation scores (Pearson's) for element ratio patterns after stratigraphic tuning internodes 1 & 2 and internodes 1 & 3 for each colony and their combined mean (bold)....	71
Table 4.5   (a) Linear and (b) Non-linear calibration Ordinary Least Squares (OLS) and Reduced Major Axis (RMA) equations based on values extracted from the literature and published calibrations with >60 % variance explained (bold). All published equations extracted from the literature can be found in Appendix C. ....	76
Table 4.6   Temperature trends (negative indicative of cooling, positive indicative of warming) for Mg/Ca-T reconstruction between timeperiod common to <i>Keratoisis</i> sp. colonies (2003-2016) obtained from Ordinary Least Squares (OLS) and Reduced Major Axis (RMA) regressions on uninterpolated, seasonally interpolated and annual interpolated temperature data. Significant regressions are highlighted in bold. ....	81
Table 5.1   Analysis of variance (ANOVA) parametric coefficients generated from pairwise comparisons between generalised additive models (GAMs) of bioturbation potential loss in each scenario. With the exception of one scenario (station B16)	

to station B15), all local extinction events result in biodiversity-ecosystem functioning curve that are significantly (*** ) different to the regional extinction scenario (station B17 to station B13).....	106
---	-----

Table 5.2   Approximate significance of smooth terms used in generalised additive models (GAMs) of bioturbation potential loss in each extinction scenario. The edf (effective degrees of freedom of smooth terms) represents the complexity of the smoother, with an edf of 1 equivalent to a straight line between x and y. The Ref.df and F columns represent test statistics employed in an analysis of variance (ANOVA) test to ascertain the overall significance (Sig.) of the smoother. In this context, a significance level of less than 0.05 implies that it is not possible to draw a horizontal line through the 95% confidence interval of the generalized additive model.....	106
--	-----

## List of Figures

Figure 1.1 | Growth in the number of publications in the peer-reviewed scientific literature focussing on climate change research in the Arctic between 1950 and 2021. Data was extracted from the *ISI Web of Science* (accessed on 10/01/2023) using the *Advanced Search* feature, with search strings (**red**) ("Arctic" AND "climat\* chang\*"), (**blue**) ("Arctic" AND "climat\* chang\*" AND "biodiversity") and (**green**) ("Arctic" AND "climat\* chang\*" AND "biodiversity" AND benth\*) in the titles and keywords of all document types across all databases and collections. .....3

Figure 1.2 | Map adapted from Deb & Bailey, (2023) showing the current state of Arctic marine, and climate change research within each Large Marine Ecosystem (LME) of the Arctic as defined by the Arctic Council's Protection of the Arctic Marine Environment Working Group (PAME 2013). The colour of pie charts indicates the ecological subject of the studies conducted in each LME, whilst the size indicates the total number of studies. Most of the studies were conducted in Barents Sea LME (21%), followed by the Baffin Bay (8%) and Beaufort Sea (8%). Less than 2% of studies were conducted in the Aleutian Islands LME, Iceland LME and Eastern Bering Sea LME. The number of studies conducted across all LMEs (Pan-Arctic) (14%) and two or more (multiple) LMEs (16%) are also shown. .....4

Figure 1.3 | Circumpolar distribution of (a-b) Records of benthic biodiversity above 60 °N and between 1800-2020 extracted from the Ocean Biodiversity Information System [access date 25/10/2021] demonstrating (a) the national efforts of Observer and Arctic States and (b) temporal coverage of data, (c) benthic fauna density data north of 60 °N extracted from the BenBioDen database (Stratmann et al. 2020) and (d) bioturbation intensity (Db) records above 60 °N extracted from Solan et al. (2019). Records are presented within each Large Marine Ecosystem (LME) of the Arctic as defined by the Arctic Council's Protection of the Arctic Marine Environment Working Group (PAME 2013). .....7

Figure 2.1 | . The effects of species identity, location and environmental condition (ambient, open symbols; future, closed symbols) on (a,c) mean ( $\pm$  s.e.) response time and (b,d) mean ( $\pm$  s.e.) burial time for *Ctenodiscus crispatus* (**squares**) and *Cistenides hyperborea* (**triangles**) obtained from station B13 (**red**) and B16 (**blue**) in the Barents Sea and *Aequiyoulodia eightsi* (**diamond**) obtained from Rothera Point (**black**). .....20

## List of Figures

Figure 2.2 | The effects of species identity, location and environmental condition (**ambient, open symbols; future, closed symbols**) on (mean  $\pm$  s.e.) (a,b,c,d) SBR (mm), (e,f,g)  ${}^f\text{-}\text{SPI}_{\text{Lmedian}}$  (mm), (h,i,j)  ${}^f\text{-}\text{SPI}_{\text{Lmax}}$  (mm) and (k,l,m,n)  $[\Delta\text{Br}^-]$  ( $\text{mg}\cdot\text{L}^{-1}$ ) in mesocosms containing (a,b,d,h,k,l) *Astarte crenata* (**circles**) or *Ctenodiscus crispatus* (**squares**) from station B13 (**red**), B16 (**blue**) or both locations combined (**gold**), (c,f,i,m) mesocosms containing *Cistenides hyperborea* (**triangles**) obtained from station B13 and (d,g,j,n) mesocosms containing *Aequiylodia eightsi* (**diamonds**) or *Laternula elliptica* (**upside down triangles**) obtained from Rothera Point. For  $[\Delta\text{Br}^-]$ , negative values indicate increased bioirrigation. Sediment profile images and associated luminophore distribution profiles are presented in Appendix A, Figures S8-S11. .... 22

Figure 2.3 | The effects of species identity, location and environmental condition (**ambient, open symbols; future, closed symbols**) on (mean  $\pm$  s.e.) effect size of nutrient concentrations (InRR) over the experimental period as indicated by (a,b,c)  $[\text{NH}_4\text{-N}]$ , (d,e,f,g)  $[\text{NO}_2\text{-N}]$ , (h,i,j,k)  $[\text{NO}_3\text{-N}]$  and (l,m,n)  $[\text{PO}_4\text{-P}]$  in mesocosms containing (a,d,e,h,i,l) *Astarte crenata* (**circles**) or *Ctenodiscus crispatus* (**squares**) from station B13 (**red**), B16 (**blue**) or both (**gold**), (b,f,j,m) mesocosms containing *Cistenides hyperborea* (**triangles**) obtained from station B13 and (c,g,k,n) mesocosms containing *Aequiylodia eightsi* (**diamonds**) or *Laternula elliptica* (**upside down triangles**) obtained from Rothera Point. A positive effect size indicates an increase in nutrient release from the sediment into the water column over the experimental period, while a negative effect size signifies an increase in the uptake of nutrients from the water column into the sediment. .... 25

Figure 3.1 | The effects of species identity, station and environmental condition on (a-c) growth ( $\Delta$  biomass, %) and (d-e) tissue:shell (TW:SW) wet weight (mean  $\pm$  s.e.) for *Astarte crenata* (**circles**), *Ctenodiscus crispatus* (**squares**) or both (**crossed-circle**), and *Cistenides hyperborea* (**diamonds**) from station B13 (**red**) and B16 (**blue**) and *Aequiylodia eightsi* (**triangles**) under ambient (open) or future (closed) environmental conditions. .... 41

Figure 3.2 | The effects of species identity and environmental condition on (a-c) oxygen consumption ( $\text{MO}_2$ :  $\mu\text{g}\cdot\text{h}^{-1}$ ), (d-f) ammonium excretion ( $\text{NH}_4$ :  $\text{nmol}\cdot\text{h}^{-1}$ ) and (g-i) phosphate excretion ( $\text{PO}_4$ :  $\text{nmol}\cdot\text{h}^{-1}$ ) (mean  $\pm$  s.e.) for *Astarte crenata* (**circles**) *Ctenodiscus crispatus* (**squares**) or both (**crossed-circle**), *Cistenides hyperborea*

(diamonds) and <i>Aequiyoldia eightsi</i> (triangles) under ambient (open) or future (closed) environmental conditions .....	43
Figure 3.3   The effects of species identity and environmental condition on concentrations of (a-c) glucose (GLU: $\mu\text{g} \cdot \text{mg}^{-1} \text{OM}$ ) and (d-f) protein (PROT: $\mu\text{g} \cdot \text{mg}^{-1} \text{OM}$ ) (mean $\pm$ s.e.) in <i>Astarte crenata</i> (circles) <i>Ctenodiscus crispatus</i> (squares) <i>Cistenides hyperborea</i> (diamonds) and <i>Aequiyoldia eightsi</i> (triangles) under ambient (open) or future (closed) environmental conditions .....	45
Figure 4.1   Two dimensional patterns in <i>Keratoisis</i> sp. element ratios (left to right: Li/Ca, Mg/Ca, Sr/Ca, Ba/Ca and U/Ca) analysed by laser ablation and overlain onto a post-ablation SEM image of the basal internode (top row), second internode (middle row) and third internode (bottom row) of colony (a) #23-1, (b) #23-6, (c) #23-10 and (d) #23-16. Ratios that clearly match structure elements of the coral include high Li/Ca, Mg/Ca and U/Ca values confined to central axis and low Li/Ca, Mg/Ca values confined to coral wall. Banding is clear in the Barium profiles. Scale in bottom left of SEM images .....	63
Figure 4.2   Covariance (Spearman's Rank; top right subplots) and distribution (bottom left subplots) of Li/Mg, Li/Ca, Mg/Ca, Sr/Ca, Ba/Ca and U/Ca ratios within the basal internode ( <b>red</b> ), second internode ( <b>green</b> ) and third internode ( <b>blue</b> ) of <i>Keratoisis</i> sp. colonies (a) #23-1 (left) and #23-6 (right), and (b) #23-10 (left) and #23-16 (right) .....	68
Figure 4.3   Compiled published (a) Mg/Ca-T, Li/Mg-T, Sr/Ca-T, Sr/U-T and U/Ca-T calibration data and (b) Ba/Ca-T, $D_{\text{Ba}}\text{-T}$ and $[\text{Ba}]_{\text{coral}} - [\text{Ba}]_{\text{SW}}$ calibration data for aragonitic ( <b>red</b> ), high-Mg calcitic ( <b>blue</b> ) mixed mineralogy ( <b>green</b> ) corals and Corallinales compared to Octocorallia ( <b>dark blue</b> ). Full element compilation datasets adjusted for interlaboratory offsets (where standard data are available). Mean coral replicates are presented in Appendix C Figure S6 .....	74
Figure 4.4   Reconstructions of past (a) temperatures derived from Mg/Ca and (b) seawater barium derived from Ba/Ca, generated for different colonies ( <b>colour</b> ) and internodes ( <b>linetype</b> ) and evaluated without data interpolation ( <b>left column</b> ), with seasonal interpolation ( <b>middle column</b> ), and with annual interpolation ( <b>right column</b> ). <i>In-situ</i> temperature measurements taken at nearby locations ( <b>grey points</b> - K. Azestu-Scott, pers. comm., May 31, 2022; Zweng & Münchow, 2006) and the average trend of sea surface temperatures ( <b>dashed yellow line</b> ,	

## List of Figures

Reynolds et al. 2002) are displayed. The bottom row of each figure shows the reconstructed environmental conditions during the time period shared by all <i>Keratoisis</i> sp. colonies. ....	80
Figure 4.5   <i>In-situ</i> temperature data (green squares) and trend (green line, shaded area is standard error of Ordinary Least Squares regression) for Baffin Bay (Zweng & Münchow, 2006) vs annually interpolated reconstructed temperature data (purple circles, error bars denote standard error after averaging across internodes) and trend (purple line, shaded area is standard error of Ordinary Least Squares regression) in <i>Keratoisis</i> sp. colony #23-6.....	90
Figure 5.1   Basic schematic of model procedure, with logic gates for whether co-extinctions and co-compensation occurs (see Section 5.3.1.1.1).....	99
Figure 5.2     Changes in community bioturbation potential ( $BP_c$ , log) following climate-driven extinctions (upper panels), combined with interaction-derived co-extinctions (middle panels) and post-extinction compensations (bottom panels) associated with environmental transitions from stations (a,g,m) B17- B16, (b,h,n) B16 -B15 (c,i,o) B15 -Xs (d,j,p) Xs-B14 (e,k,q) B14-B13 and (f,l,r) B17-B13 in the Barents Sea. Colour intensity (grey—blue) reflects an increasing density (low to high) of data points with the pre-extinction species richness (vertical green solid line) and predicted post-extinction species richness (vertical red dashed line) represented. Coextinctions lead to an increase in colour intensity along the main species-function trajectory, whilst compensations increase the spread of data points. Simulations, n = 500 per panel.....	104
Figure 5.3   Predicted biodiversity-ecosystem function relation curves (upper row) represented with a generalised additive model (GAM, mean $\pm$ s.e., solid lines $\pm$ shaded area), following post-extinction compensations (mean $\pm$ s.d., second row) and reorganisation of functional groups characterised by their mobility (third row) and sediment reworking (fourth row) associated with environmental transitions from stations (a,g,m,s) B17-B16, (b,h,n,t) B16-B15 (c,i,o,u) B15-Xs (d,j,p,v) Xs-B14 (e,k,q,w) B14-B13 and (f,l,r,x) B17-B13 in the Barents Sea. The pre-extinction species richness (vertical green solid line) and predicted (median of observed data) post-extinction species richness (vertical red dashed line) are presented.	105

Figure 5.4 | Taxonomic reorganisation during simulated extinction events following environmental transitions from (a) Station B17 to Station B16, (b) Station B16 to Station B15 (c) Station B15 to Station Xs (d) Station Xs to Station B14 (e) Station B14 to Station B13 and (f) Station B17 to B13 in the Barents Sea. Colour shading (**low—high, white—dark blue**) represents the relative contributions of individual taxa to BPc at each sequential level of local extinction. The pre-extinction species richness (**vertical green solid line**), predicted post-extinction species richness (**vertical red dashed line**) and subset of twenty taxa that contribute most to functioning are represented, with contributions above 20% greyed out.....108

Figure 5.5 | Changes in mean extinction probability (log) of species following environmental transitions from (a,g) Station B17 to Station B16, (b,h) Station B16 to Station B15 (c,i) Station B15 to Station Xs (d,j) Station Xs to Station B14 (e,k) Station B14 to Station B13 and (f,l) Station B17 to B13 in the Barents Sea. Colours represent the extinction probability of all species going extinct (**purple**), the extinction probability of species still present within the community (**grey**), the extinction probability of species going extinct as a result of climate vulnerabilities (**blue**), the extinction probability of species going extinct as a result of species codependencies (**yellow**), the pre-extinction species richness (**vertical green solid line**) and post-extinction species richness (**vertical red dashed line**)..109



## List of Equations

Equation 3.1	Calculation of oxygen consumption rate during closed-chamber respirometry ( $\text{MO}_2$ ) .....	38
Equation 4.1	Calculation of relative dating precision for a given sampling point within a radially growing coral .....	59



## Research Thesis: Declaration of Authorship

Print name: Thomas Joshua Williams

Title of thesis: Ecological Consequences of Climatic Forcing in the Arctic Marine Benthos

I declare that this thesis and the work presented in it are my own and has been generated by me as the result of my own original research.

I confirm that:

1. This work was done wholly or mainly while in candidature for a research degree at this University;
2. Where any part of this thesis has previously been submitted for a degree or any other qualification at this University or any other institution, this has been clearly stated;
3. Where I have consulted the published work of others, this is always clearly attributed;
4. Where I have quoted from the work of others, the source is always given. With the exception of such quotations, this thesis is entirely my own work;
5. I have acknowledged all main sources of help;
6. Where the thesis is based on work done by myself jointly with others, I have made clear exactly what was done by others and what I have contributed myself;
7. None of this work has been published before submission

Signature: ..... Date: .....



## Acknowledgements

Firstly, I wish to express my thanks to my supervisor Martin Solan for his tireless support. He not only continuously encouraged me to push the boundaries of my ecologist mindset but demonstrated first-hand that you can have many spinning plates in academia. His non-judgemental support during the unknowns of the pandemic, and everything else life threw at me, was invaluable. I'll always look back fondly on the many in depth discussions regarding early electronic music and loud obnoxious vehicles.

To my supervisor Jasmin Godbold, I thank for having faith in me, as a very underwhelming MSci student, to pursue a PhD. The ChAOS research expedition was a positive turning point in my academic journey and I can safely attribute her supervision leading up to and during it. Her pragmatism and patience throughout my PhD has also been essential, especially when Martin and I go off on unrealistic “super-experiment” tangents. Vielen Dank!

I also thank my supervisor Phillip Fenberg for the opportunities to reflect on my work and offer guidance. I enjoyed our brief chats in the corridor about the potential of CTscans for macroevolutionary and macroecological analyses.

Kindest thanks also to Philippe Archambault, for the tremendous opportunity to be part of the 2021 Amundsen expedition and visit Laval the following year. I also extend my gratitude to Clement Garcia, for his constant guidance as I got to grips with predictive ecology, extinction models, and R. Deepest gratitude also to Gavin Foster, Chris Standish, Chris Hauton, Lloyd Peck and Adam Reed for their invaluable support and the dedicated scientific crew members of the Amundsen and ChAOS expeditions for cherished memories that will resonate with me forever. I look forward to collaborating more with all of you in the future.

I give thanks to the GSNOCS PhD cohorts, many of whom are dear friends, for their patience during my rants about science, and their ability to take my mind of it. I also thank my housemates Emma and Ben, encouraging that work-life balance I sorely needed at times.

I want to thank all the support staff and technicians who in no small part, helped me along my journey. Cynthia, Dan, George, John, Nicola, Matt, Robbie, without you I would have never got this far.

Finally, to my family. Mum and Dad, I will never forget your unbounded support, always accommodating my seemingly sporadic change of plans. Dee, thank you for keeping me on my toes as a sibling every should. Nan, I wish you were still here to read this – I hope I have made you proud.

Dwi ond cystal â'r bobl o'm cwmpas!

## Acknowledgements

Financial support was provided by the INSPIRE Doctoral Training Partnership programme (grant NE/S007210/1) and 'The Changing Arctic Ocean Seafloor (ChAOS) - how changing sea ice conditions impact biological communities, biogeochemical processes and ecosystems' project (NE/N015894/1 and NE/P006426/1, 2017–2021), Natural Environment Research Council (NERC) in the UK. Computed Tomography scanning was supported by the National Research Facility for Lab X-ray CT (NXCT) at the  $\mu$ -VIS X-ray Imaging Centre, University of Southampton [EPSRC grant EP/T02593X/1]. The geochemical analyses were supported by ERC Advanced Grant 884650 Microns2Reefs.

Chapter 2 was conceived and designed by Thomas Williams, Martin Solan and Jasmin Godbold. Thomas Williams, Adam Reed and Jasmin Godbold collected the Arctic fauna and Lloyd Peck collected the Antarctic fauna. Thomas Williams conducted the experiments. Thomas Williams completed the statistical analysis with assistance from Martin Solan and Jasmin Godbold.

Chapter 3 was conceived and designed by Thomas Williams, Chris Hauton and Martin Solan. Thomas Williams carried out the experiment, completed the O<sub>2</sub> consumption, dissections and biochemical analysis. Thomas Williams completed the statistical analysis with assistance from Martin Solan.

Chapter 4 was conceived and designed by Thomas Williams, Gavin Foster and Martin Solan. Thomas Williams collected the bamboo coral, prepared the samples and conducted the geochemical analysis with Chris Standish. Thomas Williams completed the statistical analysis.

Chapter 5 was conceived and designed by Thomas Williams, Martin Solan and Clement Garcia. Thomas Williams modified the model simulation code to incorporate co-extinctions and co-compensations with assistance from Clement Garcia. Thomas Williams completed the statistical analyses with assistance from Martin Solan, Jasmin Godbold and Clement Garcia on interpretation of the findings.

All co-authors read, input and approved subsequent iterations of each respective chapter.

“And I tell you, if you have the desire for knowledge and the power to give it physical expression,  
go out and explore.”

Apsley Cherry-Garrard, *The Worst Journey in the World* (1922)



## Definitions and Abbreviations

[Ba] .....	Barium concentration
[Ba] <sub>SW</sub> .....	Barium concentration in Seawater
[CO <sub>2</sub> ] .....	Carbon Dioxide concentration
[NH <sub>3</sub> ] .....	Ammonia concentration
[NH <sub>4</sub> -N] .....	Ammonium concentration
[NO <sub>2</sub> -N] .....	Nitrite concentration
[NO <sub>3</sub> -N] .....	Nitrate concentration
[PO <sub>4</sub> -P] .....	Phosphate concentration
AMAP .....	Arctic Monitoring and Assessment Programme
B13 .....	Station B13 of the Barents Sea Transect
B14 .....	Station B14 of the Barents Sea Transect
B15 .....	Station B15 of the Barents Sea Transect
B16 .....	Station B16 of the Barents Sea Transect
B17 .....	Station B17 of the Barents Sea Transect
BEF .....	Biodiversity-ecosystem functioning
BP <sub>c</sub> .....	Bioturbation Potential of the Community
BP <sub>i</sub> .....	Bioturbation Potential of the Individual
BP <sub>p</sub> .....	Bioturbation Potential of the Population
CAFF .....	Conservation of Arctic Flora and Fauna
CTD .....	Conductivity, Temperature, Depth
CTscan .....	Computed Tomography scan
IPCC .....	Intergovernmental Panel on Climate Change
JR17007 .....	2018 Barents Sea Cruise
JR18006 .....	2019 Barents Sea Cruise
LME .....	Large Marine Ecosystem
NAO .....	North Atlantic Oscillation

## Definitions and Abbreviations

O<sub>2</sub>.....Oxygen

PAME ..... Protection of the Arctic Marine Environment

pCO<sub>2</sub> ..... Partial pressure of Carbon Dioxide

TOC ..... Total Organic Carbon

Xs ..... Station Xs of the Barents Sea Transect

# Chapter 1 Introduction



As integral parts of the global ocean, atmospheric, ecological and societal systems, the polar regions are at the forefront of climate concern (Post et al. 2019; Meredith et al. 2019). In the Arctic, where approximately four million people reside (and roughly 10% are indigenous (Arctic Council, 2004)), temperature rise has far outpaced the global average (Burrows et al. 2011; Rantanen et al. 2022). Unprecedented transformations have already been observed in sea ice dynamics (Meredith et al. 2019), ocean chemistry (Terhaar et al. 2020) and circulation (Liu et al. 2019b), permafrost thaw (Swanson, 2021) and glacier melt (Sharma et al. 2020). These physical system responses do not necessarily occur in isolation (Yamamoto-Kawai et al. 2009), and can both positively (Serreze & Barry, 2011) and negatively feed back (Callaghan et al. 2011) to the climate system. Moreover, there is mounting evidence indicating that climate feedbacks in the cryosphere may extend into the mid-latitudes (Barnes & Screen, 2015; Screen, 2018) though the validity of the signals are still contested (Overland, 2015; 2016). Nevertheless, the magnitude, rate and combination of environment changes has, and will likely continue to, present novel and complex challenges for the stability (Sivel et al. 2022), structure (composition, Frainer et al. 2017; diversity, Frainer et al. 2021) and functioning (Faust et al. 2020; Solan et al. 2020c) of Arctic ecosystems and provision of ecological services (O'Garra , 2017; Steiner et al. 2021) that society is so reliant on (Kaiser et al. 2016; Olsen et al. 2020). Indeed, climate change is expected to become one of the most influential drivers of change in global biodiversity in the coming decades (Leadley et al. 2010) and cooperative scientific and political engagement is urgently needed for addressing the complexities of climate feedbacks in the polar regions (Alvarez et al. 2020; Forbis Jr et al. 2018).

Scientific output on climate change in the Arctic has increased substantially from 20 publications in 1990 to 1765 in 2021 (total n = 18741 between 1950 and 2021, Figure 1.1), whilst publications focusing on the associated changes in biodiversity has been lagging behind (n = 1650 between 1950 and 2021, Figure 1.1) and predominantly skewed toward terrestrial systems (64.4%) compared to marine (26.4%) and freshwater systems (9.2%), in spite of the fact that the vulnerability of Arctic marine biota to climate change is not a recent discovery (Vibe, 1967; Gradinger, 1995). Attempts to quantify how climate change shapes large-scale ecological dynamics and trends have been, and will continue to be, moderated by spatiotemporal heterogeneity in effects (Pold et al. 2019; Hansen et al. 2019; Cassidy et al. 2020b; Godbold et al. 2013), habitats (Kortsch et al. 2019; Wohlgemuth et al. 2017; Cassidy et al. 2020a), capacities to compensate (Thomsen et al. 2017, 2019; Pan et al. 2016), alongside the time-consuming and expensive efforts for data collection in the Arctic (Mallory et al. 2018). As a result, “circumpolar” assessments of change are heavily skewed by the selective information from a limited number of regions, depths and contexts (Figure 1.2; Deb & Bailey, 2023). Furthermore, the responsiveness of

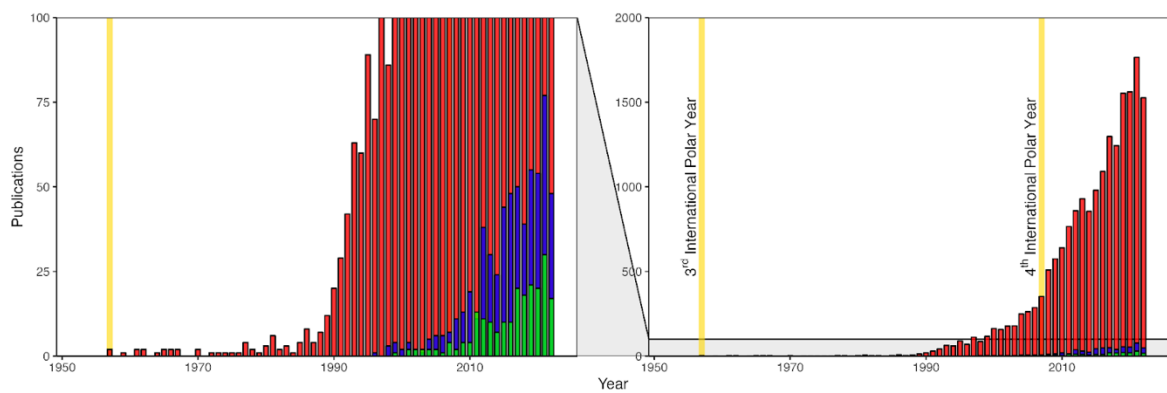


Figure 1.1 | Growth in the number of publications in the peer-reviewed scientific literature

focussing on climate change research in the Arctic between 1950 and 2021. Data was extracted from the *ISI Web of Science* (accessed on 10/01/2023) using the *Advanced Search* feature, with search strings (**red**) ("Arctic" AND "climat\* chang\*"), (**blue**) ("Arctic" AND "climat\* chang\*" AND "biodiversity") and (**green**) ("Arctic" AND "climat\* chang\*" AND "biodiversity" AND benth\*) in the titles and keywords of all document types across all databases and collections.

species to recent (Parmesan & Yohe, 2003; Root et al. 2003; Pounds et al. 1999) and past (Overpeck et al. 2002; Benton & Twitchett, 2003) climate change raises the possibility that anthropogenic climate change could act as a major cause of extinctions in the near future (Thomas et al. 2004; Hannah, 2012). Yet despite calls for the development of more realistic scenarios that integrate spatial-temporal variability in these controlling factors (Naeem, 2008), simulations on natural systems that do so are still rare (Garcia et al. 2021).

In selected Arctic regions where data is sufficient to assess trends in marine biodiversity (Figure 1.2), ecological changes that are consistent with climatic forcing have been recorded across multiple trophic levels in the pelagic, benthic, and sympagic (sea ice related) realms (Frederiksen et al. 2017; Wassman et al. 2011; Deb & Bailey, 2023). Changes in sea ice extent has already resulted in earlier and larger-celled phytoplankton blooms (Kahru et al. 2011; Fujiwara et al. 2016) whilst a proliferation of thinner first year ice cover may favour growth of microalgae and increase their contribution to primary production (Song et al. 2016). Evidence demonstrates that shifts in the spatial pattern and timing of the ice algal and phytoplankton blooms have influenced the

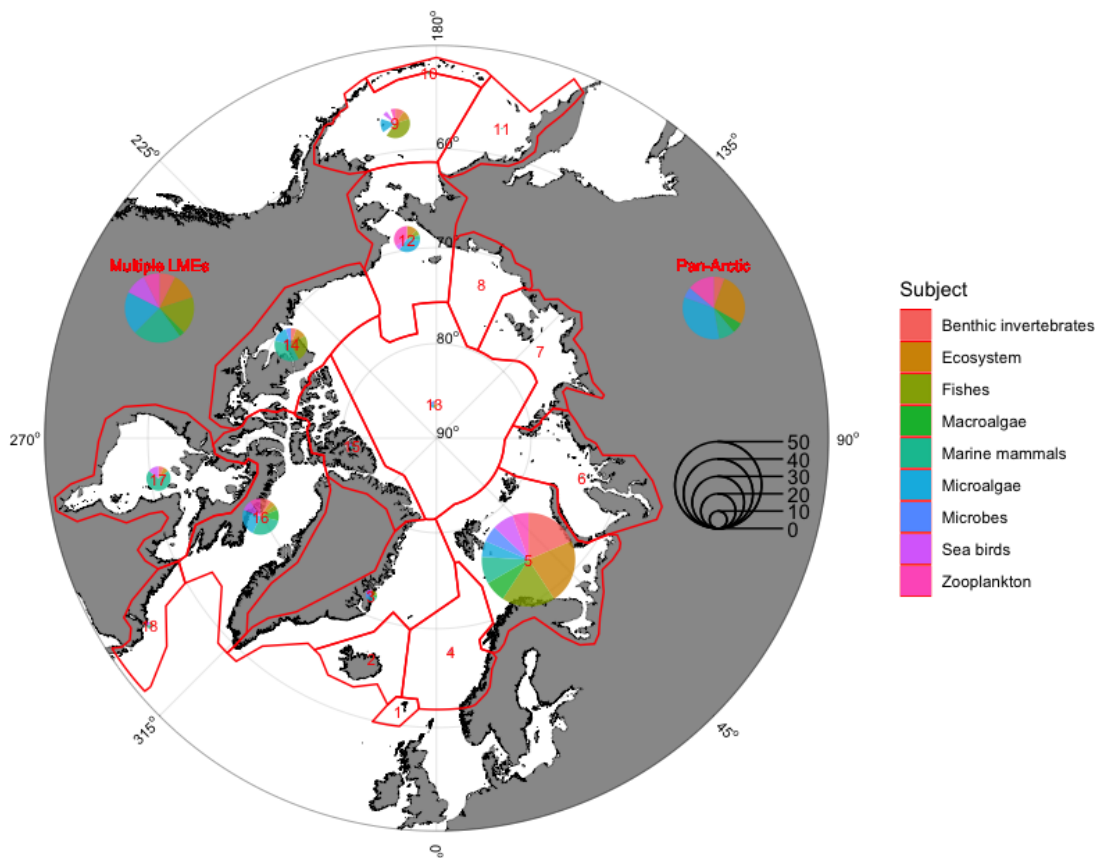


Figure 1.2 | Map adapted from Deb & Bailey, (2023) showing the current state of Arctic marine, and climate change research within each Large Marine Ecosystem (LME) of the Arctic as defined by the Arctic Council's Protection of the Arctic Marine Environment Working Group (PAME 2013). The colour of pie charts indicates the ecological subject of the studies conducted in each LME, whilst the size indicates the total number of studies. Most of the studies were conducted in Barents Sea LME (21%), followed by the Baffin Bay (8%) and Beaufort Sea (8%). Less than 2% of studies were conducted in the Aleutian Islands LME, Iceland LME and Eastern Bering Sea LME. The number of studies conducted across all LMEs (Pan-Arctic) (14%) and two or more (multiple) LMEs (16%) are also shown.

phenology, magnitude and duration of zooplankton production (Dalpadado et al. 2020) with changes in the zooplankton community composition (Skjoldal et al. 2022) and productivity (Kimura et al. 2022) also recorded. Even so, concerns over the cascading effects that sea-ice driven changes in both primary and secondary production will have on the pelagic-benthic pump (Wassman & Reigstad, 2011) are already being realised in the biodiversity and productivity at the seafloor (Link et al. 2013) as this food supply is critical for the growth and survival of benthic organisms. Indeed, within distinct hydrographic regions, benthic community patterns are directly

affected by the export production of organic matter from the overlying water column (Piepenburg et al. 1995), with assemblages often acting as long-term integrators of overlying water column processes. Observed effects of climate change on organisms, communities and biological processes at extreme depths are largely unknown. However, the likely destabilisation of ecosystem services under forthcoming temperature, oxygen and pCO<sub>2</sub> changes will be felt across all trophic levels and marine layers (Levin and Le Bris, 2015, Sweetman et al. 2017), with the largest effects projected to occur by the turn of the century (Battaglia and Joos, 2018).

Around 90% of Arctic marine invertebrates known today are benthic (CAFF, 2013) with the total known benthic species richness in the order of ~4600 species (Sirenko 2001; Bluhm et al. 2011; Piepenburg et al. 2011). Such biodiversity forms an integral component of food webs and carbon budgets in seasonally-ice covered shelf-seas (Moore & Stabeno, 2015; Jay et al. 2012), coastal margins (Rysgaard & Nielsen, 2006; Thomas, 2021) and polynyas (Grebmeier & Barry, 2007) all of which are sustained via tight benthic-pelagic interactions (Ambrose and Renaud 1995; Grebmeier et al. 2006b; Peterson & Curtis, 1980). The diversity of activity exhibited by benthic organisms in terms of their movement, feeding, burrowing and irrigation has been shown to modify, maintain and create habitats (Jones et al. 1994; Lawton, 1994), facilitate the reworking of sediment and redistribution of pore water fluids (Pearson, 2001), influence the sediment-microbial community structure and diversity (Solan & Wigham, 2005), enhance carbon sequestration (Cochrane et al. 2012 and references therein) and biogeochemical cycling at the sediment-water interface (Boudreau & Jørgensen, 2001; Furukawa, 2005). Due to the large proportion of shallow shelf seas (< 300 m) in the Arctic, parts of which have been found to exhibit biomass densities of benthic invertebrates upwards of 7000 ind.m<sup>-2</sup> (Carroll et al. 2008) and 60 g.C.m<sup>-2</sup> (Grebmeier et al. 2006a), the benthic food web is argued to be relatively more important in the Arctic than at lower latitudes (Gulliksen et al 2009).

Despite a well-received consensus of the importance of the Arctic benthos from both scientific and intergovernmental parties (Murphy et al. 2016; Whitehouse et al. 2014; CAFF, 2013), Arctic studies that link benthic biodiversity patterns to ecosystem processes on large spatial scales are scarce (e.g. Highsmith & Coyle 1990; Solan et al. 2020c) – a likely consequence of significant temporal and spatial inconsistencies in benthic biodiversity research intensity (Figure 1.3). Though we have access to a vast amount of benthic data, the temporal sequence of data collection is regionally specific. Different countries and their respective research efforts have obtained data at various times, leading to a patchwork of information that does not necessarily overlap. For instance, all pre-industrial revolution biodiversity data is concentrated in Russian-Arctic shelves (Zenkevich, 1963; Vetrov & Romankevich, 2004), while the Canadian Arctic, Barents Sea and Bering Strait were primarily investigated post-industrial revolution (Figure 1.3b). As a result,

databases that aim to be a point of reference for future studies on the distribution, biomass and functional activity of benthic fauna are limited in their spatiotemporal coverage (Stratman et al. 2020; Solan et al. 2019; Figure 1.3c-d). By extension, when taken together, this explains why studies with a benthic biodiversity focus only make up a fraction of all climate-change-related publications ( $n = 213$  between 1985 and 2022 from ISIS Web of Science; Figure 1.1) and just under 10% of investigations on impacts on Arctic marine biota (Figure 1.2, Deb & Bailey, (2023)). Despite this relatively small pool of knowledge, the expression of climate change in the Arctic is expected to have substantive effects at the seafloor (Renaud et al. 2015; Kędra et al. 2015; Solan et al. 2020c). However, macroinvertebrate assessments are largely limited to general statements about range shifts, species introductions and population dynamics (Wassman et al. (2011) and references therein; Josefson and Mokievsky, (2013); Renaud et al. (2019); Grebmeier et al. (2018); Fedewa et al. (2020); Hansen et al. (2020)). Though this type of information is a useful indicator for changes in the overlying water column (Carroll & Ambrose 2012) it does not capture impacts on benthic productivity and ecosystem processes.

The study of Arctic benthic biodiversity-ecosystem functioning (BEF) has been hindered by the sporadic availability of quality-controlled observational data (Figure 1.3) alongside a lack of understanding of the mechanisms that cause patterns of observed biodiversity change (Deb & Bailey, (2023)) and relate them to changes in ecosystem processes. In the context of climatic forcing, there is an urgent need for clear and in-depth information on the cause-and-effect relationships between environment change and Arctic benthic BEF, while also considering the interdependencies between climatic drivers (Kroeker et al. 2013), time-dependent response mechanisms such as acclimation and adaptation (Form et al. 2012; Pörtner, 2008; Isotalo et al. 2022), and context- and species-specific compensatory mechanisms (Kroeker et al. 2010; 2011; Siebel et al. 2012). It follows, therefore, that investigations at the level of the organism are critical, especially as the ability to tolerate, and adapt to, variation in changing conditions is tightly related to the biological traits they exhibit (Clarke, 1993) which can differ between conspecifics, species and spatio-temporal contexts (Cassidy et al. 2020; Godbold & Solan, 2013). In a benthic functioning perspective, the contribution of individual organisms to an ecosystem function is closely intertwined to their expression of traits (Snelgrove et al. 2014; Lam-Gordillo et al. 2020). As such, climate-driven changes in environmental conditions that affect trait expression can, subsequently, influence nutrient turnover and productivity (Bulling et al. 2010; Hicks et al. 2011; Godbold & Solan, 2013). By addressing all of these gaps, a better understanding of the complex interplay between climate change and Arctic benthic BEF can be gained, ultimately contributing to the development of more realistic biodiversity models that can be utilised for informing management strategies for this fragile ecosystem.

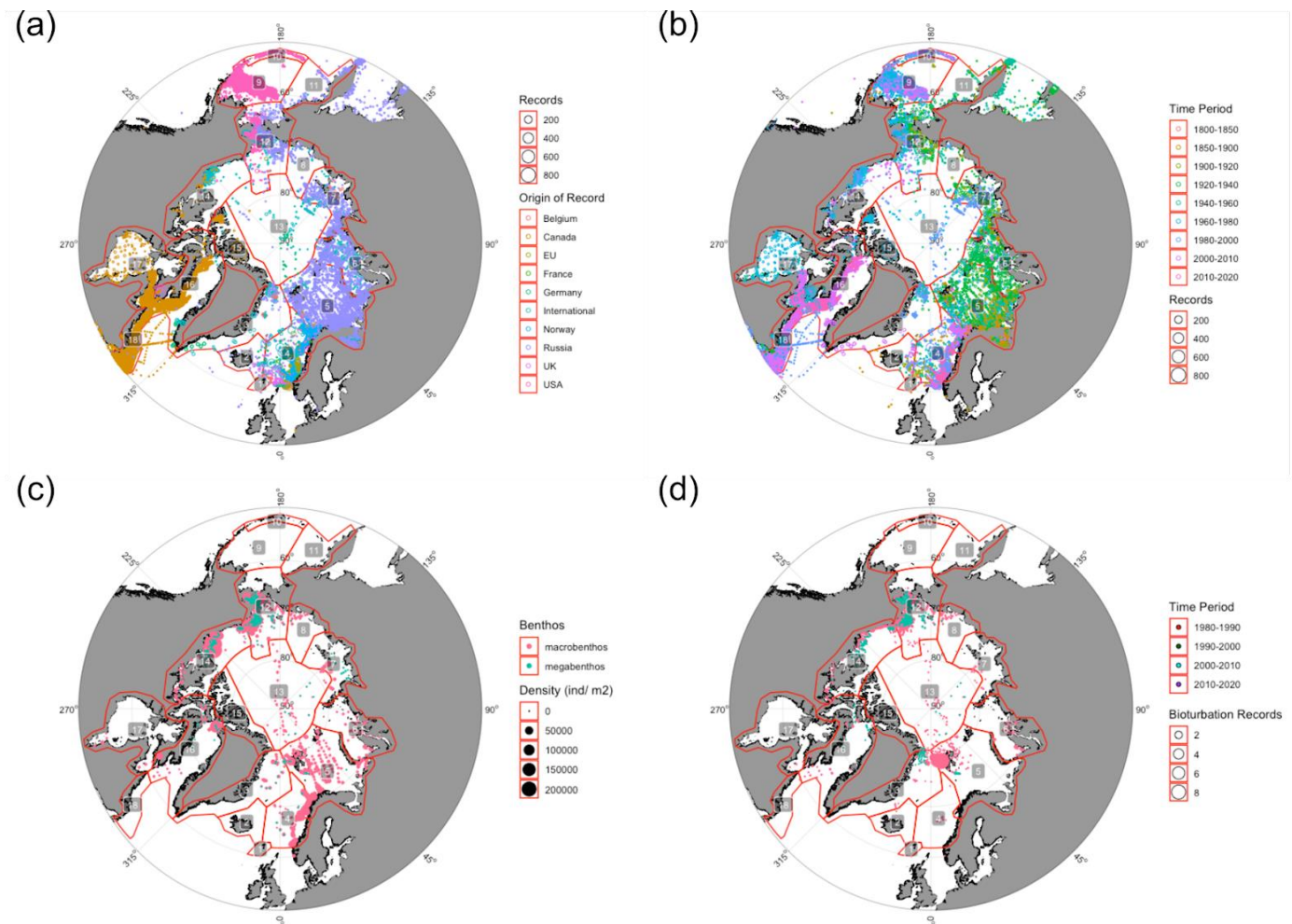


Figure 1.3 | Circumpolar distribution of (a-b) Records of benthic biodiversity above 60 °N and between 1800-2020 extracted from the Ocean Biodiversity Information System [access date 25/10/2021] demonstrating (a) the national efforts of Observer and Arctic States and (b) temporal coverage of data, (c) benthic fauna density data north of 60 °N extracted from the BenBioDen database (Stratmann et al. 2020) and (d) bioturbation intensity (Db) records above 60 °N extracted from Solan et al. (2019). Records are presented within each Large Marine Ecosystem (LME) of the Arctic as defined by the Arctic Council's Protection of the Arctic Marine Environment Working Group (PAME 2013).

## 1.1 Aims and Objectives

The aims of this thesis are to investigate:

- (i) context-specific Arctic organism responses in behaviour and the associated consequences for benthic ecosystem functioning and,
- (ii) fitness-trade-offs of Arctic benthic organisms to long-term exposure of climatic drivers.

Where Arctic benthic organisms show differences in persistence under climate change, the thesis will evaluate:

- (iii) their ability to record environmental data to bridge the gaps in instrumental records on benthic functionality and climate model estimates and,
- (iv) the context-dependent relationship between projected climate-induced changes in the environment, benthic biodiversity change and ecosystem functioning.

Specifically,

**Chapter 2** investigates the influence of species identity, intra-specific variability and environmental history on organism behaviour, sediment-reworking, ventilation activity, and nutrient concentrations at the sediment-water interface in the face of ambient and near-future climate change. To achieve this, five macroinvertebrate species (three from the Arctic and two from the Antarctic) are subjected to a 2100 climate scenario for a 3-month duration, where temperature and [CO<sub>2</sub>] are experimentally manipulated. I aim to quantify the behavioural expression of individuals and species under varying abiotic factors, identify the level of plasticity within and among cold-water taxa to environmental change, and determine the level of context-dependency in the relationship of polar benthic invertebrates and functioning.

Marine organisms that exhibit high levels of phenotypic plasticity may do so at risk of impeding other biological functions in the instance of incomplete whole organism adaptation. Hence,

**Chapter 3** explores this possibility in cold-water taxa, subjecting four species of macroinvertebrates from the Arctic and Antarctic to a 360 day exposure of a 1.5 °C rise in temperature and 550ppm [CO<sub>2</sub>] to investigate whether the rate of whole organism functions (respiration, excretion) differ between organisms in present versus near-future environmental conditions. As changes in environmental conditions can result in compensatory species responses,

**Chapter 3** also explores whether species employ different physiological compensation mechanisms to maintain whole organism performance.

Gaining a comprehensive understanding of species' responses to past environmental modifications, including climate change, is crucial for predicting their future responses to ongoing climate forcing. Due to limited instrumental records and imprecise projections of contemporary climate change, **Chapter 4** explores the feasibility of using a cold-water species of bamboo coral to analyse high-resolution archives of environmental variability in the deep Arctic Ocean.

Additionally, **Chapter 4** retrospectively investigates the influence of intra- and inter-colony "vital effects" on reconstruction uncertainty using geochemical tracers (Mg/Ca, Li/Mg, Sr/Ca, Ba/Ca and U/Ca), considering the importance of biological variation for adaptive success in response to environmental perturbations (**Chapter 2** and **3**). Assessing the effectiveness of benthic calcifiers as indirect indicators of climate change will improve our understanding of changes in the Arctic deep-sea, while also providing insights into species' responses over longer timescales than current data allows.

The functional response of surviving communities is of scientific and socio-economic concern, but existing predictive models of the ecological effects of local extinctions are limited with respect to how realistic and relevant they are to the most likely system responses to change. Hence, using data from the Barents Sea, **Chapter 5** uses a trait-based model for marine benthic communities to explore local vs regional effects of spatial variability on simulated "borealisation" of biodiversity and community functioning (community bioturbation potential,  $BP_c$ ). Contrary to previous models, here I will include co-extinctions and multiple post-perturbation compensatory mechanisms derived from a gradient of environmental change.

Collectively, these contributions will explore the magnitude, direction, and context of macrobenthic responses to past, present and future climate change – and their concomitant effects on benthic ecosystem functioning in one of the most rapidly changing environments in the world. While I expect to observe changes in organism behaviour and physiology due to climate-driven environmental change, there will likely be significant variations in response among individuals and species, as well as differences across various contexts, which will inevitably influence the reliability of living proxies for climate change and the outcomes of biodiversity-ecosystem functioning following "borealisation" events. Nevertheless, I anticipate that these responses, at both the individual and community level of biological organisation, will have a fundamental effect on benthic ecosystem functioning.



## **Chapter 2 Intra- and inter-specific differences in invertebrate behavioural trait expression moderate present and future benthic biogeochemical functioning in regions of rapid climatic transition**



## 2.1 Abstract

Climate change is known to affect the distribution and composition of species, but how associated alterations in functionally important aspects of behaviour and species-environment relations further modify ecosystem outcomes is poorly constrained. Here, using sediment-dwelling marine invertebrates from polar regions experiencing rapid rates of climate change, I examine the ecosystem ramifications of changes in invertebrate contributions to fluid and particle transport - key processes that mediate benthic nutrient cycling - in response to anticipated near-future environmental conditions (+1.5 °C, 550 ppm [pCO<sub>2</sub>]). I find, despite high levels of inter-specific variability, warming and acidification fundamentally alter species effects on the magnitude and direction of nitrate and nitrite concentrations and also lead to a reduction in intra-specific variability of behavioural trait expression. In addition, my analyses indicate that species behaviour between populations across my regions of climatic transition is not predetermined and, instead, can depend on local variations in environmental history that set species capacities for acclimation. My findings provide evidence that specific and subtle aspects of inter- and intra-specific variations in behavioural trait expression, rather than the presence or relative proportional representation of species *per se*, is an important and underappreciated determinant of benthic biogeochemical responses to climate change, and may act as an early warning for impending ecological transitions associated with progressive climatic forcing.

## 2.2 Introduction

Narratives of the ecological consequences of climate change in regions where system responses are amplified often centre on the wide-spread changes in biodiversity, food-web structure and productivity that are taking place (Kędra et al. 2015, Jørgensen et al. 2019, Cochrane et al. 2009; Garcíá Molinos et al. 2016, Solan et al. 2020c), rather than the ecological consequences of alternative subtler outcomes that typically form the prelude to compositional restructuring and/or altered levels of biodiversity (Nagelkerken & Munday, 2016; McLean et al. 2016). Species responses to climate change can include avoidance through dispersal (Loarie et al. 2009; Schloss et al. 2012), acclimation through phenotypic plasticity (Gibbin et al. 2017, Norin & Metcalfe, 2019), including adjustments to physiological regulation (Dillon et al. 2010), and adaptation through genetic modification (Williams et al. 2008; Hoffmann and Sgrò 2011). However, these alternative strategies are not always viable or, when available and integrated, are not necessarily equally weighted as an effective means of response (Magozzi & Calosi 2014). Indeed, in areas of greater risk from projected environmental change, such as those at higher latitudes, opportunities for dispersal and adaptation are often limited due to local evolutionary history and ecology (Reed et al. 2020), meaning that phenotypic plasticity becomes the primary mechanism for organisms to mediate the effects of rapid environmental change (Bonamour et al. 2018). For organisms with very long generation times, as is common in polar regions (Moss et al. 2016; Vogt, 2019), behavioural acclimatisation to novel environmental conditions can maximise an individual's

chance of survival (Woods et al. 2015; Kearney et al. 2009; Ma et al. 2018) before any potential genetic adaptation can take effect (Peck, 2011). Previous work has largely focussed on invertebrate physiological plasticity in relation to ocean warming (Clark et al. 2017; Richard et al. 2012a,b) and acidification (Cummings et al. 2011; Cross et al. 2015; Lischka & Riebesell, 2012; Wood et al. 2011), whilst behavioural plasticity has received less attention (Christiansen et al. 2015; Morley et al. 2012a), even though changes in behaviour often form the first observable and practical response to altered environmental context (Tuomainen & Candolin, 2011, Wong & Candolin, 2015), and can have significant consequences for other ecosystem attributes (Palkovacs & Dalton, 2012, Wilson et al. 2020, Snelgrove et al. 2014). Consequently, the specifics of how and when climate related change affects the way in which species behaviour modifies ecosystem functioning under near-term futures is woefully under-appreciated (Buchholz et al. 2019; Gunn et al. 2021).

The activities of sediment-dwelling invertebrates play a significant role in the redistribution of pore water fluids and sediment particles. Such behaviour can have a profound influence on sediment biogeochemistry and microbiology (Pearson, 2001; Meysman et al. 2006) and, ultimately, global carbon and nutrient cycles (Griffiths et al. 2017; Snelgrove et al. 2018). It follows, therefore, that any directional change in species behaviour or trait expression associated with a change in circumstance will have important consequences for ecosystem process and function (Godbold et al. 2009; de Smit et al. 2021). Indeed, evidence suggests that changes in behaviour and/or trait expression, although species and context dependent (Murray et al. 2014; Wohlgemuth et al. 2017, Cassidy et al. 2020), may maintain (Frid & Caswell, 2015), reduce (Murray et al. 2013) or enhance (Biles et al. 2003, Ouellette et al. 2004, Maire et al. 2010) functioning relative to that achieved under prior conditions. Consequently, it has been difficult to pinpoint alterations in ecosystem properties associated with behavioural change as the net functional position is the product of multiple species responses. Disentangling these is further frustrated by the fact that changes in behaviour are also accompanied by numeric or biomass compensatory responses (Calder-Potts et al. 2018; Thomsen et al. 2017, Thomsen et al. 2019) that affect dominance patterns (Winfree et al. 2015, Wohlgemuth et al. 2016), and other factors which can partially or wholly offset directional change in functional responses to forcing (O'Connor & Donohue 2013). Nevertheless, field observations have highlighted that a shift in the type and amount of faunal activity can lead to environmental transitions (McIlroy & Logan 1999, Solan et al. 2020c) that can exert a disproportionate influence on ecosystem properties and functioning that is additional to the effects of changes in species diversity (Emmerson et al. 2001, Solan et al. 2004a, Cardinale et al. 2012) and composition (Norling et al. 2007, Wohlgemuth et al. 2016). It is

important to note, however, that although flexible behavioural strategies can improve short-term fitness (Van Colen et al. 2020; Zhou et al. 2022), the emergence of associated functional consequences (Murray et al. 2017; Woodin et al. 2016) may not fully materialise until much later and can be hard to distinguish from other temporal changes in the system (Godbolt & Solan, 2013).

I anticipated that changes in species behaviour are likely to be more pronounced in regions of fast paced climatic change, as genetic and other coping mechanisms take longer to implement and cannot be enacted in time (Burrows et al. 2011). I speculated, given the closure of dispersal and adaptation as viable options, that adjustments to behaviour would dominate species responses to change at higher latitudes, providing opportunity to assess the relative importance of behavioural plasticity in determining functional outcomes. Here, using sediment-dwelling invertebrate species obtained from areas of the Arctic and Antarctic currently experiencing amplified levels of climatic change (Kohnemann et al. 2017; Vaughan et al. 2003), I explore the combined effects of ocean warming and acidification on important aspects of species behaviour known to influence biogeochemical cycling. As I anticipate that the direction and magnitude of change in organism behaviour will diverge between species (Nagelkerken and Munday, 2016), mirroring known interdependencies in physiological responses to multiple environmental changes (Harvey et al. 2013, Przeslawski et al. 2015), I also include fauna from two locations within the Barents Sea that contrast in ocean temperature and sea ice dynamics. For these species, my expectation is that individual species responses will be in line with previous observations (Solan et al. 2020c), but more pronounced for individuals obtained from locations experiencing a narrower environmental variation. If my expectations are met, my findings will demonstrate the importance of behavioural change and compensatory mechanisms (Thomsen et al. 2017, Thomsen et al. 2019) in moderating how benthic environments respond to external forcing, and will emphasise how inappropriate it is to ascribe the functional role of species to a priori determined fixed typologies.

## 2.3 Materials and methods

### 2.3.1 Fauna and sediment collection

I obtained individuals of the bivalve *Astarte crenata* (Gray, 1824), asteroid *Ctenodiscus crispatus* (Bruzelius, 1805) and polychaete *Cistenides hyperborea* (Malmgren, 1866) from replicate SMBA (Scottish Marine Biological Association, 50 × 50 cm) box cores and 15 minute Agassiz trawls in the Barents Sea (stations B13, 74.3 °N, 30.0 °E; B16, 80.3 °N, 30.0 °E; JCR18006, *RSS James Clark Ross*, Appendix A, Figure S1a, Table S1) in July 2019. I also collected individuals of the protobranch *Aequiyyoldia eightsi* (Jay, 1839) and bivalve *Laternula elliptica* (P. P. King, 1832) using SCUBA-

assisted divers at Rothera Point, Adelaide Island, West Antarctic Peninsula (67.3 °S, 68.1 °W, Appendix A, Figure S1b) in March-April 2019. Surficial sediment (< 5 cm depth) for the Arctic species was collected using SMBA box cores at stations B13, B14 (76.3 °N, 30.3 °E) and B16 (Appendix A, Table S1) in July 2019 and, for the Antarctic species, sediment was collected by hand from the Hamble, UK (50.9 °N, 1.3 °W). Sediment was sieved (500 µm mesh) within a seawater bath to retain the fine fraction and remove macrofauna and debris. Sediment particle size frequency distributions (Appendix A, Figure S2) were determined using a Malvern Mastersizer 2000 He-Ne LASER diffraction sizer following standard protocols at the Department of Geography, University of Cambridge (available at: [www.geog.cam.ac.uk/facilities/laboratories/techniques/](http://www.geog.cam.ac.uk/facilities/laboratories/techniques/)) to quantify mean particle size, sorting, skewness and kurtosis (Folk, 1974) using GRADISTAT (Blott & Pye, 2001). Loss on ignition was used to determine sediment organic material content (%).

### 2.3.2 Experimental design and set-up

Sediment and species were distributed across 42 clear acrylic aquaria (internal LWH: 12 x 12 x 33 cm, 3 replicates treatment<sup>-1</sup>: species x location x climate scenario; Appendix A, Table S2), designed to accommodate representative field densities (Arctic species, 2 ind. aquarium<sup>-1</sup>; Antarctic species, 1 ind. aquarium<sup>-1</sup>; (Fritschie & Olden, 2016; Appendix A, Table S3) and the size and burrowing requirements of each species (sediment depth: *A. crenata*, *C. crispatus* & *C. hyperborea*, 16 cm; *A. eightsi*, 12cm; *L. elliptica*, 19cm; Davenport, 1998; Peck et al. 2004). Aquaria were randomly placed within one of two insulated seawater reservoirs (Solan et al. 2020c, Appendix A, Figure S3). All aquaria were overlain with seawater (salinity 33, 10 µm sand filtered, UV sterilized) to a standardised water depth of ~12 cm above the sediment-water interface and maintained in the dark. Fauna were exposed to ambient (1 ± 0.5°C, ~400 ppm [CO<sub>2</sub>]) or indicative near-future (3 ± 0.5 °C, ~550 ppm [CO<sub>2</sub>]) environmental conditions (IPCC, 2018). After acclimation to ambient aquarium conditions (21 days, 09-29/09/2019), water temperature and [CO<sub>2</sub>] were increased at 0.5°C and 50 ppm increments every 7 days, to minimise any adverse physiological response to the change in environmental conditions (Form & Riebesell, 2012). During both the acclimation and experimental period (92 days, 21/10/2019 – 21/01/2020), *C. crispatus* and *C. hyperborea* were fed *ad libitum* once a week with commercially available fish food (Aquarian Tropical Flake; 0.03 g), and *A. crenata*, *A. eightsi* and *L. elliptica* were fed *ad libitum* three times per week with 15 ml of precultured phytoplankton (33:33:33 mix, *Isochrysis* sp., *Tetraselmis* sp., and *Phaeodactylum* sp.; Algal Culture Laboratory, National Oceanography Centre Southampton). To avoid accumulation of excess food and associated nutrients, partial seawater exchanges (weekly, 50% volume) with seawater (pre-conditioned to the appropriate environmental condition) were undertaken.

### 2.3.3 Seawater carbonate chemistry, temperature and salinity

Atmospheric  $\text{[CO}_2\text{]}$  (Appendix A, Figure S4) was controlled using a  $\text{CO}_2$ -air mixing system from Godbold & Solan (2013). Carbonate systems developed and equilibrated within the head-space of each aquarium. Temperature, pH (NBS scale, Mettler-Toledo InLab Expert Pro temperature-pH combination electrode), salinity (WTW™ TetraCon™ 325 Standard temperature-conductivity combination electrode) and total alkalinity ( $A_T$ , Apollo SciTech Alkalinity Titrator AS-ALK2) were periodically measured ( $T, \text{pH}, S$ : weekly;  $A_T$ : week 2, 6, and 11).  $A_T$  analysis followed standard HCl titration protocols of the Carbonate Facility, University of Southampton. DIC,  $[\text{pCO}_2]$ ,  $[\Omega_{\text{calcite}}]$ ,  $[\Omega_{\text{aragonite}}]$ ,  $[\text{NCO}_3]$  and  $[\text{CO}_3]$  were calculated using the CO2calc carbon calculator (v 4.0.9) (Robbins et al. 2010; Appendix A, Figure S5).

### 2.3.4 Behavioural response of individuals

Behavioural activity of *C. crispatus*, *C. hyperborea* and *A. eightsi* were quantified using measurements of movement and burial behaviour at the sediment surface. Individuals (morphology,  $\pm 0.01$  mm; blotted wet weight,  $\pm 0.001$  g, Appendix A, Table S5) were placed in treatment-acclimatised viewing trays containing sediment (depth 5 cm) overlain with sea water (depth 3 cm) and viewed ( $\leq 60$  minutes) with a benchtop video camera (Logitech C920 HD Pro Webcam, 1080p; Appendix A, Figure S6). The time taken for each individual to initiate movement (response time, s) and to complete burial (burial time, s) was recorded (3 frame  $\text{s}^{-1}$ , SkyStudioPro) and analysed frame-by-frame (VLC Media Player). Rather than expressing responses relative to total wet biomass (g), I opted to incorporate biomass as a random factor in the statistical analysis to account for differences in the effects of biomass between species and/or context (Zuur et al. 2009).

### 2.3.5 Effects on ecosystem process and functioning

Sediment particle reworking and ventilation activity for each of the five species under study were determined from sediment profile images of the redistribution of particulate luminophore tracers (dyed sediment, fluorescent under ultraviolet light; 30 g  $\text{aqua}^{-1}$ , 125 – 250  $\mu\text{m}$  diameter, 12 day incubation 09/01/2020-21/01/2020; Solan et al. 2004b, Schiffers et al. 2011). All four sides of each aquarium were imaged under UV light (Canon EOS 400D, 3888 x 2592 pixels, effective resolution 74 x 74  $\mu\text{m}$  per pixel) stitched together (Adobe Photoshop CC 2019; Appendix A, Figures S7 to S11) and the redistribution of luminophores was analysed using a semi-automated plugin within ImageJ (version 1.46r; Solan et al. 2004b). From these profile data (Appendix A, Figure S12), I calculated the mean ( ${}^f\text{-SPL}_{\text{mean}}$ , time dependent indication of mixing), median ( ${}^f\text{-SPL}_{\text{med}}$ , typical

short-term depth of mixing) and maximum ( $f\text{-SPL}_{max}$ , maximum extent of mixing over the long-term) mixed depth of particle redistribution. Given the shape of the vertical distribution of luminophores,  $f\text{-SPL}_{mean}$  was determined to be an unsuitable descriptor of the redistribution profile and was not considered for statistical analysis. The rugosity of the sediment-water interface (upper – lower limit = surface boundary roughness, SBR) provided an indication of surficial activity.

Ventilatory behaviour - the active transfer of fluid by infaunal organisms (Solan et al. 2019) - was estimated from absolute changes in the concentration of the inert tracer sodium bromide [NaBr]. Since water depth varied between aquaria of different species, dissolved [NaBr] was standardised across all aquaria (mean starting concentration =  $1353.816 \pm 317.264 \text{ mg L}^{-1}$ ) and [NaBr] was determined using a Tecator flow injection auto-analyser (FIA Star 5010 series). Negative values of change in [NaBr] ( $\Delta[\text{Br}^-] \text{ mg L}^{-1}$ ) over an 8 hour period are indicative of increased infaunal ventilatory activity.

As nutrient concentrations at the sediment-water interface are mediated by benthic fauna activity, I determined water column  $[\text{NH}_4\text{-N}]$ ,  $[\text{NO}_3\text{-N}]$ ,  $[\text{NO}_2\text{-N}]$  and  $[\text{PO}_4\text{-P}]$  ( $\mu\text{mol L}^{-1}$ ) from filtered samples ( $\sim 10\text{ml}$ ,  $0.45 \mu\text{m}$  NALGENE nylon matrix) once a month (Appendix A, Figure S13) using a QuAAstro 39 continuous flow auto-analyser (SEAL Analytical). As nutrient concentrations *per se* would reflect differences in the volume of sediment between species treatments, I calculated the log response ratio ( $\text{lnRR} = \text{ln}[\text{conc}_{\text{before}}/\text{conc}_{\text{after}}]$ ; Hedges et al. 1999), a formal effect size measure that quantifies proportionate change, rather than absolute values. As patterns of  $[\text{NO}_x\text{-N}]$  are reciprocal to those of  $[\text{NH}_4\text{-N}]$ , because bioturbation stimulates denitrification within the nitrogen cycle (Solan, 2016), lnRR values for  $[\text{NO}_2\text{-N}]$  and  $[\text{NO}_3\text{-N}]$  are multiplied by -1 to align the effect sizes with a positive direction of ecosystem functioning.

### 2.3.6 Statistical analysis

Analysis of Variance (ANOVA) models were developed for each dependent variable (behaviour: response time, burial time; ecosystem process: SBR,  $f\text{-SPL}_{median}$ ,  $f\text{-SPL}_{max}$ ,  $\Delta[\text{Br}^-]$ ; ecosystem functioning:  $[\text{NH}_4\text{-N}]$ ,  $[\text{NO}_3\text{-N}]$ ,  $[\text{NO}_2\text{-N}]$ ,  $[\text{PO}_4\text{-P}]$ ). For *A. crenata* and *C. crispatus*, I determined the effects of the independent variables environmental condition (2 levels: ambient, future), location (2 levels: stations B13 and B16), species identity (2 levels), and their interactions, whilst for *A. eightsi* and *L. elliptica*, I determined the effects, alone and in combination, of the independent variables environmental condition (2 levels) and species identity (2 levels). As *C. hyperborea* was found at a single station, I determined only the effects of the independent variable environmental

condition (2 levels). The extent of intra-specific variability in response within treatment levels was determined using the coefficient of variation.

Model assumptions (homogeneity of variance, normality, outliers) were visually assessed using standardised residuals vs fitted values plots, Q-Q plots and Cook's distance (Zuur et al. 2010). Where there was a violation of homogeneity of variance, I used a varIdent variance-covariance structure and generalised least-squares (GLS) estimation (Pinheiro & Bates 2000, West et al. 2014), to allow residual spread to differ between the explanatory variables. I determined the optimal fixed-effects structure using backward selection informed by Akaike Information Criteria (AIC) and inspection of model residual patterns. For the GLS analysis, I determined the optimal variance-covariance structure using restricted maximum-likelihood (REML) estimation by comparing the initial ANOVA model without variance structure to equivalent GLS models incorporating specific variance terms. These models were compared for suitability against the initial ANOVA model using the AIC informed by visualisation of model residuals. I determined the optimal fixed structure of the most suitable model by applying backward selection using the likelihood ratio test with maximum-likelihood (ML) estimation (West et al. 2014, Zuur et al. 2010). For ANOVA models with interactions, I calculated the effect size ( $\omega^2$ , Graham & Edwards 2001) of each independent variable in R (R Core Team, 2022) using the *effectsize* package (Ben-Shachar et al. 2020). For GLS models with interactions, I determined the relative importance of each independent variable by comparing the minimal adequate model with a model with the independent variable of interest, and all of its interactions, removed using likelihood ratio (L-ratio) in the *nlme* package (Pinheiro and Bates, 2000). Details of initial and minimal adequate models (Model S1 to S29) and all data are provided in Appendix A.

## 2.4 Results

I find evidence that individual behaviour, sediment reworking, burrow ventilation, and associated nutrient concentrations, are dependent on environmental condition, location or species identity (Models S1 to S29), with observed effects seldomly (8 of 29 models) resulting from full factorial interactions. Despite observing mortalities in *A. crenata* (2 individuals, 1 from each climate), *C. crispatus* (4 individuals, 3 from ambient climate and 1 from future climate), and *C. hyperborea* (1 individual from ambient climate), it was still possible to relate my response variables in ecosystem process and functioning to species behaviour in all aquaria. Differences in mortality were accounted for by using total biomass of aquaria as a random effect, which was found to be insignificant across all models.

#### 2.4.1 Effects on individual behaviour

All individuals of *C. crispatus* ( $n_T = 18$ ) initiated movement within 60 minutes of being placed onto the sediment surface, with 16 individuals completing reburial (mean  $\pm$  s.e. =  $684.3 \pm 113.5$  s, range 1722 – 222 s), but I found no evidence that response time was affected by environmental condition, location or their interaction (intercept only model: L-ratio = 1.420, d.f. = 1,  $p = 0.234$ ; Figure 2.1a). However, mean response time ( $\pm$  s.e.) was less variable among individuals from station B13 ( $370.9 \pm 48.3$  s; CV = 34.5%) relative to between individuals from B16 ( $492.3 \pm 93.3$  s; CV = 62.9%). Regardless of location, mean burial time of *C. crispatus* was influenced by environmental condition ( $F_{[1,12]} = 5.285$ ,  $p < 0.05$ ), with reburial time (mean  $\pm$  s.e.) halving under future conditions (ambient,  $995.0 \pm 199.6$  s; future,  $497.9 \pm 103.8$  s; Figure 2.1b). For *C. hyperborea*, 9 individuals ( $n_T = 11$ ) responded within 60 minutes, with comparable response rates across two environmental conditions ( $F_{[1,7]} < 0.001$ ,  $p = 0.992$ ; Figure 2.1a). However, only three individuals under future conditions reburied within the 60 minute period, an insufficient number for reliable statistical analysis. For *A. eightsi*, mean ( $\pm$  s.e.) response time ( $378.5 \pm 201.5$  s, range, 1322 – 44 s,  $n = 6$ ) was not dependent on environmental condition (intercept only model, L-ratio = 2.277, d.f. = 1,  $p = 0.131$ ; Figure 2.1c), despite a substantive reduction in intra-specific variability under future conditions (CV: ambient, 95.7 %; future, 51.5%). The effect of environmental condition on the burial time of *A. eightsi* was weak (L-ratio = 3.5943, d.f. = 1,  $p = 0.0580$ ), despite a reduction in intra-specific variability (CV: ambient = 42.3%, future = 28.4%) and burial time (mean  $\pm$  s.e.: ambient,  $144.3 \pm 35.3$  s; future,  $67.3 \pm 11.1$  s ; Figure 2.1d). I found no effect of biomass as a random factor in any of these models.

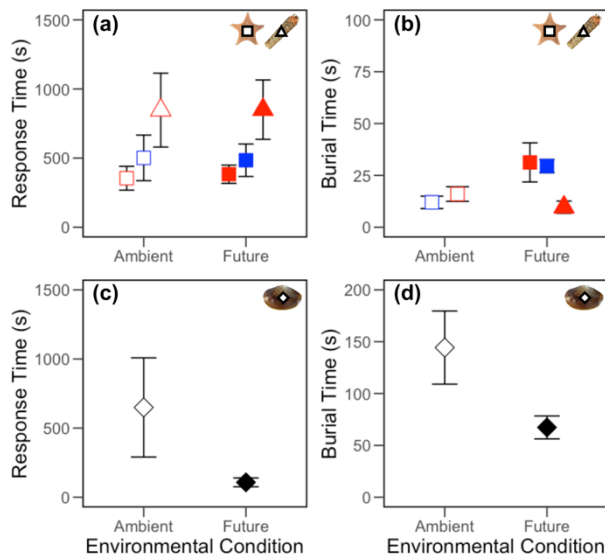


Figure 2.1 | . The effects of species identity, location and environmental condition (ambient, open symbols; future, closed symbols) on (a,c) mean ( $\pm$  s.e.) response time and (b,d) mean ( $\pm$  s.e.) burial time for *Ctenodiscus crispatus* (squares) and *Cistenides hyperborea* (triangles) obtained from station B13 (red) and B16 (blue) in the Barents Sea and *Aequioldia eightsi* (diamond) obtained from Rothera Point (black).

#### 2.4.2 Effects on ecosystem process

Surface boundary roughness in the presence of *A. crenata* and *C. crispatus* (Figure 2.2a, b) was dependent on the independent effects of species ( $L$ -ratio = 10.056, d.f. = 1,  $p < 0.01$ ; *A. crenata*:  $16.42 \pm 1.63$  mm, *C. crispatus*:  $10.16 \pm 0.62$  mm) and location ( $L$ -ratio = 4.010, d.f. = 1,  $p < 0.05$ ; B13,  $14.28 \pm 1.30$  mm, B16,  $12.30 \pm 1.72$  mm), but not environmental condition ( $L$ -ratio = 3.238, d.f. = 1,  $p = 0.072$ ). For *C. hyperborea*, I also found no evidence that surface boundary roughness was affected by changes in environmental condition ( $L$ -ratio = 0.025, d.f. = 1,  $p = 0.8740$ ) despite an increase in intra-specific variability under future conditions (CV: ambient, 2.5%; future, 31.4%; Figure 2.2c). For *A. eightsi* and *L. elliptica*, I found no effect of environmental condition, species identity, or their interactions, on surface boundary roughness ( $F_{[1,8]} = 3.005$ ,  $p = 0.121$ ; Figure 2.2d).

The median mixed depth of particle reworking ( ${}^f\text{-SPI}L_{\text{med}}$ ) for *A. crenata* and *C. crispatus* was dependent on the independent effect of environmental condition (mean  $\pm$  s.e.; *A. crenata*: ambient,  $3.035 \pm 0.342$  mm, future,  $2.680 \pm 0.196$  mm; *C. crispatus*: ambient,  $3.687 \pm 0.526$  mm, future,  $2.294 \pm 0.433$  mm;  $F_{[1,18]} = 5.2018$ ,  $p < 0.05$ ; Figure 2.2e). However, there was no effect of environmental condition on  ${}^f\text{-SPI}L_{\text{med}}$  for *C. hyperborea* ( $L$ -ratio = 0.338, d.f. = 1,  $p = 0.126$ ; Figure 2.2f) or for *A. eightsi* and *L. elliptica* ( $F_{[1,8]} = 2.955$ ,  $p = 0.124$ ; Figure 2.2g). In contrast, maximum

mixed depth ( $f\text{-SPI}_{L_{\max}}$ ) was dependent on an interaction between species identity  $\times$  location for *A. crenata* and *C. crispatus* ( $F_{[1,20]} = 7.8123$ ,  $p < 0.05$ , Figure 2.2h), with species identity ( $\omega^2 = 0.537$ ) more influential than location ( $\omega^2 = 0.316$ ). Specifically, mean  $f\text{-SPI}_{L_{\max}}$  ( $\pm$  s.e.) was deeper in aquaria containing *C. crispatus* from station B16 ( $17.49 \pm 2.55$  mm) than it was in aquaria containing *A. crenata* from station B16 ( $5.72 \pm 1.03$  mm) and, to a lesser extent, station B13 (*C. crispatus*:  $15.76 \pm 1.29$  mm; *A. crenata*:  $14.48 \pm 2.20$  mm). For *C. hyperborea*,  $f\text{-SPI}_{L_{\max}}$  was not dependent on environmental condition (intercept only model:  $f\text{-SPI}_{L_{\max}}$ , L-ratio = 0.695, d.f. = 1,  $p = 0.405$ ), but there was some evidence for a reduction in intra-specific variability between treatment levels (CV: ambient, 22.8 %; future, 11.5 %; Figure 2.2i). In contrast, I found that  $f\text{-SPI}_{L_{\max}}$  for *A. eightsi* and *L. elliptica* was dependent on the interaction environmental condition  $\times$  species identity ( $F_{[1,8]} = 7.962$ ,  $p < 0.05$ ), with species identity ( $\omega^2 = 1.103$ ) more influential than environmental condition ( $\omega^2 = 0.907$ ). Specifically, mean ( $\pm$  s.e.)  $f\text{-SPI}_{L_{\max}}$  was deeper for *A. eightsi* relative to *L. elliptica*, with a larger difference observed under future conditions (ambient: *A. eightsi*,  $9.52 \pm 1.82$  mm and *L. elliptica*,  $5.82 \pm 0.75$  mm; future: *A. eightsi*,  $17.62 \pm 0.30$  mm and *L. elliptica*,  $7.11 \pm 1.37$  mm; Figure 2.2j).

The burrow ventilation behaviour ( $[\Delta Br^-]$ ) of *A. crenata* and *C. crispatus* was dependent on an interaction between environmental condition  $\times$  location  $\times$  species identity ( $F_{[1,16]} = 7.910$ ,  $p < 0.05$ ). Computation of effect sizes revealed that species identity was the most influential independent variable ( $\omega^2 = 0.678$ ), followed by location ( $\omega^2 = 0.481$ ) and environmental condition ( $\omega^2 = 0.376$ ). In individuals from station B13, irrespective of species identity, ventilation activity was unchanged by environmental conditions (Figure 2.2k). However, whilst the ventilation activity of *A. crenata* individuals from station B16 was negligible ( $[\Delta Br^-]$  values were positive) in both ambient and future environmental conditions, ventilation activity for *C. crispatus* increased 7-fold ( $[\Delta Br^-]$  values more negative) under the future environmental condition (mean  $\pm$  s.e.; future,  $-966.08 \pm 139.24$  mg L $^{-1}$ , ambient,  $-138.30 \pm 123.14$  mg L $^{-1}$ ; Figure 2.2l). Mean ( $\pm$  s.e.) burrow ventilation behaviour of *C. hyperborea*, was also affected by environmental conditions (L-ratio = 5.879, d.f. = 1,  $p < 0.05$ ), increasing from  $71.61 \pm 178.82$  mg L $^{-1}$  under ambient environmental conditions to  $-564.24 \pm 86.32$  mg L $^{-1}$  under future environmental conditions (Figure 2.2m). In contrast, there was no effect of environmental condition or species identity on ventilatory activity for *A. eightsi* and *L. elliptica* (intercept only; L-ratio = 0.764, d.f. = 1,  $p = 0.382$ ; Figure 2.2n), but I did observe a reduction in intra-specific variability between treatments (CV: ambient, 713 %; future, 293 %).

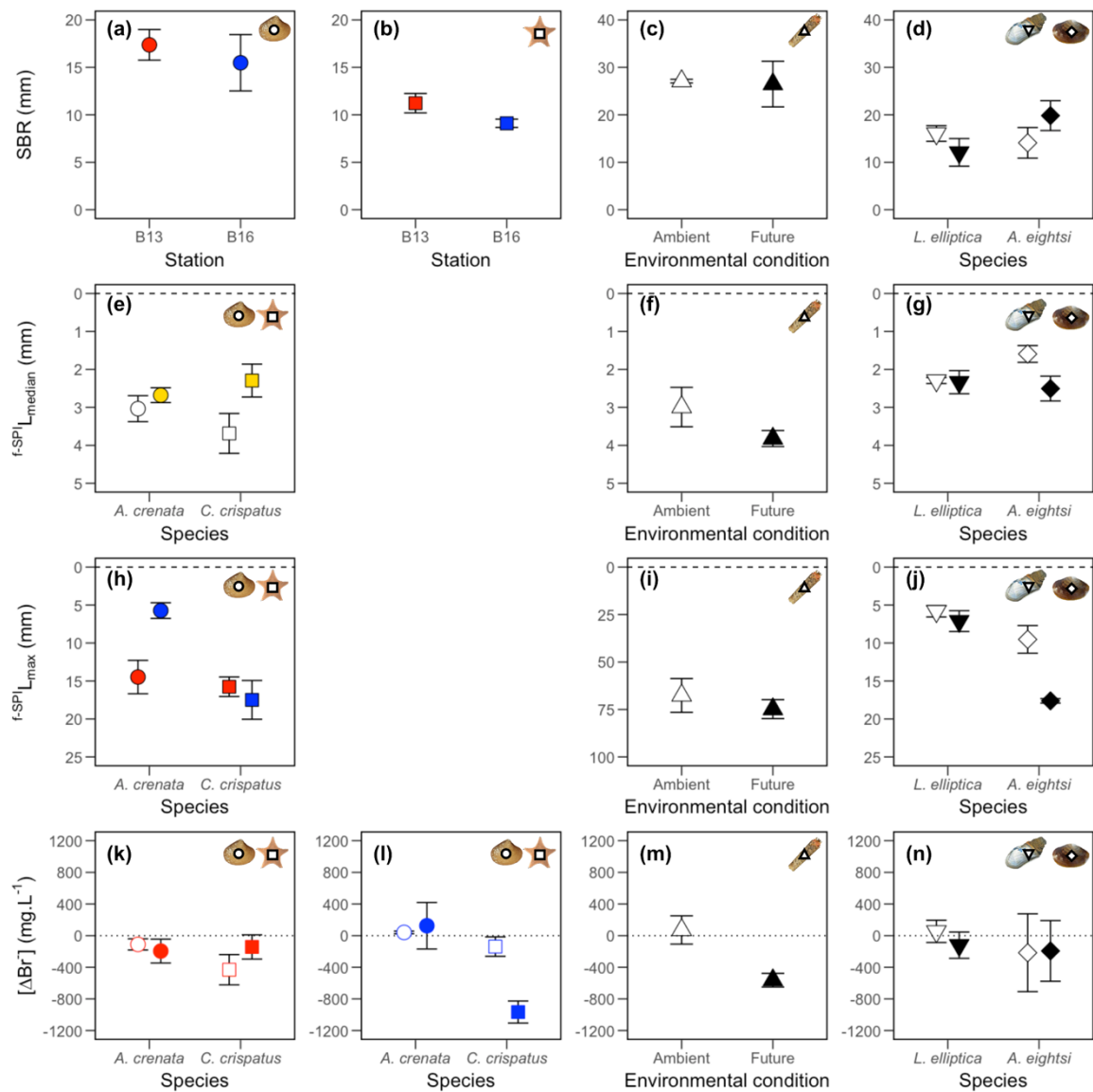
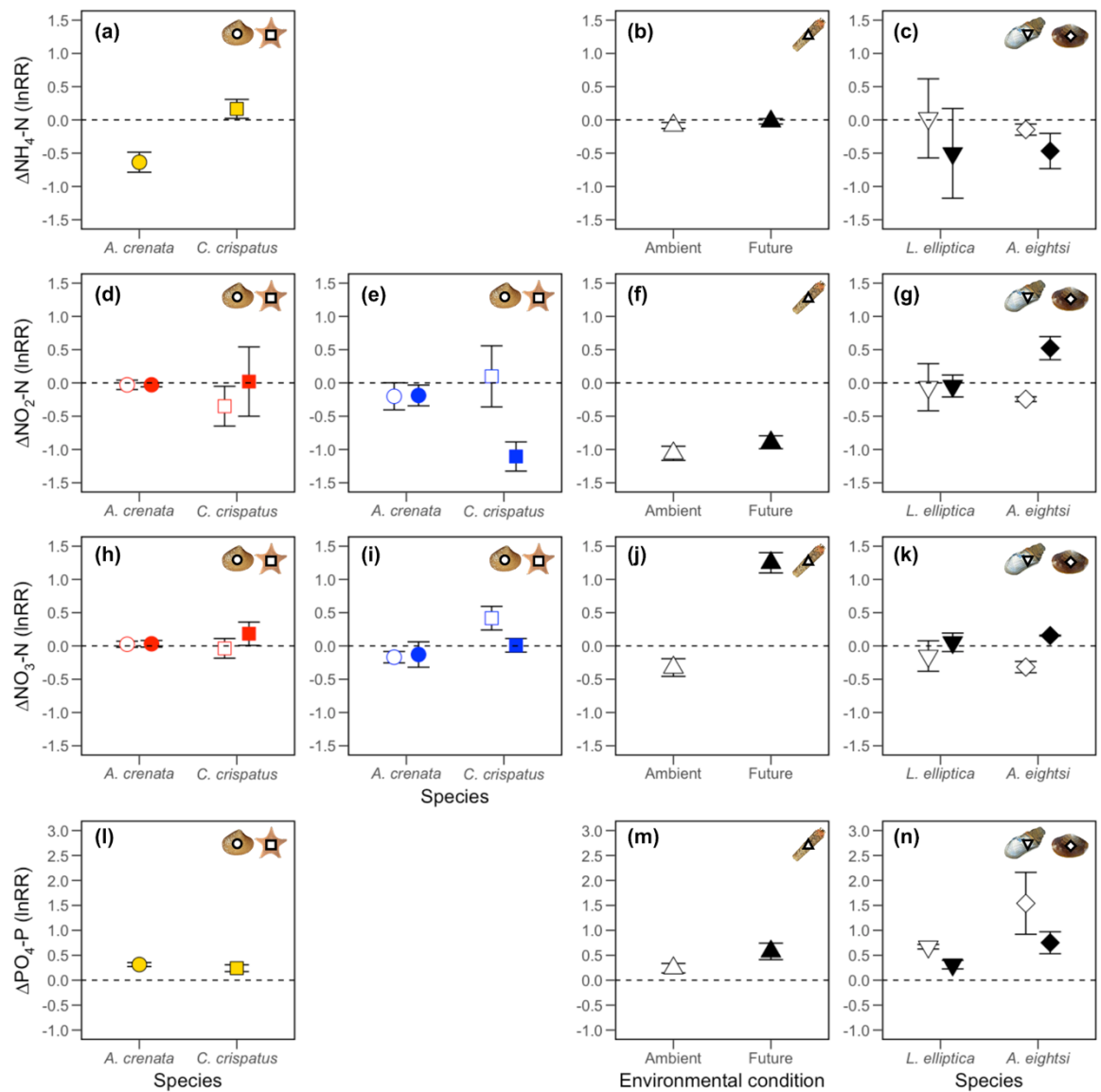


Figure 2.2 | The effects of species identity, location and environmental condition (ambient, open symbols; future, closed symbols) on (mean  $\pm$  s.e.) (a,b,c,d) SBR (mm), (e,f,g)  $f\text{-SPI}_L$  median (mm), (h,i,j)  $f\text{-SPI}_L$  max (mm) and (k,l,m,n)  $[\Delta\text{Br}^-]$  (mg.L $^{-1}$ ) in mesocosms containing (a,b,d,h,k,l) *Astarte crenata* (circles) or *Ctenodiscus crispatus* (squares) from station B13 (red), B16 (blue) or both locations combined (gold), (c,f,i,m) mesocosms containing *Cistenides hyperborea* (triangles) obtained from station B13 and (d,g,j,n) mesocosms containing *Aequiyyoldia eightsi* (diamonds) or *Laternula elliptica* (upside down triangles) obtained from Rothera Point. For  $\Delta[\text{Br}^-]$ , negative values indicate increased bioirrigation. Sediment profile images and associated luminophore distribution profiles are presented in Appendix A, Figures S8-S11.

### 2.4.3 Effects on ecosystem functioning

My analyses reveal that, for *A. crenata* and *C. crispatus*, [NH<sub>4</sub>-N] was influenced by the independent effect of species identity ( $F_{1,22} = 14.951$ ,  $p < 0.0001$ ), with response values ranging from positive lnRRs in aquaria containing *C. crispatus* (mean  $\pm$  s.e.,  $0.17 \pm 0.14$ ) to negative lnRRs in aquaria containing *A. crenata* (mean  $\pm$  s.e.,  $-0.64 \pm 0.15$ ; Figure 2.3a). I find that the effect size for [NH<sub>4</sub>-N] is not dependent on environmental condition in the presence of *C. hyperborea* (intercept only models: [NH<sub>4</sub>-N],  $F_{1,4} = 1.047$ ,  $p = 0.364$ ; Figure 2.3b), *A. eightsi* or *L. elliptica* (intercept only model, L-ratio = 0.009, d.f. = 1,  $p = 0.925$ ; Figure 2.3c). For [NO<sub>2</sub>-N], whilst there is evidence of a weak dependence of the effect size on environmental condition in the presence of *L. elliptica* and *A. eightsi* (mean  $\pm$  s.e.: ambient,  $-0.15 \pm 0.16$ ; future,  $0.23 \pm 0.17$ ; L-ratio = 3.532, d.f. = 1,  $p = 0.060$ ; Figure 2.3g), the effect size of [NO<sub>2</sub>-N] in the presence of *A. crenata* and *C. crispatus* was dependent on an interaction between environmental condition  $\times$  location  $\times$  species identity (L-ratio = 4.629, d.f. = 1,  $p < 0.05$ ). For the latter, closer examination of model coefficients revealed that location was the most influential independent variable (L-ratio = 7.714, d.f. = 4,  $p = 0.103$ ), followed by species identity (L-ratio = 6.955, d.f. = 4,  $p = 0.138$ ) and environmental condition (L-ratio = 5.952, d.f. = 4,  $p = 0.203$ ). In aquaria containing infauna from station B13 (*A. crenata* and *C. crispatus*), irrespective of species identity, and for *A. crenata* in station B16, the effect size of [NO<sub>2</sub>-N] was not affected by environmental condition (Figure 2.3d,e). For station B16, however, the effect size of [NO<sub>2</sub>-N] in aquaria containing *C. crispatus* decreased from  $0.10 \pm 0.46$  under ambient conditions to  $-1.11 \pm 0.22$  under future conditions. Similarly, the effect size for [NO<sub>3</sub>-N] in the presence of *A. crenata* or *C. crispatus* was dependent on the three-way interaction between environmental condition  $\times$  location  $\times$  species identity ( $F_{1,16} = 3.057$ ,  $p = 0.09$ ). Computation of effect sizes revealed that species identity was the most influential independent variable ( $\omega^2 = 0.281$ ) for [NO<sub>3</sub>-N], followed by location ( $\omega^2 = 0.207$ ) and environmental condition ( $\omega^2 = 0.136$ ). Notably, environmental condition had no effect on the activities of species at station B13, but did influence the behaviour of *C. crispatus* at station B16 (mean  $\pm$  s.e.: ambient,  $0.42 \pm 0.18$ ; future,  $0.01 \pm 0.10$ ; Figure 2.3h,i). In contrast, for aquaria with *C. hyperborea*, I find no influence of environmental condition on the effect size of [NO<sub>2</sub>-N] (mean  $\pm$  s.e.:  $-0.97 \pm 0.07$ ,  $F_{1,4} = 1.324$ ,  $p = 0.314$ ; Figure 2.3f), but the effect size of [NO<sub>3</sub>-N] did increase under future conditions (mean  $\pm$  s.e.: ambient,  $-0.32 \pm 0.13$ ; future,  $1.25 \pm 0.15$ ;  $F_{1,4} = 60.821$ ,  $p < 0.01$ ; Figure 2.3j). For *L. elliptica* and *A. eightsi*, the effect size of [NO<sub>3</sub>-N] was dependent on the independent effect of environmental condition (L-ratio = 9.720, d.f. = 1,  $p < 0.01$ ; Figure 2.3k), with higher [NO<sub>3</sub>-N] under future

conditions for both *L. elliptica* (mean  $\pm$  s.e.: ambient,  $-0.15 \pm 0.23$ ; future,  $0.05 \pm 0.14$ ) and *A. eightsi* (mean  $\pm$  s.e.: ambient,  $-0.32 \pm 0.08$ ; future,  $0.16 \pm 0.01$ ).



**Figure 2.3 | The effects of species identity, location and environmental condition (ambient, open symbols; future, closed symbols) on (mean  $\pm$  s.e.) effect size of nutrient concentrations (lnRR) over the experimental period as indicated by (a,b,c) [ $\Delta\text{NH}_4\text{-N}$ ], (d,e,f,g) [ $\Delta\text{NO}_2\text{-N}$ ], (h,i,j,k) [ $\Delta\text{NO}_3\text{-N}$ ] and (l,m,n) [ $\Delta\text{PO}_4\text{-P}$ ] in mesocosms containing (a,d,e,h,i,l) *Astarte crenata* (circles) or *Ctenodiscus crispatus* (squares) from station B13 (red), B16 (blue) or both (gold), (b,f,j,m) mesocosms containing *Cistenides hyperborea* (triangles) obtained from station B13 and (c,g,k,n) mesocosms containing *Aequioldia eightsi* (diamonds) or *Laternula elliptica* (upside down triangles) obtained from Rothera Point. A positive effect size indicates an increase in nutrient release from the sediment into the water column over the experimental period, while a negative effect size signifies an increase in the uptake of nutrients from the water column into the sediment.**

The effect size for  $[PO_4-P]$  was not dependent on any of my explanatory variables (intercept only model; Figure 2.3l) for aquaria containing *A. crenata* and *C. crispatus*, although I did find independent effects of environmental condition for aquaria containing *C. hyperborea* (ambient,  $0.24 \pm 0.10$ ; future,  $0.58 \pm 0.17$ ; L-ratio = 3.123, d.f. = 1, p = 0.078; Figure 2.3m) and independent effects of condition (ambient,  $1.12 \pm 0.34$ ; future,  $0.53 \pm 0.14$ ; L-ratio = 7.865, d.f. = 1, p < 0.01) and species identity (*A. eightsi*,  $1.15 \pm 0.34$ ; *L. elliptica*,  $0.49 \pm 0.09$ ; L-ratio = 4.662, d.f. = 1, p < 0.05) for *A. eightsi* and *L. elliptica* (Figure 2.3n). The onset of future conditions decreased intra-specific variability (CV) in the effect size for  $[PO_4-P]$  for *A. eightsi* (ambient, 69.7%; future, 50.6%) and *C. hyperborea* (ambient, 68.6%; future, 49.7%), but increased for *L. elliptica* (ambient, 11.7%; future, 47.6%).

## 2.5 Discussion

My findings demonstrate that conditions representative of anticipated near-future climate change can lead to fundamental shifts in functionally important aspects of sediment-dwelling invertebrate behaviour. These effects can be substantive; for *A. eightsi* for example, I observed a doubling of burial rate, deepening of particle mixing and a change in the magnitude and direction of biogeochemical dynamics that are sufficient to change the functional role of a species (Wohlgemuth et al. 2017). This observation is important, because alterations in individual functional capacity that are distinct from functional shifts caused by changes in community composition and/or novel environmental conditions are common (Godbold & Solan 2009, Solan et al. 2020c), and likely result from changes in the strength and nature of species interactions (Connell et al. 2010, Ghedini et al. 2015), various compensatory mechanisms (Thomsen et al. 2017, 2019) and other subtle phenotypic responses that collectively form a dynamic portfolio of sublethal responses to changing circumstances (Godbold & Solan, 2013, Renaud et al. 2019). Negligible changes in macronutrient cycling under climatic forcing is not trivial to detect (Godbold et al. 2017), however, and may be masked by the pH buffering effects of  $[CO_2]$  driven alkalinity changes (Gattuso & Hansson, 2011; Laverock et al. 2013) on microbial mediated pathways of nutrient recycling (Tait et al. 2013).

Whilst the effects of a near-future climate did not feature prominently in the outcomes of my experiments, consistent with theoretical expectations (Pörtner et al. 2008), I did note a reduction in intra-specific variation that reflected changes in environmental context and location (Cassidy et al. 2020). Intra-specific variation in response (= burrowing) and effect (= bioturbation) trait expression has previously been noted to be very important for maintaining populations (Dingemanse & Wolf, 2013), enabling adaptation to changing environmental conditions (Henn et

al. 2018) and for stability in ecosystem functioning (Wright et al. 2016). I recognise, however, that though sublethal responses may enable species to persist to changes in immediate circumstance, this might entail other phenotypic costs that constrain or inhibit the ability to adjust further (Wood et al. 2008; Gilbert & Miles, 2019). My results indicate that reductions in intra-specific variation may serve as an early warning for impending ecological transitions associated with progressive forcing, reinforcing the need for continual monitoring of faunal mediated functioning and the ecological constraints that modify functionally important aspects of species behaviour (Sheaves et al. 2021, Schmidt-Traub 2021).

The observed variation in intra-specific behaviour exhibited here under enhanced warming and  $[CO_2]$  is consistent with previous behavioural studies (Ferrari et al. 2011) and physiological responses observed in polar benthic species (Clark et al. 2017) as well as regional contextualisation (Reed et al. 2020). Whilst not explicitly designed to examine species range shifts or gradients of environmental change, an important feature of my study design was that my locations were positioned to the north and south of the oceanographic polar front which contrast in benthic biogeography (Jørgensen et al. 2015), bioturbation activity and functioning (Solan et al. 2020). Hence, I was able to show that individuals that are predisposed to a wider inter-annual thermal range south of the polar front exhibit a more reserved behavioural response (= ventilatory activity) to change than those individuals that inhabit areas with a narrower thermal range (Schaum et al. 2012). Thus, plasticity in response mirrors the level of local environmental fluctuation (Joshi et al. 2001). Whilst spatial associations between environmental temperature range and physiological thermal tolerances are not atypical in ectothermic species found in this biome (Morley et al. 2012b) or elsewhere (Reed et al. 2020; Mermilliod-Blondin et al. 2013), this feature of high latitude populations does mean that populations may be at greater risk of local extinction over the long term. As thermal tolerance narrows with decreasing seasonality in temperature towards the poles (Sunday et al. 2011), and is expected to be further constrained as the Arctic warms (Screen, 2014), populations already at the edge of their thermal limits will most likely have less scope to compensate and adapt to change (Davis & Shaw, 2001). Temperature-driven responses are, however, typically complicated by interactions with other abiotic drivers (Pörtner & Farrell, 2008) and, at least for Arctic regions, are likely to lead to both amplified and dampened effects in spatially stochastic ecosystems (Arrigo et al. 2020). Despite this, previous studies investigating the influence of climate change on benthic ecosystems have predominantly focused on spatial distributions of species turnover (Renaud et al. 2019), functional diversity (Frainer et al. 2017; Liu et al. 2019a) and redundancy (Aune et al. 2018), with little emphasis placed on characterising the intra-specific variability of species-environment interactions. The latter can be a more important

driver of the short-term functional response of communities than changes in species composition, dominance and richness (Blois et al. 2013, Nagelkerken et al. 2015; Des Roches et al. 2018). For example, previous work has suggested that the shallower burrowing activity of invertebrates held under more acidified conditions (Clements and Hunt, 2014; Clements et al. 2016) allows species to evade the physiological effects of decreasing pH, but simultaneous responses to warming may negate the need for such avoidance behaviour (Clements et al. 2017) because species also alter their rate of burrow ventilation (Ouellette et al. 2004) and type of burrowing activity to maintain environmental continuity (Przeslawski et al. 2009; Munguia et al. 2017). Over the longer term, the cumulative effect of short-term behavioural responses like these are likely to be decisive for the composition (Wong et al. 2015), population dynamics (Hoover & Tylianakis, 2012), connectivity (Valdovinos et al. 2010) and functioning (Jones et al. 2021) of post-change benthic communities, albeit further moderated by seasonal timing (Godbolt & Solan, 2013) and local circumstance (Griffith et al. 2019; Wohlgemuth et al. 2017, Reed et al. 2020), including interannual variability (Solan et al. 2020c).

*In-situ* evaluations of climate-driven shifts in marine biodiversity face challenges arising from complex interactions between climate and non-climate factors. *Ex-situ* experiments, as demonstrated in this study, offer a method to isolate the impacts of specific combinations of drivers necessary to develop a mechanistic understanding of how organisms respond and, in turn, affect the environment. However, the advantages of these experiments are counterbalanced by their limitations, trading realism for meticulous control and replication. This is particularly evident in single-species investigations that disregard ecological responses arising from shifts in species interactions (Carpenter, 1996), where effects from interaction changes can rival or surpass those driven solely by species tolerances (Kordas et al. 2011) though the effects from interaction changes are not universally applicable (Queirós et al. 2015). Regardless, a greater integration of controlled experiments and expansive field studies (Wernberg et al. 2012) will aid in understanding how subtle effects at the level of the organism scale toward broader ecosystem dynamics, which is necessary for accurately predicting the repercussions of climate change within intricate community landscapes.

Quantitative information on the functional role of individual species is rare for both polar regions (Solan et al. 2019), yet understanding, and accounting for, species responses to climate change is fundamental to improving the likelihood of determining the most realistic ecosystem future (Post et al. 2019, Garcia et al. 2021). My findings suggest that this task will be frustrated by context-dependent variation in both intra- and inter-specific responses to forcing, which cannot be readily captured using fixed trait modalities (Murray et al. 2014, Hale et al. 2014). Where the overall outcome of species responses remains largely unresolved, I contend that reductions in the

Intra- and inter-specific differences in invertebrate behavioural trait expression moderate present and future benthic biogeochemical functioning in regions of rapid climatic transition

variation of conspecific responses (Bolnick et al. 2011; Des Roches et al. 2018), although not consistently observed across all my measured responses, may still form a viable alternative for some predictive models. Furthermore, my findings lend support to the growing view that location-dependent variation in behavioural responses can be attributed to localised thermal plasticity driven by exposure to divergent temperature seasonality trends (Joshi et al. 2001). Inter- and intra-specific variations in vulnerability, effect-and-response traits (Des Roches et al. 2018; Gervais et al. 2020) and interactions between species (Clare et al. 2016; Mauro et al. 2022) can facilitate functional redundancy and/or post-change compensations (Thomsen et al. 2017, 2019). A mechanistic approach that explicitly tests suspected abiotic and biological signals would assist in establishing patterns of response (McEntire et al. 2022) across multiple levels of biological organisation (Borer et al. 2014; Barner et al. 2018), enabling more likely projections of the functional consequences of change.



## **Chapter 3 Intra-specific variability in physiological responses underpin acclimation capacities in high-latitude marine invertebrates**



### 3.1 Abstract

Species make physiological adjustments to improve performance and maintain fitness in response to gradual changing conditions associated with climate forcing, but few studies have considered the acclimation capacity of high latitude species experiencing amplified rates of climate expression. Here, I investigate how four sediment-dwelling invertebrate species from high-latitude environments adjust growth, respiration, excretion, and metabolism over 360 days under near-future (+1.5 °C/550 ppm atmospheric [CO<sub>2</sub>]) conditions. I find that species maintained inter-specific respiration and ammonium excretion rates over a 360-day period by making distinct physiological and biochemical adjustments. However, individuals from a higher latitude location expressed more variable growth responses relative to those from a lower latitude location. I find that the maintenance of whole-organism performance does not guarantee that an organism will operate at full functional capacity, and that conspecific variability in physiological responses reflects locally adapted resilience to environmental change. My study provides evidence that variation in how species and individuals respond to changing conditions can alter the capacity for recovery following disturbances. Hence, there is a need to consider the functional ramifications of the context dependency of intra-specific variability in responses, rather than focus on whether a species is present or otherwise, in efforts that aim to predict hotspots of climate-driven alterations in marine ecosystems.

### 3.2 Introduction

There is unequivocal evidence for the influence of climate change on marine species (Doney et al. 2012; Poloczanska et al. 2013; 2016) but efforts to project ecosystem futures under progressive climatic forcing are burdened by ambiguous mechanistic detail of how species are able to remodel their physiology to compensate for the adverse effects of environmental change (Schmidt-Nielsen, 1972; Hochachka & Somero, 2002). Physiological plasticity can improve resilience to environmental perturbation (Chevin et al. 2010; Hoffmann & Sgrò, 2011), so long as any invoked compensatory responses do not impede other biological functions; species that are already close to their physiological limits have less capacity to respond to further directional forcing (e.g. climate change, Stillman, 2003; Somero, 2010). The various ways in which species respond to components of climate change alone, and in combination, are well known (growth, Pörtner & Knust, 2007; Berge et al. 2006; reproduction, Moreira et al. 2018a; Weydmann et al. 2012; biochemical regulation and metabolic processes, Collins et al. 2020; Freitas et al. 2017a; Freitas et al. 2017b; Moreira et al. 2018b), and include emergent additive, synergistic, and antagonistic effects on organism development (Arnberg et al. 2013; Gianguzza et al. 2013; Padilla-Gamino et al. 2013; Reed et al. 2021; Wangensteen et al. 2013), physiology (Byrne, 2012; Costa et al. 2020; Matoo et al. 2013; Melatunian, et al. 2011; Nardi et al. 2017; Small et al. 2015), and other life history traits (Byrne, 2011; Byrne & Przeslawski, 2013; Kroeker et al. 2013; Pistevos, et al. 2011;

Small et al. 2015). However, physiological sensitivity is perceived to be extremely variable among and within species (Kroeker et al. 2013; Przeslawski et al. 2015; Whiteley, 2011; Wittman and Pörtner, 2013), and any discrepancy in response capability between individuals, long been considered as noise (McGill et al. 2006), is now recognised as meaningful phenotypic variation and an integral part of a species' plasticity (Guscelli et al. 2019). For species and populations with high levels of intra-specific variability, the risk of local extinction will be significantly reduced (Forsman and Wennersten, 2016). Yet, the extent to which the physiological flexibility of an individual determines a species' ability to cope with changing circumstances is not well constrained.

The degree to which intra-specific trait expression alters across ecological and environmental gradients (Williams et al. submitted; Jones & Cheung, 2018; Hamilton et al. 2019; Cassidy et al. 2020, Solan et al. 2020c) offers the possibility of determining the relative importance of context-dependent responses for maintaining ecosystem resilience (Richard et al. 2012b; Des Roches et al. 2018). Trends and variability in ocean warming and acidification tend to be more pronounced in parts of the Arctic and Antarctic than for their respective hemispheres or the globe as a whole (Serreze & Barry, 2011; Feely et al. 2009; Auger et al. 2021), with responses of biodiversity to the most amplified rates of environmental change (Convey & Peck, 2019; Gutt et al. 2015; Morley et al. 2019; Wassmann et al. 2011) aiding understanding of likely responses at lower latitudes (di Prisco et al. 2012). In these regions, as many species are sessile (Clarke et al. 2004; Degen et al. 2019) and have a long life expectancy (Moss et al. 2016; Vogt, 2019), macrophysiological studies have predominantly focused on the effect of single environmental stressors (warming, Clark et al. 2017; Richard et al. 2012a,b; acidification, Cummings et al. 2011; Cross et al. 2015) on sediment-dwelling invertebrates (Clark et al. 2017; Cummings et al. 2011; Cross et al. 2015; Lischka & Riebesell, 2012; Richard et al. 2012a,b; Wood et al. 2011) over short time periods (days-months) that exclude opportunities (Carey et al. 2014) to explore seasonally variable (Godbolt & Solan, 2013) or delayed responses (Frolova et al. 2007; Alexander et al. 2018) which may moderate long-term persistence and performance. The latter is not a trivial omission, as species with relatively poor physiological plasticity may maintain performance over the long term if pressures are transient, whilst being at heightened risk during certain times of the year or when subject to specific periodic circumstances (Peck, 2005). It follows, therefore, where species distributions envelope significant environmental gradients (fronts, Loeng, 1991, Cochrane et al. 2012, Jørgensen et al. 2015), locally conditioned resilience may influence how populations respond to future environmental change (Calosi et al. 2017; Bennett et al. 2019).

The applicability of aggregated acclimation estimations across studies, particularly those employing diverse stress assessment methods (Form et al. 2012; Gilbert & Miles, 2019; Markle & Kozak, 2018; Peck et al. 2014; Richard et al. 2012a), is limited in its utility as a standardised metric or when applied to a singular generalised context, such as average climate warming (Terblanche & Hoffman, 2020). Here, I experimentally explore the scope of long-term acclimation (Bishop et al. 1950; Schmidt-Nielsen, 1990) to near-term warming and acidification for a range of abundant (Jørgensen et al. 2015; Pasotti et al. 2015; Solan et al. 2020c) sediment-dwelling marine invertebrates experiencing amplified rates of climate change that contrast in environmental history (Arctic vs Antarctic, Reed et al. 2020). I were motivated to evaluate the importance of context-dependant intra-specific expression for mediating physiological plasticity by including conspecifics from two separate locations, because responses of species in similar habitats can be modified by setting and environmental history (Wohlgemuth et al. 2017, Reed et al. 2020). If this holds true, and is a common feature of areas in receipt of differential climate expression, that would indicate that acclimation capacity of an individual may diverge from expectation as species responses align with the magnitude and timing of environmental forcing. As I speculated that the response of an individual or species would be equivalent to the net contribution of multiple responses, my aim was to identify a diverse array of mechanisms that underpin physiological compensatory strategies. Hence, I focus on altered rates of growth, respiration, excretion, and/or biochemical regulation, to assess the plasticity and condition of each species and gain predictive insight into its vulnerability to future change (Hoffmann & Sgrò, 2011; Magozzi & Calosi, 2015).

### 3.3 Materials and methods

#### 3.3.1 Fauna and sediment collection

Individuals of the bivalve *Astarte crenata* (Gray, 1824), asteroid *Ctenodiscus crispatus* (Bruzelius, 1805) and polychaete *Cistenides hyperborea* (Malmgren, 1866) were collected from replicate SMBA (Scottish Marine Biological Association) box cores and 15 minute Agassiz trawls (Appendix B Table S1) at two stations (B13: 74.3 °N, 30.0 °E; B16: 80.3 °N, 30.0 °E) in the Barents Sea (30/06/2019-01/08/2019, RRS James Clark Ross JR18006 research cruise, Barnes et al. 2019). *Astarte crenata* and *Ctenodiscus crispatus* were abundant at both sampling stations, whereas *C. hyperborea* were only present in sufficient numbers at stations B13. Individuals of the protobranch *Aequiyloldia eightsi* (Jay, 1839) were hand collected during by divers in March-April 2019 at Rothera Point, Adelaide Island, West Antarctic Peninsula (67.3 °S, 68.1 °W) and transported to the *Biodiversity and Ecosystem Futures Facility*, University of Southampton. Surficial sediment (uppermost 5 cm) was collated from replicate SMBA (Scottish Marine Biological

Association) box cores (*A. crenata*; *C. crispatus*, *C. hyperborea*; B13, n = 13; B14, n = 2 [76.3 °N, 30.3 °E]; B16, n = 13), and from the Hamble, UK (*A. eightsi*; 50.9 °N, 1.3 °W), sieved (500 µm mesh) in a seawater bath to remove macrofauna and debris whilst retaining the fine fraction and allowed to settle for 48 hours, before the supernatant seawater was removed and sediment homogenized.

### 3.3.2 Experimental design and set-up

Each of the four invertebrate species (*A. crenata*, *C. crispatus*, *C. hyperborea*, *A. eightsi*; Appendix B Table S2) were assigned to transparent acrylic aquaria (internal LWH: 12 x 12 x 33 cm, wall thickness: 0.5 cm) held in the dark in insulated fibreglass seawater baths (LWH: 1.2×1.2×0.8 m, Tanks Direct, UK; Appendix B Figure S2; Solan et al. 2020c) at a representative ambient summer bottom temperature (Appendix B Table S3, 1.0 ± 0.5°C; Titan 1500 chiller unit, AquaMedic) and present-day level atmospheric CO<sub>2</sub> (~400 ppm [CO<sub>2</sub>], following Godbold & Solan, 2013). Species density (*A. crenata*, *C. crispatus* & *C. hyperborea*, 2 ind. aquarium<sup>-1</sup>; *A. eightsi*, 1 ind. aquarium<sup>-1</sup>) and sediment depth (*A. crenata*, *C. crispatus* & *C. hyperborea*, 16cm; *A. eightsi*, 12cm) of aquaria was set based on the size (mean body length (L) per aquarium ± se; *A. crenata*, 24.79 ± 1.01 mm ; *C. crispatus*, 16.15 ± 0.72 mm ; *C. hyperborea*, 56.43 ± 1.32 mm ; *A. eightsi*, 20.21 ± 0.37 mm) and known burrowing activities of each species (Davenport, 1998; Peck et al. 2004). All aquaria were overlain with seawater (UV sterilized; *A. crenata*, *C. crispatus* & *C. hyperborea*, ~ 6 L; *A. eightsi*, ~ 7.6 L) to a combined sediment and water depth of 31 cm. After a period of adjustment to allow for transfer to mesocosm conditions (21 days), water temperature and atmospheric CO<sub>2</sub> was maintained (ambient treatment) or gradually increased (near-future treatment) stepwise at 0.5°C and 50 ppm increments at intervals of 7 days, until reaching 2.5 °C (± 0.5 °C) and 550 ppm. Aquaria were maintained under ambient [1/0 ± 0.5 °C, ~400 ppm [CO<sub>2</sub>]] and near-future ([2.5 ± 0.5 °C, ~550 ppm [CO<sub>2</sub>]]) conditions based on IPCC future projections for 2050-2080; IPCC 2018) for a period of 360 days (21/10/2019 to 15/10/2020). All fauna were fed *ad libitum* with commercially sourced flaked fish food (Aquarian Tropical Flake: *C. crispatus* and *C. hyperborea*, 0.03g aquarium<sup>-1</sup> week<sup>-1</sup>) or precultured algae (*Isochrysis* sp., *Tetraselmis* sp., and *Phaeodactylum* sp., mixed in 5 L batches at peak culture densities of 15.6 × 10<sup>6</sup> cells ml<sup>-1</sup>, 8.6 × 10<sup>5</sup> cells ml<sup>-1</sup>, and 14.2 × 10<sup>6</sup> cells ml<sup>-1</sup>, respectively: *A. crenata* and *A. eightsi*, 100 ml, 3 times week<sup>-1</sup>). To avoid accumulation of nutrients and metabolites associated with feeding, I performed weekly partial (50%) seawater changes .

### 3.3.3 Carbonate chemistry

Total alkalinity ( $A_T$ ) was monitored monthly and analysed by titration (Apollo SciTech Alkalinity Titrator AS-ALK2) following standard protocols (Carbonate Facility, National Oceanography Centre, Southampton). Calculated  $A_T$ , temperature, pH (NBS scale, Mettler-Toledo InLab Expert Pro temperature-pH combination electrode) and salinity (WTW™ TetraCon™ 325 Standard temperature-conductivity combination electrode) values were plotted in CO2SYS software (Robbins et al. 2010), and carbonate chemistry parameters (bicarbonate, carbonate and  $pCO_2$ ; Appendix B Figure S3) were calculated from pH,  $A_T$ , temperature and salinity using dissociation constants K1 and K2 from Mehrbach et al. (1973) refit by Dickson and Millero (1987), and  $KSO_4$  from Dickson (1990).

### 3.3.4 Effects on growth and body condition

Taxonomic-specific morphometric measurements ( $\pm 0.01$  mm; Appendix B Figure S4) and blot-wet weight ( $\pm 0.001$  g) of each species (24 individuals: *A. crenata*, *C. crispatus*; 20 individuals: *C. hyperborea*, *A. eightsi*), taken after a 24-h starvation period to evacuate the gut, were obtained on day 0 and day 360. For *C. crispatus*, sediment was removed from the body cavity prior to weighing by rinsing with seawater. As removal of *C. hyperborea* from its tube can result in mortality, I used geometric dimensions as a proxy for body size. From these measurements, I determined growth as  $\Delta$  biomass (% change) over the experimental period (360 d). For *A. crenata* and *A. eightsi*, I calculated a tissue to shell blot-weight ratio (TW:SW) as a measurement of body condition, as body condition, shell mass, biomass, and calcification rates in molluscs are known to respond to prolonged exposure to elevated  $pCO_2$  (Parker et al. 2013).

### 3.3.5 Effects on respiration and excretion

To avoid the window of peak specific dynamic action of feeding (SDA, 24-hour post-feeding; Chapelle et al. 1994), the rate of oxygen consumption ( $MO_2$ ), ammonium excretion ( $\Delta[NH_4]$ ) and phosphate excretion ( $\Delta[PO_4-P]$ ) was measured ( $n = 36 + 6$  control; 3 ind. per species x station x environmental condition, sets of 4) on fasted individuals (48 h, species *Astarte crenata*, *Aequioldia eightsi*; 96 h species *Ctenodiscus crispatus*, *Cistenides hyperborea*) using closed-chamber constant volume aquatic respirometry adapted from Lighton (2008; Appendix B Figure S5). Oxygen consumption was measured in glass respirometric chambers (120 ml volume) using non-invasive optical optodes with integrated temperature compensation (YSI ODO/T probe) connected to portable DO meters (YSI ProODO). A two-point calibration was performed as per the manufacturer's instructions (daily) using reverse osmosis water (0 PSU) saturated with sodium

sulphite anhydrous (0 % O<sub>2</sub> saturation) and air-saturated reverse osmosis water (0 PSU, 100 % O<sub>2</sub> saturation). Chambers were submerged in the seawater baths housing the aquaria in the dark. Prior to, and between each trial, chambers were emptied and refilled with artificial seawater adjusted to treatment conditions and the sensor was salinity-corrected (WTW™ TetraCon™ 325 Standard temperature-conductivity combination electrode). Between trial days, chambers were emptied, rinsed with freshwater and air dried to minimise microbial growth. Any algal and faunal growth on my experimental species were also removed. To minimise elevated oxygen consumption associated with transfer and acclimatisation, specimens were placed in unsealed chambers (continuously flushed with air-saturated seawater) without a sensor for 30 minutes prior to measurement. Chambers were sealed with a rubber bung and attached oxygen probe, ensuring that there was no formation of air bubbles. Following a further adjustment period (30 min), oxygen concentration ( $\pm 0.01 \text{ mg.L}^{-1}$ ) was recorded every 5 minutes for 300 minutes. During this time, oxygen saturation did not fall below 80 % ( $\pm 0.1$ ). To estimate rates of excretion ( $\Delta[\text{NH}_4]$ ,  $\Delta[\text{PO}_4\text{-P}]$ ; Tecator flow injection auto-analyser, FIA Star 5010 series), water samples (15 ml, syringed approx. 7 cm water depth into chamber, 0.45  $\mu\text{m}$  NALGENE nylon matrix filter) were collected before (- 30 min) and immediately after (300 min) respirometry trials. Following each incubation, the wet soft tissue weight (WTW) of each individual was measured ( $\pm 0.0001 \text{ g}$ ) before being rinsed with distilled water, flash frozen with liquid nitrogen and stored at -80 °C.

### **3.3.6 Effects on biochemical status**

Whole individuals from the respirometry trials were processed to determine the general biochemical status of benthic invertebrates (De Marchi et al. 2018; Freitas et al. 2016; 2017; 2019) due to small body sizes (< 1 g WTW) and indistinct organs (Lau et al. 2018). Frozen soft tissues (n = 36; 3 ind. species x station x environmental condition<sup>-1</sup>) were manually homogenised using a mortar and pestle with liquid nitrogen and separated into 0.05 g aliquots. Organic matter content (OM) was determined as the difference between dry and ashed weight of a single aliquot (Slattery and McClintock 1995; Appendix B Table S4). Energy-related biochemical parameters (Glucose content, GLU; total protein content, PROT) were analysed (2 ind.<sup>-1</sup>, accompanied by blanks and standard samples for quality control and background correction) from the remaining aliquots. Frozen tissue of *Cerastoderma edule*, analysed alongside samples, contained (mean  $\pm$  s.d.) 3.5  $\pm$  0.1 g GLU and 10.9  $\pm$  1.7 g PROT per 100 g tissue, consistent with nutrition information values provided (Appendix B Figure S6).

Extraction was performed with specific buffers for each biomarker (Appendix B Table S5; Andrade et al. 2019; Coppola et al. 2019). Before extraction, aliquots were re-homogenized for 30 s using a

vortexer and centrifuged for 10 min at 10,000 g. Supernatants were re-stored at -80 °C or immediately used. GLU was quantified using the D-Glucose (HK) Coulometric Assay Kit (Megazyme™, Ireland) following the manufacturer's protocol and absorption measured at  $\lambda = 340$  nm. PROT was quantified using a Bicinchoninic Acid (BCA) Protein Assay Kit (Thermo Scientific™ Pierce™, United States) following the manufacturer's protocol and absorption measured at  $\lambda = 562$  nm. Results are presented in  $\mu\text{g GLU/PROT .mg}^{-1}_{\text{OM}}$ .

### 3.3.7 Data analysis

I estimated individual oxygen consumption rates using total least square regression of oxygen concentration over time (Supplementary Figure S7). To remove any effect of microbial and algal activity (error: Supplementary Table S6), triplicate measurements in the absence of fauna for each environmental condition were subtracted from faunal measurements (Clark et al. 2013). Rates were adjusted for the water volume of the chamber following Bushnell et al. (1994) and Schurmann and Steffensen (1992).

Equation 3.1 Calculation of oxygen consumption rate during closed-chamber respirometry

$$(\text{MO}_2)$$

$$\text{MO}_2 = [\text{O}_2]_{\text{TLS.slope}} \times \text{VOL}_{\text{resp}}$$

where  $\text{MO}_2$  ( $\mu\text{g [O}_2\text{]. hr}^{-1}$ ) =  $\text{O}_2$  consumption,  $[\text{O}_2]_{\text{TLS.slope}}$  ( $\mu\text{g [O}_2\text{]. L}^{-1}\text{. hr}^{-1}$ ) =  $\Delta\text{O}_2 \cdot \Delta\text{time}^{-1}$  and  $\text{VOL}$  is the volume of the chamber after displacement by faunal volume. Rather than standardising to WTW, whole-animal values for  $[\text{MO}_2]$  were incorporated as a random factor in mixed effect models (Zuur et al. 2009) to give an estimation of the overall sum of all energy consuming processes and avoid presuming that biomass comparably scales across all taxon and contexts (Kiørboe & Hirst, 2014; Hirst & Forster, 2013; Glazier, 2005). Excretion rates were converted to nmol  $[\text{NH}_4]$   $\text{hr}^{-1}$  and nmol  $[\text{PO}_4]$   $\text{hr}^{-1}$  based on the volume of water contained in each incubation chamber. I subtracted mean ( $n = 3$ ) rate of controls (ambient: +0.01 nmol  $[\text{NH}_4]$   $\text{min}^{-1}$ , ranging from -0.07 to +0.13 nmol  $[\text{NH}_4]$   $\text{min}^{-1}$ , -0.02 nmol  $[\text{PO}_4]$   $\text{min}^{-1}$ , ranging from -0.04 to 0.00 nmol  $[\text{PO}_4]$   $\text{min}^{-1}$ ; future: +0.04 nmol  $[\text{NH}_4]$   $\text{min}^{-1}$ , ranging from -0.04 to +0.08 nmol  $[\text{NH}_4]$   $\text{min}^{-1}$ , +0.01 nmol  $[\text{PO}_4]$   $\text{min}^{-1}$ , ranging from -0.01 to +0.04 nmol  $[\text{PO}_4]$   $\text{min}^{-1}$ ) from the measured macrofaunal rates to distinguish background microbial and meiofaunal production.

All statistical analyses were performed in R (R Core Team, 2020) using the *nlme* package (Pinheiro and Bates, 2000). Analysis of variance models (ANOVAs) were developed for each of the response variables ( $\Delta$  biomass: %, TW:SW; oxygen consumption & excretion:  $[\text{MO}_2]$ ,  $\Delta[\text{NH}_4]$ ,  $\Delta[\text{PO}_4]$ ; biochemical status: CARB, PROT) to investigate the effects of (i) environmental condition (2 levels:

ambient, future), station (2 levels: B13, B16), species identity (2 levels), and any interactions, for *A. crenata* and *C. crispatus*, and (ii) environmental condition (2 levels) for *C. hyperborea* and, separately, *A. eightsi*. The extent of intra-specific variability in response within treatment levels was determined using the coefficient of variation.

Model assumptions (homogeneity of variance, normality, presence of influential outliers) were visually assessed using standardised residuals vs fitted values plots, Q-Q plots and Cooks distance (Zuur et al. 2010). Where homogeneity of variance was violated, data were analysed using *varIdent* variance-covariance structure and generalised least-squares (GLS) estimation (Pinheiro & Bates 2000, West et al. 2014) to allow residual spread to differ between the individual explanatory variables. The optimal fixed-effects structure (and random-effects for  $[\text{MO}_2]$ ,  $\Delta[\text{NH}_4]$  and  $\Delta[\text{PO}_4]$ ) in each ANOVA model was determined using backward selection informed by Akaike Information Criteria (AIC) and inspection of model residual patterns (Zuur et al. 2009). I determined the optimal variance-covariance structure for the GLS analysis by using the restricted maximum-likelihood (REML) estimation method which involved comparing the initial ANOVA model without variance structure to equivalent GLS models incorporating specific variance terms. These models were compared against the initial ANOVA model using the AIC and visualisation of model residuals. The optimal fixed structure of the most suitable model is then determined by applying backward selection using the likelihood ratio test with maximum-likelihood (ML) estimation method (West et al. 2014, Zuur et al. 2010). In GLS models with interactions, I determined the significance of each independent variable by comparing the minimal adequate model to a model with the independent variable of interest and all of its interactions removed. This comparison was performed using likelihood ratio (L-ratio) in the *nlme* package (Pinheiro and Bates, 2000). Details of initial and minimal adequate models, and all data are provided in Appendix B.

## 3.4 Results and Discussion

### 3.4.1 Effects on growth and body condition

I found that the context-dependence of trait expression (Reed et al. 2020; Cassidy et al. 2020; Wohlgemuth et al. 2017) and behavioural responses to climate change (Williams et al. submitted; Morley et al. 2012) also extends to physiological responses, as growth in *A. crenata* and *C. crispatus* did not differ between the two species (L ratio = 1.004, d.f. = 1, p = 0.316) but was weakly influenced by an interaction between location and environmental condition (L ratio = 3.936, d.f = 1, p = 0.047), with environmental condition of more importance (L ratio = 13.497, d.f.

= 2,  $p = 0.001$ ) than location (L ratio = 4.129, d.f. = 2,  $p = 0.127$ ). Specifically, individuals from station B16 exhibited little overall difference but increased variability in mean ( $\pm$  s.e.) growth rates under the future environmental condition (ambient,  $10.88 \pm 6.92\%$  ( $CV = 180\%$ ); future,  $11.30 \pm 17.57\%$  ( $CV = 491.8\%$ )), whilst individuals from station B13 experienced increased growth rates under the future environmental condition (ambient:  $2.44 \pm 3.03\%$ , future:  $6.40 \pm 3.31\%$ ; Figure 3.1Figure 3.1a). Inter-specific responses to climatic drivers in marine calcifiers are common (Ries et al. 2009), however, and I found growth was not dependant on the environmental condition in *C. hyperborea* (intercept only model;  $F_{1,17} = 0.876$ ,  $p = 0.362$ ) and *A. eightsi* (intercept only model: L-ratio = 1.142, d.f. = 1,  $p = 0.285$ ), respectively, despite evidence of negative growth under the ambient environmental condition in *C. hyperborea* (mean  $\pm$  s.e.: ambient,  $-5.00 \pm 3.47\%$ ; future,  $-0.40 \pm 3.46\%$ ; Figure 3.1b) and evidence of a substantial increase in variability and decrease in mean ( $\pm$  s.e.) growth rate under the future environmental condition in *A. eightsi* (mean  $\pm$  s.e.: ambient,  $9.00 \pm 4.16\%$  ( $CV = 146.3\%$ ); future,  $0.10 \pm 7.54\%$  ( $CV = 23853.5\%$ ); Figure 3.1c). The ratio of tissue to shell wet weight (TW:SW) in *A. crenata* was dependant on the individual effects of environmental condition ( $F_{1,18} = 7.240$ ,  $p = 0.015$ ) and location ( $F_{1,18} = 20.001$ ,  $p < 0.001$ ; Figure 3.1d) with a greater mean ( $\pm$  s.e.) ratio of tissue in individuals subjected to the future environmental condition for both station B13 (ambient,  $0.27 \pm 0.02$ ; future,  $0.33 \pm 0.17$ ) and station B16 (ambient,  $0.20 \pm 0.14$ ; future,  $0.24 \pm 0.03$ ) reflecting shifts in energy allocation between muscle and tissue growth versus calcification (Bayne et al. 1985; Wood et al. 2008). Mean TW:SW in *A. eightsi* was also strongly influenced by environmental condition ( $F_{1,17} = 10.079$ ,  $p = 0.006$ ) but with a lower mean ( $\pm$  s.e.) ratio of tissue in individuals under the future environmental condition (ambient,  $1.25 \pm 0.05$ ; future,  $1.06 \pm 0.03$ ; Figure 3.1e).

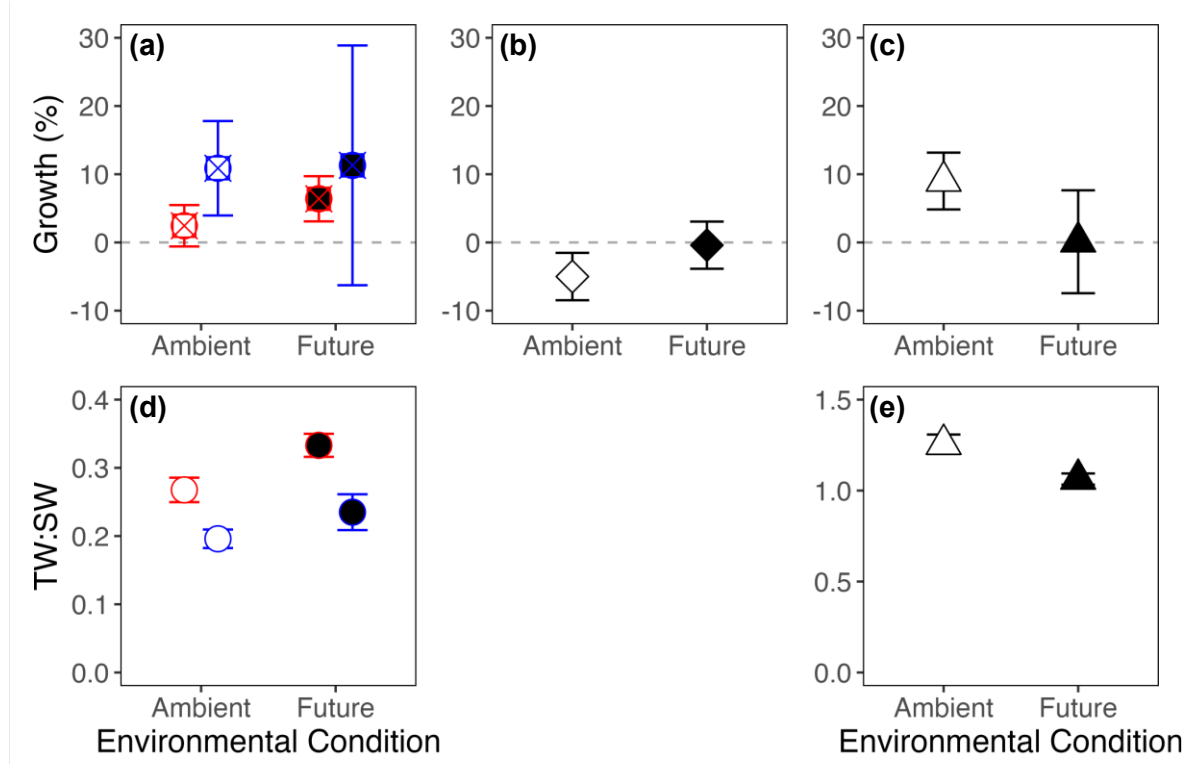


Figure 3.1 | The effects of species identity, station and environmental condition on (a-c) growth (Δ biomass, %) and (d-e) tissue:shell (TW:SW) wet weight (mean  $\pm$  s.e.) for *Astarte crenata* (circles), *Ctenodiscus crispatus* (squares) or both (crossed-circle), and *Cistenides hyperborea* (diamonds) from station B13 (red) and B16 (blue) and *Aequiyyoldia eightsi* (triangles) under ambient (open) or future (closed) environmental conditions.

### 3.4.2 Effects on respiration and excretion

My experimental design allowed us to measure oxygen consumption alongside changes in inorganic nitrogen and phosphate concentrations of the surrounding water, as an estimation of excretion rate (nitrogen: Le Borgne, 1986, Dy & Yap, 2000; Brockington & Peck, 2001; phosphate: Vink & Atkinson, 1985, Pomeroy & Bush, 1959, Gardner et al. 1981) and direct contribution to the recycling of nutrients (Gardner et al. 1993; Berezina et al. 2019), to evaluate climate-driven impacts on routine metabolic activity and functional performance. I found rates of oxygen consumption in *A. crenata* and *C. crispatus* unaffected by environmental condition ( $F_{1,20} = 0.028$ ,  $p = 0.868$ ), weakly affected by species identity ( $F_{1,20} = 3.759$ ,  $p = 0.067$ ) but not their interaction ( $F_{1,20} = 2.695$ ,  $p = 0.116$ ) despite evidence of opposite changes under the future environmental condition between the two species (ambient: *A. crenata*,  $0.78 \pm 0.46$ ; *C. crispatus*,  $0.93 \pm 0.59 \mu\text{g [O}_2\text{]. L}^{-1}\text{. hr}^{-1}$ ; future: *A. crenata*,  $-0.12 \pm 0.24$ ; *C. crispatus*,  $1.67 \pm 0.62 \mu\text{g [O}_2\text{]. L}^{-1}\text{. hr}^{-1}$ ; Figure 3.2a).

Rates of oxygen consumption in both *C. hyperborea* and *A. eightsi* were also unaffected by environmental condition (intercept only models; *C. hyperborea*: L-ratio = 0.292, d.f. = 1, p = 0.589; *A. eightsi*, L-ratio = 1.000, d.f. = 1, p = 0.317, Figure 3.2b-c) despite reduced conspecific variation under the future environmental conditions (mean  $\pm$  s.e.; *C. hyperborea*: ambient,  $9.21 \pm 5.13$  (CV = 96.6 %)  $\mu\text{g} [\text{O}_2] \cdot \text{L}^{-1} \cdot \text{hr}^{-1}$ ; future,  $6.79 \pm 1.54$  (CV = 39.2 %)  $\mu\text{g} [\text{O}_2] \cdot \text{L}^{-1} \cdot \text{hr}^{-1}$ ; *A. eightsi*: ambient,  $6.55 \pm 2.57$  (CV = 67.9 %)  $\mu\text{g} [\text{O}_2] \cdot \text{L}^{-1} \cdot \text{hr}^{-1}$ ; future,  $4.22 \pm 0.61$  (CV = 24.9 %)  $\mu\text{g} [\text{O}_2] \cdot \text{L}^{-1} \cdot \text{hr}^{-1}$ ).

Ammonium excretion rates in all species were not influenced by any explanatory factors (ANOVA intercept only models; Figure 3.2d-e), though I did find mean rates ( $\pm$  s.e.) were more variable under the future environmental condition for *A. crenata* (ambient,  $5.52 \pm 1.67$  (CV = 74.2 %) nmol  $[\text{NH}_4] \text{ min}^{-1}$ ; future,  $21.82 \pm 16.62$  (CV = 170.3 %) nmol  $[\text{NH}_4] \text{ min}^{-1}$ ), *C. hyperborea* (ambient,  $3.69 \pm 0.54$  (CV = 92.8 %) nmol  $[\text{NH}_4] \text{ min}^{-1}$ ; future,  $3.62 \pm 2.28$  (CV = 395.3 %) nmol  $[\text{NH}_4] \text{ min}^{-1}$ ) and *A. eightsi* (ambient,  $55.33 \pm 9.77$  (CV = 30.6 %) nmol  $[\text{NH}_4] \text{ min}^{-1}$ ; future,  $57.83 \pm 18.46$  (CV = 55.3 %) nmol  $[\text{NH}_4] \text{ min}^{-1}$ ). Phosphate excretion rates of *A. crenata* and *C. crispatus* did not differ between the two species (L-ratio = 0.816, d.f. = 1, p = 0.366) or location (L-ratio = 0.707, d.f. = 1, p = 0.401) but were lower (mean  $\pm$  s.e.) under the future environmental condition (L-ratio = 4.887, d.f. = 1, p = 0.027; ambient:  $2.60 \pm 0.66$ , future:  $0.91 \pm 0.33$  nmol  $[\text{PO}_4] \text{ min}^{-1}$ ; Figure 3.2g). Phosphate excretion rates in both *C. hyperborea* and *A. eightsi* were unaffected by environmental condition (intercept only models: *C. hyperborea*: L-ratio = 1.04, d.f. = 1, p = 0.307; *A. eightsi*, L-ratio = 1.85, d.f. = 1, p = 0.173; Figure 3.2h-i) despite evidence of increased variability under the future environmental condition (mean  $\pm$  s.e.; *C. hyperborea*: ambient,  $4.65 \pm 1.41$  (CV = 52.6 %) nmol  $[\text{PO}_4] \text{ min}^{-1}$ ; future,  $3.35 \pm 0.20$  (CV = 10.6 %) nmol  $[\text{PO}_4] \text{ min}^{-1}$ ; *A. eightsi*: ambient,  $2.08 \pm 1.28$  (CV = 106.4 %) nmol  $[\text{PO}_4] \text{ min}^{-1}$ ; future,  $5.91 \pm 2.77$  (CV = 81.0 %) nmol  $[\text{PO}_4] \text{ min}^{-1}$ ).

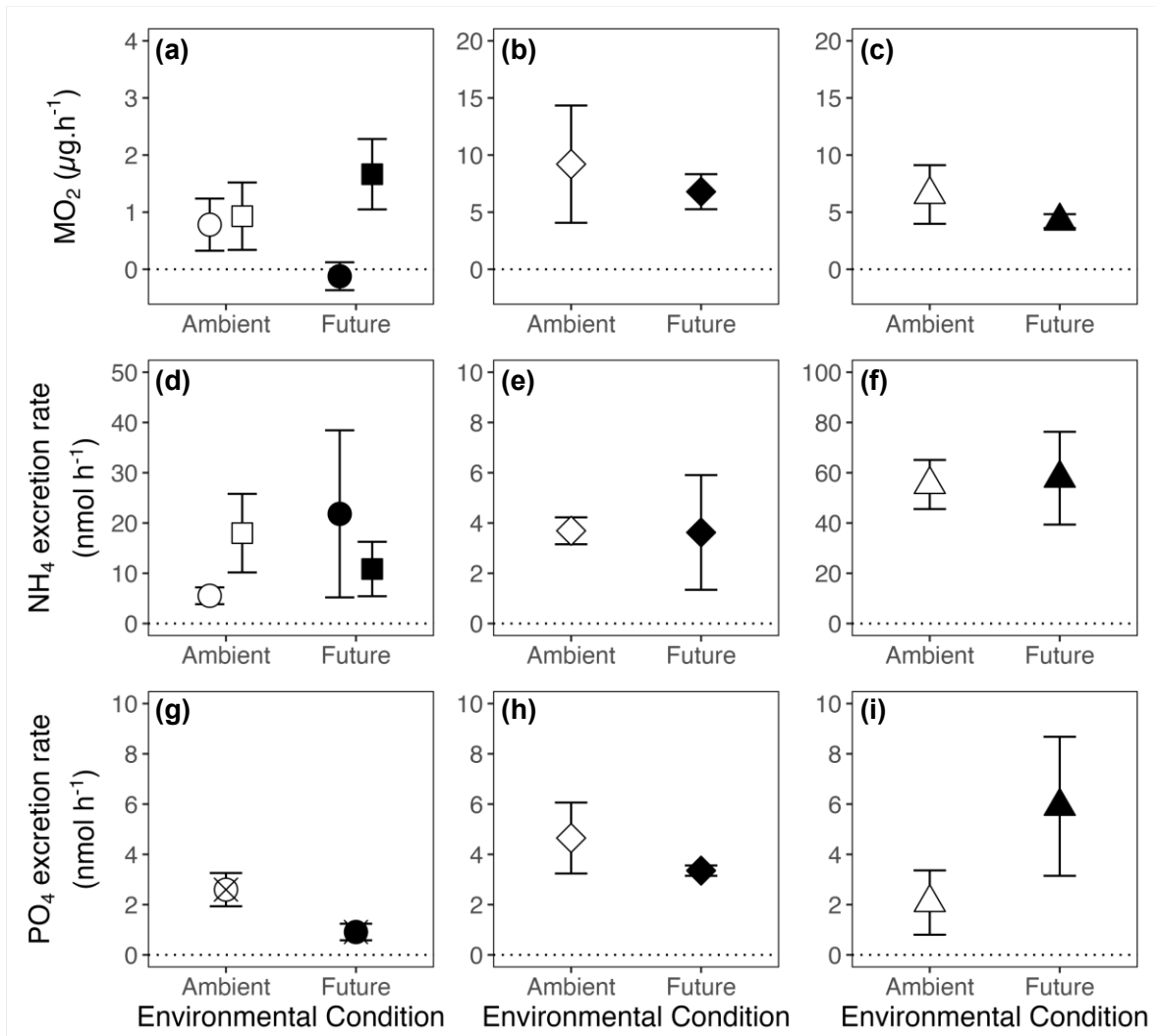


Figure 3.2 | The effects of species identity and environmental condition on (a-c) oxygen consumption ( $\text{MO}_2$ :  $\mu\text{g.h}^{-1}$ ), (d-f) ammonium excretion ( $\text{NH}_4$ :  $\text{nmol.h}^{-1}$ ) and (g-i) phosphate excretion ( $\text{PO}_4$ :  $\text{nmol.h}^{-1}$ ) (mean  $\pm$  s.e.) for *Astarte crenata* (circles) *Ctenodiscus crispatus* (squares) or both (crossed-circle), *Cistenides hyperborea* (diamonds) and *Aequiyyoldia eightsi* (triangles) under ambient (open) or future (closed) environmental conditions.

### 3.4.3 Effects on biochemical status

Quantifying the biochemical regulation of energy reserves can delve into how organisms deal with the energetic demanding processes involved with maintaining whole organism performance under a changing environment (Schmidt-Nielsen 1972; Hochachka and Somero 2002). Here, the influence of a changing climate on total protein and glucose concentrations differed between *A. crenata* and *C. crispatus* (SPID x environmental condition: PROT: L-ratio = 4.570, d.f. = 1, p = 0.033; GLU: L-ratio = 4.029, d.f. = 1, p = 0.045). Closer examination of model coefficients for both PROT

and GLU revealed that species identity was the most influential independent variable (PROT: L ratio = 11.887, d.f. = 2, p = 0.003; GLU: L ratio = 6.908, d.f. = 2, p = 0.032) followed by environmental condition (PROT: L ratio = 5.970, d.f. = 2, p = 0.051; GLU: L ratio = 4.249, d.f. = 2, p = 0.120). Specifically, under the future environmental condition, mean ( $\pm$  s.e.) total protein and glucose concentrations were higher in *A. crenata* (PROT: ambient,  $5.17 \pm 0.39 \text{ }\mu\text{g.mg}^{-1}_{\text{OM}}$ ; future,  $7.62 \pm 1.43 \text{ }\mu\text{g.mg}^{-1}_{\text{OM}}$ ; GLU: ambient,  $0.26 \pm 0.04 \text{ }\mu\text{g.mg}^{-1}_{\text{OM}}$ ; future,  $0.40 \pm 0.09 \text{ }\mu\text{g.mg}^{-1}_{\text{OM}}$ ) and lower in *C. crispatus* (PROT: ambient,  $18.77 \pm 3.74 \text{ }\mu\text{g.mg}^{-1}_{\text{OM}}$ ; future,  $10.72 \pm 2.86 \text{ }\mu\text{g.mg}^{-1}_{\text{OM}}$ ; GLU: ambient,  $0.65 \pm 0.14 \text{ }\mu\text{g.mg}^{-1}_{\text{OM}}$ ; future,  $0.39 \pm 0.11 \text{ }\mu\text{g.mg}^{-1}_{\text{OM}}$ ; Figure 3.3a,d). In *C. hyperborea*, neither total proteins nor glucose concentrations were affected by environmental condition (ANOVA intercept only models; PROT:  $F_{1,4} = 2.958$ , p = 0.161; GLU:  $F_{1,4} = 1.460$ , p = 0.294) despite evidence of decreased concentrations under the future environmental condition (PROT: ambient,  $5.68 \pm 1.03 \text{ }\mu\text{g.mg}^{-1}_{\text{OM}}$ ; future,  $3.31 \pm 0.93 \text{ }\mu\text{g.mg}^{-1}_{\text{OM}}$ ; GLU: ambient,  $0.28 \pm 0.05 \text{ }\mu\text{g.mg}^{-1}_{\text{OM}}$ ; future,  $0.19 \pm 0.05 \text{ }\mu\text{g.mg}^{-1}_{\text{OM}}$ ; Figure 3.3b,e). Total protein concentrations (mean  $\pm$  s.e.) were significantly lower in *A. eightsi* under the future environmental condition (L-ratio = 4.740, d.f. = 1, p = 0.030; ambient,  $5.73 \pm 0.08$ , future,  $0.91 \pm 0.53 \text{ }\mu\text{g.mg}^{-1}_{\text{OM}}$ ; Figure 3.3c), whilst glucose concentrations were unaffected (intercept only model: L-ratio = 0.496, d.f. = 1, p = 0.481; ambient,  $0.21 \pm 0.03 \text{ }\mu\text{g.mg}^{-1}_{\text{OM}}$ ; future,  $0.19 \pm 0.01 \text{ }\mu\text{g.mg}^{-1}_{\text{OM}}$ ; Figure 3.3f). I found no effect of biomass as a random factor in any of these models.

#### 3.4.4 Acclimation variability in polar invertebrates

Initially, my findings imply that the duration of exposure was sufficient for acclimation to transpire as respiration and ammonium excretion rates are preserved despite sustained exposure to novel environmental forcing (Schmidt-Nielsen 1972; Hochachka and Somero 2002) and reflect those expected under ambient conditions (Asnicar et al. 2021). I reveal, however, changes in inter- and intra-specific variation across multiple response variables that represent alterations in metabolic pathways (Green et al. 2017) and energy dynamics (Bayne et al. 1985; Wood et al. 2008). While it is widely recognized that physiological responses vary among species (Pörtner et al. 2012; Solan et al. 2016; Asnicar et al. 2021), my study reveals that responses also vary among individuals of the same species. This variation can result in both increased (here, *A. crenata*, *C. crispatus*, *A. eightsi*) and decreased (here, *C. hyperborea*, *A. eightsi*) intra-specific variation in trait expression, which can influence individual contributions to ecosystem processes (Williams et al. submitted) and population stability (Dingemanse & Wolf, 2013). Indeed, the ecological effects of intra-specific variation is increasingly recognised to be on par to effects of inter-specific variability when investigating changes in community composition (Des Roches et al. 2018; Bolnick et al. 2011) and

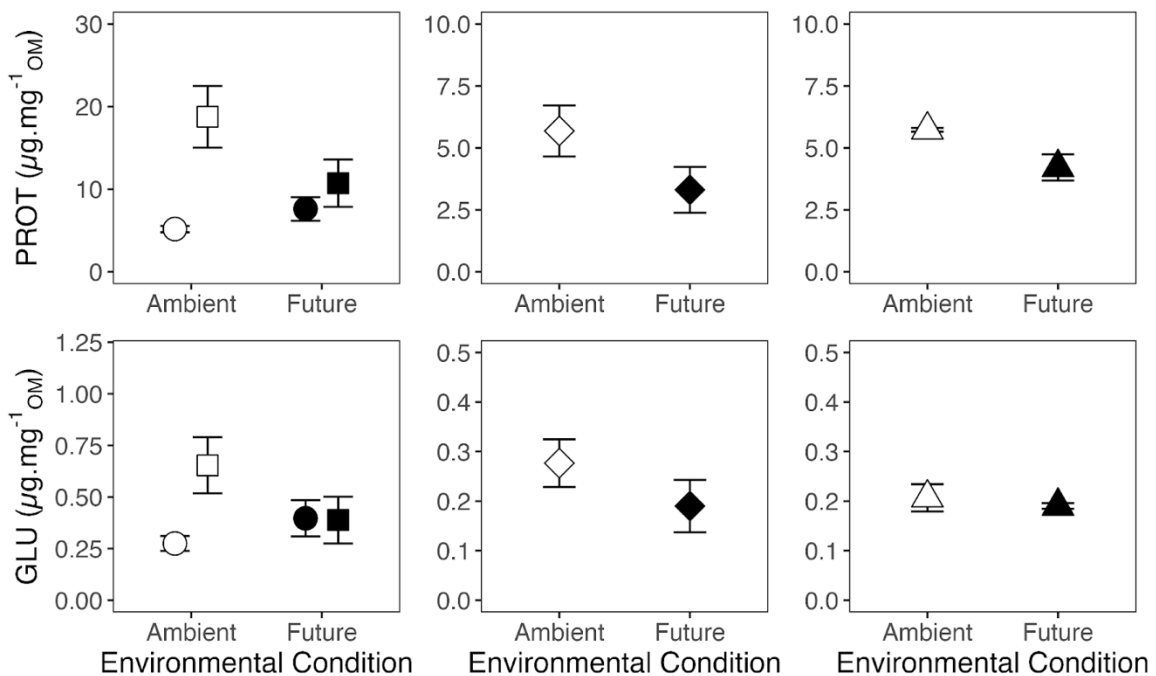


Figure 3.3 | The effects of species identity and environmental condition on concentrations of (a-c) glucose (GLU:  $\mu\text{g.mg}^{-1}\text{OM}$ ) and (d-f) protein (PROT:  $\mu\text{g.mg}^{-1}\text{OM}$ ) (mean  $\pm$  s.e.) in *Astarte crenata* (circles) *Ctenodiscus crispatus* (squares) *Cistenides hyperborea* (diamonds) and *Aequiyyoldia eightsi* (triangles) under ambient (open) or future (closed) environmental conditions

ecosystem functioning (Cassidy et al. 2020), yet despite its ecological importance and vulnerability to anthropogenic influence through selection and local extirpation (Palkovacs et al. 2012; Miraldo et al. 2016), of which can abruptly reduce population genetic diversity (Ceballos et al. 2017), empirical studies on the causes and patterns behind within-species variation are rare (Bolnick et al. 2003; Bolnick et al. 2011). As such, I emphasise the importance of accounting for biological variation in studies of species' mean responses (Applebaum et al. 2014) and add support to previous calls for greater identification of the genetic and phenotypic causes of ecological variation (Cassidy, 2020), as well as for quantification of ecological variation across multiple species, trophic levels, or entire communities to better predict how rapid, widespread changes in trait expression within species will impact communities and ecosystems (Mimura et al. 2017).

The observed variations in energy allocation and biochemical production are indicative of distinct adaptive mechanisms and differences in vulnerability to climate change (Savva et al. 2018). Acclimation of respiration and excretion processes correspond with reduced growth, tissue production, and/or protein synthesis in *C. crispatus* and *A. eightsi*. Repressed growth hampers size-dependent fecundity (Foo & Byrne, 2017) and competitiveness over time (Lord & Whitlatch,

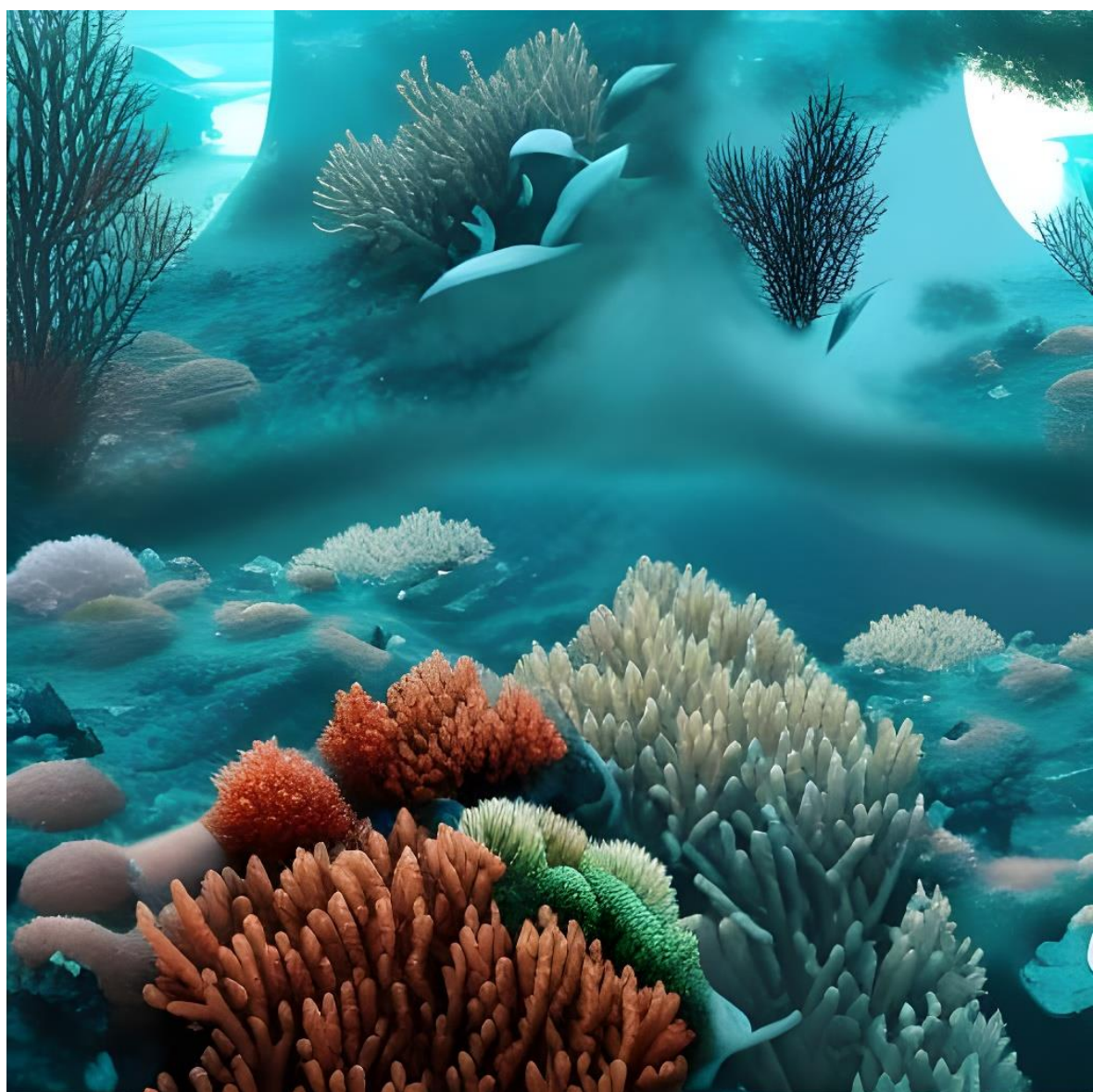
2015), which is particularly detrimental in oxygen-limited marine benthic environments (Ferguson et al. 2013). In contrast, *A. crenata* increased glucose and protein synthesis, but with reduced growth, suppressed phosphorus excretion, and evidence of decreased respiration, suggesting a shift in energy allocation to reproduction over overall organism performance (Reed et al. 2021). This focus on transgenerational success may compensate for poor phenotypic plasticity in the current generation, where parental exposure to environmental stress leads to phenotypic changes in offspring (Marshall, 2008; Ross et al. 2016). Although there were indications of metabolite downregulation and reduced growth, trait expression in *C. hyperborea* remained largely unchanged. Its resilience likely stems from being the deepest burrower among the four species (Williams et al. submitted), allowing it to physically evade adverse effects of novel environmental conditions (Woods et al. 2015; Kearney et al. 2009). Divergent responses to disturbance improves ecological resilience (Baskett et al. 2014), efficiency of resource utilisation and increases capacity for recovery following disturbances (Duffy, 2009; Bolnick et al. 2011), especially among organisms that coexist (Pagès-Escolà et al. 2018) or perform overlapping functional roles (Williams et al. submitted). Moreover, communities with diverse response capacities have a higher probability of including organisms that persist under specific environmental conditions and functionally compensate following species loss (Bernhardt et al. 2013; Hooper et al. 2005), minimising the impact on linked ecosystem services when environmental conditions fluctuate over time (Truchy et al. 2015).

While the measured responses offer valuable insights into acclimation strategies, they must be interpreted in light of the organisms that did not endure the full length of the experiment. Mortalities were evident across ambient and future conditions for all species except one (Appendix B Table S7). This could be attributed to the prolonged confinement within artificial mesocosms, potentially inducing a discernible deviation from the natural environment, which would have become increasingly evident during the experiment. This selectivity towards the proportion that are unaffected by artificial conditions may have excluded a comprehensive assessment of the species. Even so, my study illustrates the diversity of physiological strategies employed by cold-water organisms to cope with changing environmental conditions and, consistent with prior research (Uthicke et al. 2016; Wohlgemuth et al. 2017; Cassidy et al. 2020; Williams et al. submitted), emphasises the need to consider the spatial, temporal and biological context of within-species variation, which can improve forecasts of climate change vulnerability in marine systems (Valladares et al. 2014; Bennett et al. 2019).

Responses to climate change are anticipated to be more detrimental at higher latitudes (Manno et al. 2012; Figuerola et al. 2021), particularly where populations are near their geographic limits (Findlay et al. 2010). Here, limited opportunities for avoidance (i.e., dispersal, Chaine and Clobert, 2012) leave species susceptible to modifications in functional performance in the instance of unsuccessful acclimation (Pörtner et al. 2017) that reduces resilience and population recovery following disturbances (Fraser et al. 2014). Implementing local mitigation strategies at the edges of species' ranges can enhance resilience (Hughes et al. 2005) and mitigate the extent of environmental change within the limits of their ability to acclimate (Peck, 2005). However, as demonstrated here, polar invertebrates require significant time for acclimation (Peck et al. 2014) and given the swift regional pace of climate change (Auger et al. 2021), the time required to adapt to initial environmental shifts may be jeopardised by subsequent climatic forcing or other disturbances. In the context of Arctic shelf seas, benthic communities will likely experience additional challenges from melting sea ice, reduced availability of ice algae (Leu et al. 2011; Polyakov et al. 2012) and coinciding changes in phytoplankton primary production (Arrigo and van Dijken, 2020). Examining the modulation of physiological responses across environmental gradients (Telesca et al. 2019; Gaitán-Espitia et al. 2017), temporal scales (Godbold & Solan, 2013; Mardones et al. 2022; Form and Riebesell 2012), and under additional stressors (Delorme et al. 2020) would help disentangle the context-specific interactive effects of multiple drivers observed *in situ* (Ashton et al. 2017; Barnes et al. 2021) and shed light on performance trade-offs that become apparent only when multiple climate change stressors are taken into account (Laubenstein et al. 2019). Moreover, when utilised to parametrize the vulnerability of species (Magozzi & Calosi, 2015) and climate envelope models (Buckley et al. 2011), this would enable more accurate projections of where and when Arctic benthic communities will transition under conditions expected from global environmental change (Gaitán-Espitia et al. 2017).



## **Chapter 4 Inter- and intra-colony elemental systematics of a cold-water bamboo coral mediate deep- sea temperature and nutrient proxies**



## 4.1 Abstract

The impact of warming, acidification, and deoxygenation on deep-sea environments due to changes in shelf and coastal regions is a growing concern. Historical records in these deep environments are lacking, particularly at high latitudes, making climate change projections challenging. Indirect proxies, such as trace element composition of marine carbonates such as coral skeletons, can offer an alternative method to fill these data gaps. However, research on deep polar ocean coral species, like high-Mg calcitic bamboo coral from the Eastern Canadian Arctic, is limited. Here, using Laser Ablation Triple-Quadrupole Inductively Coupled Plasma Mass Spectrometry (LA-QQQ-ICP-MS), I examined micrometre-scale element variation within and between individual *Keratoisis* sp. colonies to assess the influence of biological variability on geochemical tracers for reconstructing past environmental conditions (temperature, Mg/Ca, Li/Mg, Sr/Ca, Ba/Ca, U/Ca;  $[Ba]_{sw}$ , Ba/Ca). I also refined calibrations for high-Mg calcitic Octocorals using established environmental proxies. I find reproducible ( $2\sigma$  relative coefficient of variation) values in Mg/Ca (3 %) and Ba/Ca (6 %) along the radial growth axis of all colonies and internodes of *Keratoisis* sp., indicating these signals are stable and suitable for environmental reconstructions. After revising cross-study multi-taxa calibrations for Mg/Ca ( $0.316 \pm 0.026 \text{ }^{\circ}\text{C}/\text{mmol/mol}$ ,  $R^2 = 0.87$ ,  $p < 0.001$ ) and Ba/Ca ( $[Ba/Ca \mu\text{mol/mol}] = 0.148 \pm 0.005 \text{ } [Ba_{sw} \text{ nmol/kg}]$ ,  $R^2 = 0.97$ ,  $p < 0.001$ ), I show that vital effects within and among *Keratoisis* sp. colonies strongly influence reconstructed temperature and  $[Ba]_{sw}$ , but this is improved by combining replicate internode transects into a single composite series. Despite the ontogenetic variability, all colonies reveal a gradual deep-water cooling trend since the early 21<sup>st</sup> century and synchronised, multi-year spikes in  $[Ba]_{sw}$  that suggest substantial barium inputs to the seafloor. My study confirms the reliability of Mg/Ca and Ba/Ca proxies in high-Mg bamboo corals for detecting temperature and seawater barium variations in cold-water environments. However, further investigation into micro-scale element behaviour influenced by biotic processes in these corals is needed to enhance confidence in reconstructions at finer resolutions. Employing empirical calibrations from multi-taxa multi-proxy approaches can increase the certainty of reconstructions when proxies like Li/Mg, Sr/Ca, U/Ca and Sr/U underperform, while leveraging multiple element series to account for biological-induced variability improves single colony reconstructions.

## 4.2 Introduction

High-resolution historical records of the marine environment are essential for ascertaining the effects of rapid anthropogenic climate change and reducing the uncertainty of projected future conditions. The ecological repercussions of climate change for deep sea organisms, communities and biological processes, however, remain largely unresolved, though the severe changes in temperature, oxygen,  $\text{pCO}_2$  and export of particulate organic matter projected for the seafloor (Battaglia and Joos, 2018) are likely to lead to ecological destabilisation across all trophic levels and marine layers by the turn of the century (Levin and Le Bris, 2015; Sweetman et al. 2017). Despite this, insufficient spatio-temporal coverage of in-situ measurements of temperature, salinity, and biogeochemical parameters for deep waters (>200 m), particularly in polar regions

(Buch et al. 2019; Smith et al. 2019), has resulted in a fragmented information landscape, limiting the construction of predictive models. Although preserved environmental information from paleo-proxies can help fill in the gaps, both over time and space, conventional samples such as sediment cores and ice cores do not have the requisite time resolution to study precise, modern-era changes.

So-called deep-sea corals (DSCs) offer an opportunity to access detailed records of localised environmental history within its geochemistry at sub-decadal resolution over the entire lifespan of the coral (Sherwood & Risk, 2007; Robinson et al. 2014), which can provide a more holistic understanding of anthropogenic influences within the deep benthos and improve predictions of resulting environmental changes. Previous studies demonstrate that proxy records of temperature (Smith et al. 2000; Thresher et al. 2010; Lutringer et al. 2005; Case et al. 2010; Kimball et al. 2014; Montagna et al. 2005; 2014), ocean circulation and ventilation (Adkins et al. 1998; Frank et al. 2004; Robinson et al. 2005; Sherwood et al. 2008), biological productivity and nutrient concentrations (Sherwood et al. 2005a, 2011; LaVigne et al. 2011), and the isotopic and elemental properties of seawater (Anagnostou et al. 2012; Hill et al. 2012) can be derived from patterns in trace and minor elements within the carbonate and organic matrices of the coral skeletal structure. Cold-water corals such as *Desmophyllum dianthus*, are, however, known to possess heterogeneities in microstructural chemistry, particularly around their centres of calcification (Anagnostou et al. 2012; Gagnon et al. 2007; Stewart et al. 2016) which can frustrate efforts to reliably reconstruct past environments.

Cold-water gorgonian octocorals (hereafter, bamboo coral) do not typically exhibit centres of calcification or similar microstructural heterogeneities (Noé & Dullo, 2006), and unlike aragonitic corals typically used for deep-sea paleo investigations, can grow in seawater that is undersaturated in calcite (Geyman et al. 2019; Feely et al. 2002), thus inhabiting a wider range of depths. However, deep-sea octocorals, in general, are some of the slowest-growing corals (Sherwood et al. 2009), the biomineralization processes they use is not well understood but are presumed not to precipitate in isotopic equilibrium with sea water (Farmer et al. 2015a) and therefore, if like other CWCs (Smith et al. 2000), the extent of the disequilibrium may vary widely within a particular individual. Indeed, physiological processes play a significant role in controlling microscale variations in trace and minor element compositions, which is why many proxies in bamboo corals suggest environmental variability outside of the known limits of ambient seawater conditions (Flöter, 2019). In coral paleoclimatology, explicitly evaluating the effects of intra- and inter-colony variation through the application of a multi-colony approach is a vital way of ascertaining reproducible environmentally-driven signals from ontogenetic noise (e.g. Alpert et al.

2016; Hu et al. 2018) as proxies can typically exhibit poor reproducibility between single colonies due a combination of variable vital effects related to growth rates, instrumental uncertainty, incorporation of organic material, and seasonality of the environmental signal (Sherwood et al. 2005b; Sinclair et al. 2011; Aranha et al. 2014). Within the field of ecology, accounting for inter-individual variability is also a necessary approach for understanding community dynamics (Bolnick et al. 2011), functional productivity (Cianciaruso et al. 2009) and responses to global change (Pistevos et al. 2011; Schlegel et al. 2012). In terms of within individual variation, it is recognised that improved reproducibility of geochemical records could be achieved by cross-validating replicate transects on adjacent growth paths (DeLong et al. 2007; DeLong et al. 2011; Kawakubo et al. 2014). As for Octocorals that grow radially, this can be carried out across a singular internode (Sinclair et al. 2011) or by sectioning the coral at different positions along its longitudinal axis to obtain different internode sections. By aligning replicate stratigraphies with *in-situ* environmental data (Hu et al. 2018; Cuny-Guirriez et al. 2019; Hathorne et al. 2013), this approach ultimately enhances the accuracy of paleoenvironmental reconstruction.

In cases where long-term *in-situ* environmental measurements are lacking, a possible calibration alternative is to compare the nominal proxy value with the ambient conditions at the collection site of a live coral (e.g. Thresher et al. 2016a). Combining multiple comparisons from various taxa, depths, and geographic locations can help identify universal proxies and serve as a basis for targeted studies in the future (Stewart et al. 2020) but this approach has limitations, as it overlooks any ontogenetic variability and confines lifetime response mechanisms to fluctuating environmental conditions into a single point. As such, I adopt a cross-study calibration method alongside a multi-colony multi-internode micrometre-scale analysis of trace and minor element variation in deep-water bamboo corals using laser ablation approaches to holistically assess the likelihood that the observed geochemical variability is indicative of environmental change. Specifically, multidecadal-scale geochemical information of Li/Ca, Mg/Ca, Sr/Ca, U/Ca, Li/Mg and Ba/Ca were extracted from four deep-water *Keratoisis* sp. (Subclass Octocorallia, Bayer, 1956; Watling et al. 2022; lifespan estimate, 100 years+, Neves et al. 2014) from a region of the Canadian Arctic that is undergoing rapid environmental change (Laidre et al. 2020; Nusbaumer et al. 2019). These tracers are regularly used as proxies for ambient seawater temperature (Thresher et al. 2010; Lopéz Correa et al. 2011; Flöter 2019; Flöter et al. 2019) and barium concentrations (LaVigne et al. 2011; Thresher et al. 2016a, Flöter et al. 2019; Geyman et al. 2019), the latter of which exhibits a nutrient-like profile in open oceans (Chow & Goldberg, 1960) and tracks patterns of other algal nutrients (Wolgemuth and Broeker, 1970). This selection enables us to gain insights into the dynamics of deep oceanographic processes and the circulation of refractory nutrients from the overlying water column. By employing *Keratoisis* sp. as a paleoceanographic proxy in

cold-water environments, I gain insights into species' responses over extended timescales beyond the limitations of current data. Additionally, I evaluate the efficacy of benthic calcifiers as indirect indicators of environmental changes in the Arctic deep-sea. Through examining the dependencies of various element ratios on temperature and surrounding seawater chemistry, I expect that changes in geochemical signals across the coral's lifetime will capture both long-term trends and shorter cyclic environmental variability. In cases where such correlations are absent, I instead anticipate that biological variability will serve as the dominant factor influencing the observed patterns.

## 4.3 Materials and methods

### 4.3.1 Sample collection

*Keratoisis* sp. (SubFamily *Keratoisidinae*) was collected at the Disko Fan station (67° 57.9786' N, 59° 29.6286' W, 889 m, 2<sup>nd</sup> August 2021) using the Sub-Atlantic® Comanche (Forum Energy Technologies™, USA) remotely operated submersible from the CCGS Amundsen (Geoffroy et al. 2021). Individual colonies of *Keratoisis* sp. were collected along the planned (~ 1 km) dive transect (Appendix C Table S1 and Figure S1 for geo- and timestamps) and extracted close to the basal internode (near the base of the colony).

### 4.3.2 Sample processing

External debris and fauna were removed by hand, before the *Keratoisis* sp. colonies (n = 4) were photographed (NIKON D3300, AF-S DX VR Nikkor 18-55mm Lens, f/3.5-5.6G II; Appendix C Figure S2), sealed in Ziplock bags and placed in -20 °C for 72 hours. After the initial freezing, tissue was removed from the *Keratoisis* sp. skeletons with jets of re-circulated 0.45 µm membrane-filtered seawater at 4 °C using a WaterPik™ (Johannes & Wiebe 1970). Two separate washes of 60 to 80 ml filtered seawater were used on each internode, and 20 ml was used to rinse the remainder of the skeleton, WaterPik™ reservoir, and to flush the WaterPik™ pump. The cleaned *Keratoisis* sp. skeleton portions were then vacuum sealed in PVC tubing, sealed with Parafilm®, and transported to the National Oceanography Centre, Southampton, UK.

### 4.3.3 Hydrographic data

The environmental data and sources are provided in Table 1. To calibrate *Keratoisis* sp. element values (Li/Mg, Mg/Ca, Sr/Ca, Sr/U, U/Ca) to *in-situ* environment conditions, proximal deep-water

temperature values at the point of sampling and during previous research cruises (K. Azestu-Scott, pers. comm., May 31, 2022) were obtained from in-situ measurements using precise probe or CTD (conductivity, temperature, depth) profiles. As proximate temperature values were only available for the previous three years (2018-2021), with one value each year between June-August, these were compared to a weekly sea surface temperature (SST; 1989-12-31 to 2020-12-31 within a 2 x 2 ° grid; 67 – 69 °N, 61.5 – 59.5 °W; resolution 1°) obtained from the NOAA Optimum Interpolation SST (OISST) dataset (V2; <https://psl.noaa.gov/data/gridded/data.noaa.oisst.v2.html>; Reynolds et al. 2002) and a deep-water 20<sup>th</sup> century temperature timeseries of the Baffin Bay basin obtained from sporadic bottle- and CTD-casts within a 200 m vertical bin (1940 – 2003; 800 – 1000m; 62 – 80 °N; 85 – 50 °W; irregular time intervals; Figure 7 in Zweng & Münchow, 2006) to achieve a longer, more complete history of environmental conditions.

Proximal dissolved barium concentrations ( $[Ba]_{sw}$ ) data were compiled from GEOTRACES (GEOTRACES Intermediate Data Product Group, 2021) to investigate the relationship with *Keratoisis* sp. Ba/Ca values and calculate the partition coefficient,  $D_{Ba}$ . The geographically closest  $[Ba]_{sw}$  profile was identified (66.857 °N; 59.064 °W; 2015-08-03; Thomas et al. 2021) and a representative (matched the sample depth of each *Keratoisis* sp. colony)  $[Ba]_{sw}$  value was calculated (linear interpolation between the nearest two measurement depths; 669.7m and 998.6m). Data reported in units of nM, assuming atmospheric pressure and ambient room temperature, were converted to nmol/kg using a seawater density of 1.025 kg/m<sup>3</sup>.  $[Ba]_{sw}$  measurements in the modern ocean remain sparse, especially in the Eastern Canadian Arctic, yet the distance between sampling station and the  $[Ba]_{sw}$  profile was less than 130 km (colony-specific distances, depths and interpolated  $[Ba]_{sw}$  values reported in Appendix C Table S2). Uncertainty on matched  $[Ba]_{sw}$  values was estimated using analytical uncertainty of  $\pm 1$  nmol/kg which was calculated by applying a representative, high-end analytical uncertainty from the  $[Ba]_{sw}$  dataset used ( $\pm 2.5\%$ ; Thomas et al. 2021) to the highest  $[Ba]_{sw}$  value in my dataset (59 nmol/kg).  $[Ba]_{sw}$  was converted to seawater Ba/Ca ratios ( $\mu\text{mol/mol}$ ) using a  $[Ca]_{sw}$  value of 10.3 mmol/kg (Nozaki, 1997). Seawater [Ca] was assigned an error of  $\pm 5\%$  to account for variations in salinity. Calculated barium partition coefficients were compared to previous studies by LaVigne et al. (2016) and Kershaw et al. (2023) to cross-reference values with other Octocorals.

Table 4.1 | Geographic coordinates and depths of the coral colonies analysed in this study alongside hydrographic data, carbonate system parameters, estimated age (yr) and uncertainty. Temperature (T), salinity (S) and dissolved oxygen ( $O_2$ ) from conductivity-temperature-depth (CTD) casts taken nearby the coral sample sites are provided. For ageing estimation and uncertainty methodology, refer to Section 4.3.5.1.

SITE	LAT.	LONG.	DEPTH (M)	ID	TAXON.	SEAWATER PARAMETERS			ESTIMATED AGE (YR)	AGE UNCERTAINTY (RANGE, YEARS)
						T(°C)	Salinity	$O_2$ (μmol/kg)		
<b>EASTERN CANADIAN ARCTIC</b>										
DISKO FAN (CANADA)	67.96629	-59.49069	885	23-1	<i>Keratoisis</i> sp.	1.12	33.47	200.1	27	9-31
DISKO FAN (CANADA)	67.96631	-59.4899	883	23-6	<i>Keratoisis</i> sp.	1.12	33.47	200.1	56	20-64
DISKO FAN (CANADA)	67.96631	-59.48892	879.9	23-10	<i>Keratoisis</i> sp.	1.12	33.47	200.1	28	10-32
DISKO FAN (CANADA)	67.9663	-59.48768	876.2	23-16	<i>Keratoisis</i> sp.	1.12	33.47	200.1	22	8-25

#### 4.3.4 Analytical procedures

##### 4.3.4.1 Micro CT scanning

I analysed 4 colonies of *Keratoisis* sp. using three-dimensional models constructed with the custom-built X-ray microfocus computed tomography system (Nikon XT microCT) at the  $\mu$ -VIS Imaging Centre, University of Southampton, UK. Two-dimensional image reconstructions of each colony from matrices of scan slices (voxel resolution 50  $\mu$ m) were assembled using a proprietary ImageJ plugin “LinkedView” (Ho et al. 2020) to locate three separate internodes along the colony for sample sectioning (see Section 4.3.4.1). Slice data derived from the scans were further manipulated in the 3D visualisation software Dragonfly $\circledR$  (v2022.1; Li et al. 2020) and exported as fly-through timelapse videos (Appendix C Figure S3).

##### 4.3.4.2 Geochemical analysis

###### 4.3.4.2.1 Sample preparation

Each sample of *Keratoisis* sp. was sectioned (20 – 30 mm thickness, perpendicular to main axis) across three separate internodes, embedded in epoxy resin, hand polished (1200 to 4000 grit) and then polished using a petrological polishing machine (6 polishing cycles over 280 minutes, starting at 9 microns particulate down to 0.3 microns). To achieve an analytical grade polish, sections were processed for a further 20 minutes at 0.1 micron and visually quality checked under a digital microscope (AmScope) (Appendix C Figure S4).

###### 4.3.4.2.2 Laser ablation Quadrupole ICP-MS

*Keratoisis* sp. sections were analysed using an Agilent (Agilent Technologies Inc., CA, USA) 8900 Triple Quadrupole ICP mass spectrometer coupled to an Elemental Scientific Lasers (Bozeman, MT, USA) NWR193 excimer laser ablation system with a TwoVol2 ablation chamber, housed in the Geochemistry laboratory at the University of Southampton. The isotopes  $^{7}\text{Li}$ ,  $^{25}\text{Mg}$ ,  $^{43}\text{Ca}$ ,  $^{86}\text{Sr}$   $^{137}\text{Ba}$  and  $^{238}\text{U}$  were selected for analysis to investigate the applicability of commonly used geochemistry temperature proxies (Table 4.2 Thresher et al. 2010; Lopéz Correa et al. 2011; Flöter 2019; Flöter et al. 2019) and the seawater barium proxy (LaVigne et al. 2011; Thresher et al. 2016a, Flöter et al. 2019; Geyman et al. 2019). Samples and standards were ablated in line-mode, where standard analyses consisted of ca. 230 integration cycles of 0.52 s (1.2 mm lines). For sample analysis, five adjacent 50  $\mu$ m wide transects were ablated on 12 *Keratoisis* sp. sections (four colonies with three internodes each), where each transect consisted of ca. 240 – 638 integration cycles of 0.52 s (min 1.2 mm; max 3.2 mm). Prior to data collection, samples and

standards were ablated to remove any surface contamination (laser power density of  $0.6 \text{ J cm}^{-2}$ , repetition rate of 40 Hz, and tracking speed of  $400 \mu\text{m s}^{-1}$ ). Typical operating conditions during data collection are fully outlined in Appendix C Table S3. An on-peak gas blank subtraction was performed to the raw counts using the mean of bracketing gas blank analyses. Blank bracketing cut-offs were calculated using a 4-step rolling difference, where the maximum positive and negative change in  $^{43}\text{Ca}$  across the 4-step are indicative of where the resin-coral boundaries are located. Element/Ca ratios were corrected for instrumental drift and mass bias by standard-sample bracketing with glass reference material NIST SRM612 using the values published by Jochum et al. (2011). In addition, a pressed pellet of *Porites* sp. coral JCp-1 (Hathorne et al. 2013) was analysed as an internal consistency standard. For data processing and outlier rejection, I followed Standish et al. (2019). Briefly, outliers defined as  $\pm 3$  times the interquartile range of raw counts (within the blanks and analysis brackets) were removed from each set of the standards to eliminate anomalous values due to laser intensity variability. External reproducibility of the consistency standards ( $2\sigma$ ,  $n = 14$  per standard) are shown in Table 4.2. Element ratios of the *Keratoisis* sp. sections were secondary normalised using the JCp-1 (Table 4.2).

#### 4.3.4.2.3 Elemental mapping

Outliers were removed from each laser line for elements of the *Keratoisis* sp. sections using a standard deviation (SD) rejection and data was smoothed using a 5 point moving average. Selection of the number of SD was dependent on an initial examination of the data patterns and the degree of synchrony of variability observed for each element (Appendix C Table S4). For each section, 5 separate smoothed laser lines were mapped onto an equal spaced grid using their X and Y spatial coordinates from the laser ablation system. The dimensions of the grid were governed by the resolution of the data and was constructed using the “raster” function of the terra package (Hijmans, 2022) in R (R Core Team, 2022), achieving a resolution of  $5 \times 40$  microns  $\text{pixel}^{-1}$ . To orientate the elemental mapping onto the coral sections, cleaned coral skeletons were mounted (carbon coated) to conductive carbon tape and examined with a Leo 1450VP (Carl Zeiss) variable pressure scanning electron microscope.

Table 4.2 | Selected average JCp-1 elemental ratios normalised to NIST612 as determined over two sessions in May 2022. \* refers to the deviation the average element ratios compared with GeoRem preferred compositions <sup>a</sup>Hathorne et al. 2013. Isotopes measured: <sup>7</sup>Li, <sup>26</sup>Mg, <sup>43</sup>Ca, <sup>88</sup>Sr, <sup>138</sup>Ba, <sup>238</sup>U.

Elemental ratio	Average (n = 13)	2 s.d.	2 s.d. (%)	Difference from reference (%) <sup>a</sup>
Li/Ca (μmol/mol)	6.73	0.50	7.37	8.77 <sup>a</sup>
Mg/Ca (mmol/mol)	4.36	0.18	4.04	3.76 <sup>a</sup>
Sr/Ca (mmol/mol)	8.43	0.17	2.00	-4.64 <sup>a</sup>
Ba/Ca (μmol/mol)	5.36	0.58	10.90	-28.27 <sup>a</sup>
U/Ca (μmol/mol)	1.09	0.03	3.12	-8.67 <sup>a</sup>

#### 4.3.5 Paleo-environmental reconstructions

##### 4.3.5.1 Age model

Coral elemental ratios need to be translated from length to time to make direct comparisons to the observational temperature and [Ba]<sub>sw</sub> record. For timeseries analysis of my geochemical mapping data, I broadly follow Flöter et al. (2019). First, I compiled published linear radial growth rates for *Keratoisis* sp. by searching the Thomson Reuters Web of Science collection (<http://www.webofknowledge.com>, accessed 30/09/2022) using an ‘Advanced Search’ across all databases with the search term *Keratoisis* AND “growth rate” in the titles, key words and abstracts of all document types, in all languages, for the publication years 1950 to 2021. Citation returns (n = 13, Appendix C Table S5) were manually searched for reported values of linear radial growth rates, associated environmental metadata (latitude, longitude, water depth, temperature), information on the methodology used, and details about timing (year) and ecoregion (following accepted biogeographical typologies; Bailey et al. 1998; Spalding et al. 2007), reducing the number of records to 11 papers. Although more complex nonlinear growth modes have been proposed for bamboo corals (e.g., Frenkel et al. 2017) to allow for ontogenetic changes in growth rates (Farmer et al. 2015b), I prefer to opt for a linear model given the limited available chronological data. Non-linearity in growth could be identified by counting periodic bands (Thresher et al. 2004; Roark et al. 2005), however, banding was irregular and frequently ambiguous in the colonies presented in this study (μCTscan, digital microscope images, Appendix C Figure S4; SEM images, Appendix C Figure S5). An absolute (calendar) age model was established for these colonies using the collection year (2021), estimated median growth rate (51  $\mu\text{m.yr}^{-1}$ ), and upper and lower quartiles (31  $\mu\text{m.yr}^{-1}$ ; 59  $\mu\text{m.yr}^{-1}$ ) across all colonies from the literature (n = 21, Appendix C Table S6). To estimate the relative dating precision for a given sampling point, I started with the sampling year (2021) and integrated one-sided dating uncertainty in years, calculated as follows:

Equation 4.1 Calculation of relative dating precision for a given sampling point within a radially growing coral

$$\Delta t_{+;-} = \left| \left( \frac{d}{GR_m} + A_{abs} \right) - \left( \frac{d}{GR_{+;-}} + A_{abs} \right) \right|$$

where  $d$  is the distance from the outer rim in  $\mu\text{m}$ ,  $GR_m$  is the mean growth rate in  $\mu\text{m yr}^{-1}$ ,  $GR_{+;-}$  are the respective upper and lower growth rate quartiles in  $\mu\text{m yr}^{-1}$ , and  $A_{abs}$  is the year of sampling. Maximum uncertainty values alongside estimated ages for each colony are presented in Table 4.1.

#### 4.3.5.2 Intra-individual covariance and reproducibility

Covariance and monotonic relationships between raw Element/Calcium ratio (hereafter, E/Ca) signals were first compared between each internode of the same colony using the “*ggpairs*” R function of the GGally package (v2.1.2; Schloerke et al. 2021). Intra-individual reproducibility in E/Ca signals was analysed using a stratigraphic correlation technique. To accomplish this, the five ablation tracks per internode were first averaged into one transect along the growth axis. Anchor points were assigned by identifying unique peaks and troughs present across the transects of the basal and other two internodes in that colony using the “*QAnalySeries*” software (v 1.5.1, Kotov & Pälike, 2018). Barium profiles were selected as the basis for assigning anchor points due to their high reproducibility in marine carbonates, allowing for precise alignment of different tracks (Sinclair et al. 2011). The age model established by stratigraphic tuning of Ba/Ca signals was then applied to each of the remaining 5 ratios (Li/Ca, Li/Mg, Mg/Ca, Sr/Ca and U/Ca) to obtain tuned element tracks in each internode (linearly interpolated back to 50 $\mu\text{m}$  intervals) and intra-specific Pearson’s correlation scores.

#### 4.3.5.3 Multi-element, multi-species paleoenvironment calibrations

In conjunction to section 4.3.5.1, I evaluated the systematics of the “Li/Mg”, “Mg/Ca”, “Sr/Ca”, “Ba/Ca”, “U/Ca” and “Sr-U” multispecies palaeothermometry in published literature for coral and coralline algae. This was carried out by searching the Thomson Reuters Web of Science collection (<http://www.webofknowledge.com>, accessed 30/09/2022) using an ‘Advanced Search’ across all databases with the search term (*Li/Mg OR Mg/Ca OR Sr/Ca OR Ba/Ca OR U/Ca OR Sr-U*) AND (*coral OR coralline algae*) AND (*temperature OR thermometry OR thermometer*) AND (*calibration*) in the titles, key words and abstracts of all document types, in all languages, for the publication years 1950 to 2021. Unique citation returns ( $n = 193$ , Appendix C Table S7) were manually

searched for reported values of the five element ratios (standard corrected), associated environmental metadata (latitude, longitude, water depth, temperature), information on the methodology used, type of marine calcifier, mineralogy, details about timing and ecoregion (following accepted biogeographical typologies; Bailey et al. 1998; Spalding et al. 2007). I include culture experiments in my search, incorporating data where seawater carbonate chemistry has not been manipulated. Where data is compiled from other sources, I extracted from the original publication. Data that was only presented graphically (with decipherable individual data points) were extracted using *WebPlotDigitiser* (v4.6; Rohatgi, 2022). Papers that focused solely on reconstructing temperature from derived empirical calibrations without supporting *in-situ* instrument measurements (either used to directly compare against element signals or to correlate against satellite derived temperature) were excluded from data extraction, leaving 2650 unique data points across 56 papers (Appendix C Figure S6). Alongside data from Kershaw et al. (2023), citation returns were also manually searched for reported values of  $[\text{Ba}]_{\text{SW}}$ , associated metadata (latitude, longitude, water depth, temperature, salinity, pH), type of marine calcifier and mineralogy, leaving 329 unique data points across 12 papers (Appendix C Figure S6). Published element ratio-temperature (E/Ca-T) and  $[\text{Ba}/\text{Ca}]_{\text{coral}} - [\text{Ba}]_{\text{SW}}$  calibration equations were compiled and compared with my own calibrations that evaluate the influence of: (i) mineralogy and (ii) taxa.

#### 4.3.5.4 Inter-individual reproducibility in reconstructed environmental conditions

Stratigraphically tuned E/Ca determinations in the distance domain (i.e.,  $\mu\text{m}$  from coral wall) were converted to the time domain using the age model. Reconstructed temperature and  $[\text{Ba}]_{\text{SW}}$  was carried out using the derived calibration equations (Section 4.3.5.3) for multispecies high-Mg corals and compared across internodes and between colonies. Reconstructions were linearly interpolated to 4 points a year (seasonal) and 1 point a year (annual) using the “*spline*” function from the stats R package (R Core Team, 2022). Mean  $[\text{Ba}]_{\text{SW}}$ , mean temperature, and temperature trend ( $^{\circ}\text{C yr}^{-1}$ ) were calculated over the shared time period among all colonies, with the latter subsequently compared to trends in SST and deep-water temperature obtained during Section 4.3.3.

When conducting element analysis for palaeoceanographic reconstructions, it is crucial to account for coral skeletal heterogeneities and potential contamination sources. Differences in E/Ca behaviour between outer and central bands suggest distinct mechanisms controlling element uptake in these regions, including but not limited to, skeletal heterogeneity, diagenesis, heat stress, contamination from organic materials, and non-linear growth rates (Adkins et al. 2003; Anagnostou et al. 2011; Gagnon et al. 2007; Stewart et al. 2016; Clarke et al. 2019; Cuny-Guiriec

et al. 2019; Lazareth et al. 2016; Thresher et al. 2016b, Flöter, 2019, Flöter et al. 2019, 2022). While the absence of calcification centres (COCs) and amorphous carbonate infilling in *Keratoisis* spp. distinguishes them from other bamboo corals (Noé and Dullo, 2006; Thresher et al. 2004; Andrews et al. 2009; Thresher et al. 2010; Farmer et al. 2015b), reduced and elevated E/Ca values near the central axis and coral wall are still observable (Figure 4.1; Flöter et al. 2019) and hence, these sections were removed prior to temperature reconstruction. Despite these exclusions, the majority of the coral internode sections (mean: 85.9%, range: 73.7 % to 95.5 %) were considered for paleotemperature reconstruction.

#### 4.3.5.5 Statistical analysis

Tests for intra-individual covariance among *Keratoisis* sp. elements ( $n = 7$ ) were carried out using Spearman's rank (monotonic) correlations. To establish an empirical relationship between coral E/Ca and *in-situ* environmental conditions (Section 4.3.5.3), and reconstructed temperature vs time calculations (Section 4.3.5.4), I used an ordinary least squares (OLS) regression technique (type I; Alibert and McCulloch 1997; Quinn & Sampson 2002) and compared with a reduced major axis (RMA) regression model (type II; Cobb, 1998), with temperature as the independent variable and coral element/Ca as the dependent variable. The OLS technique assumes error only in the measurement of the dependent variable, whilst a RMA assumes error in the measurement of both the dependent and independent variables and is more suitable for use with geologic data. The slope of the equation produced by the RMA regression is equal to the slope of the equation of the OLS regression divided by the correlation coefficient (e.g., Cobb, 1998).

To test the individual and interactive effects of between-individual (colony) and within-individual (internode) variation on: (i) the mean reconstructed temperature (intercept) and trend (slope) calculated using the element paleothermometry proxy, and (ii) the mean reconstructed  $[\text{Ba}]_{\text{sw}}$  calculating using the Ba/Ca- $[\text{Ba}]_{\text{sw}}$  proxy, repeated measures two-factor analysis of variance models (ANOVAs) were created. As internodes were sampled repeatedly (to achieve different interpolations), I accounted for pseudoreplication by incorporating interpolation as a random factor (random intercepts) in linear mixed effect (LME) models (Zuur et al. 2009). I assessed model assumptions by visual inspection of standardised residuals vs fitted values plots, Q-Q plots, and Cooks distance (Zuur et al. 2010). When homogeneity of variance was violated, I utilised a *varIdent* variance-covariance structure and generalised least-squares (GLS) estimation (Pinheiro et al. 2022; Pinheiro & Bates, 2000; West et al. 2014), which allows residual spread to differ between the individual explanatory variables. I determined the optimal fixed-effects structure using backward selection informed by Akaike Information Criteria (AIC) and inspection of model

residual patterns. For the GLS analysis, I determined the optimal variance-covariance structure through restricted maximum-likelihood (REML) estimation by comparing the initial ANOVA model without variance structure to equivalent GLS models incorporating specific variance terms. The suitability of these models was compared against the initial ANOVA model using the AIC and by visualising model residuals. Finally, I determined the optimal fixed structure of the most suitable model through backward selection using the likelihood ratio test with maximum-likelihood (ML) estimation (West et al. 2014; Zuur et al. 2010).

All data processing was carried out in R (v4.2.2, R Core Team 2022) using the GGally (Schloerke et al. 2021), lmodel2 (Legendre, 2018), nlme (Pinheiro et al. 2022; Pinheiro & Bates, 2000), patchwork (Pedersen, 2022), stats (R Core Team, 2022), terra (Hijmans, 2022) tidyverse (Wickham et al. 2019) and viridis packages (Garnier et al. 2021). All code is available on Github (tjw-benth/BambooCoral-LAICPMS) and a summary of statistical models is included in Appendix C.

## 4.4 Results

### 4.4.1 Patterns in coral elements

The co-located 2D maps of skeletal element composition exhibit coherent lateral variability across each colony's internode, suggesting that these patterns are representative of *Keratoisis* sp. (Figure 4.1). The following patterns are typically evident in each image: elevated Li/Ca, Mg/Ca, U/Ca and depleted Sr/Ca are observable near the central axis, with depleted Li/Ca, Mg/Ca, Sr/Ca and elevated U/Ca found near the coral wall. Examination of SEM and digital microscope images reveal a less dense boundary of calcite at the coral radial wall which suffered acute cracking during the ablation (Appendix C Figure S5) and a denser band of calcite that encompasses the hollow central axis (Appendix C Figure S4). The Sr/Ca images demonstrate significant heterogeneity in both dimensions, with elevated values near minute stress fractures along the laser tracks, indicating that this element ratio does not follow a clear structure over time. Radial banding in Ba/Ca is visible across all colonies, with each band of raised concentrations reproduced further from the coral wall from the basal internode upward, suggesting these are time locked to repeating events. Outside of the elevated U/Ca at the outer edge of the coral, ratio values are fairly constant throughout the internode with some banding visible in the larger colonies.

Figure 4.1(a)

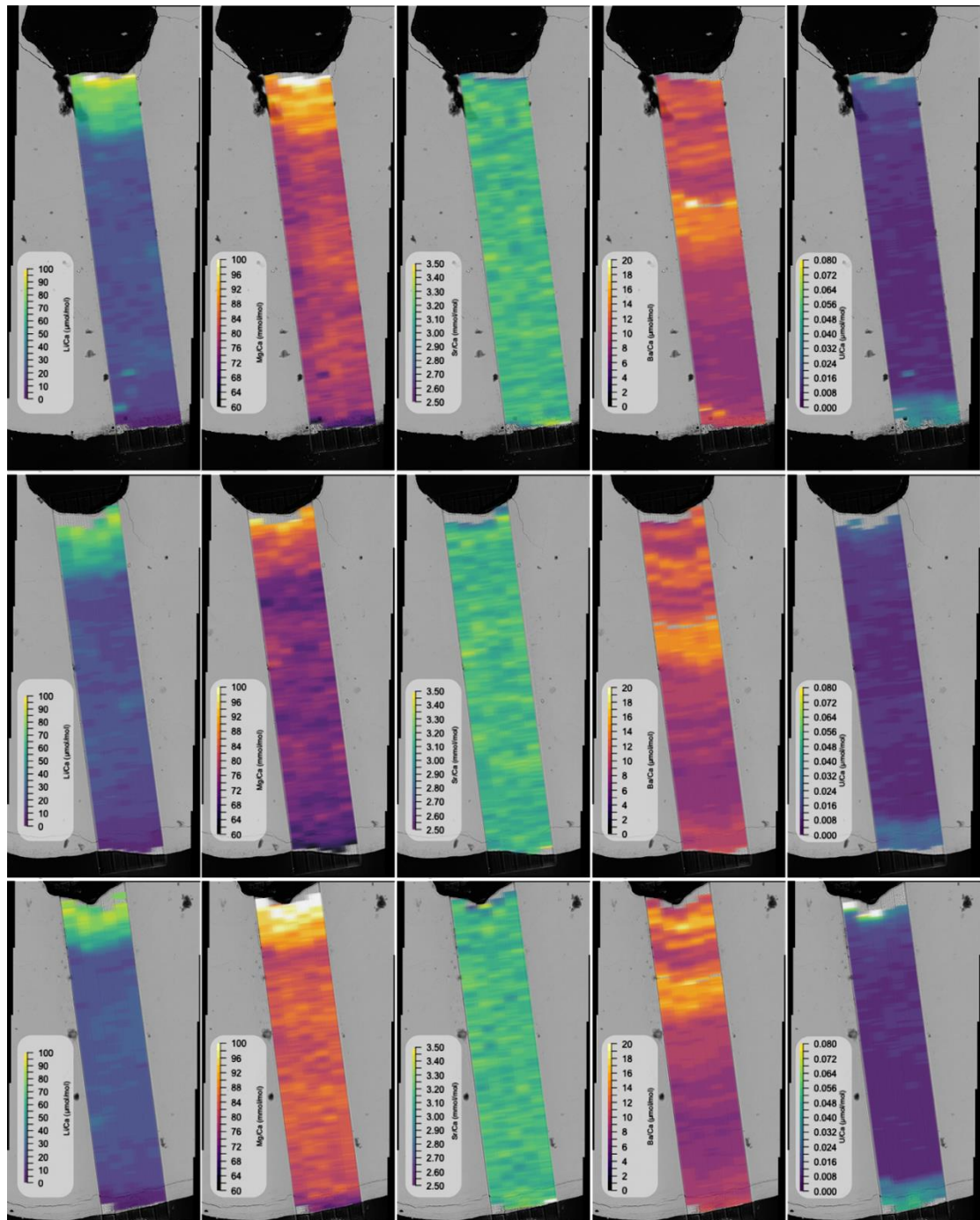


Figure 4.1 | Two dimensional patterns in *Keratoisis* sp. element ratios (left to right: Li/Ca, Mg/Ca, Sr/Ca, Ba/Ca and U/Ca) analysed by laser ablation and overlain onto a post-ablation SEM image of the basal internode (top row), second internode (middle row) and third internode (bottom row) of colony (a) #23-1, (b) #23-6, (c) #23-10 and (d) #23-16. Ratios that clearly match structure elements of the coral include high Li/Ca, Mg/Ca and U/Ca values confined to central axis and low Li/Ca, Mg/Ca values confined to coral wall. Banding is clear in the Barium profiles. Scale in bottom left of SEM images.

Figure 4.1(b)

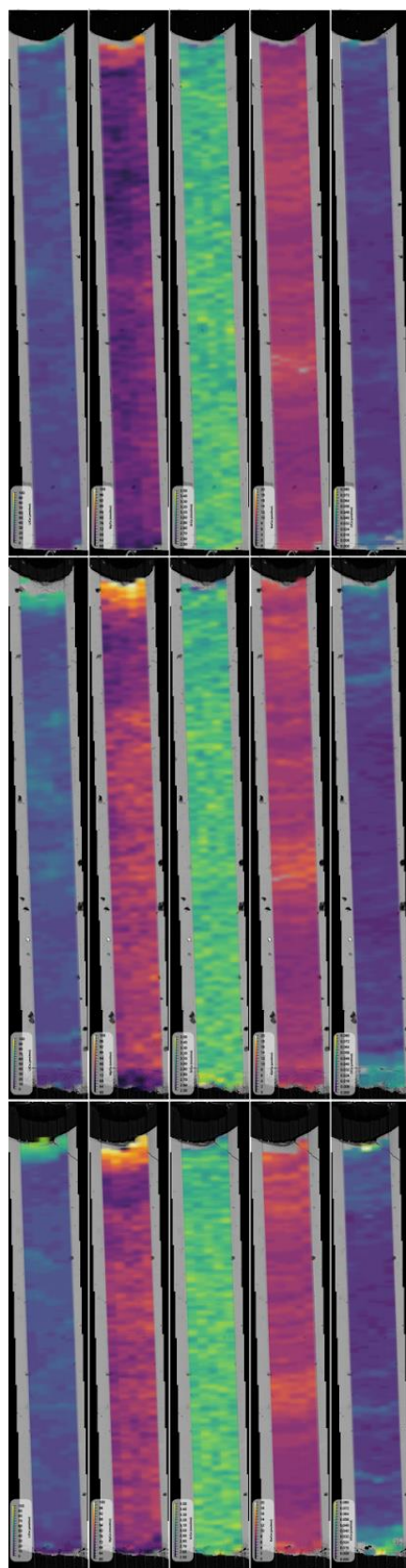


Figure 4.1(c)

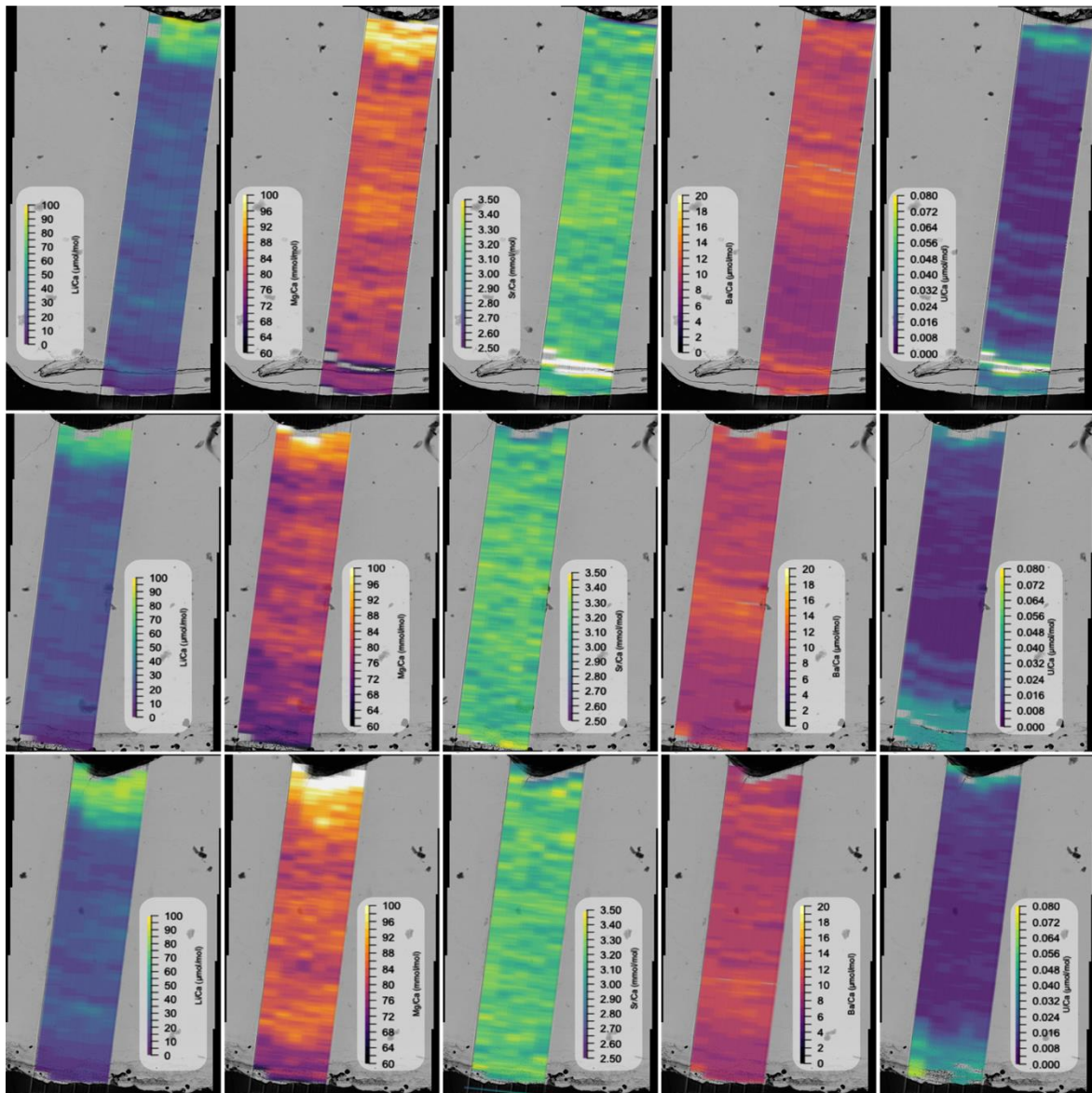
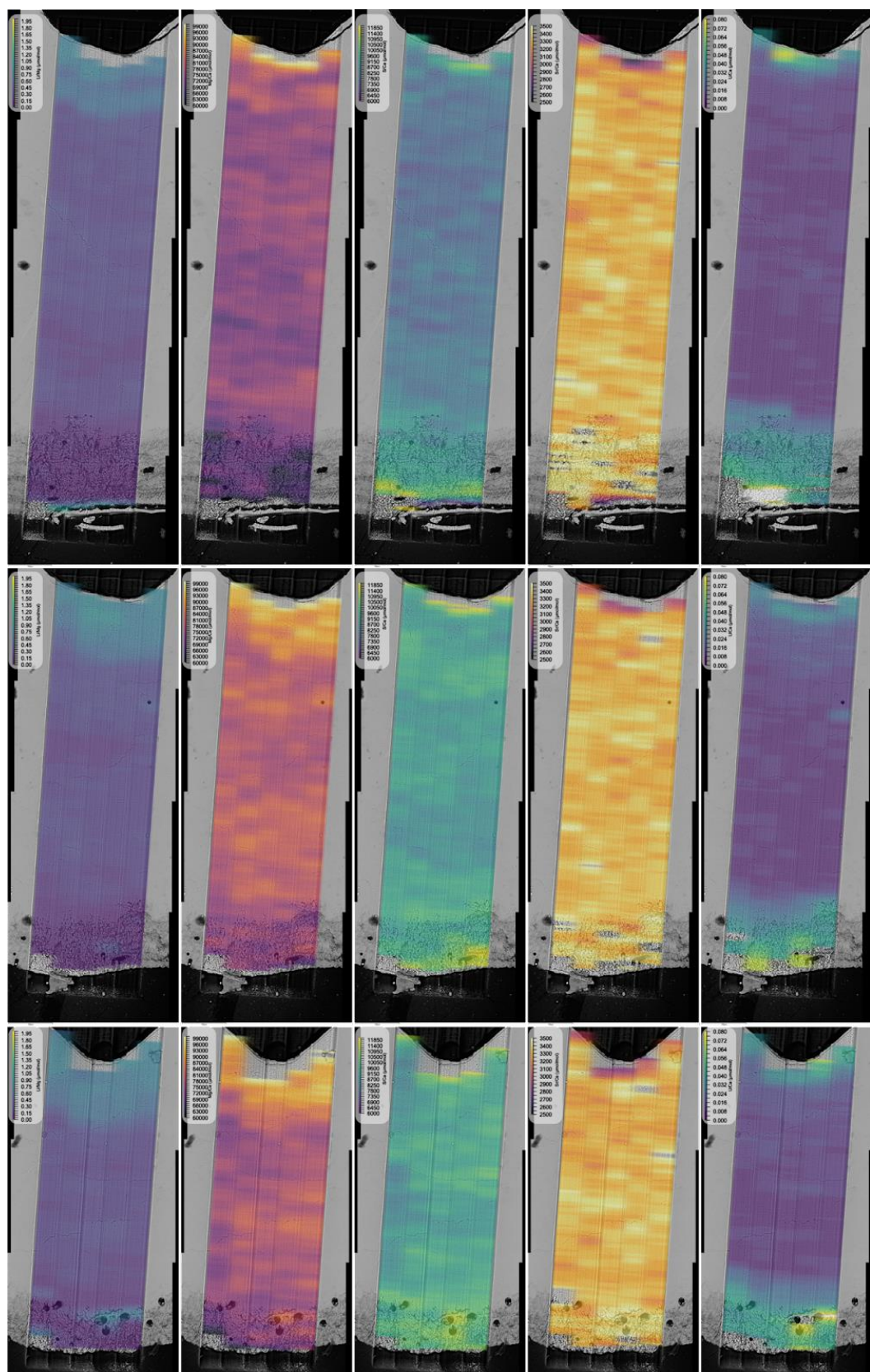


Figure 4.1(d)



#### **4.4.2 Intra-individual E/Ca variability and reproducibility**

Frequency distributions of skeletal elements in *Keratoisis* sp. from Baffin Bay (Figure 4.2) reveal that all elements, with the exception of Mg/Ca, exhibit overlapping distributions between internodes. Three out of the four colonies exhibited greatest variance in element ratios in the basal internode. Overall, I find a reproducible positive covariance between Mg/Ca and Li/Ca within all colonies ( $p < 0.001$ ), with monotonic correlation scores (range, 0.226 – 0.857 in Spearman’s rank). Sr/Ca and U/Ca exhibit a weak negative covariance (Spearman’s rank, range: -0.057 to -0.281,  $p < 0.001$ ), although this is not present in one colony (Figure 4.2d) and the third internode of two other colonies (Figure 4.2a,c). Ba/Ca exhibits a consistent positive co-variance within all colonies and individual internodes with Li/Mg ( $p < 0.001$ ; Spearman’s rank 0.176–0.578) and Li/Ca ( $p < 0.001$ , Spearman’s rank 0.171–0.549) but not Mg/Ca, Sr/Ca or U/Ca.

#### **4.4.3 Inter-individual E/Ca variability and reproducibility**

I find a decrease in values with increasing distance from the central axis across all corals and their internodes for Li/Ca and Mg/Ca (Li/Ca: OLS slope range -0.46 to -0.81,  $R^2$  range, 0.21 – 0.68, all  $p < 0.001$ ; Mg/Ca: OLS slope range -0.2 to -0.81,  $R^2$  range, 0.04 – 0.66, all  $p < 0.001$ ; Table 4.3), with both ratios exhibiting respectively large ranges (Li/Ca: 4.54 – 113.23  $\mu\text{mol/mol}$ ; Mg/Ca: 41.03 – 126.69  $\text{mmol/mol}$ ) but different coefficients of variation (Li/Ca: 9 – 19 %; Mg/Ca: 2 – 4 %). In colony #23-6, mean ( $\pm$  s.e.) Mg/Ca in the basal internode is much lower ( $71.27 \pm 0.96 \text{ mmol/mol}$ ) than the other replicates (#23-1:  $80.42 \pm 1.23 \text{ mmol/mol}$ ; #23-10:  $81.90 \pm 1.15 \text{ mmol/mol}$ ; #23-16:  $74.31 \pm 1.10 \text{ mmol/mol}$ ), with weaker trends across each internode (OLS slope range, -0.2 to -0.35) and a poor level of explained variance ( $R^2$  range, 0.04 – 0.12). I found low coefficients of variation in raw Sr/Ca values across all colonies and a positive trend (increasing values with distance from central axis;  $p < 0.01$  –  $<0.001$ ; Table 4.3c), albeit with a much lower amount of variance explained (median  $R^2$  : 0.15) relative to that observed for Li/Ca and Mg/Ca (Li/Ca: median  $R^2$ , 0.51; Mg/Ca: median  $R^2$ , 0.53). For U/Ca, I observed positive trends in two out of the four colonies, with the strongest trends within the first two internodes (OLS slope range: 0.25 to 0.41,  $p < 0.001$ ;  $R^2$  range,  $< 0.01$  – 0.17) albeit with high coefficients of variation (13 – 21 %; Table 4.3d)

Figure 4.2(a)

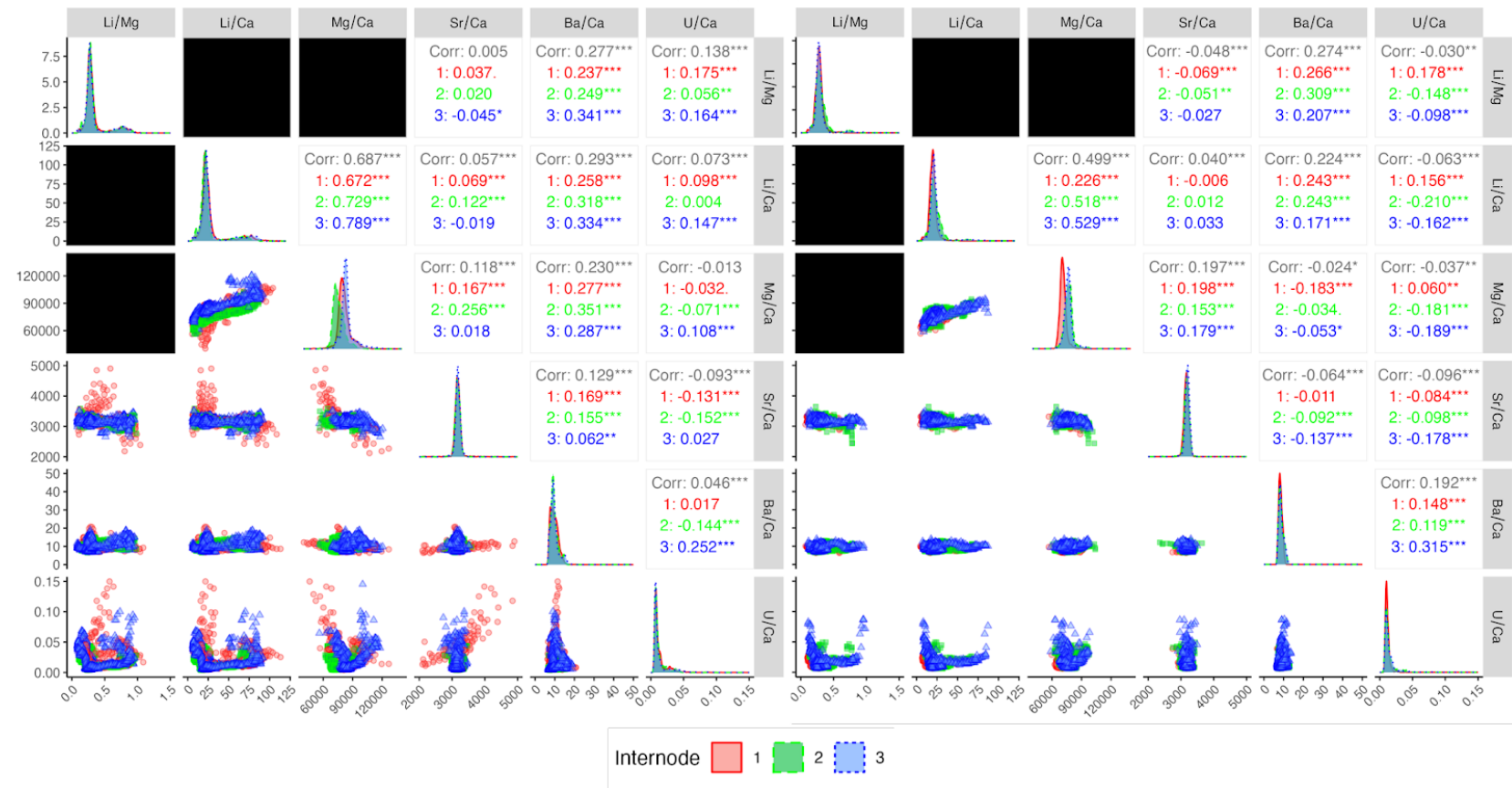


Figure 4.2 | Covariance (Spearman's Rank; top right subplots) and distribution (bottom left subplots) of Li/Mg, Li/Ca, Mg/Ca, Sr/Ca, Ba/Ca and U/Ca ratios within the basal internode (red), second internode (green) and third internode (blue) of *Keratoisis* sp. colonies (a) #23-1 (left) and #23-6 (right), and (b) #23-10 (left) and #23-16 (right).

Figure 4.2(b)

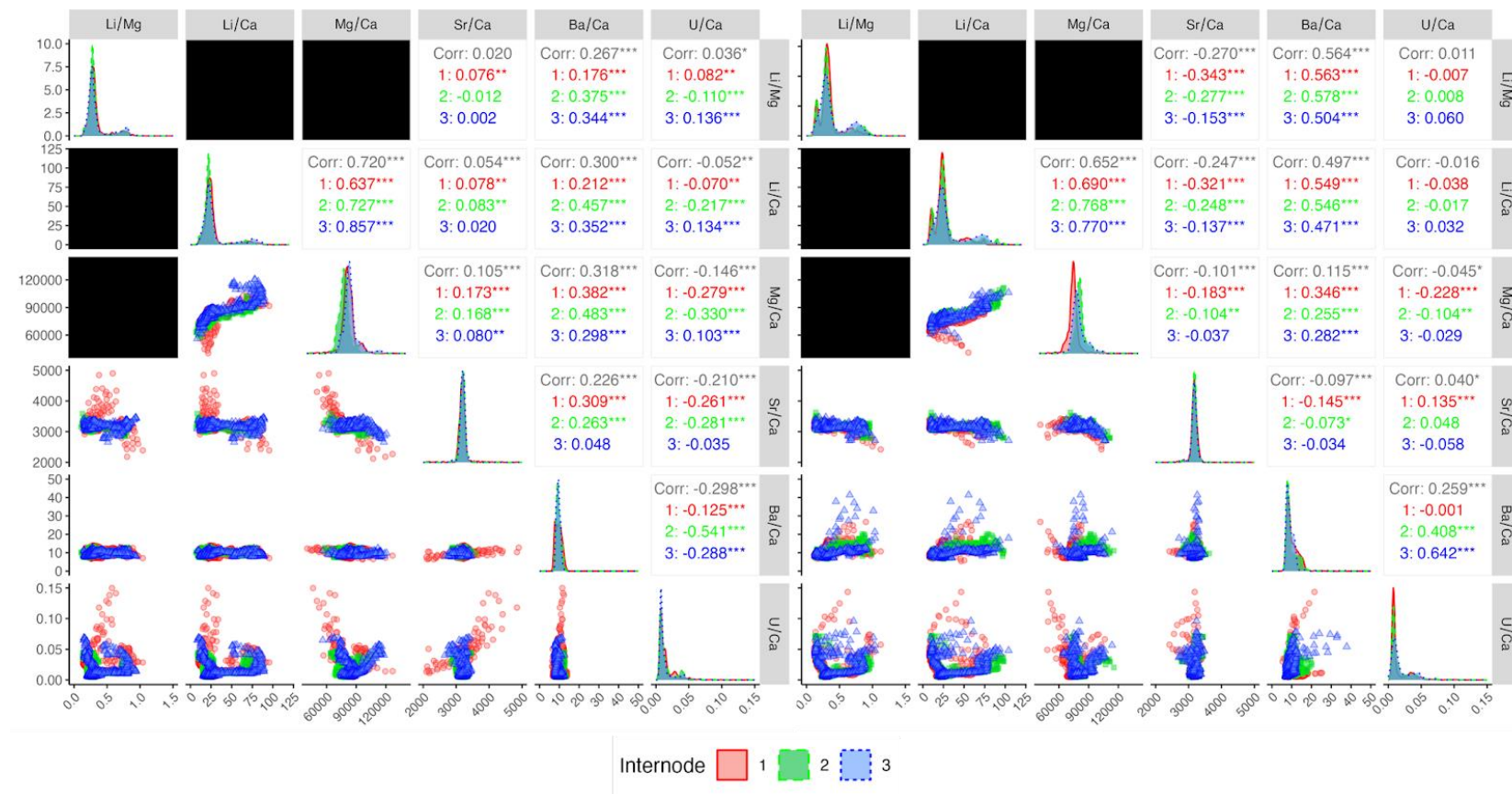


Table 4.3 | Summary table of mean element ratios ( $\pm 2$  standard deviations) measured in each internode across all *Keratoisis* sp. colonies. Coefficient of variation (CV) and range of values are also presented. Significance of OLS regression: \*,  $p<0.05$ ; \*\*,  $p<0.01$ ; \*\*\*,  $p<0.001$

<i>E/Ca</i>		<i>Specimen</i>	<i>Internode</i>	<i>Mean <math>\pm 2sd</math></i>	<i>CV</i>	<i>Range</i>	<i>Slope</i>	<i>Significance</i>	<i>R</i> <sup>2</sup>
<b>Li/Ca</b>	$\mu\text{mol/mol}$	#23-1	1	$30.73 \pm$ 12%	12%	113.23—	<b>-0.73</b>	***	<b>0.54</b>
			2	$27.93 \pm$ 9%	9%	86.55—6.05	<b>-0.75</b>	***	<b>0.57</b>
			3	$30.02 \pm$ 9%	9%	91.58—5.45	<b>-0.73</b>	***	<b>0.53</b>
		#23-10	1	$27.6 \pm 7.06$	12%	95.60—9.24	<b>-0.61</b>	***	<b>0.37</b>
			2	$25.86 \pm$ 10%	10%	79.59—6.69	<b>-0.66</b>	***	<b>0.44</b>
			3	$31.64 \pm 7.6$	12%	89.48—8.22	<b>-0.73</b>	***	<b>0.53</b>
		#23-16	1	$28.01 \pm 6.3$	11%	76.24—7.68	<b>-0.63</b>	***	<b>0.4</b>
			2	$31.77 \pm$ 12%	12%	98.24—9.67	<b>-0.81</b>	***	<b>0.66</b>
			3	$35.81 \pm$ 19%	19%	104.04—	<b>-0.83</b>	***	<b>0.68</b>
		#23-6	1	$19.95 \pm$ 12%	12%	50.24—4.54	<b>-0.69</b>	***	<b>0.48</b>
			2	$24.17 \pm$ 11%	11%	69.54—9.57	<b>-0.5</b>	***	<b>0.25</b>
			3	$23.25 \pm$ 11%	11%	87.07—7.38	<b>-0.46</b>	***	<b>0.21</b>
<b>Mg/Ca</b>	$\text{mmol/mol}$	#23-1	1	$80.42 \pm$ 3%	3%	112.94—	<b>-0.73</b>	***	<b>0.53</b>
			2	$74.23 \pm$ 2%	2%	98.61—	<b>-0.72</b>	***	<b>0.52</b>
			3	$84.55 \pm 3.7$	2%	111.69—	<b>-0.64</b>	***	<b>0.4</b>
		#23-10	1	$81.9 \pm 5.14$	3%	126.69—	<b>-0.75</b>	***	<b>0.56</b>
			2	$78.13 \pm$ 3%	3%	109.32—	<b>0.75</b>	***	<b>0.56</b>
			3	$85.47 \pm$ 3%	3%	120.54—	<b>-0.69</b>	***	<b>0.47</b>
		#23-16	1	$74.31 \pm$ 3%	3%	106.66—	<b>-0.74</b>	***	<b>0.55</b>
			2	$82.39 \pm$ 3%	3%	115.48—	<b>-0.74</b>	***	<b>0.55</b>
			3	$81.24 \pm$ 4%	4%	113.64—	<b>-0.81</b>	***	<b>0.66</b>
		#23-6	1	$71.27 \pm$ 3%	3%	91.30—	<b>-0.21</b>	***	<b>0.04</b>
			2	$77.06 \pm$ 3%	3%	103.91—	<b>-0.2</b>	***	<b>0.04</b>
			3	$76.82 \pm$ 3%	3%	98.12—	<b>-0.35</b>	***	<b>0.12</b>
<b>Ba/Ca</b>	$\mu\text{mol/mol}$	#23-1	1	$9.97 \pm 1.42$	7%	20.76—6.83			
			2	$10.01 \pm$ 7%	7%	16.2—6.56			
			3	$10.05 \pm$ 6%	6%	19.02—6.7			
		#23-10	1	$9.68 \pm 1.11$	6%	14.01—6.33			
			2	$9.65 \pm 1.1$	6%	13.27—7.41			
			3	$9.46 \pm 1.09$	6%	12.46—7.66			
		#23-16	1	$10.36 \pm 1.8$	8%	26.73—5.4			
			2	$9.87 \pm 1.52$	7%	20.16—6.58			
			3	$9.74 \pm 2.78$	11%	41.4—6.84			
		#23-6	1	$8.41 \pm 0.73$	4%	11.3—6.28			
			2	$8.78 \pm 0.88$	5%	13.02—6.51			
			3	$8.83 \pm 0.95$	5%	13.99—6.63			
<b>Sr/Ca</b>	$\text{mmol/mol}$	#23-1	1	$3.15 \pm 0.11$	2%	3.57—2.73	<b>0.14</b>	*	<b>0.02</b>
			2	$3.15 \pm 0.11$	2%	3.50—2.77	-0.04		<0.01
			3	$3.15 \pm 0.11$	2%	3.51—2.66	<b>0.32</b>	***	<b>0.1</b>
		#23-10	1	$3.2 \pm 0.17$	3%	5.78—1.67	<b>0.17</b>	**	<b>0.03</b>

		2	3.19 ± 0.12	2%	3.59–2.85	<b>0.28</b>	***	<b>0.08</b>
		3	3.18 ± 0.12	2%	3.47–2.66	<b>0.32</b>	***	<b>0.1</b>
	#23-16	1	3.17 ± 0.14	2%	3.42–2.42	<b>0.45</b>	***	<b>0.2</b>
		2	3.18 ± 0.12	2%	3.63–2.79	<b>0.64</b>	***	<b>0.41</b>
		3	3.17 ± 0.14	2%	3.47–2.71	<b>0.58</b>	***	<b>0.33</b>
	#23-6	1	3.16 ± 0.12	2%	3.43–2.74	<b>0.48</b>	***	<b>0.23</b>
		2	3.17 ± 0.13	2%	3.64–2.36	<b>0.52</b>	***	<b>0.27</b>
		3	3.19 ± 0.11	2%	3.49–2.87	<b>0.52</b>	***	<b>0.27</b>
<b>U/Ca</b>	nmol/mol	#23-1	1	11.99 ±	17%	46.02–4.19	0.08	<0.01
			2	10.67 ±	15%	28.98–3.84	0.02	<0.01
			3	14.53 ± 5.2	16%	145.18–	0.09	<0.01
	#23-10	1	16.41 ±	21%	149.8–4.84	<b>0.25</b>	***	<b>0.06</b>
		2	15.48 ±	17%	46.88–4.38	<b>0.41</b>	***	<b>0.17</b>
		3	17.18 ±	18%	68.86–4.4	0.06		<0.01
	#23-16	1	18 ± 7.93	18%	154.65–	<b>0.34</b>	***	<b>0.11</b>
		2	17.9 ± 5.99	18%	71.68–4.56	<b>0.38</b>	***	<b>0.15</b>
		3	20.98 ±	19%	96.01–4.16	<b>0.23</b>	**	<b>0.05</b>
	#23-6	1	11.74 ±	14%	38.92–6.05	-0.02		<0.01
		2	14.02 ±	13%	49.47–6.13	0.06		<0.01
		3	15.13 ±	16%	87.27–5.57	0.07		<0.01

Table 4.4 | Correlation scores (Pearson's) for element ratio patterns after stratigraphic tuning internodes 1 & 2 and internodes 1 & 3 for each colony and their combined mean (bold).

<i>Element ratio</i>	<i>Specimen ID</i>	<i>Internode</i>	<i>Correlation after tuning</i>
Ba/Ca	#23-1	1 & 2	0.953
		1 & 3	0.956
#23-10		1 & 2	0.840
		1 & 3	0.713
#23-16		1 & 2	0.971
		1 & 3	0.614
#23-6		1 & 2	0.750
		1 & 3	0.903
<b>Mean</b>		<b>1 &amp; 2</b>	<b>0.879</b>
		<b>1 &amp; 3</b>	<b>0.797</b>
Li/Ca	#23-1	1 & 2	0.923
		1 & 3	0.869
#23-10		1 & 2	0.964
		1 & 3	0.113
#23-16		1 & 2	0.660
		1 & 3	0.410
#23-6		1 & 2	0.618
		1 & 3	0.258
<b>Mean</b>		<b>1 &amp; 2</b>	<b>0.791</b>
		<b>1 &amp; 3</b>	<b>0.413</b>
Li/Mg	#23-1	1 & 2	0.907
		1 & 3	0.854
#23-10		1 & 2	0.943

		1 & 3	0.042
	#23-16	1 & 2	0.438
		1 & 3	0.123
	#23-6	1 & 2	0.610
		1 & 3	0.320
	<b>Mean</b>	<b>1 &amp; 2</b>	<b>0.725</b>
		<b>1 &amp; 3</b>	<b>0.335</b>
<hr/>			
Mg/Ca	#23-1	1 & 2	0.895
		1 & 3	0.829
	#23-10	1 & 2	0.814
		1 & 3	0.029
	#23-16	1 & 2	0.623
		1 & 3	0.553
	#23-6	1 & 2	0.513
		1 & 3	0.296
	<b>Mean</b>	<b>1 &amp; 2</b>	<b>0.711</b>
		<b>1 &amp; 3</b>	<b>0.427</b>
<hr/>			
Sr/Ca	#23-1	1 & 2	0.022
		1 & 3	0.275
	#23-10	1 & 2	-0.012
		1 & 3	0.489
	#23-16	1 & 2	-0.208
		1 & 3	0.032
	#23-6	1 & 2	0.343
		1 & 3	0.237
	<b>Mean</b>	<b>1 &amp; 2</b>	<b>0.036</b>
		<b>1 &amp; 3</b>	<b>0.258</b>
<hr/>			
U/Ca	#23-1	1 & 2	0.811
		1 & 3	0.568
	#23-10	1 & 2	0.680
		1 & 3	0.624
	#23-16	1 & 2	0.913
		1 & 3	0.763
	#23-6	1 & 2	0.834
		1 & 3	0.786
	<b>Mean</b>	<b>1 &amp; 2</b>	<b>0.810</b>
		<b>1 &amp; 3</b>	<b>0.685</b>

With the exception of Sr/Ca, stratigraphic tuning using the Ba/Ca-based age model revealed strong synchronicity in element signals between the basal and adjacent internodes of *Keratoisis* sp. (mean correlation score  $\pm$  s.d;  $0.838 \pm 0.132$ ,  $n = 12$ ; Appendix C Figure S7). However, the magnitude of reproducibility widely differed between the colonies and element signals were generally reproduced better between the basal and second internode than the basal and third internode (Table 4.4). Specifically, element signal pattern synchronicity (mean correlation score  $\pm$  s.d,  $n = 12$ ) was greatest in U/Ca ( $0.747 \pm 0.115$ ) and worst in Sr/Ca ( $0.147 \pm 0.227$ ), with Li/Ca, Mg/Ca and Li/Mg all exhibiting similar correlation strengths ( $0.602 \pm 0.317$ ,  $0.569 \pm 0.294$  and  $0.530 \pm 0.357$ , respectively).

#### 4.4.4 Multi-element, multi-species paleoenvironment calibrations

I find a high degree of similarity (+- 1 s.e.) in the gradient and intercept values in my regressions (Table 5). Here, consistent with previous studies, I present ordinary least squares (OLS) regression calibrations but it is important to note that I find, in practice, that outcomes are not regression method dependent. I find significant linear temperature dependency in aragonitic, high-Mg calcite and Octocoral Mg/Ca, Sr/Ca, U/Ca and Ba/Ca (Figure 4.3; Table 4.5a:  $p = 0.001$ ), whilst Li/Mg demonstrates an exponential relationship with temperature in both aragonitic and high-Mg calcitic taxa and a linear relationship in Octocorals (Figure 4.3a; Table 4.5b). Due to the inherent limitations of nonlinear models, I encountered difficulties in determining the variance explained by temperature for aragonitic and high-Mg calcitic Li/Mg (Spiess & Neumeyer, 2010).

Nevertheless, my calibration constant aligns with previous studies, providing consistency in my findings (Table 4.5b; Montagna et al. 2014; Stewart et al. 2020). Ranking Octocoral E/Ca temperature relationships variance explained ( $R^2$ ) alongside proxy sensitivity (element unit change per  $^{\circ}\text{C}$ ) from highest to lowest gives an order of  $\text{Mg/Ca} > \text{U/Ca} > \text{Ba/Ca} > \text{Li/Mg} > \text{Sr/U} > \text{Sr/Ca}$  (Table 4.5a), indicating that Mg/Ca and U/Ca are strong paleothermometry prospects in high-Mg calcitic Octocorals.

The barium partition coefficient ( $D_{\text{Ba}}$ ) is negatively correlated with temperature in aragonitic corals with evidence of a linear correlation in high-Mg calcitic Styelasteridae, though uncertainty ( $\pm 2$  s.d.) is high for both the intercept ( $\pm 23.6$ ) and gradient ( $\pm 396$ ). I did not have enough data to calculate the relationship between  $D_{\text{Ba}}$  and temperature in Octocorals, and  $D_{\text{Ba}}$  varied across the four *Keratoisis* colonies examined here ( $\pm 0.1$  within colonies,  $\pm 0.4$  across colonies).  $\text{Ba/Ca}-[\text{Ba}]_{\text{sw}}$  demonstrates a linear relationship across all taxa and mineralogies (Table 4.5a; Figure 4.3b) with the steepest  $[\text{Ba}]_{\text{sw}}-\text{Ba/Ca}$  regression (forced through a zero-intercept) exhibited in high-Mg Styelasteridae ( $[\text{Ba}]_{\text{sw}} = 7.260 (\pm 0.169) * \text{Ba/Ca}$ ,  $R^2 = 0.99$ ). Although I display data from mixed mineralogy corals, they were not used in any of the regression analyses and, for simplicity, I only compare to published equations with the highest degree of variance explained ( $R^2 > 0.6$ , Table 4.5; full listing in Appendix C Table S8). In brief, the literature search revealed no previous Sr/U, U/Ca, Ba/Ca and  $D_{\text{Ba}}$  temperature calibrations for high-Mg calcitic corals, with Mg/Ca and Sr/Ca temperature calibrations only found for high-Mg coralline algae.

Figure 4.3 (a)

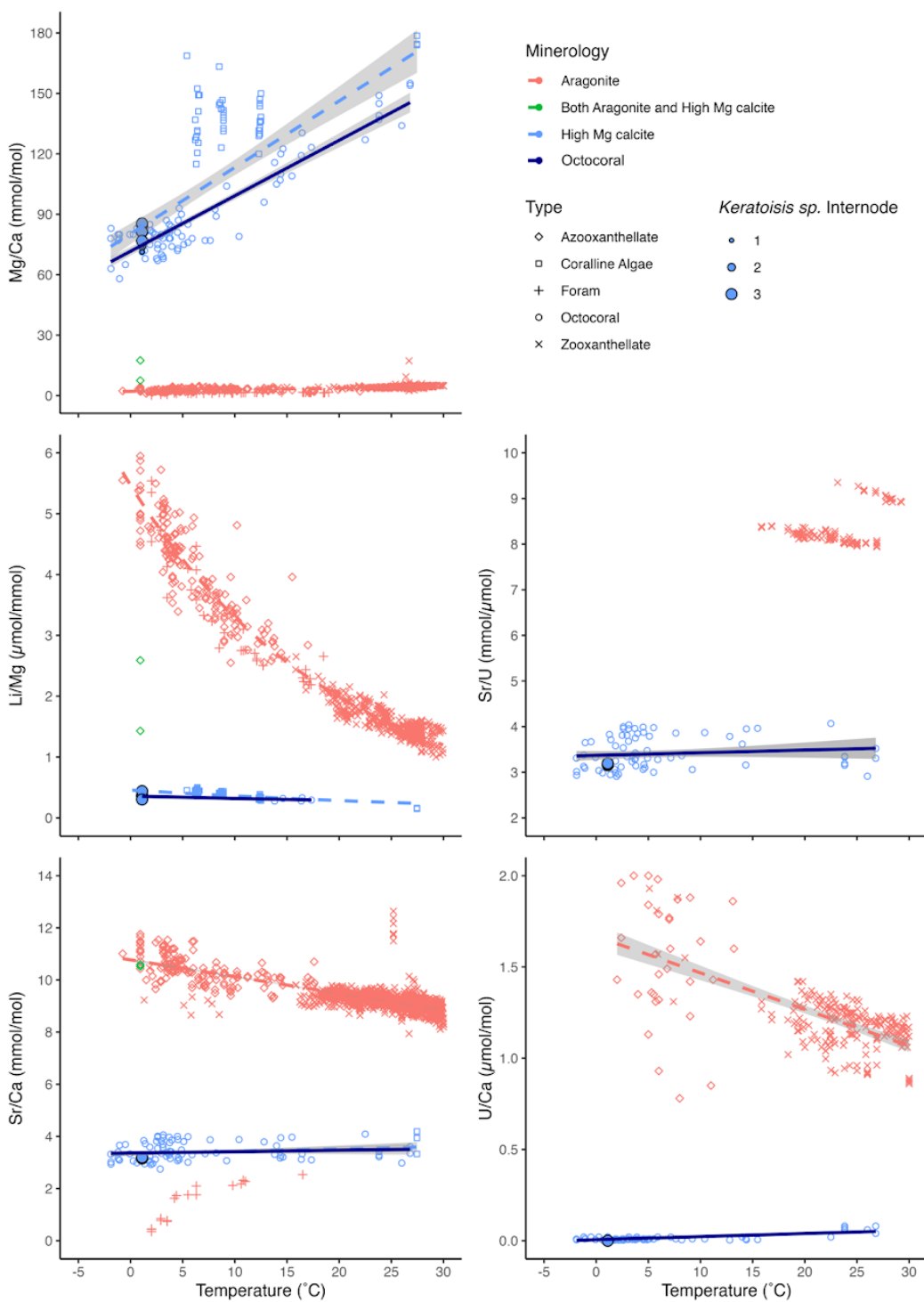


Figure 4.3 | Compiled published (a) Mg/Ca-T, Li/Mg-T, Sr/Ca-T, Sr/U-T and U/Ca-T calibration data and (b) Ba/Ca-T, D<sub>Ba</sub>-T and [Ba]<sub>coral</sub>-[Ba]<sub>sw</sub> calibration data for aragonitic (red), high-Mg calcitic (blue) mixed mineralogy (green) corals and Corallinales compared to Octocorallia (dark blue). Full element compilation datasets adjusted for interlaboratory offsets (where standard data are available). Mean coral replicates are presented in Appendix C Figure S6.

Figure 4.3(b)

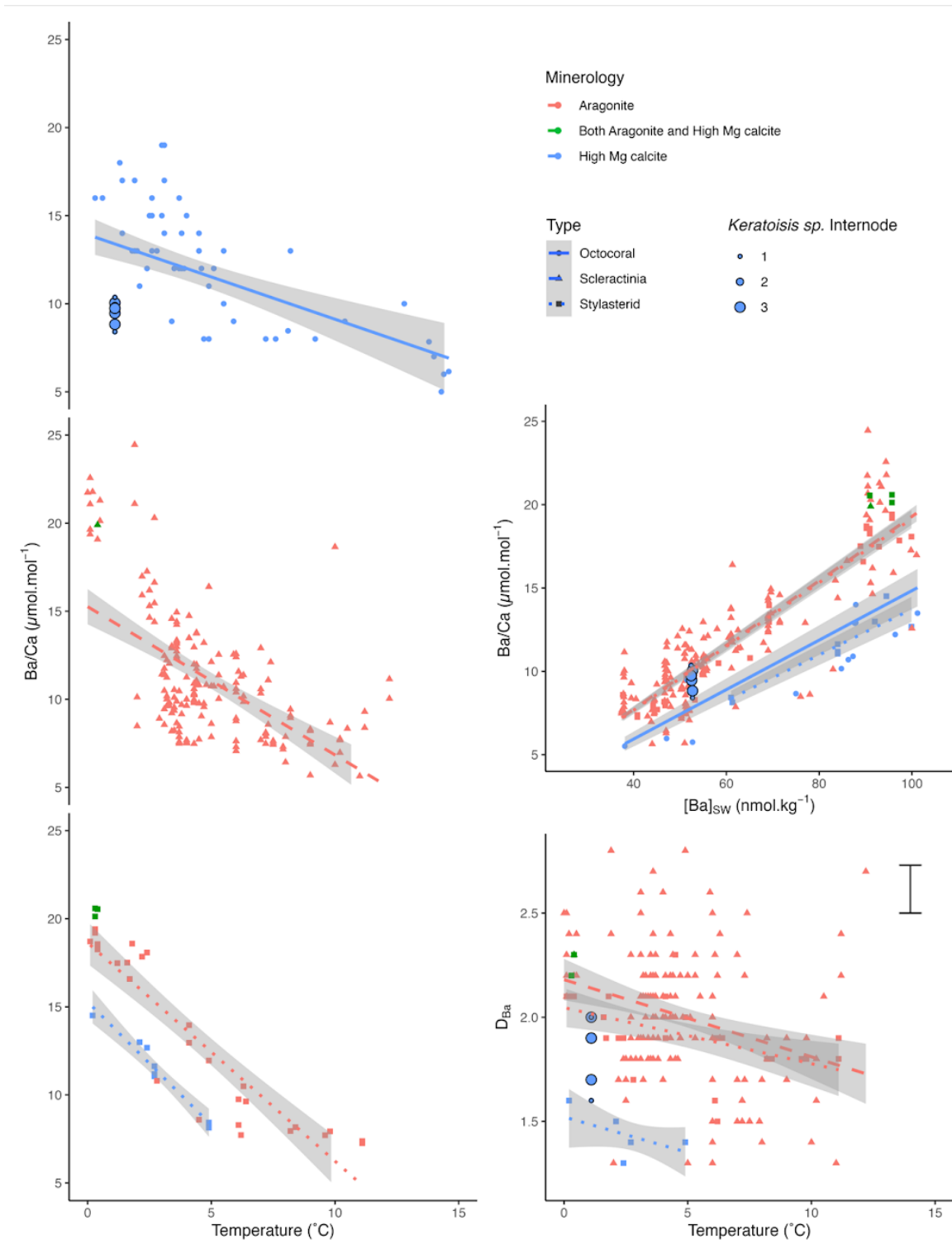


Table 4.5 | (a) Linear and (b) Non-linear calibration Ordinary Least Squares (OLS) and Reduced Major Axis (RMA) equations based on values extracted from the literature and published calibrations with >60 % variance explained (bold). All published equations extracted from the literature can be found in Appendix C.

Table 4.5 (a)

Relationship	x unit	y unit	Mineralogy	Taxon Group	Source	n	r	R <sup>2</sup>	Type of regression	p	Gradient	± 2SD	Intercept	± 2SD
[Ba]SW ~ Ba/Ca + 0	µmol/mol	nmol.kg	Aragonite	<i>Scleractinia</i>	This study	172		0.97	OLS	0.001	5.040	0.065		
				<i>Stylasteridae</i>	This study	28		0.99	OLS	0.001	5.190	0.073		
			High-Mg calcite	Octocorallia	This study	45		0.97	OLS	0.001	6.530	0.237		
				<i>Stylasteridae</i>	This study	8		0.99	OLS	0.001	7.260	0.169		
			Aragonite	<i>Scleractinia</i>	Anagnostou et al. 2011	17		0.60	OLS		1.400	0.300	0	2
Temperature ~ Ba/Ca	µmol/mol	°C	Aragonite	<i>Scleractinia</i>	This study	174	-0.58	0.34	OLS	0.001	-0.394	0.082	9.272	0.974
									RMA	0.001	-0.690	0.163	12.590	1.464
				<i>Stylasteridae</i>	This study	28	-0.92	0.85	OLS	0.001	-0.682	0.118	13.383	1.649
									RMA	0.001	-0.729	0.135	14.005	1.561
			High-Mg calcite	Octocorallia	This study	91	-0.73	0.54	OLS	0.001	-1.332	0.260	21.082	3.105
									RMA	0.001	-1.863	0.409	27.056	3.706
				<i>Stylasteridae</i>	This study	8	-0.98	0.95	OLS	0.001	-0.680	0.154	10.525	1.770
									RMA	0.001	-0.696	0.177	10.709	1.621
Temperature ~ DBa	-	°C	Aragonite	<i>Scleractinia</i>	This study	172	-0.22	0.05	OLS	0.004	-1.682	1.110	8.173	2.245
									RMA	0.004	-12.163	17.925	29.086	10.849
				<i>Stylasteridae</i>	This study	28	-0.55	0.30	OLS	0.003	-11.121	6.863	25.818	13.288
									RMA	0.003	-27.149	35.099	56.730	22.137

## Inter- and intra-colony elemental systematics of a cold-water bamboo coral mediate deep-sea temperature and nutrient proxies

	High-Mg calcite	<i>Stylasteridae</i>	This study	8	-0.59	0.34	OLS	0.051	-10.091	13.904	17.205	19.846		
							RMA	0.041	-18.345	395.398	28.966	23.548		
<hr/>														
Temperature ~ Mg/Ca	mmol/mol	°C	Aragonite	All taxon	This study	576	0.67	0.45	OLS	0.001	5.419	0.487	-1.862	1.816
							RMA	0.001	11.581	0.957	-23.500	4.004		
	High-Mg calcite	All taxon	This study	93	0.93	0.87	OLS	0.001	0.317	0.026	-22.065	2.361		
							RMA	0.001	0.345	0.027	-24.467	2.615		
		Octocorallia	This study	91	0.93	0.87	OLS	0.001	0.316	0.026	-21.881	2.336		
							RMA	0.001	0.342	0.027	-24.173	2.576		
	High-Mg calcite	Corallinales	Hetzinger et al. 2018	164	0.88		OLS	0.001	0.345	0.015	-41.834	2.163		
Temperature ~ Li/Mg	μmol/mmol	°C	High-Mg calcite	Octocorallia	This study	17	-0.55	0.30	OLS	0.008	-82.140	68.650	33.180	23.410
							RMA	0.008	-201.280	104.020	73.460	210.440		
Temperature ~ Sr/Ca	mmol/mol	°C	Aragonite	All taxon	This study	2013	-0.24	0.06	OLS	0.001	-1.813	0.315	39.509	2.922
							RMA	0.001	-26.228	5.501	264.986	35.916		
	High-Mg calcite	All taxon	This study	92	0.14	0.02	OLS	0.094	3.041	4.540	-4.339	15.440		
							RMA	0.094	25.060	24.324	-78.853	-675.793		
		Octocorallia	This study	90	0.12	0.01	OLS	0.137	2.643	4.662	-2.890	15.900		
							RMA	0.137	28.456	30.297	-90.495	-286.162		
	High-Mg calcite	Corallinales	Kamenos et al. 2008	0.88	0.77		OLS	0.001	3.137	0.166	-2.060	0.730		
Temperature ~ Sr/U	mmol/mol	°C	Aragonite	All taxon	This study	103	0.45	0.20	OLS	0.001	4.106	1.610	-10.980	13.421
							RMA	0.001	8.068	2.790	-43.969	31.770		

	High-Mg calcite	Octocorallia	This study	81	0.13	0.02	OLS	0.121	2.704	4.795	-3.652	16.393		
							RMA	0.121	9.525	16.353	-26.856	99.647		
	Aragonite	All taxon	Ross et al. 2019	33	0.89	OLS	0.001	-0.035		8.920				
Temperature ~ U/Ca	µmol/mol	°C	Aragonite	All taxon	This study	245	-0.72	0.52	OLS	0.001	-18.913	2.297	45.241	3.022
							RMA	0.001	-32.525	4.414	62.650	4.579		
	High-Mg calcite	Octocorallia	This study	81	0.75	0.56	OLS	0.001	334.277	66.002	0.500	1.471		
							RMA	0.001	472.536	83.521	-1.587	1.612		
	Aragonite	<i>Porites cylindrica</i>	Armid et al. 2011			0.78	OLS		-0.021	0.002	1.488	0.048		

Table 4.5 (b)

Relationship	x unit	y unit	Mineralogy	Taxon Group	Source	n	a	p	± SE	b	p	± SE
Li/Mg ~ a*e <sup>[b*Temperature]</sup>	°C	µmol/mmol	Aragonite	All taxon	This study	597	5.469	0.001	0.030	-0.051	0.001	0.000
			High Mg calcite	All taxon	This study	59	0.458	0.001	0.019	-0.046	0.001	0.005
			Aragonite	All taxon	Montagna et al. 2014	49	5.41			-0.05		0.002
			High Mg calcite	All taxon	Steward et al. 2020	49	0.63		0.02	-0.05		0.002

#### 4.4.5 Paleo-environment reconstructions

##### 4.4.5.1 Temperature

As Mg/Ca demonstrates consistent intra-individual patterns (Table 4.4) and the strongest correlation and sensitivity to temperature ( $r = 0.93$ ,  $p < 0.001$ ,  $R^2 = 0.87$ ;  $0.316 \pm 0.026 \text{ } ^\circ\text{C}/\text{mmol/mol}$ ; Table 4.5a; Figure 4.3), I focus on temperature reconstructed using the *Keratoisis*-specific age model, the Octocoral-derived calibration equation and the stratigraphically tuned Mg/Ca signals. Overall, the Mg/Ca proxy demonstrates significant sub-seasonal, seasonal, annual and interannual variation within all colonies (Figure 4.4a). Mean predicted temperature (solid line) timeseries are offset by up to  $2 \text{ } ^\circ\text{C}$  within internodes from the same individual and up to  $5 \text{ } ^\circ\text{C}$  among individuals (colonies). However, in colony #23-6 (and arguably #23-16 and #23-1) the mean reconstructed temperature timeseries overlaps the range of *in-situ* measurements from previous records for deep-water Baffin Bay ( $0.39 \text{ } ^\circ\text{C}$  to  $1.36 \text{ } ^\circ\text{C}$ ). There are also synchronised multiannual cycles in reconstructed temperature between 3 out of the 4 colonies. Assuming each internode is of equal importance within a colony, leveraging each replicate timeseries (averaging) reduced the uncertainty (95% CI's) of reconstructed temperature from  $\pm 4.25 \text{ } ^\circ\text{C}$  (range:  $3.99 - 4.52 \text{ } ^\circ\text{C}$ ) to  $\pm 1.92 \text{ } ^\circ\text{C}$  (range:  $0.02 - 5.91 \text{ } ^\circ\text{C}$ ) when seasonally interpolated and  $\pm 4.25 \text{ } ^\circ\text{C}$  (range:  $3.99 - 4.52 \text{ } ^\circ\text{C}$ ) to  $\pm 2.20 \text{ } ^\circ\text{C}$  (range:  $< 0.01 - 4.63 \text{ } ^\circ\text{C}$ ) when annual interpolated.

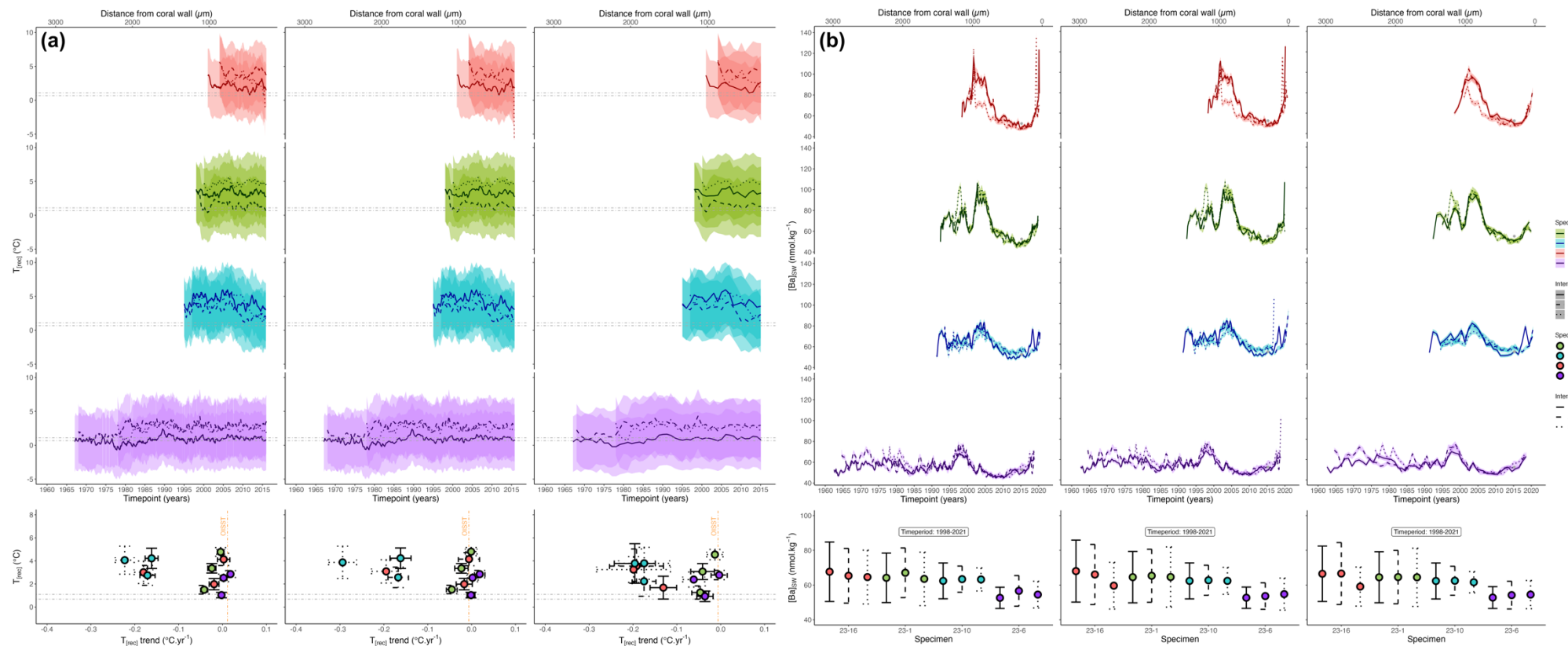


Figure 4.4 | Reconstructions of past (a) temperatures derived from Mg/Ca and (b) seawater barium derived from Ba/Ca, generated for different colonies (**colour**) and internodes (**linetype**) and evaluated without data interpolation (**left column**), with seasonal interpolation (**middle column**), and with annual interpolation (**right column**). *In-situ* temperature measurements taken at nearby locations (**grey points** - K. Azestu-Scott, pers. comm., May 31, 2022; Zweng & Münchow, 2006) and the average trend of sea surface temperatures (**dashed yellow line**, Reynolds et al. 2002) are displayed. The bottom row of each figure shows the reconstructed environmental conditions during the time period shared by all *Keratoisis* sp. colonies.

Table 4.6 | Temperature trends (negative indicative of cooling, positive indicative of warming) for Mg/Ca-T reconstruction between timeperiod common to *Keratoisis* sp. colonies (2003-2016) obtained from Ordinary Least Squares (OLS) and Reduced Major Axis (RMA) regressions on uninterpolated, seasonally interpolated and annual interpolated temperature data. Significant regressions are highlighted in bold.

Relationship	x unit	y unit	Interpolation	Specimen ID	Internode	n	r	R <sup>2</sup>	Regression Type	p	Gradient	± 2SD
Temperature ~ Time	Year	°C	Uninterpolated	#23-1	1	130	<b>-0.22</b>	0.0	OLS	<b>0.007</b>	-0.02	0.02
						130	<b>-0.22</b>	0.0	RMA	<b>0.007</b>	-0.06	0.05
					2	140	<b>-0.40</b>	0.2	OLS	<b>0.001</b>	-0.04	0.02
						140	<b>-0.40</b>	0.2	RMA	<b>0.001</b>	-0.08	0.03
					3	132	-0.04	0.0	OLS	0.315	0.00	0.02
						132	-0.04	0.0	RMA	0.315	-0.01	0.05
				#23-10	1	130	<b>-0.69</b>	0.5	OLS	<b>0.001</b>	-0.16	0.03
						130	<b>-0.69</b>	0.5	RMA	<b>0.001</b>	-0.23	0.05
					2	101	<b>-0.70</b>	0.5	OLS	<b>0.001</b>	-0.17	0.03
						101	<b>-0.70</b>	0.5	RMA	<b>0.001</b>	-0.24	0.05
					3	91	<b>-0.74</b>	0.5	OLS	<b>0.001</b>	-0.22	0.04
						91	<b>-0.74</b>	0.5	RMA	<b>0.001</b>	-0.29	0.06
				#23-16	1	132	-0.15	0.0	OLS	0.051	-0.02	0.02
						132	-0.15	0.0	RMA	0.051	-0.04	0.04
					2	109	0.02	0.0	OLS	0.415	0.00	0.03
						109	0.02	0.0	RMA	0.415	0.00	0.05
					3	78	-0.17	0.0	OLS	0.064	-0.04	0.05
						78	-0.17	0.0	RMA	0.064	-0.08	0.13
				#23-6	1	129	-0.04	0.0	OLS	0.308	0.00	0.01
						129	-0.04	0.0	RMA	0.308	-0.01	0.04
					2	176	<b>0.25</b>	0.1	OLS	<b>0.001</b>	0.02	0.01
						176	<b>0.25</b>	0.1	RMA	<b>0.001</b>	0.02	0.01
					3	116	0.03	0.0	OLS	0.383	0.00	0.02
						116	0.03	0.0	RMA	0.383	0.01	0.05

Seasonal	#23-1	1	52	-0.21	0.0	OLS	0.071	-0.02	0.03
			52	-0.21	0.0	RMA	0.071	-0.07	0.15
		2	52	<b>-0.46</b>	<b>0.2</b>	OLS	<b>0.001</b>	<b>-0.05</b>	<b>0.02</b>
			52	<b>-0.46</b>	<b>0.2</b>	RMA	<b>0.001</b>	<b>-0.08</b>	<b>0.05</b>
		3	52	-0.01	0.0	OLS	0.462	0.00	0.03
			52	-0.01	0.0	RMA	0.462	0.00	0.14
	#23-10	1	52	<b>-0.69</b>	<b>0.5</b>	OLS	<b>0.001</b>	<b>-0.16</b>	<b>0.05</b>
			52	<b>-0.69</b>	<b>0.5</b>	RMA	<b>0.001</b>	<b>-0.23</b>	<b>0.08</b>
		2	52	<b>-0.71</b>	<b>0.5</b>	OLS	<b>0.001</b>	<b>-0.17</b>	<b>0.05</b>
			52	<b>-0.71</b>	<b>0.5</b>	RMA	<b>0.001</b>	<b>-0.23</b>	<b>0.07</b>
		3	52	<b>-0.79</b>	<b>0.6</b>	OLS	<b>0.001</b>	<b>-0.29</b>	<b>0.06</b>
			52	<b>-0.79</b>	<b>0.6</b>	RMA	<b>0.001</b>	<b>-0.38</b>	<b>0.09</b>
	#23-16	1	52	-0.13	0.0	OLS	0.184	-0.02	0.04
			52	-0.13	0.0	RMA	0.184	-0.03	0.07
		2	48	-0.04	0.0	OLS	0.415	-0.01	0.05
			48	-0.04	0.0	RMA	0.415	-0.02	0.18
		3	48	-0.13	0.0	OLS	0.176	-0.03	0.07
			48	-0.13	0.0	RMA	0.176	-0.07	0.20
	#23-6	1	52	-0.02	0.0	OLS	0.431	0.00	0.02
			52	-0.02	0.0	RMA	0.431	-0.01	-
		2	52	0.22	0.0	OLS	0.055	0.02	0.02
			52	0.22	0.0	RMA	0.055	0.04	0.05
		3	52	0.02	0.0	OLS	0.445	0.00	0.03
			52	0.02	0.0	RMA	0.445	0.01	0.25
Annual	#23-1	1	20	-0.35	0.1	OLS	0.07	-0.04	0.05
			20	-0.35	0.1	RMA	0.07	-0.06	0.11
		2	21	<b>-0.50</b>	<b>0.3</b>	OLS	<b>0.01</b>	<b>-0.05</b>	<b>0.04</b>

			21	<b>-0.50</b>	<b>0.3</b>	RMA	<b>0.01</b>	<b>-0.08</b>	<b>0.10</b>
		3	20	-0.17	0.0	OLS	0.213	-0.01	0.04
			20	-0.17	0.0	RMA	0.213	-0.06	NA
	#23-10	1	21	<b>-0.71</b>	<b>0.5</b>	OLS	<b>0.001</b>	<b>-0.20</b>	<b>0.09</b>
			21	<b>-0.71</b>	<b>0.5</b>	RMA	<b>0.001</b>	<b>-0.24</b>	<b>0.14</b>
		2	21	<b>-0.84</b>	<b>0.7</b>	OLS	<b>0.001</b>	<b>-0.17</b>	<b>0.05</b>
			21	<b>-0.84</b>	<b>0.7</b>	RMA	<b>0.001</b>	<b>-0.20</b>	<b>0.07</b>
		3	17	<b>-0.64</b>	<b>0.4</b>	OLS	<b>0.008</b>	<b>-0.17</b>	<b>0.12</b>
			17	<b>-0.64</b>	<b>0.4</b>	RMA	<b>0.008</b>	<b>-0.27</b>	<b>0.29</b>
	#23-16	1	19	<b>-0.74</b>	<b>0.6</b>	OLS	<b>0.001</b>	<b>-0.13</b>	<b>0.06</b>
			19	<b>-0.74</b>	<b>0.6</b>	RMA	<b>0.001</b>	<b>-0.16</b>	<b>0.09</b>
		2	17	<b>-0.65</b>	<b>0.4</b>	OLS	<b>0.002</b>	<b>-0.19</b>	<b>0.12</b>
			17	<b>-0.65</b>	<b>0.4</b>	RMA	<b>0.002</b>	<b>-0.25</b>	<b>0.20</b>
		3	17	<b>-0.55</b>	<b>0.3</b>	OLS	<b>0.013</b>	<b>-0.12</b>	<b>0.10</b>
			17	<b>-0.55</b>	<b>0.3</b>	RMA	<b>0.013</b>	<b>-0.16</b>	<b>0.18</b>
	#23-6	1	19	<b>-0.44</b>	<b>0.2</b>	OLS	<b>0.037</b>	<b>-0.04</b>	<b>0.04</b>
			19	<b>-0.44</b>	<b>0.2</b>	RMA	<b>0.037</b>	<b>-0.06</b>	<b>0.10</b>
		2	19	-0.05	0.0	OLS	0.44	0.00	0.04
			19	-0.05	0.0	RMA	0.44	-0.01	0.10
		3	19	<b>-0.53</b>	<b>0.3</b>	OLS	<b>0.009</b>	<b>-0.06</b>	<b>0.05</b>
			19	<b>-0.53</b>	<b>0.3</b>	RMA	<b>0.009</b>	<b>-0.10</b>	<b>0.12</b>

Over the period common to all corals (2003 to 2016), I find that Mg/Ca reconstructed deep-water temperatures exhibited subtle, but significant, cooling trends (Table 4.6) though the rate of cooling and mean reconstructed temperature differed across colonies and internodes (Figure 4.4a). Similar to the multi-taxa calibrations previously demonstrated (Table 4.5; Figure 4.3), the gradients of both ordinary least squares (OLS) and reduced major axis (RMA) regressions displayed a notable degree of resemblance. The disparities between the two regression methods were found to be within one standard error, leading us to exclusively refer to OLS regressions for the sake of consistency. I found strong and marginal random effects of interpolation on OLS intercepts ( $T_{[rec]}$  mean; L-ratio = 25.666, d.f. = 1,  $p < 0.0001$ ) and slopes ( $T_{[rec]}$  trend; L-ratio = 2.154, d.f. = 1,  $p = 0.071$ ), respectively, and hence, the random effects were kept in both models. Linear mixed models revealed strong dependency of  $T_{[rec]}$  mean and  $T_{[rec]}$  trend on an interaction between colony and internode ( $T_{[rec]}$  mean: L-ratio = 117.338, d.f. = 6,  $p < 0.0001$ ;  $T_{[rec]}$  trend: L-ratio = 20.63, d.f. = 6,  $p < 0.01$ ; Appendix C model S1 and S2). Investigating the individual effects demonstrated that colony was more important than internode for the  $T_{[rec]}$  trend (Colony: L-ratio = 66.93, d.f. = 9,  $p < 0.0001$ ; Internode: L-ratio = 20.76, d.f. = 8,  $p < 0.01$ ) whilst internode was more important for the  $T_{[rec]}$  mean (Colony: L-ratio = 175.82, d.f. = 9,  $p < 0.0001$ ; Internode: L-ratio = 189.08, d.f. = 8,  $p < 0.0001$ ). Mean  $T_{[rec]}$  (un-interpolated  $\pm$  s.e.) across this time period ranged from  $4.77 \pm 0.03$  to  $1.04 \pm 0.02$  °C (Figure 4.4a). A stronger cooling  $T_{[rec]}$  trend was reconstructed in one colony (23-10;  $-0.22 \pm 0.04$  to  $-0.16 \pm 0.03$  °C.yr $^{-1}$ ) compared to the other three colonies in this study, which all exhibited  $T_{[rec]}$  trends similar to OISST data (dashed vertical yellow line, Figure 4.4a). Mean  $T_{[rec]}$  became more uncertain ( $\pm$  s.e.) as the data was interpolated to longer timeframes (uninterpolated:  $\pm 0.021$  to 0.155; seasonally interpolated:  $\pm 0.034$  to 0.195; annual interpolated:  $\pm 0.093$  to 0.374) with an overall weaker cooling  $T_{[rec]}$  trend when the data was seasonally interpolated.

#### 4.4.5.2 [Ba]<sub>sw</sub>

Using the Ba/Ca<sub>Octocoral</sub>–[Ba]<sub>sw</sub> calibration calculated in Section 3.1.2., I find highly reproducible reconstructions in seawater barium in my *Keratoisis* sp. colonies (Figure 4.4b) with mean uncertainty (95% CI's) of  $\pm 2.24$  nmol.kg $^{-1}$  (range: 1.62–4.94 nmol.kg $^{-1}$ ) and strong sub-seasonal, seasonal and annual variation recorded. A reproducible, multi-year spike in [Ba]<sub>sw</sub> between 2000 and 2005 is observable across three colonies (#23-16, #23-10 and #23-1) with evidence of this event occurring  $\sim$ 2 years earlier in the remaining colony. Over the period common to all colonies (1998–2021), mean [Ba]<sub>sw</sub> was dependent on an interaction between colony and internode (L-ratio = 32.23, d.f. = 6,  $p < 0.0001$ ; Appendix C model S3) with both variables exhibiting a strong independent effect (Colony: L-ratio = 104.14, d.f. = 9,  $p < 0.0001$ ; Internode: L-ratio = 32.98, d.f. =

8,  $p < 0.0001$ ) but I found no influence of interpolation as a random effect ( $L$ -ratio = 0.009, d.f. = 1,  $p = 0.461$ ). Specifically, un-interpolated mean  $[Ba]_{sw}$  ( $\pm$  s.e.) ranged from 52.6 ( $\pm$  0.4) nmol.kg<sup>-1</sup> to 67.7 ( $\pm$  1.2) nmol.kg<sup>-1</sup> across the different colonies. There is no consistent change in mean  $[Ba]_{sw}$  from the basal internode upward, but there is evidence of a decreasing mean  $[Ba]_{sw}$  and reduced variability in  $[Ba]_{sw}$  when moving from the smallest colony (23-16) to the largest (23-6).

## 4.5 Discussion

### 4.5.1 Multi-taxa element analysis

#### 4.5.1.1 Mg/Ca

The cross-study comparison of multi-taxa calibrations demonstrates a strong positive abiotic Mg/Ca temperature relationship in high-Mg calcitic Octocorals found between -2 to 27 °C. Mg/Ca temperature sensitivity is well documented in several gorgonian families (Weinbauer et al. 2000; Sherwood et al. 2005b) albeit with taxon-specific slopes and intercepts (Sinclair et al. 2011; Thresher, 2009). The calibration slope utilised in this study ( $0.316 \pm 0.026$  °C/mmol/mol) is much steeper than previous gorgonian calculations (Thresher et al. 2010, 2016a) and has a tighter distribution of residuals, with 87% of bulk Mg/Ca explained by ambient temperature. Here, I observe differences in bulk Mg/Ca within and between individuals of *Keratoisis* sp. (Figure 4.3), leading to variable offsets in paleotemperature reconstructions from *in-situ* temperature measurements when using a SubClass-level calibration. Whilst I could have opted for a calibration specific to the *Keratoisidinae* SubFamily, it would have resulted in a substantially weaker regression and flatter gradient ( $[T$  °C] =  $0.12 \pm 0.08$  [Mg/Ca mmol/mol] –  $6.64 \pm 6.63$ ;  $R^2 = 0.13$ ) calculated over a smaller range of temperatures (-1.9 to 10 °C) with 95% confidence intervals of  $\pm$  10 °C. As such, despite the offsets within individuals of *Keratoisis* sp., the robustness of the linear calibration model derived from the combined Octocoral data instils confidence in the suitability of Mg/Ca for estimating past temperatures.

#### 4.5.1.2 Ba/Ca

Superficially, bulk Octocoral Ba/Ca also appears to be related to *in-situ* temperature much like other taxon- and mineralogy-specific relationships (Figure 4.3b). However, similar studies on other cold-water species demonstrated a strong covariance between  $[Ba]_{sw}$  and T (Scleractinia, Spooner et al. 2018), and a relatively minor dependence on coral Ba/Ca on T has been reported in a warm water species (*Favia fragum*, Gonreea et al. 2017). Here, Ba/Ca values for *Keratoisis* sp. colonies fall outside of the linear relationship with temperature, suggesting that the correlation

between Ba/Ca and temperature in Octocorals is predominantly driven by the dependence of Ba/Ca on  $[Ba]_{sw}$  (LaVigne et al. 2011; Thresher et al. 2016, Flöter et al. 2019; Geyman et al. 2019). This is important because this proxy could provide an insight into the dynamics and circulation of refractory nutrients from the overlying water column (Chow & Goldberg, 1960; Wolgemuth and Broeker, 1970).

Octocoral Ba/Ca versus  $[Ba]_{sw}$  calibration suggests a well-defined, linear relationship, despite the inclusion of samples from different regions of the globe and gorgonian families:  $[Ba/Ca \mu\text{mol/mol}] = 0.148 \pm 0.005 \text{ [Ba}_{sw} \text{ nmol/kg}], R^2 = 0.97, p < 0.001$  (Figure 4.3b). This relationship has a steeper slope than demonstrated in other high-Mg corals, assuming that the only source of Ba to the skeleton is from the dissolved pool in seawater (i.e. if  $[Ba]_{sw} = 0$ , then the coral skeleton Ba/Ca ratio = 0). However, I find evidence of ontogenetic variability in  $D_{Ba}$  for *Keratoisis* (Figure 4.3b), indicating that such an assumption may be incorrect due to genus- (vital-) and/or site-specific effects (Flöter et al. 2019). Regardless, the empirical calibration model of Ba/Ca vs  $[Ba]_{sw}$  that emerges from the combined Octocoral data (Table 4.5) appears to be robust, despite inclusion of different genus and methodologies, providing confidence in its applicability to estimate past  $[Ba]_{sw}$ .

#### 4.5.2 Microscale trace element discrepancies

When interpreting any paleoceanographic record it is important to consider the fidelity with which a proxy is able reproduce the hydrographic parameter of choice. When using the Octocoral derived calibration, Mg/Ca values in my *Keratoisis* sp. colonies suggest a maximum temperature variability of  $\pm 3.78^\circ\text{C}$  across the timeframe common to all colonies and maximum prediction uncertainty of  $\pm 4.52^\circ\text{C}$  when reconstructing temperature for any given timepoint. This exceeds the temperature variability documented at parallel depths during a long-term monitoring across the Davis Strait (Curry et al. 2010), entire Baffin Bay basin (Zweng & Munchow, 2006; Birch et al. 1983), and even proximate deep-water CTD casts from the past three years (pers. comm., Azetsu-Scott). One explanation for this might be that the newly refined multi-taxa calibration, which uses globally distributed Octocoral colonies derived from multiple water depths, is not appropriate for *Keratoisis* sp. and/or for the high-resolution Mg/Ca mapping approach. An alternative explanation is that the enhanced reconstructed temperature variability of this species reflects variable physiological processes that influence Mg-uptake rather than issues relating to calibration (Alpert et al. 2016; DeLong et al. 2011; Hu et al. 2018). If the latter is the case, biological variability exerts a major control on the ability of this species to accurately preserve environmental information, but it is unclear whether these inter- and intra-colony offsets differ from site to site or represent an intrinsic feature of this species of *Keratoisis* as is it poorly characterised by available studies.

#### 4.5.2.1 Variation within and among individuals

Observations of element signals across internodes reveal asynchronous variability between E/Ca transects, indicating that variability in contemporaneous skeletal composition is large enough to adjust paleoenvironmental reconstructions that are based on sub-annual, annual and interannual element chronologies even after stratigraphic tuning. The examination of replicate E/Ca transects per analysed colony can assist in unravelling the influence of environmental factors versus physiological effects (Sinclair et al. 2011; DeLong et al. 2007; Kawakubo et al. 2014) and demonstrated here by leveraging the data from different internodes into a singular timeline, which reduced the prediction uncertainty of seasonally interpolated and annually interpolated temperature reconstruction by an average of 55% and 48%, respectively. However, it is important to exercise caution when predicting seawater conditions, as this approach primarily assesses the consistency of the relationship within living proxies. Enhancing accuracy requires *in-situ* measurements to adjust the linear or non-linear regression between the coral's element proxy and the environmental variable of interest. This is regularly employed in tropical (Hu et al. 2018; Cuny-Guirriec et al. 2019; Hathorne et al. 2013) and temperate (Montagna et al. 2014) studies due to the abundance of hydrological stations, buoys, and satellite information within these regions.

Though long-term reconstructed T and [Ba]<sub>sw</sub> variability is very coherent across the coral colonies, most sub-annual fluctuations occurred at different timepoints, suggesting that ontogenetic variation between colonies collected from the same location can influence paleoenvironment reconstructions at seasonal resolution and below. Numerous studies have observed inconsistencies between colonies of tropical *Porites* species sampled close to one another (Cahyarini et al. 2008, 2009; Pfeiffer et al. 2019; Hu et al. 2018) where differences are often attributed to localised temperature, photosynthetic effects or environmental stress (Marshall and McCulloch, 2002; Linsley et al. 2004; DeLong et al. 2007). As physical conditions tend to coalesce with depth (Rogers, 2015) I contend that the interannual and sub annual variations of *Keratoisis*-derived temperature and [Ba]<sub>sw</sub> may not be driven by localised oceanographic variability (Figure 4.4). Where coral element variability cannot solely be explained by small-scale environment fluctuations, vital effects are considered the main contributor (Cohen et al. 2001; Allison and Finch, 2004; Sinclair et al. 2011; DeLong et al. 2011; Gaetani et al. 2011; Hill et al. 2011; Robinson et al. 2014). Indeed, correlations between vital effects and specific features of aragonitic deep-sea corals (Shirai et al. 2005; Gagnon et al. 2007), as well as in high-Mg bamboo corals (Hill et al. 2011; Flöter et al. 2019), have been documented, with several mechanisms (Rayleigh fractionation, ion-specific pumping, and Ca/proton exchange) investigated to explain the distribution of Na and S

(Flöter et al. 2022). To better understand the differences in element behaviour across growth lines in coral colonies, future studies should investigate the controlling mechanisms of element uptake in these regions. This could involve examining the effects of non-linear growth rates (Farmer et al. 2015b) on element incorporation in *Keratoisis* and other bamboo coral species under varying environmental conditions to establish more robust chronologies, as growth rates are known to vary within fossilised individuals of other *Keratoisis* spp. (Noé et al. 2008). Faster growth rates in this area may cause elevated Mg/Ca via enhanced Mg partitioning at higher calcite precipitation rates – an explanation supported by other studies of *Keratoisis* (Thresher et al. 2016a, 2016b; Flöter, 2019, Flöter et al. 2019, 2022) and the fact that Sr incorporation is negatively correlated with the calcification rate (Ferrier-Pages et al. 2002). This, alongside revised calcification models, can help predict element behaviour, disentangle environmental influences from physiological drivers of the calcitic skeletal composition (Flöter et al. 2022) and, therefore, enable confident exploration of environmental reconstructions at finer temporal resolutions.

#### **4.5.2.2 Sr/Ca, U/Ca, Sr/U and Li/Mg in high-Mg calcitic Octocorallia**

Other than Mg/Ca, correlations between temperature and E/Ca ratios were found to be extremely weak in high-Mg calcitic Octocorals. Environmental effects on Sr/Ca values are known to vary between gorgonian taxa (Weinbauer and Velimirov, 1995; Heikoop et al. 2002) and in other bamboo coral species track ambient Sr/Ca ratios rather than temperature (Hill et al. 2012). There have been few studies exploring the Li/Mg temperature relationship in high-Mg cold water Octocorals, but sensitivity is similar to the Sr/Ca proxy in warm water counterparts (Chaabane et al. 2019). Interestingly, U/Ca demonstrated high reproducibility at the micrometre scale in *Keratoisis* sp. and a significant abiotic Mg/Ca temperature relationship across high-Mg Octocorals is observed (Figure 4.3) which argues against previous investigations with temperature (DeCarlo et al. 2015, 2016). Correlated variability between tracers can be a strong constraint on vital effect mechanisms (Sinclair et al. 2006), but was not observed here and the mechanisms causing the observed U/Ca variations remain unknown. Few studies have directly compared the utility of the range of available temperature proxies (U/Ca, Sr/Ca, Li/Mg, and Sr-U) at sub annual resolution (e.g. Ross et al. 2019) or across overlapping growth periods within the same specimen, so whether temperature sensitivity is universal across taxa is unknown.

#### **4.5.3 Prospect for a E/Ca paleothermometer in *Keratoisis* sp.**

Temperature reconstructions over the shared timeframe for all colonies reveal a notable but minor cooling trend in deep-water during the past 20 years (Figure 4.4). The accuracy of this reconstruction is challenging to determine due to the lack of complete continuous *in-situ*

temperature datasets for alignment; nonetheless, it aligns with trends observed in OISST (Figure 4.4). When considering the entire 20<sup>th</sup> century, a gradual warming trend has been observed in the deep-water layer of the Baffin Bay basin (Zweng & Münchow, 2006; Birch et al. 1983) and is most likely caused by an increase in temperature of the inflowing Atlantic waters of the West Greenland Current, a speculation supported by a significant correlation of subsurface (~900 m) temperature fluctuations with the NAO over the same timeframe (Zweng & Münchow, 2006). As Baffin Bay is a semi enclosed basin to the north of the Labrador Sea, any hydrographic changes here may indicate potential climate shifts because water exiting Baffin Bay enters the Labrador Sea, one of the two or possibly three deep convection sites in the Northern Hemisphere (Pickart et al. 2002, 2003). Though all available *in-situ* measurements predate 2003 and are outside the timeframe of this study, the deep-water warming trend (OLS regression  $\pm$  95 CI) determined from sporadic bottle- and CTD-casts within a 200 m vertical bin (1967-1998, 800-1000 m,  $n_T = 10$ ;  $0.016 \pm 0.013$  °C/yr; Zweng & Münchow, 2006) is smaller than the Mg/Ca reconstructed temperature trend (annual interpolated) in my longest-lived colony over the same timeframe (averaged over internodes,  $n_T = 31$ ,  $0.060 \pm 0.017$  °C/yr; Figure 4.5). As both the coral and direct measurements demonstrate a warming period, this provides confidence in the derived relationship between Mg/Ca of *Keratoisis* sp. and ambient temperature. Furthermore, the agreement between the mean Mg/Ca of *Keratoisis* sp. and the abiotic Mg/Ca temperature relationship at a single temperature point is promising, if somewhat preliminary, for the development of a Mg/Ca paleothermometer. However, improved precision is necessary because even when leveraging replicate transects, the external error of my current Mg/Ca method corresponds to roughly 2 °C using the slope of the relationship between Mg/Ca and temperature for high-Mg calcitic Octocorals. In the context of cold-water environments this error can account for a near 100% difference from mean temperatures. Although Mg/Ca in the outer section of *Keratoisis* sp. exhibits low variance, and accepting the limitations of analytical error, I remain confident that regional analyses are likely to yield an improved test of a Mg /Ca paleothermometer when more *in-situ* temperature data becomes available. Nevertheless, inside the band surrounding the central axis, vital effects will still present a challenge to the development of a Mg/Ca deep-sea cold-water paleothermometer.

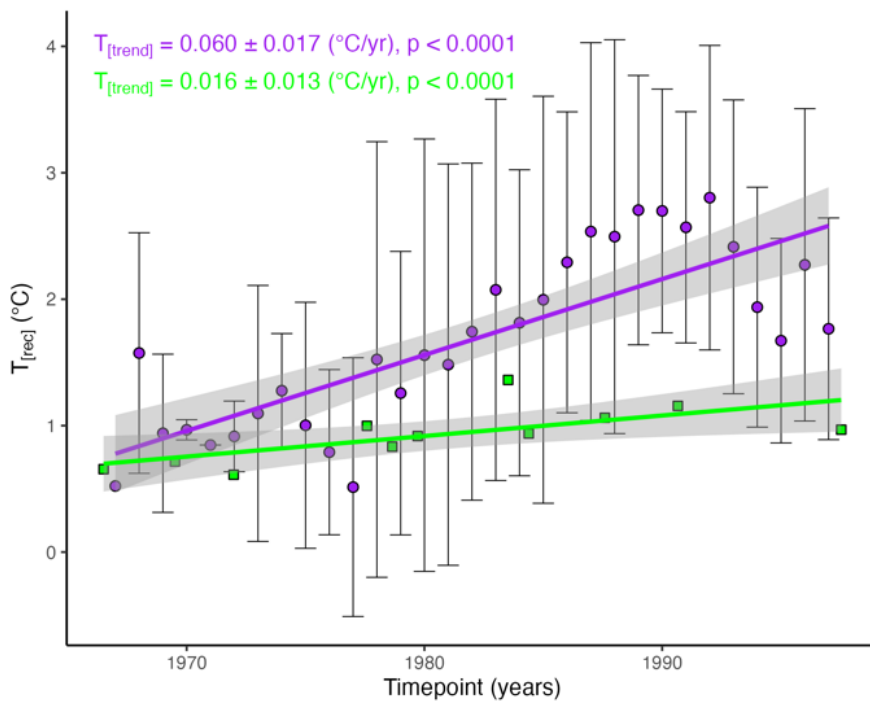


Figure 4.5 | *In-situ* temperature data (green squares) and trend (green line, shaded area is standard error of Ordinary Least Squares regression) for Baffin Bay (Zweng & Münchow, 2006) vs annually interpolated reconstructed temperature data (purple circles, error bars denote standard error after averaging across internodes) and trend (purple line, shaded area is standard error of Ordinary Least Squares regression) in *Keratoisis* sp. colony #23-6.

#### 4.5.4 Prospect for a nutrient tracer in *Keratoisis* sp.

The existence of Ba/Ca variability in coral skeletons related to variability in [Ba]<sub>sw</sub> is well documented (e.g., Hart et al. 1997; Tanzil et al. 2019). In coastal regions where input from rivers is significant, flooding can cause sudden increases in the Ba/Ca ratio of seawater and, thereby, produce sharp Ba/Ca “spikes” in coral skeleton (Alibert et al. 2003; Sinclair and McCulloch, 2004). The presence of a broad anomalous peak in these corals, however, suggests a slow and diffusive input of Ba to the seafloor, while the consistent Ba enrichment across all corals indicates that the driving factor behind these peaks extends beyond their immediate environment. Despite the corals not being coastal, they inhabit a sizable submarine sedimentary trough-mouth fan adjacent to Disko Bay, which has experienced historical meltwater sediment delivery (Ó Cofaigh et al. 2018), suggesting that large-scale variations in Ba content of riverine inputs might be responsible for the anomalous Ba peak. However, it is important to consider the compositions of other inputs such as glacial meltwaters, groundwaters, submarine discharge, sea-ice, and snowpack. Meteoric water, primarily glacial meltwater from the Greenland Ice Sheet, is the dominant source of

freshwater in the Davis Strait region (Azetsu-Scott et al. 2012), from which barium bound to transported particulates may slowly sink towards the deep water. Although limited ice discharge data prior to 2000 is available, a noticeable increase in ice discharge, particularly from the Jakobshavn Glacier flowing into the Disko Bay region, is observed during the early 21st century and from 2012 to 2015 (Mankoff et al. 2020). The observed peaks in barium concentrations in my corals align with this pattern, providing compelling evidence for the utility of barium as a proxy for glacial meltwaters. Small, intense localised barium (Ba) inputs cannot be ruled out, as fluctuations in Ba concentration across the coral colonies suggest sharp and brief pulse events. In oceanic corals, upwelling serves as a potential source of pulsed Ba input, associated with increased local productivity and sedimentation of particulates and planktonic tests. Periodic upwelling from April to October has been observed further down the western Greenland coast (Juul-Pedersen et al. 2006), and studies on pelagic productivity and food web structure in Disko Bay have documented strong benthic-pelagic coupling with springtime blooms (Heide-Jørgensen et al. 2007) and the prevalence of large calanoid copepods, bacterioplankton, and unicellular zooplankton (Nielsen and Hansen, 1995; Nielsen and Hansen, 1999; Hansen et al. 2003). However, caution must be exercised when using barium as a benthic-pelagic tracer in the Arctic, as previous research indicates non-conservative behaviour even during low biological productivity periods, likely due to sea-ice microenvironment processes (Hendry et al. 2018). Coral spawning, which significantly affects coral physiology (Gagan et al. 1994; Gagan et al. 1996), may also contribute to the anomalous Ba peaks. Tracey et al. (2007) suggest that reproduction can influence the element composition in bamboo corals, and the existence of an annual reproductive cycle in a lower-latitude Canadian bamboo coral (*Keratoisis ornata*; Mercier and Hamel, 2011) aligns with the hypothesis of synchronous annual Ba concentration cycles between colonies. While the influence of temperature on spawning has been observed in tropical corals (*Montastraea annularis*; Mendes & Woodley 2002), its impact has not been investigated in *Keratoisis* spp. If any climate-driven environmental variables also affect spawning in this context, it would further undermine the reliability of barium as a nutrient tracer.

## 4.6 Conclusions and Outlook

The micrometre-scale analysis of the chemical composition of deep-sea bamboo coral, *Keratoisis* sp., alongside a calibration comparison with other taxa and evaluation against environmental conditions, reveals that Mg/Ca ratios demonstrate the strongest correlation with ambient temperature among high-Mg calcitic Octocorals. Ba/Ca ratios in high-Mg Octocorals are positively correlated with ambient  $[Ba]_{sw}$  and exhibit a steeper gradient compared to high-Mg calcitic

*Stylasteridae* and *Scleractinia*. However, significant ontogenetic variability in Mg/Ca and D<sub>Ba</sub> is observed within and among individuals of the *Keratoisis* sp., suggesting caution in the interpretation of variability in reconstructed environmental conditions. Replicate transects and colony-specific calibrations improve the reliability of geochemical records and help differentiate true paleoenvironmental variation from ontogenetic discrepancies. At the microscale, distinct geochemical features are observed in the *Keratoisis* sp. skeletons, with a high-density skeletal layer near the central axis and a less dense layer lining the outer edge of the internode. Mg/Ca and Li/Ca covary positively within the skeletal structure, while Sr/Ca and U/Ca exhibit a weak negative covariance. Ba/Ca covaries positively with Mg/Ca and Li/Mg, showing significant banding across the internode. The central section of the internode is deemed the most suitable location for paleo-environmental reconstruction due to potential chemistry manipulation effects at the coral edge and faster calcification near the central axis. Careful selection of representative sections is necessary to minimise vital effects and enhance the statistical precision of climate reconstructions

In the deep-water basin of Baffin Bay, *Keratoisis* sp. plays a crucial role in supporting benthic functioning (Pierrejean et al. 2020), and previous studies have highlighted the significant influence of paleoclimate on biodiversity dynamics and its lasting effects on contemporary patterns (Svenning et al. 2015). However, limited empirical research has been conducted on the legacies of paleoclimate on ecosystem functioning (Svenning et al. 2015). Future investigations should therefore prioritise elucidating the intricate dynamics between oceanographic conditions and proximate functioning. Despite uncertainties stemming from taxonomic-derived age models and ontogenetic variability among *Keratoisis* sp. colonies, my application of the Mg/Ca proxy reveals a gradual cooling trend over the past 20 years and a 20th-century warming trend in the longest-lived coral, which aligns with available in-situ records. While my findings suggest limited evidence of temperature influencing barium, which exhibits a nutrient-like profile in open oceans and tracks the patterns of other algal nutrients (Chow & Goldberg, 1960; Wolgemuth and Broeker, 1970), the reproducible reconstructions of pronounced and frequent spikes in [Ba]<sub>sw</sub> indicate potential influences from sea-ice, upwelling, phytoplankton blooms, and/or spawning events, which themselves can be affected by climate-driven environmental factors. Consequently, the reliability of this nutrient tracing proxy may be indirectly influenced by climate change. To enhance confidence in utilising this coral species for deep-water paleoenvironmental reconstructions, future studies should incorporate colony-specific growth rates, site-specific calibrations based on *in-situ* measurements of environmental data, and direct metrics of functioning such as sediment oxygen demand and carbon context. This comprehensive approach will improve the resolution of reconstructed environmental variability *Keratoisis* sp. and provide

Inter- and intra-colony elemental systematics of a cold-water bamboo coral mediate deep-sea temperature and nutrient proxies

insights into the potential influences of temperature and other climate-driven environmental factors on benthic ecosystem functioning.



## Chapter 5 **Species co-dependency and vulnerability**

### **moderate ecological consequences of species loss**



## 5.1 Abstract

Climate-driven changes in marine environments can disrupt ecosystem functioning and increase extinction risk. However, conventional risk assessments often overlook the role of species interactions in shaping ecosystem responses to perturbation. Here, I parameterise trait-based extinction models that adjust the probability of species extirpation and/or compensation by taking into account species interdependencies. I show that co-extinctions can intensify the degradation of a crucial ecosystem process - bioturbation, the faunal mixing of sediments - beyond that expected from independent instances of species loss. However, compensatory mechanisms from the local and regional species pool reduce the influence of co-extinctions and introduce uncertainty in biodiversity-ecosystem functioning extinction trajectories. My study demonstrates the influence of community dynamics in determining the ecosystem consequences of local alterations to biodiversity associated with climatic forcing.

## 5.2 Introduction

The accelerating pace (Burrows et al. 2011) and amplification (Rantanen et al. 2022) of climate change continues to generate concern over the potential ecological consequences of local alterations to biodiversity (Cardinale et al. 2012). Localised species loss is generally expected to reduce ecosystem functioning (Cardinale et al. 2012), but the magnitude of reduction depends on how the functional traits of individual species covary with their risk of extinction (Solan et al. 2004a), the influence of post-extinction community dynamics (McIntyre et al. 2007, Thomsen et al. 2017, Thomsen et al. 2019) and the relative vulnerabilities of individual species to extinction (Garcia et al. 2021). Yet, the fundamental role of interactions in predicting the fate of taxa facing multiple simultaneous pressures has not been incorporated in efforts attempting to project the ecosystem consequences of environmental forcing (Brook et al. 2008). It is important to recognise that the consequences of biodiversity adjustments are not limited solely to functional role of the extirpated species, but extend and are expressed through changes to species interactions, including resource partitioning (Gross & Cardinale, 2005), competitive release (Godbolt et al. 2009), interaction simplification (Burkepile and Hay, 2007, Hughes et al. 2012) and adjustments to the nature of mutualistic, parasitic (Kovats et al. 2001), symbiotic and discriminate predator-prey relationships (Edwards and Richardson, 2004). If we are to advance realistic and relevant projections of future ecosystems, it will be vital to recognise and consider the full span of community responses to environmental forcing.

Co-extinction—the loss of species caused by direct or indirect effects that stem from other extinctions (Brodie et al. 2014; Koh et al. 2004)—is a major contributor to global biodiversity loss and amplifies the effect of primary extinctions (Sanders et al. 2015, Strona, 2015, Valiente-Banuet

et al. 2015, Strona & Bradshaw, 2018, Strona & Bradshaw 2022). Yet, few studies have made comprehensive predictions regarding the differential functional consequences between co-extinctions and singular extinctions (Ives & Cardinale 2004). Conflicting conclusions exist regarding diversity (Viera et al. 2013, Petchey, 2008), redundancy (Sanders et al. 2018, Biggs et al. 2020), and implied effects on ecological processes and functions (Kehoe et al. 2020, Raine et al. 2018). In cases where ecosystem properties were concurrently measured, the significance of co-extinctions was heavily influenced by taxonomic connectivity although primary extinctions were assumed to be random (Thébaud, 2007). Moreover, none of these studies have explored the significance of compensatory mechanisms and population dynamics in moderating the impacts of locally-altered biodiversity and sustaining functional resilience amidst environmental perturbations (Gonzalez et al. 2009, Pan et al. 2016, Thomsen et al. 2017, 2019, Garcia et al. 2021). However, assessing the relative importance of these mechanisms under variable contexts (Wardle and Zackrisson, 2005) where species tend to differ in their functional roles (Fetzer et al. 2015), expression of traits (Wohlgemuth et al. 2017, Cassidy et al. 2020), response to disturbance (Williams et al. in press), interaction with the environment (Dolbeth et al. 2019) and other species (Bimler et al. 2018) remains a complex challenge.

In this study, I use probabilistic trait-based models of marine benthic communities to investigate how climate-driven change alters the biological mediation of seabed functioning. My simulations assume that the sequence of species loss are ordered by extinction risk to climate change, that vary across a gradient of forcing in the Barents Sea (Solan et al. 2020c). Here, recent changes in the timing of sea ice formation and retreat, along with increasing seawater temperature, are driving poleward shifts in distribution (i.e., “borealization”), abundance and overall community composition of benthic invertebrates (Grebmeier, 2012). I hypothesised that as the benthic community is incrementally subjected to increasingly boreal environmental conditions (Wang et al. 2020) the diversity, structure and functioning of the community will modify (Csapó et al. 2021, Ingvaldsen et al. 2021), generating interaction-driven co-extinctions. I also postulated that boreal-adapted species will migrate poleward and further adjust community dynamics (Kortsch et al. 2015, Fauchald et al. 2021). I compare these probabilistic distributions to further simulations in which populations of surviving species exhibit numeric compensation. Anticipating context-dependent species turnover and considering interdependencies in vulnerabilities (McLean et al. 2019) and interactions (Bimler et al. 2018), my expectation was that the level and influence of co-extinction on ecosystem response would maximise at the polar front, and be less important at the northerly and southerly ends of the environmental gradient. If my expectations are met, my findings will highlight the importance of including the full suite of species responses to

perturbations when attempting to project the most likely ecosystem consequences of environmental forcing.

## 5.3 Material and methods

### 5.3.1 Study location and environmental gradient

I use a benthic survey of 6 stations (4 replicate deployments per station) in the Northwestern part of the Barents Sea shelf (Appendix D data S1, figure S1), to parametrise models that predict how alterations to biodiversity associated with climate-driven change in environmental conditions affect seabed function. The selected transect of stations (B13-B17, Xs; Appendix D figure S1) intersects a well recognised polar front (Loeng, 1991, Jorgensen et al. 2015) and a clear North-South separation in faunal assemblages (Solan et al. 2020c) . I investigate differences in the magnitude and extent of forcing by parameterising my models with sequential station-to-station species vulnerabilities, and compare these simulations to equivalent extinctions based on the full gradient of change. Hence, the most northerly and most southerly stations in my transect represent the polar and boreal, respectively, pre-extinction community. Stepped scenarios between these conditions comprise a northernmost station as the pre-extinction community, and the neighbouring southern station as the post-extinction community.

#### 5.3.1.1 Modelling tool

Using a probabilistic trait-based model developed for exploring the effects of local extinction scenarios and the associated compensatory response of natural communities (Figure 5.1; Solan et al. 2004a), I predict how altered diversity associated with climatic-driven environmental change is likely to affect seabed functioning in the Arctic. I establish the relationships between an index of community-level bioturbation potential ( $BP_c$ ; (Solan et al. 2004a)), estimated from per capita contributions of sediment-dwelling invertebrates to sediment reworking based on average body-size (across the entire transect;  $B_{ind}$ ), abundance ( $A_i$ ), level of movement ( $M_i$ ) and sediment reworking mode ( $R_i$ ).

Climate-driven Atlantification will transform current benthic communities through the selective removal of vulnerable taxa (Jørgensen et al. 2019), subsequently triggering compensatory responses, co-extinctions and increasing dominance of boreal-adapted taxa (Csapó et al. 2021). To simulate this, my model selectively eliminates taxa from the starting species pool before calculating the response of the surviving community through compensatory mechanisms established for the regional species pool. The probability-based order of extinctions and compensations are derived from ranked vulnerabilities to each step in the climatic-driven

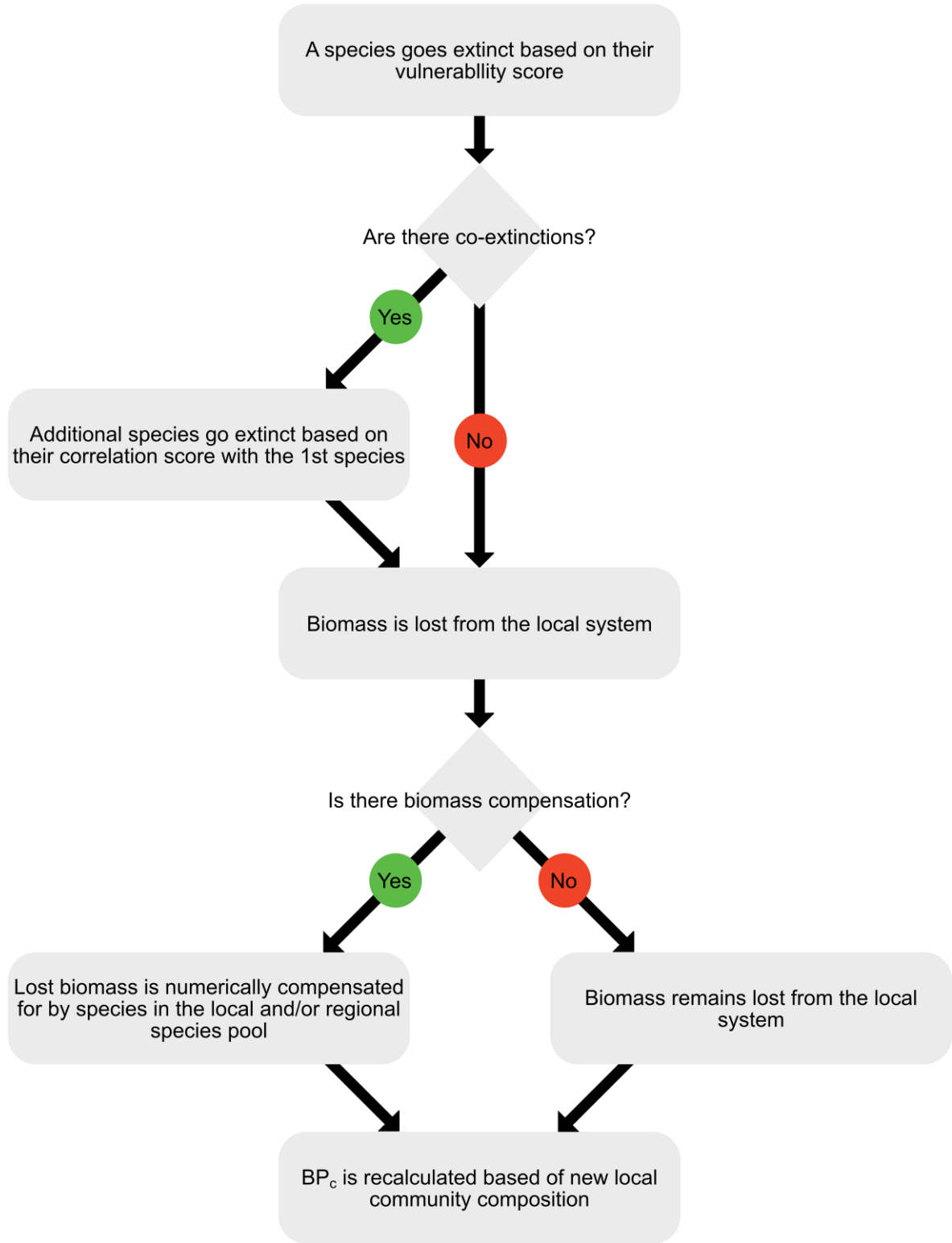


Figure 5.1 | Basic schematic of model procedure, with logic gates for whether co-extinctions and co-compensation occurs (see Section 5.3.1.1.1).

environmental transition, calculated from the percentage differences in sediment-dwelling invertebrate biomass between the pre-extinction community (northernmost station) and the reference post-extinction community (southernmost station) for all taxa in the regional species pool (Appendix D table S1, Appendix E code S1). I took this approach rather than using specific

tolerances to climatic drivers to parameterize the model because such information is scarce for a lot of Arctic invertebrates (Degen et al. 2019), not accurately described (Hale et al. 2014), behaviour dependant (Cassidy et al. 2020), and the relation to fitness is under question (Calosi et al. 2008; Sæther et al. 2015). Instead, I establish changes in the proportional abundances of individual species as an indicator of species vulnerability and, reciprocally, compensation, across the environmental gradient (Solan et al. 2020c; Jørgensen et al. 2015; Loeng, 1991). This means that a taxon with a high vulnerability score (i.e. present at the starting station but absent at the reference station) is deemed to have both a high probability of going extinct and a low probability to compensate (Appendix D figure S2).

As taxa are sequentially extirpated and the surviving community numerically compensates, a revised community  $BP_c$  is calculated. Alongside the revised community bioturbation potential, taxa-specific contributions to  $BP_c$  are also modified when they increase or decrease in number. I calculated these per-capita contributions ( $BP_{species}$ ) for all taxa in the regional community at each iteration. I run my simulations until all taxa become locally extinct, but my expectation is that each simulation is only valid to the level of biodiversity typically observed at my stations. That is, I assume the species richness of each station reflects the carrying capacity of the community.

Similarly, I only allow for species to compensate up to the median abundance for either side of the polar benthic front (Solan et al. 2020c) to prevent any taxa increasing in number beyond carrying capacity (Appendix E code S2). As any alteration in local communities associated with climate change may be offset by more resilient taxa from a wider area (Ingvaldsen et al. 2021), I allow for taxa present in the regional species pool (Northern pool: B17, B16; Southern pool: B15, Xs, B14, B13; Appendix D figure S3; Solan et al. 2020c) that were not present in the starting assemblage to be introduced and compensate (Garcia et al. 2021). Inclusion of taxa that are present (abundance greater than zero and at risk of local extinction) or absent (abundance equal to zero, no risk of local extinction) allows for the possibility that taxa from the absent pool can arrive and contribute to the present pool as would happen in a natural system.

### **5.3.1.1.1 Correlations, Co-extinctions and Co-compensations**

Biotic interactions build up complex ecological networks through which the loss of one species can alter the vulnerability of other species, a cascade process known as ‘co-extinction’ (Sanders et al. 2015; Strona, 2015; Valiente-Banuet et al. 2015). Here, interactions between taxa were estimated from positive and negative correlations in biomass across all station deployments ( $n = 24$ ) between species (abundance  $> 1$  across all stations) in the regional species pool ( $n = 69$ , Appendix D figure S4a). However, as species can be correlated with one another but not necessarily be codependent on each other, I only select correlations that are 1.5 standard

deviations outside the mean correlation score (0.0397; Appendix D figure S4b table S2; 466 correlations, Appendix E code S3). Positive correlations were used to calculate the probability of taxa going extinct during the same iteration as the primary extinction (hereafter co-extinctions, Appendix E code S4) and reduce their probability of compensating when they do not undergo co-extinction. Assuming that surviving taxa have a higher chance of compensation when their antagonist is removed, I recalculated the probability of compensation within the remaining community by utilising negative correlations between taxa removed during each extinction step (primary and co-extinctions) and the remaining community (Appendix E code S5). Once a taxon becomes locally extinct, I assume conditions are no longer supportive (Appendix E code S5) and do not allow any extirpated taxa to compensate a second time.

To achieve realistic simulations of biodiversity change (Naeem 2008), I acknowledge that multiple species have the capacity to compensate after an extinction event, particularly when the initial compensatory efforts of the first species do not fully replace all the lost biomass (Appendix E code S6; Appendix D figure S5). Hence, I only allow taxa to compensate up to the median abundance observed in the field, potentially allowing several compensators to respond to an extirpation. If there are several compensating species introduced from the regional species pool during initial extinction events, this can lead to an increase in local species diversity. When the median abundance of all species is reached during a simulation, biomass is lost from the system and a sequence of uncompensated extinction events is initiated. This continues until the next species from the regional species pool is introduced into the system.

### 5.3.2 Statistical analyses

I use a series of linear models to evaluate the vulnerability of taxa going extinct vs taxa remaining in the community as species richness declines.

Given the non-linear nature of each simulated biodiversity-function relationship, I use Generalised Additive Models (GAMs) with species richness as a smoothing function and climatic-driven environmental transition as an interaction term. This allows the relationship between  $BP_c$  and species richness to differ under each spatially explicit extinction scenario. I also calculated the standard error around each prediction (Appendix E code S7).

All statistical analysis, data exploration and plotting were performed using the R statistical and programming environment (R Core Team, 2022) and the R packages ‘qgraph’ (visual correlation networks; (Epskamp et al. 2022)), ‘MetBrewer’ (formatting graphical outputs; (Mills, 2022)), ‘mgcv’ (Generalised Additive Models; (Wood, 2011; Wood, 2017)), ‘stats’ (correlation calculations and matrices; (R Core Team, 2022)) and ‘tidyverse’ (data exploration and plotting; (Wickham et al.

2019)). Code for creating model output figures can be found at the end of the electronic supplementary material (Appendix E code S8).

## 5.4 Results

### 5.4.1 Projected ecosystem futures

In the absence of co-extinction and compensatory dynamics (Figure 5.2a–f), the form of the biodiversity-function curve approximates expectations (accelerating loss of function with declining species richness, moderated by climate vulnerability of the underlying community) though notable differences in the form of the curve occur between scenarios. A bifurcation of bioturbation potential with species loss is a common feature across most of my scenarios (except B15 to Xs, Figure 5.2c), and reflect the presence of species that disproportionately contribute to function (Solan et al. 2004a, McIntyre et al. 2007, Thomsen et al. 2017). These bifurcations become more pronounced when extinctions, ordered by climate vulnerability, incorporate co-extinctions (Figure 5.2g–l), whilst co-compensatory mechanisms temper the functional consequences associated with species loss (Figure 5.2m–r). .

I find that there are exclusive outcomes for each projected scenario (Table 5.1), and that the shape of the species-function trajectory is non-linear, significant (Table 5.2) and starts to saturate as species loss extends below carrying capacity (=dashed red vertical line, Figure 5.3). Post-extinction compensation intensities (maximum and mean number of compensating species per taxa extinction) also demonstrate divergent patterns within each scenario, with the largest numbers of compensating species observed within Xs-B14 and B14-B13 (Figure 5.3g–l). Across all scenarios, the first taxa to be lost from the local community are typically those inhabiting fixed tubes (Figure 5.3m–r) and surficial modifiers (Figure 5.3s–x), whilst species that inhabit burrow systems, live above the sediment and/or exhibit conveyor feeding increase in number. My probabilistic trajectories also indicate that diversity levels may extend above pre-extinction carrying capacity (=solid green vertical line, Figure 5.3), although the extent of such an increase and effect on functioning is dependent on scenario.

My findings show that progressive forcing (here, across a latitudinal gradient) result in stepped changes in the way in which species interact with one another that have functional consequences. In the transition from B17-B16, bioturbation consistently decreases with declining species richness (Figure 5.3a). Moving from B16 to B15, the species-function curve initially shows a shallow and consistent pattern during early species loss (Figure 5.3b; s.e. negligible). However, as species richness continues to decline towards the post-extinction community average (dashed red

vertical), functioning decay becomes sharper and more unpredictable. Transitioning from B15 to Xs results in a consistently flat biodiversity-function trajectory with high uncertainty in the early extinctions (Figure 5.3c). A shift from Xs to B14 demonstrates that initial species loss has minimal impact on functioning, but as species richness decreases towards the post-extinction community average, there is a sharpening loss in functioning and increased uncertainty in its trajectory (Figure 5.3d). Transitioning from B14 to B13 maintains the bioturbation potential similar to the pre-extinction state at first (solid green vertical), but then experiences a sharp and increasingly variable decline as species richness matches the post-extinction community state (Figure 5.3e). Overall, a region-wide transition from B17 to B13 exhibits a shallow biodiversity-function trajectory with minimal uncertainty in the early extinctions (Figure 5.3f).

I find that the most intense compensation effect within each scenario shifts as I move southward across the latitudinal gradient. Compensatory responses during the transition from B17 to B16 are highest at high species richness levels (mean  $\pm$  s.d.:  $4.67 \pm 2.51$  compensating species at 52 species richness; Figure 5.3g) while for B16-B15, compensation intensity remains consistent but low (range: 2.84 to 1.00 compensating species; Figure 5.3h). Compensation intensity is highest at the start of the extinctions when simulating an environmental transition from B15 to Xs and gradually declines with decreasing species richness (mean  $\pm$  s.d.,  $3.58 \pm 1.80$ , at 41 species richness; Figure 5.3i). When shifting from Xs to B14, a consistently high maximum compensation intensity is observed, accompanied by increasing mean compensation intensity as species richness decreases (Figure 5.3j). In the change from B14 to B13, compensation intensity is projected to peak in the middle of the extinction scenario (mean  $\pm$  s.d.:  $5.95 \pm 3.38$  at 16 species richness; Figure 5.3k) before rapidly declining. In a region-wide transition from B17 to B13, compensation intensity is highest at the beginning of the extinction scenario (mean  $\pm$  s.d.:  $3.76 \pm 1.82$  at 51 species richness) and then stabilises at a consistent level (Figure 5.3l).

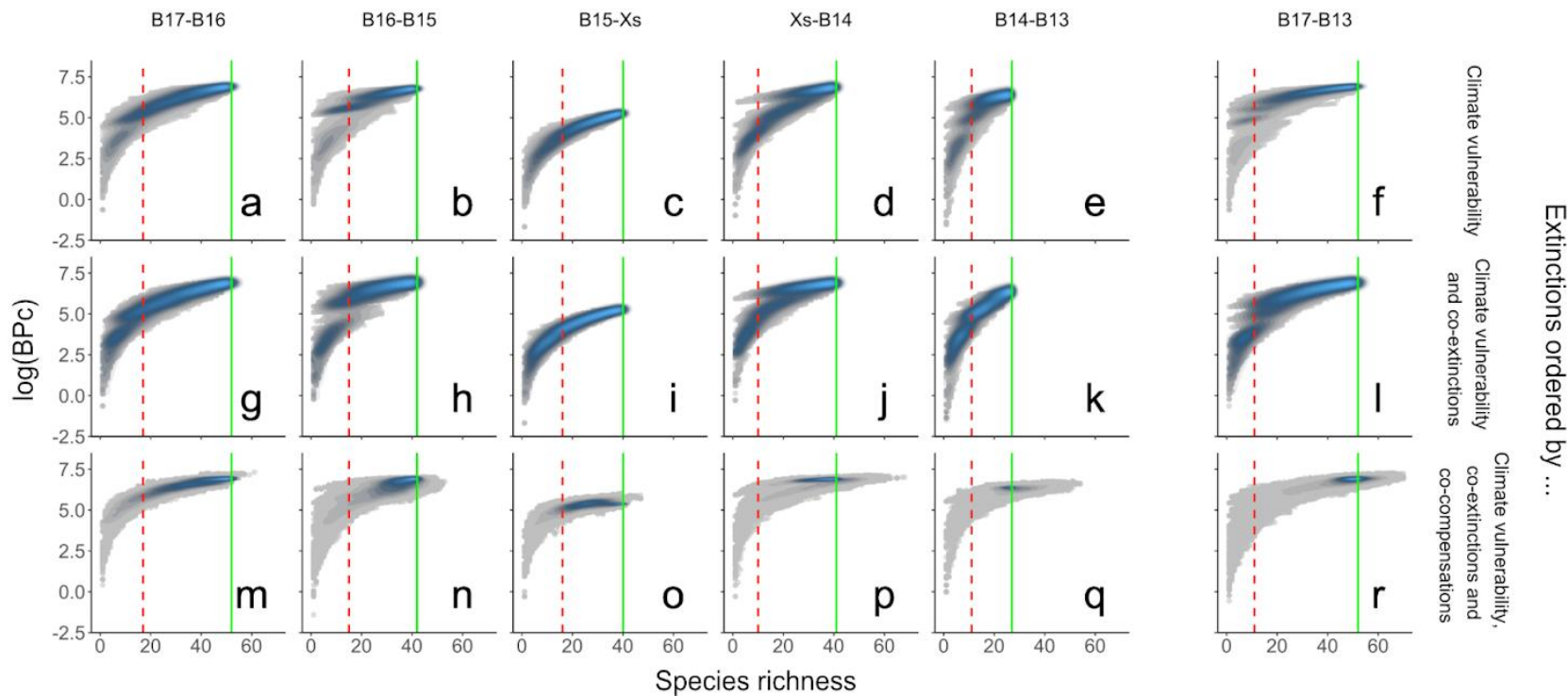


Figure 5.2 | Changes in community bioturbation potential ( $\text{BP}_c$ ,  $\log$ ) following climate-driven extinctions (**upper panels**), combined with interaction-derived co-extinctions (**middle panels**) and post-extinction compensations (**bottom panels**) associated with environmental transitions from stations (*a,g,m*) B17- B16, (*b,h,n*) B16 -B15 (*c,i,o*) B15 -Xs (*d,j,p*) Xs-B14 (*e,k,q*) B14-B13 and (*f,l,r*) B17-B13 in the Barents Sea. Colour intensity (**grey—blue**) reflects an increasing density (low to high) of data points with the pre-extinction species richness (**vertical green solid line**) and predicted post-extinction species richness (**vertical red dashed line**) represented. Coextinctions lead to an increase in colour intensity along the main species-function trajectory, whilst compensations increase the spread of data points. Simulations,  $n = 500$  per panel.

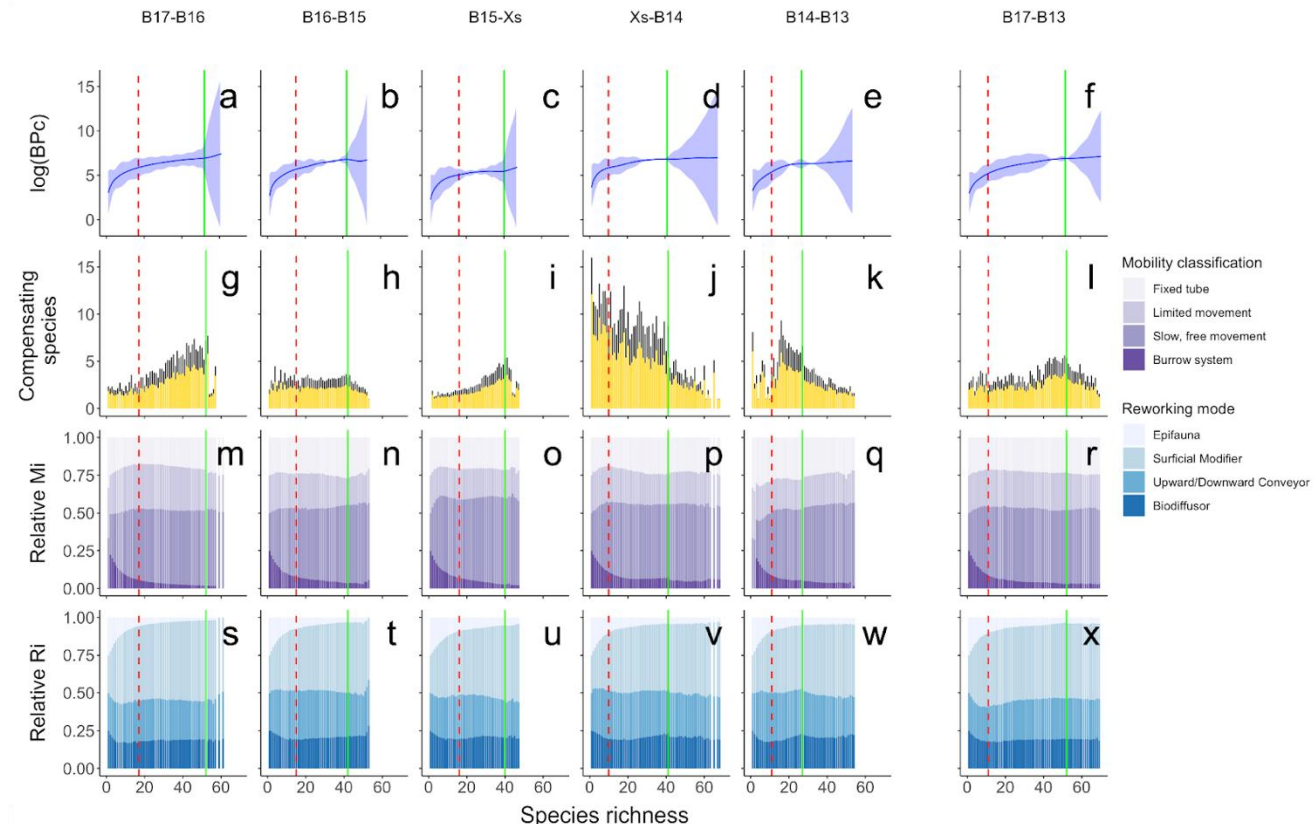


Figure 5.3 | Predicted biodiversity-ecosystem function relation curves (**upper row**) represented with a generalised additive model (GAM, mean  $\pm$  s.e., solid lines  $\pm$  shaded area), following post-extinction compensations (mean  $\pm$  s.d., **second row**) and reorganisation of functional groups characterised by their mobility (**third row**) and sediment reworking (**fourth row**) associated with environmental transitions from stations (a,g,m,s) B17-B16, (b,h,n,t) B16-B15 (c,i,o,u) B15-Xs (d,j,p,v) Xs-B14 (e,k,q,w) B14-B13 and (f,l,r,x) B17-B13 in the Barents Sea. The pre-extinction species richness (**vertical green solid line**) and predicted (median of observed data) post-extinction species richness (**vertical red dashed line**) are presented.

Table 5.1 | Analysis of variance (ANOVA) parametric coefficients generated from pairwise comparisons between generalised additive models (GAMs) of bioturbation potential loss in each scenario. With the exception of one scenario (station B16 to station B15), all local extinction events result in biodiversity-ecosystem functioning curve that are significantly (\*\*\*\*) different to the regional extinction scenario (station B17 to station B13).

Pairwise comparison	Mean difference	Std. error	t value	Significance
<b>B17-B13 to B17-B16</b>	67.63	1.1841	57.116	<0.0001
<b>B17-B13 to B16-B15</b>	-8.8338	16.4569	-0.0537	0.591
<b>B17-B13 to B15-Xs</b>	-277.52	58.9241	-4.71	<0.0001
<b>B17-B13 to Xs-B14</b>	15.9213	0.8482	219.203	<0.0001
<b>B17-B13 to B14-B13</b>	-41.1690	1.6076	-25.609	<0.0001

Table 5.2 | Approximate significance of smooth terms used in generalised additive models (GAMs) of bioturbation potential loss in each extinction scenario. The edf (effective degrees of freedom of smooth terms) represents the complexity of the smoother, with an edf of 1 equivalent to a straight line between x and y. The Ref.df and F columns represent test statistics employed in an analysis of variance (ANOVA) test to ascertain the overall significance (Sig.) of the smoother. In this context, a significance level of less than 0.05 implies that it is not possible to draw a horizontal line through the 95% confidence interval of the generalized additive model.

Extinction Scenario	edf	Ref.df	F	Sig.
<b>B17-B13</b>	8.675	8.961	48548	<0.0001
<b>B17-B16</b>	8.642	8.879	28951	<0.0001
<b>B16-B15</b>	8.952	8.998	28529	<0.0001
<b>B15-Xs</b>	8.846	8.997	1171	<0.0001
<b>Xs-B14</b>	9.722	8.941	26252	<0.0001
<b>B14-B13</b>	6.633	6.999	11097	<0.0001

#### 5.4.2 Functional contributions of surviving taxa

My projections indicate that taxa contributing most to community-level ecosystem functioning (%  $BP_c$ ) undergo a scenario-exclusive transition from those of an annelid dominant pre-extinction community (solid green line in lower panels of Figure 5.4a–e) such as *Nephasoma procera* and *Maldane sarsi*, to those of a more taxa-diverse post-extinction community (dashed red line in lower panels of Figure 5.4a–e). When simulating a change from station B15 to Xs and Xs to B14, the flat pattern of  $BP_c$  values following initial taxa losses indicates high levels of functional redundancy in the intermediate subset of taxa (Figure 5.3c). Nevertheless, a consistent feature of the projected post-extinction communities, regardless of scenario, is that the surviving assemblage yields a lower  $BP_c$  relative to that of the pre-extinction state (Figure 5.3), even when (mean) compensating intensity increased with species loss (station Xs to B14, station B14 to B13; Figure 5.3d and Figure 5.4e).

#### 5.4.3 Climate vulnerability vs order of extinctions

As species richness declines from the initial community (green vertical lines, Figure 5.5a–f) to the expected level in the post-extinction community (red dashed vertical lines), the relative vulnerability of all species undergoing extinction decreases (purple regression lines; vulnerability ~ -species richness, Pearson correlation coefficient “r”, range: -0.03 to -0.19, median: -0.12,  $p < 0.001$ ) though unexplained variability is high ( $R^2$ , range: < 0.01 to 0.09, median: 0.04). The overall climate vulnerability of the remaining taxa (hereafter, assemblage vulnerability; grey regression lines, Figure 5.5a–f) decreases as species go extinct within each step-wise transition ((B17-B16)  $r = -0.37$ ,  $R^2 = 0.14$ ,  $p < 0.001$ ; (B15-Xs)  $r = -0.11$ ,  $R^2 = 0.01$ ,  $p < 0.001$ ; (Xs-B14)  $r = -0.18$ ,  $R^2 = 0.03$ ,  $p < 0.001$ ; (B14-B13)  $r = -0.54$ ,  $R^2 = 0.29$ ,  $p < 0.001$ ) and across the entire latitudinal gradient ((B17-B13)  $r = -0.29$ ,  $R^2 = 0.09$ ,  $p < 0.001$ ). The only exception is B16-B15, where assemblage vulnerability marginally increases as taxa are selectively removed ( $r = 0.03$ ,  $R^2 < 0.01$ ,  $p < 0.001$ ). However, the relationship between climate-driven biomass-based vulnerability and the order of co-extinctions (yellow regression lines) exhibits variations as I move down the latitudinal gradient (Figure 5.5g–l), and notably differs within the central section (Figure 5.5i).

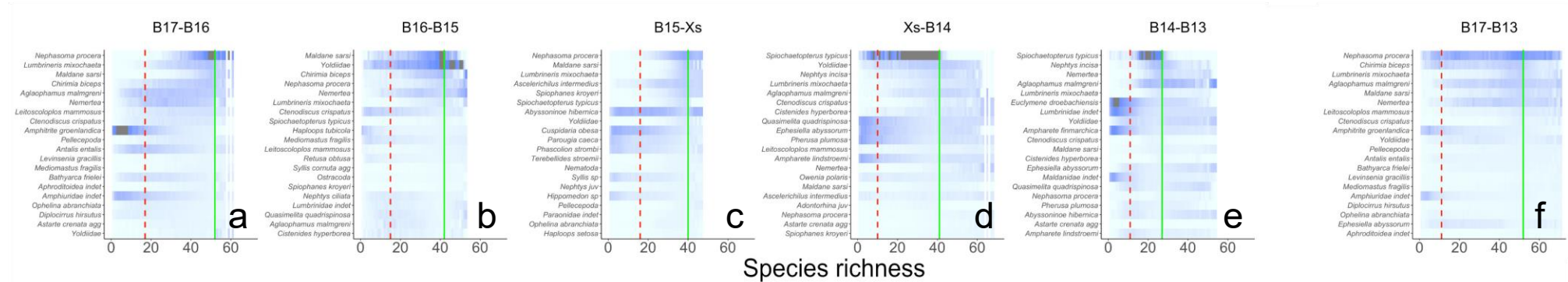


Figure 5.4 | Taxonomic reorganisation during simulated extinction events following environmental transitions from (a) Station B17 to Station B16, (b) Station B16 to Station B15 (c) Station B15 to Station Xs (d) Station Xs to Station B14 (e) Station B14 to Station B13 and (f) Station B17 to B13 in the Barents Sea. Colour shading (low—high, white—dark blue) represents the relative contributions of individual taxa to BPC at each sequential level of local extinction. The pre-extinction species richness (vertical green solid line), predicted post-extinction species richness (vertical red dashed line) and subset of twenty taxa that contribute most to functioning are represented, with contributions above 20% greyed out.

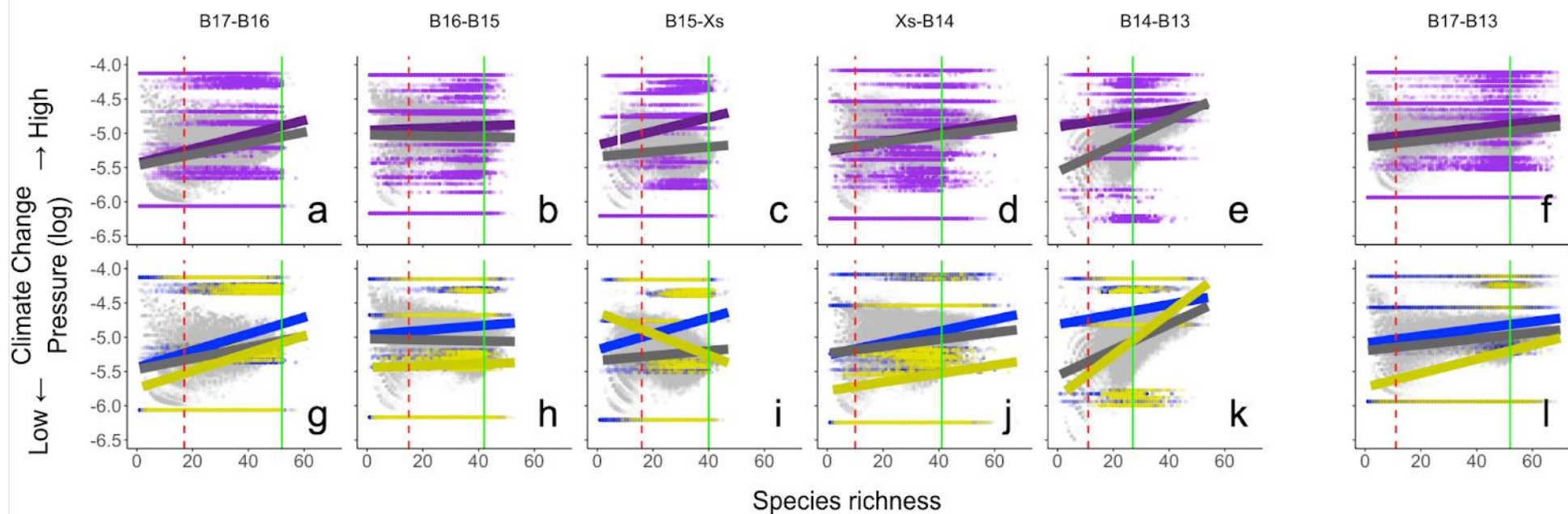


Figure 5.5 | Changes in mean extinction probability (log) of species following environmental transitions from (a,g) Station B17 to Station B16, (b,h) Station B16 to Station B15 (c,i) Station B15 to Station Xs (d,j) Station Xs to Station B14 (e,k) Station B14 to Station B13 and (f,l) Station B17 to B13 in the Barents Sea. Colours represent the extinction probability of all species going extinct (purple), the extinction probability of species still present within the community (grey), the extinction probability of species going extinct as a result of climate vulnerabilities (blue), the extinction probability of species going extinct as a result of species codependencies (yellow), the pre-extinction species richness (vertical green solid line) and post-extinction species richness (vertical red dashed line).

From station B17-B16, the models predict that co-extinctions (indicated by yellow regression lines) will preferentially eliminate taxa most susceptible to climate-driven environmental changes (Figure 5.5g; vulnerability  $\sim$  species richness,  $r = -0.19$ ,  $R^2 = 0.04$ ,  $p < 0.001$ ). For B16-B15, co-extinctions still target the most vulnerable species, but to a lesser extent (Figure 5.5h;  $r = -0.02$ ,  $R^2 = < 0.01$ ,  $p = 0.006$ ). In the shift from B15 to Xs, co-extinctions selectively remove the least vulnerable species to climate-driven environmental change (Figure 5.5i;  $r = 0.14$ ,  $R^2 = 0.02$ ,  $p < 0.001$ ). For Xs-B14, B14-B13 and the regional-wide scenario (B17-B13), co-extinctions will preferentially eliminate taxa most susceptible to climate-driven environmental changes (Figure 5.5j–k; (Xs-B14)  $r = -0.10$ ,  $R^2 < 0.01$ ,  $p < 0.001$ ; (B14-B13)  $r = -0.26$ ,  $R^2 = 0.07$ ,  $p < 0.001$ ; (B17-B13)  $r = -0.16$ ,  $R^2 = 0.03$ ,  $p < 0.001$ ).

## 5.5 Discussion

This study provides evidence of how projected climate change related pressures alter the biological-mediation of seabed functioning. I have demonstrated that projected local outcomes strongly differ from the conclusions derived from region wide assessments because the expression of climate forcing at the seafloor is not spatially homogeneous (Jørgensen et al. 2019; Orlova et al. 2015) and alters the way in which species respond. My simulations confirm the role of the surviving community in compensating for the loss, or change in, the relative abundance of species, but emphasises the importance of species co-dependencies that act to suppress (multiple compensators) or intensify (co-extinctions) the functional consequences associated with biodiversity loss. This is important because, when species co-dependency's are acknowledged, they lead to different biodiversity-function trajectories to those that are currently anticipated, lending support to the view that improved levels of ecological realism are necessary to support the generation of sensible environmental futures (Naeem 2008; Bracken et al 2008; Dolbeth et al. 2019; Garcia et al. 2021). Here, I embraced the modifying effects of biotic interactions on ecological performance (Montoya et al. 2010; Blois et al. 2013) where the rearrangement of species traits and changes in dominance patterns (Wohlgemuth et al. 2017) within the post-disturbance community are not just a function of specific extinctions and associated compensatory responses by the surviving community.

Co-extinctions are expected to hasten the loss of species (Dunn et al. 2009; Memmott et al. 2004) and minimise functional diversity (Sellman et al. 2016). My model projections reveal amplified, sharper losses of biodiversity and, subsequently, ecosystem functioning, indicating an erosion of functional capacity. Though this is in broad agreement with global simulations (Strona & Bradshaw, 2018; 2022), I recognise that the effects of secondary extinctions on ecosystem functioning are likely to be population and context-dependent (Wohlgemuth et al. 2017). Indeed,

resilient species may be removed from the system faster than preconceptions based on direct vulnerabilities may dictate but this does not directly correlate with a compounded impact on ecosystem functioning because species that are susceptible to perturbation may not be functional pivotal in the same context (Fetzer et al. 2015). In regions experiencing amplified levels of climate change (here, the Arctic), whether the functional architecture of communities lead to the decline, maintenance or enhancement of ecosystem functioning is also dependent on the extent of species migration and how post-borealization species interactions (and resulting compensatory responses) are realised (Thomsen et al. 2017; 2019), as well as the level of functional redundancy within replacement taxa (Garcia et al. 2021). I found that incorporating multi-taxa compensatory mechanisms sufficiently reduced the ecological consequences of species loss in each of my scenarios and lessened the effect of losing dominant, highly productive species from local communities with low functional redundancy. Further I note that, the rate of introduction of non-local species can exceed the rate of extinction of native species in the same habitat (Ellis, Antill, & Kreft, 2012; Sax, Gaines, & Brown, 2002), leading to stasis or increase in local biodiversity with concomitant effects on functioning. Higher diversity is often assumed to have a positive effect on ecosystems (Salo & Gustafsson, 2016; Arese Lucini et al. 2020), my results indicate that the effect of increased levels of diversity above carrying capacity can be highly variable. Such an effect is, however, likely be transitory as the carrying capacity of the local habitat shifts with environmental change (Woodworth-Jefcoats et al. 2017) and may lead to introduced species causing additional native extinctions (Catford et al. 2018) through, for example, predation (Pyšek et al. 2017) and competition (Castorani & Hovel, 2005) though the latter is not expected to be widespread (Davis, 2003).

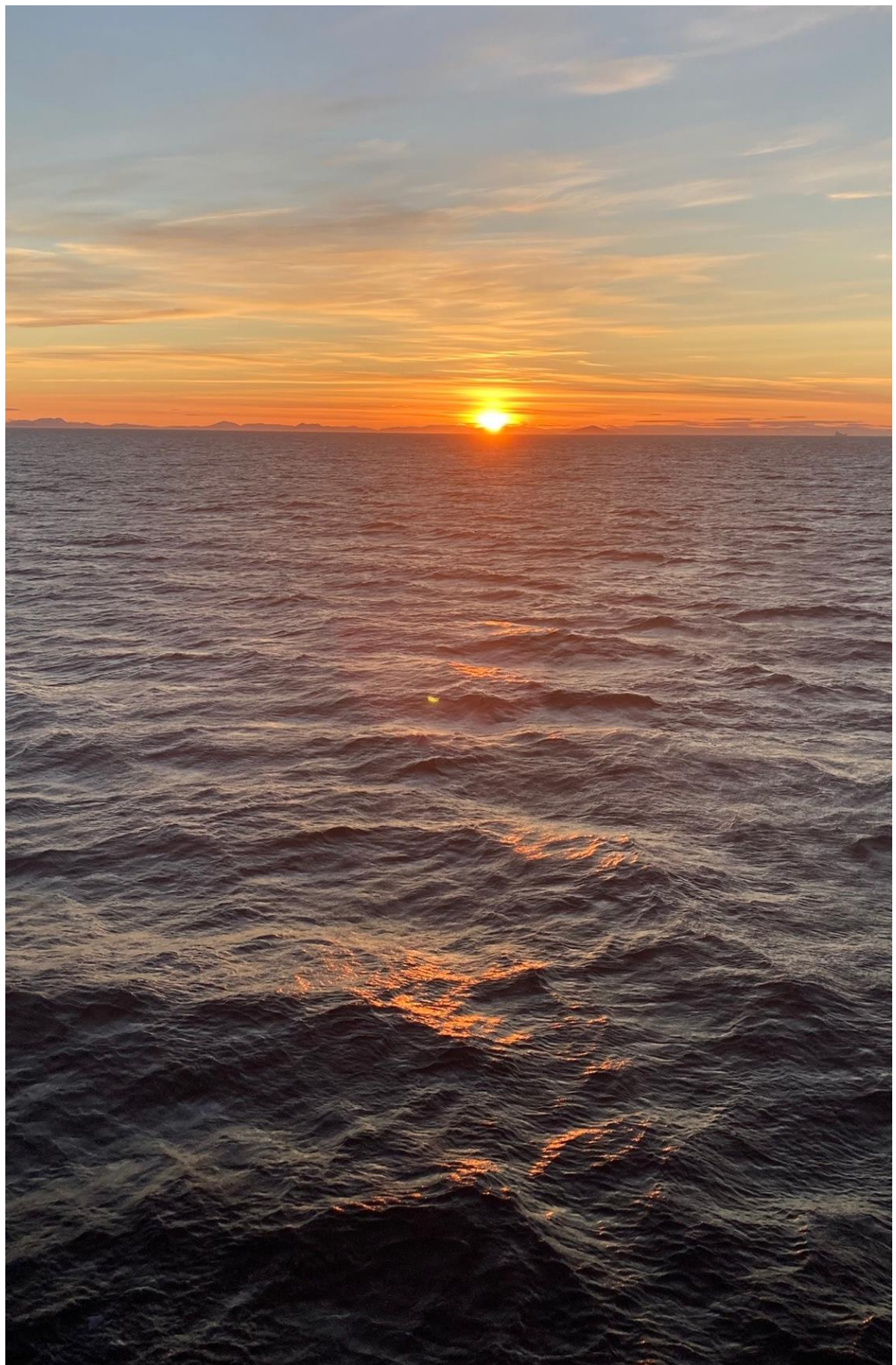
While my model predicts a decline in ecosystem functioning with increased "borealisation" across all my scenarios, the weakest effect occurs at the polar front transition where an admixture of species and functional groups from the northern and southern species pools are supported. Although the precise physical location of the front is contested (Oziel et al. 2016; 2017), the zone exhibits a relatively stationary behaviour (Onarheim & Teigen, 2018) and is becoming more persistent (Barton et al. 2018). As species are extirpated, co-extinctions selectively remove the most resistant taxa first, which may have acted to delay the effects of community homogenisation (Ellingsen et al. 2020; Frainer et al. 2017; Frainer et al. 2021; McKinney and Lockwood, 1999) and associated decline in ecosystem functioning (Tilman et al. 1997). A second possibility is that the seabed within this location experiences significant environmental fluctuations (Appendix D figure S1) and as disturbance history can condition resilience (Keith et al. 2008; Renes et al. 2020), this may also have suppressed any decline in functioning. This finding is important because it argues that complex relationships exist between patterns of species turnover and ecosystem functioning,

and that the short- and long-term dimensions of species functionality are not sufficiently well-constrained in current ecosystem models.

My study design allowed us to compare the response of northern and southern pools of species (Jørgensen et al. 2015; Solan et al. 2020c), allowing establishment of any generalities associated with species loss under climate change. I find that species contributions to functioning are dominated by a subset of taxa and that the greatest losses of functioning occur at low levels of perturbation despite high numbers of compensating species. Hence, the potential or probability for compensatory dynamics countering the consequences of biodiversity loss will depend on the level and extent of functional redundancy (Naeem & Wright, 2003) and the replacement taxa (Garcia et al. 2021), the mechanisms of both are known to depend on the factors driving local extinction (Fetzer et al. 2015); if pivotal species are among the most susceptible to changing conditions, then there is more certainty that ecosystem functioning will decline (Jonsson et al. 2003; Solan et al. 2004a). Indeed, having functionally dominant species that are unique to the community, or a selection of taxa that affect functioning similarly, but also exhibit similar responses to perturbations, could lead to an acceleration in functional decline due to insufficient functional replacement.

A contemporary focus in ecology is deciphering variations in the relationship between biodiversity and ecosystem function across local and regional spatio-temporal scales (Gonzalez et al. 2020). My findings reveal that the shape, magnitude, and variability of post-extinction community functioning are moderated by the local environmental conditions (Ratcliffe et al. 2017) and acknowledge the significance of environmental heterogeneity (Bulling et al. 2008, Boyd et al. 2016; Wohlgemuth et al. 2017, Gammal et al. 2020), species arrangement (Wohlgemuth et al. 2016), vulnerability (McLean et al. 2019), and the expression of response traits (Williams et al. in press; Cassidy et al. 2020). Progression in this area will need to assess the suitability of conducting binary extinction assessments across extensive environmental gradients (Fukami & Wardle, 2005), as these are most likely to overlook the critical processes and compensatory effects that occur at the local scale and may lead to over- or underestimations of local biodiversity-ecosystem functioning changes (Yan et al. 2022). I contend that management and conservation efforts will benefit from considering the non-lethal effects of the climate crisis and, as climate change does not act alone (Brook et al. 2008, Hewitt et al. 2016), integrate the presence and intensity of other pressures that alter the context in which forcing occurs.

## Chapter 6    Synthesis



The Arctic Ocean's benthic ecosystems face rapidly increasing climate stress, but research on the direct implications is limited in comparison to non-benthic ecosystems (Deb and Bailey, 2023). However, simultaneous alterations in the diversity, composition (Degen, 2015; Grebmeier et al. 2015; Waga et al. 2020) and trophic structure of assemblages (Kędra et al. 2019) are being documented. Even so, literature that only focuses on changes in the presence or proportional representation of species fails to capture subtle responses exhibited in behaviour, morphology and biochemical processes that are exhibited before these realised ecological changes (Stark et al. 2019; Peck, 2011). These responses can also subsequently modify biologically mediated biogeochemical processes (Furukawa, 2005) and resistance to further change (Wood et al. 2008; 2011), preclude ecosystem-wide changes (Hooper et al. 2012) and impact ecological goods and services for human wellbeing (Snelgrove et al. 2014). To achieve a comprehensive understanding of the Arctic benthos' vulnerability to climate change, which is necessary for effective conservation efforts, it is imperative to investigate the cause, effects and generality of these underpinning responses (Pörtner & Peck, 2010; Williams et al. 2008).

The chapters in this thesis provide insight into how the expression of climatic forcing under context-specific circumstances affects benthic macroinvertebrate behavioural, physiological, and functional performance in Arctic environments. Here, I demonstrate that;

By altering their expression of behaviour (**Chapter 2**) and physiology (**Chapter 3**) in response to a change in temperature and [CO<sub>2</sub>], species modify aspects of their sediment reworking and burrow ventilation activity (**Chapter 2**) which in turn, has a fundamental effect on the magnitude and direction of benthic nutrient cycling (**Chapter 2**)

Biological variation (within individuals (**Chapter 3**, **Chapter 4**), within species (**Chapter 2**, **Chapter 3**) and between species (**Chapter 2**, **Chapter 3**, **Chapter 5**), species-interactions (**Chapter 5**) and environmental context (**Chapter 2**, **Chapter 3**, **Chapter 5**) are all critical in mediating organism and community-level responses to climatic forcing.

It is evident that species and conspecific individuals inherently vary in trait expression (Cassidy 2020) due to a diversity of biotic and environmental conditions (Alibert et al. 2010). These variations can impact functional processes (Wohlgemuth et al. 2017), community net behaviours

(Cassidy et al. 2020), and ecosystem functioning (Bolnick et al. 2011; Godbold et al. 2011). By manipulating seawater conditions that simulate the effects of ocean warming and acidification, I revealed that species and conspecifics also exhibit variable responses in their behaviour (**Chapter 2**) and physiology (**Chapter 3**) to climate-driven environmental changes, that led to alterations in their mediation of nutrient cycling at the sediment-water interface (**Chapter 2**). Behavioural and physiological responses to climatic forcing are not novel findings (Briffa et al. 2012; Kroeker et al. 2013) nor is the fact that it coincided with a change in related levels of ecosystem functioning (Godbold & Solan, 2013; Connell et al. 2013). However, ocean warming and acidification also reduced intra-specific variability in trait expression (**Chapters 2 and 3**), and as this can alter the capacity of species to adjust further (Wood et al. 2008; Gilbert & Miles, 2019), is indicative of the constraining effect climatic forcing has on phenotypic plasticity (Bonamour et al. 2019; and references therein) and subsequently, stability of ecosystem functioning (Wright et al. 2016).

Polar-adapted marine ectotherms that survive a change in environmental conditions can exhibit whole organism performance levels that are evident of successful acclimation (Peck et al. 2014), but this outcome may take extended periods of time to develop (Peck, 2011; Peck et al. 2014) and risks impeding other biological functions in the process (Peck et al. 2004). After a year-long experimental exposure to near-future ocean warming and acidification, I observed no significant differences in species-specific respiration and excretion rates, reflecting acclimation (Asnicar et al. 2021), but did find intra- and inter-specific changes in growth and/or biochemical status (**Chapter 3**) suggesting that multiple strategies within and between species may be utilised to cope with climatic forcing. The diversity in response capacities among coexisting (Pagès-Escolà et al. 2018), competing (Baskett et al. 2014), and functionally similar organisms (**Chapter 2**) increases the probability of some organisms persisting through environmental conditions and functionally compensating for the loss of vulnerable species following environmental perturbations (Bernhardt et al. 2013; Hooper et al. 2005). However, persistence alone does not guarantee maintained contributions to functional processes (**Chapter 2**), as compromising physiological processes within metabolic pathways (**Chapter 3**) may not ensure future tolerance (Heuer & Grosell, 2014). This is especially relevant as climate forcing intensifies over time and environmental thresholds are approached (Pucko et al. 2011). Therefore, it is crucial to assess multiple proxies for both acute and chronic physiological responses to avoid false positives regarding acclimation capacities and ensure accurate predictions of species vulnerability to climatic forcing (Magozzi & Calosi, 2015).

The diversity of responses I observed underlines an important consideration in the context of ecosystem conservation, especially when the practice of trait groups (such as size groups, or functional groups) is a commonly used way of reducing complexity and attempting to carry sufficient information between levels (Wardle & Zackrisson, 2005; Michaud et al. 2005). This

approach generalises response patterns when assessing the ecological impacts of environmental change to simplify complex natural communities for management efforts, but this is not consistent with the findings of my research and leaves projections subject to a great deal of uncertainty (Clark et al. 2011; Evans, 2012). Indeed, organisms with varying capacities to respond in terms of behaviour (**Chapter 2**; Ferrari et al. 2011) and physiology (**Chapter 3**; Clark et al. 2017) often display distinct vulnerabilities to climatic forcing (McKinney, 1997; Van Colen et al. 2020). Moreover, as the magnitude of climate change increases and the interactive effects of multiple anthropogenic perturbations progress, species responses may become increasingly divergent and lead to shifts in dominance patterns (Pucko et al. 2011) and subsequent changes in biodiversity-ecosystem functioning (**Chapter 5**), particularly in the presence of context-specific environmental thresholds (Stevens, 1989; **Chapters 2 and 3**). Therefore, climate change adaptation strategies should move away from uniform grouping approaches (Murray et al. 2014; Hale et al. 2014) and instead consider the presence of intra-specific responses to climate change (Stralberg et al. 2015; Cianciaruso et al. 2009; Des Roches et al. 2018; McEntire et al. 2022), particularly in situations where trait expression naturally varies within species (Cassidy et al. 2020). This can provide a more complete view of communities and the processes driving their assembly (Siefert, 2012) and in some contexts, mirror patterns of inter-specific variation (Albert et al. 2010; Brousseau et al. 2013) where processes affecting within-population diversity may be the same as those that caused species divergence.

The functional role of a species is not only contingent upon the environmental setting (Fetzer et al. 2015) but individuals from different abiotic and biotic contexts can also exhibit divergent behaviors and functional contributions (Cassidy et al. 2020; Wohlgemuth et al. 2017). Through studying an environmental transition zone, I discovered that the impact of climate-driven environmental change is also context-dependent for individuals, species (**Chapters 2 and 3**), and entire communities (**Chapter 5**). Indeed, organisms originating from more heterogeneous environments are expected to display greater phenotypic plasticity when confronted with climatic stressors (Peck et al. 2014; von Dassow et al. 2015) as environmental variability expands the thermal tolerance range (Stevens, 1989; Stearns, 1992; Sunday et al. 2011; Somero, 2010). However, this advantage will likely be temporally constrained as the combined effect of environmental fluctuations and multifaceted climate change may expose organisms to extremes that exceed their thresholds of tolerance long before mean climate change exerts such influence (Hollander and Butlin, 2010; Service, 2012; Flynn et al. 2015). The importance of including natural environmental fluctuations in climate change manipulation experiments cannot be overstated. Differences in species' responses to environmental fluctuations stabilise community dynamics (Leary & Petchey, 2009) but also cause fluctuations in ecosystem functioning by strengthening the

dominance of species that perform best under those conditions (Yachi & Loreau, 1999). As a result, studies that incorporate such fluctuations have produced different outcomes from those that do not (Cornwall et al. 2013). Moreover, modelling simulations suggest that climate variability, in addition to mean climate change, will intensify in the coming decades (Bathiany et al. 2018, IPCC, 2021). Consequently, environmental heterogeneity, and its effects on system behaviour (Bulling et al. 2008; Godbold et al. 2011) is set to increase, highlighting the need for more realistic biological manipulation experiments that incorporate natural fluctuations (Boyd et al. 2016, Godbold and Solan, 2013).

As currently coexisting species exhibit variable sensitivities and responses to climate change (**Chapters 2 & 3**), we will likely observe the emergence of no-analog communities in the near future (Lurgi et al. 2012), leading to the disruption of already established interactions and facilitation of novel ones (Montoya and Raffaelli, 2010, Woodward et al. 2010). Although sophisticated, multi-component diagenetic models of biodiversity change and ecosystem functioning already exist (Garcia et al. 2021, Thomsen et al. 2017), these projections do not regularly integrate the complexities of interactions between coexisting taxa despite its role in facilitating ecosystem functioning (Clare et al. 2016, Emmerson et al. 2001). By using positive and negative correlations between coexisting species to parameterise co-dependencies (**Chapter 5**), I found this leads to exclusive patterns of species turnover in response to climate-driven environmental change compared to without co-dependencies. Furthermore, integrating co-dependencies led to both an enhanced loss of functioning through localised co-extinctions (Strona and Bradshaw, 2018) and reduced loss of functioning via an enhanced compensation effect from both local and immigrating taxa. Species that are initially functionally redundant within the local community may functionally compensate for the loss of others (Thomsen et al. 2017; 2019), and even instigate greater functioning than before (Mulder et al. 2001) by becoming essential performers or partners in the new inter-specific interactions (Fetzer et al. 2015) with facilitative taxa immigrating from the regional species pool (Garcia et al. 2021). The impact of climate change is indeed both shaped by (Hughes, 2012) and shapes (Harley, 2011; Blois et al. 2013) species interactions, with the results of altered species interactions ranging from species becoming rare to disproportionately abundant (Van der Putten, 2010). Therefore, if we do not incorporate codependent responses into our analyses, we risk making inaccurate predictions about biodiversity change (Alexander et al. 2015) that will feed into ineffective mitigation strategies on the effects of climate change on ecosystem functioning.

Multifaceted relationships between biodiversity and ecosystem function are known across a range of spatial and temporal scales (Gonzalez et al. 2020, and references therein), but assessments primarily focus on broader systems (Walther et al. 2002, Walther, 2010) which

neglect neighbouring communities that exhibit distinct structures, resulting in divergent resilience and response mechanisms when exposed to similar climatic influences. Here, I find that the trajectory of functioning following local extinction events diverge across the Polar Front, reflecting compositional changes (Solan et al. 2020c; Jørgensen et al. 2015) of surviving communities (**Chapter 5**). As each local assemblage contains its own assortment of interactions (Fetzer et al. 2015), response capacities (**Chapters 2 and 3**), and spread of taxa-specific contributions to functioning (Solan et al. 2020c), the level of functional redundancy and capacity to compensate (Thomsen et al. 2017, 2019) differs and leads to distinctive differences in the direction and magnitude of net functioning. Where the communities meet, characterised by greatest environmental variability and admixture of species from the North and South assemblages (Solan et al. 2020c; Jørgensen et al. 2015), I find that the impact of localised species loss on ecosystem function is at its weakest (**Chapter 5**). Habitat heterogeneity and connectivity play crucial roles in enhancing the resilience of communities in the face of extreme events such as local extinction events (Pelletier et al. 2020; and references therein) but the magnitude of effect depends on the scale of investigation (Pedruski & Arnott, 2011; Williams et al. 2010; Van Gaever et al. 2010). Furthermore, the response and recovery processes of communities following disturbances are also dependent on the size and extent of the affected area (Zajac et al. 1998). Addressing context and scale dependence of responses to climate change (**Chapters 2 to 5**) is essential for reducing uncertainty in large-scale assessments (Yan et al. 2022; Catford et al. 2022), unravelling BEF relationships (Gonzales et al. 2020), and producing reliable estimates of ecosystem dynamics (Evans 2012). Therefore, integrating long-term studies, considering environmental and biological variability, and incorporating paleoclimatology research are imperative to enhance our understanding and inform effective conservation strategies.

Even though human-driven global warming is not a recent discovery (Callendar, 1938) the bulk of our understanding on biodiversity responses to climate change are from short term experiments (Wernberg et al. 2012), with few exceptions (Godbold & Solan, 2013). Considering that the short- and long-term results of these experiments can fluctuate (Godbold & Solan, 2013; Melillo et al. 2017), the length of time required to provide definitive results is unknown. Additionally, many studies use shock-type stressor exposure at rates much faster than projected change (Cummings et al. 2011; Richard et al. 2012a; Byrne et al. 2020) and as such, whether these short-term studies truly capture the nature of organism responses to climate change is up for debate. In my investigation of species responses to historical climate change, I found evidence of variability in both long-term trends and short-term fluctuations of deep-water temperature and seawater barium, a proxy for nutrient cycling in open waters (Chow & Goldberg, 1960), and influence of biological variability at both the inter-individual and intra-individual levels (**Chapter 4**).

Paleoclimate has had strong impacts on past biodiversity dynamics and left legacies in contemporary patterns (Svenning et al. 2015), but little empirical work has been done on footprints in ecosystem functioning. Utilising long-lived organisms for the purpose of paleoclimatology is a promising avenue for understanding how complex interactions between biodiversity-ecosystem functioning and climate change evolves over time. Although still in its early stages, the integration of paleo studies (**Chapter 4**), and investigations of context (**Chapters 2, 3 and 5**), into ecological response research frameworks enables a more holistic codetermination of the capacity of species to undergo niche shifts in response to environmental changes (Fritz et al. 2013; Jezkova et al. 2011). This information is crucial for predicting biotic responses to future environmental changes.

## 6.1 Future directions

This thesis highlights the crucial importance of considering both environmental and biological contexts when studying the responses of organisms to climatic forcing. At the Arctic seafloor, I provide robust evidence that climatic forcing has, is, and will continue to be a major influence on biodiversity and ecosystem functioning, and the degree of variation in organism responses significantly affects the outcome in *per capita* functional contributions and community net output. It is anticipated that the coming decades will see unprecedented change in the environmental context (IPCC, 2021), biological composition (Mulder et al. 2015), and functional contributions (Thébault et al. 2014, Douglas et al. 2019) of natural systems with biodiversity either adapting, dispersing, or going extinct (Parmesan, 2006, Aitken et al. 2008, Dawson et al. 2011; Hoffman and Sgrò 2011). One frequently debated proposition on Arctic change is that longer and more extensive open water conditions, especially across shelf seas, could lead to substantive changes in ecological dynamics (Arrigo and van Dijken, 2015, Slagstad et al. 2015, Post et al. 2013). Indeed, available evidence suggests that environmental conditions across the Barents Sea, and other Arctic inflow shelves, will become more akin to those of sub-Arctic seas (Ingvaldsen et al. 2021; Csapo et al. 2021) though the dynamics controlling the Polar Front are still poorly pinned down (Oziel et al. 2016; Barton et al. 2018). To holistically assess how this will impact the Arctic benthos, and build upon the findings from this thesis, emphasis is now needed within the following areas.

**Greater integration of unambiguous, hypothesis-driven investigations to unravel the key mechanisms, alone and in concert, driving Arctic ecosystem responses is paramount for advancing predictive capabilities of impacts of climatic forcing.** The current capacity to explore the interactions (additive, synergistic, or otherwise) among climate change factors in the Arctic is limited, and *in-situ* benthic assessments have been primarily confined to confirmatory

observations of change (Degen, 2015, Waga et al. 2020, Kędra et al. 2015) and assumed/extrapolated predictions (Renaud et al. 2019). The timescales over which the mean climate-change signature will become dominant, relative to natural fluctuations, will vary for both the various levels of biological organisation (Stark et al. 2019, Peck, 2011) and individual ecological properties (Boyd et al. 2016). Furthermore, any of the environmental changes driven by climatic forcing has the potential to individually affect biodiversity and ecosystem functioning, but as these changes rarely occur in isolation, it is necessary to consider the influence of multiple changes in concert (Gamfeldt, Roger, 2017) which is difficult to predict. Experimental research, which involves falsification of hypotheses and identifying mechanisms, is generally more persuasive than modelling studies, observations, logical arguments, or anecdotes, due to the statistical rigor and power of data analysis (Lawton, 1996) and ability to isolate factors of interest whilst controlling others. However, there is always a trade-off to consider between the spatial and temporal scales of investigation, the degree of replication (Raffaelli and Moller, 2000). By confining each investigation to a singular timepoint of sampling, I acknowledge the risk that the recorded responses may be a by-product of natural variation, an anomalous year, or a consequence of interactive effects from other driving factors before sampling, but still present a persuasive case through replicated experiments. To mirror the intricate structural and temporal context of natural communities under climatic forcing, alternative reconstruction approaches (**Chapter 4**) or the establishment of large-scale benthic model systems for long-term multi-trophic investigations (e.g., Goldenberg et al. 2018, Kim et al. 2018) are potential strategies. However, the latter is challenging to support within the constraints of short funding cycles in academia. In a blue-skies scenario, assembling communities in a controlled manner, focusing on specific functional groups, indicator species, and their interactions, could enable more precise monitoring and interpretation. The principles learned from both small- and large-scale experimental approaches, in combination with observational work, can be combined in models that will provide insights into the ecosystem consequences of climate-driven biodiversity loss (Naeem, 2006).

**A coordinated strategy concerning the timing, location, frequency, and methods of our future efforts is crucial for effectively directing our scientific actions and maximising their impact.** Not only are the functional roles of many benthic species still poorly constrained (Degen and Faulwetter, 2019) but the underlying evidence base is frustrated by the major spatiotemporal biases in scientific coverage (Figure 1.2, Figure 1.3) and subsequently outdated information of species inventories (Piepenburg et al. 2011). Where data has been collected, faunal composition and responses to climate change reflect proximity to Arctic vs boreal conditions (Jørgensen et al. 2015; **Chapters 2, 3, 5**), and baseline faunal activity is moderated by seasonal variations in sea ice extent that influence food supply to the benthos (Solan et al. 2020c). Both seasonal and

interannual variability are identified to modify processes at the base of the food chain, with consequent effects through microbial and faunal processing, up to trophic interactions reaching top predators (Hutchison et al. 2020). However, trying to decipher the spatiotemporal paradigms of the Arctic benthos is not a straightforward process (e.g. (Berge et al. 2015)), with sea ice dynamics limiting available areas for year-round scientific expeditions but also moderating the effects of other anthropogenic drivers, such as trawling (Fauchald et al. 2021), and contaminants (Krumpen et al. 2019) which may make ecosystems more fragile and interact with climate in novel ways (Zscheischler et al. 2018). While longer and more extensive expeditions have proven to be both feasible and valuable (Nicolaus et al. 2022, Rabe et al. 2022, Shupe et al. 2022), embracing cutting-edge technologies such as remote sensing and Digital Twin environments will enhance accessibility to this outlying region (Yusuf, 2022) and ensure that our research efforts are conducted in an environmentally responsible manner.

**Effective incorporation of novel digital technologies is urgently required to revamp investigative frameworks and enhance the realism of predictive models.** Climate change intertwines with the exploitation of natural resources (Smalås et al. 2019), land use changes (Strona & Bradshaw, 2022), invasive species (Vetter et al. 2020), and pollutants (Alava et al. 2018), exerting cumulative pressures on ecosystems (IPCC, 2023). Consequently, predicting the trajectory of ecological responses is obscured with uncertainty as approaches are burdened with sacrificing scale, generality, realism, and/or precision (Evans, 2012). However, the convergence of key technological enablers like Cloud Computing, Big Data and Explainable Artificial Intelligence is poised to revolutionize ecological research (Goodwin et al. 2022; Yang et al. 2013; Pichler et al. 2019; 2023), comparable to what was witnessed during the emergence of the Internet of Things (Allan et al. 2018). Although there is a plausible cause for concern about the risk of accessible intelligent technologies for security (Iswarya, 2014), education and ethical research integrity (Abdalla and Abdalla, 2021), we cannot ignore the rapidly increasing presence in the daily lives of the public, industry and academia. AI applications and advanced digital technologies can optimize production efficiency (Shepley et al. 2021) and alleviate the burden of mundane administrative tasks, enabling ecologists to focus on data collection and addressing fundamental questions. Furthermore, these technologies have significant potential in integrating complex interactions within natural systems (Ashraf et al. 2015, Keller et al. 1997). Combined with theoretical frameworks and empirical data that link the causes, consequences, and variability of responses (**Chapters 2 to 5**) to multiple global change factors (Zhou et al. 2023) across different levels of biological organization (McEntire et al. 2022; Woodward et al. 2010), this, in turn, would support active management initiatives in inferring when and where ecosystem conservation efforts are

necessary (Lapeyrolerie et al. 2022) to enhance resilience in the face of rapidly changing environmental conditions.

**Production of a solution-based narrative that recognises biodiversity as a key ally in mitigating climate change impacts is essential for effective decision-making and policy formulation.**

Maintaining high levels of species richness and functional diversity can, for example, improve ecosystem resilience and stability by providing a large pool of species with potentially relevant traits under changing environmental conditions (Mulder et al. 2001, Fetzer et al. 2015). Transiting from documenting the negative impacts of change to formulating a socio-ecological, solution-based narrative will be effective in providing evidence to support decision- and policy-making across the Arctic (Solan et al. 2020b). To be successful, approaches involving multiple disciplines that mobilise and build on indigenous and local knowledge are urgently required (Falardeau et al. 2018, Falardeau and Bennett, 2020) and need to be supplemented by socio-ecological contributions to aid our understanding of cross-system dynamics. Unfortunately, the historical compartmentalization of terrestrial and marine disciplines (Raffaelli et al. 2005) has left large gaps in our understanding of the extent to which different landscapes are interconnected (Ward et al. 2017) and though a solution-based narrative has recently been proposed for the Arctic marine benthos (Solan et al. 2020a) a more unified assessment of its socio-ecological (Burgass et al. 2018) and socio-economic systems (Crepin et al. 2017, Scharffenberg et al. 2020, Townhill et al. 2022) is sorely needed.

## Appendix A      Appendix for Chapter 2

Figure S1 | The location of (a) the stations B13 and B16 in the Barents Sea relative to the generally accepted position of the oceanographic (Loeng, 1991, **grey line**) and benthic (Jørgensen et al. 2015, **dashed black line**) polar front, and (b) the Rothera Point station, western Antarctica.

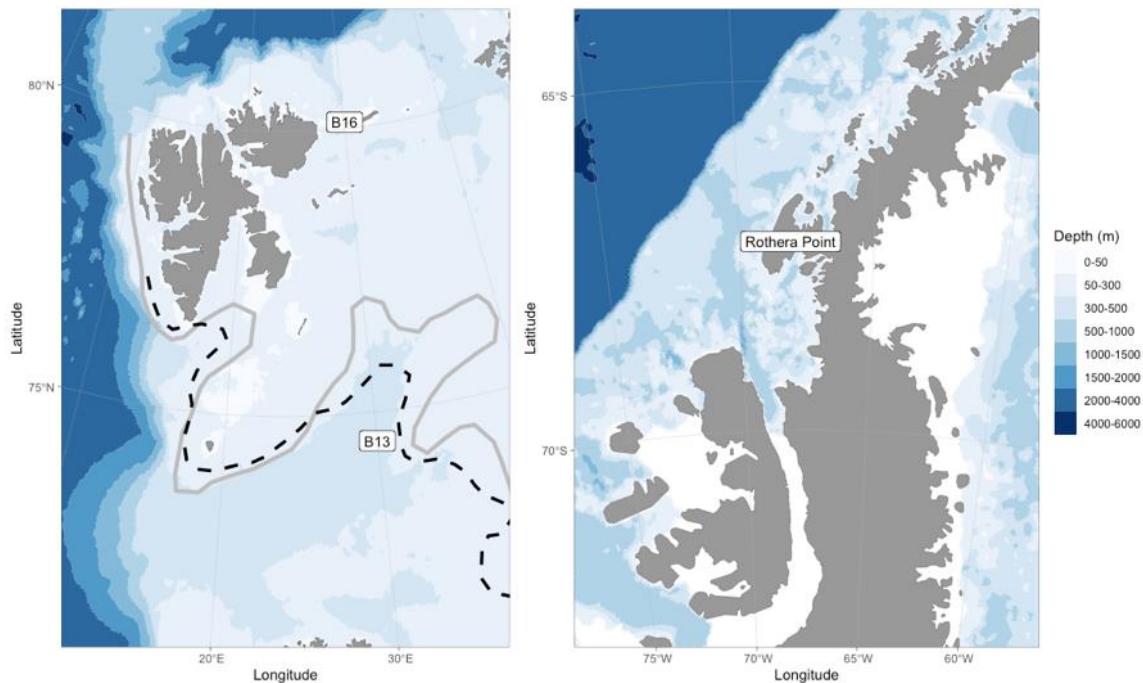


**Table S1 (next two pages):** Summary of the cruise event number from the ship log, date, timing, geographical position and water column depth for each (a) box core and (b) trawl obtained for the collection of sediment (S) and/or sediment-dwelling macrofaunal invertebrates (F) obtained during research cruise JR18006, RRS James Clark Ross (Barnes et al. 2018).

Table S1(a)

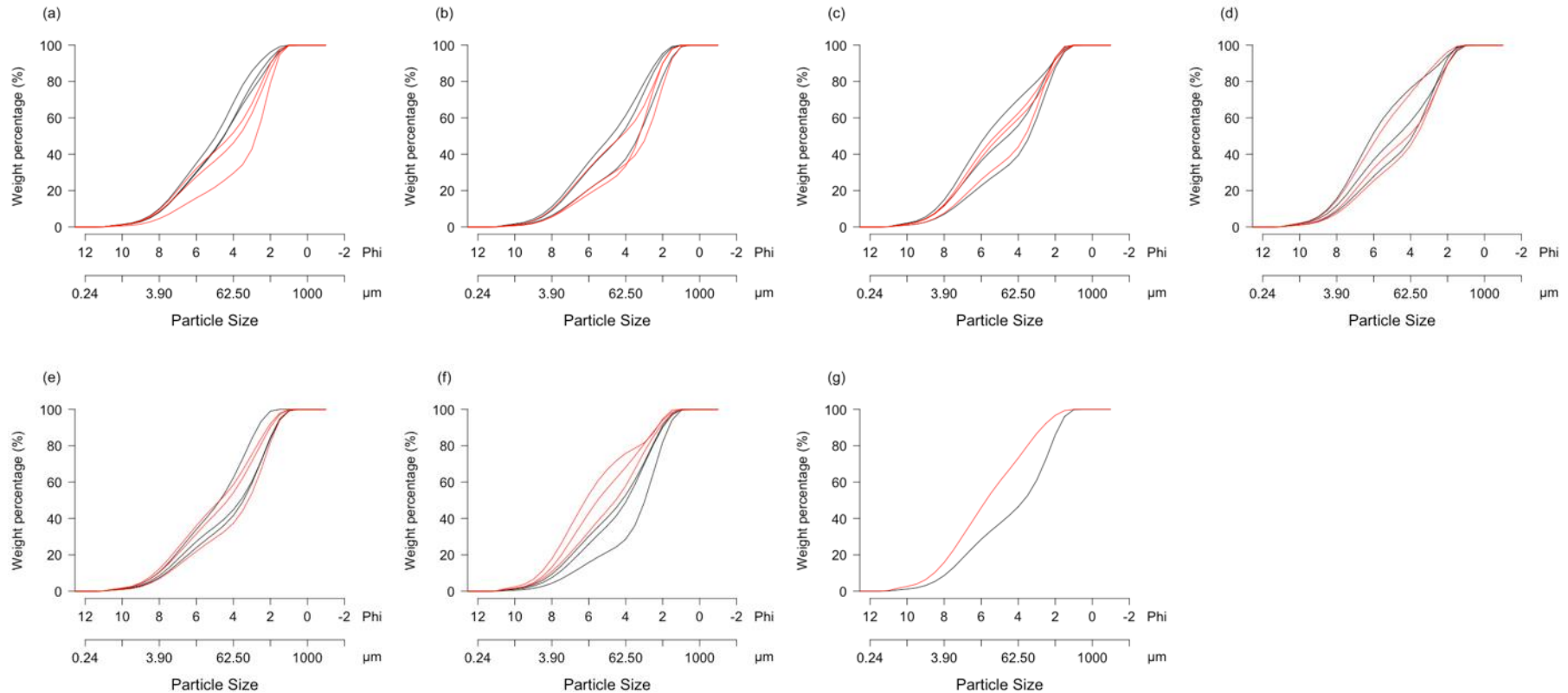
Station	Event	Date	Lat (°N)	Long (°E)	Time (UTC)	Depth (m)
B13	32 <sub>S,F</sub>	08/07/2019	74.46607	30.11835	18:14:45	354.59
B13	33 <sub>S,F</sub>	08/07/2019	74.46613	30.11831	18:52:08	354.21
B13	34 <sub>S,F</sub>	08/07/2019	74.46614	30.1184	19:23:06	354.19
B13	35 <sub>S,F</sub>	08/07/2019	74.46621	30.1184	20:02:01	357.10
B13	36 <sub>S,F</sub>	08/07/2019	74.46618	30.11864	20:33:04	354.41
B13	37 <sub>S,F</sub>	08/07/2019	74.46623	30.11868	21:05:04	354.38
B13	38 <sub>S,F</sub>	08/07/2019	74.46619	30.119	21:50:21	353.99
B13	39 <sub>S,F</sub>	08/07/2019	74.46626	30.11901	22:29:06	254.18
B13	40 <sub>S,F</sub>	08/07/2019	74.46625	30.1191	23:05:50	353.91
B13	41 <sub>S,F</sub>	08/07/2019	74.46627	30.11932	23:36:46	353.82
B13	42 <sub>S,F</sub>	09/07/2019	74.46632	30.1194	00:18:57	353.97
B13	43 <sub>S,F</sub>	09/07/2019	74.46632	30.11948	00:53:47	353.50
B13	44 <sub>S,F</sub>	09/07/2019	74.46631	30.11958	01:30:14	354.32
B14	105 <sub>S</sub>	13/07/2019	76.55291	30.61992	09:00:16	281.47
B14	106 <sub>S</sub>	13/07/2019	76.55282	30.61963	09:38:10	281.41
B16	161 <sub>S,F</sub>	17/07/2019	80.08478	30.15126	06:00:25	263.00
B16	162 <sub>S,F</sub>	17/07/2019	80.08561	30.14997	06:28:22	264.00
B16	163 <sub>S,F</sub>	17/07/2019	80.08785	30.1499	07:04:36	264.00

Table S1(b)

Station	Event	Date	Latitude (°N)			Longitude (°E)			Time (HH:MM, UTC)			Trawl time (mins)	Depth(m)
			On bottom	Trawl Start	Left bottom	On bottom	Trawl Start	Left bottom	On bottom	Trawl Start	Left bottom		
B13	53 <sub>F</sub>	09/07/2019	74.4972	74.49767	74.49857	30.0744	30.07926	30.08872	10:39	10:49	11:09	00:19	361.86
B13	54 <sub>F</sub>	09/07/2019	74.50071	74.50109	74.50149	30.11158	30.11768	30.12638	12:24	12:36	12:53	00:17	351.78
B13	171 <sub>F</sub>	24/07/2019	74.49889	74.4973	74.4963	29.99775	29.98403	29.97519	16:43	17:12	17:30	00:18	362.15
B13	172 <sub>F</sub>	24/07/2019	74.49567	74.49566	74.49568	29.9643	29.95472	29.94587	18:11	18:29	18:46	00:17	367.31
B13	173 <sub>F</sub>	24/07/2019	74.4964	74.49767	74.49861	29.93578	29.92737	29.92129	19:30	19:49	20:02	00:13	371.81
B13	174 <sub>F</sub>	24/07/2019	74.50068	74.50213	74.50327	29.90772	29.89843	29.89113	21:02	21:22	21:38	00:16	374.83
B13	175 <sub>F</sub>	24/07/2019	74.50524	74.50657	74.50765	29.87843	29.86988	29.86281	22:25	22:44	23:00	00:15	372.55
B13	176 <sub>F</sub>	24/07/2019	74.51009	74.5109	74.51229	29.84718	29.84188	29.83291	23:46	00:03	00:20	00:17	372.81
B13	177 <sub>F</sub>	25/07/2019	74.51637	74.51866	74.52021	29.81048	29.80509	29.80134	01:13	01:33	01:46	00:13	369.16

## Appendix A

**Figure S2 (next two pages):** Cumulative sediment particle size distributions ( $n = 3$ ) for the sediments used in aquaria containing *Astarte crenata* from (a) station B13 and (b) station B16, *Ctenodiscus crispatus* from (c) station B13 and (d) station B16, (e) *Cistenides hyperborea* from station B13, (f) *Aequiyyoldia eightsi* and (g) *Laternula elliptica*. Line colour indicates aquaria maintained under ambient (black) versus future (red) climate conditions.



**Table S2.** Summary of experimental design for investigating the effects of enhanced temperature and atmospheric [CO<sub>2</sub>] on species-specific behaviour and associated contributions to ecosystem process and functioning.

Species	Polar Region	Station	total <i>n</i> <sub>aquaria</sub>	Climate regimes	
<i>Astarte crenata</i>	Arctic	B13, B16	12	1°C, 400 <sub>[CO<sub>2</sub>]</sub> ppm	2.5°C, 550 <sub>[CO<sub>2</sub>]</sub> ppm
<i>Ctenodiscus crispatus</i>	Arctic	B13, B16	12	1°C, 400 <sub>[CO<sub>2</sub>]</sub> ppm	2.5°C, 550 <sub>[CO<sub>2</sub>]</sub> ppm
<i>Cistenides hyperborea</i>	Arctic	B13	6	1°C, 400 <sub>[CO<sub>2</sub>]</sub> ppm	2.5°C, 550 <sub>[CO<sub>2</sub>]</sub> ppm
<i>Aequiyyoldia eightsi</i>	Antarctic	Rothera	6	1°C, 400 <sub>[CO<sub>2</sub>]</sub> ppm	2.5°C, 550 <sub>[CO<sub>2</sub>]</sub> ppm
<i>Laternula elliptica</i>	Antarctic	Rothera	6	1°C, 400 <sub>[CO<sub>2</sub>]</sub> ppm	2.5°C, 550 <sub>[CO<sub>2</sub>]</sub> ppm

**Table S3 (next three pages):** Morphological measurements of (a) *Astarte crenata* (b) *Ctenodiscus crispatus* (c) *Cistenides hyperborea* (d) *Aequiylodia eightsi* and (e) *Laternula elliptica* listed by each climate treatment group (ambient vs future) .

Table S3(a)

Climate	Station	Shell Length (mm)	Shell Height (mm)	Shell Width (mm)
Ambient	B13	25.87	21.97	11.81
Ambient	B13	20.09	17.58	9.15
Ambient	B13	24.72	19.91	10.70
Ambient	B13	22.95	18.43	9.05
Ambient	B13	27.58	24.57	11.18
Ambient	B13	25.07	20.28	11.18
Ambient	B16	28.12	24.78	12.65
Ambient	B16	28.29	21.55	11.69
Ambient	B16	23.97	19.52	11.75
Ambient	B16	22.97	18.98	11.39
Ambient	B16	28.76	23.90	12.69
Ambient	B16	22.97	18.98	11.39
Future	B13	24.28	20.51	10.48
Future	B13	22.37	18.65	10.28
Future	B13	19.49	16.16	7.48
Future	B13	21.08	18.13	8.88
Future	B13	18.14	16.51	8.89
Future	B13	17.68	14.61	7.38
Future	B16	29.63	24.77	12.44
Future	B16	30.16	25.37	12.55
Future	B16	29.19	24.71	12.97
Future	B16	28.40	22.95	11.71
Future	B16	27.14	22.26	13.21
Future	B16	26.04	20.47	12.37

Table S3(b)

Climate	Station	Arm length (mm)	Pit length (mm)
Ambient	B13	17.53	10.38
Ambient	B13	13.13	8.41
Ambient	B13	18.17	11.11
Ambient	B13	16.98	10.48
Ambient	B13	13.90	10.88
Ambient	B13	17.25	10.13
Ambient	B16	23.33	16.13
Ambient	B16	17.78	10.10
Ambient	B16	10.64	8.32
Ambient	B16	14.79	7.33
Ambient	B16	18.78	10.88
Ambient	B16	11.52	6.98

Future	B13	16.75	11.08
Future	B13	19.49	12.38
Future	B13	17.05	11.05
Future	B13	15.32	9.44
Future	B13	11.74	9.27
Future	B13	14.40	8.66
Future	B16	16.83	10.88
Future	B16	17.13	9.07
Future	B16	17.08	11.65
Future	B16	15.99	10.06
Future	B16	15.12	9.45
Future	B16	11.70	7.99

Table S3(c)

Climate	Station	Cone length (mm)	Anterior aperture (mm)
Ambient	B13	60.68	8.08
Ambient	B13	57.09	7.14
Ambient	B13	57.98	8.03
Ambient	B13	67.38	8.69
Ambient	B13	66.07	6.98
Ambient	B13	35.78	6.74
Future	B13	55.18	7.36
Future	B13	56.23	7.58
Future	B13	40.88	5.95
Future	B13	61.38	7.88
Future	B13	59.16	7.78
Future	B13	48.74	6.88

Table S3(d)

Climate	Shell Length (mm)	Shell Height (mm)	Shell Width (mm)
Ambient	22.42	14.11	6.41
Ambient	16.36	11.00	3.99
Ambient	19.11	11.75	5.90
Future	19.28	12.56	5.80
Future	24.12	15.01	7.55
Future	20.90	13.43	6.66

Table S3(e)

Climate	Shell Length (mm)	Shell Height (mm)	Shell Width (mm)
Ambient	64.71	44.88	34.20
Ambient	61.97	41.85	27.63
Ambient	66.98	49.33	34.09
Future	50.82	38.41	26.53
Future	48.38	36.52	27.48

## Appendix A

Future	72.63	50.61	37.16
--------	-------	-------	-------

**Figure S3:** System of (a) interconnected insulated fibreglass seawater baths (lids removed, LWH: 1.2 x 1.2 x 0.8m) used to house the aquaria (following Table S1), with temperature controlled by a chiller (located top left of panel (a)). Aquaria were randomly allocated to water baths within a climate treatment, randomly positioned within each water bath, and (b) continually aerated by bubbling through a glass pipette linked to a controllable air supply (grey ducting). The green coloration in each aquarium are the luminophore particulate tracers used to track infaunal particle mixing. Water bath temperatures were controlled ( $\pm 1^{\circ}\text{C}$ ). Water buckets pictured were used for routine partial water exchanges and pre-chilled to match the temperature of each climate treatment.

Figure S3(a)

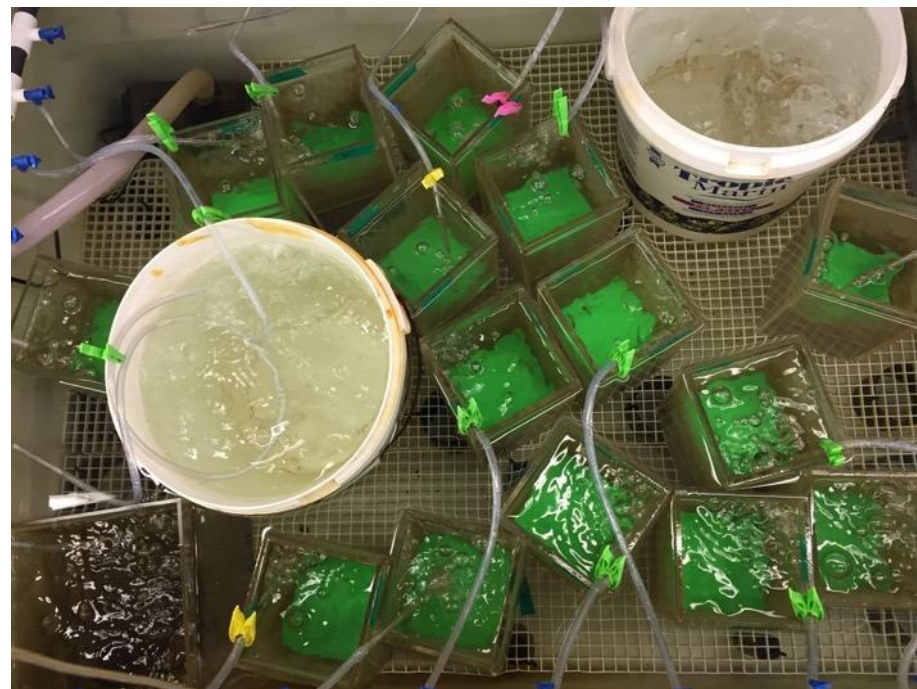
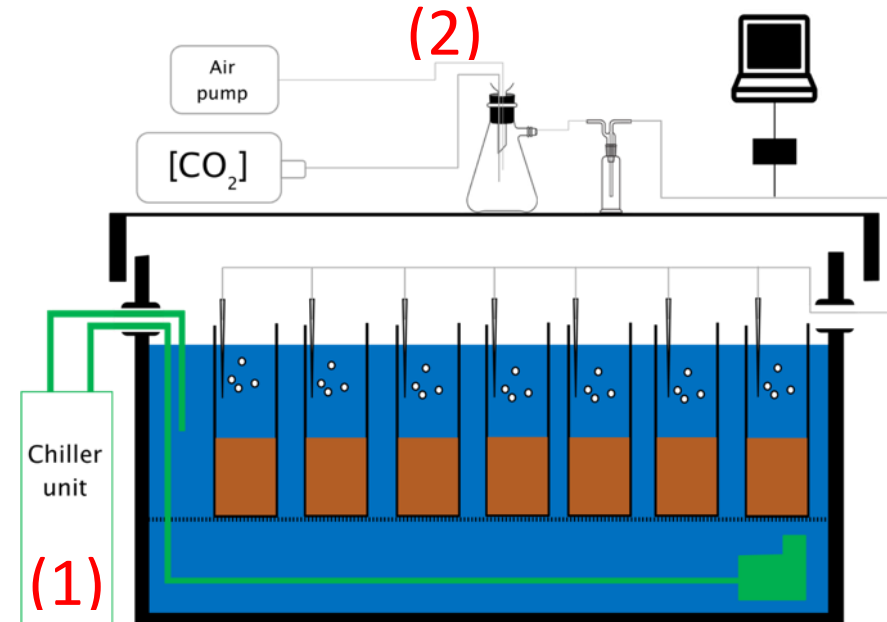
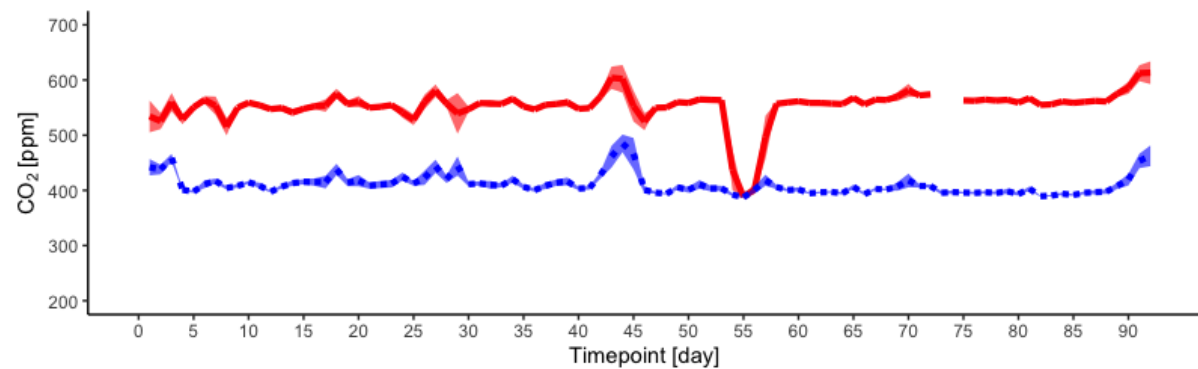


Figure S3(b)



**Figure S4:** Recorded mean daily  $[\text{CO}_2]$  in all aquaria maintained under ambient (blue dot-dash line) and future (red line) environmental conditions (92 days; 21<sup>st</sup> October 2019 to 21<sup>st</sup> January 2020).  $[\text{CO}_2]$  concentrations were measured continuously with an infrared gas analyser (Licor LI-840A). Filled area around the trend is representative of 1 standard deviation.



**Figure S5:** Monthly seawater carbonate chemistry measurements in aquaria maintained under ambient (blue) and future (red) climate conditions. Temperature ( $^{\circ}\text{C}$ ), Salinity,  $\text{pH}_{\text{NBS}}$  and total alkalinity ( $\text{A}_T$ ,  $\mu\text{mol kgSW}^{-1}$ ) were measured directly from each aquarium and were used to calculate dissolved organic carbon (DIC,  $\mu\text{mol kgSW}^{-1}$ ),  $\text{pCO}_2^{\text{SW}}$  ( $\mu\text{Atm}$ ), saturation states for calcite ( $\Omega_{\text{Calcite}}$ ) and aragonite ( $\Omega_{\text{Aragonite}}$ ), bicarbonate ( $\text{HCO}_3$ ,  $\mu\text{mol kgSW}^{-1}$ ) and carbonate ( $\text{CO}_3$ ,  $\mu\text{mol kgSW}^{-1}$ ) were calculated using *CO2calc* (Robbins et al. 2010).

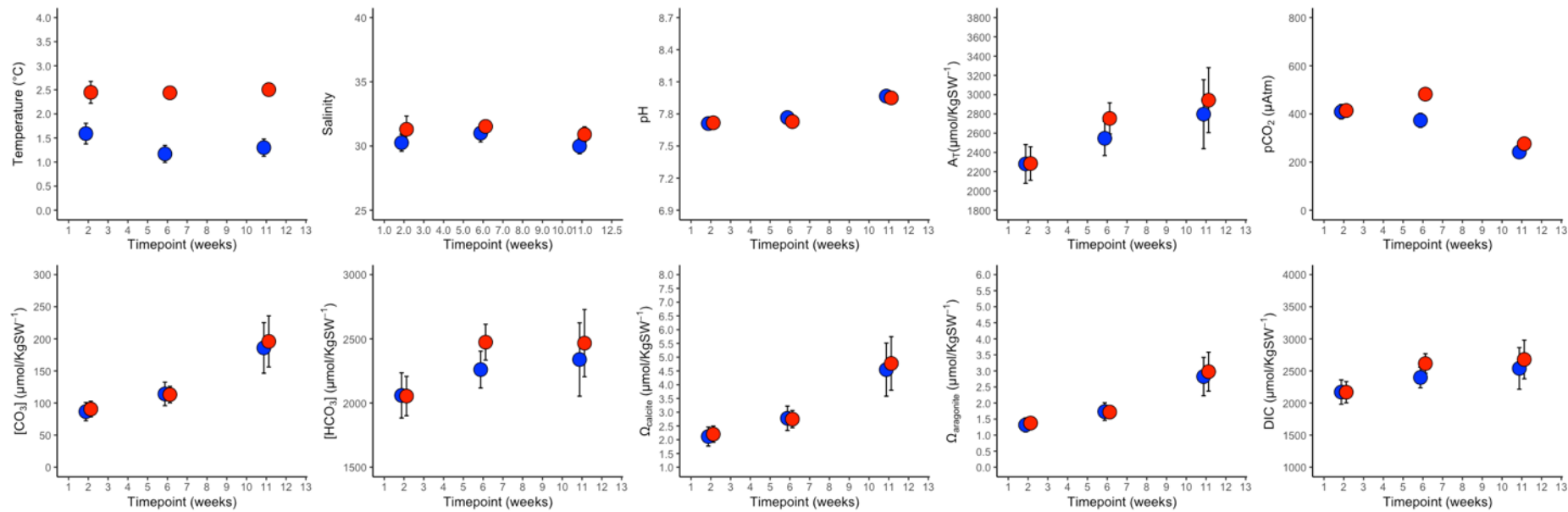


**Table S5 (next three pages):** Morphological and biomass measurements of (a) *Ctenodiscus crispatus* (b) *Cistenides hyperborea* (c) *Aequiyooldia eightsi* used for behaviour measurements.

Table S5(a)

Climate	Station	Arm length (mm)	Pit length (mm)	Biomass (g)
Ambient	B13	19.50	11.80	2.36
Ambient	B13	21.30	11.50	3.29
Ambient	B13	16.90	10.50	2.46
Ambient	B16	18.90	11.00	2.76
Ambient	B16	21.30	11.60	4.87
Ambient	B16	10.90	6.00	0.54
Ambient	B16	15.30	9.00	1.02
Ambient	B16	12.20	7.20	0.91
Future	B13	13.30	9.50	1.40
Future	B13	20.60	9.00	3.89
Future	B13	13.10	8.50	0.92
Future	B13	14.50	9.30	1.58
Future	B16	18.90	10.40	2.64
Future	B16	11.50	9.10	2.09
Future	B16	18.50	9.20	2.22
Future	B16	12.60	10.50	2.21
Future	B16	14.40	9.50	1.29
Future	B16	12.30	7.60	0.82

Table S5(b)

Climate	Station	Cone length (mm)	Anterior aperture (mm)	Biomass (g)
Ambient	B13	61.60	8.00	2.21
Ambient	B13	57.20	7.90	1.77
Ambient	B13	57.40	8.00	1.92
Ambient	B13	66.50	7.90	1.98
Ambient	B13	42.10	6.60	1.15
Future	B13	55.70	7.00	1.48
Future	B13	54.70	7.70	2.19
Future	B13	62.10	6.80	2.05
Future	B13	42.80	6.00	0.82
Future	B13	62.50	7.50	1.71
Future	B13	49.80	6.70	1.17

Table S5(c)

Climate	Shell Length (mm)	Shell Height (mm)	Shell Width (mm)	Biomass (g)
Ambient	22.40	19.70	6.20	1.52
Ambient	16.20	10.10	5.00	0.66
Ambient	18.80	12.40	5.90	0.99
Future	19.80	13.20	6.60	1.00
Future	24.00	14.70	6.60	1.77
Future	21.00	13.30	6.60	1.23

**Figure S6** Selected time-lapse (3 frame s<sup>-1</sup>, SkyStudioPro) images capturing movements of (a) *Aequiyyoldia eightsi* (left viewing tray) and *Ctenodiscus crispatus* (right viewing tray) under future climate treatment (file: timelapse1.mp4), (b) *Ctenodiscus crispatus* (left viewing tray) and *Cistenides hyperborea* (right viewing tray) under ambient climate treatment (file: timelapse2.mp4). Frames are timestamped.

Figure S6(a)



Figure S6(b)



**Figure S7 (next four pages):** Replicate ( $n = 3$ ) stitched f-SPI images for aquaria containing (a) *Astarte crenata* from (a) station B13 under ambient conditions (b) station B13 under future climate conditions (c) station B16 under ambient conditions and (d) station B16 under future climate conditions. The images (four aquarium sides, each 19cm, stitched together) are presented. The green coloration is the luminophore tracers after 10 days of incubation.

Figure S7(a)

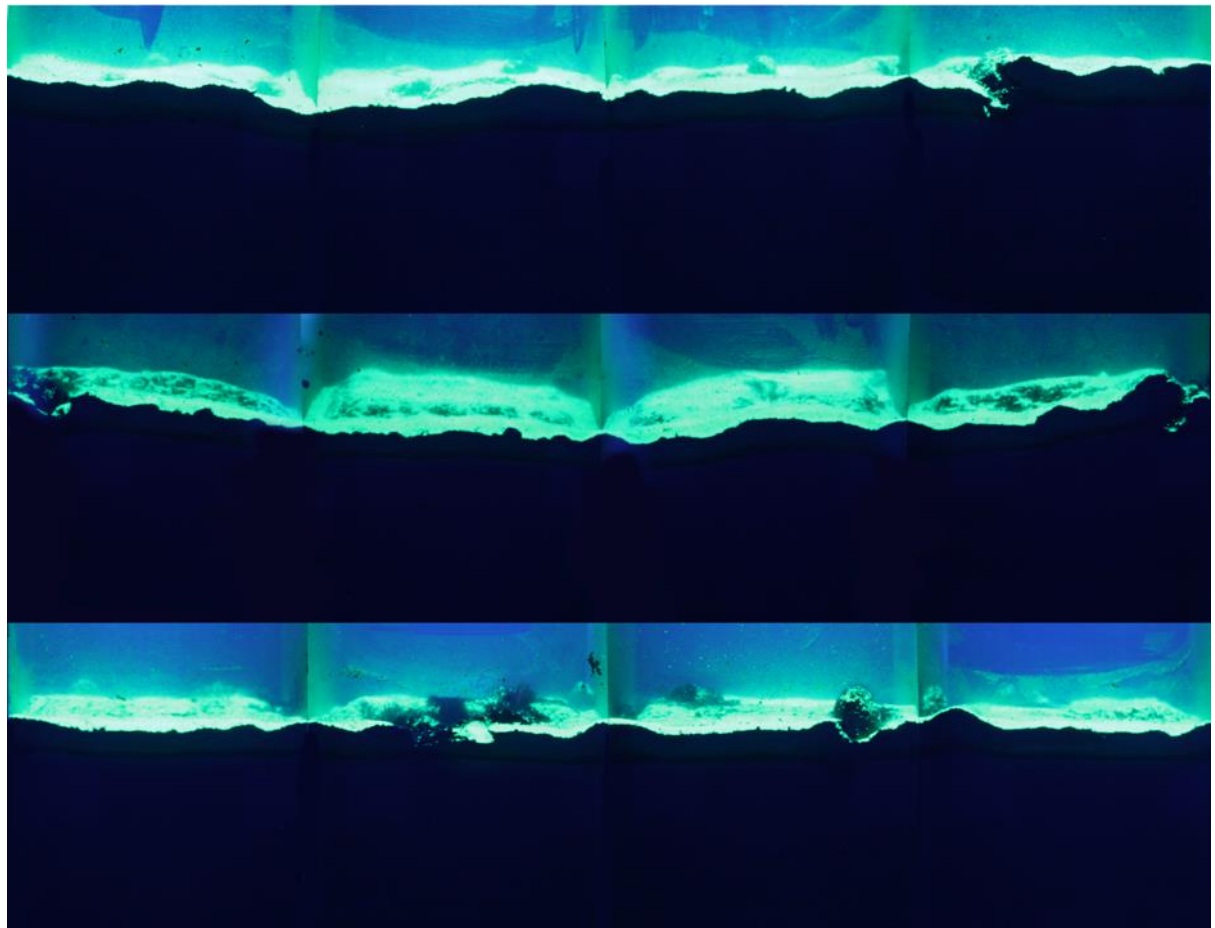


Figure S7(b)

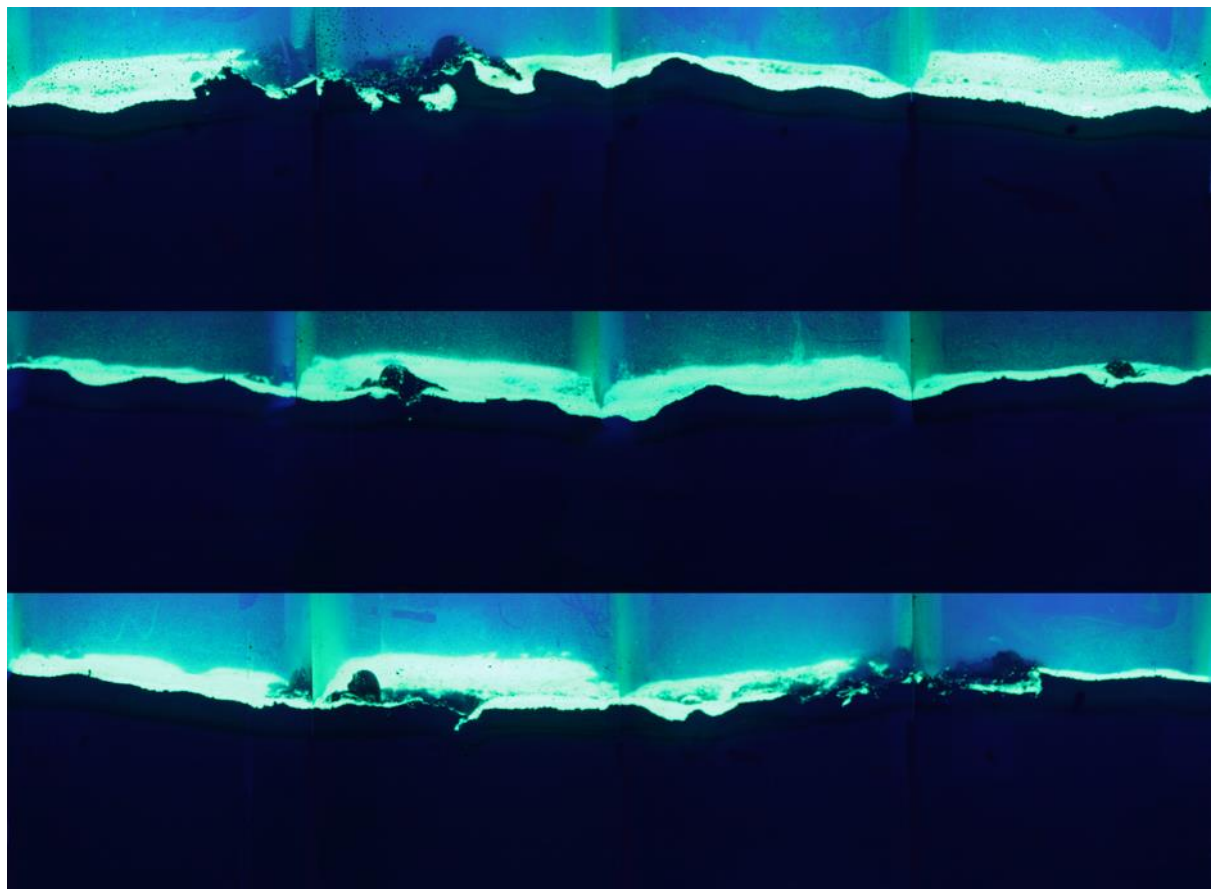


Figure S7(c)

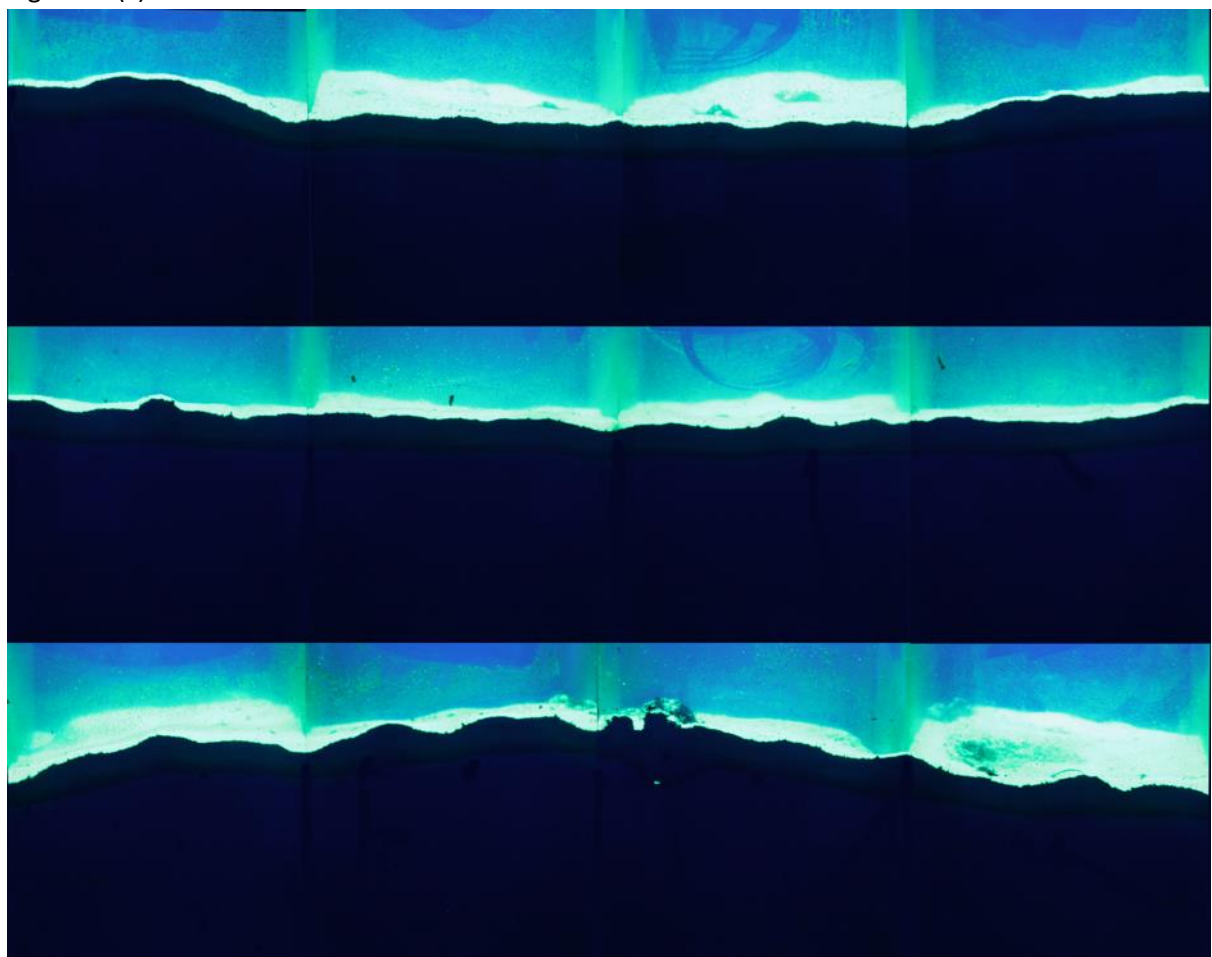
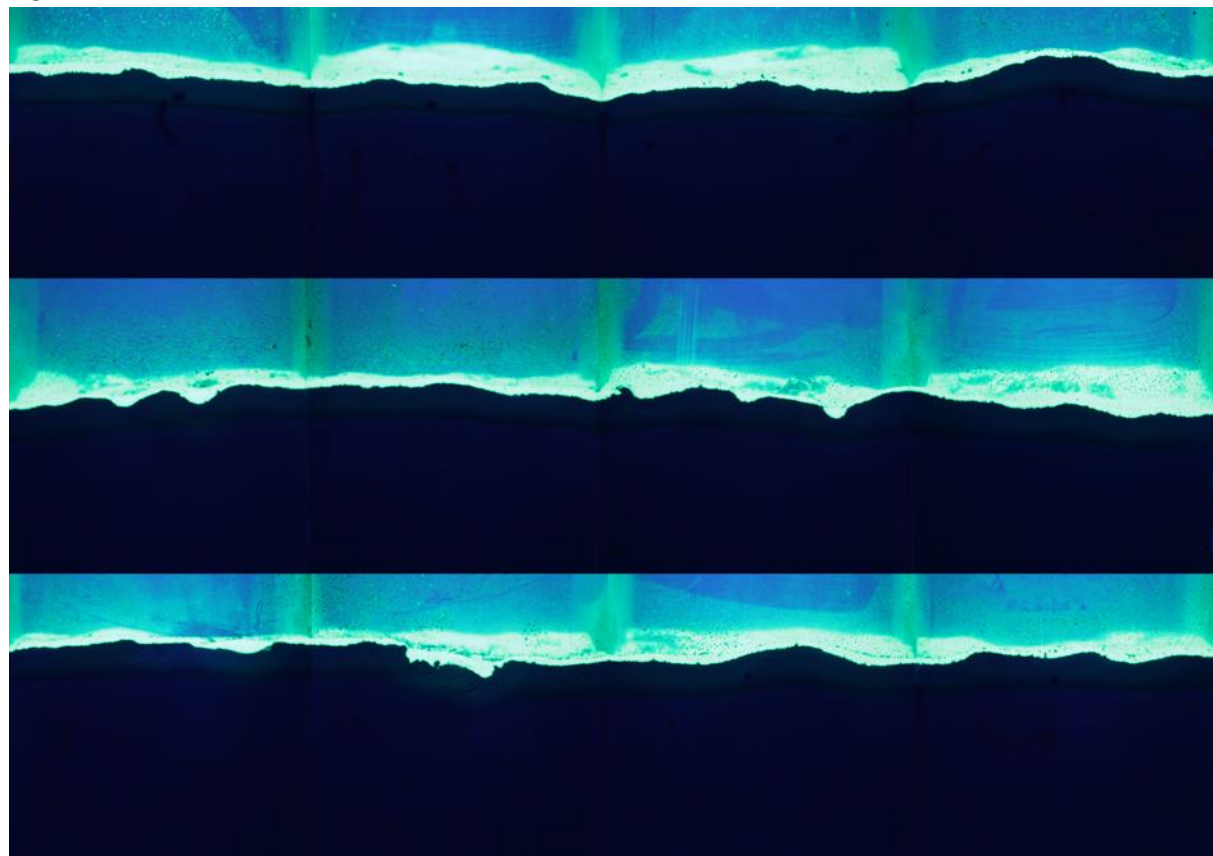
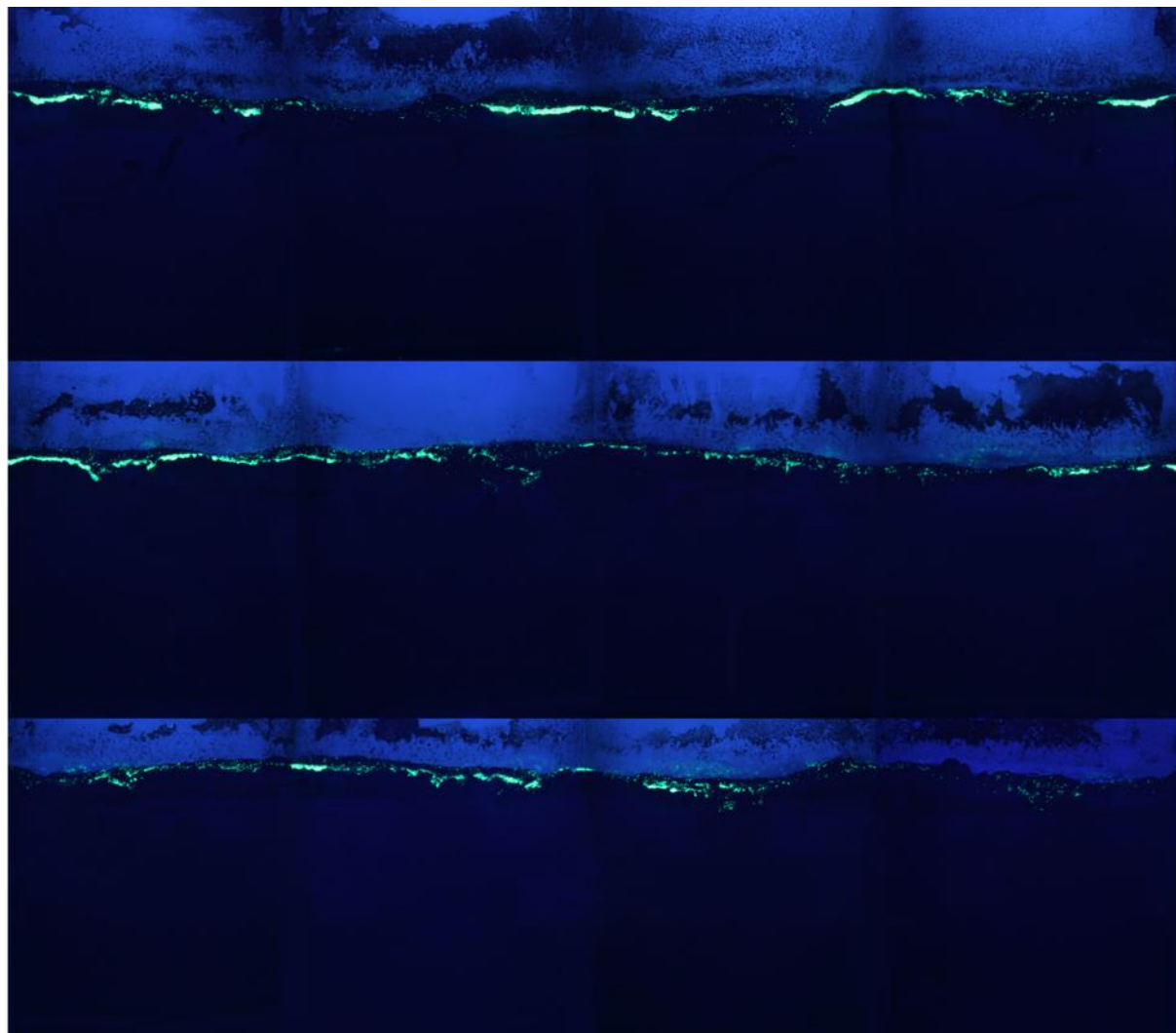


Figure S7(d)



**Figure S8 (next four pages):** Replicate ( $n = 3$ ) stitched f-SPI images for aquaria containing (a) *Ctenodiscus crispatus* from (a) station B13 under ambient conditions (b) station B13 under future climate conditions (c) station B16 under ambient conditions and (d) station B16 under future climate conditions. The images (four aquarium sides, each 19cm, stitched together) are presented. The green coloration is the luminophore tracers after 10 days of incubation.

Figure S8(a)



Appendix A

Figure S8(b)

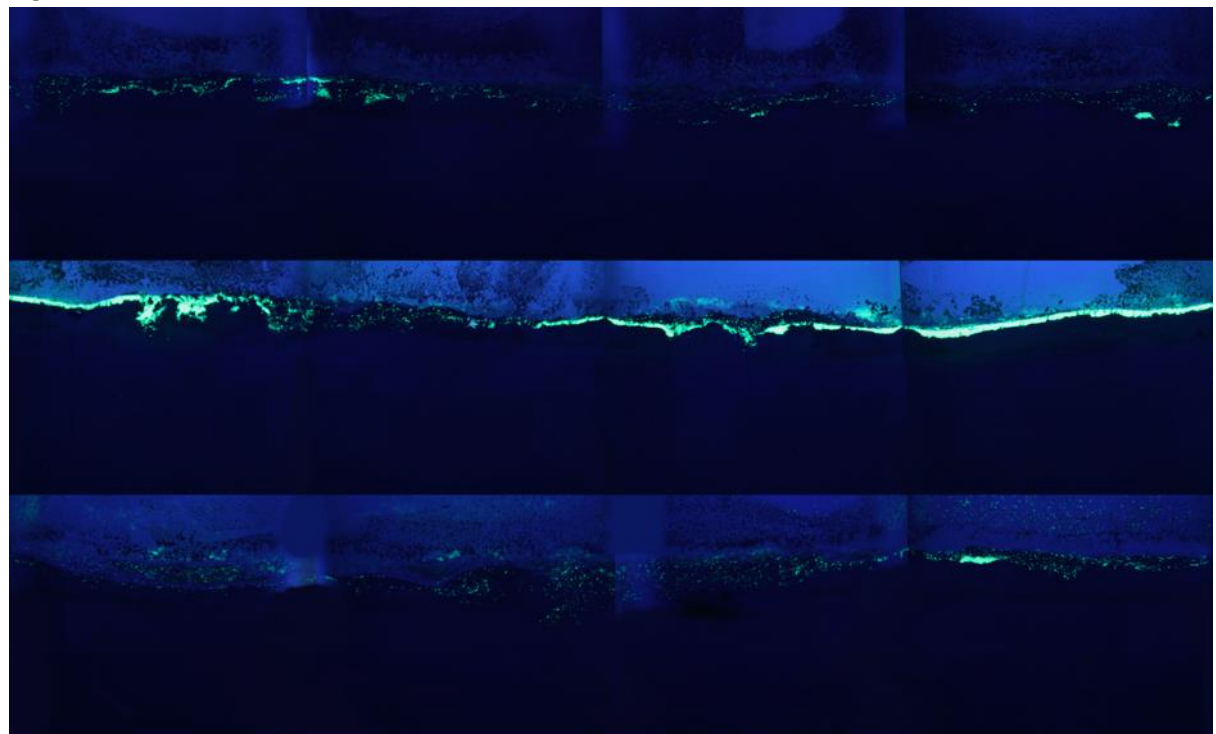
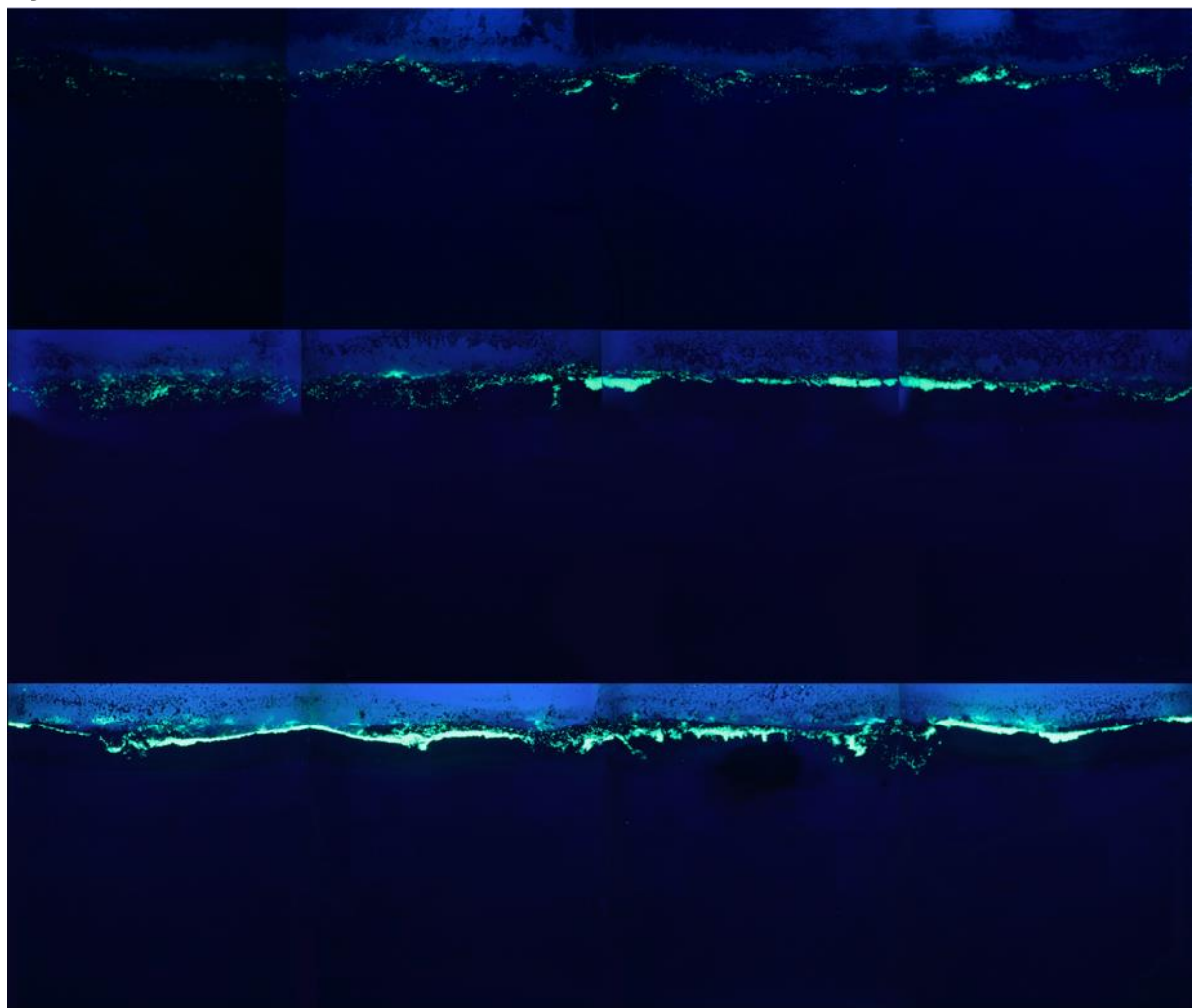
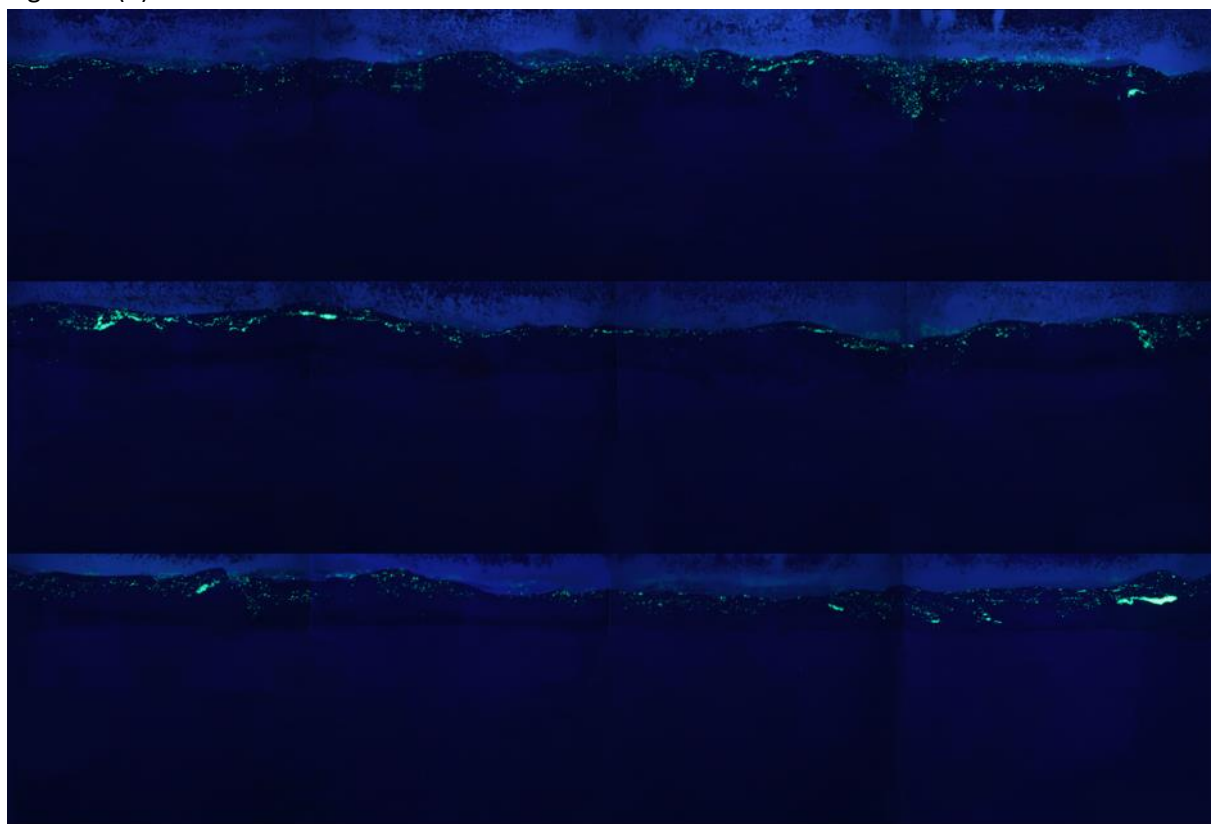


Figure S8(c)



Appendix A

Figure S8(d)



**Figure S9 (next two pages):** Replicate ( $n = 3$ ) stitched f-SPI images for aquaria containing *Cistenides hyperborea* from (a) station B13 under ambient conditions (b) station B13 under future climate conditions. The images (four aquarium sides, each 19cm, stitched together) are presented. The green coloration is the luminophore tracers after 10 days of incubation.

Figure S9(a)

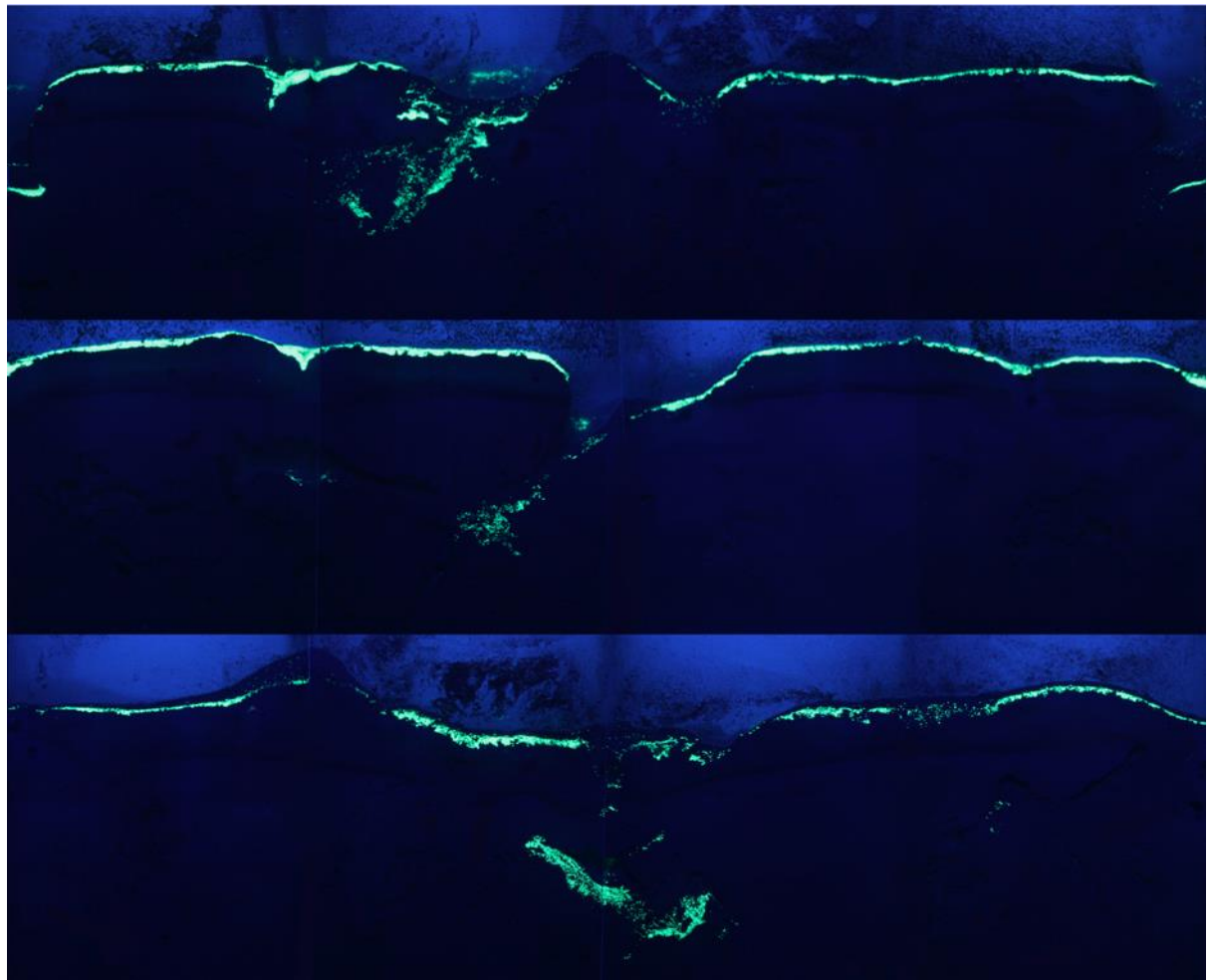
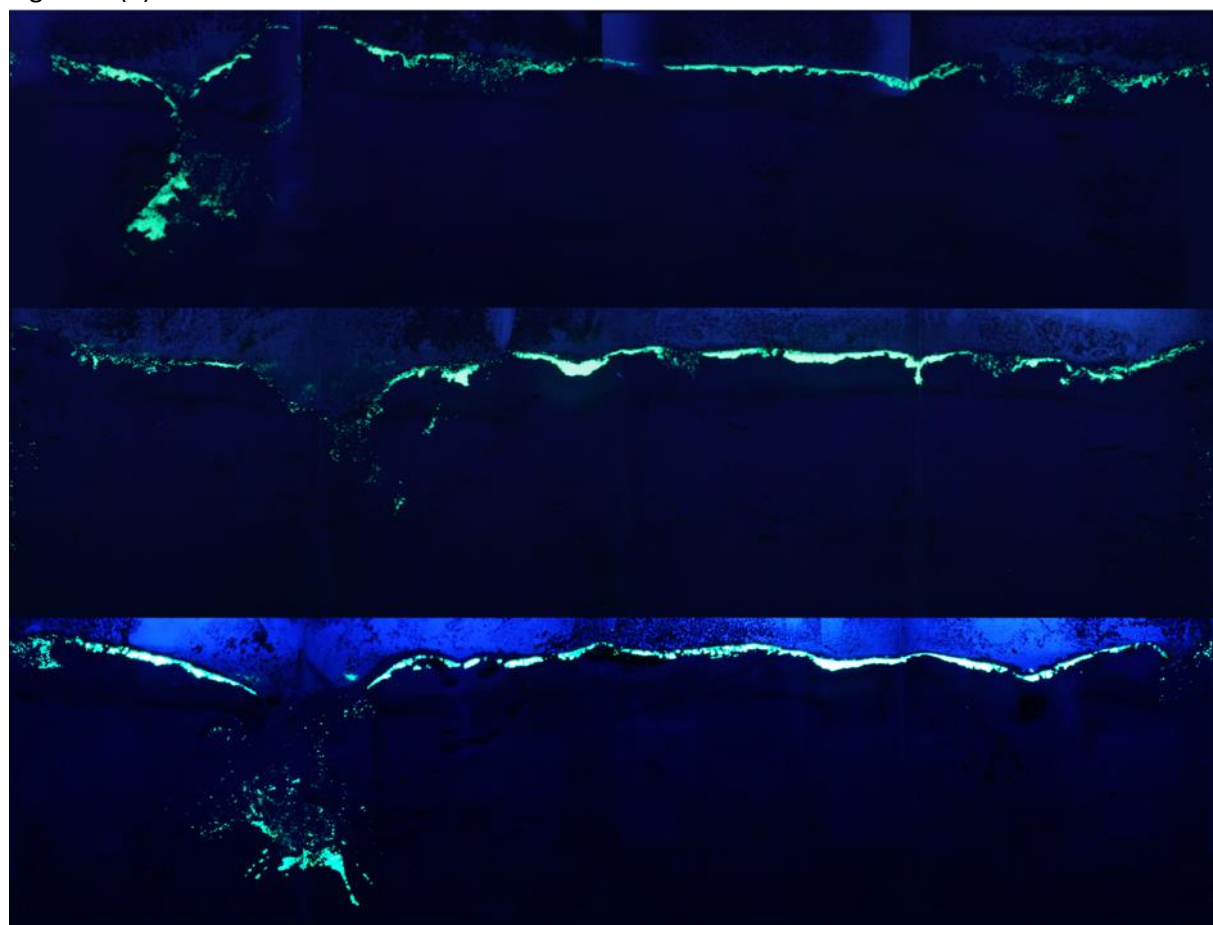


Figure S9(b)



**Figure S10 (next two pages):** Replicate ( $n = 3$ ) stitched f-SPI images for aquaria containing *Aequioldia eightsi* from (a) adjacent cove to Rothera research station under ambient conditions (b) adjacent cove to Rothera research station under future climate conditions. The images (four aquarium sides, each 19cm, stitched together) are presented. The green coloration is the luminophore tracers after 10 days of incubation.

Figure S10(a)

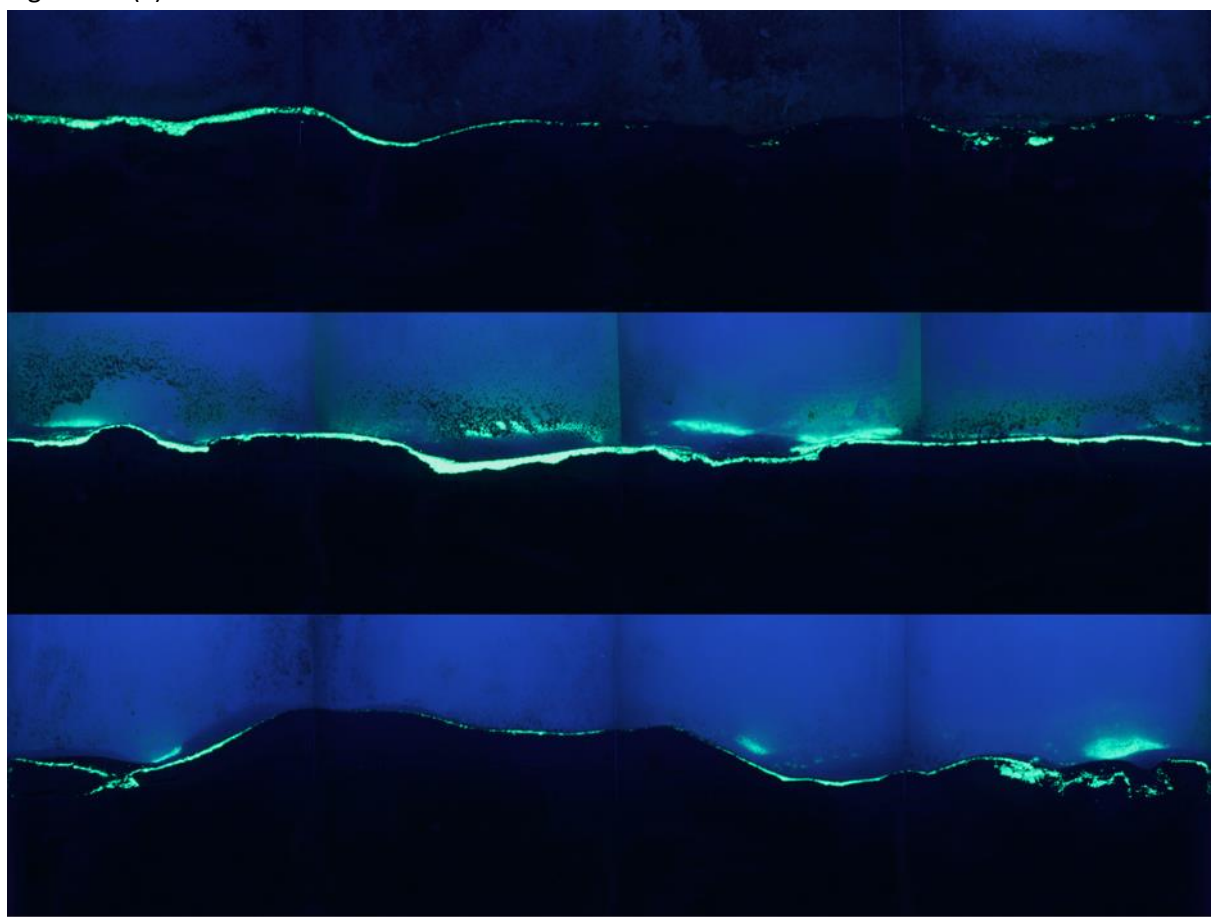
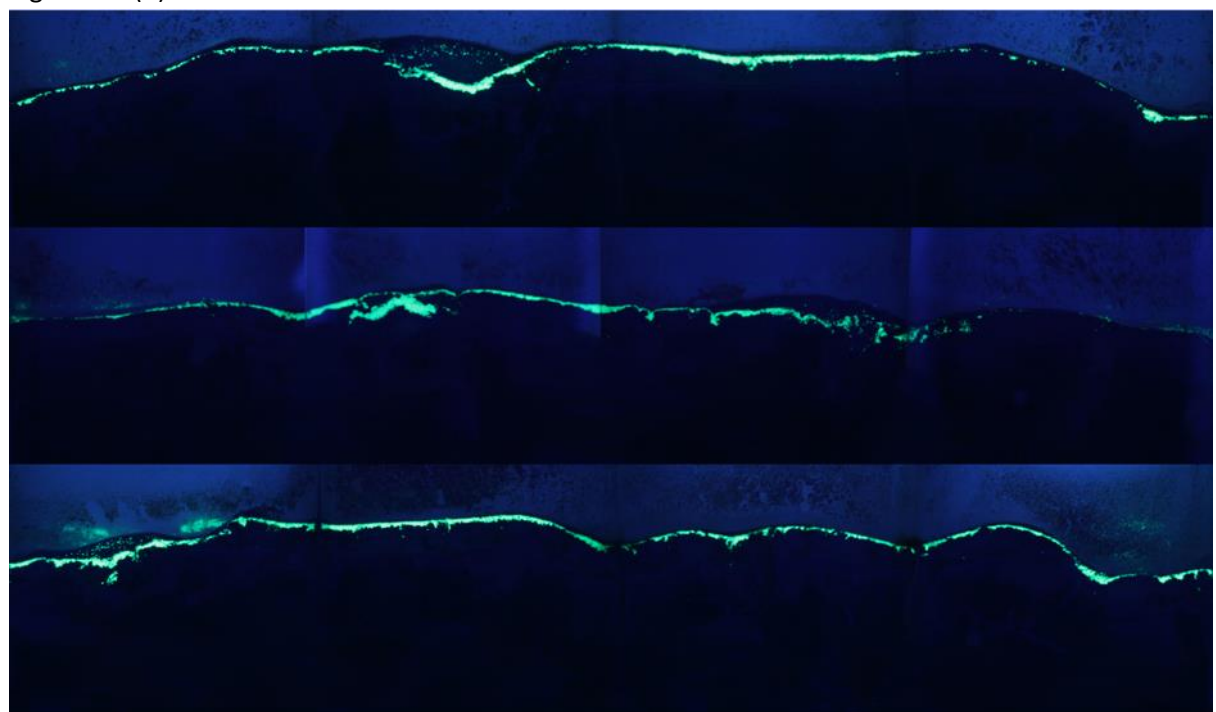
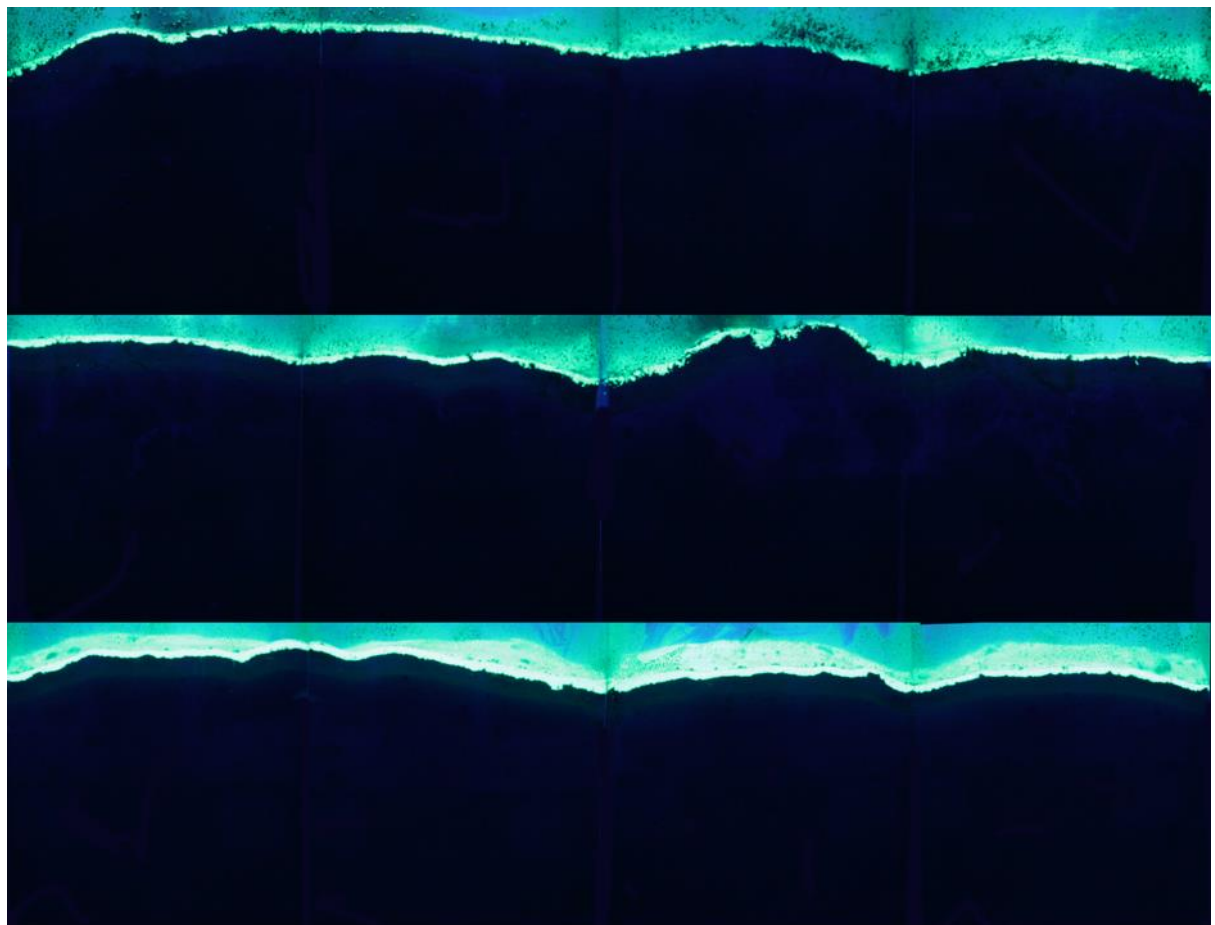


Figure S10(b)



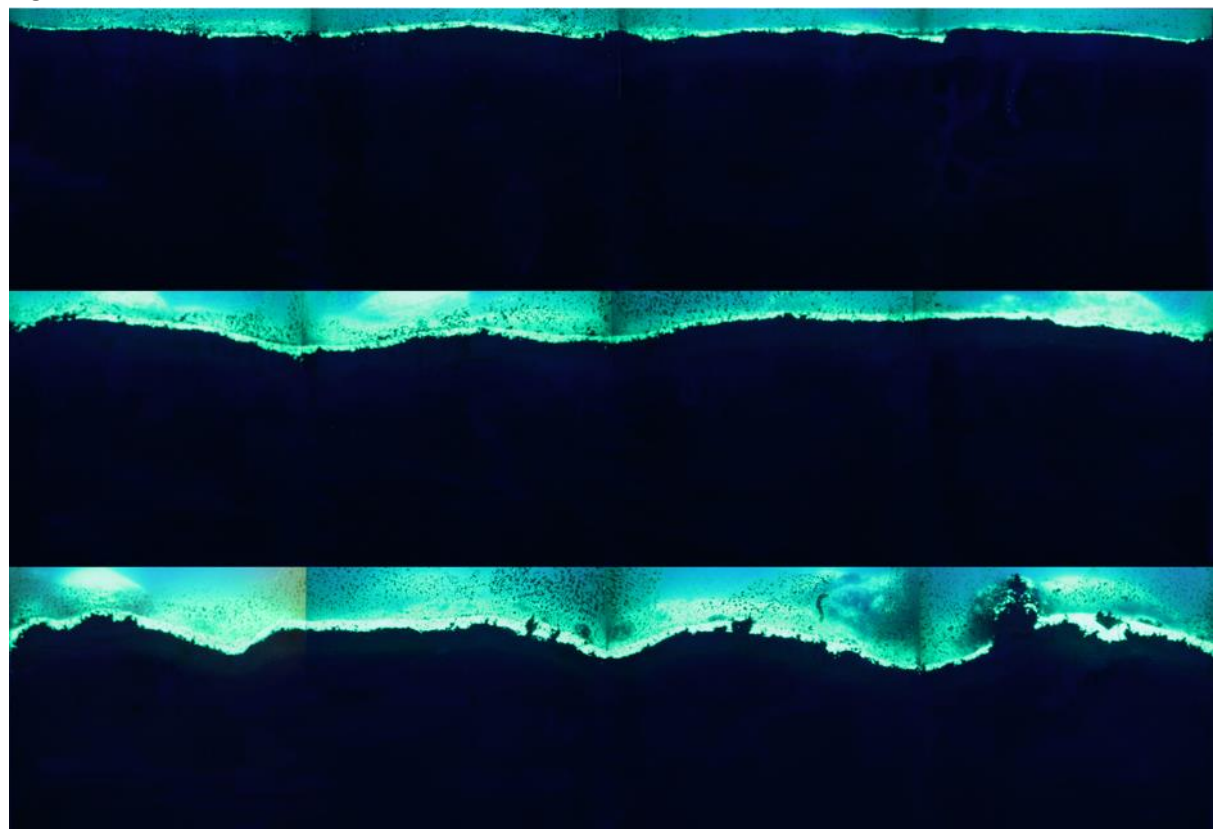
**Figure S11 (next two pages):** Replicate ( $n = 3$ ) stitched f-SPI images for aquaria containing *Laternula elliptica* from (a) adjacent cove to Rothera research station under ambient conditions (b) adjacent cove to Rothera research station under future climate conditions. The images (four aquarium sides, each 19cm, stitched together) are presented. The green coloration is the luminophore tracers after 10 days of incubation.

Figure S11(a)

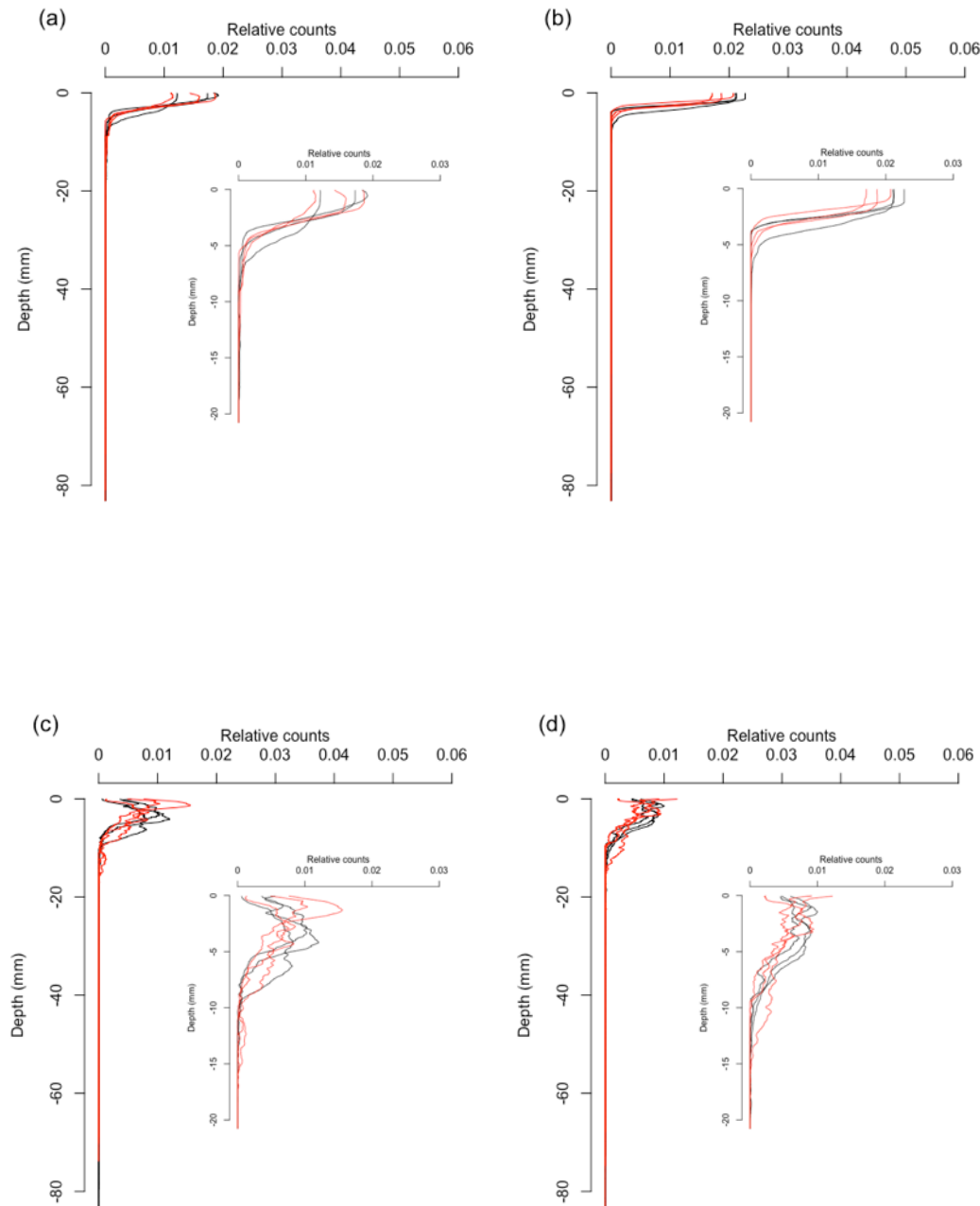


Appendix A

Figure S11(b)



**Figure S12 (next two pages):** Sediment particle reworking profiles ( $n=3$ ) derived from f-SPI images for (a) *Astarte crenata* from station B13 (b) *Astarte crenata* from B16 (c) *Ctenodiscus crispatus* from station B13 (d) *Ctenodiscus crispatus* from station B16 (e) *Cistenides hyperborea* from station B13 (f) *Aequiylodia eightsi* and (g) *Laternula elliptica*. Line colour indicates environmental condition (ambient, black; future, red). Inserts show detail of the upper portion of the main figure.



## Appendix A

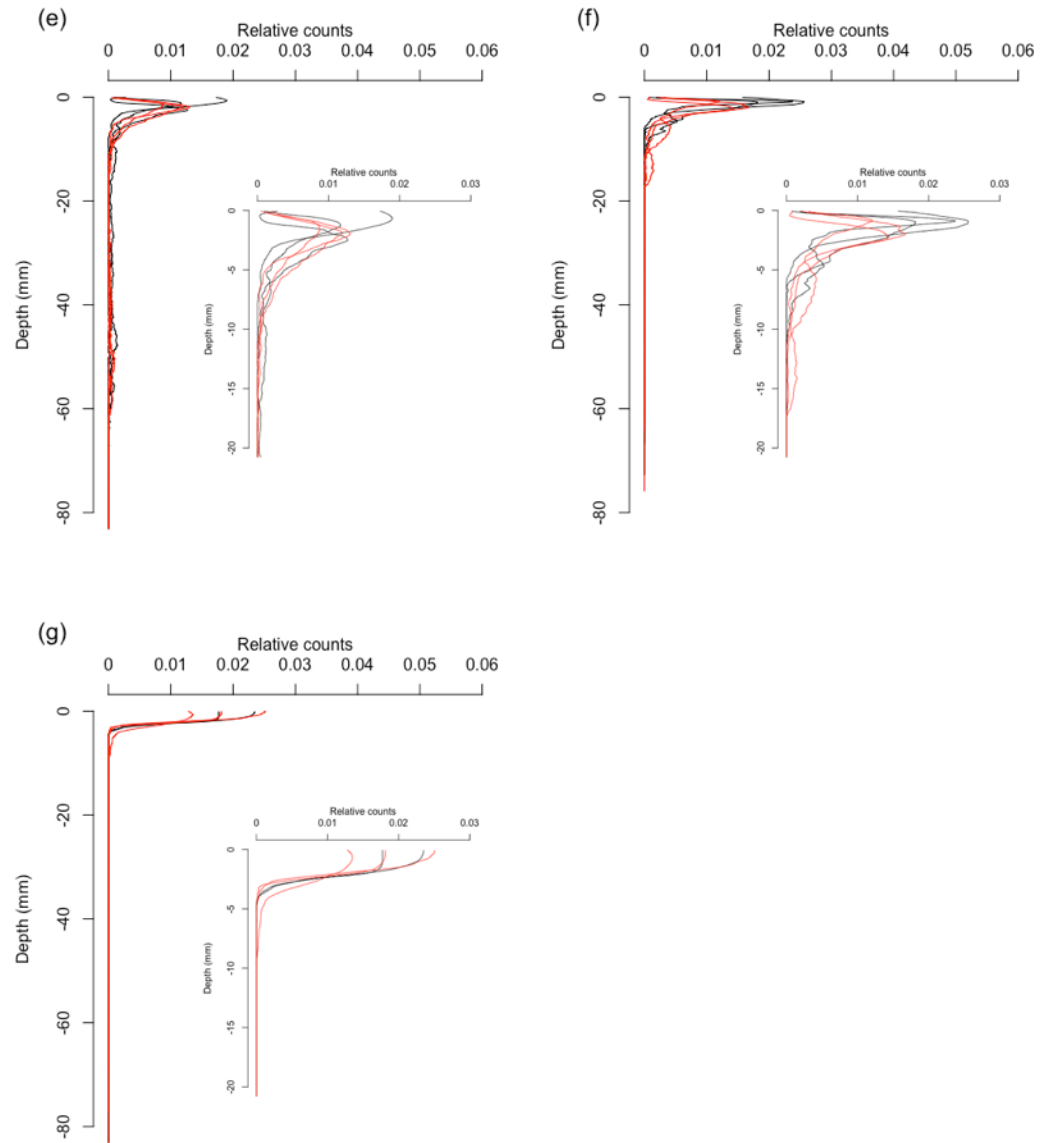


**Figure S13:** Monthly nutrient ( $[\text{NH}_4\text{-N}]$ ;  $[\text{NO}_2\text{-N}]$ ;  $[\text{NO}_3\text{-N}]$ ;  $[\text{PO}_4\text{-P}]$ ) concentrations in aquaria maintained under ambient ( $1\text{ }^{\circ}\text{C}$ ,  $400\text{ ppm [CO}_2\text{]}$ ; open symbols) and future ( $2.5\text{ }^{\circ}\text{C}$ ,  $550\text{ ppm [CO}_2\text{]}$ ; closed symbols) environmental conditions containing *Astarte crenata* (circles) and *Ctenodiscus crispatus* (squares) from station B13 (red symbols) and B16 (blue symbols); *Cistenides hyperborea* (triangles); *Aequiyyoldia eightsi* (diamonds) and *Laternula eightsi* (inverted triangles).

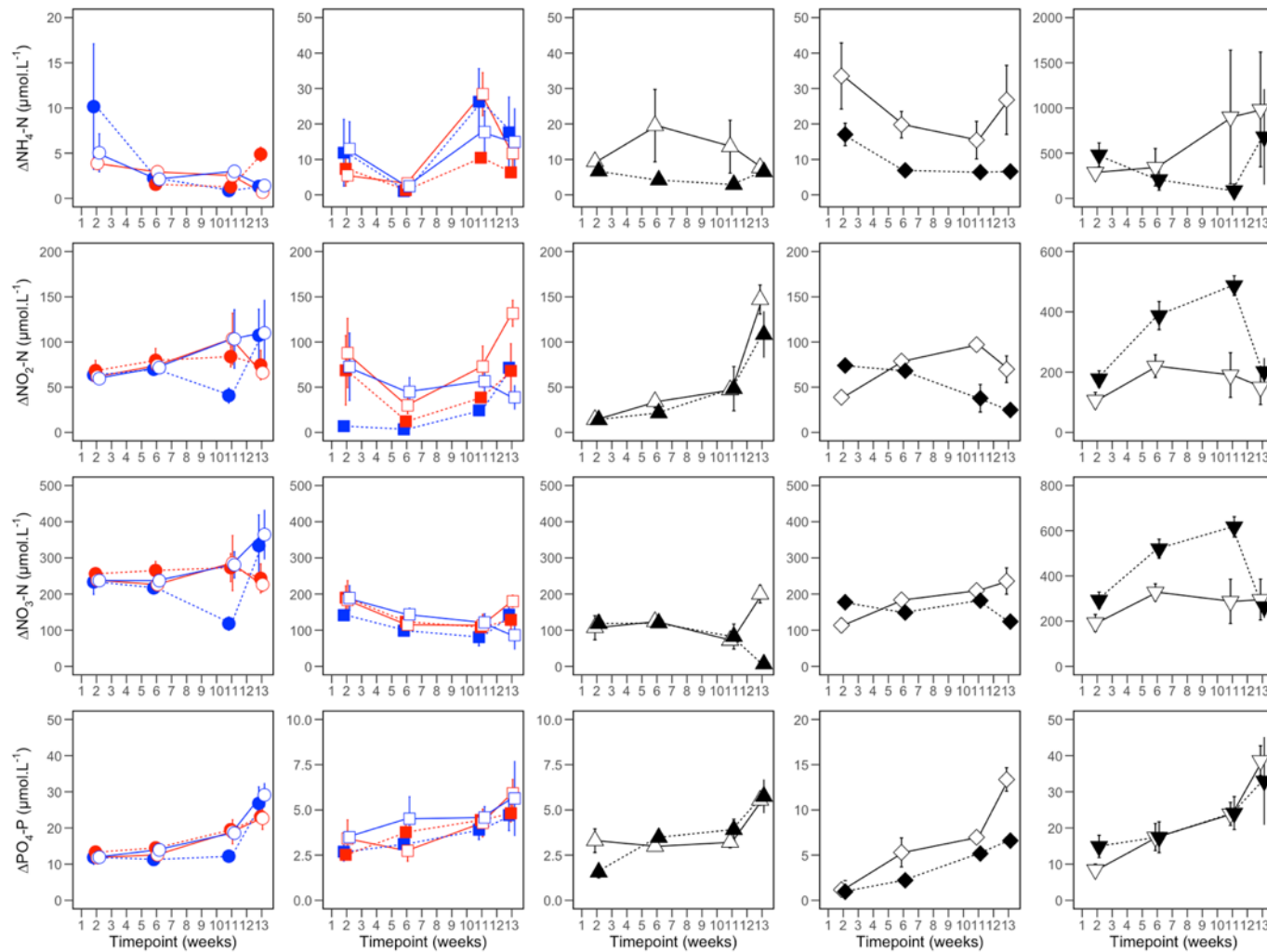


**Table S4 (next two pages):** Summary of sediment particle size statistics for each replicate aquaria determined from profile distributions of particle size using GRADISTAT (Blott & Pye, 2001). Mean, sorting, skewness, kurtosis, the percentage of sample less than 63 µm and organic matter content (%) are presented for all aquaria maintained in (i) ambient and (ii) future climate conditions. Superscripts provide descriptive terminology as outlined by Blott & Pye (2001). Mean,  $\bar{x}$ : vfs, very fine sand, fs, fine sand; ms, medium silt; cs, coarse silt; vcs, very coarse silt. Sorting,  $\sigma$ : ps, poorly sorted; vps, very poorly sorted. Skewness,  $Sk$ : sy, symmetrical; vfsk, very fine skewed; fsk, fine skewed; csk, coarse skewed. Kurtosis,  $K$ : mk, mesokurtic; lk, leptokurtic; pk, platykurtic.

Table S4

Species identity	Station	Climate	Mean ( $\bar{x}$ , µm)	Sorting ( $\sigma$ , µm)	Skewness ( $Sk$ , µm)	Kurtosis ( $K$ , µm)	Sample <63 µm (%)	Organic matter content (%)	Sediment type
<b>(i) Ambient</b>									
<i>Astarte crenata</i>	B13	Ambient	51.86 <sup>vcs</sup>	4.444 <sup>vps</sup>	-0.183 <sup>fsk</sup>	0.855 <sup>pk</sup>	50.180	4.547	Very Coarse Silty Very Fine Sand
<i>Astarte crenata</i>	B13	Ambient	39.50 <sup>vcs</sup>	4.233 <sup>vps</sup>	-0.150 <sup>fsk</sup>	0.878 <sup>pk</sup>	58.250	4.569	Very Fine Sandy Very Coarse Silt
<i>Astarte crenata</i>	B13	Ambient	54.08 <sup>vcs</sup>	4.762 <sup>vps</sup>	-0.142 <sup>fsk</sup>	0.828 <sup>pk</sup>	50.480	4.625	Very Fine Sandy Very Coarse Silt
<i>Astarte crenata</i>	B16	Ambient	91.19 <sup>vcs</sup>	4.644 <sup>vps</sup>	-0.423 <sup>vfsk</sup>	0.910 <sup>mk</sup>	31.940	4.911	Coarse Silty Fine Sand
<i>Astarte crenata</i>	B16	Ambient	43.40 <sup>vfs</sup>	4.716 <sup>vps</sup>	-0.164 <sup>fsk</sup>	0.781 <sup>pk</sup>	53.990	4.957	Fine Sandy Medium Silt
<i>Astarte crenata</i>	B16	Ambient	53.49 <sup>vcs</sup>	4.642 <sup>vps</sup>	-0.267 <sup>fsk</sup>	0.772 <sup>pk</sup>	47.590	4.591	Medium Silty Fine Sand
<i>Ctenodiscus crispatus</i>	B13	Ambient	32.58 <sup>vcs</sup>	5.424 <sup>vps</sup>	0.134 <sup>csk</sup>	0.794 <sup>pk</sup>	65.120	5.004	Medium Sandy Medium Silt
<i>Ctenodiscus crispatus</i>	B13	Ambient	81.62 <sup>cs</sup>	4.588 <sup>vps</sup>	-0.460 <sup>csk</sup>	0.863 <sup>mk</sup>	34.260	4.910	Medium Silty Fine Sand
<i>Ctenodiscus crispatus</i>	B13	Ambient	48.03 <sup>vcs</sup>	5.163 <sup>vps</sup>	-0.207 <sup>fsk</sup>	0.719 <sup>pk</sup>	50.670	5.100	Fine Sandy Medium Silt
<i>Ctenodiscus crispatus</i>	B16	Ambient	63.32 <sup>vcs</sup>	4.620 <sup>vps</sup>	-0.378 <sup>fsk</sup>	0.789 <sup>pk</sup>	41.620	5.353	Coarse Silty Fine Sand
<i>Ctenodiscus crispatus</i>	B16	Ambient	27.01 <sup>vfs</sup>	4.983 <sup>vps</sup>	0.193 <sup>vfsk</sup>	0.901 <sup>pk</sup>	71.450	5.223	Medium Sandy Medium Silt
<i>Ctenodiscus crispatus</i>	B16	Ambient	47.69 <sup>vfs</sup>	5.388 <sup>vps</sup>	-0.114 <sup>vfsk</sup>	0.728 <sup>pk</sup>	52.550	5.125	Fine Sandy Medium Silt
<i>Cistenides hyperborea</i>	B13	Ambient	80.77 <sup>vfs</sup>	4.850 <sup>vps</sup>	-0.422 <sup>vfsk</sup>	0.818 <sup>pk</sup>	36.410	4.322	Medium Silty Medium Sand
<i>Cistenides hyperborea</i>	B13	Ambient	73.97 <sup>vfs</sup>	5.209 <sup>vps</sup>	-0.380 <sup>vfsk</sup>	0.760 <sup>pk</sup>	39.690	4.876	Medium Silty Medium Sand
<i>Cistenides hyperborea</i>	B13	Ambient	42.26 <sup>vcs</sup>	4.280 <sup>vps</sup>	-0.246 <sup>fsk</sup>	0.796 <sup>pk</sup>	53.590	4.853	Fine Sandy Very Coarse Silt
<i>Aequiyyoldia eightsi</i>	Rothera	Ambient	57.41 <sup>vcs</sup>	4.900 <sup>vps</sup>	-0.267 <sup>fsk</sup>	0.780 <sup>pk</sup>	46.180	4.898	Medium Silty Fine Sand
<i>Aequiyyoldia eightsi</i>	Rothera	Ambient	115.6 <sup>vfs</sup>	3.963 <sup>ps</sup>	-0.500 <sup>vfsk</sup>	1.188 <sup>lk</sup>	24.490	4.392	Coarse Silty Fine Sand
<i>Aequiyyoldia eightsi</i>	Rothera	Ambient	66.30 <sup>vfs</sup>	4.574 <sup>vps</sup>	-0.311 <sup>vfsk</sup>	0.837 <sup>pk</sup>	41.720	4.750	Very Coarse Silty Fine Sand
<i>Laternula elliptica</i>	Rothera	Ambient	70.28 <sup>vfs</sup>	5.090 <sup>vps</sup>	-0.375 <sup>vfsk</sup>	0.732 <sup>pk</sup>	41.660	4.616	Medium Silty Medium Sand

(ii) Future									
<i>Astarte crenata</i>	B13	Future	122.0 <sup>vfs</sup>	4.024 <sup>vps</sup>	-0.575 <sup>vfsk</sup>	1.067 <sup>mk</sup>	25.630	4.668	Very Coarse Silty Medium Sand
<i>Astarte crenata</i>	B13	Future	58.32 <sup>vcs</sup>	5.055 <sup>vps</sup>	-0.271 <sup>fsk</sup>	0.728 <sup>pk</sup>	46.440	4.961	Medium Silty Fine Sand
<i>Astarte crenata</i>	B13	Future	70.10 <sup>vfs</sup>	5.019 <sup>vps</sup>	-0.372 <sup>vfsk</sup>	0.755 <sup>pk</sup>	41.010	4.962	Medium Silty Medium Sand
<i>Astarte crenata</i>	B16	Future	104.9 <sup>vfs</sup>	4.708 <sup>vps</sup>	-0.536 <sup>vfsk</sup>	0.844 <sup>pk</sup>	31.060	5.184	Medium Silty Medium Sand
<i>Astarte crenata</i>	B16	Future	57.16 <sup>vcs</sup>	5.095 <sup>vps</sup>	-0.247 <sup>fk</sup>	0.722 <sup>pk</sup>	47.620	5.295	Medium Silty Fine Sand
<i>Astarte crenata</i>	B16	Future	92.39 <sup>vfs</sup>	3.997 <sup>ps</sup>	-0.491 <sup>vfsk</sup>	1.096 <sup>mk</sup>	28.100	4.448	Very Coarse Silty Fine Sand
<i>Ctenodiscus crispatus</i>	B13	Future	40.20 <sup>vcs</sup>	5.263 <sup>vps</sup>	0.014 <sup>sy</sup>	0.722 <sup>pk</sup>	57.550	4.671	Fine Sandy Medium Silt
<i>Ctenodiscus crispatus</i>	B13	Future	69.43 <sup>vfs</sup>	4.487 <sup>vps</sup>	-0.448 <sup>vfsk</sup>	0.790 <sup>pk</sup>	38.460	4.600	Medium Silty Fine Sand
<i>Ctenodiscus crispatus</i>	B13	Future	45.91 <sup>vcs</sup>	5.394 <sup>vps</sup>	-0.036 <sup>sy</sup>	0.716 <sup>pk</sup>	54.690	5.098	Medium Sandy Medium Silt
<i>Ctenodiscus crispatus</i>	B16	Future	71.50 <sup>vfs</sup>	4.614 <sup>vps</sup>	-0.390 <sup>vfsk</sup>	0.809 <sup>pk</sup>	38.790	5.147	Medium Silty Fine Sand
<i>Ctenodiscus crispatus</i>	B16	Future	59.65 <sup>vcs</sup>	5.063 <sup>vps</sup>	-0.279 <sup>fsk</sup>	0.717 <sup>pk</sup>	46.430	4.963	Medium Silty Fine Sand
<i>Ctenodiscus crispatus</i>	B16	Future	29.09 <sup>cs</sup>	4.698 <sup>vps</sup>	0.074 <sup>sy</sup>	0.831 <sup>pk</sup>	67.570	7.282	Very Fine Sandy Medium Silt
<i>Cistenides hyperborea</i>	B13	Future	54.81 <sup>vcs</sup>	5.097 <sup>vps</sup>	-0.238 <sup>fsk</sup>	0.777 <sup>pk</sup>	47.800	7.210	Coarse Silty Fine Sand
<i>Cistenides hyperborea</i>	B13	Future	45.47 <sup>vcs</sup>	5.192 <sup>vps</sup>	-0.155 <sup>fsk</sup>	0.758 <sup>pk</sup>	52.480	7.985	Fine Sandy Medium Silt
<i>Cistenides hyperborea</i>	B13	Future	91.16 <sup>vfs</sup>	4.791 <sup>vps</sup>	-0.478 <sup>vfsk</sup>	0.847 <sup>pk</sup>	32.820	8.059	Coarse Silty Medium Sand
<i>Aequioldia eightsi</i>	Rothera	Future	34.43 <sup>vcs</sup>	4.981 <sup>vps</sup>	0.061 <sup>sy</sup>	0.779 <sup>pk</sup>	62.490	8.481	Fine Sandy Medium Silt
<i>Aequioldia eightsi</i>	Rothera	Future	27.23 <sup>cs</sup>	5.448 <sup>vps</sup>	0.210 <sup>csk</sup>	0.865 <sup>pk</sup>	72.010	8.275	Medium Sandy Medium Silt
<i>Aequioldia eightsi</i>	Rothera	Future	48.88 <sup>vcs</sup>	4.922 <sup>vps</sup>	-0.200 <sup>fsk</sup>	0.818 <sup>pk</sup>	50.670	8.123	Fine Sandy Coarse Silt
<i>Laternula elliptica</i>	Rothera	Future	28.32 <sup>cs</sup>	4.812 <sup>vps</sup>	0.029 <sup>sy</sup>	0.834 <sup>pk</sup>	66.860	8.026	Very Fine Sandy Medium Silt

## Statistical model summary

Summary of the statistical models analysing each species group (Arctic: *A. crenata* & *C. crispatus*; *C. hyperborea*; Antarctic: *A. eightsi* & *L. elliptica*) separately (Model S1 to S29). For each model I list the initial linear regression model and the minimal adequate model. When homogeneity of variance was violated I used a linear regression with generalised least squares (GLS) estimation. I present a summary of the coefficient tables for single terms. The coefficients indicate the relative performance of each factor level in relation to the re-levelled baseline (as indicated). Coefficients  $\pm$  SE, t-values and respective significance values are presented.

## Abbreviations

### (i) Explanatory variables

Climate, environmental condition

Station, cruise station

SPID, species Identity

### (ii) Response variables

Response Time, time to initiate movement (s)

Burial Time, time to complete burial (s)

SBR, surface boundary roughness (mm)

$f\text{-SPI}_{L_{\text{median}}}$ , median mixed depth of particle reworking (mm)

$f\text{-SPI}_{L_{\text{max}}}$ , maximum mixed depth of particle reworking (mm)

$\Delta[\text{Br}^-]$ , burrow ventilation ( $\text{mg L}^{-1}$ )

$\Delta[\text{NH}_4\text{-N}]$ ,  $\text{NH}_4\text{-N}$  (lnRR)

$\Delta[\text{NO}_2\text{-N}]$ ,  $\text{NO}_2\text{-N}$  (lnRR)

$\Delta[\text{NO}_3\text{-N}]$ ,  $\text{NO}_3\text{-N}$  (lnRR)

$\Delta[\text{PO}_4\text{-P}]$ ,  $\text{PO}_4\text{-P}$  (lnRR)

**Data:** All data used in the analyses are provided as Table S6.

## Arctic species

### Model S1 Time to initiate movement (Response Time, s) - *Ctenodiscus crispatus*

Initial linear regression model:

```
lm(Response Time ~ Climate + Station + Climate:Station)
```

Minimal adequate model:

```
gls(Response Time ~ 1, weights = varIdent(form = ~
1|Station), method = "REML")
```

### Model S2 Time to complete burial (Burial Time, s) - *Ctenodiscus crispatus*

Initial linear regression model:

```
lm(Burial Time ~ Climate + Station + Climate:Station)
```

Minimal adequate model:

```
lm(Burial Time ~ Climate)
```

Intercept  $\pm$  SE (when baseline is for Ambient for Climate):  $995.0 \pm 160.6$ ,  $t = 6.1978$ , **p < 0.0001**

Coefficient table for Climate

	Ambient	Future
Ambient	/	$-497.1 \pm 203.1$ $-2.448$

## Appendix A

		<b>0.0282</b>
Future	$-497.1 \pm 203.1$ $-2.448$ <b>0.0282</b>	/

### Model S3 Surface boundary roughness (SBR, mm) – *Astarte crenata*\* *Ctenodiscus crispatus*

Initial linear regression model:

```
lm(SBR ~ Climate + Station + SPID + Climate:Station +
  Climate:SPID + Station:SPID + Climate:Station:SPID)
```

Minimal adequate model:

```
gls(SBR ~ Station + SPID, weights = varIdent(form = ~1|SPID),
  method = "REML")
```

Intercept  $\pm$  SE (when baseline is for B13 for Station and *A. crenata* for SPID):  $17.452 \pm 1.701$ .  $t = 10.259$ , **p = 0**

Coefficient table for Station

	B13	B16
B13	/	$-2.096 \pm 1.045$ $-2.007$ $0.058$
B16	$-2.096 \pm 1.045$	/

	-2.007	
	0.058	

Coefficient table for SPID

	<i>Astarte crenata</i>	<i>Ctenodiscus crispatus</i>
<i>Astarte crenata</i>	/	-6.261 ± 1.709 -3.663 <b>0.002</b>
<i>Ctenodiscus crispatus</i>	-6.261 ± 1.709 -3.663 <b>0.002</b>	/

**Model S4** Median mixing depth ( ${}^f\text{-SPI}L_{\text{median}}$ , mm) – *Astarte crenata*\**Ctenodiscus crispatus*

Initial linear regression model:

```
lm({}^f\text{-SPI}L_{\text{median}} ~ Climate + Station + SPID + Climate:Station +
Climate:SPID + Station:SPID + Climate:Station:SPID)
```

Minimal adequate model:

```
lm({}^f\text{-SPI}L_{\text{median}} ~ Climate + Station + SPID + Climate:SPID +
Station:SPID)
```

**Model S5** Maximum mixing depth ( ${}^f\text{-SPI}L_{\max}$ , mm) – *Astarte crenata*\* *Ctenodiscus crispatus*

Initial linear regression model:

```
lm({}^f\text{-SPI}L_{\max} ~ Climate + Station + SPID + Climate:Station +  
Climate:SPID + Station:SPID + Climate:Station:SPID)
```

Minimal adequate model:

```
lm({}^f\text{-SPI}L_{\max} ~ Station + SPID + Station:SPID)
```

Intercept  $\pm$  SE:  $5.714 \pm 1.875$ ,  $t = 3.052$ , **p < 0.01**

**Model S6** Burrow ventilation ( $\Delta[\text{Br}^-]$ , mg L $^{-1}$ ) – *Astarte crenata*\* *Ctenodiscus crispatus*

Initial linear regression model:

```
lm(\Delta[\text{Br}^-] ~ Climate + Station + SPID + Climate:Station +  
Climate:SPID + Station:SPID + Climate:Station:SPID)
```

Minimal adequate model:

```
lm(\Delta[\text{Br}^-] ~ Climate + Station + SPID + Climate:Station +  
Climate:SPID + Station:SPID + Climate:Station:SPID)
```

**Model S7** NH<sub>4</sub>-N flux ( $\Delta[\text{NH}_4\text{-N}]$ , lnRR) – *Astarte crenata*\* *Ctenodiscus crispatus*

Initial linear regression model:

$lm(\Delta[\text{NH}_4\text{-N}] \sim \text{Climate} + \text{Station} + \text{SPID} + \text{Climate:Station} + \text{Climate:SPID} + \text{Station:SPID} + \text{Climate:Station:SPID})$

Minimal adequate model:

$lm(\Delta[\text{NH}_4\text{-N}] \sim \text{SPID})$

Intercept  $\pm$  SE (when baseline is for *Astarte crenata* for SPID):  $-0.636 \pm 0.147$ ,  $t = -4.336$ , **p < 0.001**

Coefficient table for Climate

	<i>Astarte crenata</i>	<i>Ctenodiscus crispatus</i>
<i>Astarte crenata</i>	/	$0.802 \pm 0.207$ 3.867 <b>&lt;0.001</b>
<i>Ctenodiscus crispatus</i>	$0.802 \pm 0.207$ 3.867 <b>&lt;0.001</b>	/

**Model S8**  $\text{NO}_2\text{-N}$  flux ( $\Delta[\text{NO}_2\text{-N}]$ , lnRR) – *Astarte crenata*\**Ctenodiscus crispatus*

Initial linear regression model:

$lm(\Delta[\text{NO}_2\text{-N}] \sim \text{Climate} + \text{Station} + \text{SPID} + \text{Climate:Station} + \text{Climate:SPID} + \text{Station:SPID} + \text{Climate:Station:SPID})$

## Appendix A

Minimal adequate model:

```
gls(Δ[NO2-N] ~ Climate + Station + SPID + Climate:Station +  
Climate:SPID + Station:SPID + Climate:Station:SPID, weights =  
= varIdent(form = ~1|SPID), method = "REML")
```

### **Model S9** NO<sub>3</sub>-N flux (Δ[NO<sub>3</sub>-N], lnRR) – *Astarte crenata*\* *Ctenodiscus crispatus*

Initial linear regression model:

```
lm(Δ[NO3-N] ~ Climate + Station + SPID + Climate:Station +  
Climate:SPID + Station:SPID + Climate:Station:SPID)
```

Minimal adequate model:

```
lm(Δ[NO3-N] ~ Climate + Station + SPID + Climate:Station +  
Climate:SPID + Station:SPID + Climate:Station:SPID)
```

### **Model S10** PO<sub>4</sub>-P flux (Δ[PO<sub>4</sub>-P], lnRR) – *Astarte crenata*\* *Ctenodiscus crispatus*

Initial linear regression model:

```
lm(Δ[PO4-P] ~ Climate + Station + SPID + Climate:Station +  
Climate:SPID + Station:SPID + Climate:Station:SPID)
```

Minimal adequate model:

```
lm(Δ[PO4-P] ~ 1)
```

### **Model S11** Time to initiate movement (Response Time, s) - *Cistenides hyperborea*

Initial linear regression model:

```
lm(Response Time ~ Climate)
```

Minimal adequate model:

```
lm(Response Time ~ 1)
```

**Model S12** Surface boundary roughness (SBR, mm) – *Cistenides hyperborea*

Initial linear regression model:

```
lm(SBR ~ Climate)
```

Minimal adequate model:

```
gls(SBR ~ 1, weights = varIdent(form = ~1|Climate), method = "REML")
```

**Model S13** Median mixing depth ( ${}^f\text{-SPI}L_{\text{median}}$ , mm) – *Cistenides hyperborea*

Initial linear regression model:

```
lm({}^f\text{-SPI}L_{\text{median}} ~ Climate)
```

Minimal adequate model:

```
gls({}^f\text{-SPI}L_{\text{median}} ~ 1, weights = varIdent(form = ~1|Climate), method = "REML")
```

## Appendix A

### Model S14 Maximum mixing depth ( ${}^{\text{f-SPI}}\text{L}_{\text{max}}$ , mm) – *Cistenides hyperborea*

Initial linear regression model:

```
lm ({}^{\text{f-SPI}}\text{L}_{\text{max}} ~ Climate)
```

Minimal adequate model:

```
gls ({}^{\text{f-SPI}}\text{L}_{\text{max}} ~ 1, weights = varIdent(form = ~1|Climate),  
method = "REML")
```

### Model S15 Burrow ventilation ( $\Delta[\text{Br}^-]$ , mg L<sup>-1</sup>) – *Cistenides hyperborea*

Initial linear regression model:

```
lm (Δ [Br-] ~ Climate)
```

Minimal adequate model:

```
gls (Δ [Br-] ~ Climate, weights = varIdent(form = ~1|Climate),  
method = "REML")
```

Intercept  $\pm$  SE (when baseline is for Ambient for Climate):

$71.611 \pm 178.821$ ,  $t = 0.400$ ,  $p = 0.709$

Coefficient table for Climate

	Ambient	Future
Ambient	/	$-634.850 \pm 198.567$  $-3.197$  <b>0.033</b>
Future	$634.850 \pm 198.567$	/

	-3.197	
	<b>0.033</b>	

**Model S16** NH<sub>4</sub>-N flux ( $\Delta[\text{NH}_4\text{-N}]$ , lnRR) – *Cistenides hyperborea*

Initial linear regression model:

$$\text{lm}(\Delta[\text{NH}_4\text{-N}] \sim \text{Climate})$$

Minimal adequate model:

$$\text{lm}(\Delta[\text{NH}_4\text{-N}] \sim 1)$$

**Model S17** NO<sub>2</sub>-N flux ( $\Delta[\text{NO}_2\text{-N}]$ , lnRR) – *Cistenides hyperborea*

Initial linear regression model:

$$\text{lm}(\Delta[\text{NO}_2\text{-N}] \sim \text{Climate})$$

Minimal adequate model:

$$\text{lm}(\Delta[\text{NO}_2\text{-N}] \sim 1)$$

**Model S18** NO<sub>3</sub>-N flux ( $\Delta[\text{NO}_3\text{-N}]$ , lnRR) – *Cistenides hyperborea*

Initial linear regression model:

$$\text{lm}(\Delta[\text{NO}_3\text{-N}] \sim \text{Climate})$$

## Appendix A

Minimal adequate model:

$$\text{lm}(\Delta[\text{NO}_3-\text{N}] \sim \text{Climate})$$

Intercept  $\pm$  SE (when baseline is for Ambient for Climate):

$$0.325 \pm 0.143, t = 2.273, p = 0.085$$

Coefficient table for Climate

	Ambient	Future
Ambient	/	$-1.574 \pm 0.202$ $-7.799$ <b>0.002</b>
Future	$-1.574 \pm 0.202$ $-7.799$ <b>0.002</b>	/

## Model S19 PO<sub>4</sub>-P flux ( $\Delta[\text{PO}_4-\text{P}]$ , lnRR) – *Cistenides hyperborea*

Initial linear regression model:

$$\text{lm}(\Delta[\text{PO}_4-\text{P}] \sim \text{Climate})$$

Minimal adequate model:

$$\text{gls}(\Delta[\text{PO}_4-\text{P}] \sim 1, \text{weights} = \text{varIdent}(\text{form} = \sim 1 \mid \text{Climate}), \text{method} = \text{"REML"})$$

## Antarctic species

### **Model S20** Time to initiate movement (Response Time, s) - *Aequiyoldia eightsi*

Initial linear regression model:

```
lm(Response Time ~ Climate)
```

Minimal adequate model:

```
gls(Response Time ~ 1, weights = varIdent(form = ~1|Climate),  
method = "REML")
```

### **Model S21** Time to complete burial (Burial Time, s) - *Aequiyoldia eightsi*

Initial linear regression model:

```
lm(Response Time ~ Climate)
```

Minimal adequate model:

```
gls(Response Time ~ 1, weights = varIdent(form = ~1|Climate),  
method = "REML")
```

### **Model S22** Surface boundary roughness (SBR, mm) – *Laternula elliptica*\**Aequiyoldia eightsi*

Initial linear regression model:

```
lm(SBR ~ Climate + SPID + Climate:SPID)
```

## Appendix A

Minimal adequate model:

```
lm(SBR ~ Climate + SPID + Climate:SPID)
```

**Model S23** Median mixing depth ( ${}^f\text{-SPI}L_{\text{median}}$ , mm) – *Laternula elliptica*\**Aequiyoldia eightsi*

Initial linear regression model:

```
lm({}^f\text{-SPI}L_{\text{median}} ~ Climate + SPID + Climate:SPID)
```

Minimal adequate model:

```
lm({}^f\text{-SPI}L_{\text{median}} ~ Climate + SPID + Climate:SPID)
```

**Model S24** Maximum mixing depth ( ${}^f\text{-SPI}L_{\text{max}}$ , mm) – *Laternula elliptica*\**Aequiyoldia eightsi*

Initial linear regression model:

```
lm({}^f\text{-SPI}L_{\text{max}} ~ Climate + SPID + Climate:SPID)
```

Minimal adequate model:

```
lm({}^f\text{-SPI}L_{\text{max}} ~ Climate + SPID + Climate:SPID)
```

**Model S25** Burrow ventilation ( $\Delta[\text{Br}^-]$ , mg L $^{-1}$ ) – *Laternula elliptica*\**Aequiyoldia eightsi*

Initial linear regression model:

```
lm(\Delta[\text{Br}^-] ~ Climate + SPID + Climate:SPID)
```

Minimal adequate model:

```
gls( $\Delta[\text{Br}^-]$  ~ 1, weights = varIdent(form = ~1|SPID), method = "REML")
```

**Model S26** NH<sub>4</sub>-N flux ( $\Delta[\text{NH}_4\text{-N}]$ , lnRR) – *Laternula elliptica*\**Aequiyoldia eightsi*

Initial linear regression model:

```
lm( $\Delta[\text{NH}_4\text{-N}]$  ~ Climate + SPID + Climate:SPID)
```

Minimal adequate model:

```
gls( $\Delta[\text{NH}_4\text{-N}]$  ~ 1, weights = varIdent(form = ~ 1|SPID*Climate, method = "REML")
```

**Model S27** [NO<sub>2</sub>-N] flux ( $\Delta[\text{NO}_2\text{-N}]$ , lnRR) – *Laternula elliptica*\**Aequiyoldia eightsi*

Initial linear regression model:

```
lm( $\Delta[\text{NO}_2\text{-N}]$  ~ Climate + SPID + Climate:SPID)
```

Minimal adequate model:

```
gls( $\Delta[\text{NO}_2\text{-N}]$  ~ 1, weights = varIdent(form = ~ 1|SPID*Climate, method = "REML")
```

**Model S28** NO<sub>3</sub>-N flux ( $\Delta[\text{NO}_3\text{-N}]$ , lnRR) – *Laternula elliptica*\**Aequiyoldia eightsi*

## Appendix A

Initial linear regression model:

`lm(Δ[NO3-N] ~ Climate + SPID + Climate:SPID)`

Minimal adequate model:

`lm(Δ[NO3-N] ~ Climate, weights = varIdent(form = ~ 1 | SPID*Climate, method = "REML")`

Intercept ± SE (when baseline is for Ambient for Climate and *Laternula elliptica* for SPID):

$0.295 \pm 0.077$ ,  $t = 3.810$ , **p < 0.01**

Coefficient table for Climate

	Ambient	Future
Ambient	/	$-0.451 \pm 0.078$ $-5.801$ <b>&lt;0.001</b>
Future	$-0.451 \pm 0.078$ $-5.801$ <b>&lt;0.001</b>	/

**Model S29** PO<sub>4</sub>-P flux ( $\Delta[\text{PO}_4\text{-P}]$ , lnRR) – *Laternula elliptica*\**Aequiyyoldia eightsi*

Initial linear regression model:

`lm(Δ[PO4-P] ~ Climate + SPID + Climate:SPID)`

Minimal adequate model:

```
gls( $\Delta[\text{PO}_4-\text{P}] \sim \text{Climate} + \text{SPID}$ , weights = varIdent(form =
~1 | SPID*Climate), method = "REML")
```

Intercept  $\pm$  SE (when baseline is Ambient for Climate and *Laternula elliptica* for SPID):

$0.676 \pm 0.068$ ,  $t = 9.934$ , **p < 0.0001**

Coefficient table for Climate

	Ambient	Future
Ambient	/	$-0.369 \pm 0.096$ $-3.861$ <b>&lt;0.01</b>
Future	$-0.369 \pm 0.096$ $-3.861$ <b>&lt;0.01</b>	/

Coefficient table for SPID

	<i>Laternula elliptica</i>	<i>Aequioldia eightsi</i>
<i>Laternula elliptica</i>	/	$0.655 \pm 0.313$ $2.089$ $0.066$
<i>Aequioldia eightsi</i>	$0.655 \pm 0.313$ $2.089$ $0.066$	/

**Table S6 (the next three pages):** Summary of (a) intra-specific behavioural activity and (b) ecosystem process and functioning used in my statistical analyses. Climate = environmental condition (ambient vs future), Station = location (B13 = station B13, B16 = station B16).

\* indicates individuals that did not respond within my maximum observation period (3600s).

Table S6(a)

Climate	Station	Species identity	Replicate	Response Time (s)	Burial Time (s)
Ambient	B13	<i>Ctenodiscus crispatus</i>	1	215	683
Ambient	B13	<i>Ctenodiscus crispatus</i>	2	512	1722
Ambient	B13	<i>Ctenodiscus crispatus</i>	3	336	670
Ambient	B16	<i>Ctenodiscus crispatus</i>	1	122	1480
Ambient	B16	<i>Ctenodiscus crispatus</i>	2	253	*
Ambient	B16	<i>Ctenodiscus crispatus</i>	3	722	886
Ambient	B16	<i>Ctenodiscus crispatus</i>	4	1026	*
Ambient	B16	<i>Ctenodiscus crispatus</i>	5	385	529
Ambient	B13	<i>Cistenides hyperborea</i>	1	787	*
Ambient	B13	<i>Cistenides hyperborea</i>	2	1577	*
Ambient	B13	<i>Cistenides hyperborea</i>	3	731	*
Ambient	B13	<i>Cistenides hyperborea</i>	4	293	*
Ambient	Rothera	<i>Aequiyoldia eightsi</i>	1	529	175
Ambient	Rothera	<i>Aequiyoldia eightsi</i>	2	1322	184
Ambient	Rothera	<i>Aequiyoldia eightsi</i>	3	97	74
Future	B13	<i>Ctenodiscus crispatus</i>	1	296	575
Future	B13	<i>Ctenodiscus crispatus</i>	2	548	1331
Future	B13	<i>Ctenodiscus crispatus</i>	3	260	231
Future	B13	<i>Ctenodiscus crispatus</i>	4	429	222
Future	B16	<i>Ctenodiscus crispatus</i>	1	386	318
Future	B16	<i>Ctenodiscus crispatus</i>	2	458	682
Future	B16	<i>Ctenodiscus crispatus</i>	3	631	459
Future	B16	<i>Ctenodiscus crispatus</i>	4	978	486
Future	B16	<i>Ctenodiscus crispatus</i>	5	173	377
Future	B16	<i>Ctenodiscus crispatus</i>	6	281	298
Future	B13	<i>Cistenides hyperborea</i>	1	193	1034
Future	B13	<i>Cistenides hyperborea</i>	2	1263	*
Future	B13	<i>Cistenides hyperborea</i>	3	538	2376
Future	B13	<i>Cistenides hyperborea</i>	4	1309	*
Future	B13	<i>Cistenides hyperborea</i>	5	950	775
Future	Rothera	<i>Aequiyoldia eightsi</i>	1	44	70
Future	Rothera	<i>Aequiyoldia eightsi</i>	2	134	85
Future	Rothera	<i>Aequiyoldia eightsi</i>	3	145	47

Table S6(b)

Climate	Station	Species identity	Replicate	SBR (mm)	f-SPI <sub>L<sub>median</sub></sub> (mm)	f-SPI <sub>L<sub>max</sub></sub> (mm)	Δ[Br <sup>-</sup> ] (mg L <sup>-1</sup> )	Δ[NH <sub>4</sub> -N] (lnRR)	Δ[NO <sub>2</sub> -N] (lnRR)	Δ[NO <sub>3</sub> -N] (lnRR)	Δ[PO <sub>4</sub> -P] (lnRR)
Ambient	B13	<i>Astarte crenata</i>	1	18.864	2.955	19.659	-246.343	-0.699	-0.081	-0.102	0.136
Ambient	B13	<i>Astarte crenata</i>	2	23.222	4.556	22.111	-8.974	-0.976	0.006	-0.031	0.326
Ambient	B13	<i>Astarte crenata</i>	3	11.150	2.450	9.100	-76.436	-0.587	0.160	0.057	0.364
Ambient	B16	<i>Astarte crenata</i>	1	16.348	2.472	4.382	52.534	-0.140	-0.186	0.005	0.353
Ambient	B16	<i>Astarte crenata</i>	2	9.323	2.396	3.906	7.825	-0.963	0.503	0.295	0.475
Ambient	B16	<i>Astarte crenata</i>	3	28.309	3.382	10.515	61.468	-0.693	0.286	0.208	0.339
Ambient	B13	<i>Ctenodiscus crispatus</i>	1	11.979	4.375	20.990	-490.463	0.417	0.947	0.332	0.666
Ambient	B13	<i>Ctenodiscus crispatus</i>	2	8.688	4.750	21.688	-728.410	0.354	0.036	-0.130	0.048
Ambient	B13	<i>Ctenodiscus crispatus</i>	3	8.796	3.102	14.907	-74.363	0.046	0.066	-0.092	0.137
Ambient	B16	<i>Ctenodiscus crispatus</i>	1	8.827	1.888	12.245	-305.589	0.952	0.792	-0.320	0.059
Ambient	B16	<i>Ctenodiscus crispatus</i>	2	7.585	2.797	11.398	101.869	-0.466	-0.737	-0.762	-0.079
Ambient	B16	<i>Ctenodiscus crispatus</i>	3	9.158	5.211	24.053	-211.187	-0.505	-0.352	-0.170	0.492
Ambient	B13	<i>Cistenides hyperborea</i>	1	27.088	2.912	52.198	-268.773	-0.014	1.266	0.576	0.368
Ambient	B13	<i>Cistenides hyperborea</i>	2	27.767	2.136	67.670	146.754	-0.068	0.917	0.271	0.299
Ambient	B13	<i>Cistenides hyperborea</i>	3	26.429	3.929	82.976	336.853	-0.167	0.989	0.126	0.054
Ambient	Rothera	<i>Aequiyooldia eightsi</i>	1	11.183	1.613	11.129	596.093	-0.077	0.316	0.297	0.916
Ambient	Rothera	<i>Aequiyooldia eightsi</i>	2	10.562	1.966	5.899	-142.498	-0.311	0.194	0.183	0.926
Ambient	Rothera	<i>Aequiyooldia eightsi</i>	3	20.529	1.202	11.538	-1102.750	-0.048	0.222	0.474	2.781
Ambient	Rothera	<i>Laternula elliptica</i>	1	17.188	2.135	6.146	270.931	0.486	0.261	0.280	0.663
Ambient	Rothera	<i>Laternula elliptica</i>	2	18.177	2.396	6.927	-209.815	0.741	-0.623	-0.295	0.597
Ambient	Rothera	<i>Laternula elliptica</i>	3	12.832	2.345	4.381	100.282	-1.157	0.555	0.468	0.753
Future	B13	<i>Astarte crenata</i>	1	15.924	3.361	14.874	-486.898	-1.431	0.067	0.065	0.261
Future	B13	<i>Astarte crenata</i>	2	16.833	2.833	10.333	15.398	-0.217	0.050	-0.061	0.248
Future	B13	<i>Astarte crenata</i>	3	18.211	2.632	10.789	-114.633	0.199	-0.033	-0.101	0.204
Future	B16	<i>Astarte crenata</i>	1	18.211	2.737	5.211	699.360	-0.225	0.322	0.199	0.362
Future	B16	<i>Astarte crenata</i>	2	9.837	1.870	3.984	-52.708	-1.515	0.365	0.418	0.598
Future	B16	<i>Astarte crenata</i>	3	10.865	2.644	6.346	-270.559	-0.384	-0.123	-0.231	0.095
Future	B13	<i>Ctenodiscus crispatus</i>	1	10.891	3.168	15.941	163.403	0.540	0.482	0.025	0.337
Future	B13	<i>Ctenodiscus crispatus</i>	2	11.274	2.217	13.160	-282.644	0.355	-1.062	-0.533	0.150
Future	B13	<i>Ctenodiscus crispatus</i>	3	15.577	0.865	17.308	-309.883	-0.493	0.518	-0.042	0.348
Future	B16	<i>Ctenodiscus crispatus</i>	1	9.767	3.488	22.907	-769.134	0.073	0.673	-0.211	-0.076

Appendix A

Future	B16	<i>Ctenodiscus crispatus</i>	2	10.709	1.231	9.478	-894.046	0.817	1.386	0.121	0.475
Future	B16	<i>Ctenodiscus crispatus</i>	3	8.713	2.794	15.404	-1235.051	-0.099	1.258	0.062	0.333
Future	B13	<i>Cistenides hyperborea</i>	1	22.525	3.990	71.061	-417.178	0.004	0.944	-1.309	0.420
Future	B13	<i>Cistenides hyperborea</i>	2	36.031	4.072	84.691	-715.989	-0.101	0.703	-1.478	0.402
Future	B13	<i>Cistenides hyperborea</i>	3	20.850	3.400	68.700	-556.549	0.034	1.028	-0.962	0.907
Future	Rothera	<i>Aequiyoldia eightsi</i>	1	23.739	2.838	17.477	-955.795	-0.157	-0.737	-0.166	1.082
Future	Rothera	<i>Aequiyoldia eightsi</i>	2	13.611	1.852	18.194	260.590	-0.994	-0.179	-0.159	0.836
Future	Rothera	<i>Aequiyoldia eightsi</i>	3	22.120	2.826	17.174	115.246	-0.251	-0.653	-0.143	0.336
Future	Rothera	<i>Laternula elliptica</i>	1	7.718	1.845	6.262	-417.679	-1.732	-0.021	-0.079	0.303
Future	Rothera	<i>Laternula elliptica</i>	2	10.909	2.273	5.289	157.486	-0.367	-0.200	-0.282	0.168
Future	Rothera	<i>Laternula elliptica</i>	3	17.603	2.893	9.793	-102.498	0.593	0.358	0.197	0.465

## A.1 References

BARNES, D. K. A., ANDRADE, L., BRAUN, J., BROAD, E., BRUNNER, L., DOWNES, P., DIXON, J., ENSOR, N., EVANS, J., FAUST, J., GODBOLD, J., HENLEY, S., JONES, R., MAY, R., MCAFEE, C., MESHER, T., MURDOCH, I., OWEN, R., REED, A., RÜHL, S., SALES DE FREITAS, F., STEVENSON, M., VENABLES, E., VINCENT, S., WALKINSHAW, C., WILLIAMS, T., WOOD, C., ZAENCKER, B. & ZINDORF, M. 2019. Changing Arctic Ocean Seafloor JR18006 Cruise Report.

BLOTT, S. J. & PYE, K. 2001. GRADISTAT: A grain size distribution and statistics package for the analysis of unconsolidated sediments. *Earth Surface Processes and Landforms*, 26, 1237-1248.

JØRGENSEN, L. L., LJUBIN, P., SKJOLDAL, H. R., INGVALDSEN, R. B., ANISIMOVA, N. & MANUSHIN, I. 2015. Distribution of benthic megafauna in the Barents Sea: baseline for an ecosystem approach to management. *ICES Journal of Marine Science*, 72, 595-613.

LOENG, H. 1991. Features of the Physical Oceanographic Conditions of the Barents Sea. *Polar Research*, 10, 5-18.

ROBBINS, L. L., HANSEN, M. E., KLEYPAS, J. A. & MEYLAN, S. C. 2010. CO2calc: A user-friendly carbon calculator for Windows, Mac OS X, and iOS (iPhone) *Florida Shelf Ecosystems Response to Climate Change Project*. U.S. Geological Survey.



## Appendix B Appendix for Chapter 3

**Table S1 (next two pages):** Log summary of Arctic faunal and sediment collection **(a)** from replicate SMBA cores and **(b)** replicate Agassiz trawls onboard the JR18006 cruise (Barnes 2019). Events were for collection of sediment (**s**) and/or fauna (**f**).

**Table S1(a)**

Station	Event	Date	Lat (°N)	Long (°E)	Time (GMT)	Depth (m)
B13	32 <sub>S,F</sub>	08/07/2019	74.46607	30.11835	18:14:45	354.59
B13	33 <sub>S,F</sub>	08/07/2019	74.46613	30.11831	18:52:08	354.21
B13	34 <sub>S,F</sub>	08/07/2019	74.46614	30.1184	19:23:06	354.19
B13	35 <sub>S,F</sub>	08/07/2019	74.46621	30.1184	20:02:01	357.10
B13	36 <sub>S,F</sub>	08/07/2019	74.46618	30.11864	20:33:04	354.41
B13	37 <sub>S,F</sub>	08/07/2019	74.46623	30.11868	21:05:04	354.38
B13	38 <sub>S,F</sub>	08/07/2019	74.46619	30.119	21:50:21	353.99
B13	39 <sub>S,F</sub>	08/07/2019	74.46626	30.11901	22:29:06	254.18
B13	40 <sub>S,F</sub>	08/07/2019	74.46625	30.1191	23:05:50	353.91
B13	41 <sub>S,F</sub>	08/07/2019	74.46627	30.11932	23:36:46	353.82
B13	42 <sub>S,F</sub>	09/07/2019	74.46632	30.1194	00:18:57	353.97
B13	43 <sub>S,F</sub>	09/07/2019	74.46632	30.11948	00:53:47	353.50
B13	44 <sub>S,F</sub>	09/07/2019	74.46631	30.11958	01:30:14	354.32
B14	105 <sub>S</sub>	13/07/2019	76.55291	30.61992	09:00:16	281.47
B14	106 <sub>S</sub>	13/07/2019	76.55282	30.61963	09:38:10	281.41
B16	161 <sub>S,F</sub>	17/07/2019	80.08478	30.15126	06:00:25	263.00
B16	162 <sub>S,F</sub>	17/07/2019	80.08561	30.14997	06:28:22	264.00
B16	163 <sub>S,F</sub>	17/07/2019	80.08785	30.1499	07:04:36	264.00

Cruise reports for this research programme can be obtained from the British Oceanographic Data Centre at: [https://www.bodc.ac.uk/resources/inventories/cruise\\_inventory/results/](https://www.bodc.ac.uk/resources/inventories/cruise_inventory/results/)

Barnes D. 2019 RRS James Clark Ross cruise, JR18006.

Cruise reports for JR16006 and JR17007 are not relevant to the present manuscript, but listed here as they forms sister cruises for this research programme:

Cottier FR. 2017 RRS James Clark Ross cruise, JR16006

Solan M. 2018 RRS James Clark Ross cruise, JR17007

**Table S1(b)**

Station	Event	Date	Latitude (°N)			Longitude (°E)			Time (HH:MM)		Trawl time (mins)	Depth(m)	
			On bottom	Trawl Start	Left bottom	On bottom	Trawl Start	Left bottom	On bottom	Trawl Start			
B13	53 <sub>F</sub>	09/07/2019	74.4972	74.49767	74.49857	30.0744	30.07926	30.08872	10:39	10:49	11:09	00:19	361.86
B13	54 <sub>F</sub>	09/07/2019	74.50071	74.50109	74.50149	30.11158	30.11768	30.12638	12:24	12:36	12:53	00:17	351.78
B13	171 <sub>F</sub>	24/07/2019	74.49889	74.4973	74.4963	29.99775	29.98403	29.97519	16:43	17:12	17:30	00:18	362.15
B13	172 <sub>F</sub>	24/07/2019	74.49567	74.49566	74.49568	29.9643	29.95472	29.94587	18:11	18:29	18:46	00:17	367.31
B13	173 <sub>F</sub>	24/07/2019	74.4964	74.49767	74.49861	29.93578	29.92737	29.92129	19:30	19:49	20:02	00:13	371.81
B13	174 <sub>F</sub>	24/07/2019	74.50068	74.50213	74.50327	29.90772	29.89843	29.89113	21:02	21:22	21:38	00:16	374.83
B13	175 <sub>F</sub>	24/07/2019	74.50524	74.50657	74.50765	29.87843	29.86988	29.86281	22:25	22:44	23:00	00:15	372.55
B13	176 <sub>F</sub>	24/07/2019	74.51009	74.5109	74.51229	29.84718	29.84188	29.83291	23:46	00:03	00:20	00:17	372.81
B13	177 <sub>F</sub>	25/07/2019	74.51637	74.51866	74.52021	29.81048	29.80509	29.80134	01:13	01:33	01:46	00:13	369.16

**Table S2:** Summary of experimental design for investigating the effects of enhanced temperature and atmospheric [CO<sub>2</sub>] on species-specific physiological and biochemical processes.

Species	Origin	Station	total <i>n</i> <sub>aquaria</sub>	Environmental condition	
<i>Astarte crenata</i>	Arctic	B13, B16	12	1°C, 400 <sub>[CO<sub>2</sub>]</sub> ppm	2.5°C, 550 <sub>[CO<sub>2</sub>]</sub> ppm
<i>Ctenodiscus crispatus</i>	Arctic	B13, B16	12	1°C, 400 <sub>[CO<sub>2</sub>]</sub> ppm	2.5°C, 550 <sub>[CO<sub>2</sub>]</sub> ppm
<i>Cistenides hyperborea</i>	Arctic	B13	6	1°C, 400 <sub>[CO<sub>2</sub>]</sub> ppm	2.5°C, 550 <sub>[CO<sub>2</sub>]</sub> ppm
<i>Aequiyledia eightsi</i>	Antarctic	Rothera	6	1°C, 400 <sub>[CO<sub>2</sub>]</sub> ppm	2.5°C, 550 <sub>[CO<sub>2</sub>]</sub> ppm

**Figure S2:** Experimental water bath system housed at the *Biodiversity and Ecosystem Futures Facility*, University of Southampton in **(a)** a fibreglass seawater bath (lid removed, LWH: 1.20 x 1.20 x 0.80 m) used to house the aquaria (LWH: 0.20 x 0.20 x 0.33 m) during the experimental period and **(b)** schematic of the air-CO<sub>2</sub> gas mixture and delivery apparatus (Godbold & Solan, 2013) . I accommodated aquaria subjected to ambient environmental conditions (2 water baths) and future environmental conditions (2 water baths) . In each seawater bath, aquaria were randomly positioned within each environmental condition across both treatment baths. Bath temperatures were controlled by a **(1)** chiller (Titan 1500, AquaMedic, modified to add chill-heat regulation capability) and the desired atmospheric CO<sub>2</sub> (ambient, ~400 ppm, future, ~550 ppm ) continuously bubbled into each aquarium through glass pipettes was controlled from a **(2)** CO<sub>2</sub>-air mixing system controlled by an infra-red gas analyser (Licor LI-840A).

Figure S2(a)

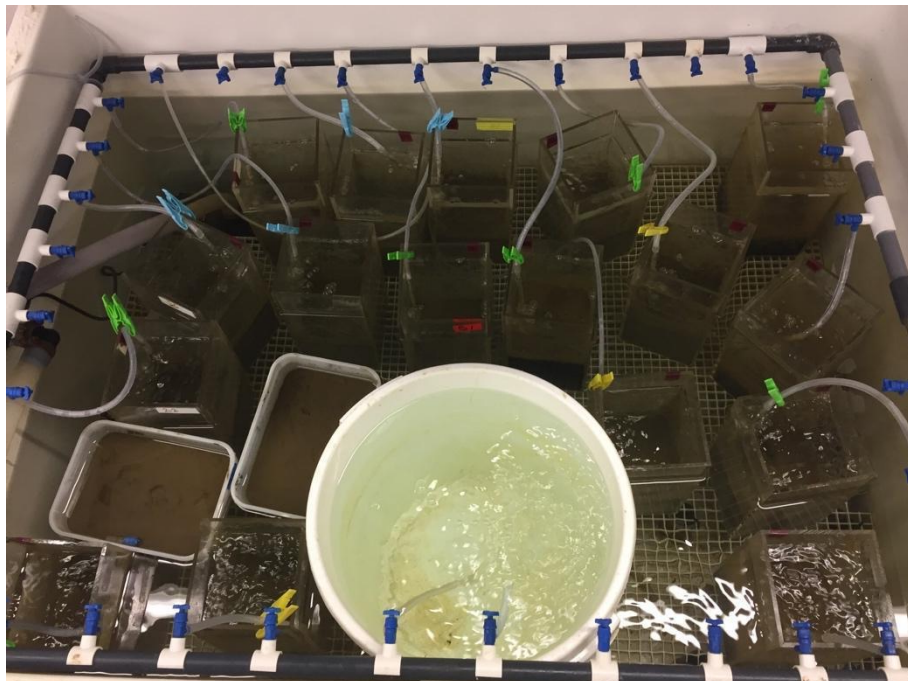
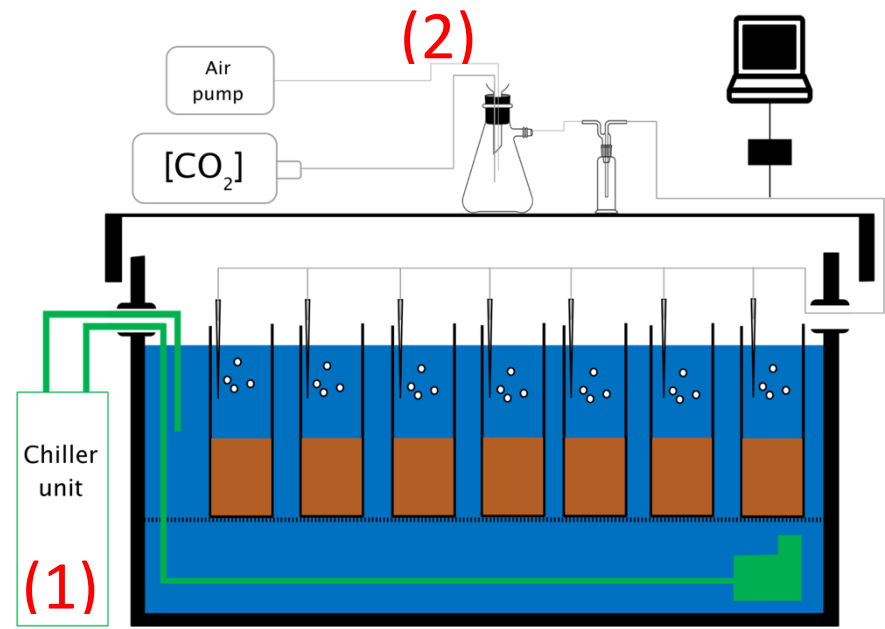


Figure S2(b)



**Table S3:** Summary of summer near-bottom temperatures at **(a)** stations B13 and B16 in the Arctic obtained from two independent sensors (Temperature #1 and #2) on proximate CTD casts: Data courtesy of Dr. Sian Henley, University of Edinburgh) and **(b)** Rothera Oceanographic and Biological Time Series station 3 (Latitude 67.577514 °S; Longitude 68.215232 °W; closest CTD cast maximum depth 495.4 m; averaged using all available data between 1<sup>st</sup> December and 28<sup>th</sup> February; extracted from <https://www.bodc.ac.uk/resources/inventories/edmed/report/4278/>).

Table S3(a)

Station	Latitude (N)	Longitude (E)	Depth (m)	Bottle depth (m)	Temperature #1 (°C) (mean)	Temperature #2 (°C) (mean)	Date (ddmmyy) and Time (UTC)
JCR16006							
	B13	74.4998	29.9982	346	345.7	2.418	2.418 01/08/2017 01:27
JCR17007	B16	80.1513	29.9146	294	277.6	-1.436	-1.438 22/07/2017 08:02
JCR18006	B13	74.5000	30.0002	357	350.6	0.802	0.801 28/07/2018 03:54
	B16	80.1167	30.0683	280	270.6	0.387	0.386 22/07/2018 10:18
	B13	74.50003	30.00062	359.1	350	1.480	07/07/2019 16:32
	B16	80.04295	30.0193	287.7	269	-1.830	16/07/2019 03:51

Table S3(b)

Year	Temperature (°C)
2000	1.14
2003	0.743
2004	1.1
2005	1.1
2006	1.11
2007	1.13
2008	1.07
2009	1.13
2010	1.14
2011	1.16

**Figure S3:** Monthly seawater measurements in aquaria under ambient ( $1\text{ }^{\circ}\text{C}$ ,  $400\text{ ppm [CO}_2\text{]}$ ; blue circles) and future ( $2.5\text{ }^{\circ}\text{C}$ ,  $550\text{ ppm [CO}_2\text{]}$ ; red squares) environmental conditions. Temperature ( $^{\circ}\text{C}$ ), Salinity,  $\text{pH}_{\text{NBS}}$  and total alkalinity ( $\text{A}_T, \mu\text{mol kgSW}^{-1}$ ) were measured directly from each mesocosm and were used to calculate dissolved organic carbon (DIC,  $\mu\text{mol kgSW}^{-1}$ ),  $\text{pCO}_2^{\text{SW}}$  ( $\mu\text{Atm}$ ), saturation states for calcite ( $\Omega_{\text{Calcite}}$ ) and aragonite ( $\Omega_{\text{Aragonite}}$ ), bicarbonate ( $\text{HCO}_3, \mu\text{mol kgSW}^{-1}$ ) and carbonate ( $\text{CO}_3, \mu\text{mol kgSW}^{-1}$ ) using *CO2calc* (Robbins et al. 2010). The absence of intermediate data (weeks 12-48) coincides with the 2020 Covid pandemic UK lockdown period where access was constrained.

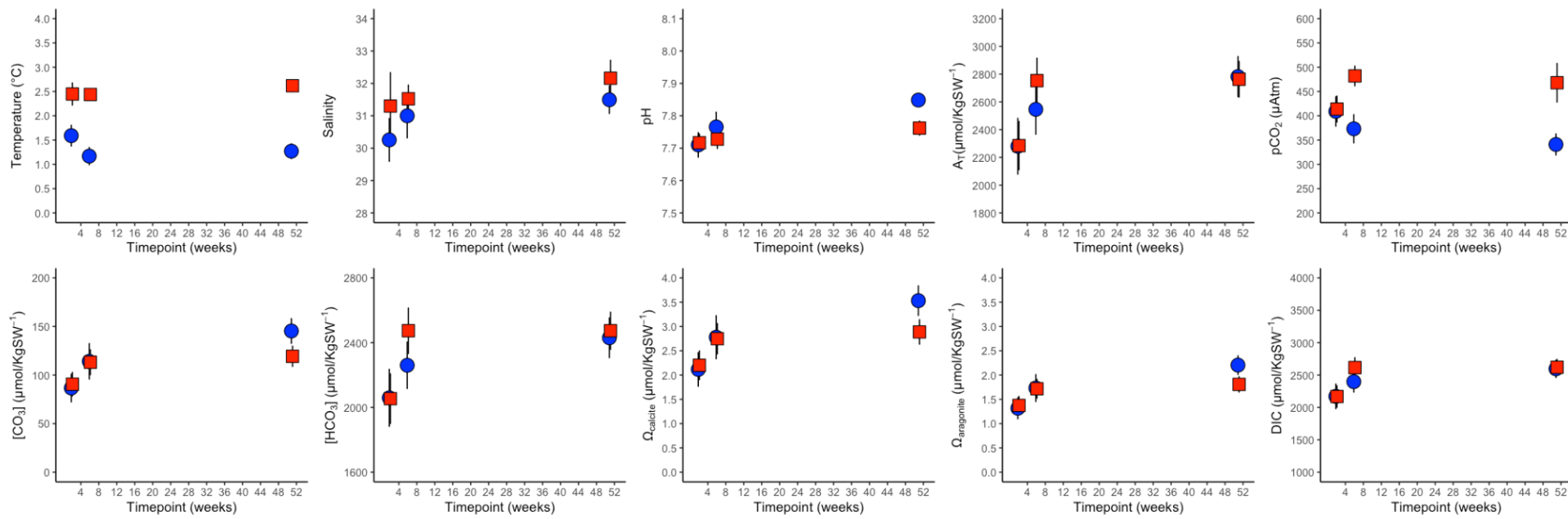


**Figure S4:** Photographs of the morphological measurements for (a) *Astarte crenata* (b) *Ctenodiscus crispatus* (c) *Cistenides hyperborea* (d) *Aequiyoldia eightsi*. Red arrows demonstrate the measurements taken for each species (SL: shell length; SW: shell width; SH: shell height; AL: arm length; PL: pit length; TL: tube length; AOD: aperture opening diameter). Scale indicated with cm rule.

Figure S4 (a)

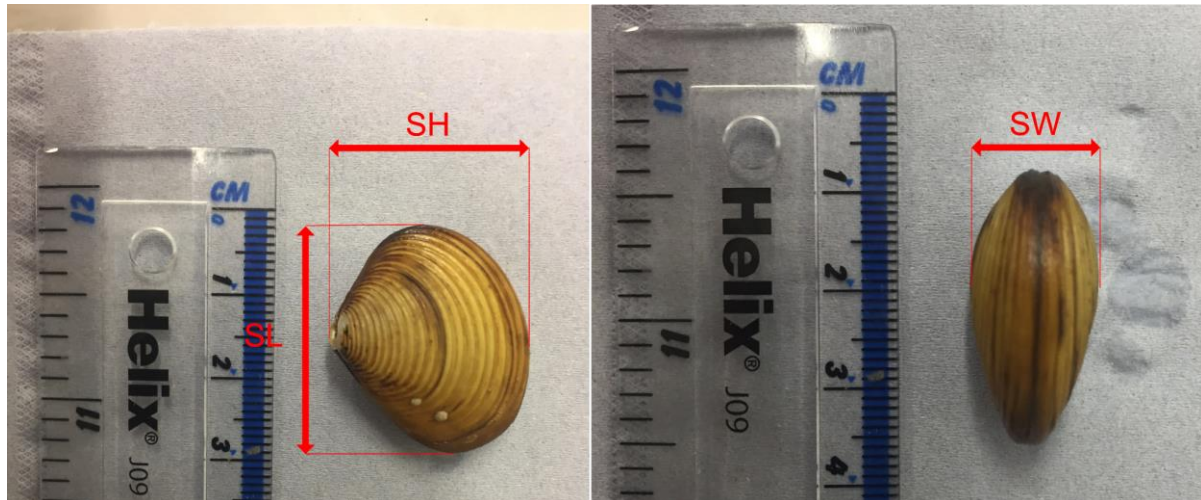


Figure S4(b)

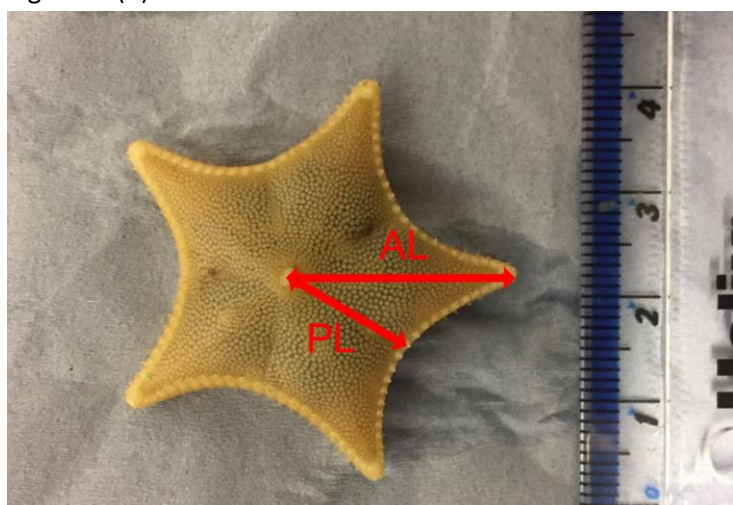
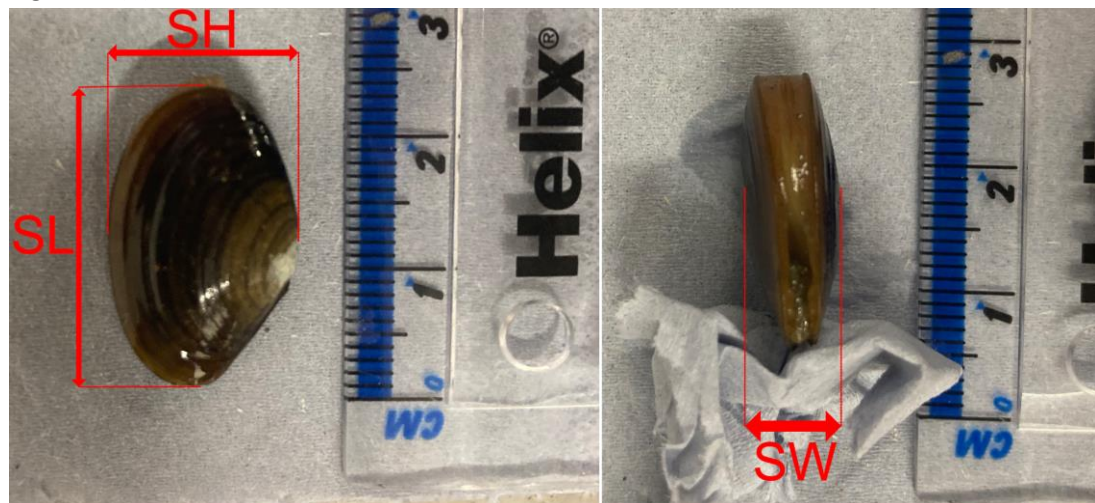


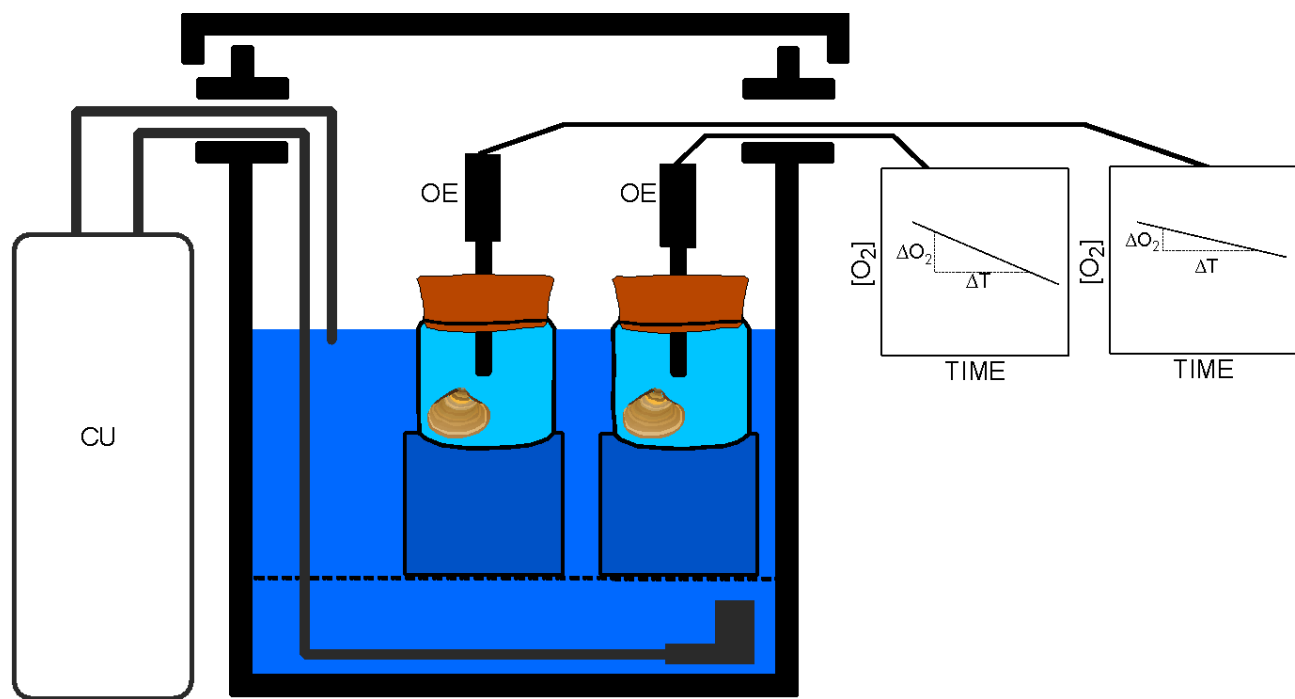
Figure S4(c)



Figure S4(d)



**Figure S5:** A schematic of the closed-chamber constant volume respirometry system used during the experiment, adapted from Lighton (2008). A total of four glass chambers (120 ml volume) with salinity-corrected oxygen electrodes (OE) were run in parallel within the temperature controlled seawater baths with an accompanying chiller unit (CU; see Figure S2). The rate of decline of the measured  $O_2$  concentration in the chamber water, in combination with the volume of the chamber (minus the displacement from the organism), yields the rate of  $O_2$  consumption of the organism.



Appendix B

**Table S4 (next two pages):** Table of loss of ignition results for calculating organic matter content in individuals from (a) ambient and (b) future environmental condition treatments

Table S4(a)

Environmental condition	Species	Station	Dry weight [DW] (g)	Ashed weight (g)	Organic matter [OM] (g)	OM g DW <sup>-1</sup> (g)	OM g WTW <sup>-1</sup>	OM DW <sup>-1</sup> (%)	OM WTW <sup>-1</sup> (%)
Ambient	<i>Aequiyyoldia eightsi</i>	Rothera	0.009	0.002	0.007	0.805	0.158	80	16
Ambient	<i>Aequiyyoldia eightsi</i>	Rothera	0.009	0.004	0.006	0.591	0.097	59	10
Ambient	<i>Aequiyyoldia eightsi</i>	Rothera	0.013	0.003	0.010	0.800	0.159	80	16
Ambient	<i>Astarte crenata</i>	B13	0.008	0.001	0.007	0.845	0.152	85	15
Ambient	<i>Astarte crenata</i>	B13	0.007	0.001	0.006	0.814	0.131	81	13
Ambient	<i>Astarte crenata</i>	B13	0.019	0.012	0.007	0.347	0.140	35	14
Ambient	<i>Astarte crenata</i>	B16	0.010	0.003	0.007	0.691	0.109	69	11
Ambient	<i>Astarte crenata</i>	B16	0.015	0.008	0.007	0.467	0.092	47	9
Ambient	<i>Astarte crenata</i>	B16	0.008	0.002	0.006	0.738	0.094	74	9
Ambient	<i>Ctenodiscus crispatus</i>	B13	0.032	0.029	0.003	0.102	0.047	10	5
Ambient	<i>Ctenodiscus crispatus</i>	B13	0.027	0.024	0.003	0.103	0.042	10	4
Ambient	<i>Ctenodiscus crispatus</i>	B13	0.022	0.019	0.003	0.138	0.046	14	5
Ambient	<i>Ctenodiscus crispatus</i>	B16	0.031	0.025	0.006	0.197	0.081	20	8
Ambient	<i>Ctenodiscus crispatus</i>	B16	0.041	0.037	0.003	0.084	0.034	8	3
Ambient	<i>Ctenodiscus crispatus</i>	B16	0.035	0.033	0.002	0.057	0.027	6	3
Ambient	<i>Cistenides hyperborea</i>	B13	0.015	0.009	0.006	0.412	0.097	41	10
Ambient	<i>Cistenides hyperborea</i>	B13	0.009	0.005	0.005	0.505	0.109	51	11
Ambient	<i>Cistenides hyperborea</i>	B13	0.008	0.003	0.005	0.613	0.115	61	12

Table S4(b)

Environmental condition	Species	Station	Dry weight [DW] (g)	Ashed weight (g)	Organic matter [OM] (g)	OM per g DW <sup>-1</sup> (g)	OM per g WTW <sup>-1</sup>	OM per DW (%)	OM per WTW (%)
Future	<i>Aequioldia eightsi</i>	Rothera	0.014	0.003	0.011	0.772	0.191	77	19
Future	<i>Aequioldia eightsi</i>	Rothera	0.013	0.002	0.011	0.867	0.179	87	18
Future	<i>Aequioldia eightsi</i>	Rothera	0.010	0.004	0.006	0.621	0.143	62	14
Future	<i>Astarte crenata</i>	B13	0.006	0.004	0.002	0.393	0.060	39	6
Future	<i>Astarte crenata</i>	B13	0.003	0.002	0.001	0.412	0.080	41	8
Future	<i>Astarte crenata</i>	B13	0.008	0.002	0.006	0.733	0.130	73	13
Future	<i>Astarte crenata</i>	B16	0.014	0.005	0.009	0.638	0.119	64	12
Future	<i>Astarte crenata</i>	B16	0.010	0.004	0.007	0.650	0.121	65	12
Future	<i>Astarte crenata</i>	B16	0.008	0.007	0.001	0.157	0.031	16	3
Future	<i>Ctenodiscus crispatus</i>	B13	0.019	0.008	0.011	0.603	0.190	60	19
Future	<i>Ctenodiscus crispatus</i>	B13	0.033	0.030	0.003	0.076	0.032	8	3
Future	<i>Ctenodiscus crispatus</i>	B13	0.030	0.025	0.004	0.148	0.059	15	6
Future	<i>Ctenodiscus crispatus</i>	B16	0.032	0.028	0.004	0.124	0.052	12	5
Future	<i>Ctenodiscus crispatus</i>	B16	0.024	0.015	0.009	0.388	0.151	39	15
Future	<i>Ctenodiscus crispatus</i>	B16	0.026	0.020	0.006	0.246	0.092	25	9
Future	<i>Cistenides hyperborea</i>	B13	0.004	0.002	0.002	0.421	0.291	42	29
Future	<i>Cistenides hyperborea</i>	B13	0.016	0.011	0.005	0.302	0.108	30	11
Future	<i>Cistenides hyperborea</i>	B13	0.010	0.005	0.005	0.495	0.097	49	10

**Figure S6:** Summary of the nutritional values and associated information of frozen *Cerastoderma edule* tissue used in the biochemical analyses as a standard. *Cerastoderma edule* was found to contain (mean  $\pm$  s.d., n = 6)  $3.5 \pm 0.1$  g GLU and  $10.9 \pm 1.7$  g PROT per 100g tissue, consistent with the carbohydrate and protein nutrition information values provided.

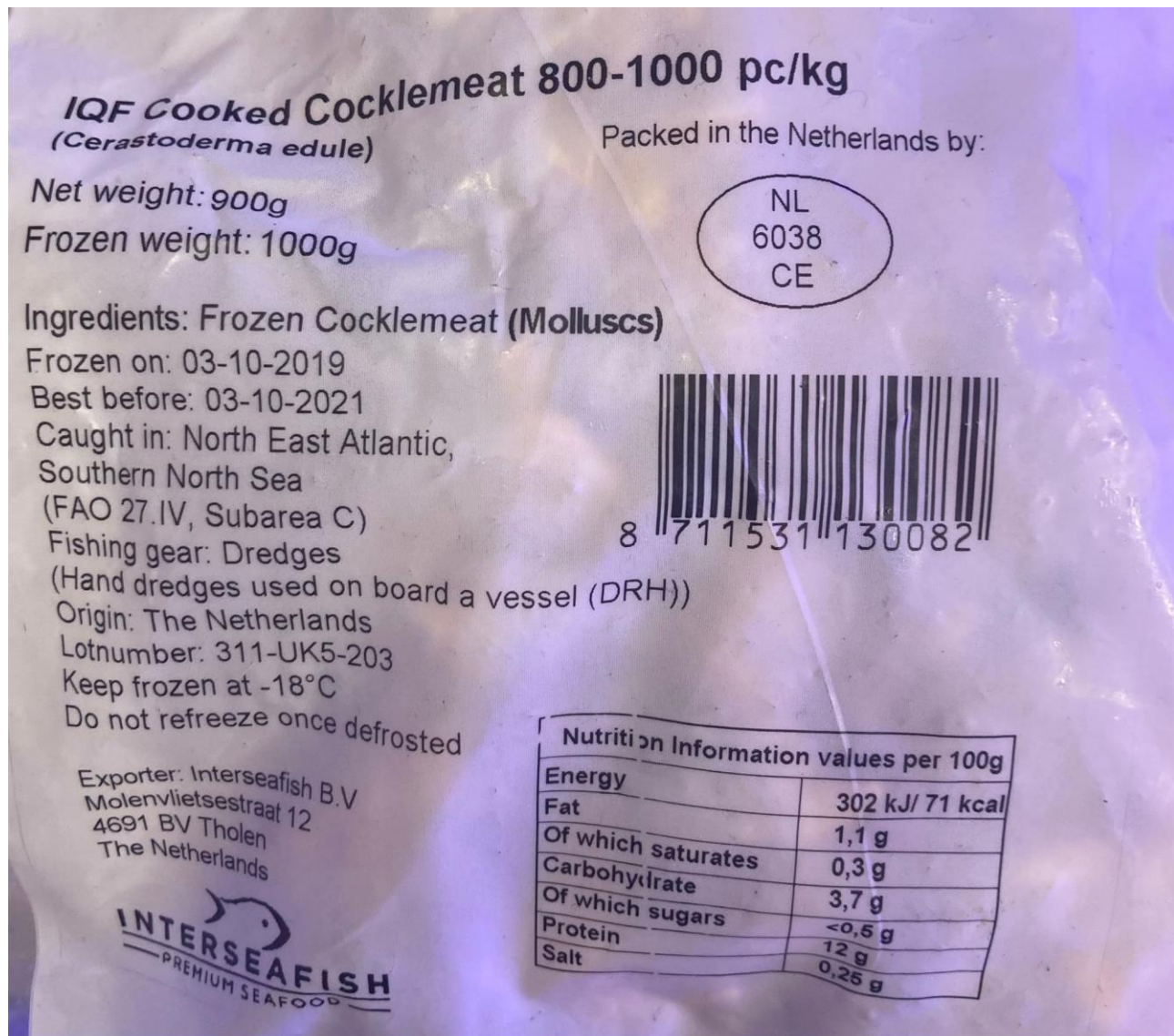


**Table S5:** List of reagents used for the extraction of (a) total proteins and (b) D-glucose from marine invertebrate tissues

Table S5(a)

Reagent Name	Brand	Supplier
Tissue Extraction Reagent II	Invitrogen™	FisherScientific
Protease Inhibitor Tablets	Thermo Scientific™	FisherScientific

Table S5(b)

Reagent Name	Brand	Supplier
Carrez I solution	Chem Lab™	FisherScientific
Zinc Sulphate	Alfa Aesar™	FisherScientific
Sodium Hydroxide	Fisher Chemical	FisherScientific

**Figure S7 (next three pages):** Total least square regressions of oxygen decline over time during closed-chamber constant volume respirometry of (a-b) *Astarte crenata* from station B13; (c-d) *Astarte crenata* from station B16; (e-f) *Ctenodiscus crispatus* from station B13; (g-h) *Ctenodiscus crispatus* from station B16 (i-j) *Cistenides hyperborea*; (k-l) *Aequioidia eightsi* from the (a,c,e,g,i,k) ambient (blue) and (b,d,f,h,j,l) future (red) environmental condition treatments.

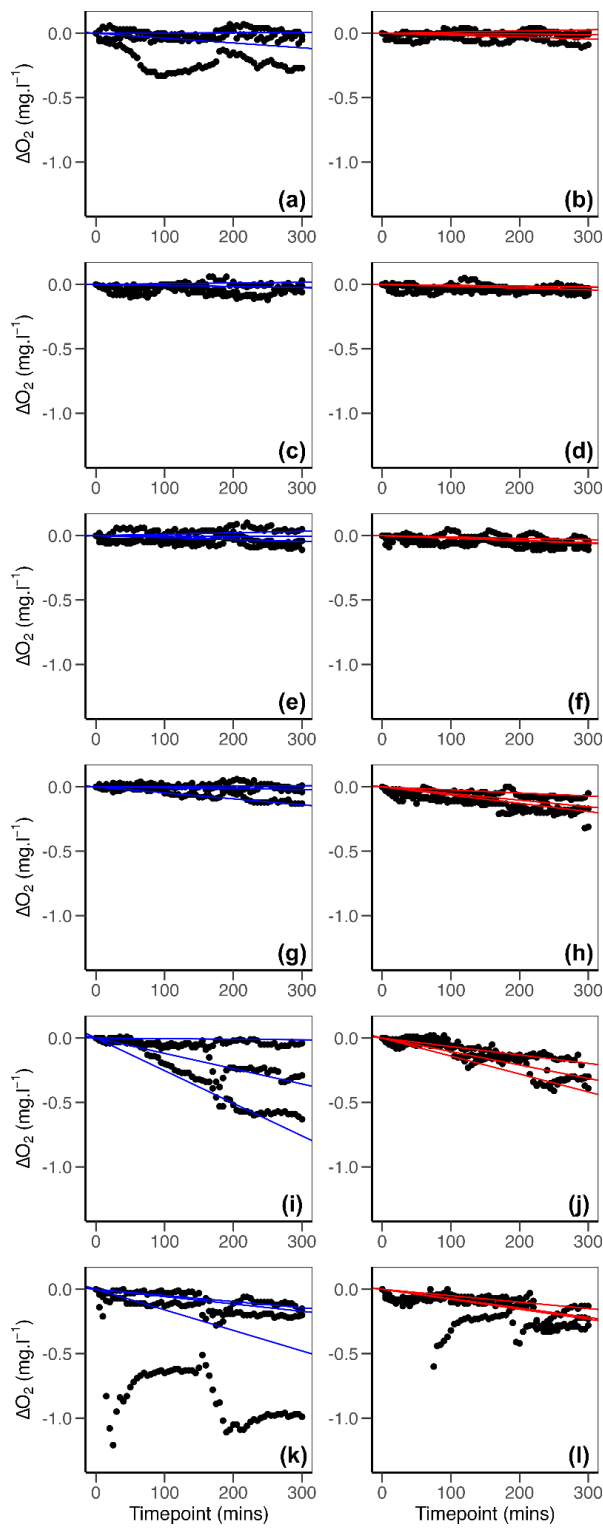


**Table S6:** Table of errors for (a) oxygen consumption (b) ammonium excretion and (c) phosphate excretion in individuals from each species and their summarised mean (bold) from the ambient and future environmental condition treatments.

Table S6(a)

Species	Environmental condition	Mean $[\text{MO}_2]_{\text{ctrl}}$ ( $\mu\text{g.h}^{-1}$ )	Mean $[\text{MO}_2]_{\text{ctrl}}$ (%) species	SE (%) species
<b>ALL</b>	Ambient	<b>0.2721</b>	5	<b>22</b>
<i>Astarte crenata</i>	Ambient	0.2721	-57	46
<i>Ctenodiscus crispatus</i>	Ambient	0.2721	23	45
<i>Cistenides hyperborea</i>	Ambient	0.2721	30	20
<i>Aequiyooldia eightsi</i>	Ambient	0.2721	6	1
<b>ALL</b>	Future	<b>-0.5358</b>	<b>43</b>	<b>16</b>
<i>Astarte crenata</i>	Future	-0.5358	-83	43
<i>Ctenodiscus crispatus</i>	Future	-0.5358	-36	9
<i>Cistenides hyperborea</i>	Future	-0.5358	-8	0
<i>Aequiyooldia eightsi</i>	Future	-0.5358	-12	1

Table S6(b)

Species	Environmental condition	Mean $\Delta[\text{NH}_4]_{\text{ctrl}}$ ( $\text{nmol.h}^{-1}$ )	Mean $\Delta[\text{NH}_4]_{\text{ctrl}}$ (%) species	SE (%) species
<b>ALL</b>	Ambient	<b>0.6</b>	<b>10</b>	<b>3</b>
<i>Astarte crenata</i>	Ambient	0.6	13	6
<i>Ctenodiscus crispatus</i>	Ambient	0.6	9	7
<i>Cistenides hyperborea</i>	Ambient	0.6	15	2
<i>Aequiyooldia eightsi</i>	Ambient	0.6	1	0
<b>ALL</b>	Future	<b>2.3</b>	<b>39</b>	<b>19</b>
<i>Astarte crenata</i>	Future	2.3	79	50
<i>Ctenodiscus crispatus</i>	Future	2.3	16	11
<i>Cistenides hyperborea</i>	Future	2.3	54	21
<i>Aequiyooldia eightsi</i>	Future	2.3	5	1

Table S6(c)

Species	Environmental condition	Mean $\Delta[\text{PO}_4]_{\text{ctrl}}$ ( $\text{nmol.h}^{-1}$ )	Mean $\Delta[\text{PO}_4]_{\text{ctrl}}$ (%) species	SE (%) species
<b>ALL</b>	Ambient	<b>-1.4</b>	<b>20</b>	<b>77</b>
<i>Astarte crenata</i>	Ambient	-1.4	46	70
<i>Ctenodiscus crispatus</i>	Ambient	-1.4	84	225

Appendix B

<i>Cistenides hyperborea</i>	Ambient	-1.4	-113	83
<i>Aequiyyoldia eightsi</i>	Ambient	-1.4	-27	54
<b>ALL</b>	<b>Future</b>	<b>0.6</b>	<b>90</b>	<b>38</b>
<i>Astarte crenata</i>	Future	0.6	34	6
<i>Ctenodiscus crispatus</i>	Future	0.6	222	99
<i>Cistenides hyperborea</i>	Future	0.6	14	1
<i>Aequiyyoldia eightsi</i>	Future	0.6	12	3

**Table S7:** Table of mortality rates of species from ambient and future environmental condition treatments after 360 days.

Environmental condition	Species	Station	Mortality (%)
Ambient	<i>Astarte crenata</i>	B13	0.0
Ambient	<i>Astarte crenata</i>	B16	33.3
Ambient	<i>Ctenodiscus crispatus</i>	B13	50.0
Ambient	<i>Ctenodiscus crispatus</i>	B16	33.3
Ambient	<i>Cistenides hyperborea</i>	B13	10.0
Ambient	<i>Aequioldia eightsi</i>	Rothera	0.0
Future	<i>Astarte crenata</i>	B13	0.0
Future	<i>Astarte crenata</i>	B16	16.7
Future	<i>Ctenodiscus crispatus</i>	B13	33.3
Future	<i>Ctenodiscus crispatus</i>	B16	16.7
Future	<i>Cistenides hyperborea</i>	B13	0.0
Future	<i>Aequioldia eightsi</i>	Rothera	0.0

## Statistical model summary

Summary of the statistical models analysing each species group (Arctic: *A. crenata* & *C. crispatus*; Arctic 2: *C. hyperborea*; Antarctic: *A. eightsi*) separately (Model S1 to S20). For each model I list the initial linear regression model and the minimal adequate model. When variance homogeneity was violated, I used a linear regression with generalized least squares (GLS) estimation. I present a summary of the coefficient tables for single terms. The coefficients indicate the relative performance of each factor level in relation to the re-levelled baseline (as indicated). Coefficients  $\pm$  SE, t-values and respective significance values are presented. As mortalities were observed in *A. crenata* (16.7 %, ambient environmental condition, 8.4 % future environmental condition), *C. crispatus* (41.7 % ambient environmental condition, 25 % future environmental condition) and *C. hyperborea* (10 % ambient environmental condition) after the over the 360 day experimental period, the statistical analyses of growth and body condition were based on the remaining individuals (see table S4).

## Abbreviations

### (i) Explanatory variables

#### Fixed factors

Environmental condition, environmental condition throughout the experimental period (two levels: Ambient | Future)

Station, cruise station (two levels: B13 | B16)

Species, species identity (number of levels dependant on the model)

#### Random factors

WTW, wet tissue weight (g)

### (ii) Response variables

$\Delta$ Biomass, growth over experimental period (% change from initial weight)

TW:SW, tissue:shell wet weight ratio

MO<sub>2</sub>, oxygen consumption ( $\mu\text{g h}^{-1}$ )

$\Delta$ [NH4], ammonium excretion (nmol  $\text{h}^{-1}$ )

$\Delta$ [PO4], phosphate excretion (nmol  $\text{h}^{-1}$ )

PROT, whole organism total protein tissue concentration ( $\mu\text{g mg}^{-1}$  OM)

GLU, whole organism D-glucose tissue concentration ( $\mu\text{g mg}^{-1}$  OM)

**Data:** All data used in the analyses are provided as Table S6.

**Model S1** – growth over experimental period – *Astarte crenata*\**Ctenodiscus crispatus*

Initial linear regression model:

```
lm(formula = ΔBiomass ~ as.factor(Environmental
condition)*as.factor(Species)*as.factor(Station))
```

Minimal adequate model:

```
glm(formula = ΔBiomass ~ as.factor(Environmental condition) + as.factor(Station) +
as.factor(Environmental condition):as.factor(Station),
varIdent(form = ~1|as.factor(Station)*as.factor(Species),
method = "REML")
```

**Model S2** – growth over experimental period – *Cistenides hyperborea*

Initial linear regression model:

```
lm(formula = ΔBiomass ~ as.factor(Environmental condition))
```

Minimal adequate model:

```
lm(formula = ΔBiomass ~ 1)
```

**Model S3** – growth over experimental period – *Aequiyyoldia eightsi*

Initial linear regression model:

```
lm(formula = ΔBiomass ~ as.factor(Environmental condition))
```

Minimal adequate model:

```
glm(formula = ΔBiomass ~ 1,
weights = 1|as.factor(Environmental condition))
```

**Model S4 – tissue:shell wet weight ratio – *Astarte crenata***

Initial linear regression model:

```
lm(formula = TW:SW ~ as.factor(Environmental
condition) *as.factor(Station))
```

Minimal adequate model:

```
lm(formula = TW:SW ~ as.factor(Environmental condition) +
as.factor(Station))
```

Intercept  $\pm$  SE (when baseline is for Ambient for Environmental condition and B13 for Station):

$0.273 \pm 0.015$ ,  $t = 17.668$ , **p < 0.0001**

Coefficient table for Environmental condition

	Ambient	Future
Ambient	/	$0.055 \pm 0.019$ 2.993 <b>0.0089</b>
Future	$0.055 \pm 0.019$ 2.993 <b>0.0089</b>	/

Coefficient table for Station

	B13	B16
B13	/	$-0.084 \pm 0.019$

		-4.472 <b>0.0003</b>
B16	-0.084 ± 0.019 -4.472 <b>0.0003</b>	/

### Model S5 – tissue:shell wet weight ratio – *Aequiyyoldia eightsi*

Initial linear regression model:

```
lm(formula = TW:SW ~ as.factor(Environmental condition))
```

Minimal adequate model:

```
lm(formula = TW:SW ~ as.factor(Environmental condition))
```

Intercept ± SE (when baseline is for Ambient for Environmental condition):  $1.254 \pm 0.044$ ,  $t = 28.674$ , **p < 0.0001**

Coefficient table for Environmental condition

	Ambient	Future
Ambient	/	-0.191 ± 0.060 -3.175 <b>0.0055</b>
Future	-0.191 ± 0.060 -3.175 <b>0.0055</b>	/

**Model S6 – oxygen consumption – *Astarte crenata*\**Ctenodiscus crispatus***

Initial linear regression model:

```
lme(formula = MO2 ~ as.factor(Environmental  
condition)*as.factor(Species)*as.factor(Station),  
  
random = 1|WTW/Species)
```

Minimal adequate model:

```
lm(formula = MO2 ~ as.factor(Environmental condition) +  
as.factor(Species) + as.factor(Environmental  
condition):as.factor(Species))
```

**Model S7 – oxygen consumption – *Cistenides hyperborea***

Initial linear regression model:

```
lme(formula = MO2 ~ as.factor(Environmental condition),  
  
random = 1|WTW)
```

Minimal adequate model:

```
gls(formula = MO2 ~ 1,  
  
weights = 1|as.factor(Environmental condition),  
  
method = "REML")
```

**Model S8 – oxygen consumption – *Aequiylodia eightsi***

Initial linear regression model:

```
lme(formula = MO2 ~ as.factor(Environmental condition),
random = 1 | WTW)
```

Minimal adequate model:

```
gls(formula = MO2 ~ 1,
weights = 1 | as.factor(Environmental condition),
method = "REML")
```

### **Model S9 – ammonium excretion – *Astarte crenata*\**Ctenodiscus crispatus***

Initial linear regression model:

```
lme(formula = Δ[NH4] ~ as.factor(Environmental
condition)*as.factor(Species)*as.factor(Station),
random = 1 | WTW)
```

Minimal adequate model:

```
lm(formula = Δ[NH4] ~ as.factor(Environmental condition) + as.factor(Species) +
as.factor(Environmental condition):as.factor(Species))
```

### **Model S10 – ammonium excretion – *Cistenides hyperborea***

Initial linear regression model:

```
lme(formula = Δ[NH4] ~ as.factor(Environmental condition),
Random = 1 | WTW)
```

Minimal adequate model:

```
gls(formula = Δ[NH4] ~ 1,
weights = 1 | as.factor(Environmental condition),
method = "REML")
```

**Model S11 – ammonium excretion – *Aequiyyoldia eightsi***

Initial linear regression model:

```
lme(formula = Δ[NH4] ~ as.factor(Environmental condition),  
random = 1|WTW)
```

Minimal adequate model:

```
gls(formula = Δ[NH4] ~ 1,  
weights = 1|as.factor(Environmental condition),  
method = "REML")
```

**Model S12 - phosphate excretion - *Astarte crenata*\**Ctenodiscus crispatus***

Initial linear regression model:

```
lme(formula = Δ[PO4] ~ as.factor(Environmental  
condition)*as.factor(Species)*as.factor(Station),  
random = 1|WTW)
```

Minimal adequate model:

```
gls(formula = Δ[PO4] ~ as.factor(Environmental condition), weights =  
1|as.factor(Environmental condition),  
method = "REML")
```

**Model S13 – phosphate excretion – *Cistenides hyperborea***

Initial linear regression model:

```
lme(formula = Δ[PO4] ~ as.factor(Environmental condition),  
random = 1|WTW)
```

Minimal adequate model:

```
gls(formula = Δ[NH4] ~ 1,  
weights = 1|as.factor(Environmental condition),
```

```
method = "REML")
```

**Model S14 – phosphate excretion – *Aequiyyoldia eightsi***

Initial linear regression model:

```
lme(formula = Δ[PO4] ~ as.factor(Environmental condition),
random = 1|WTW)
```

Minimal adequate model:

```
glm(formula = Δ[NH4] ~ 1,
weights = 1|as.factor(Environmental condition),
method = "REML")
```

**Model S15 – whole organism total protein tissue concentration – *Astarte crenata*\**Ctenodiscus crispatus***

Initial linear regression model:

```
lm(formula = PROT ~ as.factor(Environmental
condition)*as.factor(Species)*as.factor(Station))
```

Minimal adequate model:

```
glm(formula = PROT ~ as.factor(Environmental condition) + as.factor(Species) +
as.factor(Environmental condition):as.factor(Species),
weights = varIdent(form = ~1|as.factor(Species)),
method = "REML")
```

**Model S16 – whole organism total protein tissue concentration – *Cistenides hyperborea***

## Appendix B

Initial linear regression model:

```
lm(formula = PROT ~ as.factor(Environmental condition))
```

Minimal adequate model:

```
lm(formula = PROT ~ as.factor(Environmental condition))
```

Intercept  $\pm$  SE (when baseline is for Ambient for Environmental condition):  $5.683 \pm 0.977$ ,  $t = 5.817$ , **p = 0.0044**

Coefficient table for Environmental condition

	Ambient	Future
Ambient	/	$-2.377 \pm 1.382$ $-1.720$ $0.161$
Future	$-2.377 \pm 1.382$ $-1.720$ $0.161$	/

## Model S17 – whole organism total protein tissue concentration – *Aequioldia eightsi*

Initial linear regression model:

```
lm(formula = PROT ~ as.factor(Environmental condition))
```

Minimal adequate model:

```
glm(formula = PROT ~ as.factor(Environmental condition),  
weights = 1|as.factor(Environmental condition),  
method = "REML")
```

Intercept  $\pm$  SE (when baseline is for Ambient for Environmental condition):  $5.733 \pm 0.088$ ,  $t = 65.010$ , **p < 0.0001**

Coefficient table for Environmental condition

	Ambient	Future
Ambient	/	$-1.533 \pm 0.558$ $-2.749$ <u>0.051</u>
Future	$-1.533 \pm 0.558$ $-2.749$ <u>0.051</u>	/

**Model S18** – whole organism D-glucose tissue concentration – *Astarte crenata*\**Ctenodiscus crispatus*

Initial linear regression model:

```
lm(formula = GLU ~ as.factor(Environmental
condition)*as.factor(Species)*as.factor(Station))
```

Minimal adequate model:

```
glm(formula = GLU ~ as.factor(Environmental condition) + as.factor(Species) +
as.factor(Environmental condition):as.factor(Species),
weights = varIdent(form = ~1|as.factor(Species),
method = "REML")
```

**Model S19** – whole organism D-glucose tissue concentration – *Cistenides hyperborea*

## Appendix B

Initial linear regression model:

```
lm(formula = GLU ~ as.factor(Environmental condition))
```

Minimal adequate model:

```
lm(formula = 1)
```

### **Model S20** – whole organism D-glucose tissue concentration – *Aequiyyoldia eightsi*

Initial linear regression model:

```
lm(formula = GLU ~ as.factor(Environmental condition))
```

Minimal adequate model:

```
gls(formula = GLU ~ 1,  
weights = 1|as.factor(Environmental condition))
```

**Table S6 (next three pages):** Data for (a) growth data and (b) O<sub>2</sub> consumption, ammonium excretion and biochemical processes used for statistical analysis. Station = cruise station (B13 = station B13, B16 = station B16).

\*measurement below instrument detection threshold

Table S6(a)

Environmental condition	Station	Species	Growth (%)	Wet TW (g)	Wet SW (g)	TW:SW
Ambient	B13	<i>Astarte crenata</i>	-0.152	0.76	2.639	0.288
Ambient	B13	<i>Astarte crenata</i>	0.018	0.24	1.17	0.205
Ambient	B13	<i>Astarte crenata</i>	0.011	0.514	1.86	0.276
Ambient	B13	<i>Astarte crenata</i>	0.054	0.366	1.386	0.264
Ambient	B13	<i>Astarte crenata</i>	0.125	0.619	2.585	0.239
Ambient	B13	<i>Astarte crenata</i>	-0.010	0.631	1.891	0.334
Ambient	B13	<i>Ctenodiscus crispatus</i>	0.600			
Ambient	B13	<i>Ctenodiscus crispatus</i>	-0.253			
Ambient	B13	<i>Ctenodiscus crispatus</i>	0.049			
Ambient	B13	<i>Cistenides hyperborea</i>	-0.279			
Ambient	B13	<i>Cistenides hyperborea</i>	0.027			
Ambient	B13	<i>Cistenides hyperborea</i>	-0.359			
Ambient	B13	<i>Cistenides hyperborea</i>	-0.292			
Ambient	B13	<i>Cistenides hyperborea</i>	-0.002			
Ambient	B13	<i>Cistenides hyperborea</i>	0.088			
Ambient	B13	<i>Cistenides hyperborea</i>	0.139			
Ambient	B13	<i>Cistenides hyperborea</i>	-0.216			
Ambient	B13	<i>Cistenides hyperborea</i>	-0.107			
Ambient	B16	<i>Astarte crenata</i>	-0.064	0.842	4.245	0.198
Ambient	B16	<i>Astarte crenata</i>	1.167	0.554	3.254	0.17
Ambient	B16	<i>Astarte crenata</i>	-0.156	0.716	3.909	0.183
Ambient	B16	<i>Astarte crenata</i>	-0.043	0.727	3.116	0.233
Ambient	B16	<i>Ctenodiscus crispatus</i>	-0.051			
Ambient	B16	<i>Ctenodiscus crispatus</i>	0.476			
Ambient	B16	<i>Ctenodiscus crispatus</i>	0.147			
Ambient	B16	<i>Ctenodiscus crispatus</i>	0.269			
Ambient	Rothera	<i>Aequiyoldia eightsi</i>	0.189	0.720	0.470	1.532
Ambient	Rothera	<i>Aequiyoldia eightsi</i>	0.119	0.512	0.439	1.166
Ambient	Rothera	<i>Aequiyoldia eightsi</i>	-0.021	0.453	0.427	1.06

Appendix B

Ambient	Rothera	<i>Aequiyyoldia eightsi</i>	-0.021	0.780	0.560	1.393
Ambient	Rothera	<i>Aequiyyoldia eightsi</i>	0.042	0.450	0.390	1.154
Ambient	Rothera	<i>Aequiyyoldia eightsi</i>	0.092	0.527	0.501	1.052
Ambient	Rothera	<i>Aequiyyoldia eightsi</i>	0.115	0.516	0.403	1.280
Ambient	Rothera	<i>Aequiyyoldia eightsi</i>	0.110	0.350	0.270	1.296
Ambient	Rothera	<i>Aequiyyoldia eightsi</i>	0.080	0.530	0.390	1.359
Ambient	Rothera	<i>Aequiyyoldia eightsi</i>	-0.036	0.550	0.430	1.279
Future	B13	<i>Astarte crenata</i>	0.137	0.569	1.931	0.295
Future	B13	<i>Astarte crenata</i>	0.140	0.797	1.972	0.404
Future	B13	<i>Astarte crenata</i>	0.088	0.396	1.175	0.337
Future	B13	<i>Astarte crenata</i>	0.106	0.246	0.75	0.329
Future	B13	<i>Astarte crenata</i>	0.060	0.331	1.147	0.289
Future	B13	<i>Astarte crenata</i>	0.081	0.234	0.681	0.344
Future	B13	<i>Ctenodiscus crispatus</i>	0.251			
Future	B13	<i>Ctenodiscus crispatus</i>	-0.104			
Future	B13	<i>Ctenodiscus crispatus</i>	0.261			
Future	B13	<i>Ctenodiscus crispatus</i>	-0.151			
Future	B13	<i>Cistenides hyperborea</i>	-0.070			
Future	B13	<i>Cistenides hyperborea</i>	-0.291			
Future	B13	<i>Cistenides hyperborea</i>	0.152			
Future	B13	<i>Cistenides hyperborea</i>	-0.252			
Future	B13	<i>Cistenides hyperborea</i>	0.006			
Future	B13	<i>Cistenides hyperborea</i>	-0.077			
Future	B13	<i>Cistenides hyperborea</i>	0.205			
Future	B13	<i>Cistenides hyperborea</i>	0.210			
Future	B13	<i>Cistenides hyperborea</i>	0.043			
Future	B13	<i>Cistenides hyperborea</i>	-0.130			
Future	B16	<i>Astarte crenata</i>	-0.185	0.868	4.203	0.206
Future	B16	<i>Astarte crenata</i>	-0.149	1.378	4.183	0.330
Future	B16	<i>Astarte crenata</i>	-0.239	0.830	3.376	0.246
Future	B16	<i>Astarte crenata</i>	-0.246	0.665	3.783	0.176
Future	B16	<i>Astarte crenata</i>	-0.124	0.731	3.363	0.217
Future	B16	<i>Ctenodiscus crispatus</i>	-0.966			
Future	B16	<i>Ctenodiscus crispatus</i>	-0.721			
Future	B16	<i>Ctenodiscus crispatus</i>	-0.452			
Future	B16	<i>Ctenodiscus crispatus</i>	1.185			
Future	B16	<i>Ctenodiscus crispatus</i>	1.080			
Future	Rothera	<i>Aequiyyoldia eightsi</i>	-0.037	0.466	0.412	1.132
Future	Rothera	<i>Aequiyyoldia eightsi</i>	-0.044	0.450	0.540	0.833

Future	Rothera	<i>Aequiyoldia eightsi</i>	0.280	0.580	0.540	1.074
Future	Rothera	<i>Aequiyoldia eightsi</i>	0.054	0.450	0.43	1.047
Future	Rothera	<i>Aequiyoldia eightsi</i>	-1.025	0.330	0.300	1.100
Future	Rothera	<i>Aequiyoldia eightsi</i>	0.007	0.340	0.330	1.030
Future	Rothera	<i>Aequiyoldia eightsi</i>	-0.232	0.467	0.393	1.189
Future	Rothera	<i>Aequiyoldia eightsi</i>	-0.006	0.612	0.532	1.149
Future	Rothera	<i>Aequiyoldia eightsi</i>	-0.129	0.440	0.430	1.023
Future	Rothera	<i>Aequiyoldia eightsi</i>	0.027	0.399	0.377	1.056

Table S6(b)

Environmental condition	Station	Species	WTW (g)	MO <sub>2</sub> (µg [O <sub>2</sub> ]. L <sup>-1</sup> . hr <sup>-1</sup> )	Δ[NH <sub>4</sub> ] (nmol. min <sup>-1</sup> )	Δ[PO <sub>4</sub> ] (nmol. min <sup>-1</sup> )	CARB (µg.mg <sup>-1</sup> OM)	PROT (µg.mg <sup>-1</sup> OM)
Ambient	B13	<i>Astarte crenata</i>	0.76	0.610	1.72	0.85	0.15	3.48
Ambient	B13	<i>Astarte crenata</i>	0.514	0.094	4.42	2.19	0.42	5.26
Ambient	B13	<i>Astarte crenata</i>	0.619	0.369	1.20	0.78	0.25	5.29
Ambient	B13	<i>Cistenides hyperborea</i>	0.906	0.586	2.64	1.89	0.32	3.78
Ambient	B13	<i>Cistenides hyperborea</i>	0.989	0.659	4.40	5.52	0.33	5.97
Ambient	B13	<i>Cistenides hyperborea</i>	1.01	0.830	4.03	6.54	0.18	7.30
Ambient	B13	<i>Ctenodiscus crispatus</i>	5.019	4.589	53.77	7.99	0.43	14.59
Ambient	B13	<i>Ctenodiscus crispatus</i>	3.412	2.852	16.75	2.57	0.56	32.53
Ambient	B13	<i>Ctenodiscus crispatus</i>	2.398	1.888	0.81	1.27	0.51	9.20
Ambient	B16	<i>Astarte crenata</i>	0.842	0.582	12.28	4.13	0.26	5.66
Ambient	B16	<i>Astarte crenata</i>	0.554	0.294	6.10	4.48	0.26	6.39
Ambient	B16	<i>Astarte crenata</i>	0.716	0.406	7.41	-1.04	0.31	4.95
Ambient	B16	<i>Ctenodiscus crispatus</i>	1.071	0.771	5.93	2.75	0.30	10.01
Ambient	B16	<i>Ctenodiscus crispatus</i>	3.233	2.273	22.25	3.42	0.96	24.98
Ambient	B16	<i>Ctenodiscus crispatus</i>	0.946	-0.214	8.40	1.77	1.16	21.32
Ambient	Rothera	<i>Aequiyoldia eightsi</i>	0.453	0.283	74.43	2.75	0.17	5.85
Ambient	Rothera	<i>Aequiyoldia eightsi</i>	0.527	0.267	49.33	-0.39	0.26	5.75
Ambient	Rothera	<i>Aequiyoldia eightsi</i>	0.512	0.322	42.22	3.89	0.19	5.59
Future	B13	<i>Astarte crenata</i>	0.569	0.009	*	1.90	0.56	13.12
Future	B13	<i>Astarte crenata</i>	0.396	0.016	14.28	1.16	0.38	5.96
Future	B13	<i>Astarte crenata</i>	0.331	0.131	-1.53	0.71	0.20	4.20
Future	B13	<i>Cistenides hyperborea</i>	0.883	0.793	7.94	3.45	0.09	1.60
Future	B13	<i>Cistenides hyperborea</i>	1.132	0.922	2.75	3.65	0.21	4.78
Future	B13	<i>Cistenides hyperborea</i>	0.832	0.562	0.18	2.96	0.27	3.54
Future	B13	<i>Ctenodiscus crispatus</i>	3.81	3.700	17.98	3.11	0.11	4.38
Future	B13	<i>Ctenodiscus crispatus</i>	1.42	0.580	-7.70	0.76	0.84	22.8
Future	B13	<i>Ctenodiscus crispatus</i>	1.797	1.457	4.55	-0.46	0.34	12.54
Future	B16	<i>Astarte crenata</i>	0.868	0.568	87.43	2.28	0.30	5.38
Future	B16	<i>Astarte crenata</i>	0.83	0.630	1.72	0.35	0.20	6.31
Future	B16	<i>Astarte crenata</i>	0.665	-0.075	7.20	1.65	0.74	10.72
Future	B16	<i>Ctenodiscus crispatus</i>	3.459	2.889	22.15	0.03	0.57	11.26
Future	B16	<i>Ctenodiscus crispatus</i>	1.495	1.365	1.85	-0.43	0.13	3.34
Future	B16	<i>Ctenodiscus crispatus</i>	2.909	2.569	26.24	-0.13	0.34	10.02

Future	Rothera	<i>Aequiyoldia eightsi</i>	0.466	0.286	31.92	3.35	0.18	3.64
Future	Rothera	<i>Aequiyoldia eightsi</i>	0.612	0.422	93.56	11.44	0.19	5.26
Future	Rothera	<i>Aequiyoldia eightsi</i>	0.399	0.199	48.01	2.95	0.20	3.73



## B.1 References

Godbold, J. A. & Solan, M. 2013. Long-term effects of warming and ocean acidification are modified by seasonal variation in species responses and environmental conditions. *Philos Trans R Soc Lond B Biol Sci*, 368, 20130186.

Robbins, L. L., Hansen, M. E., Kleypas, J. A. & Meylan, S. C. 2010. CO2calc: A user-friendly carbon calculator for Windows, Mac OS X, and iOS (iPhone) *Florida Shelf Ecosystems Response to Climate Change Project*. U.S. Geological Survey.

Lighton, J. R. B. 2008. *Measuring metabolic rates: a manual for scientists*, Oxford University Press.



## Appendix C Appendix for Chapter 4

**Table S1** | Summary of activity during the *CCGS Amundsen* 2021 expedition (Geoffroy et al. 2021) associated with the collection of *Keratoisis* sp. from station *Disko Fan*.

Time (UTC)	Station Type	Station Activity	Latitude	Longitude	Depth (m)	Dive #	Sample #	Species	Wet Biomass (g)	Height (mm)	Thickest internode (mm)
02/08/2021 15:06	ROV/Benthic	ROV	67.96629	-59.49069	885	R23	23-1	<i>Keratoisis</i> sp.	27	730	3.44
02/08/2021 15:54	ROV/Benthic	ROV	67.96631	-59.4899	883	R23	23-6	<i>Keratoisis</i> sp.	54	900	6.65
02/08/2021 16:21	ROV/Benthic	ROV	67.96631	-59.48892	879.9	R23	23-10	<i>Keratoisis</i> sp.	7	220	3.62
02/08/2021 17:02	ROV/Benthic	ROV	67.9663	-59.48768	876.2	R23	23-16	<i>Keratoisis</i> sp.	35	650	3.82

## Appendix C

**Figure S1** | Collection of *Keratoisis* sp. colonies from station *Disko Fan* with the Sub-Atlantic® Comanche (Forum Energy Technologies™, USA) remotely operated vehicle during the CCGS Amundsen 2021 expedition (Geoffroy et al. 2021). Panels show (a) collection of *Keratoisis* sp. colony #23-1, (b) collection of *Keratoisis* sp. colony #23-6, (c) collection of *Keratoisis* sp. colony #23-10 and (d) collection of *Keratoisis* sp. colony #23-16. Collected specimens are held in the frame. Scale (green laser guides) = 10 cm. Associated metadata are provided in Table S1.

Figure S1(a)



Figure S1(b)

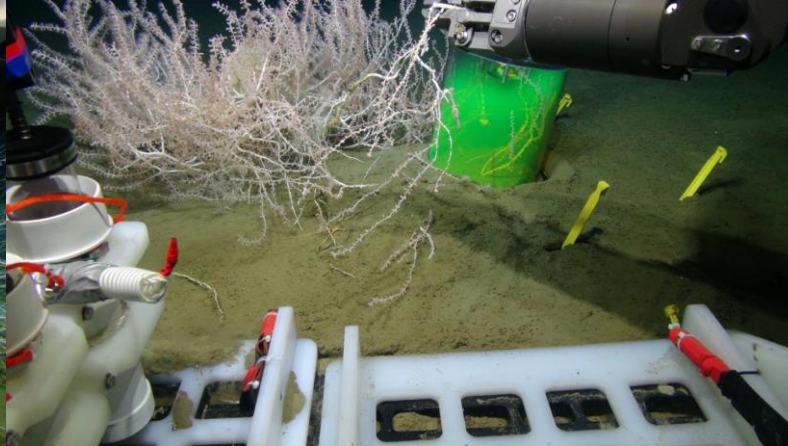


Figure S1(c)

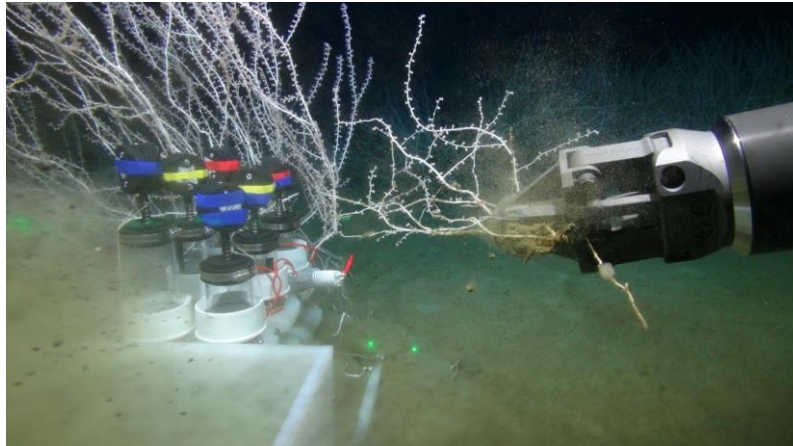


Figure S1(d)

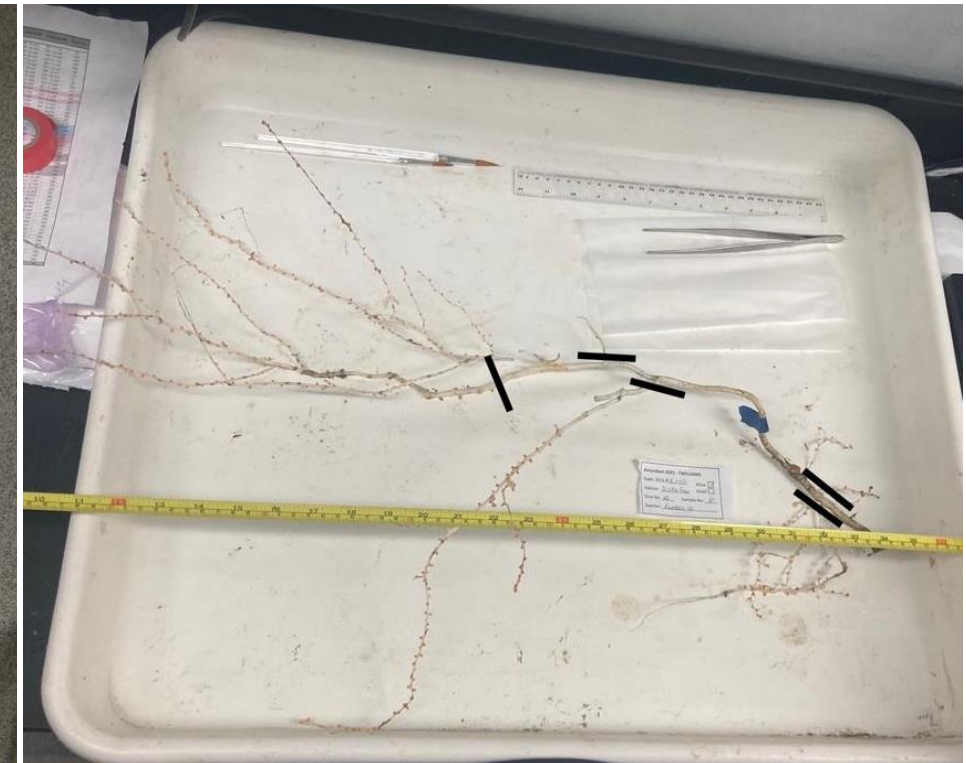


**Figure S2 |** Sectioning of *Keratoisis* sp. colonies collected from station *Disko Fan*. Black lines highlight the locations where cuts were made to section off the area of the main colony branch prior to CT scanning for sample (a) #23-1, (b) #23-6, (c) #23-10, and (d) #23-16. Sample tray = 80 × 60 cm.

Figure S2(a)



Figure S2(b)



Appendix C

Figure S2(c)



Figure S2(d)



**Table S2 |** *Keratoisis* sp. colony-specific distances, water depths and linear interpolated [Ba]<sub>sw</sub> values from the geographically closest *in-situ* profile (66.857 °N; 59.064 °W; 2021-08-03; Thomas et al. 2021; GEOTRACES Intermediate Data Product Group, 2021)

Colony	Latitude	Longitude	Depth (m)	Distance to profile (km)	Ba (nmol/kg)
#23-1	67.96629	-59.49069	885	124.48	52.7315909
#23-6	67.96631	-59.4899	883	124.48	52.6591162
#23-10	67.96631	-59.48892	879.9	124.47	52.5467803
#23-16	67.9663	-59.48768	876.2	124.46	52.412702

## Appendix C

Figure S3 | Representative longitudinal plane reconstruction of a *Keratoisis* sp. section obtained via micro computed tomography ( $\mu$ CT). Three-dimensional models were created by segmentation and rendered in Dragonfly $\circledcirc$  (v2022.1). Specific locations chosen for sectioning are highlighted (blue, green and red squares) alongside adjacent transverse SEM scanning images (insets). Scale (lower left) = 10 mm.

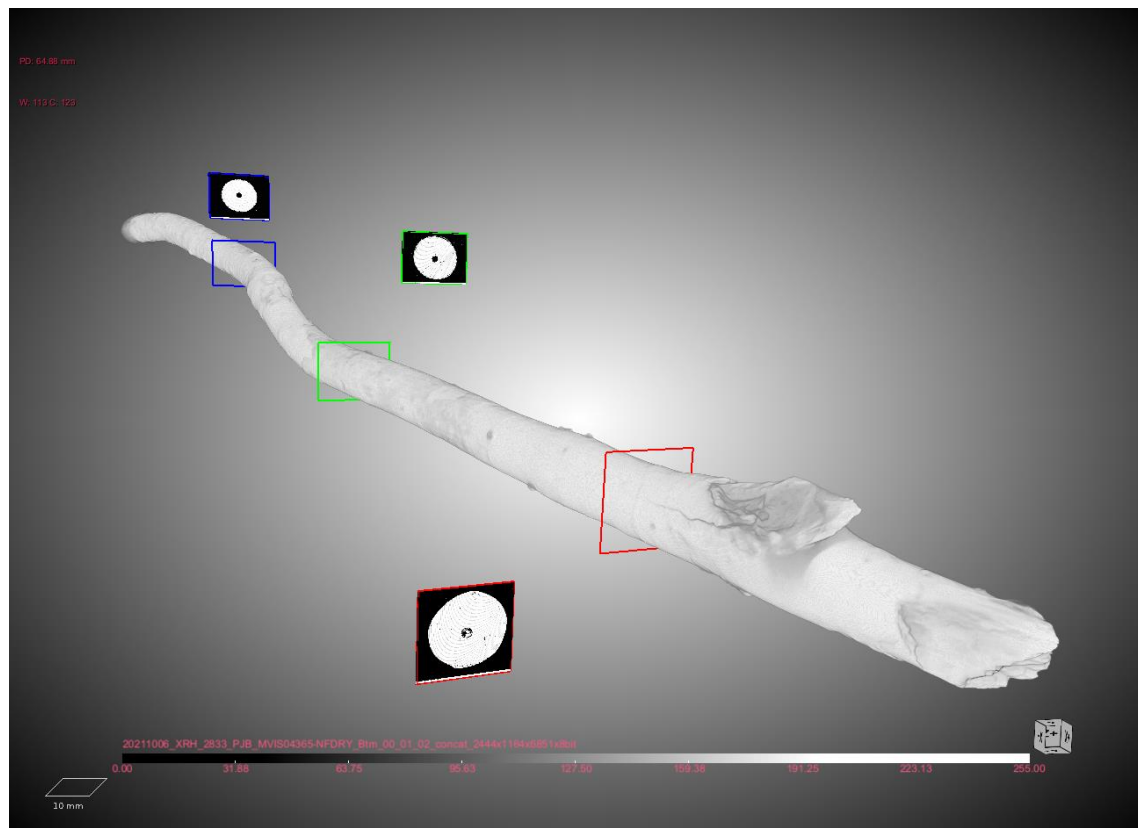


**Figure S4 |** Sections of *Keratoisis* sp. internodes photographed under a digital Dual-illumination microscope (AmScope, 2x magnification) for colony (a) #23-1, (b) #23-6, (c) #23-10, and (d) #23-16. Scale = 1 mm.

Figure S4(a)

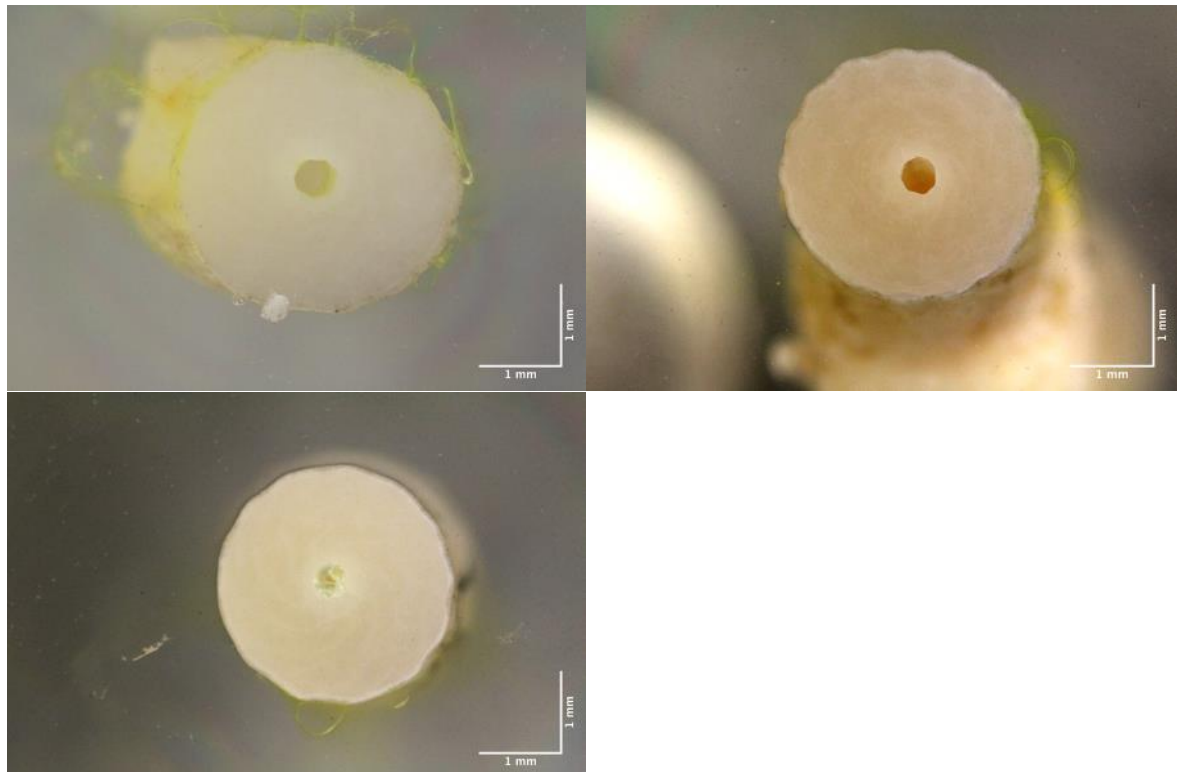
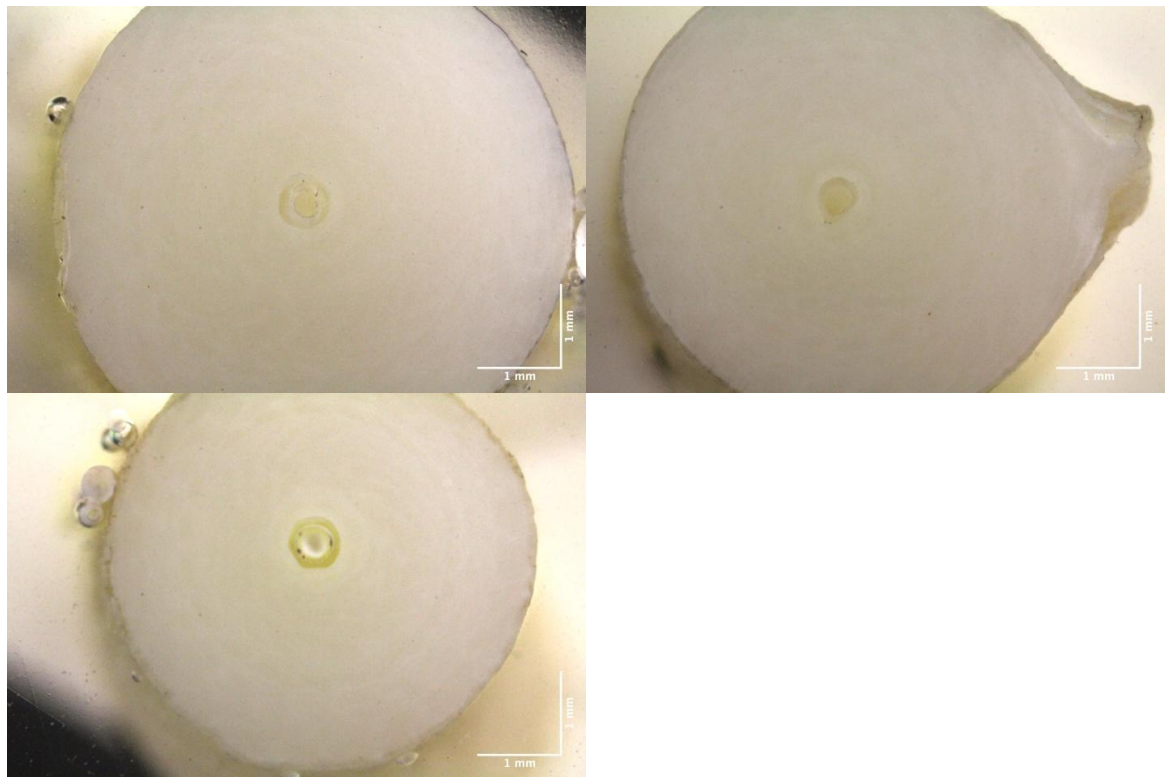


Figure S4(b)



Appendix C

Figure S4(c)

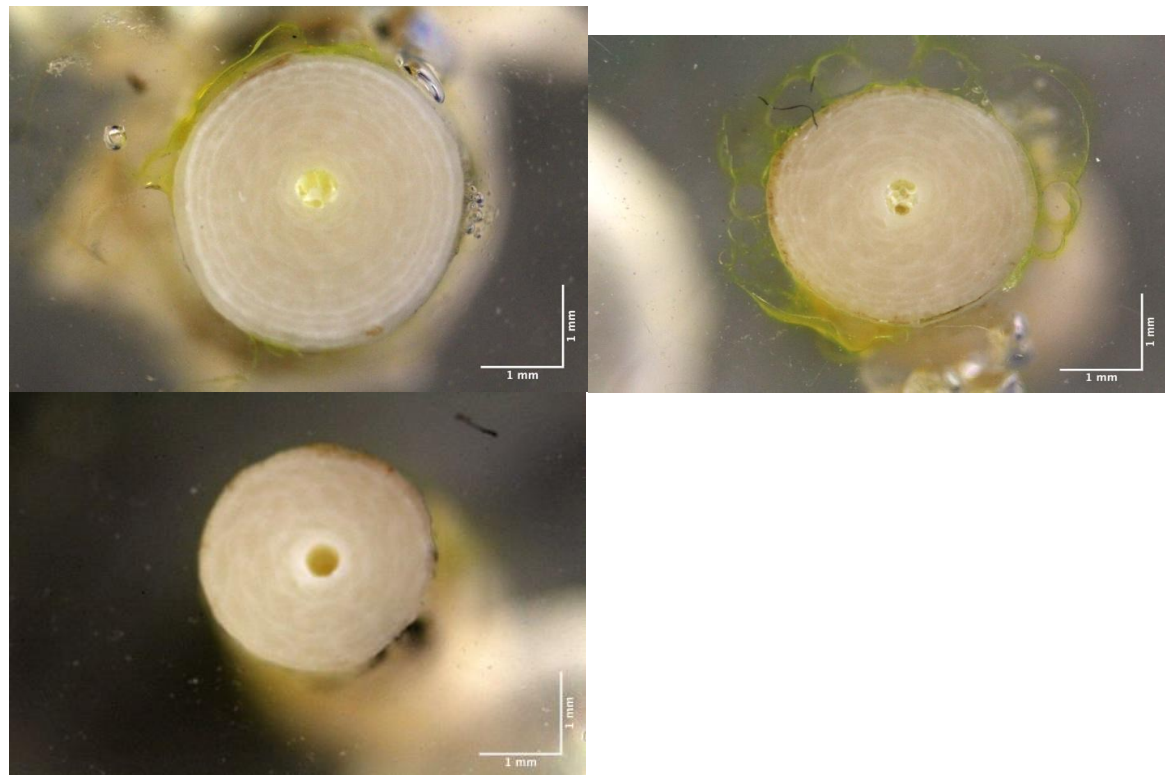


Figure S4(d)

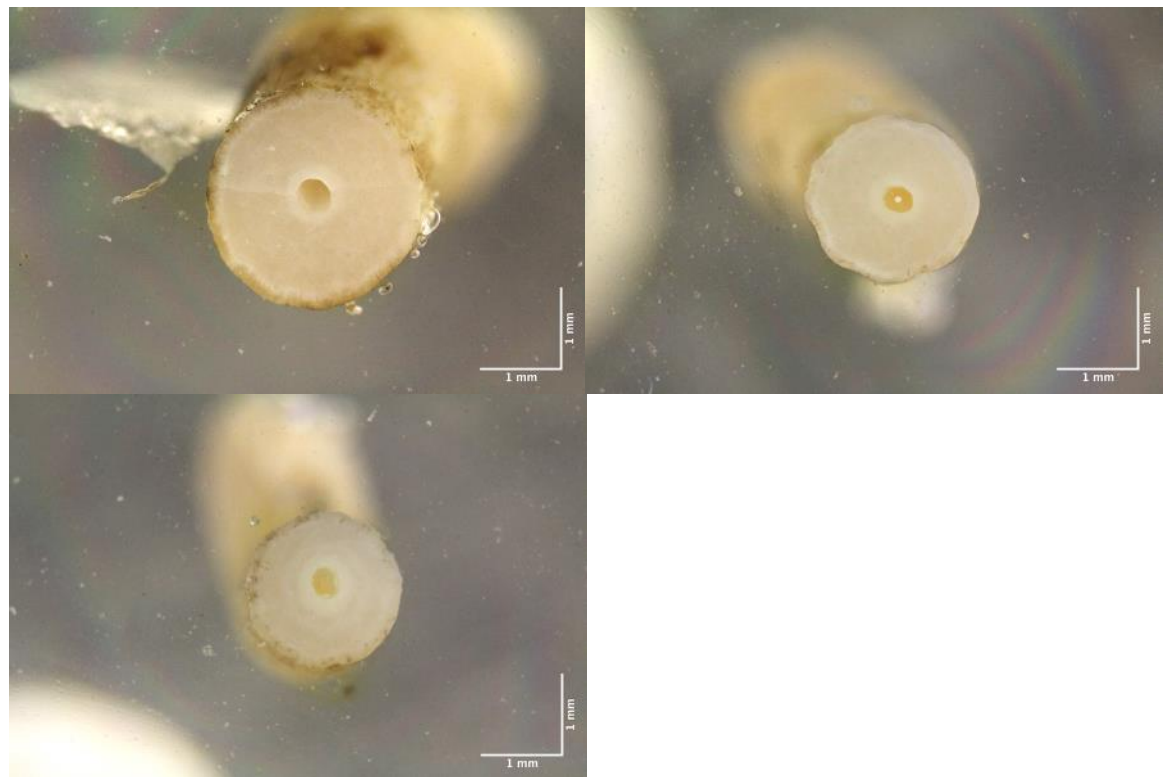


Table S3 | Typical operating conditions for laser ablation trace element QQQ-ICP-MS analysis.

<b>Instrument</b>					
<i>Mass Spectrometer</i>	Agilent (Agilent Technologies Inc., CA, USA) 8900 Triple Quadrupole inductively coupled plasma mass spectrometer				
<i>Laser Ablation System</i>	Elemental Scientific Lasers (Bozeman, MT, USA) NWR193 excimer laser with a TwoVol2 ablation chamber				
<i>RF Power</i>	1550 W				
<i>Cones</i>	Standard nickel sample cone and XT skimmer				
<b>Gas Flows</b>					
<i>Cooling Gas (argon)</i>	13 l min <sup>-1</sup>				
<i>Auxiliary Gas (argon)</i>	0.56 l min <sup>-1</sup>				
<i>Make-up gas (argon)</i>	1.1 l min <sup>-1</sup>				
<i>Ablation cell carrier gas (helium)</i>	0.8 l min <sup>-1</sup>				
<i>Additional Gas (nitrogen)</i>	0.014 l min <sup>-1</sup>				
<b>Ablation Conditions</b>					
<i>Laser power density</i>	~3.5 J cm <sup>-2</sup>				
<i>Laser repetition rate</i>	12 Hz				
<i>Laser spot size</i>	50 x 20 $\mu$ m				
<i>Laser tracking speed</i>	10 $\mu$ m s <sup>-1</sup>				
<i>Ablation mode</i>	Line or raster				

**Table S4 |** Summary of the number of trace element standard deviations used for rejection and simple moving average calculation during elemental mapping.

<b>Ratio</b>	<b>Level of rejection (standard deviation)</b>
Li/Ca	3
Mg/Ca	4
Li/Mg	3
Sr/Ca	3
Ba/Ca	2
U/Ca	2

**Table S5 |** List of publications that included measured growth rates of *Keratoisis* sp. identified using a Thomson Reuters Web of Science collection (<http://www.webofknowledge.com>, accessed 30/09/2022) 'Advanced Search' across all databases in the titles, key words and abstracts of all document types, in all languages, with the search term "Keratoisis" AND "growth rate" for publication years 1950 to 2021. Eligible literature (reported values of linear radial growth rates, associated environmental metadata) are highlighted with an \*

\*Andrews, A.H., Cailliet, G.M., Kerr, L.A., Coale, K.H., Lundstrom, C., & DeVogelaere, A.P. (2003).

Investigations of age and growth for three deep-sea corals from the Davidson Seamount off central California. In 2nd International Symposium on Deep-Sea Corals (pp. 1021-1038). Springer-Verlag Berlin, Erlangen, GERMANY.

\*Andrews, A.H., Stone, R.P., Lundstrom, C.C., & DeVogelaere, A.P. (2009). Growth rate and age determination of bamboo corals from the northeastern Pacific Ocean using refined 210Pb dating. *Marine Ecology Progress Series*, 397, 173-185.

\*Farmer, J.R., Robinson, L.F., & Honisch, B. (2015). Growth rate determinations from radiocarbon in bamboo corals (genus *Keratoisis*). *Deep Sea Research Part I: Oceanographic Research Papers*, 105, 26-40.

Frenkel, M.M., LaVigne, M., Miller, H.R., Hill, T.M., McNichol, A., & Gaylord, M.L. (2017). Quantifying bamboo coral growth rate nonlinearity with the radiocarbon bomb spike: A new model for paleoceanographic chronology development. *Deep Sea Research Part I: Oceanographic Research Papers*, 125, 26-39. doi:10.1016/j.dsr.2017.04.006

\*Flöter, S., Fietzke, J., Gutjahr, M., Farmer, J., Hönnisch, B., Nehrke, G., & Eisenhauer, A. (2019). The influence of skeletal micro-structures on potential proxy records in a bamboo coral. *Geochimica et Cosmochimica Acta*, 248, 43-60.

\*Noé, S.U., Lembke-Jene, L., & Dullo, W.C. (2008). Varying growth rates in bamboo corals: sclerochronology and radiocarbon dating of a mid-Holocene deep-water gorgonian skeleton (*Keratoisis* sp.: Octocorallia) from Chatham Rise (New Zealand). *Facies*, 54, 151-166.

\*Sherwood, O.A., & Edinger, E.N. (2009). Ages and growth rates of some deep-sea gorgonian and antipatharian corals of Newfoundland and Labrador. *Canadian Journal of Fisheries and Aquatic Sciences*, 66, 142-152.

\*Sherwood, O.A., Thresher, R.E., Fallon, S.J., Davies, D.M., & Trull, T.W. (2009). Multi-century time-series of N-15 and C-14 in bamboo corals from deep Tasmanian seamounts: evidence for stable oceanographic conditions. *Marine Ecology Progress Series*, 397, 209-218.

## Appendix C

\*Sinclair, D.J., Williams, B., Allard, G., Ghaleb, B., Fallon, S., Ross, S.W., & Risk, M. (2011). Reproducibility of trace element profiles in a specimen of the deep-water bamboo coral *Keratoisis* sp. *Geochimica Et Cosmochimica Acta*, 75, 5101-5121.

\*Thresher, R.E. (2009). Environmental and compositional correlates of growth rate in deep-water bamboo corals (Gorgonacea; Isididae). *Marine Ecology Progress Series*, 397, 187-196.

\*Thresher, R.E., MacRae, C.M., Wilson, N.C., & Fallon, S. (2009). Feasibility of age determination of deep-water bamboo corals (Gorgonacea; Isididae) from annual cycles in skeletal composition. *Deep Sea Research Part I: Oceanographic Research Papers.*, 56, 442-449.

\*Tracey, D.M., Neil, H., Marriott, P., Andrews, A.H., Cailliet, G.M., & Sanchez, J.A. (2007). Age and growth of two genera of deep-sea bamboo corals (family Isididae) in New Zealand waters. *Bulletin of Marine Science*, 81, 393-408.

Yoshimura, T., Wakaki, S., Iwasaki, N., Ishikawa, T., & Ohkouchi, N. (2022). Stable Sr isotope ( $^{88}\text{Sr}/^{86}\text{Sr}$ ) fractionation in calcite precious corals. *Frontiers in Marine Science*, 9. doi:10.3389/fmars.2022.104590.

**Figure S5** | Transverse section of sectioned internodes of *Keratoisis* sp. photographed under a Leo 1450VP (Carl Zeiss) variable pressure scanning electron microscope at 25x magnification for sample (a) #23-1, (b) #23-6, (c) #23-10, and (d) #23-16. Scale = 1 mm

Figure S5(a) 23-1

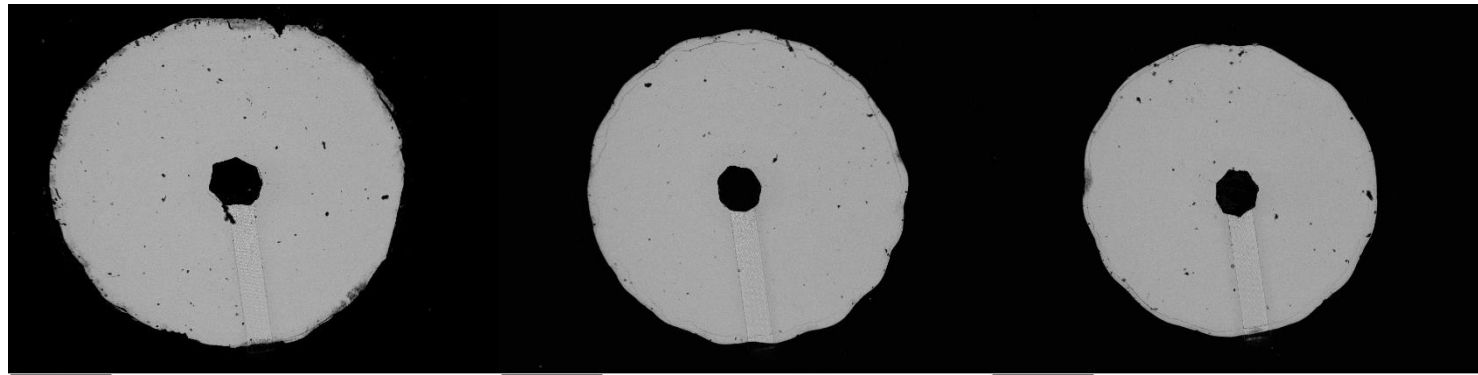
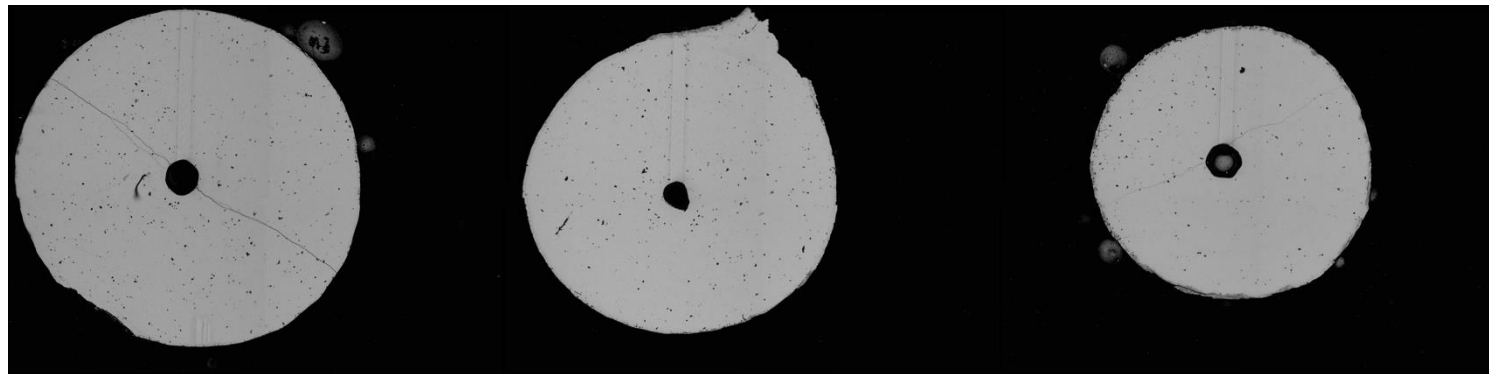


Figure S5(b) 23-6



Appendix C

Figure S5(c) 23-10

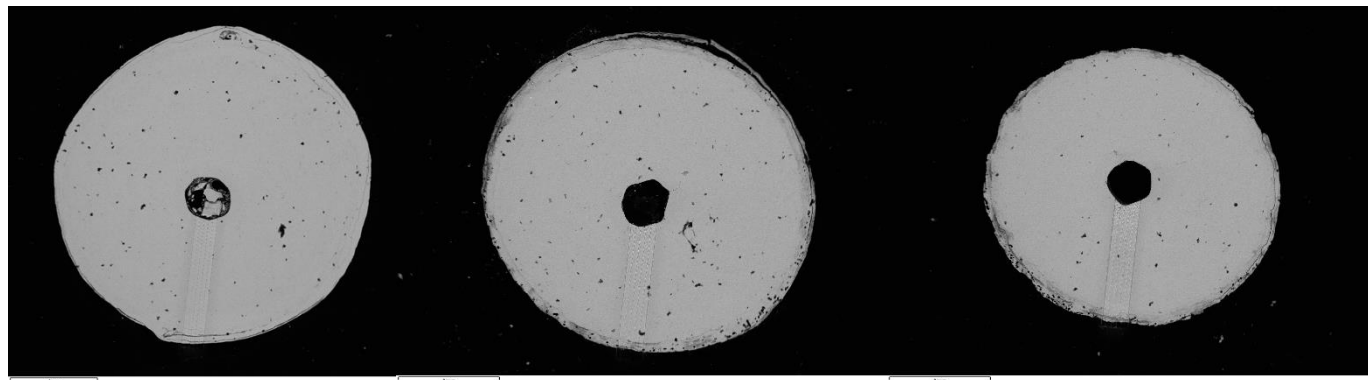
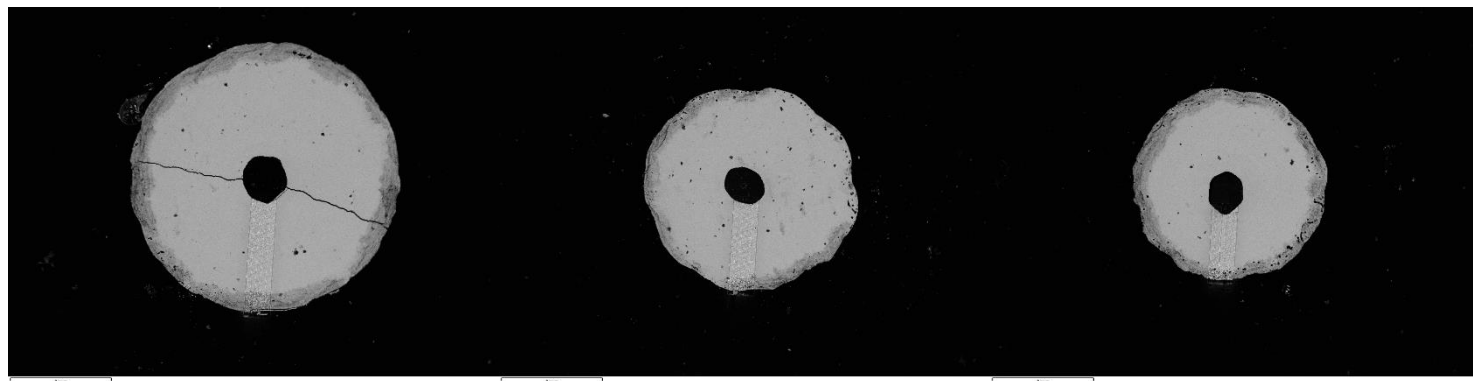


Figure S5(d) 23-16



**Table S6** | Reported values for *Keratoisis* sp. growth rate and associated environmental parameters extracted from the scientific literature listed by marine ecoregion. Data are compiled from the following sources in Table S5 (indicated by superscripted letters in the Specimen ID column):(a) Andrews et al. 2009; (b) Farmer et al. 2005; (c) Hill et al. 2011; (d) Noe et al. 2011; (e) Sherwood and Edinger, 2009; (f) Sinclair et al. 2011; (g) Thresher, 2009; (h) Thresher et al. 2009. Error is expressed as two standard deviations outside the mean growth rate.

Specimen ID	Genus ID	EcoRegion	Coral depth (m)	Lat (°N)	Long (°E)	T (°C)	Mean growth rate (μm/yr)	Error (± 2σ)	Technique	no. discrete samples
GOA99 <sup>a</sup>	<i>Keratoisis</i> sp.	Cold Temperate North Pacific	746	57.89	-137.49	3.67	56.00	15.50	210Pb	7
T428-A10 <sup>a</sup>	<i>Keratoisis</i> sp.	Cold Temperate North Pacific	1425	35.77	-122.70	2.50	51.00	17.50	210Pb	8
T948-A2 <sup>a</sup>	<i>Keratoisis</i> sp.	Cold Temperate North Pacific	1574	35.73	-122.71	2.60	57.00	2.50	210Pb	12
SS_320m <sup>b</sup>	<i>Keratoisis</i> sp.	Cold Temperate North Atlantic	320	44.22	-58.03	7.19	59.00	10.00	Calcite <sup>14</sup> C	4
BS_963m <sup>b</sup>	<i>Keratoisis</i> sp.	Cold Temperate North Atlantic	963	40.26	-67.69	4.22	21.00	2.00	14C Plateau	8
BS_963m <sup>b</sup>	<i>Keratoisis</i> sp.	Cold Temperate North Atlantic	963	40.26	-67.69	4.22	12.00	3.00	Bomb <sup>14</sup> C	2
BS_1299m <sup>b</sup>	<i>Keratoisis</i> sp.	Cold Temperate North Atlantic	1299	39.88	-67.47	3.83	60.00	14.00	Calcite <sup>14</sup> C	8
BS_1917m <sup>b</sup>	<i>Keratoisis</i> sp.	Cold Temperate North Atlantic	1917	39.92	-67.40	3.33	41.00	3.00	Calcite <sup>14</sup> C	4
BS_1917m <sup>b</sup>	<i>Keratoisis</i> sp.	Cold Temperate North Atlantic	1917	39.92	-67.40	3.33	12.00	2.00	Calcite <sup>14</sup> C	4
EF_805m <sup>b</sup>	<i>Keratoisis</i> sp.	Warm Temperate North Atlantic	805	30.73	-79.43	10.88	31.00	10.00	Calcite <sup>14</sup> C	4
T664-A17 <sup>c</sup>	<i>Keratoisis</i> sp.	Cold Temperate North Pacific	1295	33.13	-120.91	3.30	46.00	12.00	Calcite <sup>14</sup> C	2

Appendix C

T668-A13 <sup>c</sup>	<i>Keratoisis</i> sp.	Cold Temperate North Pacific	2136	31.91	-120.05	2.08	54.00	12.00	Calcite <sup>14</sup> C	2
C2 <sup>d</sup>	<i>Keratoisis</i> sp.	Southern New Zealand	682	-44.75.	174.39	-	40.00	23.00	Bomb <sup>14</sup> C	9
1449 <sup>e</sup>	<i>Keratoisis</i> sp.	Arctic	1193	61.60	-60.38	3.37	75.00	11.00	Bomb <sup>14</sup> C	22
2452 <sup>e</sup>	<i>Keratoisis</i> sp.	Cold Temperate North Atlantic	601	44.83	-54.47	4.36	74.00	6.00	Bomb <sup>14</sup> C	4
1343 <sup>e</sup>	<i>Keratoisis</i> sp.	Cold Temperate North Atlantic	713	44.13	-52.93	4.00	53.00	9.00	Bomb <sup>14</sup> C	24
JSL-4683 <sup>f</sup>	<i>Keratoisis</i> sp.	Warm Temperature North Atlantic	549	30.52	-79.66	13.15	33.00	10.00	<sup>14</sup> C and <sup>210</sup> Pb	9
K22 <sup>g</sup>	<i>Keratoisis</i> sp.	Continental High Antarctic	2355.5	-61.95	55.88	-0.4	15.50	-	Calcite <sup>14</sup> C	-
K2 <sup>g</sup>	<i>Keratoisis</i> sp.	Southern New Zealand	1000	-43.88	150.42	4.66	104.00	12.00	Calcite <sup>14</sup> C	39
K8 <sup>g</sup>	<i>Keratoisis</i> sp.	Southern New Zealand	2000	-43.3	148.03	2.40	15.40	-	Calcite <sup>14</sup> C	-
K6 <sup>h</sup>	<i>Keratoisis</i> sp.	Southern New Zealand	925	-47.47	148.78	5.41	67.00	12.00	Calcite <sup>14</sup> C	-

**Table S7 |** List of publications that investigated paleothermometry of corals and coralline algae, identified using a Thomson Reuters Web of Science collection (<http://www.webofknowledge.com>, accessed 30/09/2022) 'Advanced Search' across all databases in the titles, key words and abstracts of all document types, in all languages, with the search term ("Li/Mg" OR "Mg/Ca" OR "Sr/Ca" OR "Ba/Ca" OR "U/Ca" OR "Sr-U") AND ("coral" OR "coralline algae") AND ("temperature" OR "thermometry" OR "thermometer") AND ("calibration") for publication years 1950 to 2021.

Alibert, C., Kinsley, L., (2008). A 170-year Sr/Ca and Ba/Ca coral record from the western Pacific warm pool: 1. What can we learn from an unusual coral record? *Journal of Geophysical Research-Oceans*, 113(C4).

Alibert, C., McCulloch, M.T., (1997). Strontium/calcium ratios in modern *Porites* corals from the Great Barrier Reef as a proxy for sea surface temperature: Calibration of the thermometer and monitoring of ENSO. *Paleoceanography*, 12(3): 345-363.

Allison, N., Finch, A.A., (2005). High-resolution Sr/Ca records in modern *Porites lobata* corals: Effects of skeletal extension rate and architecture. *Geochemistry Geophysics Geosystems*, 5.

Alpert, A.E. et al. (2016). Comparison of equatorial Pacific sea surface temperature variability and trends with Sr/Ca records from multiple corals. *Paleoceanography*, 31(2): 252-265.

Alpert, A.E. et al. (2017). Twentieth century warming of the tropical Atlantic captured by Sr-U paleothermometry. *Paleoceanography*, 32(2): 146-160.

Amir, L., Mohamed, C.A.R., (2019). A First Look at Monthly Fluctuations of Sr/Ca in *Porites* sp. from the East and West Coast of Peninsular Malaysia. *Sains Malaysiana*, 48(11): 2367-2380.

Anagnostou, E. et al. (2011). Seawater nutrient and carbonate ion concentrations recorded as P/Ca, Ba/Ca, and U/Ca in the deep-sea coral *Desmophyllum dianthus*. *Geochimica et Cosmochimica Acta*, 75(9): 2529-2543.

Anagnostou, E., Williams, B., Westfield, I., Foster, G.L., Ries, J.B., (2019). Calibration of the pH-delta B-11 and temperature-Mg/Li proxies in the long-lived high-latitude crustose coralline red alga *Clathromorphum compactum* via controlled laboratory experiments. *Geochimica et Cosmochimica Acta*, 254: 142-155.

Anonymous, (2014). Dry Tortugas National Park Coral Sr/Ca data for 1734 to 2008, NOAA Paleoclimatology.

Armid, A. et al. (2011). Seawater temperature proxies based on D-Sr, D-Mg, and D-U from culture experiments using the branching coral *Porites cylindrica*. *Geochimica et Cosmochimica Acta*, 75(15): 4273-4285.

## Appendix C

Asami, R. et al. (2009). Evidence for tropical South Pacific climate change during the Younger Dryas and the Bolling-Allerod from geochemical records of fossil Tahiti corals. *Earth and Planetary Science Letters*, 288(1-2): 96-107.

Asami, R., (2009). A review of paleoenvironmental studies on Sr/Ca ratios and oxygen isotopes from fossil corals. *Fossils (Tokyo)*(86): 67-78.

Azmy, K., Edinger, E., Lundberg, J., Diegor, W., (2010). Sea level and paleotemperature records from a mid-Holocene reef on the North coast of Java, Indonesia. *International Journal of Earth Science*, 99(1): 231-244.

Ballantyne, A.P., Lavine, M., Crowley, T.J., Liu, J., Baker, P.B., (2005). Meta-analysis of tropical surface temperatures during the Last Glacial Maximum. *Geophysical Research Letters*, 32(5).

Bell, T. et al. (2017). Temperature-controlled culture experiments with primary polyps of coral *Acropora digitifera*: Calcification rate variations and skeletal Sr/Ca, Mg/Ca, and Na/Ca ratios. *Palaeogeography Palaeoclimatology Palaeoecology*, 484: 129-135.

Boerner, N. et al. (2013). Ostracod shell chemistry as proxy for paleoenvironmental change. *Quaternary International*, 313: 17-37.

Bolton, A. et al. (2014). Paired *Porites* coral Sr/Ca and delta O-18 from the western South China Sea: Proxy calibration of sea surface temperature and precipitation. *Palaeogeography Palaeoclimatology Palaeoecology*, 410: 233-243.

Bolton, A., Goodkin, N.F., Druffel, E.R.M., Griffin, S., Murty, S.A., (2016). Upwelling of Pacific Intermediate Water in the South China Sea Revealed by Coral Radiocarbon Record. *Radiocarbon*, 58(1): 37-53.

Bonifacie, M. et al. (2017). Calibration of the dolomite clumped isotope thermometer from 25 to 350 degrees C, and implications for a universal calibration for all (Ca, Mg, Fe) CO<sub>3</sub> carbonates. *Geochimica et Cosmochimica Acta*, 200: 255-279.

Brenner, L.D. et al. (2020). Coral Record of Younger Dryas Chronozone Warmth on the Great Barrier Reef. *Paleoceanography and Paleoclimatology*, 35(12).

Brenner, L.D., Linsley, B.K., Potts, D.C., (2017). A modern Sr/Ca-delta O-18-sea surface temperature calibration for *Isopora* corals on the Great Barrier Reef. *Paleoceanography*, 32(2): 182-194.

Brocas, W.M., Felis, T., Mudelsee, M., (2019). Tropical Atlantic Cooling and Freshening in the Middle of the Last Interglacial from Coral Proxy Records. *Geophysical Research Letters*, 46(14): 8289-8299.

Cahyarini, S.Y. et al. (2014). Twentieth century sea surface temperature and salinity variations at Timor inferred from paired coral delta O-18 and Sr/Ca measurements. *Journal of Geophysical Research-Oceans*, 119(7): 4593-4604.

Cahyarini, S.Y., Pfeiffer, M., Dullo, W.C., (2009). Improving SST reconstructions from coral Sr/Ca records: multiple corals from Tahiti (French Polynesia). *International Journal of Earth Science*, 98(1): 31-40.

Cahyarini, S.Y., Pfeiffer, M., Timm, O., Dullo, W.-C., Schoenberg, D.G., (2008). Reconstructing seawater delta O-18 from paired coral delta O-18 and Sr/Ca ratios: Methods, error analysis and problems, with examples from Tahiti (French Polynesia) and Timor (Indonesia). *Geochimica et Cosmochimica Acta*, 72(12): 2841-2853.

Case, D.H., Robinson, L.F., Auro, M.E., Gagnon, A.C., (2010). Environmental and biological controls on Mg and Li in deep-sea scleractinian corals. *Earth and Planetary Science Letters*, 300(3-4): 215-225.

Chen, S., Littley, E.F.M., Rae, J.W.B., Charles, C.D., Adkins, J.F., (2021). Table\_1\_Uranium Distribution and Incorporation Mechanism in Deep-Sea Corals: Implications for Seawater [CO32-] Proxies.XLSX, Figshare.

Chen, S., Littley, E.F.M., Rae, J.W.B., Charles, C.D., Adkins, J.F., (2021). Uranium Distribution and Incorporation Mechanism in Deep-Sea Corals: Implications for Seawater [CO32 (-)] Proxies. *Frontiers in Earth Science*, 9.

Chen, T., Li, S., Shi, Q., Chen, T., (2016). Cold tolerance of subtropical *Porites lutea* from the northern South China Sea. *Acta Oceanologica Sinica*, 35(12): 58-64.

Chen, T., Yu, K., Chen, T., (2013). Sr/Ca-sea surface temperature calibration in the coral *Porites lutea* from subtropical northern South China Sea. *Palaeogeography Palaeoclimatology Palaeoecology*, 392: 98-104.

Cheung, A.H. et al. (2021). Fidelity of the Coral Sr/Ca Paleothermometer Following Heat Stress in the Northern Galapagos. *Paleoceanography and Paleoclimatology*, 36(12).

Clarke, H., D'Olivo, J.P., Conde, M., Evans, R.D., McCulloch, M.T., (2019). Coral Records of Variable Stress Impacts and Possible acclimatization to recent Marine Heat Wave Events on the Northwest Shelf of Australia. *Paleoceanography and Paleoclimatology*, 34(11): 1672-1688.

Cohen, A.L., Hart, S.R., (2005). Deglacial sea surface temperatures of the western tropical Pacific: A new look at old coral. *Paleoceanography*, 19(4).

Cohen, A.L., Owens, K.E., Layne, G.D., Shimizu, N., (2002). The effect of algal symbionts on the accuracy of Sr/Ca paleotemperatures from coral. *Science*, 296(5566): 331-333.

Cohen, A.L., Thorrold, S.R., (2007). Recovery of temperature records from slow-growing corals by fine scale sampling of skeletons. *Geophysical Research Letters*, 34(17).

Cole, C. et al. (2021). The K-D Sr/Ca in cultured massive *Porites* spp. corals are reduced at low seawater pCO(2). *Geochimica et Cosmochimica Acta*, 314: 55-67.

## Appendix C

Cole, C., Finch, A., Hintz, C., Hintz, K., Allison, N., (2016). Understanding cold bias: Variable response of skeletal Sr/Ca to seawater pCO<sub>2</sub> in acclimated massive *Porites* corals. *Scientific Reports*, 6.

Cole, C., Finch, A.A., Hintz, C., Hintz, K., Allison, N., (2016). Understanding cold bias: Variable response of skeletal Sr/Ca to seawater pCO<sub>2</sub> in acclimated massive *Porites* corals, PANGAEA.

Crowley, T.J., Quinn, T.M., Hyde, W.T., (1999). Validation of coral temperature calibrations.

*Paleoceanography*, 14(5): 605-615.

D'Olivo, J., (2018). Data for: A universal multi-trace element calibration for reconstructing sea surface temperatures from long-lived *Porites* corals: Removing vital-effects, Mendeley Data.

D'Olivo, J.P. et al. (2019). Long-Term Impacts of the 1997-1998 Bleaching Event on the Growth and Resilience of Massive *Porites* Corals from the Central Red Sea. *Geochemistry Geophysics Geosystems*, 20(6): 2936-2954.

D'Olivo, J.P., Sinclair, D.J., Rankenburg, K., McCulloch, M.T., (2018). A universal multi-trace element calibration for reconstructing sea surface temperatures from long-lived *Porites* corals: Removing 'vital-effects'. *Geochimica et Cosmochimica Acta*, 239: 109-135.

de Villiers, S., Greaves, M., Elderfield, H., (2002). An intensity ratio calibration method for the accurate determination of Mg/Ca and Sr/Ca of marine carbonates by ICP-AES. *Geochemistry Geophysics Geosystems*, 3.

DeLong, K.L. et al. (2014). A reconstruction of sea surface temperature variability in the Southeastern Gulf of Mexico from 1734 to 2008 CE using cross-dated Sr/Ca records from the coral *Siderastrea siderea*.

*Paleoceanography*, 29(5): 403-422.

DeLong, K.L. et al. (2014). Dry Tortugas National Park Coral Sr/Ca data for 1734 to 2008, NOAA Paleoclimatology.

DeLong, K.L., Flannery, J.A., Maupin, C.R., Poore, R.Z., Quinn, T.M., (2011). A coral Sr/Ca calibration and replication study of two massive corals from the Gulf of Mexico. *Palaeogeography Palaeoclimatology Palaeoecology*, 307(1-4): 117-128.

DeLong, K.L., Flannery, J.A., Maupin, C.R., Poore, R.Z., Quinn, T.M., (2011). Dry Tortugas *Siderastrea* and *Montastraea* Coral Sr/Ca Data, 1992-2008, NOAA Paleoclimatology.

DeLong, K.L., Quinn, T.M., Shen, C.-C., Lin, K., (2011). Reply to comment by Cahyarini et al. on "A snapshot of climate variability at Tahiti at 9.5 ka using a fossil coral from IODP Expedition 310". *Geochemistry Geophysics Geosystems*, 12.

Deng, W. et al. (2010). High-precision analysis of Sr/Ca and Mg/Ca ratios in corals by laser ablation inductively coupled plasma optical emission spectrometry. *Journal of Analytical Atomic Spectrometry*, 25(1): 84-87.

Devilliers, S., Shen, G.T., Nelson, B.K., (1994). The Sr/Ca-Temperature Relationship in Coralline Aragonite - Influence of Variability in (Sr/Ca)Seawater and Skeletal Growth-Parameters. *Geochimica et Cosmochimica Acta*, 58(1): 197-208.

Ellis, B., Grant, K., Mallela, J., Abram, N., (2019). Is XRF core scanning a viable method for coral palaeoclimate temperature reconstructions? *Quaternary International*, 514: 97-107.

Fallon, S.J., McCulloch, M.T., Alibert, C., (2003). Examining water temperature proxies in *Porites* corals from the Great Barrier Reef: a cross-shelf comparison. *Coral Reefs*, 22(4): 389-404.

Fallon, S.J., McCulloch, M.T., Guilderson, T.P., (2005). Interpreting environmental signals from the coralline sponge *Astrosclera willeyana*. *Palaeogeography Palaeoclimatology Palaeoecology*, 228(1-2): 58-69.

Felis, T. et al. (2012). Pronounced interannual variability in tropical South Pacific temperatures during Heinrich Stadial 1. *Nature Communications*, 3.

Felis, T. et al. (2014). Intensification of the meridional temperature gradient in the Great Barrier Reef following the Last Glacial Maximum. *Nature Communications*, 5.

Fernandez, D.P., Gagnon, A.C., Adkins, J.F., (2011). An Isotope Dilution ICP-MS Method for the Determination of Mg/Ca and Sr/Ca Ratios in Calcium Carbonate. *Geostandards and Geoanalytical Research*, 35(1): 23-37.

Fernando Vasquez-Bedoya, L., Cohen, A.L., Oppo, D.W., Blanchon, P., (2012). Corals record persistent multidecadal SST variability in the Atlantic Warm Pool since 1775 AD. *Paleoceanography*, 27.

Flannery, J.A., Poore, R.Z., (2013). Sr/Ca Proxy Sea-Surface Temperature Reconstructions from Modern and Holocene *Montastraea faveolata* Specimens from the Dry Tortugas National Park, Florida, USA. *Journal of Coastal Research*: 20-31.

Flannery, J.A., Richey, J.N., Thirumalai, K., Poore, R.Z., DeLong, K.L., (2017). Multi-species coral Sr/Ca-based sea-surface temperature reconstruction using *Orbicella faveolata* and *Siderastrea siderea* from the Florida Straits. *Palaeogeography Palaeoclimatology Palaeoecology*, 466: 100-109.

Flannery, J.A., Richey, J.N., Toth, L.T., Kuffner, I.B., Poore, R.Z., (2018). Quantifying Uncertainty in Sr/Ca-Based Estimates of SST from the Coral *Orbicella faveolata*. *Paleoceanography and Paleoclimatology*, 33(9): 958-973.

## Appendix C

Forouzan, F., Ghazban, F., Ardestani, M., (2014). Sea Surface Temperature and Salinity Reconstruction from Geochemical Tracers of a Massive Coral in the Persian Gulf. *International Journal of Environmental Research*, 8(4): 1135-1144.

Fowell, S.E. et al. (2016). Intrareef variations in Li/Mg and Sr/Ca sea surface temperature proxies in the Caribbean reef-building coral *Siderastrea siderea*. *Paleoceanography*, 31(10): 1315-1329.

Gaetani, G.A., Cohen, A.L., Wang, Z., Crusius, J., (2011). Rayleigh-based, multi-element coral thermometry: A biomineralization approach to developing climate proxies. *Geochimica et Cosmochimica Acta*, 75(7): 1920-1932.

Gagan, M.K., Dunbar, G.B., Suzuki, A., (2012). Skeletal density of *Porites*, PANGAEA.

Gagan, M.K., Dunbar, G.B., Suzuki, A., (2012). The effect of skeletal mass accumulation in *Porites* on coral Sr/Ca and delta O-18 paleothermometry. *Paleoceanography*, 27.

Gallup, C.D. et al. (2006). Sr/Ca-Sea surface temperature calibration in the branching Caribbean coral *Acropora palmata*. *Geophysical Research Letters*, 33(3).

Giry, C., Felis, T., Koelling, M., Scheffers, S., (2010). Geochemistry and skeletal structure of *Diploria strigosa*, implications for coral-based climate reconstruction. *Palaeogeography Palaeoclimatology Palaeoecology*, 298(3-4): 378-387.

Giry, C., Felis, T., Kolling, M., Scheffers, S., (2010). (Figure 4 and Figure 5) 10-year long Sr/Ca and stable isotope records from individual skeletal element of coral sample BON-9-A, PANGAEA.

Giry, C., Felis, T., Kolling, M., Scheffers, S., (2010). (Figure 6) Sr/Ca and stable isotope records across a single thecal wall of coral sample BON-9-A, PANGAEA.

Giry, C., Felis, T., Kolling, M., Scheffers, S., (2010). (Figure 7) Sr/Ca and stable isotope anomalies across the thecal wall of three different *Diploria strigosa* coral colonies, PANGAEA.

Giry, C., Felis, T., Kolling, M., Scheffers, S.R., (2010). Sr/Ca and stable isotope records of *Diploria strigosa* coral sample BON-9-A from the east coast of Bonaire, PANGAEA.

Gischler, E. et al. (2005). Coral climate proxy data from a marginal reef area, Kuwait, northern Arabian-Persian Gulf. *Palaeogeography Palaeoclimatology Palaeoecology*, 228(1-2): 86-95.

Goodkin, N.F., Hughen, K.A., Cohen, A.L., (2007). A multicoral calibration method to approximate a universal equation relating Sr/Ca and growth rate to sea surface temperature. *Paleoceanography*, 22(1).

Goodkin, N.F., Hughen, K.A., Cohen, A.L., Smith, S.R., (2005). Record of Little Ice Age sea surface temperatures at Bermuda using a growth-dependent calibration of coral Sr/Ca. *Paleoceanography*, 20(4).

Goodkin, N.F., Hughen, K.A., Curry, W.B., Doney, S.C., Ostermann, D.R., (2008). Sea surface temperature and salinity variability at Bermuda during the end of the Little Ice Age. *Paleoceanography*, 23(3).

Grottoli, A.G., Chapron, L., Gava, D., Olesik, J.W., (2020). Natural Variability of Skeletal Elemental Phosphorus (P/Ca), Lead (Pb/Ca), and Barium (Ba/Ca) in the Western Pacific Sclerosponges *Acanthocheatetes wellsi* and *Astrosclera welleyana*. *Geochemistry Geophysics Geosystems*, 21(12).

Grove, C.A. et al. (2013). Confounding effects of coral growth and high SST variability on skeletal Sr/Ca: Implications for coral paleothermometry. *Geochemistry Geophysics Geosystems*, 14(4): 1277-1293.

Haase-Schramm, A. et al. (2003). Sr/Ca ratios and oxygen isotopes from sclerosponges: Temperature history of the Caribbean mixed layer and thermocline during the Little Ice Age. *Paleoceanography*, 18(3).

Hathorne, E.C., Felis, T., Suzuki, A., Kawahata, H., Cabioch, G., (2013). Lithium in the aragonite skeletons of massive *Porites* corals: A new tool to reconstruct tropical sea surface temperatures. *Paleoceanography*, 28(1).

Hathorne, E.C., Felis, T., Suzuki, A., Kawahata, H., Cabioch, G., (2013). (Table S1) Original element/Ca data for the OGA and Tahiti corals, PANGAEA.

Hemsing, F. et al. (2018). Barium isotopes in cold-water corals. *Earth and Planetary Science Letters*, 491: 183-192.

Hennekam, R. et al. (2018). Cocos (Keeling) Corals Reveal 200 Years of Multidecadal Modulation of Southeast Indian Ocean Hydrology by Indonesian Throughflow. *Paleoceanography and Paleoclimatology*, 33(1): 48-60.

Heslop, D., Paul, A., (2011). Can oceanic paleothermometers reconstruct the Atlantic Multidecadal Oscillation? *Climate of the Past*, 7(1): 151-159.

Hetzinger, S. et al. (2018). Reproducibility of *Clathromorphum compactum* coralline algal Mg/Ca ratios and comparison to high-resolution sea surface temperature data. *Geochimica et Cosmochimica Acta*, 220: 96-109.

Hetzinger, S., (2008). Oxygen isotopes and age for coral core Roq 6, PANGAEA.

Hetzinger, S., (2008). Oxygen isotopes, trace elements and age for coral core Gua 1, slab A, PANGAEA.

Hetzinger, S., (2008). Oxygen isotopes, trace elements and age for coral core Gua 1, slab B-F, PANGAEA.

Hetzinger, S., (2008). Stable isotope ratios and chemistry on corals from the Caribbean Sea, PANGAEA.

Hetzinger, S., (2008). Trace elements and age for coral core Roq 6, PANGAEA.

## Appendix C

Hetzinger, S., Pfeiffer, M., Dullo, W.-C., Ruprecht, E., Garbe-Schoenberg, D., (2006). Sr/Ca and delta O-18 in a fast-growing *Diploria strigosa* coral: Evaluation of a new climate archive for the tropical Atlantic. *Geochemistry Geophysics Geosystems*, 7.

Hetzinger, S., Pfeiffer, M., Dullo, W.C., Ruprecht, E., Garbe-Schonberg, D., (2012). Guadeloupe 41 Year Monthly Coral d18O and Sr/Ca Data, NOAA Paleoclimatology.

Hu, M., Chen, T., Zhang, W., (2018). Inter-species and inter-colony differences of Sr/Ca-SST calibration in *Porites*. *Journal of Tropical Oceanography*, 37(6): 74-84.

Ikhsani, I.Y., Dida, E.N., Cahyarini, S.Y., (2017). Evaluation of the Use of Faas For Sr/Ca Concentration Analysis of *Porites* from Ambon Bay and Jukung Island Coral. *Jurnal Ilmu Dan Teknologi Kelautan Tropis*, 9(1): 247-253.

Juillet-Leclerc, A., Reynaud, S., Dissard, D., Tisserand, G., Ferrier-Pages, C., (2014). Light is an active contributor to the vital effects of coral skeleton proxies. *Geochimica et Cosmochimica Acta*, 140: 671-690.

Kamenos, N.A., Cusack, M., Moore, P.G., (2008). Coralline algae are global palaeothermometers with bi-weekly resolution. *Geochimica et Cosmochimica Acta*, 72(3): 771-779.

Kawakubo, Y. et al. (2014). Precise determination of Sr/Ca by laser ablation ICP-MS compared to ICP-AES and application to multi-century temperate corals. *Geochemical Journal*, 48(2): 145-152.

Khare, A., Hughes, H.P., Kilbourne, K.H., Schijf, J., (2021). An ICP-AES method for routine high-precision measurement of seawater Sr/Ca ratios to validate coral paleothermometry calibrations. *Limnology and Oceanography-Methods*, 19(6): 416-430.

Kilbourne, K.H. et al. (2010). Coral windows onto seasonal climate variability in the northern Caribbean since 1479. *Geochemistry Geophysics Geosystems*, 11.

Kroh, A., Nebelsick, J.H., (2010). Echinoderms and Oligo-Miocene carbonate systems: potential applications in sedimentology and environmental reconstruction. in: Mutti, M., Piller, W., Betzler, C. (Eds.), *Carbonate Systems During the Oligocene-Miocene Climate Transition*, pp. 201-228.

Kuffner, I.B., Jokiel, P.L., Rodgers, K.u.S., Andersson, A.J., Mackenzie, F.T., (2012). An apparent "vital effect" of calcification rate on the Sr/Ca temperature proxy in the reef coral *Montipora capitata*. *Geochemistry Geophysics Geosystems*, 13.

Kuffner, I.B., Roberts, K.E., Flannery, J.A., Morrison, J.M., Richey, J.N., (2017). Fidelity of the Sr/Ca proxy in recording ocean temperature in the western Atlantic coral *Siderastrea siderea*. *Geochemistry Geophysics Geosystems*, 18(1): 178-188.

Kuhnert, H., Cruger, T., Patzold, J., (2005). NAO signature in a Bermuda coral Sr/Ca record. *Geochemistry Geophysics Geosystems*, 6.

LaVigne, M., Grottoli, A.G., Palardy, J.E., Sherrell, R.M., (2016). Multi-colony calibrations of coral Ba/Ca with a contemporaneous in situ seawater barium record. *Geochimica et Cosmochimica Acta*, 179: 203-216.

Lawman, A.E. et al. (2020). Developing a Coral Proxy System Model to Compare Coral and Climate Model Estimates of Changes in Paleo-ENSO Variability. *Paleoceanography and Paleoclimatology*, 35(7).

LeCorne, F., Correge, T., (1997). Determination of uranium to calcium and strontium to calcium ratios in corals by inductively coupled plasma mass spectrometry. *Journal of Analytical Atomic Spectrometry*, 12(9): 969-973.

Li, Z. et al. (2018). Evidence of solar insolation and internal forcing of sea surface temperature changes in the eastern tropical Indian Ocean during the Holocene. *Quaternary International*, 490: 1-9.

Light, T. et al. (2018). Advancing Mg/Ca Analysis of Coralline Algae as a Climate Proxy by Assessing LA-ICP-OES Sampling and Coupled Mg/Ca-delta O-18 Analysis. *Geochemistry Geophysics Geosystems*, 19(9): 2876-2894.

Linol, B. et al. (2021). Towards disentangling climatic and tectonic changes of southernmost Africa using strontium isotope stratigraphy and clumped isotope thermometry. *South African Journal of Geology*, 124(2): 537-564.

Linsley, B.K., Wellington, G.M., Schrag, D.P., (2000). Decadal sea surface temperature variability in the subtropical South Pacific from 1726 to 1997 AD. *Science*, 290(5494): 1145-1148.

Liu, C. et al. (2019). Temperature seasonality and ENSO variability in the northern South China Sea during the Medieval Climate Anomaly interval derived from the Sr/Ca ratios of Tridacna shell. *Journal of Asian Earth Sciences*, 180.

Maeda, A. et al. (2017). Evaluation of oxygen isotope and Mg/Ca ratios in high-magnesium calcite from benthic foraminifera as a proxy for water temperature. *Journal of Geophysical Research-Biogeosciences*, 122(1): 185-199.

Marshall, J.F., McCulloch, M.T., (2001). Evidence of El Nino and the Indian Ocean Dipole from Sr/Ca derived SSTs for modern corals at Christmas Island, Eastern Indian Ocean. *Geophysical Research Letters*, 28(18): 3453-3456.

Maupin, C.R., Quinn, T.M., Halley, R.B., (2008). Extracting a climate signal from the skeletal geochemistry of the Caribbean coral *Siderastrea siderea*. *Geochemistry Geophysics Geosystems*, 9.

## Appendix C

McCoy, S.J., Kamenos, N.A., (2015). Coralline Algae (Rhodophyta) in A Changing World: Integrating Ecological, Physiological, and Geochemical Responses to Global Change. *Journal of Phycology*, 51(1): 6-24.

McCulloch, M.T., Gagan, M.K., Mortimer, G.E., Chivas, A.R., Isdale, P.J., (1994). A High-Resolution Sr/Ca and Delta-O-18 Coral Record from the Great-Barrier-Reef, Australia, and the 1982-1983 El-Nino. *Geochimica et Cosmochimica Acta*, 58(12): 2747-2754.

McGregor, H.V., Gagan, M.K., (2003). Diagenesis and geochemistry of *Porites* corals from Papua New Guinea: Implications for paleoclimate reconstruction. *Geochimica et Cosmochimica Acta*, 67(12): 2147-2156.

Meibom, A. et al. (2003). Monthly Strontium/Calcium oscillations in symbiotic coral aragonite: Biological effects limiting the precision of the paleotemperature proxy. *Geophysical Research Letters*, 30(7).

Mishima, M. et al. (2009). Reconstruction of the East China Sea palaeoenvironment at 16 ka by comparison of fossil and modern Faviidae corals from the Ryukyus, southwestern Japan. *Journal of Quaternary Science*, 24(8): 928-936.

Mitsuguchi, T., Dang, P.X., Kitagawa, H., Uchida, T., Shibata, Y., (2008). Coral Sr/Ca and Mg/Ca records in Con Dao Island off the Mekong Delta: Assessment of their potential for monitoring ENSO and East Asian monsoon. *Global and Planetary Change*, 63(4): 341-352.

Mitsuguchi, T., Matsumoto, E., Uchida, T., (2003). Mg/Ca and Sr/Ca ratios of *Porites* coral skeleton: Evaluation of the effect of skeletal growth rate. *Coral Reefs*, 22(4): 381-388.

Mohtar, A.T. et al. (2021). Coral-based proxy calibrations constrain ENSO-driven sea surface temperature and salinity gradients in the Western Pacific Warm Pool. *Palaeogeography Palaeoclimatology Palaeoecology*, 561.

Montagna, P. et al. (2014). Li/Mg systematics in scleractinian corals: Calibration of the thermometer. *Geochimica et Cosmochimica Acta*, 132: 288-310.

Montone, L.M., (2010). A coral skeleton geochemical record of surface water properties in the Oman upwelling region, Rutgers University Community Repository.

Morimoto, M., Kayanne, H., Abe, O., McCulloch, M.T., (2007). Intensified mid-Holocene Asian monsoon recorded in corals from Kikai Island, subtropical northwestern Pacific. *Quaternary Research*, 67(2): 204-214.

Muller, A., Gagan, M.K., McCulloch, M.T., (2001). Early marine diagenesis in corals and geochemical consequences for paleoceanographic reconstructions. *Geophysical Research Letters*, 28(23): 4471-4474.

Murty, S.A. et al. (2018). Spatial and Temporal Robustness of Sr/Ca-SST Calibrations in Red Sea Corals: Evidence for Influence of Mean Annual Temperature on Calibration Slopes. *Paleoceanography and Paleoclimatology*, 33(5): 443-456.

Ng, J.Y. et al. (2016). Assessing multi-site delta O-18-climate calibrations of the coralline alga *Clathromorphum* across the high-latitude Northern Hemisphere. *Geochimica et Cosmochimica Acta*, 194: 279-290.

O'Connor, G.K. et al. (2021). Coral Oxygen Isotopic Records Capture the 2015/2016 El Nino Event in the Central Equatorial Pacific. *Geophysical Research Letters*, 48(24).

Ohkouchi, N., Kawamura, K., Nakamura, T., Taira, A., (1994). Small Changes in the Sea-Surface Temperature During the Last 20,000 Years - Molecular Evidence from the Western Tropical Pacific. *Geophysical Research Letters*, 21(20): 2207-2210.

Ourbak, T. et al. (2006). A high-resolution investigation of temperature, salinity, and upwelling activity proxies in corals. *Geochemistry Geophysics Geosystems*, 7.

Pereira, N.S. et al. (2017). The potential of the coral species *Porites astreoides* as a paleoclimate archive for the Tropical South Atlantic Ocean. *Journal of South American Earth Sciences*, 77: 276-285.

Pfeiffer, M. et al. (2019). 20th Century delta O-18 Seawater and Salinity Variations Reconstructed from Paired delta O-18 and Sr/Ca Measurements of a La Reunion Coral. *Paleoceanography and Paleoclimatology*, 34(12): 2183-2200.

Prendergast, A.L., Versteegh, E.A.A., Schoene, B.R., (2017). New research on the development of high-resolution palaeoenvironmental proxies from geochemical properties of biogenic carbonates. *Palaeogeography Palaeoclimatology Palaeoecology*, 484: 1-6.

Quinn, T.M., Sampson, D.E., (2002). A multiproxy approach to reconstructing sea surface conditions using coral skeleton geochemistry. *Paleoceanography*, 17(4).

Ramos, R.D., Goodkin, N.F., Siringan, F.P., Hughen, K.A., (2017). *Diploastrea heliopora* Sr/Ca and O-18 records from northeast Luzon, Philippines: An assessment of interspecies coral proxy calibrations and climate controls of sea surface temperature and salinity. *Paleoceanography*, 32(4): 424-438.

Razak, T.B. et al. (2017). Use of skeletal Sr/Ca ratios to determine growth patterns in a branching coral *Isopora palifera*. *Marine Biology*, 164(4).

Razak, T.B., Roff, G., Lough, J.M., Mumby, P.J., (2020). Growth responses of branching versus massive corals to ocean warming on the Great Barrier Reef, Australia. *Science of the Total Environment*, 705.

## Appendix C

Reynaud-Vaganay, S., Gattuso, J.P., Cuif, J.P., Jaubert, J., Juillet-Leclerc, A., (1999). A novel culture technique for scleractinian corals: application to investigate changes in skeletal delta O-18 as a function of temperature. *Marine Ecology Progress Series*, 180: 121-130.

Rodriguez, L.G. et al. (2019). Mid-Holocene, Coral-Based Sea Surface Temperatures in the Western Tropical Atlantic. *Paleoceanography and Paleoclimatology*, 34(7): 1234-1245.

Rodriguez, M., Not, C., (2021). Calibration of Mg/Ca and Sr/Ca in coastal marine ostracods as a proxy for temperature. *Biogeosciences*, 18(6): 1987-(2001).

Rosenheim, B.E. et al. (2005). High-resolution Sr/Ca records in sclerosponges calibrated to temperature in situ. *Geology*, 32(2): 145-148.

Rosenthal, Y., Boyle, E.A., Slowey, N., (1997). Temperature control on the incorporation of magnesium, strontium, fluorine, and cadmium into benthic foraminiferal shells from Little Bahama Bank: Prospects for thermocline paleoceanography. *Geochimica et Cosmochimica Acta*, 61(17): 3633-3643.

Ross, C.L., DeCarlo, T.M., McCulloch, M.T., (2019). Calibration of Sr/Ca, Li/Mg and Sr-U Paleothermometry in Branching and Foliose Corals. *Paleoceanography and Paleoclimatology*, 34(8): 1271-1291.

Russon, T. et al. (2010). Inter-hemispheric asymmetry in the early Pleistocene Pacific warm pool. *Geophysical Research Letters*, 37.

Sadler, J., Nguyen, A.D., Leonard, N.D., Webb, G.E., Nothdurft, L.D., (2016). *Acropora* interbranch skeleton Sr/Ca ratios: Evaluation of a potential new high-resolution paleothermometer. *Paleoceanography*, 31(4): 505-517.

Sadler, J., Webb, G.E., Leonard, N.D., Nothdurft, L.D., Clark, T.R., (2016). Reef core insights into mid-Holocene water temperatures of the southern Great Barrier Reef. *Paleoceanography*, 31(10): 1395-1408.

Saenger, C., Cohen, A.L., Oppo, D.W., Hubbard, D., (2008). (Table 1) Summary of coral geochemical data and reconstructed SST, PANGAEA.

Saenger, C., Cohen, A.L., Oppo, D.W., Hubbard, D., (2008). Interpreting sea surface temperature from strontium/calcium ratios in Montastrea corals: Link with growth rate and implications for proxy reconstructions. *Paleoceanography*, 23(3).

Sagar, N. et al. (2016). High-resolution Sr/Ca ratios in a *Porites lutea* coral from Lakshadweep Archipelago, southeast Arabian Sea: An example from a region experiencing steady rise in the reef temperature. *Journal of Geophysical Research-Oceans*, 121(1): 252-266.

Schrag, D.P., (1999). Rapid analysis of high-precision Sr/Ca ratios in corals and other marine carbonates. *Paleoceanography*, 14(2): 97-102.

Seo, I. et al. (2013). A skeletal Sr/Ca record preserved in *Dipsastraea* (*Favia*) *speciosa* and implications for coral Sr/Ca thermometry in mid-latitude regions. *Geochemistry Geophysics Geosystems*, 14(8): 2873-2885.

Shen, C.C. et al. (1996). The calibration of D[Sr/Ca] versus sea surface temperature relationship for *Porites* corals. *Geochimica et Cosmochimica Acta*, 60(20): 3849-3858.

Shen, G.T. et al. (1992). Surface Ocean Variability At Galapagos from 1936-1982: Calibration of Geochemical Tracers in Corals. *Paleoceanography*, 7(5): 563-588.

Sinclair, D.J., Kinsley, L.P.J., McCulloch, M.T., (1998). High resolution analysis of trace elements in corals by laser ablation ICP-MS. *Geochimica et Cosmochimica Acta*, 62(11): 1889-1901.

Singh, A., (2021). Trace element and stable isotope variations in larger benthic foraminifer *Baculogypsina sphaerulata*: A potential proxy of seawater temperature. *Journal of Earth System Science*, 130(2).

Smith, J.M., Quinn, T.M., Helmle, K.P., Halley, R.B., (2006). Reproducibility of geochemical and climatic signals in the Atlantic coral *Montastraea faveolata*. *Paleoceanography*, 21(1).

Sosdian, S. et al. (2006). Strontium to calcium ratios in the marine gastropod *Conus ermineus*: Growth rate effects and temperature calibration. *Geochemistry Geophysics Geosystems*, 7.

Stewart, J.A. et al. (2020). Refining trace metal temperature proxies in cold-water scleractinian and stylasterid corals. *Earth and Planetary Science Letters*, 545.

Stewart, J.A. et al. (2021). NIST RM 8301 Boron Isotopes in Marine Carbonate (Simulated Coral and Foraminifera Solutions): Inter-laboratory delta B-11 and Trace Element Ratio Value Assignment. *Geostandards and Geoanalytical Research*, 45(1): 77-96.

Stewart, J.A., Anagnostou, E., Foster, G.L., (2016). An improved boron isotope pH proxy calibration for the deep-sea coral *Desmophyllum dianthus* through sub-sampling of fibrous aragonite. *Chemical Geology*, 447: 148-160.

Sun, M., Chiu, C.H., Shen, C.C., Lee, T., (1999). Sr thermometer for *Porites* corals: Little need to measure Ca? *Geochemical Journal*, 33(5): 351-354.

Sun, Y., Sun, M., Lee, T., Nie, B., (2005). Influence of seawater Sr content on coral Sr/Ca and Sr thermometry. *Coral Reefs*, 24(1): 23-29.

Sun, Y.L., Sun, M., (2002). Simultaneous determination of major, minor and trace elements in biocarbonates by inductively coupled plasma mass spectrometry. *Analytical and Bioanalytical Chemistry*, 374(7-8): 1338-1340.

Sun, Y.L., Sun, M., (2003). Inductively coupled plasma atomic emission spectrometry: An efficient tool for precise determination of Mg/Ca and Sr/Ca ratios in biocarbonates. *Applied Spectroscopy*, 57(6): 711-714.

## Appendix C

Swart, P.K., Elderfield, H., Greaves, M.J., (2002). A high-resolution calibration of Sr/Ca thermometry using the Caribbean coral *Montastraea annularis*. *Geochemistry Geophysics Geosystems*, 3.

Tanzil, J.T.I. et al. (2019). Multi-colony coral skeletal Ba/Ca from Singapore's turbid urban reefs: Relationship with contemporaneous in-situ seawater parameters. *Geochimica et Cosmochimica Acta*, 250: 191-208.

Thiagarajan, N., Adkins, J., Eiler, J., (2011). Carbonate clumped isotope thermometry of deep-sea corals and implications for vital effects. *Geochimica et Cosmochimica Acta*, 75(16): 4416-4425.

Thresher, R.E., Neil, H., (2016). Scale dependence of environmental and physiological correlates of delta O-18 and delta C-13 in the magnesium calcite skeletons of bamboo corals (Gorgonacea; Isididae). *Geochimica et Cosmochimica Acta*, 187: 260-278.

Tripati, A.K. et al. (2010). C-13-O-18 isotope signatures and 'clumped isotope' thermometry in foraminifera and coccoliths. *Geochimica et Cosmochimica Acta*, 74(20): 5697-5717.

Vasquez-Bedoya, L.F., Cohen, A.L., Oppo, D.W., Blanchon, P., (2012). Yucatan coral growth rate-based SST since 1775, NOAA Paleoclimatology.

Villaescusa, J.A., Carriquiry, J.D., (2005). Calibration of Sr/Ca and Mg/Ca paleothermometers in coral *Porites* sp from San Benedicto Island, Revillagigedo Archipelago, Mexico. *Ciencias Marinas*, 30(4): 603-618.

Wang, Z. et al. (2013). Experimental calibration of Mg isotope fractionation between aragonite and seawater. *Geochimica et Cosmochimica Acta*, 102: 113-123.

Watanabe, T., Winter, A., Oba, T., (2001). Seasonal changes in sea surface temperature and salinity during the Little Ice Age in the Caribbean Sea deduced from Mg/Ca and O-18/O-16 ratios in corals. *MARINE Geology*, 173(1-4): 21-35.

Watanabe, T.K., Watanabe, T., Ohmori, K., Yamazaki, A., (2020). Improving analytical method of Sr/Ca ratios in coral skeletons for paleo-SST reconstructions using ICP-OES. *Limnology and Oceanography-Methods*, 18(6): 297-310.

Watanabe, T.K., Watanabe, T., Ohmori, K., Yamazaki, A., (2021). Coral Ba/Ca Analysis Using ICP-OES With an Ultrasonic Nebulizer. *Geochemistry Geophysics Geosystems*, 22(8).

Wei, G.J., Sun, M., Li, X.H., Nie, B.F., (2000). Mg/Ca, Sr/Ca and U/Ca ratios of a *Porites* coral from Sanya Bay, Hainan Island, South China Sea and their relationships to sea surface temperature. *Palaeogeography Palaeoclimatology Palaeoecology*, 162(1-2): 59-74.

Wei, H., Jiang, S., Xiao, Y., Hemming, N.G., (2014). Boron isotopic fractionation and trace element incorporation in various species of modern corals in Sanya Bay, South China Sea. *Journal of Earth Science*, 25(3): 431-444.

Williams, S. et al. (2018). Effects of light and temperature on Mg uptake, growth, and calcification in the proxy climate archive *Clathromorphum compactum*. *Biogeosciences*, 15(19): 5745-5759.

Wu, H.C., Linsley, B.K., Dassie, E.P., Schiraldi, B., DeMenocal, P.B., (2013). Annual average Sr/Ca measurements from *Porites lutea* coral at Ha'afera Island, Tonga, PANGAEA.

Wu, H.C., Linsley, B.K., Dassie, E.P., Schiraldi, B., deMenocal, P.B., (2013). Oceanographic variability in the South Pacific Convergence Zone region over the last 210 years from multi-site coral Sr/Ca records. *Geochemistry Geophysics Geosystems*, 14(5): 1435-1453.

Wu, H.C., Linsley, B.K., Dassie, E.P., Schiraldi, B., Jr., DeMenocal, P.B., (2013). Ha'afera Island, Tonga Annual Average Sr/Ca *Porites lutea* Data from 1791-2003 AD, NOAA Paleoclimatology.

Wu, W.-z., Wei, G.-j., Xie, L.-h., Liu, Y., (2014). Variations of Sr/Ca, Mg/Ca ratios in seawater of the Sanya Bay and response of coral trace element thermometer. *Marine Sciences (Beijing)*, 38(3): 46-55.

Wu, Y., Fallon, S.J., Cantin, N.E., Lough, J.M., (2021). Assessing multiproxy approaches (Sr/Ca, U/Ca, Li/Mg, and B/Mg) to reconstruct sea surface temperature from coral skeletons throughout the Great Barrier Reef. *Science of the Total Environment*, 786.

Xiao, Y. et al. (2014). Correlation between delta O-18, Sr/Ca and Mg/Ca of coral *Acropora* and seawater temperature from coral culture experiments. *Science China-Earth Sciences*, 57(5): 1048-1060.

Xu, J., (2019). Reconstruction of dust storm frequency in China using the SST signals recorded in coral reefs. *Theoretical and Applied Climatology*, 137(3-4): 2257-2269.

Xu, Y.-Y., Pearson, S., Kilbourne, K.H., (2015). Assessing coral Sr/Ca-SST calibration techniques using the species *Diploria strigosa*. *Palaeogeography Palaeoclimatology Palaeoecology*, 440: 353-362.

Yan, H., Shao, D., Wang, Y., Sun, L., (2013). Sr/Ca profile of long-lived *Tridacnidae* bivalves from South China Sea: A new high-resolution SST proxy. *Geochimica et Cosmochimica Acta*, 112: 52-65.

Yan, H., Shao, D., Wang, Y., Sun, L., (2014). Sr/Ca differences within and among three *Tridacnidae* species from the South China Sea: Implication for paleoclimate reconstruction. *CHEMICAL Geology*, 390: 22-31.

Yu, K.F. et al. (2001). The high-resolution climate recorded in the delta O-18 of *Porites lutea* from the Nansha Islands of China. *Chinese Science Bulletin*, 46(24): 2097-2102.

Yu, K.F. et al. (2005). High-frequency winter cooling and reef coral mortality during the Holocene climatic optimum. *Earth and Planetary Science Letters*, 224(1-2): 143-155.

Yu, K.F. et al. (2005). delta O-18, Sr/Ca and Mg/Ca records of *Porites lutea* corals from Leizhou Peninsula, northern South China Sea, and their applicability as paleoclimatic indicators. *Palaeogeography Palaeoclimatology Palaeoecology*, 218(1-2): 57-73.

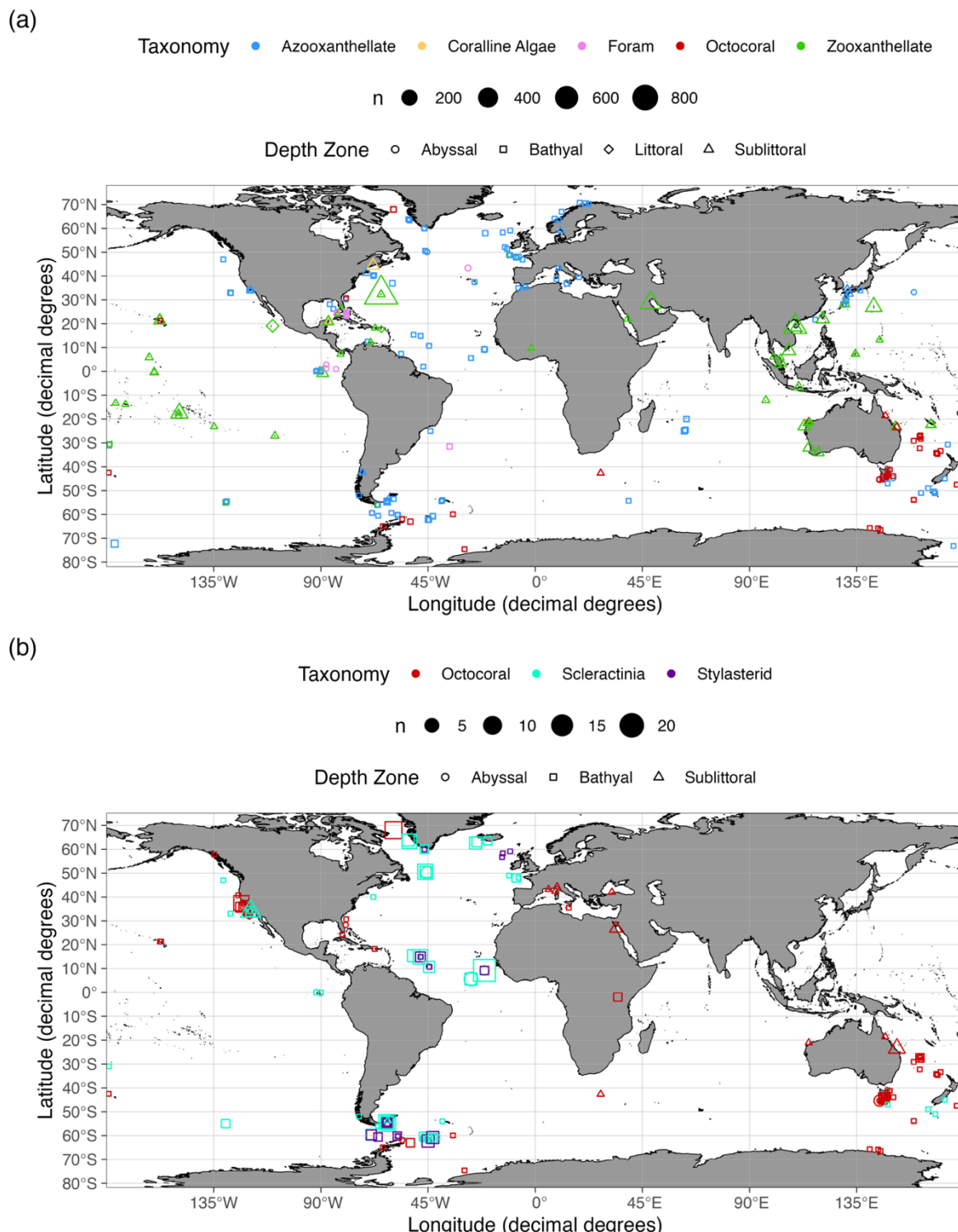
## Appendix C

Yu, K.F., Zhao, J.X., Wei, G.J., Cheng, X.R., Wang, P.X., (2005). Mid-late Holocene monsoon climate retrieved from seasonal Sr/Ca and delta O-18 records of *Porites lutea* corals at Leizhou Peninsula, northern coast of South China Sea. *Global and Planetary Change*, 47(2-4): 301-316.

Zinke, J. et al. (2019). Multi-trace-element sea surface temperature coral reconstruction for the southern Mozambique Channel reveals teleconnections with the tropical Atlantic. *Biogeosciences*, 16(3): 695-712.

Zou, J. et al. (2021). Temperature control on high-resolution SIMS oxygen isotopic compositions in *Porites* coral skeletons. *Solid Earth Sciences*, 6(2): 129-141.

**Figure S6 |** Global distribution of (a) Mg/Ca-T, Li/Mg-T, Sr/Ca-T, Sr/U-T and U/Ca-T calibration data and (b) Ba/Ca-T, D<sub>Ba</sub>-T and [Ba]<sub>coral</sub>-[Ba]<sub>SW</sub> calibration data extracted from publications identified during the multi-element, multi-species paleoenvironment calibrations literature search (section 4.3.5.3). Data without corresponding coordinates are not shown.



## Appendix C

**Figure S7 |** Summary of tuning stratigraphic element signals for *Keratoisis* sp. for sample (a) #23-1, (b) #23-6, (c) #23-10, and (d) #23-16. In each panel, tuning stratigraphic trace element signals (y-axis) are presented across basal (black solid line), second (dotted blue line) and third (dashed orange line) internodes with distance (x-axis) carried out in QAnalyseries (v 1.5.1, Kotov & Pälike, [2018]).

Figure S7(a)

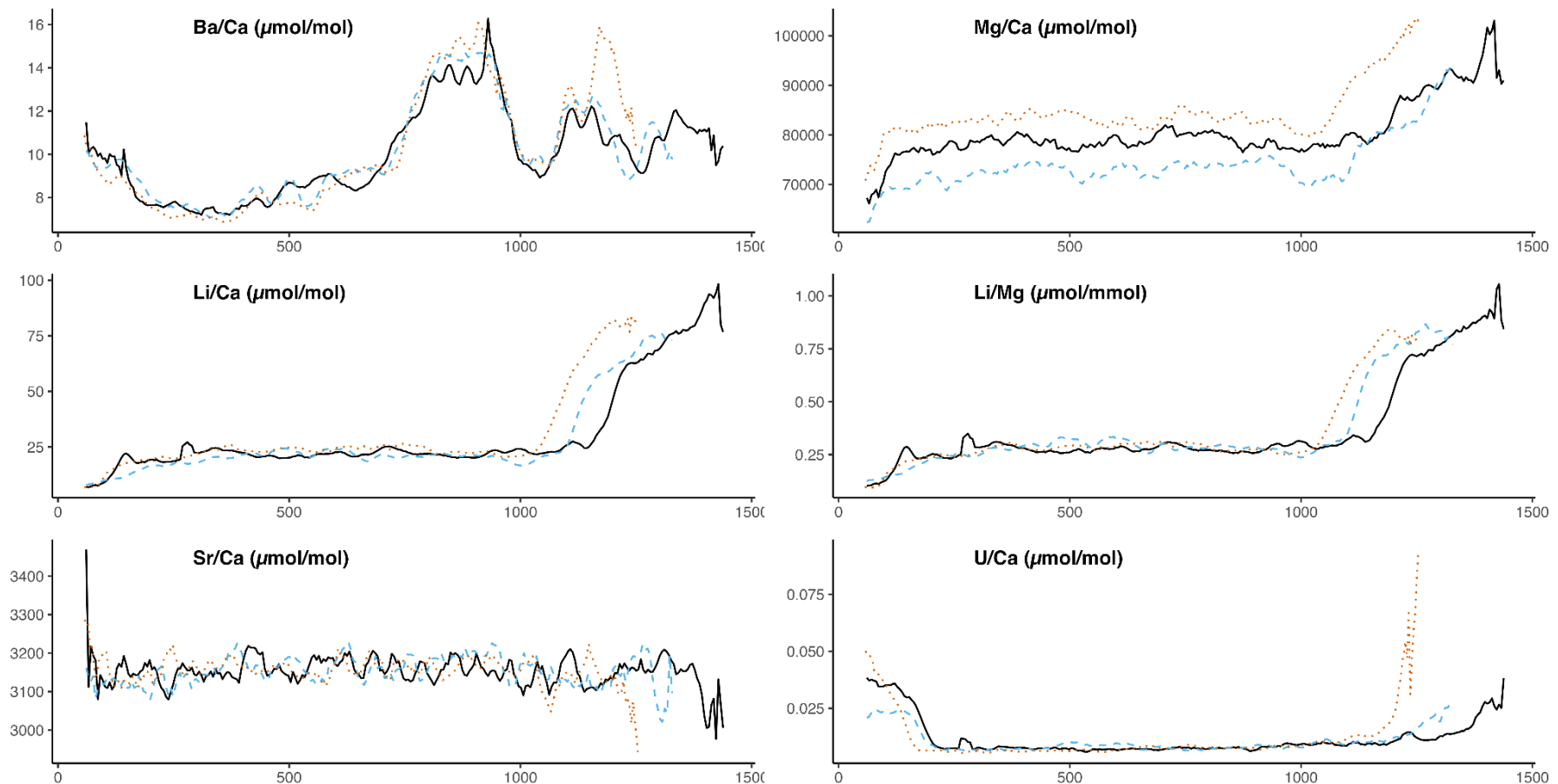
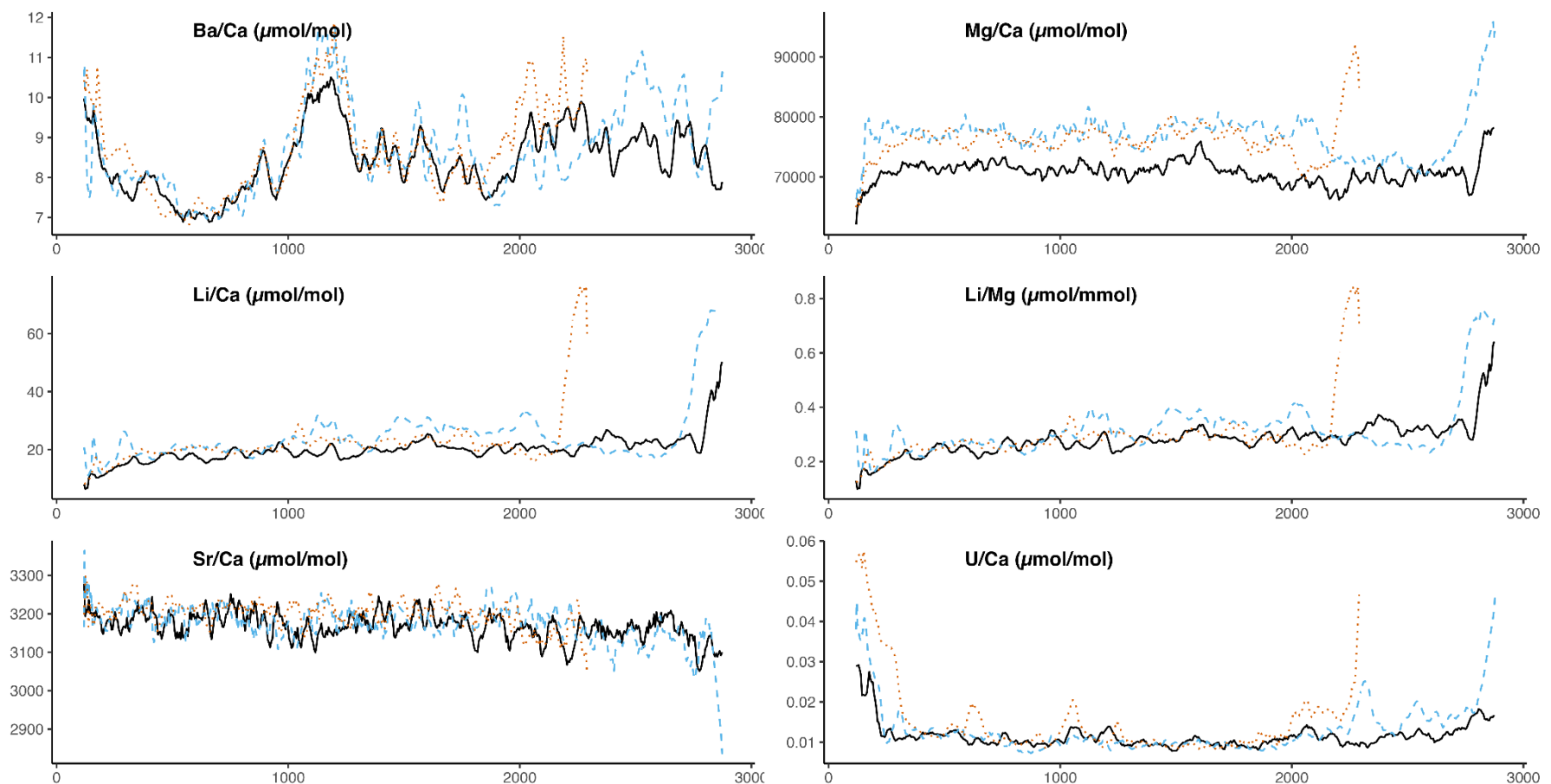


Figure S7(b)



Appendix C

Figure S7(c)

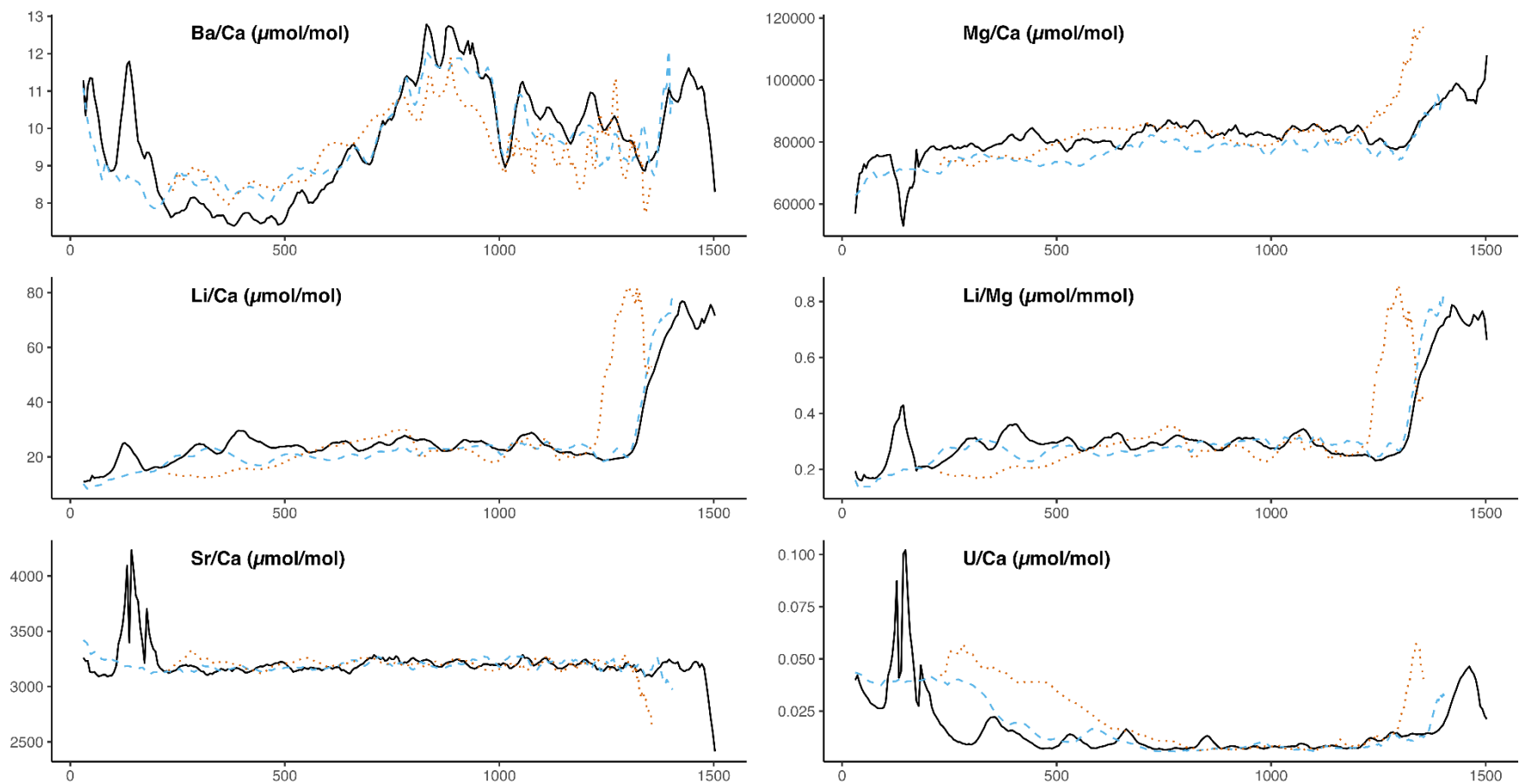
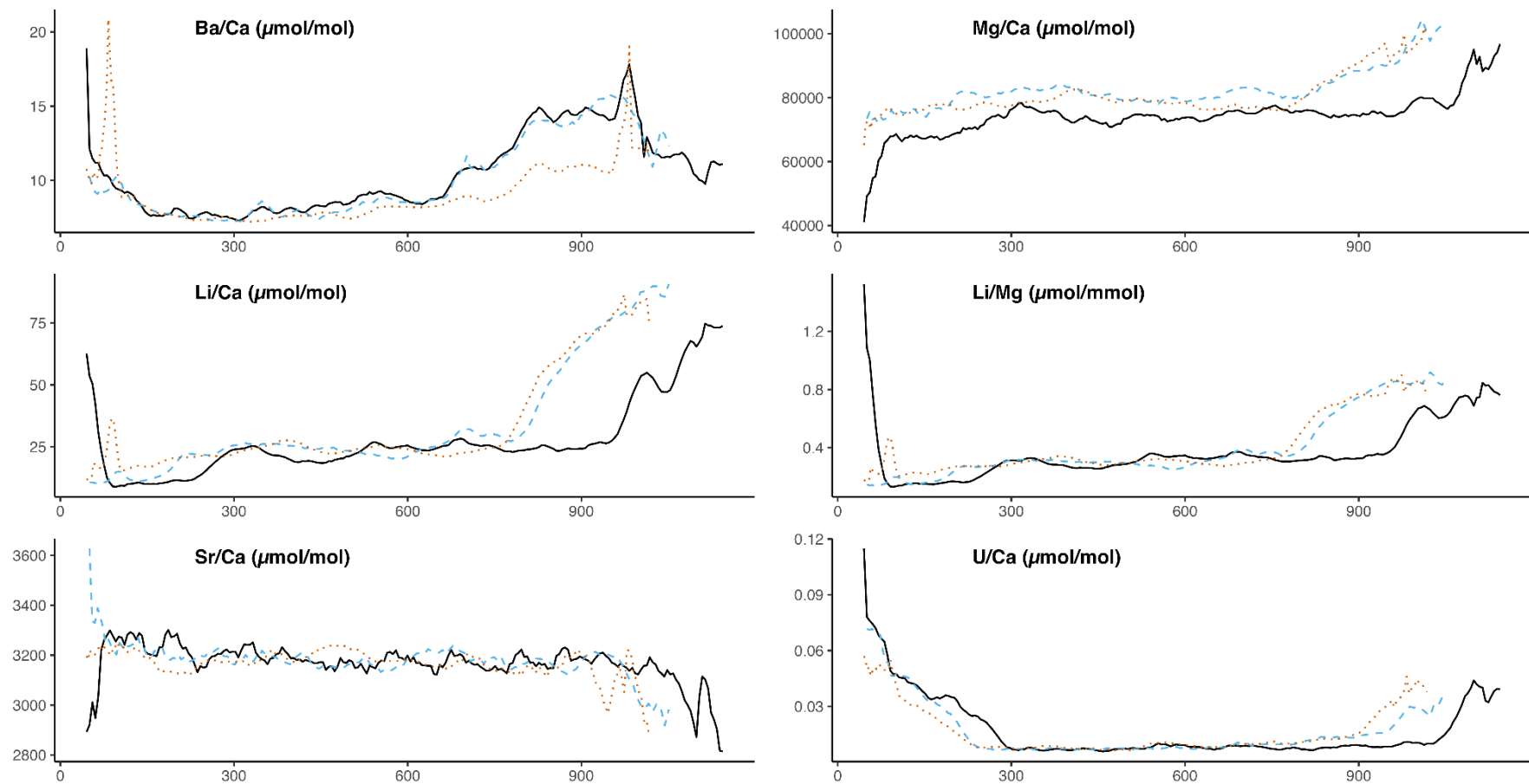


Figure S7(d)



## Appendix C

**Table S8 |** Summary of proxy calibrations extracted for the citation returns for the paleothermometry literature search of coral and coralline algae outlined in Table S7, displayed the type of relationship, the equation intercept and slope, Pearson's correlation score (r), coefficient of determination ( $R^2$ ; colour: low to high, red to green), statistical significance (p), source of temperature data, taxa and mineralogy, time resolution and temperature range.

Element ratio	units	Relationship	Publication	Journal	y	x	intercept	slope	r	$R^2$	p	Time Resolution	Temperature source	Temperature range	Coral Notes	Taxa
Li/Mg	mmol.mol	Linear	Zinke et al. 2019	Biogeosciences	Li/Mg	T	2.672	-0.045	0.94				OISST		Aragonite	<i>Porites</i> sp.
Li/Mg	mmol.mol	Linear	Zinke et al. 2019	Biogeosciences	Li/Mg	T	2.739	-0.052	0.78				OISST		Aragonite	<i>Porites</i> sp.
Li/Mg	mmol.mol	Linear	Hathorne et al. 2013	Paleoceanog.	Li/Mg	T	2.76	-0.048	0.67				in-situ	19 to 28	Aragonite	<i>Porites</i> sp.
Li/Mg	mmol.mol	Linear	Hathorne et al. 2013	Paleoceanog.	Li/Mg	T	2.96	-0.060	0.64				in-situ	25 to 29	Aragonite	<i>Porites</i> sp.
Li/Mg	mmol.mol	Linear	Ross et al. 2019	Paleoceanog. Paleoceanog. Paleoclimato.	Li/Mg	T	3.59	-0.079	0.86	<0.001			in-situ		Aragonite	Multi-species
Li/Mg	mmol.mol	Exponential	Marchitto et al. 2018	Earth Planet. Sci. Lett.	Li/Mg	T	5.29	exp	0.96				in-situ	0 to 30	Aragonite	Multi-species
Li/Mg	mmol.mol	Exponential	Montagna et al. 2014	Geomchim. Cosmochim. Acta	Li/Mg	T	5.41	exp	0.975					0 to 30	Aragonite	Multi-species
Li/Mg	mmol.mol	Exponential	Steward et al. 2020	Earth and Planetary Science Letters	Li/Mg	T	5.42	exp	0.97					0 to 30	Aragonite	Multi-species
Mg/Ca	mmol.mol	Linear	Hetzinger et al. 2018	Geomchim. Cosmochim. Acta	Mg/Ca	T	-41.834	0.345	0.882	<0.001			in-situ		High Mg calcite	<i>Clathromorphum compactum</i>
Mg/Ca	mmol.mol	Linear	Watanabe et al. 2001	Marine Geology	Mg/Ca	T	-3.24	0.28	0.92			Monthly	in-situ	24 to 31	Aragonite	<i>Porites</i> sp.
Mg/Ca	ratio to Ca	Linear	Kamenos et al. 2008	Geomchim. Cosmochim. Acta	T	Mg/Ca	-0.92	49.40	0.97	0.94	<0.0001		in-situ	6 to 16	High Mg calcite	<i>Lithothamnion glaciale</i>
Mg/Ca	mmol.mol	Linear	Ourbak et al. 2006	Geochem. Geophys. Geosys.	Mg/Ca	T	0.142	0.218	0.81				in-situ	21 to 29	Aragonite	<i>Porites</i> sp.
Mg/Ca	ratio to Ca	Linear	Kamenos et al. 2010	Geomchim. Cosmochim. Acta	T	Mg/Ca	0.74	42.12	0.89	0.78	<0.0001		in-situ	6 to 16	High Mg calcite	<i>Phymatolithon calcareum</i>
Mg/Ca	mmol.mol	Linear	Yu et al. 2005	Paleo. Paleo. Paleo.	Mg/Ca	T	1.32	0.11						18 to 31	Aragonite	<i>Porites</i> sp.
Mg/Ca	mmol.mol	Linear	Villaescusa & Carriquiry, 2004	Ciencias Marinas	Mg/Ca	T	1.550	0.0956		0.906		Monthly	AVHRR	23 to 29	Aragonite	<i>Porites</i> sp.
Mg/Ca	mmol.mol	Linear	Armid et al. 2011	Geomchim. Cosmochim. Acta	Mg/Ca	T	1.973	0.1002		0.67			Culture experiment	22 to 30	Aragonite	<i>Porites</i> sp.
Mg/Ca	mmol.mol	Linear	Xiao et al. 2014	Sci. China-Earth Sciences	Mg/Ca	T	2.339	0.0497		0.25			Culture experiment		Aragonite	<i>Acropora</i>
Mg/Ca	mmol.mol	Linear	Quinn & Sampson, 2002	Paleoceanog.	Mg/Ca	T	2.638	0.105		0.61		Monthly	in-situ	18 to 28	Aragonite	<i>Porites</i> sp.
Mg/Ca	mmol.mol	Linear	Hathorne et al. 2013	Paleoceanog.	Mg/Ca	T	3.16	0.05		0.26			in-situ	19 to 28	Aragonite	<i>Porites</i> sp.
Mg/Ca	mmol.mol	Linear	Bell et al. 2017	Paleoecol.	Mg/Ca	T	3.774	-0.0342		0.53			in-situ		Aragonite	<i>Acropora digitifera</i>

Mg/Ca	mmol.mol	Linear	Hathorne et al. 2013	Paleooceanog.	Mg/Ca	T	4.54	0.014		in-situ	25 to 29	Aragonite	<i>Porites</i> sp.				
Sr-U	mmol.mol	Linear	Ross et al. 2019	Paleooceanog. Paleoclimato.	Sr-U	T	8.92	-0.035	0.89	<0.001	in-situ	Aragonite	Multi-species				
Sr-U	mmol.mol	Linear	Rodriguez et al. 2019	Paleooceanog. Paleoclimato.	Sr-U	T	15.73	-0.247	0.74	<0.001	HADISST	Aragonite	Multi-species				
Sr-U	mmol.mol	Linear	Alpert et al. 2017	Paleooceanog.	T	Sr-U	126.98	-11.00			in-situ	23 to 32	Aragonite	Multi-species			
Sr/Ca	ratio to Ca	Linear	Kamenos et al. 2011	Geomchim. Cosmochim. Acta	T	Sr/Ca	-5.86	5174	0.83	0.69	<0.0001	in-situ	6 to 16	High Mg calcite	<i>Phymatolithon calcareum</i>		
Sr/Ca	ratio to Ca	Linear	Kamenos et al. 2008	Geomchim. Cosmochim. Acta	T	Sr/Ca	-2.06	3136.7	0.88	0.77	<0.0001	OISST	6 to 16	High Mg calcite	<i>Lithothamnion glaciale</i>		
Sr/Ca	mmol.mol	Linear	Villiers et al. 1994	Geomchim. Cosmochim. Acta	Sr/Ca	T	1.956	0.079523	-	0.949	Annual maxima-minima	in-situ	22 to 27	Aragonite	<i>Porites</i> sp.		
Sr/Ca	mmol.mol	Linear	Amir et al. 2019	Sains Malaysiana	Sr/Ca	T	9.436	-0.023	-	0.36	<0.001	in-situ	Aragonite	<i>Porites</i> sp.			
Sr/Ca	mmol.mol	Linear	Cahyarini et al. 2014	JGR Oceans	Sr/Ca	T	9.713	-0.036	-0.67		<0.0001	AVHRR	Aragonite	<i>Porites</i> sp.			
Sr/Ca	mmol.mol	Linear	Gischler et al. 2005	Paleo. Paleo. Paleo.	Sr/Ca	T	9.746	-0.027	-0.642		Monthly	GISST	16 to 35	Aragonite	<i>Porites</i> sp.		
Sr/Ca	mmol.mol	Linear	Bell et al. 2017	Paleoecol.	Sr/Ca	T	9.763	-0.0283	-	0.68		in-situ	Aragonite	<i>Acropora digitifera</i>			
Sr/Ca	mmol.mol	Linear	Cahyarini et al. 2008	Geomchim. Cosmochim. Acta	Sr/Ca	T	9.83	-0.040	0.89		<0.001		28 to 30	Aragonite	<i>Porites</i> sp.		
Sr/Ca	mmol.mol	Linear	Yu et al. 2005	Glob. Planet. Change	Sr/Ca	T	9.836	-0.0424	-				18 to 31	Aragonite	<i>Porites</i> sp.		
Sr/Ca	mmol.mol	Linear	Pfeiffer et al. 2019	Paleooceanog. Paleoclimato.	Sr/Ca	T	9.844	-0.040	-	0.66		OISST	Aragonite	<i>Porites</i> sp.			
Sr/Ca	mmol.mol	Linear	DeLong et al. 2011	Paleo. Paleo. Paleo.	Sr/Ca	T	9.893	-0.027	-0.93			in-situ	Aragonite	<i>Orbicella faveolata</i>			
Sr/Ca	mmol.mol	Linear	Chen et al. 2013	Paleo. Paleo. Paleo.	Sr/Ca	T	9.91	-0.029	-0.795	0.63		in-situ	12 to 29	Aragonite	<i>Porites</i> sp.		
Sr/Ca	mmol.mol	Linear	Cahyarini et al. 2014	JGR Oceans	Sr/Ca	T	9.94	-0.044	-0.62		<0.0001	OISST	Aragonite	<i>Porites</i> sp.			
Sr/Ca	mmol.mol	Linear	Smith et al. 2006	Paleooceanog.	Sr/Ca	T	9.962	-0.0282	-0.86			in-situ & HADISST	22 to 31	Aragonite	<i>Montastraea faveolata</i>		
Sr/Ca	mmol.mol	Linear	Zinke et al. 2019	Biogeosciences	Sr/Ca	T	9.974	-0.040	-	0.92		OISST	Aragonite	<i>Porites</i> sp.			
Sr/Ca	mmol.mol	Linear	Cohen et al. 2002	Science	Sr/Ca	T	9.9806	-0.038	-		Annual maxima-minima	in-situ	24 to 29	Aragonite	<i>Porites</i> sp.		
Sr/Ca	mmol.mol	Linear	Hetzinger et al. 2006	Geochem. Geophys. Geosys.	Sr/Ca	T	9.986	-0.041	-0.67	0.45	<0.0001		SODA SST	25 to 29	Aragonite	<i>Diploria strigosa</i>	
Sr/Ca	mmol.mol	Linear	Maupin et al. 2008	Geochem. Geophys. Geosys.	Sr/Ca	T	10.008	-0.039	-0.96			in-situ & HADISST	19 to 32	Aragonite	<i>Siderastrea siderea</i>		
Sr/Ca	mmol.mol	Linear	Hetzinger et al. 2006	Geochem. Geophys. Geosys.	Sr/Ca	T	10.013	-0.042	-0.65	0.42	<0.0001	EERSST	25 to 29	Aragonite	<i>Diploria strigosa</i>		
Sr/Ca	mmol.mol	Linear	Cahyarini et al. 2009	Int. J. Earth Sci.	Sr/Ca	T	10.050	-0.05	0.83		<0.001		Annual maxima-minima	EERSST	25 to 30	Aragonite	<i>Porites</i> sp.
Sr/Ca	mmol.mol	Linear	Cohen et al. 2002	Science	Sr/Ca	T	10.065	-0.036	-			in-situ	7 to 22	Aragonite	<i>Astrangia</i> sp.		

## Appendix C

Sr/Ca	mmol.mol	Linear	Quinn & Sampson, 2002	Paleoceanog.	Sr/Ca	T	10.073	- 0.052	0.84	Monthly	in-situ	18 to 28	Aragonite	<i>Porites</i> sp.
Sr/Ca	mmol.mol	Linear	DeLong et al. 2011	Paleo. Paleo. Paleo.	Sr/Ca	T	10.081	-0.043	-0.97		in-situ		Aragonite	<i>Siderastrea siderea</i>
Sr/Ca	mmol.mol	Linear	Goodkin et al. 2005	Paleoceanog.	Sr/Ca	T	10.1	-0.0358	0.86	<0.0001	in-situ	18 to 30	Aragonite	<i>Diploria labyrinthiformis</i>
Sr/Ca	mmol.mol	Linear	Goodkin et al. 2007	Paleoceanog. Paleoceanog. Paleoclimato.	Sr/Ca	T	10.1	-0.0376	0.73	<0.0001	in-situ	18 to 30	Aragonite	<i>Diploria labyrinthiformis</i>
Sr/Ca	mmol.mol	Linear	DeLong et al. 2014	Paleoceanog.	Sr/Ca	T	10.11	-0.043			in-situ		Aragonite	<i>Siderastrea siderea</i>
Sr/Ca	mmol.mol	Linear	Cahyarini et al. 2014	JGR Oceans	Sr/Ca	T	10.148	-0.050	-0.61	<0.0001	ERSST		Aragonite	<i>Porites</i> sp.
Sr/Ca	mmol.mol	Linear	Swart et al. 2002	Geochem. Geophys. Geosys.	Sr/Ca	T	10.165	-0.471	-0.88	Monthly	in-situ	20 to 30	Aragonite	<i>Montastraea annularis</i>
Sr/Ca	mmol.mol	Linear	Kuffner et al. 2017	Geochem. Geophys. Geosys.	Sr/Ca	T	10.1655	-0.0429			in-situ		Aragonite	<i>Siderastrea siderea</i>
Sr/Ca	mmol.mol	Linear	Seo et al. 2013	Geochem. Geophys. Geosys.	Sr/Ca	T	10.184	-0.0408		OISST	12 to 29	Aragonite	<i>Diploastrea speciosa</i>	
Sr/Ca	mmol.mol	Linear	Mohtar et al. 2021	Paleo. Paleo. Paleo.	Sr/Ca	T	10.188	-0.052	-0.65	<0.0001	OISST		Aragonite	<i>Porites</i> sp.
Sr/Ca	mmol.mol	Linear	Ramos et al. 2017	Paleoceanog.	Sr/Ca	T	10.204	-0.045	0.38	0.03	IGOSS		Aragonite	<i>Diploastrea heliopora</i>
Sr/Ca	mmol.mol	Linear	Flannery and Poore, 2013	Journal of Coastal Research	Sr/Ca	T	10.205	-0.0392			in-situ	20 to 31	Aragonite	<i>Orbicella faveolata</i>
Sr/Ca	mmol.mol	Linear	Armid et al. 2011	Geomchim. Cosmochim. Acta	Sr/Ca	T	10.214	-0.0642	0.59	Culture experiment	22 to 30	Aragonite	<i>Porites</i> sp.	
Sr/Ca	mmol.mol	Linear	Ramos et al. 2017	Paleoceanog.	Sr/Ca	T	10.237	-0.049	0.59	<0.001	IGOSS		Aragonite	<i>Porites</i> sp.
Sr/Ca	mmol.mol	Linear	Zinke et al. 2019	Biogeosciences	Sr/Ca	T	10.241	-0.045	0.93		OISST		Aragonite	<i>Porites</i> sp.
Sr/Ca	mmol.mol	Linear	Ourbak et al. 2006	Geochem. Geophys. Geosys.	Sr/Ca	T	10.248	-0.054	-0.8		in-situ	21 to 29	Aragonite	<i>Porites</i> sp.
Sr/Ca	mmol.mol	Linear	Cahyarini et al. 2014	JGR Oceans	Sr/Ca	T	10.277	-0.059	-0.89	<0.0001	OMBAI		Aragonite	<i>Porites</i> sp.
Sr/Ca	mmol.mol	Linear	Goodkin et al. 2007	Paleoceanog. Paleoclimato.	Sr/Ca	T	10.3	-0.0429	0.76	<0.0001	in-situ	18 to 30	Aragonite	<i>Diploria labyrinthiformis</i>
Sr/Ca	mmol.mol	Linear	Goodkin et al. 2007	Paleoceanog. Paleoclimato.	Sr/Ca	T	10.3	-0.0436	0.85	<0.0001	in-situ	18 to 30	Aragonite	<i>Diploria labyrinthiformis</i>
Sr/Ca	mmol.mol	Linear	Shen et al. 1996	Geomchim. Cosmochim. Acta	Sr/Ca	T	10.307	-0.0505	0.91		in-situ	22 to 28	Aragonite	<i>Porites</i> sp.
Sr/Ca	mmol.mol	Linear	Hennekam et al. 2018	Paleoceanog. Paleoclimato.	Sr/Ca	T	10.307	-0.054	0.649	<0.001	in-situ		Aragonite	<i>Porites</i> sp.
Sr/Ca	mmol.mol	Linear	Shen et al. 1996	Geomchim. Cosmochim. Acta	Sr/Ca	T	10.356	-0.0528	0.96		in-situ	22 to 28	Aragonite	<i>Porites</i> sp.
Sr/Ca	mmol.mol	Linear	Marshall & McCulloch, 2001	Geophys. Res. Lett.	Sr/Ca	T	10.375	-0.0593	0.69	Weekly	IGOSS	24 to 31	Aragonite	<i>Porites</i> sp.
Sr/Ca	mmol.mol	Linear	Razak et al. 2017	Marine Biology	Sr/Ca	T	10.39	-0.0496	0.8512	<0.001	in-situ		Aragonite	<i>Isopora</i> sp.
Sr/Ca	mmol.mol	Linear	Chen et al. 2013	Paleo. Paleo. Paleo.	Sr/Ca	T	10.432	-0.048	-0.899	0.81	in-situ	24 to 29	Aragonite	<i>Porites</i> sp.
Sr/Ca	mmol.mol	Linear	Flannery et al. 2018	Paleoceanog. Paleoceanog. Paleoclimato.	Sr/Ca	T	10.460	-0.049	0.76		AVHRR		Aragonite	<i>Orbicella faveolata</i>
Sr/Ca	mmol.mol	Linear	Villaescusa & Carrquiry, 2004	Ciencias Marinas	Sr/Ca	T	10.467	-0.0524	0.894	Monthly	AVHRR	23 to 29	Aragonite	<i>Porites</i> sp.
Sr/Ca	mmol.mol	Linear	Alibert et al. 1997	Paleoceanog.	Sr/Ca	T	10.48	-0.0615	-0.98				Aragonite	<i>Porites</i> sp.

Sr/Ca	mmol.mol	Linear	Amir et al. 2019	Sains Malaysiana	Sr/Ca	T	10.485	-0.059	0.446	<0.001	in-situ	Aragonite	<i>Porites</i> sp.	
Sr/Ca	mmol.mol	Linear	Bolton et al. 2014	Paleo. Paleo. Paleo.	Sr/Ca	T	10.503	-0.052	0.77	<0.001	HADISST	Aragonite	<i>Porites</i> sp.	
Sr/Ca	mmol.mol	Linear	Caharyini et al. 2008	Geomchim. Cosmochim. Acta	Sr/Ca	T	10.52	-0.063	0.86	<0.001		28 to 30	Aragonite	<i>Porites</i> sp.
Sr/Ca	mmol.mol	Linear	Felis et al. 2012	Nat. Comm. Paleoceanog. Paleoclimato.	Sr/Ca	T	10.53	-0.057	0.69		in-situ	25 to 29	Aragonite	<i>Porites</i> sp.
Sr/Ca	mmol.mol	Linear	Cheung et al. 2021	Paleoceanog. Paleoclimato.	Sr/Ca	T	10.5464	-0.0580	0.554		OISST	Aragonite	<i>Porites</i> sp.	
Sr/Ca	mmol.mol	Linear	Mutry et al. 2018	Paleoceanog. Paleoclimato.	Sr/Ca	T	10.61	-0.055	0.72	<0.0001	AVHRR	Aragonite	<i>Porites</i> sp.	
Sr/Ca	mmol.mol	Linear	Kilbourne et al. 2010	Geochem. Geophys. Geosys.	Sr/Ca	T	10.615	-0.058			HADISST	Aragonite	<i>Orbicella faveolata</i>	
Sr/Ca	mmol.mol	Linear	Villiers et al. 1994	Geomchim. Cosmochim. Acta	Sr/Ca	T	10.646	-0.06746	0.683	Annual maxima-minima	in-situ	19 to 25	Aragonite	<i>Pavona</i> sp.
Sr/Ca	mmol.mol	Linear	Wu et al. 2013	Geochem. Geophys. Geosys.	Sr/Ca	T	10.65	-0.062	0.67		OISST	Aragonite	<i>Porites</i> sp.	
Sr/Ca	mmol.mol	Linear	Ross et al. 2019	Paleoceanog. Paleoclimato.	Sr/Ca	T	10.66	-0.055	0.68	<0.001	in-situ	Aragonite	Multi-species	
Sr/Ca	mmol.mol	Linear	Wu et al. 2013	Geochem. Geophys. Geosys.	Sr/Ca	T	10.67	-0.058	0.68		OISST	Aragonite	<i>Porites</i> sp.	
Sr/Ca	mmol.mol	Linear	Amir et al. 2019	Sains Malaysiana	Sr/Ca	T	10.683	-0.064	0.323	<0.001	in-situ	Aragonite	<i>Porites</i> sp.	
Sr/Ca	mmol.mol	Linear	Morimoto et al. 2007	Quart. Res.	Sr/Ca	T	10.77	-0.0665	0.97			20 to 30	Aragonite	<i>Porites</i> sp.
Sr/Ca	mmol.mol	Linear	Mohtar et al. 2021	Paleo. Paleo. Paleo.	Sr/Ca	T	10.861	-0.071	-0.6	<0.0001	OISST	Aragonite	<i>Porites</i> sp.	
Sr/Ca	mmol.mol	Linear	Allison et al. 2004	Geochem. Geophys. Geosys.	Sr/Ca	T	10.861	-0.080	0.919	Annual maxima-minima	in-situ	22 to 30	Aragonite	<i>Porites</i> sp.
Sr/Ca	mmol.mol	Linear	Cheung et al. 2021	Paleoceanog. Paleoclimato.	Sr/Ca	T	10.8865	-0.0703	0.659		OISST	Aragonite	<i>Porites</i> sp.	
Sr/Ca	mmol.mol	Linear	Allison et al. 2004	Geochem. Geophys. Geosys.	Sr/Ca	T	10.965	-0.067	0.871	Annual maxima-minima	in-situ	22 to 30	Aragonite	<i>Porites</i> sp.
Sr/Ca	mmol.mol	Linear	Villiers et al. 1994	Geomchim. Cosmochim. Acta	Sr/Ca	T	11.004	0.076278	0.926	Annual maxima-minima	in-situ	23 to 27	Aragonite	<i>Pocillopora</i> sp.
Sr/Ca	mmol.mol	Linear	Felis et al. 2014	Nat. Comm.	Sr/Ca	T	11.15	-0.075					Aragonite	<i>Isopora</i> sp.
Sr/Ca	mmol.mol	Linear	Gagan et al. 2013	Paleoceanog.	Sr/Ca	T	11.278	-0.084		Culture experiment			Aragonite	<i>Porites</i> sp.
Sr/Ca	mmol.mol	Linear	Goodkin et al. 2008	Paleoceanog.	Sr/Ca	T	11.3	-0.0972	0.36	in-situ & HADISST		20 to 26	Aragonite	<i>Diploria labyrinthiformis</i>
Sr/Ca	mmol.mol	Linear	Gallup et al. 2006	Geophys. Res. Lett.	Sr/Ca	T	11.32	-0.06281	0.62		COADS	25 to 29	Aragonite	<i>Acropora palmata</i>
Sr/Ca	mmol.mol	Linear	Brenner et al. 2017	Paleoceanog.	Sr/Ca	T	11.37	-0.083					Aragonite	<i>Isopora</i> sp.
Sr/Ca	mmol.mol	Linear	Sagar et al. 2015	JGR Oceans	Sr/Ca	T	11.59	-0.088	-0.85	0.72	<0.001	MODIS-Terra SST	Aragonite	<i>Porites</i> sp.
Sr/Ca	mmol.mol	Linear	Sagar et al. 2015	JGR Oceans	Sr/Ca	T	11.67	-0.089	-0.78	0.61	<0.001	ICOADS SST	Aragonite	<i>Porites</i> sp.
Sr/Ca	mmol.mol	Linear	Saenger et al. 2008	Paleoceanog. Paleoclimato.	Sr/Ca	T	11.74	-0.095			IGOSS	18 to 28	Aragonite	<i>Montastraea</i> sp.

## Appendix C

Sr/Ca	mmol.mol	Linear	Amir et al. 2019	Sains Malaysiana	Sr/Ca	T	11.921	-0.106	0.495	<0.001	in-situ	Aragonite	<i>Porites</i> sp.	
Sr/Ca	mmol.mol	Linear	Sagar et al. 2015	JGR Oceans	Sr/Ca	T	11.98	-0.101	-0.85	0.73	<0.001	OISST	Aragonite	<i>Porites</i> sp.
Sr/Ca	mmol.mol	Linear	Sagar et al. 2015	JGR Oceans	Sr/Ca	T	12.08	-0.104	-0.85	0.73	<0.001	ERSST	Aragonite	<i>Porites</i> sp.
Sr/Ca	mmol.mol	Linear	Sagar et al. 2015	JGR Oceans	Sr/Ca	T	12.09	-0.104	-0.85	0.72	<0.001	HADISST	Aragonite	<i>Porites</i> sp.
Sr/Ca	mmol.mol	Linear	Azmt et al. 2010	Int. J. Earth Sci.	Sr/Ca	T	12.389	-0.1361	0.664		OISST	27 to 30	Aragonite	<i>Porites</i> sp.
Sr/Ca	mmol.mol	Linear	Alibert et al. 2008 Forouzan et al. 2014	JGR Oceans Int. J. Environ. Res.	Sr/Ca	T	15.60	-0.23	-		TRITON	27 to 31	Aragonite	<i>Porites</i> sp.
Sr/Ca	mmol.mol	Linear			T	Sr/Ca	231.45	-22.599	0.8469		COADS		Aragonite	<i>Platygyra sinensis</i>
U/Ca	umol.mol	Linear	Armid et al. 2011 Quinn & Sampson, 2002	Geomchim. Cosmochim. Acta Paleooceanog. Geochem. Geophys. Geosys.	U/Ca	T	1.488	-0.0212	0.78		Culture experiment	22 to 30	Aragonite	<i>Porites</i> sp.
U/Ca	umol.mol	Linear	Ourbak et al. 2006		U/Ca	T	1.847	-0.029	0.44	Monthly	in-situ	18 to 28	Aragonite	<i>Porites</i> sp.
U/Ca	umol.mol	Linear			U/Ca	T	1.928	-0.033	-0.84		in-situ	21 to 29	Aragonite	<i>Porites</i> sp.

## Statistical model summary

Summary of the statistical models analysing each reconstructed environmental variable (Temperature:  $T_{[rec]}$  mean,  $T_{[rec]}$  trend; Barium:  $[Ba]_{SW}$ ) . For each model (Model S1 to S3) I list the initial linear regression model and the minimal adequate model. When homogeneity of variance was violated I used a linear regression with generalized least squares (GLS) estimation. I present a summary of the coefficient tables for single terms. The coefficients indicate the relative performance of each factor level in relation to the re-levelled baseline (as indicated). Coefficients  $\pm$  SE, t-values and significance values are presented.

## Abbreviations

### (i) Explanatory variables

Colony, coral colony

Internode, colony internode

### (ii) Response variables

$T_{[rec]}$  mean, mean reconstructed temperature between 2003 and 2016 ( $^{\circ}C$ )

$T_{[rec]}$  trend, annual reconstructed temperature trend 2003 and 2016 ( $^{\circ}C.yr^{-1}$ )

$[Ba]_{SW}$ , mean reconstructed barium between 2001 and 2021 (nmol.kg $^{-1}$ )



**Model S1** Mean reconstructed temperature between 2003 and 2016 ( $T_{[rec]}$  mean,  $^{\circ}\text{C}$ )

Initial linear regression model:

```
lm(T[rec] mean ~ Colony + Internode + Colony:Internode)
```

Minimal adequate model:

```
lme(T[rec] mean ~ Colony + Internode + Colony:Internode,
    random = ~ 1 | Interpolation,
    weights = varIdent(form = ~ 1 | Colony),
    method = "REML")
```

**Model S2** Annual reconstructed temperature trend 2003 and 2016 ( $T_{[rec]}$  trend,  $^{\circ}\text{C.yr}^{-1}$ )

Initial linear regression model:

```
lm(T[rec] trend ~ Colony + Internode + Colony:Internode)
```

Minimal adequate model:

```
lme(T[rec] trend ~ Colony + Internode + Colony:Internode,
    random = ~ 1 | Interpolation,
    weights = varIdent(form = ~ 1 | Colony * Internode),
    method = "REML")
```

**Model S3** Mean reconstructed barium between 2001 and 2021 ( $[\text{Ba}]_{\text{sw}}$ ,  $\text{nmol.kg}^{-1}$ )

Initial linear regression model:

## Appendix D

```
lm([Ba]sw ~ Colony + Internode + Colony:Inernode)
```

Minimal adequate model:

```
lme([Ba]sw ~ Colony + Internode + Colony:Inernode,  
random = ~1|Interpolation,  
weights = varIdent(form = ~ 1|Colony*Inernode),  
method = "REML")
```



## C.1 References

Geoffroy, M., Algar, C., Archambault, P., Cote, D., Edinger, E., Hubert, C., Laing, R., Limoges, A., Mercier, A., Neves, B. R. D. M., Normandeau, A., Robert, K., Sherwood, O., Snelgrove, P., Hayes, V. W. & Zedel1, L. 2021. Leg 2 - Labrador Sea, Davis Strait and Baffin Bay. *Amundsen Field Report 2021*. Amundsen Science..

Thomas, H., Mucci, A., Mears, C., Charette, M. A. & Dehairs, F. 2021. Inorganic Carbon, Ra, Ba and,  $\delta^{18}\text{O}$  tracer distribution in the Canadian Arctic Archipelago from the 2015 Canadian GEOTRACES expedition. PANGAEA.

GEOTRACES-INTERMEDIATE-DATA-PRODUCT-GROUP 2021. The GEOTRACES Intermediate Data Product 2021 (IDP2021). <https://www.geotrades.org/geotrades-intermediate-data-product-2021/>: NERC EDS British Oceanographic Data Centre NOC.

## Appendix D Appendix 1 for Chapter 5

### **Data records S1.**

Data records are available *via* an unrestricted repository hosted by the Discovery Metadata System (<https://www.bas.ac.uk/project/dms/>), a data catalogue hosted by The UK Polar Data Centre (UK PDC, <https://www.bas.ac.uk/data/uk-pdc/>).

**The following data records were used in this contribution:**

**Invertebrate macrofauna (taxa identity, abundance and biomass)**

Solan, M., Godbold, J., Grange, L., Ward, E. R., Wood, C., & Reed, A. (2020). Macrofaunal abundance and biomass for replicate macrofaunal communities from the Western Barents Sea for summer 2017 and 2018 (Version 1.0) [Data set]. UK Polar Data Centre, Natural Environment Research Council, UK Research & Innovation. <https://doi.org/10.5285/7FBCA0A1-E2C1-4265-A7A5-713451CB52C0>

**The cruise reports (RRS James Clarke Ross, JR16006 and JR17007) are available here:**

[https://www.bodc.ac.uk/resources/inventories/cruise\\_inventory/reports/jr16006.pdf](https://www.bodc.ac.uk/resources/inventories/cruise_inventory/reports/jr16006.pdf)

[https://www.bodc.ac.uk/resources/inventories/cruise\\_inventory/reports/jr17007.pdf](https://www.bodc.ac.uk/resources/inventories/cruise_inventory/reports/jr17007.pdf)

## Appendix D

**Figure S1 |** Geographical distribution of benthic stations (B13-B14, Xs, B15-B17) and main oceanographic currents (Vihtakari et al. 2019; Eriksen et al. 2018) overlain with (a) bottom temperature range (°C) between 2004-2014 and (b) mean sea ice cover (fraction) between 2004-2014 obtained from BioOracle (Tyberghein et al. 2012; Assis et al. 2018) and mapped using the “sdmpredictors” R package (Bosch & Fernandez, 2021).

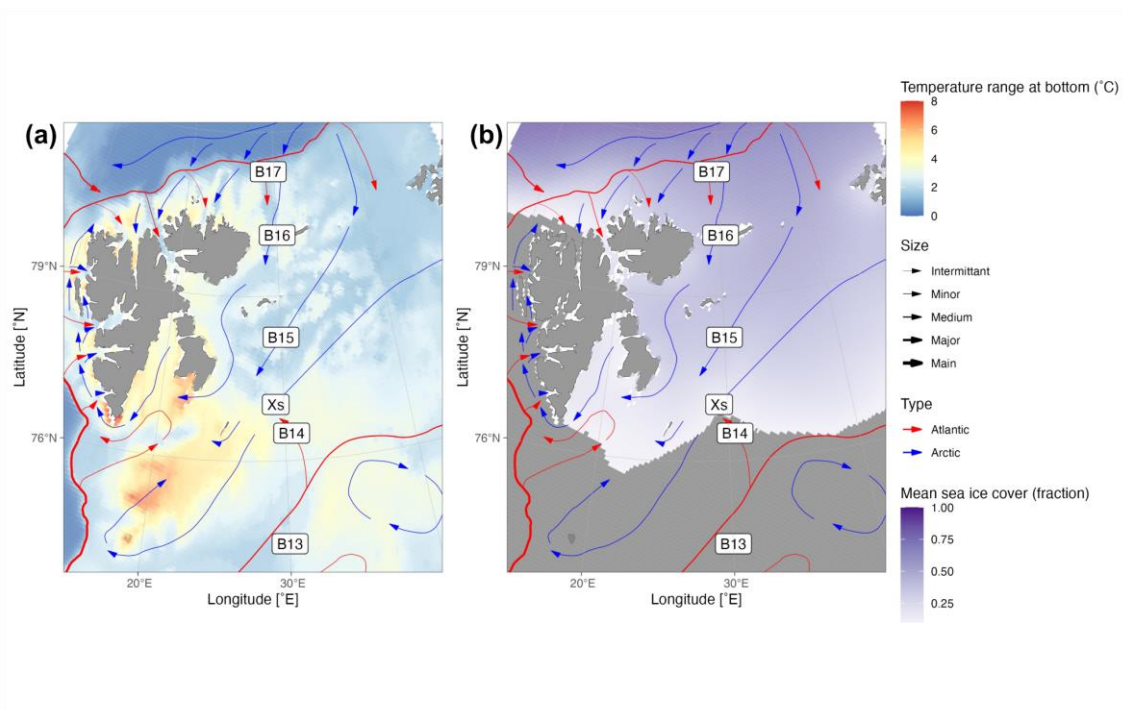


**Table S1** | Ranked (rk) vulnerabilities (alphabetically ordered) to climate-driven environmental transitions (right hand columns) based on percentage differences (left hand columns) in sediment-dwelling invertebrate biomass between the pre-extinction community (northernmost station) and the reference post-extinction community (southernmost station) for all taxa in the regional species pool (n = 69). Inf. denotes where there is no biomass in the pre-extinction community and biomass in the post-extinction community, so percentage difference = infinite.

Species	B17-B16	B16-B15	B15-Xs	Xs-B14	B14-B13	B17-B13	rk(B17-B16)	rk(B16-B15)	rk(B15-Xs)	rk(Xs-B14)	rk(B14-B13)	rk(B17-B13)
<i>Abyssinioe hibernica</i>	Inf	1.8261	-1	0	0	0	104	88	13	69	52	67
<i>Adontorhina</i> juv	-1	0	Inf	-0.942	0.3	0.3	15	60	100.5	25	84	90
<i>Aglaophamus malmgreni</i>	-1	0	Inf	-0.929	-1	-1	15	60	100.5	26	8	17
<i>Ampelisca</i> sp	0	0	0	Inf	-1	0	60.5	60	55	108.5	8	67
<i>Ampeliscidae</i>	Inf	-1	0	0	0	0	104	13.5	55	69	52	67
<i>Ampharete finmarchica</i>	0	0	0	Inf	-1	0	60.5	60	55	108.5	8	67
<i>Ampharete lindstroemi</i>	0	0	Inf	-1	0	0	60.5	60	100.5	12.5	52	67
<i>Ampharete</i> sp	Inf	-1	0	0	0	0	104	13.5	55	69	52	67
<i>Amphitrite groenlandica</i>	-1	0	0	0	0	-1	15	60	55	69	52	17
<i>Amphiuridae</i> indet	-1	0	0	0	0	-1	15	60	55	69	52	17
<i>Antalis entalis</i>	-1	0	0	Inf	17.538	-0.667	15	60	55	108.5	90	38
<i>Aphelochaeta marioni</i>	-1	0	0	0	0	-1	15	60	55	69	52	17
<i>Aphroditoidae</i> indet	-1	0	0	0	0	-1	15	60	55	69	52	17
<i>Apseudes</i> sp	0	0	0	Inf	-1	0	60.5	60	55	108.5	8	67
<i>Aricidea catherinae</i>	3	-0.95	26	-1	Inf	2.8	90	27	87	12.5	102	93
<i>Aricidea quadrilobata</i>	-1	Inf	-1	0	0	-1	15	101.5	13	69	52	17

Appendix D

<i>Aricidea suecica</i>	-1	0	Inf	-1	0	-1	15	60	100.5	12.5	52	17
<i>Ascelerichilus intermedius</i>	0	Inf	-0.966	-1	Inf	Inf	60.5	101.5	26	12.5	102	105.5
<i>Astarte crenata</i> agg	-1	0	Inf	47.815	2.11	3.2084	15	60	100.5	102	86	95
<i>Autolytinae</i> indet	0	0	0	0	Inf	Inf	60.5	60	55	69	102	105.5
<i>Bathyarca frielei</i>	-1	0	0	0	Inf	-0.967	15	60	55	69	102	34
<i>Bathyarca glacialis</i>	0	0	0	0	Inf	Inf	60.5	60	55	69	102	105.5
<i>Brachydiastylis resima</i>	-0.75	-0.5	6	-1	0	-1	32	36	80	12.5	52	17
<i>Calathura norvegica</i>	0	Inf	-1	0	0	0	60.5	101.5	13	69	52	67
<i>Calathura</i> sp	0	Inf	-1	0	0	0	60.5	101.5	13	69	52	67
<i>Capitella</i> sp	Inf	-1	0	0	0	0	104	13.5	55	69	52	67
<i>Caulleriella</i> sp A	-1	0	0	0	0	-1	15	60	55	69	52	17
<i>Chaetozone setosa</i>	-0.44	-0.857	21.5	-1	Inf	0.52	38	31	86	12.5	102	92
<i>Chirimia biceps</i>	-0.49	-1	0	0	0	-1	37	13.5	55	69	52	17
<i>Cirrophorus eliasoni</i>	-1	0	0	0	0	-1	15	60	55	69	52	17
<i>Cistenides hyperborea</i>	0	0	Inf	-0.121	0.6252	Inf	60.5	60	100.5	37	85	105.5
<i>Clymenura polaris</i>	0	Inf	-1	0	0	0	60.5	101.5	13	69	52	67
<i>Clymenura</i> sp	-1	0	0	0	0	-1	15	60	55	69	52	17
<i>Cossura</i> sp	Inf	-1	Inf	-1	0	0	104	13.5	100.5	12.5	52	67
<i>Ctenodiscus crispatus</i>	-0.809	-1	Inf	0.2042	10.217	2.8059	31	13.5	100.5	101	89	94
<i>Cuspidaria obesa</i>	0	Inf	-1	0	0	0	60.5	101.5	13	69	52	67
<i>Dialychone</i> spp	3.5526	-1	0	0	0	-1	91	13.5	55	69	52	17
<i>Diastylis lucifera</i>	-1	0	0	0	0	-1	15	60	55	69	52	17

<i>Diastyloides bisplicata</i>	-1	0	0	0	0	-1	15	60	55	69	52	17
<i>Diplocirrus hirsutus</i>	-1	0	Inf	-1	Inf	-0.518	15	60	100.5	12.5	102	41
<i>Dipolydora</i> sp	Inf	-1	0	0	0	0	104	13.5	55	69	52	67
<i>Edwardsia</i> sp	0	0	0	0	Inf	Inf	60.5	60	55	69	102	105.5
<i>Ennucula tenuis</i>	2.8611	-1	0	0	0	-1	89	13.5	55	69	52	17
<i>Ephesiella abyssorum</i>	0	0	Inf	-1	0	0	60.5	60	100.5	12.5	52	67
<i>Eteone longa</i>	0	0	Inf	-1	0	0	60.5	60	100.5	12.5	52	67
<i>Eteone</i> sp	0	0	Inf	-0.5	-1	0	60.5	60	100.5	32	8	67
<i>Euclymene droebachiensis</i>	0	0	0	Inf	-1	0	60.5	60	55	108.5	8	67
<i>Eudorella emarginata</i>	-1	0	0	0	0	-1	15	60	55	69	52	17
<i>Exogone</i> sp	0	Inf	-1	0	0	0	60.5	101.5	13	69	52	67
<i>Galathowenia oculata</i>	Inf	-1	Inf	-1	0	0	104	13.5	100.5	12.5	52	67
<i>Glyphanostomum pallescens</i>	Inf	-1	0	0	0	0	104	13.5	55	69	52	67
<i>Gnathia elongata</i>	6.25	-0.793	-1	0	0	-1	92	34	13	69	52	17
<i>Gnathia maxillaris</i>	-0.286	-1	0	0	Inf	0.4286	39	13.5	55	69	102	91
<i>Gnathiidae</i>	Inf	-1	0	0	0	0	104	13.5	55	69	52	67
<i>Haploops setosa</i>	0	Inf	-1	0	0	0	60.5	101.5	13	69	52	67
<i>Haploops tubicola</i>	55.1	-1	Inf	-0.364	8.8571	12.8	93	13.5	100.5	35	88	97
<i>Harpinia antennaria</i>	0	Inf	-1	0	0	0	60.5	101.5	13	69	52	67
<i>Harpinia</i> sp	0	Inf	-1	0	0	0	60.5	101.5	13	69	52	67
<i>Heteromastus filiformis</i>	-1	Inf	-1	0	0	-1	15	101.5	13	69	52	17
<i>Hippomedon</i> sp	0	Inf	-1	0	0	0	60.5	101.5	13	69	52	67

Appendix D

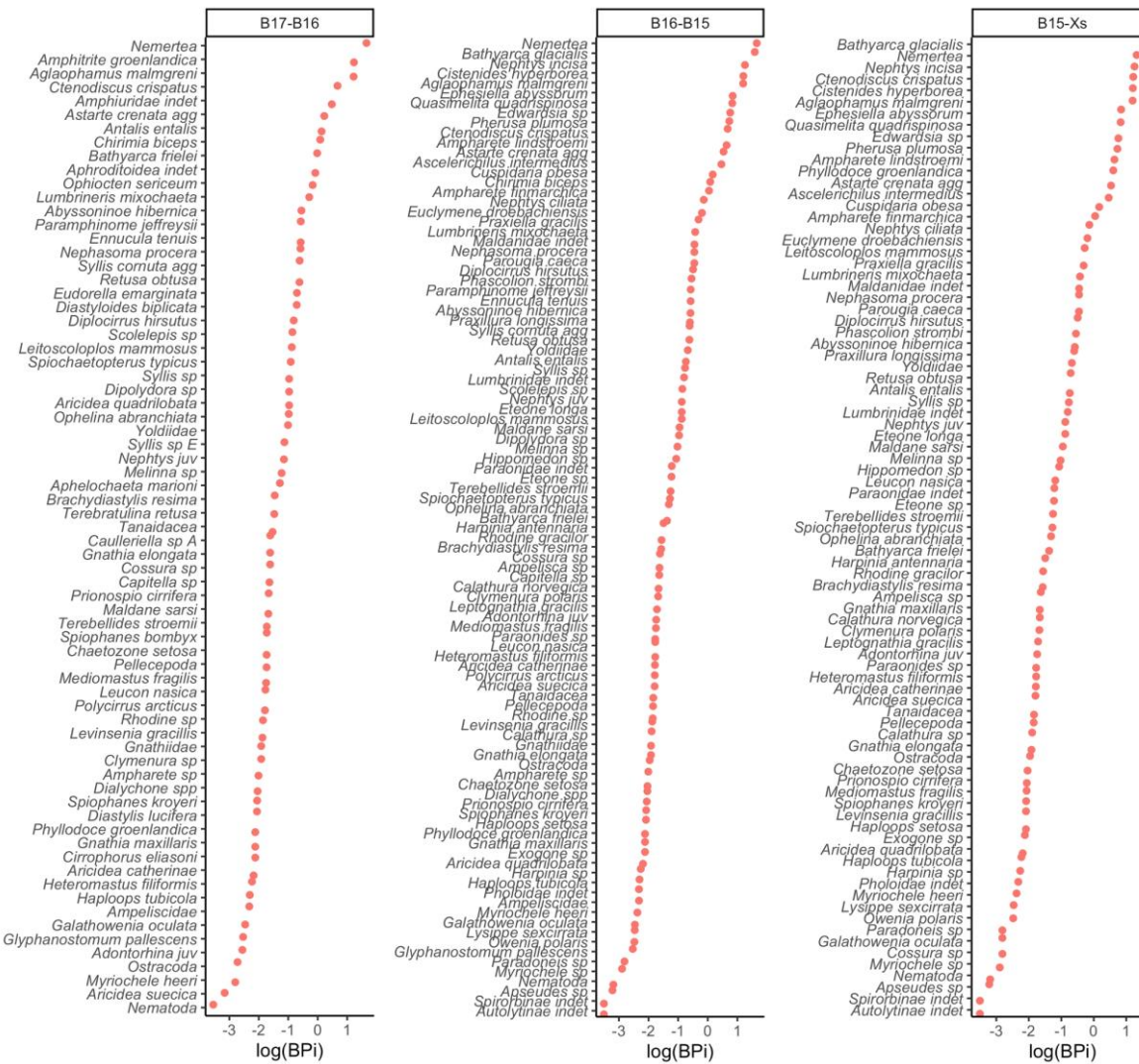
<i>Leitoscoloplos mammosus</i>	-0.695	-1	Inf	-1	Inf	-0.118	34	13.5	100.5	12.5	102	43
<i>Leptognathia gracilis</i>	0	Inf	-1	0	0	0	60.5	101.5	13	69	52	67
<i>Leucon nasica</i>	Inf	-1	Inf	-1	Inf	Inf	104	13.5	100.5	12.5	102	105.5
<i>Levinsenia gracillis</i>	-0.646	-1	Inf	-1	Inf	-0.866	35	13.5	100.5	12.5	102	36
<i>Lumbrineris mixochaeta</i>	-0.698	-0.728	6	-0.799	-0.023	-0.887	33	35	81	30	20	35
<i>Lumbrinidae</i> indet	0	0	0	Inf	-1	0	60.5	60	55	108.5	8	67
<i>Lysippe sexcirrata</i>	0	0	0	0	Inf	Inf	60.5	60	55	69	102	105.5
<i>Maldane sarsi</i>	0.5714	-0.854	2.0303	-0.297	-1	-1	85	32	79	36	8	17
<i>Maldanidae</i> indet	0	0	0	Inf	-1	0	60.5	60	55	108.5	8	67
<i>Mediomastus fragilis</i>	0.411	-1	Inf	-1	Inf	-0.521	83	13.5	100.5	12.5	102	40
<i>Melinna</i> sp	-1	0	Inf	-1	0	-1	15	60	100.5	12.5	52	17
<i>Myriochele heeri</i>	1.0833	-0.88	19.333	-0.639	-1	-1	87	30	84	31	8	17
<i>Myriochele</i> sp	0	0	Inf	-1	0	0	60.5	60	100.5	12.5	52	67
<i>Nematoda</i>	0.6	0.875	-0.933	0	-1	-1	86	87	27	69	8	17
<i>Nemertea</i>	-0.998	-1	Inf	234.5	-0.549	-0.736	30	13.5	100.5	103	18	37
<i>Nephasoma procera</i>	0.4002	-0.82	-0.291	-0.808	-1	-1	82	33	30	29	8	17
<i>Nephtys ciliata</i>	0	0	0	0	Inf	Inf	60.5	60	55	69	102	105.5
<i>Nephtys incisa</i>	0	0	Inf	-0.495	-0.949	Inf	60.5	60	100.5	33	16	105.5
<i>Nephtys</i> juv	-1	Inf	-0.667	-1	0	-1	15	101.5	29	12.5	52	17
<i>Ophelina abranchiata</i>	-1	Inf	-1	0	0	-1	15	101.5	13	69	52	17
<i>Ophiocten sericeum</i>	-1	0	0	0	0	-1	15	60	55	69	52	17
<i>Ostracoda</i>	Inf	-0.917	20	-1	0	0	104	29	85	12.5	52	67

<i>Owenia polaris</i>	0	0	Inf	-1	0	0	60.5	60	100.5	12.5	52	67
<i>Paradoneis</i> sp	0	0	0	Inf	-1	0	60.5	60	55	108.5	8	67
<i>Paramphinoe jeffreysii</i>	Inf	-1	0	0	0	0	104	13.5	55	69	52	67
<i>Paraonidae</i> indet	0	Inf	-1	0	Inf	Inf	60.5	101.5	13	69	102	105.5
<i>Paraonides</i> sp	0	Inf	-1	0	0	0	60.5	101.5	13	69	52	67
<i>Parougia caeca</i>	0	Inf	-1	0	0	0	60.5	101.5	13	69	52	67
<i>Pellecepoda</i>	-1	Inf	-1	0	0	-1	15	101.5	13	69	52	17
<i>Phascolion strombi</i>	0	Inf	-1	0	0	0	60.5	101.5	13	69	52	67
<i>Pherusa plumosa</i>	0	0	Inf	-1	0	0	60.5	60	100.5	12.5	52	67
<i>Pholoidae</i> indet	0	0	0	0	Inf	Inf	60.5	60	55	69	102	105.5
<i>Phyllodoce groenlandica</i>	Inf	-1	0	0	Inf	Inf	104	13.5	55	69	102	105.5
<i>Polycirrus arcticus</i>	Inf	-1	0	0	0	0	104	13.5	55	69	52	67
<i>Praxiella gracilis</i>	0	0	Inf	-1	Inf	Inf	60.5	60	100.5	12.5	102	105.5
<i>Praxillura longissima</i>	0	0	0	0	Inf	Inf	60.5	60	55	69	102	105.5
<i>Prionospio cirrifera</i>	-1	Inf	-1	0	Inf	-0.6	15	101.5	13	69	102	39
<i>Quasimelita quadrispinosa</i>	0	0	Inf	-1	0	0	60.5	60	100.5	12.5	52	67
<i>Retusa obtusa</i>	Inf	-1	0	0	Inf	Inf	104	13.5	55	69	102	105.5
<i>Rhodine gracilior</i>	0	Inf	-1	Inf	-1	0	60.5	101.5	13	108.5	8	67
<i>Rhodine</i> sp	Inf	-1	0	0	0	0	104	13.5	55	69	52	67
<i>Scolelepis</i> sp	Inf	-1	0	0	0	0	104	13.5	55	69	52	67
<i>Spiochaetopterus typicus</i>	0.4446	0.7086	8.2296	-0.44	-0.273	8.2765	84	85	82	34	19	96
<i>Spiophanes bombyx</i>	-1	0	0	0	0	-1	15	60	55	69	52	17

Appendix D

<i>Spiophanes kroyeri</i>	2.0638	0.8438	-0.817	-0.866	2.9231	-0.457	88	86	28	28	87	42
<i>Spirorbinae</i> indet	0	Inf	-1	0	0	0	60.5	101.5	13	69	52	67
<i>Syllis cornuta</i> agg	-0.543	-1	0	0	0	-1	36	13.5	55	69	52	17
<i>Syllis</i> sp	Inf	0.5	-1	0	0	0	104	84	13	69	52	67
<i>Syllis</i> sp E	-1	0	0	0	0	-1	15	60	55	69	52	17
<i>Tanaidacea</i>	-1	Inf	-1	Inf	-1	-1	15	101.5	13	108.5	8	17
<i>Terebellides stroemii</i>	Inf	2.6857	-0.039	-1	Inf	Inf	104	89	31	12.5	102	105.5
<i>Terebratulina retusa</i>	-1	0	0	0	0	-1	15	60	55	69	52	17
<i>Yoldiidae</i>	164.12	-0.947	14.327	-0.881	-0.945	-0.118	94	28	83	27	17	44

**Figure S2 |** Log-transformed taxa-specific BPI, from the most (top) to least (bottom) contributing taxa for all local (B17-B16 | B16-B15 | B15-Xs | Xs-B14 | B14-B13) and regional (B17-B13) environmental transitions.



Appendix D

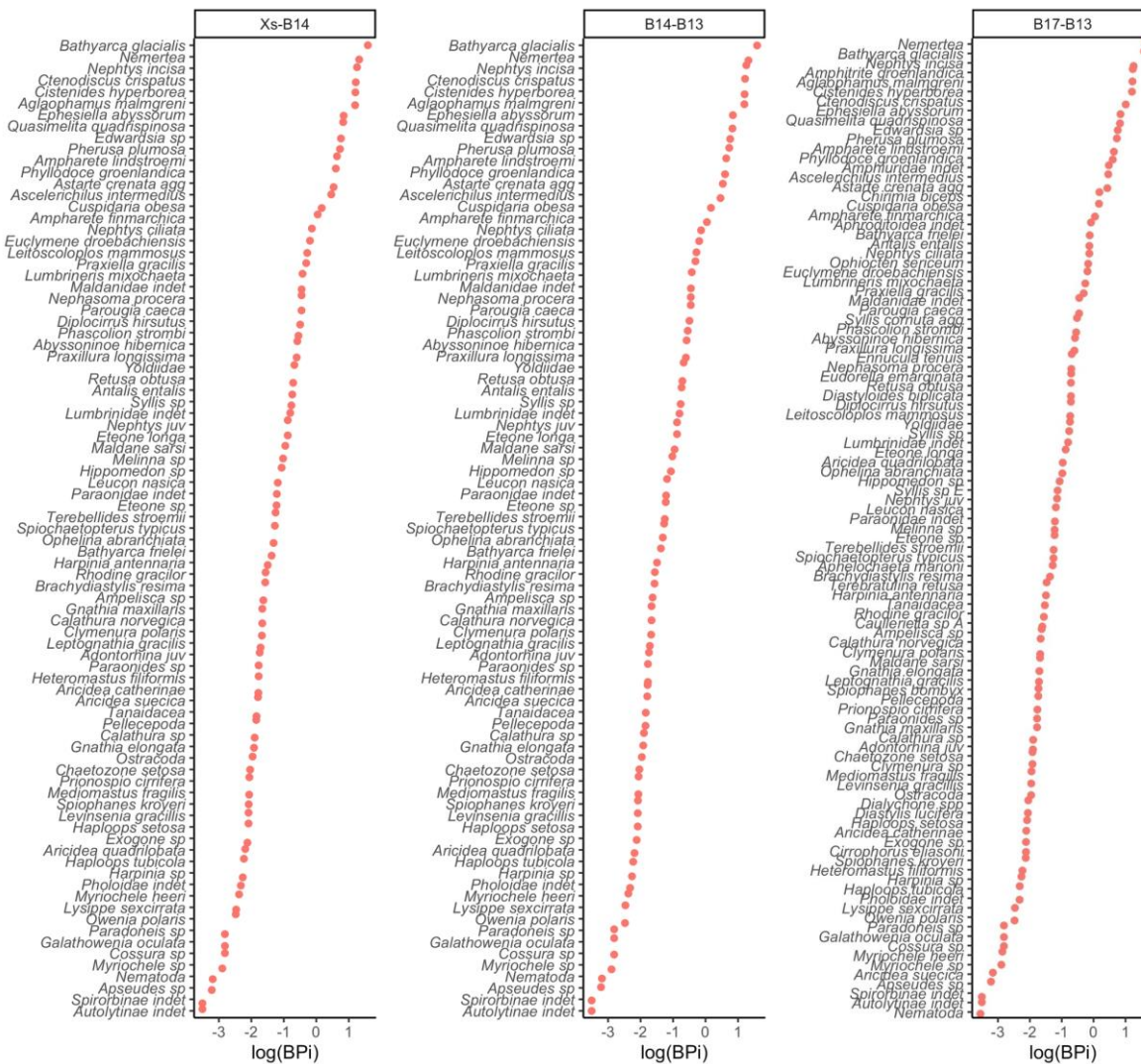
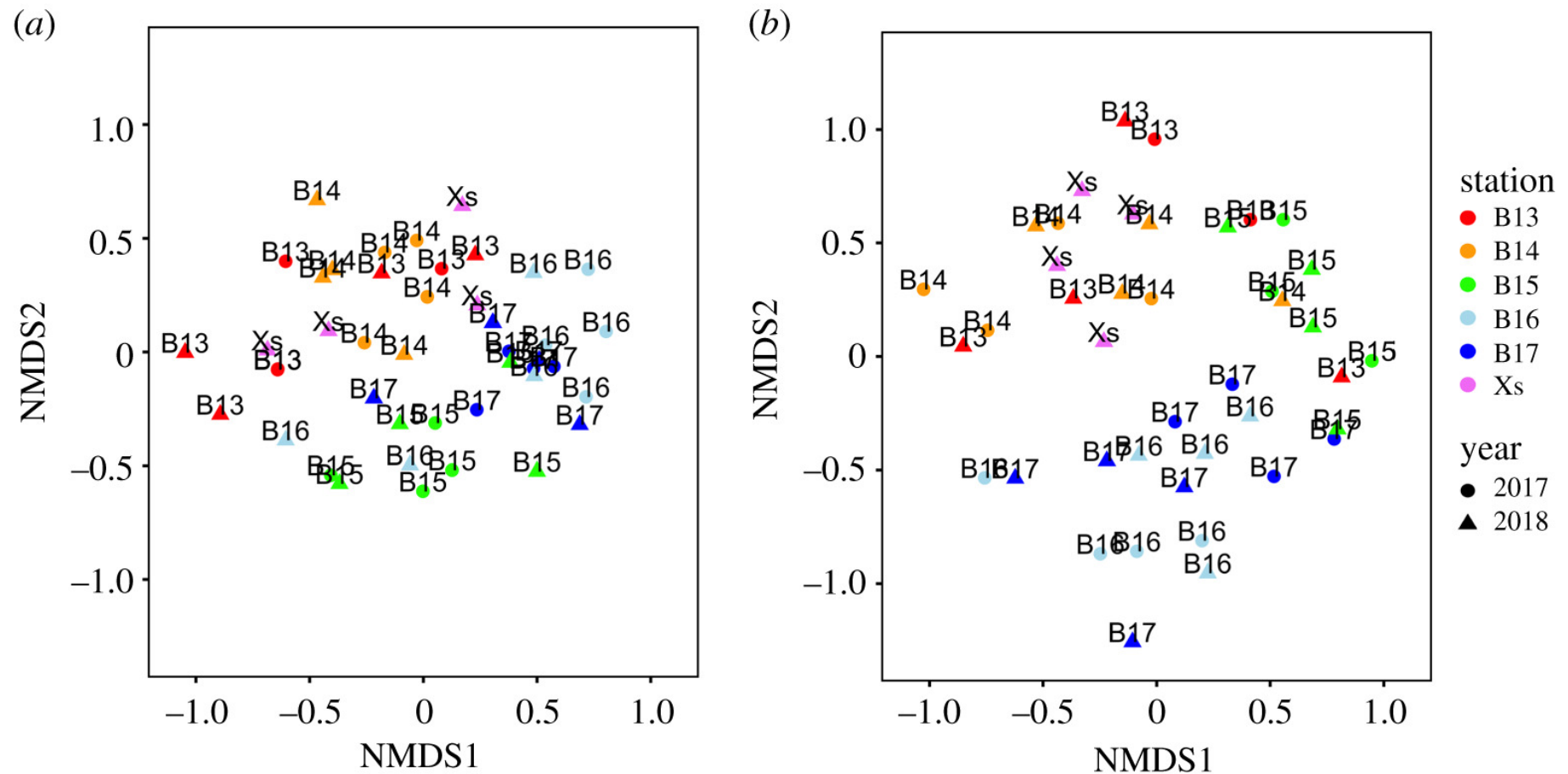


**Figure S3** | Non-metric two-dimensional (nMDS) representations of Bray–Curtis similarity matrices from Solan et al. (2020) based on (a) square root transformed abundance and (b) untransformed biomass for stations B13–B17 (indicated by colour) in 2017 (circles) and stations B13–B17 and Xs in 2018 (triangles). The classification of faunal assemblages in the Barents Sea demonstrates a distinct separation between the northern and southern stations.



## Appendix D

**Figure S4** | The (a) weighted network and (b) frequency of interactions between taxa (abundance > 1 across all stations;  $n = 69$ ) estimated from 466 correlations in biomass across all station deployments ( $n = 24$ ). Only positive (green) and negative (red) correlations  $\geq 1.5$  s.d. from the mean score (0.0397) are displayed in S3(a), where colour saturation and width of connections correspond to the absolute correlation score and scale relative to the strongest correlation score (1.0000). Cutoff (0.55) relates to the correlation value for maximum connection thickness, with all connections higher than the cutoff sharing the same thickness. Maximum relates to the maximum correlation score shown. Clustering is computed using the Fruchterman-Reingold algorithm, where nodes repel each other equally before connections create an attraction force based on the correlation score, irrespective of its sign (Fruchterman & Reingold, 1991). In S3(b), correlations mainly cluster within 1.5 standard deviations of the mean score (grey dashed horizontal bar), with more positive (green dashed horizontal bar) than negative correlations (red dashed horizontal bar) occurring outside this range.

Figure S4(a)

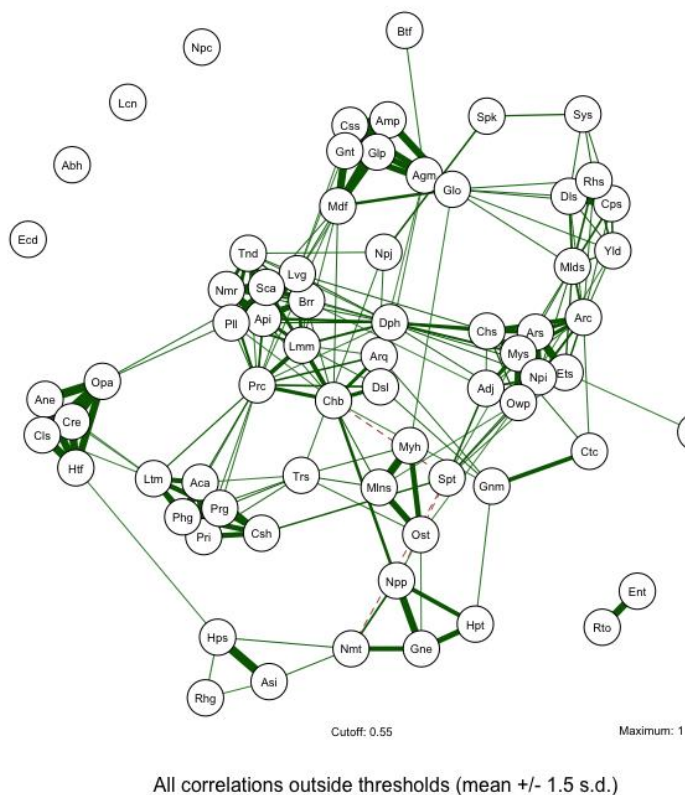
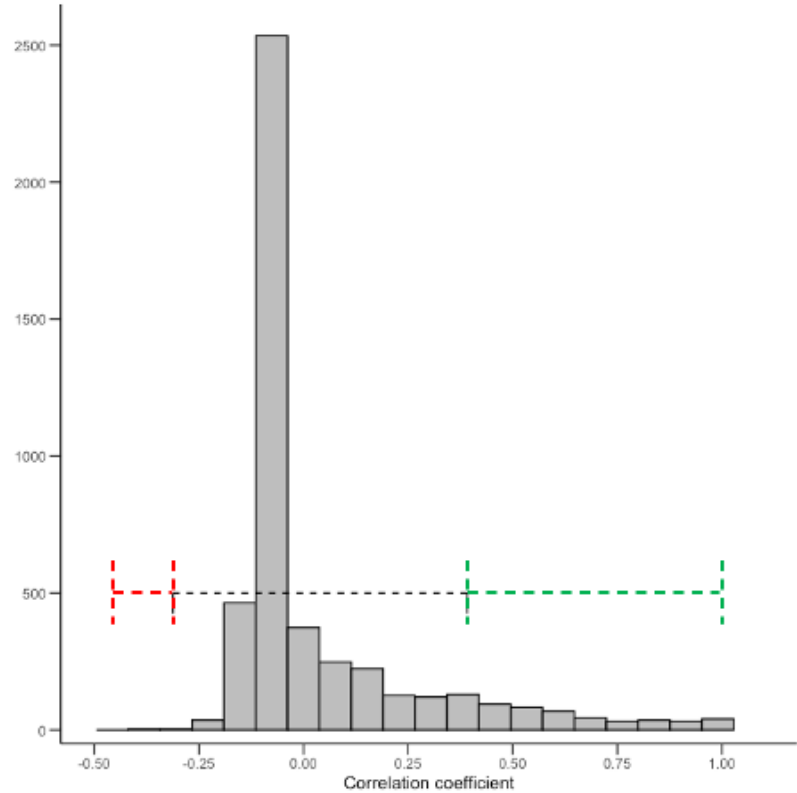


Figure S4(b)





**Table S2 |** List of sediment-dwelling invertebrate species with (a) positive (n = 460) and (b) negative correlations (n = 6)  $\geq 1.5$  standard deviations from the mean coefficient value (Figure S4).

**Table S2 (a)**

Sp1	Sp2	correlation coefficient
Adontorhina juv	<i>Aricidea catherinae</i>	0.44490047
Adontorhina juv	<i>Aricidea suecica</i>	0.65324341
Adontorhina juv	<i>Brachydiastylis resima</i>	0.39901141
Adontorhina juv	<i>Chaetozone setosa</i>	0.44925732
Adontorhina juv	<i>Eteone sp</i>	0.55942251
Adontorhina juv	<i>Myriochele sp</i>	0.65208596
Adontorhina juv	<i>Nephtys incisa</i>	0.58154394
Adontorhina juv	<i>Owenia polaris</i>	0.55005358
Adontorhina juv	<i>Spiochaetopterus typicus</i>	0.58280577
Aglaophamus malmgreni	<i>Aricidea quadrilobata</i>	0.39549028
Aglaophamus malmgreni	<i>Bathyarca frielei</i>	0.469328
Aglaophamus malmgreni	<i>Diastylis lucifera</i>	0.41354182
Ampeliscidae	<i>Cossura sp</i>	0.98666973
Ampeliscidae	<i>Galathowenia oculata</i>	0.86343044
Ampeliscidae	<i>Glyphanostomum pallescens</i>	0.99130832
Ampeliscidae	<i>Gnathiidae</i>	0.99130832
Ampeliscidae	<i>Mediomastus fragilis</i>	0.8340697
Antalis entalis	<i>Cirrrophorus eliasoni</i>	0.97355357
Antalis entalis	<i>Clymenura sp</i>	0.97355357
Antalis entalis	<i>Heteromastus filiformis</i>	0.85989273
Antalis entalis	<i>Leitoscoloplos mammosus</i>	0.40048705
Antalis entalis	<i>Ophelina abranchiata</i>	0.94265891
Aphroditoidae indet	<i>Brachydiastylis resima</i>	0.72447193
Aphroditoidae indet	<i>Chirimia biceps</i>	0.46499525
Aphroditoidae indet	<i>Diplocirrus hirsutus</i>	0.63553438
Aphroditoidae indet	<i>Levinsenia gracillis</i>	0.73574765
Aphroditoidae indet	<i>Lumbrineris mixochaeta</i>	0.66114928
Aphroditoidae indet	<i>Nemertea</i>	0.89322531
Aphroditoidae indet	<i>Pellecepoda</i>	0.91713348
Aphroditoidae indet	<i>Prionospio cirrifera</i>	0.59222719
Aphroditoidae indet	<i>Syllis cornuta agg</i>	0.90642424
Aphroditoidae indet	<i>Tanaidacea</i>	0.76019463
<i>Aricidea catherinae</i>	<i>Adontorhina juv</i>	0.44490047
<i>Aricidea catherinae</i>	<i>Aricidea suecica</i>	0.6769014
<i>Aricidea catherinae</i>	<i>Capitella sp</i>	0.48163601
<i>Aricidea catherinae</i>	<i>Chaetozone setosa</i>	0.71877728
<i>Aricidea catherinae</i>	<i>Ctenodiscus crispatus</i>	0.46770247
<i>Aricidea catherinae</i>	<i>Dialychone spp</i>	0.45636358
<i>Aricidea catherinae</i>	<i>Eteone sp</i>	0.58034329
<i>Aricidea catherinae</i>	<i>Maldane sarsi</i>	0.60755555
<i>Aricidea catherinae</i>	<i>Myriochele sp</i>	0.67995672

<b>Aricidea catherinae</b>	<i>Nephtys incisa</i>	0.5988667
<b>Aricidea catherinae</b>	<i>Owenia polaris</i>	0.57041645
<b>Aricidea catherinae</b>	<i>Rhodine sp</i>	0.48163601
<b>Aricidea catherinae</b>	<i>Yoldiidae</i>	0.49961056
<b>Aricidea quadrilobata</b>	<i>Aglaophamus malmgreni</i>	0.39549028
<b>Aricidea quadrilobata</b>	<i>Chirimia biceps</i>	0.66620934
<b>Aricidea quadrilobata</b>	<i>Diastylis lucifera</i>	0.98483334
<b>Aricidea quadrilobata</b>	<i>Gnathia maxillaris</i>	0.48409644
<b>Aricidea quadrilobata</b>	<i>Lumbrineris mixochaeta</i>	0.44188879
<b>Aricidea quadrilobata</b>	<i>Nephtys juv</i>	0.45557401
<b>Aricidea quadrilobata</b>	<i>Prionospio cirrifera</i>	0.58527962
<b>Aricidea suecica</b>	<i>Adontorhina juv</i>	0.65324341
<b>Aricidea suecica</b>	<i>Aricidea catherinae</i>	0.6769014
<b>Aricidea suecica</b>	<i>Chaetozone setosa</i>	0.67021999
<b>Aricidea suecica</b>	<i>Diplocirrus hirsutus</i>	0.61278768
<b>Aricidea suecica</b>	<i>Eteone sp</i>	0.88886812
<b>Aricidea suecica</b>	<i>Maldane sarsi</i>	0.50733476
<b>Aricidea suecica</b>	<i>Myriochele sp</i>	0.99905437
<b>Aricidea suecica</b>	<i>Nephtys incisa</i>	0.91474314
<b>Aricidea suecica</b>	<i>Owenia polaris</i>	0.87618827
<b>Ascelerichilus intermedius</b>	<i>Haploops setosa</i>	0.93926974
<b>Ascelerichilus intermedius</b>	<i>Nematoda</i>	0.4907254
<b>Ascelerichilus intermedius</b>	<i>Rhodine gracilis</i>	0.40810919
<b>Astarte crenata agg</b>	<i>Cistenides hyperborea</i>	0.67955818
<b>Astarte crenata agg</b>	<i>Leitoscoloplos mammosus</i>	0.74198895
<b>Astarte crenata agg</b>	<i>Paraonidae indet</i>	0.9265528
<b>Astarte crenata agg</b>	<i>Phyllodoce groenlandica</i>	0.92831992
<b>Astarte crenata agg</b>	<i>Praxiella gracilis</i>	0.9237353
<b>Astarte crenata agg</b>	<i>Prionospio cirrifera</i>	0.54399854
<b>Astarte crenata agg</b>	<i>Terebellides stroemii</i>	0.42223172
<b>Bathyarca frielei</b>	<i>Aglaophamus malmgreni</i>	0.469328
<b>Brachydiastylis resima</b>	<i>Adontorhina juv</i>	0.39901141
<b>Brachydiastylis resima</b>	<i>Aphroditidea indet</i>	0.72447193
<b>Brachydiastylis resima</b>	<i>Diplocirrus hirsutus</i>	0.40640716
<b>Brachydiastylis resima</b>	<i>Levinsenia gracillis</i>	0.63265662
<b>Brachydiastylis resima</b>	<i>Lumbrineris mixochaeta</i>	0.48315825
<b>Brachydiastylis resima</b>	<i>Nemertea</i>	0.61063316
<b>Brachydiastylis resima</b>	<i>Pellecepoda</i>	0.64208916
<b>Brachydiastylis resima</b>	<i>Syllis cornuta agg</i>	0.72280314
<b>Brachydiastylis resima</b>	<i>Tanaidacea</i>	0.57472834
<b>Capitella sp</b>	<i>Aricidea catherinae</i>	0.48163601
<b>Capitella sp</b>	<i>Dialychone spp</i>	0.97632349
<b>Capitella sp</b>	<i>Galathowenia oculata</i>	0.49883342
<b>Capitella sp</b>	<i>Maldane sarsi</i>	0.5929407
<b>Capitella sp</b>	<i>Rhodine sp</i>	1
<b>Capitella sp</b>	<i>Syllis sp</i>	0.52925332
<b>Capitella sp</b>	<i>Yoldiidae</i>	0.58450611
<b>Chaetozone setosa</b>	<i>Adontorhina juv</i>	0.44925732
<b>Chaetozone setosa</b>	<i>Aricidea catherinae</i>	0.71877728

Appendix D

<b>Chaetozone setosa</b>	<i>Aricidea suecica</i>	0.67021999
<b>Chaetozone setosa</b>	<i>Ctenodiscus crispatus</i>	0.51119839
<b>Chaetozone setosa</b>	<i>Diplocirrus hirsutus</i>	0.62733184
<b>Chaetozone setosa</b>	<i>Eteone sp</i>	0.57329039
<b>Chaetozone setosa</b>	<i>Levinsenia gracillis</i>	0.53210197
<b>Chaetozone setosa</b>	<i>Myriochela sp</i>	0.67338372
<b>Chaetozone setosa</b>	<i>Nephthys incisa</i>	0.59387801
<b>Chaetozone setosa</b>	<i>Owenia polaris</i>	0.5633835
<b>Chirimia biceps</b>	<i>Aphroditoidaea indet</i>	0.46499525
<b>Chirimia biceps</b>	<i>Aricidea quadrilobata</i>	0.66620934
<b>Chirimia biceps</b>	<i>Diastylis lucifera</i>	0.69050057
<b>Chirimia biceps</b>	<i>Gnathia maxillaris</i>	0.41149345
<b>Chirimia biceps</b>	<i>Levinsenia gracillis</i>	0.47536286
<b>Chirimia biceps</b>	<i>Lumbrineris mixochaeta</i>	0.71715938
<b>Chirimia biceps</b>	<i>Mediomastus fragilis</i>	0.49030427
<b>Chirimia biceps</b>	<i>Nephasoma procera</i>	0.64166231
<b>Chirimia biceps</b>	<i>Pellecepoda</i>	0.4213375
<b>Chirimia biceps</b>	<i>Prionospio cirrifera</i>	0.68226427
<b>Chirimia biceps</b>	<i>Syllis cornuta agg</i>	0.49724918
<b>Cirrophorus eliasoni</b>	<i>Antalis entalis</i>	0.97355357
<b>Cirrophorus eliasoni</b>	<i>Clymenura sp</i>	1
<b>Cirrophorus eliasoni</b>	<i>Heteromastus filiformis</i>	0.89060905
<b>Cirrophorus eliasoni</b>	<i>Leitoscoloplos mammosus</i>	0.41997644
<b>Cirrophorus eliasoni</b>	<i>Ophelina abranchiata</i>	0.97358866
<b>Cistenides hyperborea</b>	<i>Astarte crenata agg</i>	0.67955818
<b>Cistenides hyperborea</b>	<i>Leitoscoloplos mammosus</i>	0.58478494
<b>Cistenides hyperborea</b>	<i>Paraonidae indet</i>	0.75382893
<b>Cistenides hyperborea</b>	<i>Phyllodoce groenlandica</i>	0.75633975
<b>Cistenides hyperborea</b>	<i>Praxiella gracilis</i>	0.7596907
<b>Cistenides hyperborea</b>	<i>Spiochaetopterus typicus</i>	0.5747216
<b>Clymenura sp</b>	<i>Antalis entalis</i>	0.97355357
<b>Clymenura sp</b>	<i>Cirrophorus eliasoni</i>	1
<b>Clymenura sp</b>	<i>Heteromastus filiformis</i>	0.89060905
<b>Clymenura sp</b>	<i>Leitoscoloplos mammosus</i>	0.41997644
<b>Clymenura sp</b>	<i>Ophelina abranchiata</i>	0.97358866
<b>Cossura sp</b>	<i>Ampeliscidae</i>	0.98666973
<b>Cossura sp</b>	<i>Galathowenia oculata</i>	0.79342606
<b>Cossura sp</b>	<i>Glyphanostomum pallescens</i>	0.99586853
<b>Cossura sp</b>	<i>Gnathiidae</i>	0.99586853
<b>Cossura sp</b>	<i>Levinsenia gracillis</i>	0.41513559
<b>Cossura sp</b>	<i>Mediomastus fragilis</i>	0.84383606
<b>Ctenodiscus crispatus</b>	<i>Aricidea catherinae</i>	0.46770247
<b>Ctenodiscus crispatus</b>	<i>Chaetozone setosa</i>	0.51119839
<b>Ctenodiscus crispatus</b>	<i>Gnathia maxillaris</i>	0.70901712
<b>Dialychone spp</b>	<i>Aricidea catherinae</i>	0.45636358
<b>Dialychone spp</b>	<i>Capitella sp</i>	0.97632349
<b>Dialychone spp</b>	<i>Galathowenia oculata</i>	0.47612562
<b>Dialychone spp</b>	<i>Maldane sarsi</i>	0.6038821
<b>Dialychone spp</b>	<i>Rhodine sp</i>	0.97632349

<b>Dialychone spp</b>	<i>Syllis sp</i>	0.5083799
<b>Dialychone spp</b>	<i>Yoldiidae</i>	0.54771716
<b>Diastylis lucifera</b>	<i>Aglaophamus malmgreni</i>	0.41354182
<b>Diastylis lucifera</b>	<i>Aricidea quadrilobata</i>	0.98483334
<b>Diastylis lucifera</b>	<i>Chirimia biceps</i>	0.69050057
<b>Diastylis lucifera</b>	<i>Gnathia maxillaris</i>	0.50102349
<b>Diastylis lucifera</b>	<i>Lumbrineris mixochaeta</i>	0.46425117
<b>Diastylis lucifera</b>	<i>Prionospio cirrifera</i>	0.59222719
<b>Diplocirrus hirsutus</b>	<i>Aphrodoitoidea indet</i>	0.63553438
<b>Diplocirrus hirsutus</b>	<i>Aricidea suecica</i>	0.61278768
<b>Diplocirrus hirsutus</b>	<i>Brachydiastylis resima</i>	0.40640716
<b>Diplocirrus hirsutus</b>	<i>Chaetozone setosa</i>	0.62733184
<b>Diplocirrus hirsutus</b>	<i>Eteone sp</i>	0.51552062
<b>Diplocirrus hirsutus</b>	<i>Levinsenia gracillis</i>	0.5508677
<b>Diplocirrus hirsutus</b>	<i>Lumbrineris mixochaeta</i>	0.6124198
<b>Diplocirrus hirsutus</b>	<i>Myriochele sp</i>	0.60827772
<b>Diplocirrus hirsutus</b>	<i>Nemertea</i>	0.52030658
<b>Diplocirrus hirsutus</b>	<i>Nephtys incisa</i>	0.51641954
<b>Diplocirrus hirsutus</b>	<i>Owenia polaris</i>	0.50644825
<b>Diplocirrus hirsutus</b>	<i>Pellecepoda</i>	0.55385365
<b>Diplocirrus hirsutus</b>	<i>Prionospio cirrifera</i>	0.41980384
<b>Diplocirrus hirsutus</b>	<i>Syllis cornuta agg</i>	0.55221566
<b>Diplocirrus hirsutus</b>	<i>Tanaidacea</i>	0.43468053
<b>Ennucula tenuis</b>	<i>Retusa obtusa</i>	0.86549354
<b>Eteone sp</b>	<i>Adontorhina juv</i>	0.55942251
<b>Eteone sp</b>	<i>Aricidea catherinae</i>	0.58034329
<b>Eteone sp</b>	<i>Aricidea suecica</i>	0.88886812
<b>Eteone sp</b>	<i>Chaetozone setosa</i>	0.57329039
<b>Eteone sp</b>	<i>Diplocirrus hirsutus</i>	0.51552062
<b>Eteone sp</b>	<i>Lumbrinidae indet</i>	0.41561756
<b>Eteone sp</b>	<i>Maldane sarsi</i>	0.57262329
<b>Eteone sp</b>	<i>Myriochele sp</i>	0.89060905
<b>Eteone sp</b>	<i>Nephtys incisa</i>	0.97156647
<b>Eteone sp</b>	<i>Owenia polaris</i>	0.77202731
<b>Eteone sp</b>	<i>Spiochaetopterus typicus</i>	0.45335255
<b>Galathowenia oculata</b>	<i>Ampeliscidae</i>	0.86343044
<b>Galathowenia oculata</b>	<i>Capitella sp</i>	0.49883342
<b>Galathowenia oculata</b>	<i>Cossura sp</i>	0.79342606
<b>Galathowenia oculata</b>	<i>Dialychone spp</i>	0.47612562
<b>Galathowenia oculata</b>	<i>Glyphanostomum pallescens</i>	0.8001156
<b>Galathowenia oculata</b>	<i>Gnathiidae</i>	0.8001156
<b>Galathowenia oculata</b>	<i>Maldane sarsi</i>	0.48204579
<b>Galathowenia oculata</b>	<i>Mediomastus fragilis</i>	0.64157121
<b>Galathowenia oculata</b>	<i>Myriochele heeri</i>	0.42732954
<b>Galathowenia oculata</b>	<i>Rhodine sp</i>	0.49883342
<b>Galathowenia oculata</b>	<i>Yoldiidae</i>	0.46768293
<b>Glyphanostomum pallescens</b>	<i>Ampeliscidae</i>	0.99130832
<b>Glyphanostomum pallescens</b>	<i>Cossura sp</i>	0.99586853
<b>Glyphanostomum pallescens</b>	<i>Galathowenia oculata</i>	0.8001156

Appendix D

<b>Glyphanostomum pallescens</b>	<i>Gnathiidae</i>	1
<b>Glyphanostomum pallescens</b>	<i>Levinsenia gracillis</i>	0.40389708
<b>Glyphanostomum pallescens</b>	<i>Mediomastus fragilis</i>	0.84726528
<b>Gnathia elongata</b>	<i>Haploops tubicola</i>	0.77724314
<b>Gnathia elongata</b>	<i>Nematoda</i>	0.7381138
<b>Gnathia elongata</b>	<i>Nephasoma procera</i>	0.85534119
<b>Gnathia elongata</b>	<i>Ostracoda</i>	0.4197823
<b>Gnathia maxillaris</b>	<i>Aricidea quadrilobata</i>	0.48409644
<b>Gnathia maxillaris</b>	<i>Chirimia biceps</i>	0.41149345
<b>Gnathia maxillaris</b>	<i>Ctenodiscus crispatus</i>	0.70901712
<b>Gnathia maxillaris</b>	<i>Diastylis lucifera</i>	0.50102349
<b>Gnathia maxillaris</b>	<i>Haploops tubicola</i>	0.46032232
<b>Gnathiidae</b>	<i>Ampeliscidae</i>	0.99130832
<b>Gnathiidae</b>	<i>Cossura sp</i>	0.99586853
<b>Gnathiidae</b>	<i>Galathowenia oculata</i>	0.8001156
<b>Gnathiidae</b>	<i>Glyphanostomum pallescens</i>	1
<b>Gnathiidae</b>	<i>Levinsenia gracillis</i>	0.40389708
<b>Gnathiidae</b>	<i>Mediomastus fragilis</i>	0.84726528
<b>Haploops setosa</b>	<i>Ascelerichilus intermedius</i>	0.93926974
<b>Haploops setosa</b>	<i>Heteromastus filiformis</i>	0.41561756
<b>Haploops setosa</b>	<i>Nematoda</i>	0.51004797
<b>Haploops setosa</b>	<i>Rhodine gracilis</i>	0.45613448
<b>Haploops tubicola</b>	<i>Gnathia elongata</i>	0.77724314
<b>Haploops tubicola</b>	<i>Gnathia maxillaris</i>	0.46032232
<b>Haploops tubicola</b>	<i>Nephasoma procera</i>	0.71054791
<b>Heteromastus filiformis</b>	<i>Antalis entalis</i>	0.85989273
<b>Heteromastus filiformis</b>	<i>Cirrophorus eliasoni</i>	0.89060905
<b>Heteromastus filiformis</b>	<i>Clymenura sp</i>	0.89060905
<b>Heteromastus filiformis</b>	<i>Haploops setosa</i>	0.41561756
<b>Heteromastus filiformis</b>	<i>Ophelina abranchiata</i>	0.86028619
<b>Leitoscoloplos mammosus</b>	<i>Antalis entalis</i>	0.40048705
<b>Leitoscoloplos mammosus</b>	<i>Astarte crenata agg</i>	0.74198895
<b>Leitoscoloplos mammosus</b>	<i>Cirrophorus eliasoni</i>	0.41997644
<b>Leitoscoloplos mammosus</b>	<i>Cistenides hyperborea</i>	0.58478494
<b>Leitoscoloplos mammosus</b>	<i>Clymenura sp</i>	0.41997644
<b>Leitoscoloplos mammosus</b>	<i>Paraonidae indet</i>	0.73384883
<b>Leitoscoloplos mammosus</b>	<i>Phyllodoce groenlandica</i>	0.73836851
<b>Leitoscoloplos mammosus</b>	<i>Praxiella gracilis</i>	0.74208101
<b>Leitoscoloplos mammosus</b>	<i>Prionospio cirrifera</i>	0.55845291
<b>Levinsenia gracillis</b>	<i>Aphroditoidae indet</i>	0.73574765
<b>Levinsenia gracillis</b>	<i>Brachydiastylis resima</i>	0.63265662
<b>Levinsenia gracillis</b>	<i>Chaetozone setosa</i>	0.53210197
<b>Levinsenia gracillis</b>	<i>Chirimia biceps</i>	0.47536286
<b>Levinsenia gracillis</b>	<i>Cossura sp</i>	0.41513559
<b>Levinsenia gracillis</b>	<i>Diplocirrus hirsutus</i>	0.5508677
<b>Levinsenia gracillis</b>	<i>Glyphanostomum pallescens</i>	0.40389708
<b>Levinsenia gracillis</b>	<i>Gnathiidae</i>	0.40389708
<b>Levinsenia gracillis</b>	<i>Lumbrineris mixochaeta</i>	0.65467046
<b>Levinsenia gracillis</b>	<i>Mediomastus fragilis</i>	0.50073088

<b>Levinsenia gracillis</b>	<i>Nemertea</i>	0.60909048
<b>Levinsenia gracillis</b>	<i>Ophelina abranchiata</i>	0.4812985
<b>Levinsenia gracillis</b>	<i>Pellecepoda</i>	0.81887741
<b>Levinsenia gracillis</b>	<i>Prionospio cirrifera</i>	0.42803324
<b>Levinsenia gracillis</b>	<i>Syllis cornuta agg</i>	0.8511783
<b>Levinsenia gracillis</b>	<i>Tanaidacea</i>	0.49865456
<b>Lumbrineris mixochaeta</b>	<i>Aphroditidea indet</i>	0.66114928
<b>Lumbrineris mixochaeta</b>	<i>Aricidea quadrilobata</i>	0.44188879
<b>Lumbrineris mixochaeta</b>	<i>Brachydiastylis resima</i>	0.48315825
<b>Lumbrineris mixochaeta</b>	<i>Chirimia biceps</i>	0.71715938
<b>Lumbrineris mixochaeta</b>	<i>Diastylis lucifera</i>	0.46425117
<b>Lumbrineris mixochaeta</b>	<i>Diplocirrus hirsutus</i>	0.6124198
<b>Lumbrineris mixochaeta</b>	<i>Levinsenia gracillis</i>	0.65467046
<b>Lumbrineris mixochaeta</b>	<i>Mediomastus fragilis</i>	0.43705009
<b>Lumbrineris mixochaeta</b>	<i>Melinna sp</i>	0.52232368
<b>Lumbrineris mixochaeta</b>	<i>Nemertea</i>	0.56053065
<b>Lumbrineris mixochaeta</b>	<i>Pellecepoda</i>	0.60908411
<b>Lumbrineris mixochaeta</b>	<i>Prionospio cirrifera</i>	0.71553221
<b>Lumbrineris mixochaeta</b>	<i>Syllis cornuta agg</i>	0.65647107
<b>Lumbrineris mixochaeta</b>	<i>Tanaidacea</i>	0.42237943
<b>Lumbrinidae indet</b>	<i>Eteone sp</i>	0.41561756
<b>Maldane sarsi</b>	<i>Aricidea catherinae</i>	0.60755555
<b>Maldane sarsi</b>	<i>Aricidea suecica</i>	0.50733476
<b>Maldane sarsi</b>	<i>Capitella sp</i>	0.5929407
<b>Maldane sarsi</b>	<i>Dalychone spp</i>	0.6038821
<b>Maldane sarsi</b>	<i>Eteone sp</i>	0.57262329
<b>Maldane sarsi</b>	<i>Galathowenia oculata</i>	0.48204579
<b>Maldane sarsi</b>	<i>Myriochele sp</i>	0.50295976
<b>Maldane sarsi</b>	<i>Nephtys incisa</i>	0.5183831
<b>Maldane sarsi</b>	<i>Rhodine sp</i>	0.5929407
<b>Maldane sarsi</b>	<i>Yoldiidae</i>	0.56493878
<b>Mediomastus fragilis</b>	<i>Ampeliscidae</i>	0.8340697
<b>Mediomastus fragilis</b>	<i>Chirimia biceps</i>	0.49030427
<b>Mediomastus fragilis</b>	<i>Cossura sp</i>	0.84383606
<b>Mediomastus fragilis</b>	<i>Galathowenia oculata</i>	0.64157121
<b>Mediomastus fragilis</b>	<i>Glyphanostomum pallescens</i>	0.84726528
<b>Mediomastus fragilis</b>	<i>Gnathiidae</i>	0.84726528
<b>Mediomastus fragilis</b>	<i>Levinsenia gracillis</i>	0.50073088
<b>Mediomastus fragilis</b>	<i>Lumbrineris mixochaeta</i>	0.43705009
<b>Mediomastus fragilis</b>	<i>Prionospio cirrifera</i>	0.43581994
<b>Mediomastus fragilis</b>	<i>Syllis cornuta agg</i>	0.49156799
<b>Melinna sp</b>	<i>Lumbrineris mixochaeta</i>	0.52232368
<b>Melinna sp</b>	<i>Myriochele heeri</i>	0.88642033
<b>Melinna sp</b>	<i>Ostracoda</i>	0.8153058
<b>Melinna sp</b>	<i>Owenia polaris</i>	0.40387286
<b>Melinna sp</b>	<i>Terebellides stroemii</i>	0.52312745
<b>Myriochele heeri</b>	<i>Galathowenia oculata</i>	0.42732954
<b>Myriochele heeri</b>	<i>Melinna sp</i>	0.88642033
<b>Myriochele heeri</b>	<i>Ostracoda</i>	0.76351236

Appendix D

<b>Myriochele heeri</b>	<i>Terebellides stroemii</i>	0.50444763
<b>Myriochele sp</b>	<i>Adontorhina juv</i>	0.65208596
<b>Myriochele sp</b>	<i>Aricidea catherinae</i>	0.67995672
<b>Myriochele sp</b>	<i>Aricidea suecica</i>	0.99905437
<b>Myriochele sp</b>	<i>Chaetozone setosa</i>	0.67338372
<b>Myriochele sp</b>	<i>Diplocirrus hirsutus</i>	0.60827772
<b>Myriochele sp</b>	<i>Eteone sp</i>	0.89060905
<b>Myriochele sp</b>	<i>Maldane sarsi</i>	0.50295976
<b>Myriochele sp</b>	<i>Nephtys incisa</i>	0.91702917
<b>Myriochele sp</b>	<i>Owenia polaris</i>	0.8779646
<b>Myriochele sp</b>	<i>Spiochaetopterus typicus</i>	0.39150531
<b>Nematoda</b>	<i>Ascelerichilus intermedius</i>	0.4907254
<b>Nematoda</b>	<i>Gnathia elongata</i>	0.7381138
<b>Nematoda</b>	<i>Haplooops setosa</i>	0.51004797
<b>Nematoda</b>	<i>Nephasoma procera</i>	0.59547824
<b>Nemertea</b>	<i>Aphroditidea indet</i>	0.89322531
<b>Nemertea</b>	<i>Brachydiastylis resima</i>	0.61063316
<b>Nemertea</b>	<i>Diplocirrus hirsutus</i>	0.52030658
<b>Nemertea</b>	<i>Levinsenia gracillis</i>	0.60909048
<b>Nemertea</b>	<i>Lumbrineris mixochaeta</i>	0.56053065
<b>Nemertea</b>	<i>Pellecepoda</i>	0.80909715
<b>Nemertea</b>	<i>Prionospio cirrifera</i>	0.61816686
<b>Nemertea</b>	<i>Syllis cornuta agg</i>	0.79353467
<b>Nemertea</b>	<i>Tanaidacea</i>	0.66782913
<b>Nephasoma procera</b>	<i>Chirimia biceps</i>	0.64166231
<b>Nephasoma procera</b>	<i>Gnathia elongata</i>	0.85534119
<b>Nephasoma procera</b>	<i>Haplooops tubicola</i>	0.71054791
<b>Nephasoma procera</b>	<i>Nematoda</i>	0.59547824
<b>Nephasoma procera</b>	<i>Ostracoda</i>	0.4245698
<b>Nephtys incisa</b>	<i>Adontorhina juv</i>	0.58154394
<b>Nephtys incisa</b>	<i>Aricidea catherinae</i>	0.5988667
<b>Nephtys incisa</b>	<i>Aricidea suecica</i>	0.91474314
<b>Nephtys incisa</b>	<i>Chaetozone setosa</i>	0.59387801
<b>Nephtys incisa</b>	<i>Diplocirrus hirsutus</i>	0.51641954
<b>Nephtys incisa</b>	<i>Eteone sp</i>	0.97156647
<b>Nephtys incisa</b>	<i>Maldane sarsi</i>	0.5183831
<b>Nephtys incisa</b>	<i>Myriochele sp</i>	0.91702917
<b>Nephtys incisa</b>	<i>Owenia polaris</i>	0.8598009
<b>Nephtys incisa</b>	<i>Spiochaetopterus typicus</i>	0.52230307
<b>Nephtys juv</b>	<i>Aricidea quadrilobata</i>	0.45557401
<b>Nephtys juv</b>	<i>Spiophanes kroyeri</i>	0.5831241
<b>Nephtys juv</b>	<i>Tanaidacea</i>	0.47348154
<b>Nephtys juv</b>	<i>Terebellides stroemii</i>	0.45302377
<b>Ophelina abranchiata</b>	<i>Antalis entalis</i>	0.94265891
<b>Ophelina abranchiata</b>	<i>Cirrophorus eliasoni</i>	0.97358866
<b>Ophelina abranchiata</b>	<i>Clymenura sp</i>	0.97358866
<b>Ophelina abranchiata</b>	<i>Heteromastus filiformis</i>	0.86028619
<b>Ophelina abranchiata</b>	<i>Levinsenia gracillis</i>	0.4812985
<b>Ophelina abranchiata</b>	<i>Pellecepoda</i>	0.48723277

Ostracoda	<i>Gnathia elongata</i>	0.4197823
Ostracoda	<i>Melinna sp</i>	0.8153058
Ostracoda	<i>Myriochele heeri</i>	0.76351236
Ostracoda	<i>Nephasoma procera</i>	0.4245698
Ostracoda	<i>Owenia polaris</i>	0.39946195
Ostracoda	<i>Terebellides stroemii</i>	0.45937557
Owenia polaris	<i>Adontorhina juv</i>	0.55005358
Owenia polaris	<i>Aricidea catherinae</i>	0.57041645
Owenia polaris	<i>Aricidea suecica</i>	0.87618827
Owenia polaris	<i>Chaetozone setosa</i>	0.5633835
Owenia polaris	<i>Diplocirrus hirsutus</i>	0.50644825
Owenia polaris	<i>Eteone sp</i>	0.77202731
Owenia polaris	<i>Melinna sp</i>	0.40387286
Owenia polaris	<i>Myriochele sp</i>	0.8779646
Owenia polaris	<i>Nephtys incisa</i>	0.8598009
Owenia polaris	<i>Ostracoda</i>	0.39946195
Owenia polaris	<i>Spiochaetopterus typicus</i>	0.5572169
Owenia polaris	<i>Yoldiidae</i>	0.407717
Paraonidae indet	<i>Astarte crenata agg</i>	0.9265528
Paraonidae indet	<i>Cistenides hyperborea</i>	0.75382893
Paraonidae indet	<i>Leitoscoloplos mammosus</i>	0.73384883
Paraonidae indet	<i>Phyllodoce groenlandica</i>	0.99907649
Paraonidae indet	<i>Praxiella gracilis</i>	0.99592993
Paraonidae indet	<i>Prionospio cirrifera</i>	0.45446842
Paraonidae indet	<i>Terebellides stroemii</i>	0.49207222
Pellecepoda	<i>Aphroditoidae indet</i>	0.91713348
Pellecepoda	<i>Brachydiastylis resima</i>	0.64208916
Pellecepoda	<i>Chirrimia biceps</i>	0.4213375
Pellecepoda	<i>Diplocirrus hirsutus</i>	0.55385365
Pellecepoda	<i>Levinsenia gracillis</i>	0.81887741
Pellecepoda	<i>Lumbrineris mixochaeta</i>	0.60908411
Pellecepoda	<i>Nemertea</i>	0.80909715
Pellecepoda	<i>Ophelina abranchiata</i>	0.48723277
Pellecepoda	<i>Prionospio cirrifera</i>	0.51452728
Pellecepoda	<i>Syllis cornuta agg</i>	0.82144589
Pellecepoda	<i>Tanaidacea</i>	0.67715614
Phyllodoce groenlandica	<i>Astarte crenata agg</i>	0.92831992
Phyllodoce groenlandica	<i>Cistenides hyperborea</i>	0.75633975
Phyllodoce groenlandica	<i>Leitoscoloplos mammosus</i>	0.73836851
Phyllodoce groenlandica	<i>Paraonidae indet</i>	0.99907649
Phyllodoce groenlandica	<i>Praxiella gracilis</i>	0.99695853
Phyllodoce groenlandica	<i>Prionospio cirrifera</i>	0.45723194
Phyllodoce groenlandica	<i>Terebellides stroemii</i>	0.49325334
Praxiella gracilis	<i>Astarte crenata agg</i>	0.9237353
Praxiella gracilis	<i>Cistenides hyperborea</i>	0.7596907
Praxiella gracilis	<i>Leitoscoloplos mammosus</i>	0.74208101
Praxiella gracilis	<i>Paraonidae indet</i>	0.99592993
Praxiella gracilis	<i>Phyllodoce groenlandica</i>	0.99695853
Praxiella gracilis	<i>Prionospio cirrifera</i>	0.45134386

Appendix D

<b>Praxiella gracilis</b>	<i>Terebellides stroemii</i>	0.53829116
<b>Prionospio cirrifera</b>	<i>Aphroditoidaea indet</i>	0.59222719
<b>Prionospio cirrifera</b>	<i>Aricidea quadrilobata</i>	0.58527962
<b>Prionospio cirrifera</b>	<i>Astarte crenata agg</i>	0.54399854
<b>Prionospio cirrifera</b>	<i>Chirimia biceps</i>	0.68226427
<b>Prionospio cirrifera</b>	<i>Diastylis lucifera</i>	0.59222719
<b>Prionospio cirrifera</b>	<i>Diplocirrus hirsutus</i>	0.41980384
<b>Prionospio cirrifera</b>	<i>Leitoscoloplos mammosus</i>	0.55845291
<b>Prionospio cirrifera</b>	<i>Levinsenia gracillis</i>	0.42803324
<b>Prionospio cirrifera</b>	<i>Lumbrineris mixochaeta</i>	0.71553221
<b>Prionospio cirrifera</b>	<i>Mediomastus fragilis</i>	0.43581994
<b>Prionospio cirrifera</b>	<i>Nemertea</i>	0.61816686
<b>Prionospio cirrifera</b>	<i>Paraonidae indet</i>	0.45446842
<b>Prionospio cirrifera</b>	<i>Pellecepoda</i>	0.51452728
<b>Prionospio cirrifera</b>	<i>Phyllodoce groenlandica</i>	0.45723194
<b>Prionospio cirrifera</b>	<i>Praxiella gracilis</i>	0.45134386
<b>Prionospio cirrifera</b>	<i>Syllis cornuta agg</i>	0.51328323
<b>Prionospio cirrifera</b>	<i>Tanaidacea</i>	0.44373949
<b>Retusa obtusa</b>	<i>Ennucula tenuis</i>	0.86549354
<b>Rhodine gracilis</b>	<i>Ascelerichilus intermedius</i>	0.40810919
<b>Rhodine gracilis</b>	<i>Haploops setosa</i>	0.45613448
<b>Rhodine sp</b>	<i>Aricidea catherinae</i>	0.48163601
<b>Rhodine sp</b>	<i>Capitella sp</i>	1
<b>Rhodine sp</b>	<i>Dalychone spp</i>	0.97632349
<b>Rhodine sp</b>	<i>Galathowenia oculata</i>	0.49883342
<b>Rhodine sp</b>	<i>Maldane sarsi</i>	0.5929407
<b>Rhodine sp</b>	<i>Syllis sp</i>	0.52925332
<b>Rhodine sp</b>	<i>Yoldiidae</i>	0.58450611
<b>Spiochaetopterus typicus</b>	<i>Adontorhina juv</i>	0.58280577
<b>Spiochaetopterus typicus</b>	<i>Cistenides hyperborea</i>	0.5747216
<b>Spiochaetopterus typicus</b>	<i>Eteone sp</i>	0.45335255
<b>Spiochaetopterus typicus</b>	<i>Myriochele sp</i>	0.39150531
<b>Spiochaetopterus typicus</b>	<i>Nephtys incisa</i>	0.52230307
<b>Spiochaetopterus typicus</b>	<i>Owenia polaris</i>	0.5572169
<b>Spiophanes kroyeri</b>	<i>Nephtys juv</i>	0.5831241
<b>Spiophanes kroyeri</b>	<i>Syllis sp</i>	0.56566236
<b>Syllis cornuta agg</b>	<i>Aphroditoidaea indet</i>	0.90642424
<b>Syllis cornuta agg</b>	<i>Brachydiastylis resima</i>	0.72280314
<b>Syllis cornuta agg</b>	<i>Chirimia biceps</i>	0.49724918
<b>Syllis cornuta agg</b>	<i>Diplocirrus hirsutus</i>	0.55221566
<b>Syllis cornuta agg</b>	<i>Levinsenia gracillis</i>	0.8511783
<b>Syllis cornuta agg</b>	<i>Lumbrineris mixochaeta</i>	0.65647107
<b>Syllis cornuta agg</b>	<i>Mediomastus fragilis</i>	0.49156799
<b>Syllis cornuta agg</b>	<i>Nemertea</i>	0.79353467
<b>Syllis cornuta agg</b>	<i>Pellecepoda</i>	0.82144589
<b>Syllis cornuta agg</b>	<i>Prionospio cirrifera</i>	0.51328323
<b>Syllis cornuta agg</b>	<i>Tanaidacea</i>	0.67258505
<b>Syllis sp</b>	<i>Capitella sp</i>	0.52925332
<b>Syllis sp</b>	<i>Dalychone spp</i>	0.5083799

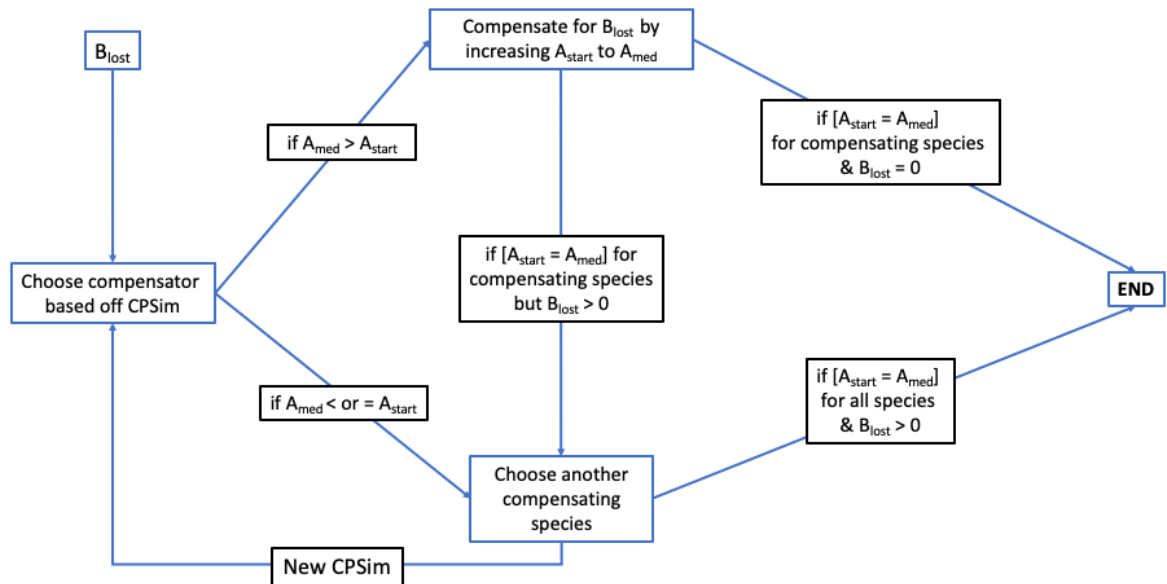
<b>Syllis sp</b>	<i>Rhodine sp</i>	0.52925332
<b>Syllis sp</b>	<i>Spiophanes kroyeri</i>	0.56566236
<b>Tanaidacea</b>	<i>Aphroditidea indet</i>	0.76019463
<b>Tanaidacea</b>	<i>Brachydiastylis resima</i>	0.57472834
<b>Tanaidacea</b>	<i>Diplocirrus hirsutus</i>	0.43468053
<b>Tanaidacea</b>	<i>Levinsenia gracillis</i>	0.49865456
<b>Tanaidacea</b>	<i>Lumbrineris mixochaeta</i>	0.42237943
<b>Tanaidacea</b>	<i>Nemertea</i>	0.66782913
<b>Tanaidacea</b>	<i>Nephtys juv</i>	0.47348154
<b>Tanaidacea</b>	<i>Pellecepoda</i>	0.67715614
<b>Tanaidacea</b>	<i>Prionospio cirrifera</i>	0.44373949
<b>Tanaidacea</b>	<i>Syllis cornuta agg</i>	0.67258505
<b>Terebellides stroemii</b>	<i>Astarte crenata agg</i>	0.42223172
<b>Terebellides stroemii</b>	<i>Melinna sp</i>	0.52312745
<b>Terebellides stroemii</b>	<i>Myriochele heeri</i>	0.50444763
<b>Terebellides stroemii</b>	<i>Nephtys juv</i>	0.45302377
<b>Terebellides stroemii</b>	<i>Ostracoda</i>	0.45937557
<b>Terebellides stroemii</b>	<i>Paraonidae indet</i>	0.49207222
<b>Terebellides stroemii</b>	<i>Phyllodoce groenlandica</i>	0.49325334
<b>Terebellides stroemii</b>	<i>Praxiella gracilis</i>	0.53829116
<b>Yoldiidae</b>	<i>Aricidea catherinae</i>	0.49961056
<b>Yoldiidae</b>	<i>Capitella sp</i>	0.58450611
<b>Yoldiidae</b>	<i>Dialychone spp</i>	0.54771716
<b>Yoldiidae</b>	<i>Galathowenia oculata</i>	0.46768293
<b>Yoldiidae</b>	<i>Maldane sarsi</i>	0.56493878
<b>Yoldiidae</b>	<i>Owenia polaris</i>	0.407717
<b>Yoldiidae</b>	<i>Rhodine sp</i>	0.58450611

Table S2 (b)

Sp1	Sp2	correlation coefficient
<i>Chirimia biceps</i>	<i>Spiochaetopterus typicus</i>	-0.3968943
<i>Nematoda</i>	<i>Spiochaetopterus typicus</i>	-0.3529203
<i>Nephasoma procera</i>	<i>Spiochaetopterus typicus</i>	-0.3138353
<i>Spiochaetopterus typicus</i>	<i>Chirimia biceps</i>	-0.3968943
<i>Spiochaetopterus typicus</i>	<i>Nematoda</i>	-0.3529203
<i>Spiochaetopterus typicus</i>	<i>Nephasoma procera</i>	-0.3138353



**Figure S5 |** Summary of the steps performed to determine the number of compensating species for each iterative extinction. As a species is extirpated, biomass is lost ( $B_{lost}$ ) and a compensating species is randomly selected based on their compensation probability (CPSim). This species will increase in abundance ( $A_{start}$ ), either up to pre-extinction median abundance ( $A_{med}$ ) or to the equivalent biomass that the extirpated species filled. . Multiple species can compensate should the original compensator's starting abundance not reach the pre-extinction median abundance. Compensation stops once lost biomass is fully replaced or all surviving species reach their assemblage median abundance. This process ensures that compensatory responses are finite and reflects the likely carrying capacity.



## D.1 References

J. Assis et al. Bio-ORACLE v2.0: Extending marine data layers for bioclimatic modelling. *Global Ecology and Biogeography* 27, 277-284 (2017).

S. Bosch, and S. Fernandez, *sdmpredictors*: Species Distribution Modelling Predictor Datasets. R package version 0.2.10. (2021). <https://CRAN.R-project.org/package=sdmpredictors>

E. Eriksen et al. From single species surveys towards monitoring of the Barents Sea ecosystem. *Progress in Oceanography* 166, 4-14 (2018).

T. M. J. Fruchterman, E. M. Reingold, Graph drawing by force-directed placement. *Software: Practice and Experience* 21, 1129-1164 (1991).

M. Solan et al. Climate-driven benthic invertebrate activity and biogeochemical functioning across the Barents Sea polar front. *Philos Trans A Math Phys Eng Sci* 378, 20190365 (2020).

L. Tyberghein et al. Bio-ORACLE: a global environmental dataset for marine species distribution modelling. *Global Ecology and Biogeography* 21, 272-281 (2012).

M. Vihtakari, A. Sundfjord, L. de Steur. Barents Sea ocean-current arrows modified from Eriksen et al. (2018). Norwegian Polar Institute and Institute of Marine Research. (2019).  
<https://github.com/MikkoVihtakari/Barents-Sea-currents>

# Appendix E Appendix 2 for Chapter 5

## Co-Extinction & Co-Compensation Supplementary Code

Thomas J Williams

2023-03-28

```
sessionInfo()

## R version 4.3.0 (2023-04-21)
## Platform: x86_64-apple-darwin20 (64-bit)
## Running under: macOS Monterey 12.2.1
##
## Matrix products: default
## BLAS:  /Library/Frameworks/R.framework/Versions/4.3-x86_64/Resources
## lib/libRblas.0.dylib
## LAPACK: /Library/Frameworks/R.framework/Versions/4.3-x86_64/Resources
## lib/libRlapack.dylib;  LAPACK version 3.11.0
##
## locale:
## [1] en_US.UTF-8/en_US.UTF-8/en_US.UTF-8/C/en_US.UTF-8/en_US.UTF-8
##
## time zone: Europe/London
## tzcode source: internal
##
## attached base packages:
## [1] stats      graphics   grDevices  utils      datasets   methods    base
##
## loaded via a namespace (and not attached):
## [1] compiler_4.3.0  fastmap_1.1.1   cli_3.6.1      formatR_1.14
## [5] tools_4.3.0    htmltools_0.5.5  rstudioapi_0.14 yaml_2.3.7
## [9] rmarkdown_2.21   knitr_1.42     xfun_0.39     digest_0.6.31
## [13] rlang_1.1.1    evaluate_0.21
```

### E.1 Supplementary code

This script performs the supplementary code required for the extinction and compensation model on local (station B17 to station B16 | station B16 to station B15 | station B15 to station Xs | station Xs to station B14 | station B14 to B13) and regional (stations B17 through to station B13) macrobenthic biodiversity data in the Barents Sea (Arctic), collected during the 2018 summer research expedition aboard the RRS James Clark Ross (Solan et al. 2020). Each supplementary code chunk is referenced in the manuscript and explained in detail below.

#### E.1.1 Loading of packages

```
packages <- c("tidyverse", "Hmisc", "qgraph", "rio", "patchwork",
           "MetBrewer", "ggpmisc", "mgcv")
# Install packages not yet installed
```

```
installed_packages <- packages %in% rownames(installed.packages())
if (any(installed_packages == FALSE)) {
  install.packages(packages[!installed_packages], repos = "http://cran
.us.r-project.org")
}

# Packages Loading
invisible(lapply(packages, library, character.only = TRUE))
```

### E.1.2 Initial load of data and data wrangling

```
ChAOS_macrofauna_2018 <- read.csv("ChAOS_macrofauna_2018_R_ready.csv")

## Stations, Habitats and Scenarios ####
ChAOS_stations_2018 <- data.frame(Station = c("B17", "B16", "B15",
  "Xs", "B14", "B13", "B17"), Habitat = c("Arctic", "Arctic",
  "Boreal", "Boreal", "Boreal", "Boreal"), Scenario = c("B17
-B16",
  "B16-B15", "B15-Xs", "Xs-B14", "B14-B13", "None", "B17-B13"))

ChAOS_macrofauna_stations_2018 <- merge(ChAOS_macrofauna_2018,
  ChAOS_stations_2018, by = "Station", all.x = T)

## mean and total abundance and biomass for 2018 ####
ChAOS_2018_mean <- ChAOS_macrofauna_stations_2018 %>%
  group_by(ScientificName_accepted, Station) %>%
  summarise(Habitat, Scenario, Mi = Mi, Ri = Ri, Bi = mean(Biomass),
    Ai = mean(Abundance), Btot = sum(Biomass), Atot = sum(Abundance)
  ) %>%
  tibble()

## Warning: Returning more (or less) than 1 row per `summarise()` group
## was deprecated in
## dplyr 1.1.0.
## [i] Please use `reframe()` instead.
## [i] When switching from `summarise()` to `reframe()`, remember that `r
## eframe()` always returns an ungrouped data frame and adjust accordingly.
## Call `lifecycle::last_lifecycle_warnings()` to see where this warning
## was
## generated.

## `summarise()` has grouped output by 'ScientificName_accepted', 'Stati
## on'. You
## can override using the ` `.groups` argument.

ChAOS_2018_mean <- unique(ChAOS_2018_mean)

# Mean biomass per North (Arctic) and South (Boreal)
# habitats as defined by an already established gradient in
# the benthos [Solan et al. 2020] and environment (Polar
# Front; [Loeng, 1991])

ChAOS_2018_mean <- ChAOS_2018_mean %>%
  group_by(ScientificName_accepted, Habitat) %>%
```

```

  summarise(Station, Scenario, Mi = Mi, Ri = Ri, Bi, Ai, Btot,
            Atot, Bind_Habitat = sum(Btot)/sum(Atot))

## Warning: Returning more (or less) than 1 row per `summarise()` group
## was deprecated in
## dplyr 1.1.0.
## [i] Please use `reframe()` instead.
## [i] When switching from `summarise()` to `reframe()`, remember that `reframe()`
##     always returns an ungrouped data frame and adjust accordingly.
## Call `lifecycle::last_lifecycle_warnings()` to see where this warning
## was
## generated.

## `summarise()` has grouped output by 'ScientificName_accepted', 'Habitat'.
## You
## can override using the ` `.groups` argument.

ChAOS_2018_mean[is.na(ChAOS_2018_mean)] <- 0

# Scenario-based Bind ####

ChAOS_2018_mean$Bind_Scenario = ChAOS_2018_mean$Bind_Habitat

# For the B16-B15 and B17-B13 scenarios, this crosses the
# Polar Front (i.e. moving from 'Arctic' to 'boreal').
# Hence, Bind is slightly different. If species are found
# at both stations, then the allocated Bind is based off
# boreal Bind. If species are only found at B16/B17, then
# the allocated Bind is based off the Arctic.
ChAOS_2018_Species <- as.character(unique(ChAOS_2018_mean$ScientificName_accepted))

for (i in ChAOS_2018_Species) {
  if (ChAOS_2018_mean[which(ChAOS_2018_mean$Station == "B16" &
    ChAOS_2018_mean$ScientificName_accepted == i), ]$Bi >
    0 && ChAOS_2018_mean[which(ChAOS_2018_mean$Station == "B15" &
    ChAOS_2018_mean$ScientificName_accepted == i),
    ]$Bi == 0) {
    ChAOS_2018_mean[which(ChAOS_2018_mean$Scenario == "B16-B15" &
      ChAOS_2018_mean$ScientificName_accepted == i), ]$Bind_Scenario <- unique(ChAOS_2018_mean[which(ChAOS_2018_mean$Habitat == "Arctic" &
        ChAOS_2018_mean$ScientificName_accepted == i), ]$Bind_Habitat)
  } else {
    ChAOS_2018_mean[which(ChAOS_2018_mean$Scenario == "B16-B15" &
      ChAOS_2018_mean$ScientificName_accepted == i), ]$Bind_Scenario <- unique(ChAOS_2018_mean[which(ChAOS_2018_mean$Habitat == "Boreal" &
        ChAOS_2018_mean$ScientificName_accepted == i), ]$Bind_Habitat)
  }
}

for (i in ChAOS_2018_Species) {
  if (ChAOS_2018_mean[which(ChAOS_2018_mean$Station == "B17" &
    ChAOS_2018_mean$Scenario == "B17-B13" & ChAOS_2018_mean$ScientificName_accepted == i), ]$Bi >
    0 && ChAOS_2018_mean[which(ChAOS_2018_mean$Station == "B16" &
    ChAOS_2018_mean$Scenario == "B16-B15" & ChAOS_2018_mean$ScientificName_accepted == i), ]$Bi == 0) {
    ChAOS_2018_mean[which(ChAOS_2018_mean$Scenario == "B17-B13" &
      ChAOS_2018_mean$ScientificName_accepted == i), ]$Bind_Scenario <- unique(ChAOS_2018_mean[which(ChAOS_2018_mean$Habitat == "Arctic" &
        ChAOS_2018_mean$ScientificName_accepted == i), ]$Bind_Habitat)
  } else {
    ChAOS_2018_mean[which(ChAOS_2018_mean$Scenario == "B17-B13" &
      ChAOS_2018_mean$ScientificName_accepted == i), ]$Bind_Scenario <- unique(ChAOS_2018_mean[which(ChAOS_2018_mean$Habitat == "Boreal" &
        ChAOS_2018_mean$ScientificName_accepted == i), ]$Bind_Habitat)
  }
}

```

```

icName_accepted ==
  i), ]$Bi > 0 && ChAOS_2018_mean[which(ChAOS_2018_mean$Station ==
  "B13" & ChAOS_2018_mean$ScientificName_accepted == i),
  ]$Bi == 0) {
  ChAOS_2018_mean[which(ChAOS_2018_mean$Scenario == "B17-B13" &
  ChAOS_2018_mean$ScientificName_accepted == i), ]$Bind_Scenar
io <- unique(ChAOS_2018_mean[which(ChAOS_2018_mean$Habitat ==
  "Arctic" & ChAOS_2018_mean$ScientificName_accepted ==
  i), ]$Bind_Habitat)
} else {
  ChAOS_2018_mean[which(ChAOS_2018_mean$Scenario == "B17-B13" &
  ChAOS_2018_mean$ScientificName_accepted == i), ]$Bind_Scenar
io <- unique(ChAOS_2018_mean[which(ChAOS_2018_mean$Habitat ==
  "Boreal" & ChAOS_2018_mean$ScientificName_accepted ==
  i), ]$Bind_Habitat)
}
}

rm(ChAOS_stations_2018)

```

### E.1.3 Code S1: Vulnerability of species

Ranked vulnerabilities to each step in the climatic-driven environmental transition (B17-B16 | B16-B15 | B15-Xs | Xs-B14 | B14-B13 | B17-B13), calculated from the percentage differences in macrofaunal biomass between the pre-extinction community (northernmost station, e.g. B17) and the reference post-extinction community (southernmost station, e.g. B16) for all taxa in the regional species pool

```

# Calculate percentage differences in biomass between
# starting station and reference station ##### B17- B16
E16 <- (ChAOS_2018_mean[which(ChAOS_2018_mean$Station == "B16"),
  ]$Bi - ChAOS_2018_mean[which(ChAOS_2018_mean$Station == "B17" &
  ChAOS_2018_mean$Scenario == "B17-B16"), ]$Bi)/ChAOS_2018_mean[which(
ChAOS_2018_mean$Station ==
  "B17" & ChAOS_2018_mean$Scenario == "B17-B16"), ]$Bi

# B16- B15
E15 <- (ChAOS_2018_mean[which(ChAOS_2018_mean$Station == "B15"),
  ]$Bi - ChAOS_2018_mean[which(ChAOS_2018_mean$Station == "B16" &
  ChAOS_2018_mean$Scenario == "B16-B15"), ]$Bi)/ChAOS_2018_mean[which(
ChAOS_2018_mean$Station ==
  "B16" & ChAOS_2018_mean$Scenario == "B16-B15"), ]$Bi

# B15- Xs
EXs <- (ChAOS_2018_mean[which(ChAOS_2018_mean$Station == "Xs"),
  ]$Bi - ChAOS_2018_mean[which(ChAOS_2018_mean$Station == "B15"),
  ]$Bi)/ChAOS_2018_mean[which(ChAOS_2018_mean$Station == "B15"),
  ]$Bi

# Xs- B14
E14 <- (ChAOS_2018_mean[which(ChAOS_2018_mean$Station == "B14"),
  ]$Bi - ChAOS_2018_mean[which(ChAOS_2018_mean$Station == "Xs"),
  ]$Bi)/ChAOS_2018_mean[which(ChAOS_2018_mean$Station == "Xs"),
  ]$Bi

```

```

# B14- B13
E13 <- (ChAOS_2018_mean[which(ChAOS_2018_mean$Station == "B13"),
  ]$Bi - ChAOS_2018_mean[which(ChAOS_2018_mean$Station == "B14"),
  ]$Bi)/ChAOS_2018_mean[which(ChAOS_2018_mean$Station == "B14"),
  ]$Bi

# B17 - B13
Eall <- (ChAOS_2018_mean[which(ChAOS_2018_mean$Station == "B13"),
  ]$Bi - ChAOS_2018_mean[which(ChAOS_2018_mean$Station == "B17" &
  ChAOS_2018_mean$Scenario == "B17-B13"), ]$Bi)/ChAOS_2018_mean[which(
ChAOS_2018_mean$Station ==
  "B17" & ChAOS_2018_mean$Scenario == "B17-B13"), ]$Bi

# row bind all the percentage differences #####
ChAOS_2018_Vulnerabilities_Biomass <- do.call(rbind, Map(data.frame,
  ScientificName_accepted = unique(ChAOS_2018_mean$ScientificName_accepted),
  E16 = E16, E15 = E15, EXs = EXs, E14 = E14, E13 = E13, Eall = Eall))
ChAOS_2018_Vulnerabilities_Biomass[is.na(ChAOS_2018_Vulnerabilities_Biomass)] <- 0

# now rank them from most to least vulnerable based on
# percetange differences #### B17 - B16
order.scores <- order(ChAOS_2018_Vulnerabilities_Biomass$E16)
ChAOS_2018_Vulnerabilities_Biomass <- ChAOS_2018_Vulnerabilities_Biomass[order.scores,
  ]
ChAOS_2018_Vulnerabilities_Biomass$Biomass_E16rank <- rank(ChAOS_2018_Vulnerabilities_Biomass$E16)
ChAOS_2018_Vulnerabilities_Biomass

# B16 - B15
order.scores <- order(ChAOS_2018_Vulnerabilities_Biomass$E15)
ChAOS_2018_Vulnerabilities_Biomass <- ChAOS_2018_Vulnerabilities_Biomass[order.scores,
  ]
ChAOS_2018_Vulnerabilities_Biomass$Biomass_E15rank <- rank(ChAOS_2018_Vulnerabilities_Biomass$E15)
ChAOS_2018_Vulnerabilities_Biomass

# B15 - Xs
order.scores <- order(ChAOS_2018_Vulnerabilities_Biomass$EXs)
ChAOS_2018_Vulnerabilities_Biomass <- ChAOS_2018_Vulnerabilities_Biomass[order.scores,
  ]
ChAOS_2018_Vulnerabilities_Biomass$Biomass_EXsrank <- rank(ChAOS_2018_Vulnerabilities_Biomass$EXs)
ChAOS_2018_Vulnerabilities_Biomass

# Xs - B14
order.scores <- order(ChAOS_2018_Vulnerabilities_Biomass$E14)
ChAOS_2018_Vulnerabilities_Biomass <- ChAOS_2018_Vulnerabilities_Biomass[order.scores,
  ]
ChAOS_2018_Vulnerabilities_Biomass$Biomass_E14rank <- rank(ChAOS_2018_Vul

```

```

nerabilities_Biomass$E14)
ChAOS_2018_Vulnerabilities_Biomass

# B14 - B13
order.scores <- order(ChAOS_2018_Vulnerabilities_Biomass$E13)
ChAOS_2018_Vulnerabilities_Biomass <- ChAOS_2018_Vulnerabilities_Biomass[order.scores,
]
ChAOS_2018_Vulnerabilities_Biomass$Biomass_E13rank <- rank(ChAOS_2018_Vulnerabilities_Biomass$E13)
ChAOS_2018_Vulnerabilities_Biomass

# B17 - B13
order.scores <- order(ChAOS_2018_Vulnerabilities_Biomass$Eall)
ChAOS_2018_Vulnerabilities_Biomass <- ChAOS_2018_Vulnerabilities_Biomass[order.scores,
]
ChAOS_2018_Vulnerabilities_Biomass$Biomass_Eallrank <- rank(ChAOS_2018_Vulnerabilities_Biomass$Eall)
ChAOS_2018_Vulnerabilities_Biomass

# Finally, merge vulnerabilities with starting data #####
ChAOS_2018_mean$B_Vulnerability <- NA

ChAOS_2018_Species <- as.character(unique(ChAOS_2018_mean$ScientificName_accepted))

for (i in ChAOS_2018_Species) {
  ChAOS_2018_mean[which(ChAOS_2018_mean$Scenario == "B17-B16" &
    ChAOS_2018_mean$ScientificName_accepted == i), ]$B_Vulnerability
  <- ChAOS_2018_Vulnerabilities_Biomass[which(ChAOS_2018_Vulnerabilities_Biomass$ScientificName_accepted ==
    i), ]$Biomass_E16rank
  ChAOS_2018_mean[which(ChAOS_2018_mean$Scenario == "B16-B15" &
    ChAOS_2018_mean$ScientificName_accepted == i), ]$B_Vulnerability
  <- ChAOS_2018_Vulnerabilities_Biomass[which(ChAOS_2018_Vulnerabilities_Biomass$ScientificName_accepted ==
    i), ]$Biomass_E15rank
  ChAOS_2018_mean[which(ChAOS_2018_mean$Scenario == "B15-Xs" &
    ChAOS_2018_mean$ScientificName_accepted == i), ]$B_Vulnerability
  <- ChAOS_2018_Vulnerabilities_Biomass[which(ChAOS_2018_Vulnerabilities_Biomass$ScientificName_accepted ==
    i), ]$Biomass_EXsrank
  ChAOS_2018_mean[which(ChAOS_2018_mean$Scenario == "Xs-B14" &
    ChAOS_2018_mean$ScientificName_accepted == i), ]$B_Vulnerability
  <- ChAOS_2018_Vulnerabilities_Biomass[which(ChAOS_2018_Vulnerabilities_Biomass$ScientificName_accepted ==
    i), ]$Biomass_E14rank
  ChAOS_2018_mean[which(ChAOS_2018_mean$Scenario == "B14-B13" &
    ChAOS_2018_mean$ScientificName_accepted == i), ]$B_Vulnerability
  <- ChAOS_2018_Vulnerabilities_Biomass[which(ChAOS_2018_Vulnerabilities_Biomass$ScientificName_accepted ==
    i), ]$Biomass_E13rank
  ChAOS_2018_mean[which(ChAOS_2018_mean$Scenario == "B17-B13" &
    ChAOS_2018_mean$ScientificName_accepted == i), ]$B_Vulnerability
  <- ChAOS_2018_Vulnerabilities_Biomass[which(ChAOS_2018_Vulnerabilities_Biomass$ScientificName_accepted ==
    i), ]$Biomass_E13rank
}

```

```

mass$ScientificName_accepted ==
  i), ]$Biomass_Eallrank
}

rm(E16, E15, EXs, E14, E13, Eall)
rm(order.scores)

```

#### E.1.4 Code S2: Calculating the median abundance above and below the ecotone Polar Front

For B16-B15 & B17-B13 scenario, switch to Amed of boreal stations (B15-B13) as that is the abundance of the incoming species from the local pool (migrating northward with Atlantification). This follows the position of the Barents Sea Polar front (Solan et al. 2020; Loeng, 1991)

```

## B17-B16 #####
ChAOS_Species_18_Compensation <- ChAOS_macrofauna_2018 %>%
  select(ScientificName_accepted, Mi, Ri, Year, Station, Replicate,
         Abundance, Biomass)
ChAOS_Species_18_Compensation$Abundance[ChAOS_Species_18_Compensation$Abundance ==
  0] <- NaN
ChAOS_Species_18_Compensation$Biomass[ChAOS_Species_18_Compensation$Biomass ==
  0] <- NaN
Species <- unique(ChAOS_Species_18_Compensation$ScientificName_accepted)

for (z in Species) {
  med_Abundance_B17_B16 <- median(ChAOS_Species_18_Compensation[which(
    ChAOS_Species_18_Compensation$ScientificName_accepted ==
      z & c(ChAOS_Species_18_Compensation$Station == "B16" |
        ChAOS_Species_18_Compensation$Station == "B17")), ]$Abundance,
    na.rm = T)

  print(med_Abundance_B17_B16)

  ChAOS_Species_18_Compensation[ChAOS_Species_18_Compensation$ScientificName_accepted ==
    z, "med_Abundance_B17_B16"] <- med_Abundance_B17_B16
}

# cant have Na!!
ChAOS_Species_18_Compensation$med_Abundance_B17_B16[is.na(ChAOS_Species_18_Compensation$med_Abundance_B17_B16)] <- 0

## B15-B13 #####
for (z in Species) {
  med_Abundance_B15_B13 <- median(ChAOS_Species_18_Compensation[which(
    ChAOS_Species_18_Compensation$ScientificName_accepted ==
      z & c(ChAOS_Species_18_Compensation$Station == "Xs" |
        ChAOS_Species_18_Compensation$Station == "B15" | ChAOS_Species_18_Compensation$Station ==
          "B14" | ChAOS_Species_18_Compensation$Station == "B13")),

```

```

    ]$Abundance, na.rm = T)
print(med_Abundance_B15_B13)

ChAOS_Species_18_Compensation[ChAOS_Species_18_Compensation$ScientificName_accepted ==
  z, "med_Abundance_B15_B13"] <- med_Abundance_B15_B13
}

# cant have Na!!
ChAOS_Species_18_Compensation$med_Abundance_B15_B13[is.na(ChAOS_Species_18_Compensation$med_Abundance_B15_B13)] <- 0

## subsetting median abundances and adding to start dataset
## for model #####
ChAOS_2018_Compensation <- ChAOS_Species_18_Compensation %>%
  select(ScientificName_accepted, med_Abundance_B17_B16, med_Abundance_B15_B13) %>%
  unique()

ChAOS_2018_mean$Amed <- NA

for (i in Species) {
  ChAOS_2018_mean[which(ChAOS_2018_mean$Scenario == "B17-B16" &
    ChAOS_2018_mean$ScientificName_accepted == i), ]$Amed <- ChAOS_2018_Compensation[which(ChAOS_2018_Compensation$ScientificName_accepted ==
    i), ]$med_Abundance_B17_B16
  ChAOS_2018_mean[which(ChAOS_2018_mean$Scenario == "B16-B15" &
    ChAOS_2018_mean$ScientificName_accepted == i), ]$Amed <- ChAOS_2018_Compensation[which(ChAOS_2018_Compensation$ScientificName_accepted ==
    i), ]$med_Abundance_B15_B13
  ChAOS_2018_mean[which(ChAOS_2018_mean$Scenario == "B15-Xs" &
    ChAOS_2018_mean$ScientificName_accepted == i), ]$Amed <- ChAOS_2018_Compensation[which(ChAOS_2018_Compensation$ScientificName_accepted ==
    i), ]$med_Abundance_B15_B13
  ChAOS_2018_mean[which(ChAOS_2018_mean$Scenario == "Xs-B14" &
    ChAOS_2018_mean$ScientificName_accepted == i), ]$Amed <- ChAOS_2018_Compensation[which(ChAOS_2018_Compensation$ScientificName_accepted ==
    i), ]$med_Abundance_B15_B13
  ChAOS_2018_mean[which(ChAOS_2018_mean$Scenario == "B14-B13" &
    ChAOS_2018_mean$ScientificName_accepted == i), ]$Amed <- ChAOS_2018_Compensation[which(ChAOS_2018_Compensation$ScientificName_accepted ==
    i), ]$med_Abundance_B15_B13
  ChAOS_2018_mean[which(ChAOS_2018_mean$Scenario == "B17-B13" &
    ChAOS_2018_mean$ScientificName_accepted == i), ]$Amed <- ChAOS_2018_Compensation[which(ChAOS_2018_Compensation$ScientificName_accepted ==
    i), ]$med_Abundance_B15_B13
}

write.csv(ChAOS_2018_mean, "ChAOS_2018_macrofauna_model_ready.csv")

```

### E.1.5 Code S3: Calculating correlations for species co-extinctions and co-compensations

```

# Removing rare species from the correlation calculations
# #####

Sum_Abundance <- ChAOS_macrofauna_2018 %>%
  group_by(ScientificName_accepted) %>%
  summarise(suma = sum(Abundance/25))

Rare_Species <- subset(Sum_Abundance, subset = suma == 1, select = ScientificName_accepted)

ChAOS_BiomassMatrix_18_no_rares <- ChAOS_macrofauna_2018 %>%
  select(ScientificName_accepted, Station, Replicate, Biomass) %>%
  pivot_wider(names_from = c(Station, Replicate), values_from = Biomass) %>%
  dplyr::filter(!ScientificName_accepted %in% Rare_Species$ScientificName_accepted) %>%
  pivot_longer(-ScientificName_accepted) %>%
  pivot_wider(names_from = ScientificName_accepted, values_from = value)

# Biomass networks - ALL stations #####

All_stations_Community <- cor(ChAOS_BiomassMatrix_18_no_rares[, 2:70], method = "pearson", use = "everything")
All_stations_Community <- cov2cor(All_stations_Community)

ChAOS_BiomassMatrix_18_allstations_Co0c <- data.frame(x = rownames(All_stations_Community)[row(All_stations_Community)],
  y = colnames(All_stations_Community)[col(All_stations_Community)],
  correlation_coefficient = c(All_stations_Community))

# remove correlations between a species and itself
ChAOS_BiomassMatrix_18_allstations_Co0c <- ChAOS_BiomassMatrix_18_allstations_Co0c[which(ChAOS_BiomassMatrix_18_allstations_Co0c$x != ChAOS_BiomassMatrix_18_allstations_Co0c$y), ]

# Getting cut off lists ##### finding out mean and standard
# deviations
qqnorm(ChAOS_BiomassMatrix_18_allstations_Co0c$correlation_coefficient)

mean(ChAOS_BiomassMatrix_18_allstations_Co0c$correlation_coefficient)
sd(ChAOS_BiomassMatrix_18_allstations_Co0c$correlation_coefficient)
uppercutoff <- mean(ChAOS_BiomassMatrix_18_allstations_Co0c$correlation_coefficient) +
  (sd(ChAOS_BiomassMatrix_18_allstations_Co0c$correlation_coefficient) *
  1.5)
lowercutoff <- mean(ChAOS_BiomassMatrix_18_allstations_Co0c$correlation_coefficient) -
  (sd(ChAOS_BiomassMatrix_18_allstations_Co0c$correlation_coefficient) *
  1.5)

```

```

ChAOS_BiomassMatrix_18_standarddev <- data.frame(mean = mean(ChAOS_BiomassMatrix_18_allstations_Co0c$correlation_coefficient),
  sd = sd(ChAOS_BiomassMatrix_18_allstations_Co0c$correlation_coefficient *
  1.5))

# Cut off determination - 1.5 s.d. either side of mean
# correlation Co-occurring species
ChAOS_BiomassMatrix_18_allstations_Co0c_cutoff <- subset(ChAOS_BiomassMatrix_18_allstations_Co0c,
  subset = correlation_coefficient >= uppercutoff)
ChAOS_BiomassMatrix_18_allstations_Co0c_cutoff$x <- gsub(" ", "_", ChAOS_BiomassMatrix_18_allstations_Co0c_cutoff$x)
ChAOS_BiomassMatrix_18_allstations_Co0c_cutoff$y <- gsub(" ", "_", ChAOS_BiomassMatrix_18_allstations_Co0c_cutoff$y)
ChAOS_BiomassMatrix_18_allstations_Co0c_cutoff$x <- as.factor(ChAOS_BiomassMatrix_18_allstations_Co0c_cutoff$x)

write.csv(ChAOS_BiomassMatrix_18_allstations_Co0c_cutoff, file = "ChAOS_2018_allstations_Co_Occurrence[based_off_Biomass].csv")

## Competing species
ChAOS_BiomassMatrix_18_allstations_Comp_cutoff <- subset(ChAOS_BiomassMatrix_18_allstations_Co0c,
  subset = correlation_coefficient <= lowercutoff)
ChAOS_BiomassMatrix_18_allstations_Comp_cutoff$x <- gsub(" ", "_", ChAOS_BiomassMatrix_18_allstations_Comp_cutoff$x)
ChAOS_BiomassMatrix_18_allstations_Comp_cutoff$y <- gsub(" ", "_", ChAOS_BiomassMatrix_18_allstations_Comp_cutoff$y)
ChAOS_BiomassMatrix_18_allstations_Comp_cutoff$x <- as.factor(ChAOS_BiomassMatrix_18_allstations_Comp_cutoff$x)

write.csv(ChAOS_BiomassMatrix_18_allstations_Comp_cutoff, file = "ChAOS_2018_allstations_Competitors[based_off_Biomass].csv")

## subsetting Co-Occurrence files by species #####
ChAOS_BiomassMatrix_18_allstations_Co0c_cutoff_list_x <- split(ChAOS_BiomassMatrix_18_allstations_Co0c_cutoff,
  with(ChAOS_BiomassMatrix_18_allstations_Co0c_cutoff, x),
  drop = TRUE)

export(ChAOS_BiomassMatrix_18_allstations_Co0c_cutoff_list_x,
  "ChAOS_2018_Coextinctionlist_Biomass.xlsx")

## subsetting Competitors files by species #####
ChAOS_BiomassMatrix_18_allstations_Comp_cutoff_list_x <- split(ChAOS_BiomassMatrix_18_allstations_Comp_cutoff,
  with(ChAOS_BiomassMatrix_18_allstations_Comp_cutoff, x),
  drop = TRUE)

export(ChAOS_BiomassMatrix_18_allstations_Comp_cutoff_list_x,
  "ChAOS_2018_Competitorlist_Biomass.xlsx")

```

### E.1.6 Code S4: Code for deciding co extinctions

```

CO_EXT <- TRUE

if (CO_EXT == T) {
  # Code S4: CO-EXTINCTION
  # Pick a second species to go extinct (species y), based on the highest
  # positive correlation with the species x
  # First, find species x co-extinction file from the list in the global
  # environment, and choose the highest co-occurring species
  # there are a few species that have no correlations - so check first
  if(!is.null(startCoextinctions[[species_x]])) {

    species_x_TopCoextinction <- top_n(startCoextinctions[[species_x]],
1, correlation_coefficient)
    species_y <- as.character(species_x_TopCoextinction$y[1])

    # sometimes there will be multiple species that have the same correlation
    # (i.e. 0.978), so need to include all of them
    # in the ChAOs data, the top correlations of nine species are with more
    # than one species
    if(nrow(species_x_TopCoextinction) >1 ) {
      species_z <- as.character(species_x_TopCoextinction$y[2])
    }

    # additionally, one or both of the top correlating species (species
    # y OR z) may have gone extinct in a previous round
    # in this case, need to re-choose species y & z
    # if ALL correlating species have already gone extinct (species y &
    # z stay NA), have to just stop looking for co-extinctions
    # run a 21x for function with conditions, as the most correlations for
    # a species is 22 (i+1)
    for (i in 1:21) {
      if(is.na(species_y) && is.na(species_z)) {break} else( # if species
      # y has already gone extinct and there is no species z, then move down
      # the correlation list of species x and re-choose species y
      if(start$EPSim[start$ScientificName_accepted == species_y] == 0
      && is.na(species_z)) {
        nth_correlation <- nth(startCoextinctions[[species_x]]$correlation_coefficient,
        i+1)
        species_x_TopCoextinctions <- startCoextinctions[[species_x]]$y[startCoextinctions[[species_x]]$correlation_coefficient == nth_correlation]
        species_y <- as.character(species_x_TopCoextinctions[1])
      } else ( # if species y has already gone extinct but species z has not,
      # then species z becomes species y
      if(start$EPSim[start$ScientificName_accepted == species_y] == 0
      && start$EPSim[start$ScientificName_accepted == species_z] != 0) {
        species_y <- species_z
        species_z <- NA
      } else ( # if species y and species z have already gone extinct,
      # then move down the correlation list of species x and re-choose species y
      # and z
      if(start$EPSim[start$ScientificName_accepted == species_y] == 0 &
      & start$EPSim[start$ScientificName_accepted == species_z] == 0) {
        nth_correlation <- nth(startCoextinctions[[species_x]]$correlation_coefficient,
        i+1)
      }
    }
  }
}

```

```

species_x_TopCoextinctions <- startCoextinctions[[species_x]]$y[startCoe
xtinctions[[species_x]]$correlation_coefficient == nth_correlation]
species_y <- as.character(species_x_TopCoextinctions[1])
species_z <- as.character(species_x_TopCoextinctions[2])
}
)
)
)
}

# Find which row species y is in the starting data
# If species y is NA, Extinct 2 becomes an empty integer
Extinct2 <- which(start == species_y, arr.ind=FALSE)
Extinct3 <- which(start == species_z, arr.ind=FALSE)
}

# How much biomass will be lost with the doomed species
## 1st species
BiomassLost <- start[Extinct, "BiSim"]

## 2nd species (if there is one)
BiomassLost2 <- if(is.null(startCoextinctions[[species_x]]) || is.na
(species_y)) {
    0} else{
    start[Extinct2, "BiSim"]}

## 3rd species (if there is one)
BiomassLost3 <- if(is.null(startCoextinctions[[species_x]]) || is.na
(species_z)) {
    0} else{
    start[Extinct3, "BiSim"]}

# total biomass lost
BiomassLost <- BiomassLost + BiomassLost2 + BiomassLost3

# Record ID of who has gone extinct at each iteration
## 1st species
output[output$Simulation == sim_count & output$Nsp==sp_count, "ExtSp"
] <- as.character(start$ScientificName_accepted[Extinct])
output[output$Simulation == sim_count & output$Nsp==sp_count, "ExtSpE
xtProb"] <- start[Extinct, "ExtProb"]

## 2nd species (if there is one)
if(!is.null(startCoextinctions[[species_x]]) && !is.na(species_y)) {
    output[output$Simulation == sim_count & output
$Nsp==sp_count, "CoExtSp"] <- as.character(start$ScientificName_accepted[
Extinct2])
    output[output$Simulation == sim_count & output
$Nsp==sp_count, "CoExtSpExtProb"] <- start[Extinct2, "ExtProb"]}

## 3rd species (if there is one)
if(!is.null(startCoextinctions[[species_x]]) && !is.na(species_z)) {
    output[output$Simulation == sim_count & output
$Nsp==sp_count, "CoExtSp2"] <- as.character(start$ScientificName_accepted
[Extinct3])
}

```

```
output[output$Simulation == sim_count & output
$Nsp==sp_count, "CoExtSp2ExtProb"] <- start[Extinct3, "ExtProb"]}
```

### E.1.7 Code S5: Recalculating species probability to compensate based on negative correlations

```
# Code S5 COMPENSATION Species going extinct (x, y and z)
# cannot compensate
start[Extinct, "CPSim"] <- 0
if (!is.na(species_y)) {
  start[Extinct2, "CPSim"] <- 0
}
if (!is.na(species_z)) {
  start[Extinct3, "CPSim"] <- 0
}

# Normalise for Loss of species
start$CPSim <- start$CPSim/sum(start$CPSim)

# Create a temp dataframe of the species that correlate
# +vely with the now extinct species, (and another temp
# dataframe for those that correlate -vely)
Positivelist <- data.frame(species = startCoextinctions[[species_x]]$y,
  CoorV = startCoextinctions[[species_x]]$correlation_coefficient)
Negativelist <- data.frame(species = startCompetitors[[species_x]]$y,
  CoorV = startCompetitors[[species_x]]$correlation_coefficient)
Combinedlist <- rbind(Positivelist, Negativelist)

# Get a list of species names from the temp dataframes
Co_species <- as.character(Combinedlist$species)

# Calculate new compensation probabilities for correlating
# species
for (i in Co_species) {
  NewCPSim <- (start[which(start$ScientificName_accepted ==
    i), ]$CPSim - (Combinedlist[which(Combinedlist$species ==
    i), ]$CoorV * start[which(start$ScientificName_accepted ==
    i), ]$CPSim)))
  start[start$ScientificName_accepted == i, "NewCPSim"] <- NewCPSim
}

# Normalise new compensation probabilities
start$NewCPSim <- start$NewCPSim/sum(start$NewCPSim) # Normalise
```

### E.1.8 Code S6: Calculating co-compensations if there is still biomass left over from the extinctions

```
counter <- 1
# Code S6
# Compensation happens, with the amount of biomass corresponding to the
# difference between starting and median abundance
# First, check there is still some lost biomass left to compensate (while
# function). Not as important first time around but very important if th
```

ere is multiple compensating species. If there is not, then compensation is complete (while function finishes).

# I use the lowest possible biomass found across the entire regional species pool as the threshold.

# Secondly, have to check if there are still species available to compensate. If there is not, then compensation is complete (while function finishes).

```

while(BiomassLost > 0.000625 &&
      sum(start[which(start$CPSim !=0),]$AiSim) < sum(start[which(start$CPSim !=0),]$Amed)) {

  # Next, check that median abundance is more than starting abundance
  # - otherwise, choose another compensating species.
  # Once I find an appropriate species, I break this loop.

  repeat{
    ifelse(start$Amed[Compensate] - start$AiSim[Compensate]<=0,
          Compensate <- which(cumsum(start$NewCPSim)>=runif(1))[1],
          break
    )
  }

  # now, I calculate the difference in abundance between the median and the starting abundance for the compensating species
  Abundancediff <- start$Amed[Compensate] - start$AiSim[Compensate]

  # next, I calculate how much biomass this will increase by
  Biomassdiff <- start$Bind[Compensate]*Abundancediff

  # if it is higher than total biomass lost from the system, I adjust the change in abundance to this maximum
  if(Biomassdiff - BiomassLost > 0) {
    Abundancediff <- BiomassLost/start$Bind[Compensate]}

  # next, I allow the compensating species to increase in number corresponding to that difference and the amount of biomass there is
  start$AiSim[Compensate] <- start$AiSim[Compensate] + Abundancediff

  # next, I re-calculate how much biomass will increase by with the new change in abundance
  Biomassdiff <- start$Bind[Compensate]*Abundancediff

  # then, I allow its biomass to increase by that amount
  start$BiSim[Compensate] <- start$BiSim[Compensate] + Biomassdiff

  # finally, I remove the compensated biomass from the lost biomass
  BiomassLost <- BiomassLost - Biomassdiff

  # now to record everything
  if (counter == 1) {

    # Record amount of compensation abundance - add output$CompRep == countvalue
    output[output$Simulation == sim_count & output$Nsp==sp_count & output$CompRep == counter,"AbnComp"] <- Abundancediff
    # Record amount of compensation biomass
    output[output$Simulation == sim_count & output$Nsp==sp_count & output$CompRep == counter,"CompBiomass"] <- Biomassdiff
  }
}

```

```

t$CompRep == counter, "BioComp"] <- Biomassdiff
  # Record the compensation species
  output[output$Simulation == sim_count & output$Nsp==sp_count & output$CompRep == counter, "CompSp"] <- as.character(start$ScientificName_accepted[Compensate])

  # Add 1 to counter
  counter <- counter + 1

} else {
  # add row into output table
  output<- output %>%
    add_row(Simulation = sim_count, # that does not change
            Nsp=sp_count, # that does not change
            CompRep = counter, # that should now be at least 2 (the 1
            would have been your normal line allocation)
            Nsp_active = Nsp_active, # does not change
            ExtSp = as.character(start$ScientificName_accepted[Extinct
            ]), # that doesn't change
            ExtSpExtProb = start[Extinct, "ExtProb"], # that doesn't change
            CoExtSp = if(!is.null(startCoextinctions[[species_x]]) &&
            !is.na(species_y)) {
              as.character(start$ScientificName_accepted[Ext
              inct2]), # that doesn't change
              CoExtSpExtProb = if(!is.null(startCoextinctions[[species_x
              ]]) && !is.na(species_y)) {
                start[Extinct2, "ExtProb"], # that doesn't change
                CoExtSp2 = if(!is.null(startCoextinctions[[species_x]]) &&
                !is.na(species_z)) {
                  as.character(start$ScientificName_accepted[Ext
                  inct3]),
                  CoExtSp2ExtProb = if(!is.null(startCoextinctions[[species_x
                  ]]) && !is.na(species_z)) {
                    start[Extinct3, "ExtProb"], # that doesn't change# that doesn't change
                    CompSp = as.character(start$ScientificName_accepted[Compensate]), # change that by the second comp species name
                    AbnComp = Abundancediff, # change that by the second comp species abundance
                    BioComp = Biomassdiff, # change that by the second comp species biomass
                    BPc = BPc, # that is just for row completion
                    TOC = TOC, # same as BPc
                    NH4 = NH4) # same as BPc

  # Add 1 to counter
  counter <- counter + 1

} # end of the else function for adding rows to output file

} # end of the else function for this round of compensating species

```

### E.1.9 Code S7: Generalised Additive Models (GAMs) of each simulated biodiversity-function relationship.

```

# Import output data from model simulations #####
# Full model (co-extinctions and co-compensations)
B17_B16_BPc <- read.csv(file.choose())

B16_B15_BPc <- read.csv(file.choose())

B15_Xs_BPc <- read.csv(file.choose())

Xs_B14_BPc <- read.csv(file.choose())

B14_B13_BPc <- read.csv(file.choose())

B17_B13_BPc <- B17_B13_BPc %>%
  add_column(Scenario = "B17-B13")

B17_B16_BPc <- B17_B16_BPc %>%
  add_column(Scenario = "B17-B16")

B16_B15_BPc <- B16_B15_BPc %>%
  add_column(Scenario = "B16-B15")

B15_Xs_BPc <- B15_Xs_BPc %>%
  add_column(Scenario = "B15-Xs")

Xs_B14_BPc <- Xs_B14_BPc %>%
  add_column(Scenario = "Xs-B14")

B14_B13_BPc <- B14_B13_BPc %>%
  add_column(Scenario = "B14-B13")

B17_B13_BPc <- B17_B13_BPc %>%
  add_column(Scenario = "B17-B13")

# bind all scenarios into one dataframe
ChAOS_Scenarios_BPc <- bind_rows(B17_B16_BPc,
                                    B16_B15_BPc,
                                    B15_Xs_BPc,
                                    Xs_B14_BPc,
                                    B14_B13_BPc,
                                    B17_B13_BPc)

ChAOS_Scenarios_BPc$Scenario <- factor(ChAOS_Scenarios_BPc$Scenario, levels = c("B17-B16", "B16-B15", "B15-Xs", "Xs-B14", "B14-B13", "B17-B13"))

# GAM #####
## https://www.sciencedirect.com/science/article/abs/pii/S0016703711001438?via%3Dihub
smooth_diff <- function(model, newdata, f1, f2, var, alpha = 0.05,
                        unconditional = FALSE) {
  xp <- predict(model, newdata = newdata, type = 'lpmatrix')

```

```

c1 <- grepl(f1, colnames(xp))
c2 <- grepl(f2, colnames(xp))
r1 <- newdata[[var]] == f1
r2 <- newdata[[var]] == f2
## difference rows of xp for data from comparison
X <- xp[r1, ] - xp[r2, ]
## zero out cols of X related to splines for other lochs
X[, ! (c1 | c2)] <- 0
## zero out the parametric cols
X[, !grepl('s\\|', colnames(xp))] <- 0
dif <- X %*% coef(model)
se <- sqrt(rowSums((X %*% vcov(model, unconditional = unconditional)) *
  X))
crit <- qt(alpha/2, df.residual(model), lower.tail = FALSE)
upr <- dif + (crit * se)
lwr <- dif - (crit * se)
data.frame(pair = paste(f1, f2, sep = '-'),
           diff = dif,
           se = se,
           upper = upr,
           lower = lwr)
}
# select only necessary columns
ChAOS_Scenarios_BPc_GAM <- ChAOS_Scenarios_BPc %>%
  select(BPc, Nsp, Nsp_active, Scenario) %>%
  filter(complete.cases(.))

hist(ChAOS_Scenarios_BPc_GAM$BPc)

# Max Nsp_active is specific for each scenario (stations have different
# starting species richness)
# Also, species richness increases beyond starting community due to inco-
# ming compensating species > species going extinct
max(ChAOS_Scenarios_BPc_GAM[which(ChAOS_Scenarios_BPc_GAM$Scenario == "B
17-B16")],]$Nsp_active) #61
max(ChAOS_Scenarios_BPc_GAM[which(ChAOS_Scenarios_BPc_GAM$Scenario == "B
16-B15")],]$Nsp_active) #53
max(ChAOS_Scenarios_BPc_GAM[which(ChAOS_Scenarios_BPc_GAM$Scenario == "B
15-Xs")],]$Nsp_active) #47
max(ChAOS_Scenarios_BPc_GAM[which(ChAOS_Scenarios_BPc_GAM$Scenario == "X
s-B14")],]$Nsp_active) #68
max(ChAOS_Scenarios_BPc_GAM[which(ChAOS_Scenarios_BPc_GAM$Scenario == "B
14-B13")],]$Nsp_active) #54
max(ChAOS_Scenarios_BPc_GAM[which(ChAOS_Scenarios_BPc_GAM$Scenario == "B
17-B13")],]$Nsp_active) #71

## GAM model with interactive term ----
GAM1.1<-gam(BPc~s(Nsp_active, by= Scenario)+Scenario,
              data=ChAOS_Scenarios_BPc_GAM)

ChAOS_Scenarios_BPc_GAM <- ChAOS_Scenarios_BPc_GAM %>%
  mutate(Scenario = factor(Scenario)) %>%
  mutate(Scenario = fct_relevel(Scenario, c("B17-B13", "B17-B16", "B16-B
15", "B15-Xs", "Xs-B14", "B14-B13")))
  levels(ChAOS_Scenarios_BPc_GAM$Scenario)

```

```

# Parametric coefficients are currently for ANOVAs of mean values between
# n B17-B13 and all other scenarios. Need releveling if want to do all pairwise
# comparisons.
# edf: effective degrees of freedom of smooth terms. This value represents the complexity of the smooth.
# An edf of 1 is equivalent to a straight line between x and y. An edf of 2 is equivalent to a quadratic curve, and so on, with higher edfs describing more wiggly curves.
# The Ref.df and F columns are test statistics used in an ANOVA test to test overall significance of the smooth.
# a significant smooth term is one where you can not draw a horizontal line through the 95% confidence interval.

AIC(GAM1.1)
sink("ChAOS_ExtScn_GAM_summary.txt")
print(summary(GAM1.1))
sink()

tiff("ChAOS_ExtScn_GAM_plots.tiff", units="in", width=10, height=10, res=600)
plot(GAM1.1, pages = 1, all.terms = TRUE, residuals = TRUE, seWithMean = TRUE, shift = coef(GAM1.1)[1], trans = log, ylim = c(-2,10))
dev.off()

## Then for the prediction; dummy data ----
# There are six Scenario factors and Nsp_active from 1 to total number of species for each scenario

DUMDAT<-data.frame(Scenario= factor(c(rep('B17-B16', 200),
                                         rep('B16-B15', 200),
                                         rep('B15-Xs', 200),
                                         rep('Xs-B14', 200),
                                         rep('B14-B13', 200),
                                         rep('B17-B13', 200)))
                                         ),
                     Nsp_active=c(rep(seq(from=1, to=61, length=200)),
                                 rep(seq(from=1, to=53, length=200)),
                                 rep(seq(from=1, to=47, length=200)),
                                 rep(seq(from=1, to=68, length=200)),
                                 rep(seq(from=1, to=54, length=200)),
                                 rep(seq(from=1, to=71, length=200)))
                     ))

# Check that the species richness matches the scenario
max(DUMDAT[which(DUMDAT$Scenario == "B17-B16"),]$Nsp_active) #61
max(DUMDAT[which(DUMDAT$Scenario == "B16-B15"),]$Nsp_active) #53
max(DUMDAT[which(DUMDAT$Scenario == "B15-Xs"),]$Nsp_active) #47
max(DUMDAT[which(DUMDAT$Scenario == "Xs-B14"),]$Nsp_active) #68
max(DUMDAT[which(DUMDAT$Scenario == "B14-B13"),]$Nsp_active) #54
max(DUMDAT[which(DUMDAT$Scenario == "B17-B13"),]$Nsp_active) #71

## Predict and bind dummy data and prediction ----

P1.1<-predict(GAM1.1, newdata=DUMDAT, se=T)

```

```

PRED1.1<-cbind(DUMDAT,P1.1)

PRED1.1$Scenario <- factor(PRED1.1$Scenario, levels = c("B17-B16", "B16-B15", "B15-Xs", "Xs-B14", "B14-B13", "B17-B13"))

## Pairwise comparison of factor-smooth interactions in the GAMS-----
COMP1.1 <- smooth_diff(GAM1.1, DUMDAT, "B17-B16", "B16-B15", "Scenario", unconditional = T)
COMP1.2 <- smooth_diff(GAM1.1, DUMDAT, "B17-B16", "B15-Xs", "Scenario", unconditional = T)
COMP1.3 <- smooth_diff(GAM1.1, DUMDAT, "B17-B16", "Xs-B14", "Scenario", unconditional = T)
COMP1.4 <- smooth_diff(GAM1.1, DUMDAT, "B17-B16", "B14-B13", "Scenario", unconditional = T)
COMP1.5 <- smooth_diff(GAM1.1, DUMDAT, "B17-B16", "B17-B13", "Scenario", unconditional = T)

COMP2.1 <- smooth_diff(GAM1.1, DUMDAT, "B16-B15", "B15-Xs", "Scenario", unconditional = T)
COMP2.2 <- smooth_diff(GAM1.1, DUMDAT, "B16-B15", "Xs-B14", "Scenario", unconditional = T)
COMP2.3 <- smooth_diff(GAM1.1, DUMDAT, "B16-B15", "B14-B13", "Scenario", unconditional = T)
COMP2.4 <- smooth_diff(GAM1.1, DUMDAT, "B16-B15", "B17-B13", "Scenario", unconditional = T)

COMP3.1 <- smooth_diff(GAM1.1, DUMDAT, "B15-Xs", "Xs-B14", "Scenario", unconditional = T)
COMP3.2 <- smooth_diff(GAM1.1, DUMDAT, "B15-Xs", "B14-B13", "Scenario", unconditional = T)
COMP3.3 <- smooth_diff(GAM1.1, DUMDAT, "B15-Xs", "B17-B13", "Scenario", unconditional = T)

COMP4.1 <- smooth_diff(GAM1.1, DUMDAT, "Xs-B14", "B14-B13", "Scenario", unconditional = T)
COMP4.2 <- smooth_diff(GAM1.1, DUMDAT, "Xs-B14", "B17-B13", "Scenario", unconditional = T)

COMP5.1 <- smooth_diff(GAM1.1, DUMDAT, "B14-B13", "B17-B13", "Scenario", unconditional = T)

COMPall <- cbind(Nsp_active=c(rep(seq(from=1, to=61, length=200),5),
                                rep(seq(from=1, to=53, length=200),4),
                                rep(seq(from=1, to=47, length=200),3),
                                rep(seq(from=1, to=68, length=200),2),
                                rep(seq(from=1, to=54, length=200),1),
                                ),
                                rbind(COMP1.1, COMP1.2, COMP1.3, COMP1.4, COMP1.5,
                                       COMP2.1, COMP2.2, COMP2.3, COMP2.4,
                                       COMP3.1, COMP3.2, COMP3.3,
                                       COMP4.1, COMP4.2,

```

```

COMP5.1))

## Pairwise comparision plotting ----
design <- "
A#####
BF#####
CGJ##
DHKM#
EILNO
"

library(ggh4x)

ChAOS_ExtScn_GAM_pairwise_plot <- ggplot(COMPall, aes(x = Nsp_active, y
= diff, group = pair)) +
  geom_ribbon(aes(ymin = lower, ymax = upper), alpha = 0.2) +
  geom_line() +
  geom_hline(yintercept = 0, linetype = 2) +
  scale_y_continuous(limits = c(-1000,1000)) +
  facet_manual(vars(pair), design = design, axes = "all", remove_labels
= "all") +
  coord_cartesian() +
  labs(x = "Species richness", y = 'Difference in BPc trend') +
  theme_classic() +
  theme(legend.position="none",
        axis.text.x = element_text(size=9),
        axis.text.y = element_text(size=9),
        plot.title = element_text(hjust = 0.5, size = 9),
        plot.subtitle = element_text(hjust = 0.5, size = 9),
        panel.grid.major = element_blank(), panel.grid.minor = element_b
lank(),
        panel.background = element_blank(), axis.line.x.bottom = element_
line(colour = "black"), axis.line.y.left = element_line(colour = "black
"),
        axis.line.x.top = element_blank(), axis.line.y.right = element_b
lank(),
        axis.ticks.x.top = element_blank(), axis.text.x.top = element_b
lank(),
        axis.ticks.y.right = element_blank(), axis.text.y.right = elemen
t_blank(),
        axis.text.x.bottom = element_text(angle = 45, hjust = 1),
        strip.background = element_blank()))

ggsave("ChAOS_ExtScn_GAM_pairwise_plot.png",
       plot = ChAOS_ExtScn_GAM_pairwise_plot,
       height = 30,
       width = 26,
       unit = "cm",
       dpi = 600,
       path = Graphs_folder)

## Plotting ----

ggplot(PRED1.1,aes(x=Nsp_active,y=log(fit), colour=Scenario, group=Scena
rio, fill=Scenario))+
  geom_line()+
  geom_ribbon(aes(ymin= log(fit) + 1.96*(log(se.fit)),
                  ymax= log(fit) - 1.96*(log(se.fit))),alpha=.3)+
```

```

theme_classic()+
  scale_y_continuous(name = "", limits = c(-2,10))+ 
  scale_x_continuous(limits=c(0,71), name="Species richness")+
  # facet_wrap(~Scenario) +
  theme(legend.position="right",
        axis.text.x = element_text(size=9),
        axis.text.y = element_text(size=9))+ 
  scale_colour_discrete(name="Climate\nScenario",
                        breaks=c("B17-B16", "B16-B15", "B15-Xs", "Xs-B14",
                                "B14-B13", "B17-B13")),
                        labels=c("B17-B16", "B16-B15", "B15-Xs", "Xs-B14",
                                "B14-B13", "B17-B13"))+
  scale_fill_discrete(name="Climate\nScenario",
                        breaks=c("B17-B16", "B16-B15", "B15-Xs", "Xs-B14",
                                "B14-B13", "B17-B13"),
                        labels=c("B17-B16", "B16-B15", "B15-Xs", "Xs-B14",
                                "B14-B13", "B17-B13"))

## Logged and facet_wrap ----
BPc.A <- ggplot(PRED1.1,aes(x=Nsp_active,y=log(fit), colour=Scenario, group=Scenario, fill=Scenario)) +
  geom_vline(data=filter(PRED1.1, Scenario=="B17-B16"), aes(xintercept=52), lty=2) + # starting community sp.richness
  geom_vline(data=filter(PRED1.1, Scenario=="B16-B15"), aes(xintercept=42), lty=2) + # starting community sp.richness
  geom_vline(data=filter(PRED1.1, Scenario=="B15-Xs"), aes(xintercept=40), lty=2) + # starting community sp.richness
  geom_vline(data=filter(PRED1.1, Scenario=="Xs-B14"), aes(xintercept=41), lty=2) + # starting community sp.richness
  geom_vline(data=filter(PRED1.1, Scenario=="B14-B13"), aes(xintercept=27), lty=2) + # starting community sp.richness
  geom_vline(data=filter(PRED1.1, Scenario=="B17-B13"), aes(xintercept=52), lty=2) + # starting community sp.richness
  geom_line()+
  geom_ribbon(aes(ymin= log(fit) + 1.96*(log(se.fit)),
                  ymax= log(fit) - 1.96*(log(se.fit))),alpha=.3)+ 
  theme_bw()+
  scale_y_continuous(name = "log(BPc)")+
  scale_x_continuous(limits=c(0,71), name="Species richness")+
  facet_grid(~Scenario) +
  theme(legend.position="right",
        axis.text.x = element_text(size=9),
        axis.text.y = element_text(size=9))+ 
  scale_colour_discrete(name="Climate\nScenario",
                        breaks=c("B17-B16", "B16-B15", "B15-Xs", "Xs-B14",
                                "B14-B13", "B17-B13")),
                        labels=c("B17-B16", "B16-B15", "B15-Xs", "Xs-B14",
                                "B14-B13", "B17-B13"))+
  scale_fill_discrete(name="Climate\nScenario",
                        breaks=c("B17-B16", "B16-B15", "B15-Xs", "Xs-B14",
                                "B14-B13", "B17-B13"),
                        labels=c("B17-B16", "B16-B15", "B15-Xs", "Xs-B14",
                                "B14-B13", "B17-B13"))

### Add space between local scenarios and region-wide scenario (B17-B13)
----
```

```
gt = ggplot_gtable(ggplot_build(BPc.A))
gt$widths[14] = 4*gt$widths[1]
grid.draw(gt)
```

### E.1.10 Code S8: Model output figures

```
# Import output data from model simulations #####
# Full model (co-extinctions and co-compensations)
B17_B16_BPc <- read.csv(file.choose())
B17_B16_Contributions <- readRDS(file.choose())
B16_B15_BPc <- read.csv(file.choose())
B16_B15_Contributions <- readRDS(file.choose())
B15_Xs_BPc <- read.csv(file.choose())
B15_Xs_Contributions <- readRDS(file.choose())
Xs_B14_BPc <- read.csv(file.choose())
Xs_B14_Contributions <- readRDS(file.choose())
B14_B13_BPc <- read.csv(file.choose())
B14_B13_Contributions <- readRDS(file.choose())
B17_B13_BPc <- read.csv(file.choose())
B17_B13_Contributions <- readRDS(file.choose())

# Reduced model (co-extinctions and no compensations)
B17_B16_CoExt_NoComp_BPc <- read.csv(file.choose())
B17_B16_CoExt_NoComp_Contributions <- readRDS(file.choose())
B16_B15_CoExt_NoComp_BPc <- read.csv(file.choose())
B16_B15_CoExt_NoComp_Contributions <- readRDS(file.choose())
B15_Xs_CoExt_NoComp_BPc <- read.csv(file.choose())
B15_Xs_CoExt_NoComp_Contributions <- readRDS(file.choose())
Xs_B14_CoExt_NoComp_BPc <- read.csv(file.choose())
Xs_B14_CoExt_NoComp_Contributions <- readRDS(file.choose())
B14_B13_CoExt_NoComp_BPc <- read.csv(file.choose())
B14_B13_CoExt_NoComp_Contributions <- readRDS(file.choose())
B17_B13_CoExt_NoComp_BPc <- read.csv(file.choose())
B17_B13_CoExt_NoComp_Contributions <- readRDS(file.choose())

# Simple model (no co-extinctions and no compensations)
B17_B16_NoCoExt_NoComp_BPc <- read.csv(file.choose())
B17_B16_NoCoExt_NoComp_Contributions <- readRDS(file.choose())
B16_B15_NoCoExt_NoComp_BPc <- read.csv(file.choose())
B16_B15_NoCoExt_NoComp_Contributions <- readRDS(file.choose())
B15_Xs_NoCoExt_NoComp_BPc <- read.csv(file.choose())
B15_Xs_NoCoExt_NoComp_Contributions <- readRDS(file.choose())
Xs_B14_NoCoExt_NoComp_BPc <- read.csv(file.choose())
Xs_B14_NoCoExt_NoComp_Contributions <- readRDS(file.choose())
B14_B13_NoCoExt_NoComp_BPc <- read.csv(file.choose())
B14_B13_NoCoExt_NoComp_Contributions <- readRDS(file.choose())
B17_B13_NoCoExt_NoComp_BPc <- read.csv(file.choose())
B17_B13_NoCoExt_NoComp_Contributions <- readRDS(file.choose())

# Figure 1: No coextinctions, no compensations, full models #####
plot1 <- ggplot(B17_B16_NoCoExt_NoComp_BPc, aes(x=Nsp_active, y=log(BPc)))
+
  geom_point(colour="grey", alpha=0.5) +
  stat_density2d(aes(fill=..level.., alpha=..level..),
```

```

        size=3, bins=20, geom='polygon') +
  geom_vline(xintercept = 17, col = "red", linetype = "dashed", size = 0
.8) +
  geom_vline(xintercept = 52, col = "green", size = 0.8) +
  scale_x_continuous(limits = c(0,70)) +
  scale_y_continuous(limits = c(-2,8)) +
  geom_text(size = 12, x = 60, y = -0.1, label = "a") +
  theme_classic()+
  theme(legend.position = "none", panel.grid.major = element_blank(), pa
nel.grid.minor = element_blank(),
        panel.background = element_blank(), axis.line = element_line(col
our = "black")) +
  labs(x = "Species richness",
       y = "log(BPc)")

plot2 <- ggplot(B17_B16_CoExt_NoComp_BPc,aes(x=Nsp_active,y=log(BPc)))+
  geom_point(colour="grey",alpha=0.5)+
  stat_density2d(aes(fill=..level.., alpha=..level..),
                 size=3, bins=20, geom='polygon') +
  geom_vline(xintercept = 17, col = "red", linetype = "dashed", size = 0
.8) +
  geom_vline(xintercept = 52, col = "green", size = 0.8) +
  scale_x_continuous(limits = c(0,70)) +
  scale_y_continuous(limits = c(-2,8)) +
  geom_text(size = 12, x = 60, y = -0.1, label = "g") +
  theme_classic()+
  theme(legend.position = "none", panel.grid.major = element_blank(), pa
nel.grid.minor = element_blank(),
        panel.background = element_blank(), axis.line = element_line(col
our = "black")) +
  labs(x = "Species richness",
       y = "log(BPc)")

plot3 <- ggplot(B17_B16_BPc,aes(x=Nsp_active,y=log(BPc)))+
  geom_point(colour="grey",alpha=0.5)+
  stat_density2d(aes(fill=..level.., alpha=..level..),
                 size=3, bins=20, geom='polygon') +
  geom_vline(xintercept = 17, col = "red", linetype = "dashed", size = 0
.8) +
  geom_vline(xintercept = 52, col = "green", size = 0.8) +
  scale_x_continuous(limits = c(0,70)) +
  scale_y_continuous(limits = c(-2,8)) +
  geom_text(size = 12, x = 60, y = -0.1, label = "m") +
  theme_classic()+
  theme(legend.position = "none", panel.grid.major = element_blank(), pa
nel.grid.minor = element_blank(),
        panel.background = element_blank(), axis.line = element_line(col
our = "black")) +
  labs(x = "Species richness",
       y = "log(BPc)")

plot4 <- ggplot(B16_B15_NoCoExt_NoComp_BPc,aes(x=Nsp_active,y=log(BPc)))
+
  geom_point(colour="grey",alpha=0.5)+
  stat_density2d(aes(fill=..level.., alpha=..level..),
                 size=3, bins=20, geom='polygon') +

```

```

geom_vline(xintercept = 15, col = "red", linetype = "dashed", size = 0
.8) +
geom_vline(xintercept = 42, col = "green", size = 0.8) +
scale_x_continuous(limits = c(0,70)) +
scale_y_continuous(limits = c(-2,8)) +
  geom_text(size = 12, x = 60, y = -0.1, label = "b") +
theme_classic()+
  theme(legend.position = "none", panel.grid.major = element_blank(), pa
nel.grid.minor = element_blank(),
        panel.background = element_blank(), axis.line = element_line(col
our = "black")) +
  labs(x = "Species richness",
       y = "log(BPc)")

plot5 <- ggplot(B16_B15_CoExt_NoComp_BPc,aes(x=Nsp_active,y=log(BPc)))+
  geom_point(colour="grey",alpha=0.5)+
  stat_density2d(aes(fill=..level.., alpha=..level..),
                 size=3, bins=20, geom='polygon') +
  geom_vline(xintercept = 15, col = "red", linetype = "dashed", size = 0
.8) +
  geom_vline(xintercept = 42, col = "green", size = 0.8) +
  scale_x_continuous(limits = c(0,70)) +
  scale_y_continuous(limits = c(-2,8)) +
  geom_text(size = 12, x = 60, y = -0.1, label = "h") +
  theme_classic()+
  theme(legend.position = "none", panel.grid.major = element_blank(), pa
nel.grid.minor = element_blank(),
        panel.background = element_blank(), axis.line = element_line(col
our = "black")) +
  labs(x = "Species richness",
       y = "log(BPc)")

plot6 <- ggplot(B16_B15_BPc,aes(x=Nsp_active,y=log(BPc)))+
  geom_point(colour="grey",alpha=0.5)+
  stat_density2d(aes(fill=..level.., alpha=..level..),
                 size=3, bins=20, geom='polygon') +
  geom_vline(xintercept = 15, col = "red", linetype = "dashed", size = 0
.8) +
  geom_vline(xintercept = 42, col = "green", size = 0.8) +
  scale_x_continuous(limits = c(0,70)) +
  scale_y_continuous(limits = c(-2,8)) +
  geom_text(size = 12, x = 60, y = -0.1, label = "n") +
  theme_classic()+
  theme(legend.position = "none", panel.grid.major = element_blank(), pa
nel.grid.minor = element_blank(),
        panel.background = element_blank(), axis.line = element_line(col
our = "black")) +
  labs(x = "Species richness",
       y = "log(BPc)")

plot7 <- ggplot(B15_Xs_NoCoExt_NoComp_BPc,aes(x=Nsp_active,y=log(BPc)))+
  geom_point(colour="grey",alpha=0.5)+
  stat_density2d(aes(fill=..level.., alpha=..level..),
                 size=3, bins=20, geom='polygon') +
  geom_vline(xintercept = 16, col = "red", linetype = "dashed", size = 0
.8) +

```

```

geom_vline(xintercept = 40, col = "green", size = 0.8) +
  scale_x_continuous(limits = c(0,70)) +
  scale_y_continuous(limits = c(-2,8)) +
  geom_text(size = 12, x = 60, y = -0.1, label = "c") +
  theme_classic()+
  theme(legend.position = "none", panel.grid.major = element_blank(), panel.grid.minor = element_blank(),
        panel.background = element_blank(), axis.line = element_line(colour = "black")) +
  labs(x = "Species richness",
       y = "log(BPc)")

plot8 <- ggplot(B15_Xs_CoExt_NoComp_BPc,aes(x=Nsp_active,y=log(BPc)))+
  geom_point(colour="grey",alpha=0.5)+
  stat_density2d(aes(fill=..level.., alpha=..level..),
                 size=3, bins=20, geom='polygon') +
  geom_vline(xintercept = 16, col = "red", linetype = "dashed", size = 0.8) +
  geom_vline(xintercept = 40, col = "green", size = 0.8) +
  scale_x_continuous(limits = c(0,70)) +
  scale_y_continuous(limits = c(-2,8)) +
  geom_text(size = 12, x = 60, y = -0.1, label = "i") +
  theme_classic()+
  theme(legend.position = "none", panel.grid.major = element_blank(), panel.grid.minor = element_blank(),
        panel.background = element_blank(), axis.line = element_line(colour = "black")) +
  labs(x = "Species richness",
       y = "log(BPc)")

plot9 <- ggplot(B15_Xs_BPc,aes(x=Nsp_active,y=log(BPc)))+
  geom_point(colour="grey",alpha=0.5)+
  stat_density2d(aes(fill=..level.., alpha=..level..),
                 size=3, bins=20, geom='polygon') +
  geom_vline(xintercept = 16, col = "red", linetype = "dashed", size = 0.8) +
  geom_vline(xintercept = 40, col = "green", size = 0.8) +
  scale_x_continuous(limits = c(0,70)) +
  scale_y_continuous(limits = c(-2,8)) +
  geom_text(size = 12, x = 60, y = -0.1, label = "o") +
  theme_classic()+
  theme(legend.position = "none", panel.grid.major = element_blank(), panel.grid.minor = element_blank(),
        panel.background = element_blank(), axis.line = element_line(colour = "black")) +
  labs(x = "Species richness",
       y = "log(BPc)")

plot10 <- ggplot(Xs_B14_NoCoExt_NoComp_BPc,aes(x=Nsp_active,y=log(BPc)))+
  geom_point(colour="grey",alpha=0.5)+
  stat_density2d(aes(fill=..level.., alpha=..level..),
                 size=3, bins=20, geom='polygon') +
  geom_vline(xintercept = 10, col = "red", linetype = "dashed", size = 0.8) +
  geom_vline(xintercept = 41, col = "green", size = 0.8) +

```

```

scale_x_continuous(limits = c(0,70)) +
scale_y_continuous(limits = c(-2,8)) +
  geom_text(size = 12, x = 60, y = -0.1, label = "d") +
theme_classic()+
  theme(legend.position = "none", panel.grid.major = element_blank(), pa
nel.grid.minor = element_blank(),
        panel.background = element_blank(), axis.line = element_line(col
our = "black")) +
  labs(x = "Species richness",
       y = "log(BPc)")

plot11 <- ggplot(Xs_B14_CoExt_NoComp_BPc,aes(x=Nsp_active,y=log(BPc)))+
  geom_point(colour="grey",alpha=0.5)+
  stat_density2d(aes(fill=..level.., alpha=..level..),
                 size=3, bins=20, geom='polygon') +
  geom_vline(xintercept = 10, col = "red", linetype = "dashed", size = 0
.8) +
  geom_vline(xintercept = 41, col = "green", size = 0.8) +
  scale_x_continuous(limits = c(0,70)) +
  scale_y_continuous(limits = c(-2,8)) +
  geom_text(size = 12, x = 60, y = -0.1, label = "j") +
theme_classic()+
  theme(legend.position = "none", panel.grid.major = element_blank(), pa
nel.grid.minor = element_blank(),
        panel.background = element_blank(), axis.line = element_line(col
our = "black")) +
  labs(x = "Species richness",
       y = "log(BPc)")

plot12 <- ggplot(Xs_B14_BPc,aes(x=Nsp_active,y=log(BPc)))+
  geom_point(colour="grey",alpha=0.5)+
  stat_density2d(aes(fill=..level.., alpha=..level..),
                 size=3, bins=20, geom='polygon') +
  geom_vline(xintercept = 10, col = "red", linetype = "dashed", size = 0
.8) +
  geom_vline(xintercept = 41, col = "green", size = 0.8) +
  scale_x_continuous(limits = c(0,70)) +
  scale_y_continuous(limits = c(-2,8)) +
  geom_text(size = 12, x = 60, y = -0.1, label = "p") +
theme_classic()+
  theme(legend.position = "none", panel.grid.major = element_blank(), pa
nel.grid.minor = element_blank(),
        panel.background = element_blank(), axis.line = element_line(col
our = "black")) +
  labs(x = "Species richness",
       y = "log(BPc)")

plot13 <- ggplot(B14_B13_NoCoExt_NoComp_BPc,aes(x=Nsp_active,y=log(BPc))
)+

  geom_point(colour="grey",alpha=0.5)+
  stat_density2d(aes(fill=..level.., alpha=..level..),
                 size=3, bins=20, geom='polygon') +
  geom_vline(xintercept = 11, col = "red", linetype = "dashed", size = 0
.8) +
  geom_vline(xintercept = 27, col = "green", size = 0.8) +
  scale_x_continuous(limits = c(0,70)) +

```

```

scale_y_continuous(limits = c(-2,8)) +
  geom_text(size = 12, x = 60, y = -0.1, label = "e") +
  theme_classic()+
  theme(legend.position = "none", panel.grid.major = element_blank(), panel.grid.minor = element_blank(),
        panel.background = element_blank(), axis.line = element_line(colour = "black")) +
  labs(x = "Species richness",
       y = "log(BPc)")

plot14 <- ggplot(B14_B13_CoExt_NoComp_BPc,aes(x=Nsp_active,y=log(BPc)))+
  geom_point(colour="grey",alpha=0.5)+
  stat_density2d(aes(fill=..level.., alpha=..level..),
                 size=3, bins=20, geom='polygon') +
  geom_vline(xintercept = 11, col = "red", linetype = "dashed", size = 0.8) +
  geom_vline(xintercept = 27, col = "green", size = 0.8) +
  scale_x_continuous(limits = c(0,70)) +
  scale_y_continuous(limits = c(-2,8)) +
  geom_text(size = 12, x = 60, y = -0.1, label = "k") +
  theme_classic()+
  theme(legend.position = "none", panel.grid.major = element_blank(), panel.grid.minor = element_blank(),
        panel.background = element_blank(), axis.line = element_line(colour = "black")) +
  labs(x = "Species richness",
       y = "log(BPc)")

plot15 <- ggplot(B14_B13_BPc,aes(x=Nsp_active,y=log(BPc)))+
  geom_point(colour="grey",alpha=0.5)+
  stat_density2d(aes(fill=..level.., alpha=..level..),
                 size=3, bins=20, geom='polygon') +
  geom_vline(xintercept = 11, col = "red", linetype = "dashed", size = 0.8) +
  geom_vline(xintercept = 27, col = "green", size = 0.8) +
  scale_x_continuous(limits = c(0,70)) +
  scale_y_continuous(limits = c(-2,8)) +
  geom_text(size = 12, x = 60, y = -0.1, label = "q") +
  theme_classic()+
  theme(legend.position = "none", panel.grid.major = element_blank(), panel.grid.minor = element_blank(),
        panel.background = element_blank(), axis.line = element_line(colour = "black")) +
  labs(x = "Species richness",
       y = "log(BPc)")

plot16 <- ggplot(B17_B13_NoCoExt_NoComp_BPc,aes(x=Nsp_active,y=log(BPc)))+
  geom_point(colour="grey",alpha=0.5)+
  stat_density2d(aes(fill=..level.., alpha=..level..),
                 size=3, bins=20, geom='polygon') +
  geom_vline(xintercept = 11, col = "red", linetype = "dashed", size = 0.8) +
  geom_vline(xintercept = 52, col = "green", size = 0.8) +
  scale_x_continuous(limits = c(0,70)) +
  scale_y_continuous(limits = c(-2,8)) +

```

```

  geom_text(size = 12, x = 60, y = -0.1, label = "f") +
  theme_classic()+
  theme(legend.position = "none", panel.grid.major = element_blank(), pa
nel.grid.minor = element_blank(),
        panel.background = element_blank(), axis.line = element_line(col
our = "black")) +
  labs(x = "Species richness",
       y = "log(BPc)")

plot17 <- ggplot(B17_B13_CoExt_NoComp_BPc,aes(x=Nsp_active,y=log(BPc)))+
  geom_point(colour="grey",alpha=0.5)+
  stat_density2d(aes(fill=..level.., alpha=..level..),
                 size=3, bins=20, geom='polygon') +
  geom_vline(xintercept = 11, col = "red", linetype = "dashed", size = 0
.8) +
  geom_vline(xintercept = 52, col = "green", size = 0.8) +
  scale_x_continuous(limits = c(0,70)) +
  scale_y_continuous(limits = c(-2,8)) +
  geom_text(size = 12, x = 60, y = -0.1, label = "l") +
  theme_classic()+
  theme(legend.position = "none", panel.grid.major = element_blank(), pa
nel.grid.minor = element_blank(),
        panel.background = element_blank(), axis.line = element_line(col
our = "black")) +
  labs(x = "Species richness",
       y = "log(BPc)")

plot18 <- ggplot(B17_B13_BPc,aes(x=Nsp_active,y=log(BPc)))+
  geom_point(colour="grey",alpha=0.5)+
  stat_density2d(aes(fill=..level.., alpha=..level..),
                 size=3, bins=20, geom='polygon') +
  geom_vline(xintercept = 11, col = "red", linetype = "dashed", size = 0
.8) +
  geom_vline(xintercept = 52, col = "green", size = 0.8) +
  scale_x_continuous(limits = c(0,70)) +
  scale_y_continuous(limits = c(-2,8)) +
  geom_text(size = 12, x = 60, y = -0.1, label = "r") +
  theme_classic()+
  theme(legend.position = "none", panel.grid.major = element_blank(), pa
nel.grid.minor = element_blank(),
        panel.background = element_blank(), axis.line = element_line(col
our = "black")) +
  labs(x = "Species richness",
       y = "log(BPc)")

ylab0 <- "Extinctions ordered by....."

Super_BPc_plot <- wrap_elements(grid::textGrob("B17-B16", vjust = 5, ro
t = 0, gp = grid::gpar(fontsize = 16))) + wrap_elements(grid::textGrob(
"B16-B15", vjust = 5, rot = 0, gp = grid::gpar(fontsize = 16))) +
  wrap_elements(grid::textGrob("B15-Xs", vjust = 5, rot = 0, gp = grid::
gpar(fontsize = 16))) +
  wrap_elements(grid::textGrob("Xs-B14", vjust = 5, rot = 0, gp = grid::
gpar(fontsize = 16))) +
  wrap_elements(grid::textGrob("B14-B13", vjust = 5, rot = 0, gp = grid:
:gpar(fontsize = 16))) + plot_spacer() +

```

```

  wrap_elements(grid::textGrob("B17-B13", vjust = 5, rot = 0, gp = grid::gpar(fontsize = 16))) +
  plot_spacer() +
  (plot1 & theme(axis.title.x = element_blank(),
                 axis.title.y = element_blank(),
                 axis.text.x = element_blank(),
                 axis.text.y = element_text(size = 16))) +
  (plot4 & theme(axis.title.x = element_blank(),
                 axis.title.y = element_blank(),
                 axis.text.x = element_blank(),
                 axis.text.y = element_blank())) +
  (plot7 & theme(axis.title.x = element_blank(),
                 axis.title.y = element_blank(),
                 axis.text.x = element_blank(),
                 axis.text.y = element_blank())) +
  (plot10 & theme(axis.title.x = element_blank(),
                  axis.title.y = element_blank(),
                  axis.text.x = element_blank(),
                  axis.text.y = element_blank())) +
  (plot13 & theme(axis.title.x = element_blank(),
                  axis.title.y = element_blank(),
                  axis.text.x = element_blank(),
                  axis.text.y = element_blank())) + plot_spacer() +
  (plot16 & theme(axis.title.x = element_blank(),
                  axis.title.y = element_blank(),
                  axis.text.x = element_blank(),
                  axis.text.y = element_text(size = 16))) +
  wrap_elements(grid::textGrob("Climate vulnerability", vjust = 4, rot = -90, gp = grid::gpar(fontsize = 16))) +
  (plot2 & theme(axis.title.x = element_blank(),
                 axis.title.y = element_blank(),
                 axis.text.x = element_blank(),
                 axis.text.y = element_text(size = 16))) +
  (plot5 & theme(axis.title.x = element_blank(),
                 axis.title.y = element_blank(),
                 axis.text.x = element_blank(),
                 axis.text.y = element_blank())) +
  (plot8 & theme(axis.title.x = element_blank(),
                 axis.title.y = element_blank(),
                 axis.text.x = element_blank(),
                 axis.text.y = element_blank())) +
  (plot11 & theme(axis.title.x = element_blank(),
                  axis.title.y = element_blank(),
                  axis.text.x = element_blank(),
                  axis.text.y = element_blank())) +
  (plot14 & theme(axis.title.x = element_blank(),
                  axis.title.y = element_blank(),
                  axis.text.x = element_blank(),
                  axis.text.y = element_blank())) + plot_spacer()
+
  (plot17 & theme(axis.title.x = element_blank(),
                  axis.title.y = element_blank(),
                  axis.text.x = element_blank(),
                  axis.text.y = element_text(size = 16))) +
  wrap_elements(grid::textGrob("Climate vulnerability \n and co-extinctions", vjust = 1.8, rot = -90, gp = grid::gpar(fontsize = 16))) +

```

```

(plot3 & theme(axis.title.x = element_blank(),
               axis.title.y = element_blank(),
               axis.text.x = element_text(size = 16),
               axis.text.y = element_text(size = 16))) +
(plot6 & theme(axis.title.x = element_blank(),
               axis.title.y = element_blank(),
               axis.text.x = element_text(size = 16),
               axis.text.y = element_blank())) +
(plot9 & theme(axis.title.x = element_blank(),
               axis.title.y = element_blank(),
               axis.text.x = element_text(size = 16),
               axis.text.y = element_blank())) +
(plot12 & theme(axis.title.x = element_blank(),
                 axis.title.y = element_blank(),
                 axis.text.x = element_text(size = 16),
                 axis.text.y = element_blank())) +
(plot15 & theme(axis.title.x = element_blank(),
                 axis.title.y = element_blank(),
                 axis.text.x = element_text(size = 16),
                 axis.text.y = element_blank())) + plot_spacer() +
(plot18 & theme(axis.title.x = element_blank(),
                 axis.title.y = element_blank(),
                 axis.text.x = element_text(size = 16),
                 axis.text.y = element_text(size = 16))) +
wrap_elements(grid::textGrob("Climate vulnerability, \n co-extinctions and \n co-compensations", vjust = 1.2, rot = -90, gp = grid::gpar(fontsize = 16))) +
plot_layout(ncol = 8, nrow = 4, widths = c(1,1,1,1,1,0.3,1,1))

# Super_BPc_plot & theme(axis.title.x = element_blank(),
#                         axis.title.y = element_blank(),
#                         axis.text.x = element_text(size = 6),
#                         axis.text.y = element_text(size = 6))

ggsave(
  "2018_all_models_BPc_superplot.tiff",
  plot = Super_BPc_plot,
  device = tiff,
  scale = 2,
  width = 24,
  height = 12,
  units = c("cm"),
  dpi = 300
)

# Figure 2: GAMS, compensation graphs #####
## GAMS #####
split_GAMs <- split(PRED1.1, PRED1.1$Scenario)

B17_B16_GAM <- ggplot(split_GAMs[["B17-B16"]], aes(x=Nsp_active, y=log(fit)))+
  geom_vline(aes(xintercept=52), lty=1, col="green", size = 0.8) +
  geom_vline(aes(xintercept=17), lty=2, col="red", size = 0.8) +
  geom_line(col = "blue") +
  geom_ribbon(aes(ymin= log(fit) + 1.96*(log(se.fit)),

```

```

        ymax= log(fit) - 1.96*(log(se.fit))), alpha=.3, fill =
"blue")+
  theme_classic()+
  theme(axis.line.y = element_line()) +
  scale_y_continuous(name = "log(BPc)", limits = c(-1,16), breaks = c(0,5
,10,15))+ 
  scale_x_continuous(limits=c(0,71), name="Species richness")+
  geom_text(size = 12, x = 65, y = 14, label = "a") +
  theme(legend.position="right",
        axis.text.x = element_text(size=9),
        axis.text.y = element_text(size=9))

B16_B17_GAM <- ggplot(split_GAMs[["B16-B17"]], aes(x=Nsp_active,y=log(fi
t)))+
  geom_vline(aes(xintercept=42), lty=1, col="green", size = 0.8) +
  geom_vline(aes(xintercept=22), lty=2, col="red", size = 0.8) +
  geom_line(col = "blue") + facet_wrap(~Scenario) +
  geom_ribbon(aes(ymin= log(fit) + 1.96*(log(se.fit)),
                  ymax= log(fit) - 1.96*(log(se.fit))), alpha=.3, fill =
"blue")+
  theme_classic()+
  theme(axis.line.y = element_line()) +
  scale_y_continuous(name = "log(BPc)", limits = c(-1,16), breaks = c(0,5
,10,15))+ 
  scale_x_continuous(limits=c(0,71), name="Species richness")+
  theme(legend.position="right",
        axis.text.x = element_text(size=9),
        axis.text.y = element_text(size=9))

B16_B15_GAM <- ggplot(split_GAMs[["B16-B15"]], aes(x=Nsp_active,y=log(fi
t)))+
  geom_vline(aes(xintercept=42), lty=1, col="green", size = 0.8) +
  geom_vline(aes(xintercept=15), lty=2, col="red", size = 0.8) +
  geom_line(col = "blue") +
  geom_ribbon(aes(ymin= log(fit) + 1.96*(log(se.fit)),
                  ymax= log(fit) - 1.96*(log(se.fit))), alpha=.3, fill =
"blue")+
  theme_classic()+
  theme(axis.line.y = element_line()) +
  scale_y_continuous(name = "log(BPc)", limits = c(-1,16), breaks = c(0,5
,10,15))+ 
  scale_x_continuous(limits=c(0,71), name="Species richness")+
  geom_text(size = 12, x = 65, y = 14, label = "b") +
  theme(legend.position="right",
        axis.text.x = element_text(size=9),
        axis.text.y = element_text(size=9))

B15_Xs_GAM <- ggplot(split_GAMs[["B15-Xs"]], aes(x=Nsp_active,y=log(fit)
))+ 
  geom_vline(aes(xintercept=40), lty=1, col="green", size = 0.8) +
  geom_vline(aes(xintercept=16), lty=2, col="red", size = 0.8) +
  geom_line(col = "blue") +
  geom_ribbon(aes(ymin= log(fit) + 1.96*(log(se.fit)),
                  ymax= log(fit) - 1.96*(log(se.fit))), alpha=.3, fill =
"blue")+

```

```

theme_classic()+
  theme(axis.line.y = element_line()) +
  scale_y_continuous(name = "log(BPc)", limits = c(-1,16), breaks = c(0,5
,10,15))+ 
  scale_x_continuous(limits=c(0,71), name="Species richness")+
  geom_text(size = 12, x = 65, y = 14, label = "c") +
  theme(legend.position="right",
        axis.text.x = element_text(size=9),
        axis.text.y = element_text(size=9))

Xs_B14_GAM <- ggplot(split_GAMs[["Xs-B14"]], aes(x=Nsp_active,y=log(fit)
))+ 
  geom_vline(aes(xintercept=41), lty=1, col="green", size = 0.8) +
  geom_vline(aes(xintercept=10), lty=2, col="red", size = 0.8) +
  geom_line(col = "blue") +
  geom_ribbon(aes(ymin= log(fit) + 1.96*(log(se.fit)),
                  ymax= log(fit) - 1.96*(log(se.fit))),alpha=.3, fill =
"blue")+
  theme_classic()+
  theme(axis.line.y = element_line()) +
  scale_y_continuous(name = "log(BPc)", limits = c(-1,16), breaks = c(0,5
,10,15))+ 
  scale_x_continuous(limits=c(0,71), name="Species richness")+
  geom_text(size = 12, x = 65, y = 14, label = "d") +
  theme(legend.position="right",
        axis.text.x = element_text(size=9),
        axis.text.y = element_text(size=9))

B14_B13_GAM <- ggplot(split_GAMs[["B14-B13"]], aes(x=Nsp_active,y=log(fi
t)))+
  geom_vline(aes(xintercept=27), lty=1, col="green", size = 0.8) +
  geom_vline(aes(xintercept=11), lty=2, col="red", size = 0.8) +
  geom_line(col = "blue") +
  geom_ribbon(aes(ymin= log(fit) + 1.96*(log(se.fit)),
                  ymax= log(fit) - 1.96*(log(se.fit))),alpha=.3, fill =
"blue")+
  theme_classic()+
  theme(axis.line.y = element_line()) +
  scale_y_continuous(name = "log(BPc)", limits = c(-1,16), breaks = c(0,5
,10,15))+ 
  scale_x_continuous(limits=c(0,71), name="Species richness")+
  geom_text(size = 12, x = 65, y = 14, label = "e") +
  theme(legend.position="right",
        axis.text.x = element_text(size=9),
        axis.text.y = element_text(size=9))

B17_B13_GAM <- ggplot(split_GAMs[["B17-B13"]], aes(x=Nsp_active,y=log(fi
t)))+
  geom_vline(aes(xintercept=52), lty=1, col="green", size = 0.8) +
  geom_vline(aes(xintercept=11), lty=2, col="red", size = 0.8) +
  geom_line(col = "blue") +
  geom_ribbon(aes(ymin= log(fit) + 1.96*(log(se.fit)),
                  ymax= log(fit) - 1.96*(log(se.fit))),alpha=.3, fill =
"blue")+
  theme_classic()+
  theme(axis.line.y = element_line()) +

```

```

  scale_y_continuous(name = "log(BPc)", limits = c(-1,16), breaks = c(0,5
,10,15))+
  scale_x_continuous(limits=c(0,71), name="Species richness")+
  geom_text(size = 12, x = 65, y = 14, label = "f") +
  theme(legend.position="right",
        axis.text.x = element_text(size=9),
        axis.text.y = element_text(size=9))

B16_B13_GAM <- ggplot(split_GAMs[["B16-B13"]], aes(x=Nsp_active,y=log(fi
t)))+
  geom_vline(aes(xintercept=42), lty=1, col="green", size = 0.8) +
  geom_vline(aes(xintercept=11), lty=2, col="red", size = 0.8) +
  geom_line(col = "blue") + facet_wrap(~Scenario) +
  geom_ribbon(aes(ymin= log(fit) + 1.96*(log(se.fit))),
              ymax= log(fit) - 1.96*(log(se.fit))),alpha=.3, fill =
"blue")+
  theme_classic()+
  theme(axis.line.y = element_line()) +
  scale_y_continuous(name = "log(BPc)", limits = c(-1,16), breaks = c(0,5
,10,15))+
  scale_x_continuous(limits=c(0,71), name="Species richness")+
  theme(legend.position="right",
        axis.text.x = element_text(size=9),
        axis.text.y = element_text(size=9))

## Compensation graphs ####

B17_B16_Compensation_graph <- B17_B16_BPc %>%
  filter(!is.na(CompSp)) %>%
  select(Simulation, Nsp, Nsp_active, CompRep, CompSp) %>%
  left_join(ChAOS_2018_ranges, by = c("CompSp" = "ScientificName_accepted")) %>%
  group_by(Nsp_active) %>%
  summarise(CompRep.mean = mean(CompRep),
            CompRep.sd = sd(CompRep),
            CompRep.max = max(CompRep)) %>%
  ggplot(aes(x= Nsp_active, y=CompRep.mean))+
  # geom_bar(stat = "identity", fill="purple4", alpha=.8, aes(y = CompRe
p.max))+
  geom_bar(stat="identity", fill="gold", alpha=.8, aes(y = CompRep.mean))+
  geom_errorbar(aes(ymin=CompRep.mean, ymax=CompRep.mean+(CompRep.sd/2))
, width=.2, col = "black") +
  geom_vline(xintercept = 17, col = "red", linetype = "dashed", size = 0
.8, alpha = 0.8) +
  geom_vline(xintercept = 52, col = "green", size = 0.8, alpha = 0.8) +
  scale_x_continuous(limits = c(0,70)) +
  scale_y_continuous(limits = c(0,16)) +
  geom_text(size = 12, x = 65, y = 14, label = "g") +
  theme_classic()+
  theme(legend.position="right", panel.grid.major = element_blank(), pan
el.grid.minor = element_blank(),
        panel.background = element_blank(), axis.line = elem
ent_line(colour = "black")) +
  labs(x = "Species richness",
       y = "Compensating \n species")

```

```

B16_B15_Compensation_graph <- B16_B15_BPc %>%
  filter(!is.na(CompSp)) %>%
  select(Simulation, Nsp, Nsp_active, CompRep, CompSp) %>%
  left_join(ChAOS_2018_ranges, by = c("CompSp" = "ScientificName_accepted"))
  ) %>%
  group_by(Nsp_active) %>%
  summarise(CompRep.mean = mean(CompRep),
            CompRep.sd = sd(CompRep),
            CompRep.max = max(CompRep)) %>%
  ggplot(aes(x= Nsp_active, y=CompRep.mean))+
  # geom_bar(stat = "identity", fill="purple4", alpha=.8, aes(y = CompRep.max))+
  geom_bar(stat="identity", fill="gold", alpha=.8, aes(y = CompRep.mean))+
  geom_errorbar(aes(ymin=CompRep.mean, ymax=CompRep.mean+(CompRep.sd/2)),
  width=.2, col = "black") +
  geom_vline(xintercept = 15, col = "red", linetype = "dashed", size = 0.8, alpha = 0.8) +
  geom_vline(xintercept = 42, col = "green", size = 0.8, alpha = 0.8) +
  scale_x_continuous(limits = c(0,70)) +
  scale_y_continuous(limits = c(0,16)) +
  geom_text(size = 12, x = 65, y = 14, label = "h") +
  theme_classic()+
  theme(legend.position="right", panel.grid.major = element_blank(), panel.grid.minor = element_blank(),
        panel.background = element_blank(), axis.line = element_line(colour = "black"))+
  labs(x = "Species richness",
       y = "Compensating \n species")

B15_Xs_Compensation_graph <- B15_Xs_BPc %>%
  filter(!is.na(CompSp)) %>%
  select(Simulation, Nsp, Nsp_active, CompRep, CompSp) %>%
  left_join(ChAOS_2018_ranges, by = c("CompSp" = "ScientificName_accepted"))
  ) %>%
  group_by(Nsp_active) %>%
  summarise(CompRep.mean = mean(CompRep),
            CompRep.sd = sd(CompRep),
            CompRep.max = max(CompRep)) %>%
  ggplot(aes(x= Nsp_active, y=CompRep.mean))+
  # geom_bar(stat = "identity", fill="purple4", alpha=.8, aes(y = CompRep.max))+
  geom_bar(stat="identity", fill="gold", alpha=.8, aes(y = CompRep.mean))+
  geom_errorbar(aes(ymin=CompRep.mean, ymax=CompRep.mean+(CompRep.sd/2)),
  width=.2, col = "black") +
  geom_vline(xintercept = 16, col = "red", linetype = "dashed", size = 0.8, alpha = 0.8) +
  geom_vline(xintercept = 40, col = "green", size = 0.8, alpha = 0.8) +
  scale_x_continuous(limits = c(0,70)) +
  scale_y_continuous(limits = c(0,16)) +
  geom_text(size = 12, x = 65, y = 14, label = "i") +
  theme_classic()+
  theme(legend.position="right", panel.grid.major = element_blank(), panel.grid.minor = element_blank(),
        panel.background = element_blank(), axis.line = element_line(colour = "black"))

```

```

            panel.background = element_blank(), axis.line = element_line(colour = "black")) +
  labs(x = "Species richness",
       y = "Compensating \n species")

Xs_B14_Compensation_graph <- Xs_B14_BPc %>%
  filter(!is.na(CompSp)) %>%
  select(Simulation, Nsp, Nsp_active, CompRep, CompSp) %>%
  left_join(ChAOS_2018_ranges, by = c("CompSp" = "ScientificName_accepted")) %>%
  group_by(Nsp_active) %>%
  summarise(CompRep.mean = mean(CompRep),
            CompRep.sd = sd(CompRep),
            CompRep.max = max(CompRep)) %>%
  ggplot(aes(x= Nsp_active, y=CompRep.mean))+
  # geom_bar(stat = "identity", fill="purple4", alpha=.8, aes(y = CompRep.max))+
  geom_bar(stat="identity", fill="gold", alpha=.8, aes(y = CompRep.mean))+
  geom_errorbar(aes(ymin=CompRep.mean, ymax=CompRep.mean+(CompRep.sd/2)),
                width=.2, col = "black") +
  geom_vline(xintercept = 10, col = "red", linetype = "dashed", size = 0.8, alpha = 0.8) +
  geom_vline(xintercept = 41, col = "green", size = 0.8, alpha = 0.8) +
  scale_x_continuous(limits = c(0,70)) +
  scale_y_continuous(limits = c(0,16)) +
  geom_text(size = 12, x = 65, y = 14, label = "j") +
  theme_classic()+
  theme(legend.position="right", panel.grid.major = element_blank(), panel.grid.minor = element_blank(),
        panel.background = element_blank(), axis.line = element_line(colour = "black")) +
  labs(x = "Species richness",
       y = "Compensating \n species")

B14_B13_Compensation_graph <-B14_B13_BPc %>%
  filter(!is.na(CompSp)) %>%
  select(Simulation, Nsp, Nsp_active, CompRep, CompSp) %>%
  left_join(ChAOS_2018_ranges, by = c("CompSp" = "ScientificName_accepted")) %>%
  group_by(Nsp_active) %>%
  summarise(CompRep.mean = mean(CompRep),
            CompRep.sd = sd(CompRep),
            CompRep.max = max(CompRep)) %>%
  ggplot(aes(x= Nsp_active, y=CompRep.mean))+
  # geom_bar(stat = "identity", fill="purple4", alpha=.8, aes(y = CompRep.max))+
  geom_bar(stat="identity", fill="gold", alpha=.8, aes(y = CompRep.mean))+
  geom_errorbar(aes(ymin=CompRep.mean, ymax=CompRep.mean+(CompRep.sd/2)),
                width=.2, col = "black") +
  geom_vline(xintercept = 11, col = "red", linetype = "dashed", size = 0.8, alpha = 0.8) +
  geom_vline(xintercept = 27, col = "green", size = 0.8, alpha = 0.8) +
  scale_x_continuous(limits = c(0,70)) +
  scale_y_continuous(limits = c(0,16)) +

```

```

geom_text(size = 12, x = 65, y = 14, label = "k") +
  theme_classic() +
  theme(legend.position="right", panel.grid.major = element_blank(), panel.grid.minor = element_blank(),
        panel.background = element_blank(), axis.line = element_line(colour = "black")) +
  labs(x = "Species richness",
       y = "Compensating \n species")

B17_B13_Compensation_graph <- B17_B13_BPc %>%
  filter(!is.na(CompSp)) %>%
  select(Simulation, Nsp, Nsp_active, CompRep, CompSp) %>%
  left_join(ChAOS_2018_ranges, by = c("CompSp" = "ScientificName_accepted")) %>%
  group_by(Nsp_active) %>%
  summarise(CompRep.mean = mean(CompRep),
            CompRep.sd = sd(CompRep),
            CompRep.max = max(CompRep)) %>%
  ggplot(aes(x = Nsp_active, y = CompRep.mean)) +
  # geom_bar(stat = "identity", fill="purple4", alpha=.8, aes(y = CompRep.max)) +
  geom_bar(stat="identity", fill="gold", alpha=.8, aes(y = CompRep.mean)) +
  geom_errorbar(aes(ymin=CompRep.mean, ymax=CompRep.mean+(CompRep.sd/2)),
                width=.2, col = "black") +
  geom_vline(xintercept = 11, col = "red", linetype = "dashed", size = 0.8, alpha = 0.8) +
  geom_vline(xintercept = 52, col = "green", size = 0.8, alpha = 0.8) +
  scale_x_continuous(limits = c(0,70)) +
  scale_y_continuous(limits = c(0,16)) +
  geom_text(size = 12, x = 65, y = 14, label = "l") +
  theme_classic() +
  theme(legend.position="right", panel.grid.major = element_blank(), panel.grid.minor = element_blank(),
        panel.background = element_blank(), axis.line = element_line(colour = "black")) +
  labs(x = "Species richness",
       y = "Compensating \n species")

## Mi #####
B17_B16_Mi <- B17_B16_Contributions %>%
  filter(AiSim != 0) %>% #remove species that are not alive
  unique() %>% # remove duplicates of same species during co-compensations
  select(Simulation, Iteration, Nsp_active, Mi, Ri) %>%
  group_by(Nsp_active, Simulation, Iteration, Mi) %>%
  dplyr::summarise(freq = n()) %>%
  group_by(Nsp_active, Mi) %>%
  dplyr::summarise(mean = mean(freq),
                  median = median(freq)) %>%
  filter(!is.na(Mi)) %>%
  ggplot() +
  geom_bar(aes(x = Nsp_active, fill = as.factor(Mi), y = mean), na.rm = T, position = "fill", stat = "identity") +
  geom_vline(xintercept = 17, col = "red", linetype = "dashed", size = 0.8, alpha = 0.8) +

```

```

geom_vline(xintercept = 52, col = "green", size = 0.8, alpha = 0.8) +
  geom_text(size = 12, x = 65, y = 0.9, label = "m") +
  scale_x_continuous(name = "Species richness", limits = c(0,70)) +
  scale_y_continuous(name = "Relative Mi") +
  scale_fill_brewer(palette = "Purples", name = "Mobility classification",
", labels = c("Fixed tube", "Limited movement", "Slow, free movement", "Burrow system")) +
  theme_classic()

B16_B15_Mi <- B16_B15_Contributions %>%
  filter(AiSim != 0) %>% #remove species that are not alive
  unique() %>% # remove duplicates of same species during co-compensations
  select(Simulation, Iteration, Nsp_active, Mi, Ri) %>%
  group_by(Nsp_active, Simulation, Iteration, Mi) %>%
  dplyr::summarise(freq = n()) %>%
  group_by(Nsp_active, Mi) %>%
  dplyr::summarise(mean = mean(freq),
                  median = median(freq)) %>%
  filter(!is.na(Mi)) %>%
  ggplot() +
  geom_bar(aes(x = Nsp_active, fill = as.factor(Mi), y = mean), na.rm =
T, position = "fill", stat = "identity") +
  geom_vline(xintercept = 15, col = "red", linetype = "dashed", size = 0
.8, alpha = 0.8) +
  geom_vline(xintercept = 42, col = "green", size = 0.8, alpha = 0.8) +
  geom_text(size = 12, x = 65, y = 0.9, label = "n") +
  scale_x_continuous(name = "Species richness", limits = c(0,70)) +
  scale_y_continuous(name = "Relative Mi") +
  scale_fill_brewer(palette = "Purples", name = "Mobility classification",
", labels = c("Fixed tube", "Limited movement", "Slow, free movement", "Burrow system")) +
  theme_classic()

B15_Xs_Mi <- B15_Xs_Contributions %>%
  filter(AiSim != 0) %>% #remove species that are not alive
  unique() %>% # remove duplicates of same species during co-compensations
  select(Simulation, Iteration, Nsp_active, Mi, Ri) %>%
  group_by(Nsp_active, Simulation, Iteration, Mi) %>%
  dplyr::summarise(freq = n()) %>%
  group_by(Nsp_active, Mi) %>%
  dplyr::summarise(mean = mean(freq),
                  median = median(freq)) %>%
  filter(!is.na(Mi)) %>%
  ggplot() +
  geom_bar(aes(x = Nsp_active, fill = as.factor(Mi), y = mean), na.rm =
T, position = "fill", stat = "identity") +
  geom_vline(xintercept = 16, col = "red", linetype = "dashed", size = 0
.8, alpha = 0.8) +
  geom_vline(xintercept = 40, col = "green", size = 0.8, alpha = 0.8) +
  geom_text(size = 12, x = 65, y = 0.9, label = "o") +
  scale_x_continuous(name = "Species richness", limits = c(0,70)) +
  scale_y_continuous(name = "Relative Mi") +
  scale_fill_brewer(palette = "Purples", name = "Mobility classification",
", labels = c("Fixed tube", "Limited movement", "Slow, free movement", "Burrow system"))

```

```

Burrow system")) +
  theme_classic()

Xs_B14_Mi <- Xs_B14_Contributions %>%
  filter(AiSim != 0) %>% #remove species that are not alive
  unique() %>% # remove duplicates of same species during co-compensations
  select(Simulation, Iteration, Nsp_active, Mi, Ri) %>%
  group_by(Nsp_active, Simulation, Iteration, Mi) %>%
  dplyr::summarise(freq = n()) %>%
  group_by(Nsp_active, Mi) %>%
  dplyr::summarise(mean = mean(freq),
                   median = median(freq)) %>%
  filter(!is.na(Mi)) %>%
  ggplot() +
  geom_bar(aes(x = Nsp_active, fill = as.factor(Mi), y = mean), na.rm =
T, position = "fill", stat = "identity") +
  geom_vline(xintercept = 10, col = "red", linetype = "dashed", size = 0.8, alpha = 0.8) +
  geom_vline(xintercept = 41, col = "green", size = 0.8, alpha = 0.8) +
  geom_text(size = 12, x = 65, y = 0.9, label = "p") +
  scale_x_continuous(name = "Species richness", limits = c(0,70)) +
  scale_y_continuous(name = "Relative Mi") +
  scale_fill_brewer(palette = "Purples", name = "Mobility classification",
                   labels = c("Fixed tube", "Limited movement", "Slow, free movement", "Burrow system")) +
  theme_classic()

B14_B13_Mi <- B14_B13_Contributions %>%
  filter(AiSim != 0) %>% #remove species that are not alive
  unique() %>% # remove duplicates of same species during co-compensations
  select(Simulation, Iteration, Nsp_active, Mi, Ri) %>%
  group_by(Nsp_active, Simulation, Iteration, Mi) %>%
  dplyr::summarise(freq = n()) %>%
  group_by(Nsp_active, Mi) %>%
  dplyr::summarise(mean = mean(freq),
                   median = median(freq)) %>%
  filter(!is.na(Mi)) %>%
  ggplot() +
  geom_bar(aes(x = Nsp_active, fill = as.factor(Mi), y = mean), na.rm =
T, position = "fill", stat = "identity") +
  geom_vline(xintercept = 11, col = "red", linetype = "dashed", size = 0.8, alpha = 0.8) +
  geom_vline(xintercept = 27, col = "green", size = 0.8, alpha = 0.8) +
  geom_text(size = 12, x = 65, y = 0.9, label = "q") +
  scale_x_continuous(name = "Species richness", limits = c(0,70)) +
  scale_y_continuous(name = "Relative Mi") +
  scale_fill_brewer(palette = "Purples", name = "Mobility classification",
                   labels = c("Fixed tube", "Limited movement", "Slow, free movement", "Burrow system")) +
  theme_classic()

B17_B13_Mi <- B17_B13_Contributions %>%
  filter(AiSim != 0) %>% #remove species that are not alive
  unique() %>% # remove duplicates of same species during co-compensatio

```

```

ns
  select(Simulation, Iteration, Nsp_active, Mi, Ri) %>%
  group_by(Nsp_active, Simulation, Iteration, Mi) %>%
  dplyr::summarise(freq = n()) %>%
  group_by(Nsp_active, Mi) %>%
  dplyr::summarise(mean = mean(freq),
                   median = median(freq)) %>%
  filter(!is.na(Mi)) %>%
  ggplot() +
  geom_bar(aes(x = Nsp_active, fill = as.factor(Mi), y = mean), na.rm =
T, position = "fill", stat = "identity") +
  geom_vline(xintercept = 11, col = "red", linetype = "dashed", size = 0
.8, alpha = 0.8) +
  geom_vline(xintercept = 52, col = "green", size = 0.8, alpha = 0.8) +
  geom_text(size = 12, x = 65, y = 0.9, label = "r") +
  scale_x_continuous(name = "Species richness", limits = c(0,70)) +
  scale_y_continuous(name = "Relative Mi") +
  scale_fill_brewer(palette = "Purples", name = "Mobility classification",
                   labels = c("Fixed tube", "Limited movement", "Slow, free movement", "Burrow system")) +
  theme_classic()

## Ri ####
B17_B16_Ri <- B17_B16_Contributions %>%
  filter(AiSim != 0) %>% #remove species that are not alive
  unique() %>% # remove duplicates of same species during co-compensatio
ns
  select(Simulation, Iteration, Nsp_active, Mi, Ri) %>%
  group_by(Nsp_active, Simulation, Iteration, Ri) %>%
  dplyr::summarise(freq = n()) %>%
  group_by(Nsp_active, Ri) %>%
  dplyr::summarise(mean = mean(freq),
                   median = median(freq)) %>%
  filter(!is.na(Ri)) %>%
  ggplot() +
  geom_bar(aes(x = Nsp_active, fill = as.factor(Ri), y = mean), na.rm =
T, position = "fill", stat = "identity") +
  geom_vline(xintercept = 17, col = "red", linetype = "dashed", size = 0
.8, alpha = 0.8) +
  geom_vline(xintercept = 52, col = "green", size = 0.8, alpha = 0.8) +
  geom_text(size = 12, x = 65, y = 0.9, label = "s") +
  scale_x_continuous(name = "Species richness", limits = c(0,70)) +
  scale_y_continuous(name = "Relative Ri") +
  scale_fill_brewer(name = "Reworking mode", labels = c("Epifauna", "Sur
ficial Modifier", "Upward/Downward Conveyor", "Biodiffusor", "Regenerato
r")) +
  theme_classic()

B16_B15_Ri <- B16_B15_Contributions %>%
  filter(AiSim != 0) %>% #remove species that are not alive
  unique() %>% # remove duplicates of same species during co-compensatio
ns
  select(Simulation, Iteration, Nsp_active, Mi, Ri) %>%
  group_by(Nsp_active, Simulation, Iteration, Ri) %>%
  dplyr::summarise(freq = n()) %>%
  group_by(Nsp_active, Ri) %>%

```

```

dplyr::summarise(mean = mean(freq),
                  median = median(freq)) %>%
filter(!is.na(Ri)) %>%
ggplot() +
  geom_bar(aes(x = Nsp_active, fill = as.factor(Ri), y = mean), na.rm =
T, position = "fill", stat = "identity") +
  geom_vline(xintercept = 15, col = "red", linetype = "dashed", size = 0
.8, alpha = 0.8) +
  geom_vline(xintercept = 42, col = "green", size = 0.8, alpha = 0.8) +
  geom_text(size = 12, x = 65, y = 0.9, label = "t") +
  scale_x_continuous(name = "Species richness", limits = c(0,70)) +
  scale_y_continuous(name = "Relative Ri") +
  scale_fill_brewer(name = "Reworking mode", labels = c("Epifauna", "Sur
ficial Modifier", "Upward/Downward Conveyor", "Biodiffusor", "Regenerato
r")) +
  theme_classic()

B15_Xs_Ri <- B15_Xs_Contributions %>%
  filter(AiSim != 0) %>% #remove species that are not alive
  unique() %>% # remove duplicates of same species during co-compensatio
ns
  select(Simulation, Iteration, Nsp_active, Mi, Ri) %>%
  group_by(Nsp_active, Simulation, Iteration, Ri) %>%
  dplyr::summarise(freq = n()) %>%
  group_by(Nsp_active, Ri) %>%
  dplyr::summarise(mean = mean(freq),
                  median = median(freq)) %>%
  filter(!is.na(Ri)) %>%
  ggplot() +
  geom_bar(aes(x = Nsp_active, fill = as.factor(Ri), y = mean), na.rm =
T, position = "fill", stat = "identity") +
  geom_vline(xintercept = 16, col = "red", linetype = "dashed", size = 0
.8, alpha = 0.8) +
  geom_vline(xintercept = 40, col = "green", size = 0.8, alpha = 0.8) +
  geom_text(size = 12, x = 65, y = 0.9, label = "u") +
  scale_x_continuous(name = "Species richness", limits = c(0,70)) +
  scale_y_continuous(name = "Relative Ri") +
  scale_fill_brewer(name = "Reworking mode", labels = c("Epifauna", "Sur
ficial Modifier", "Upward/Downward Conveyor", "Biodiffusor", "Regenerator
")) +
  theme_classic()

Xs_B14_Ri <- Xs_B14_Contributions %>%
  filter(AiSim != 0) %>% #remove species that are not alive
  unique() %>% # remove duplicates of same species during co-compensatio
ns
  select(Simulation, Iteration, Nsp_active, Mi, Ri) %>%
  group_by(Nsp_active, Simulation, Iteration, Ri) %>%
  dplyr::summarise(freq = n()) %>%
  group_by(Nsp_active, Ri) %>%
  dplyr::summarise(mean = mean(freq),
                  median = median(freq)) %>%
  filter(!is.na(Ri)) %>%
  ggplot() +
  geom_bar(aes(x = Nsp_active, fill = as.factor(Ri), y = mean), na.rm =
T, position = "fill", stat = "identity") +

```

```

  geom_vline(xintercept = 10, col = "red", linetype = "dashed", size = 0
.8, alpha = 0.8) +
  geom_vline(xintercept = 41, col = "green", size = 0.8, alpha = 0.8) +
  geom_text(size = 12, x = 65, y = 0.9, label = "v") +
  scale_x_continuous(name = "Species richness", limits = c(0,70)) +
  scale_y_continuous(name = "Relative Ri") +
  scale_fill_brewer(name = "Reworking mode", labels = c("Epifauna", "Sur
ficial Modifier", "Upward/Downward Conveyor", "Biodiffusor", "Regenerato
r")) +
  theme_classic()

B14_B13_Ri <- B14_B13_Contributions %>%
  filter(AiSim != 0) %>% #remove species that are not alive
  unique() %>% # remove duplicates of same species during co-compensatio
ns
  select(Simulation,Iteration,Nsp_active, Mi, Ri) %>%
  group_by(Nsp_active, Simulation,Iteration, Ri) %>%
  dplyr::summarise(freq = n()) %>%
  group_by(Nsp_active,Ri) %>%
  dplyr::summarise(mean = mean(freq),
                  median = median(freq)) %>%
  filter(!is.na(Ri)) %>%
  ggplot() +
  geom_bar(aes(x = Nsp_active, fill = as.factor(Ri), y = mean), na.rm =
T, position = "fill", stat = "identity") +
  geom_vline(xintercept = 11, col = "red", linetype = "dashed", size = 0
.8, alpha = 0.8) +
  geom_vline(xintercept = 27, col = "green", size = 0.8, alpha = 0.8) +
  geom_text(size = 12, x = 65, y = 0.9, label = "w") +
  scale_x_continuous(name = "Species richness", limits = c(0,70)) +
  scale_y_continuous(name = "Relative Ri") +
  scale_fill_brewer(name = "Reworking mode", labels = c("Epifauna", "Sur
ficial Modifier", "Upward/Downward Conveyor", "Biodiffusor", "Regenerato
r")) +
  theme_classic()

B17_B13_Ri <- B17_B13_Contributions %>%
  filter(AiSim != 0) %>% #remove species that are not alive
  unique() %>% # remove duplicates of same species during co-compensatio
ns
  select(Simulation,Iteration,Nsp_active, Mi, Ri) %>%
  group_by(Nsp_active, Simulation,Iteration, Ri) %>%
  dplyr::summarise(freq = n()) %>%
  group_by(Nsp_active,Ri) %>%
  dplyr::summarise(mean = mean(freq),
                  median = median(freq)) %>%
  filter(!is.na(Ri)) %>%
  ggplot() +
  geom_bar(aes(x = Nsp_active, fill = as.factor(Ri), y = mean), na.rm =
T, position = "fill", stat = "identity") +
  geom_vline(xintercept = 11, col = "red", linetype = "dashed", size = 0
.8, alpha = 0.8) +
  geom_vline(xintercept = 52, col = "green", size = 0.8, alpha = 0.8) +
  geom_text(size = 12, x = 65, y = 0.9, label = "x") +
  scale_x_continuous(name = "Species richness", limits = c(0,70)) +
  scale_y_continuous(name = "Relative Ri") +

```

```

  scale_fill_brewer(name = "Reworking mode", labels = c("Epifauna", "Sur-
ficial Modifier", "Upward/Downward Conveyor", "Biodiffusor", "Regenerato-
r")) +
  theme_classic()

GAM_BPc_plot <- wrap_elements(grid::textGrob("B17-B16", vjust = 4, rot =
0, gp = grid::gpar(fontsize = 16))) + wrap_elements(grid::textGrob("B16-
B15", vjust = 4, rot = 0, gp = grid::gpar(fontsize = 16))) +
  wrap_elements(grid::textGrob("B15-Xs", vjust = 4, rot = 0, gp = grid::
gpar(fontsize = 16))) +
  wrap_elements(grid::textGrob("Xs-B14", vjust = 4, rot = 0, gp = grid::
gpar(fontsize = 16))) +
  wrap_elements(grid::textGrob("B14-B13", vjust = 4, rot = 0, gp = grid::
gpar(fontsize = 16))) +
  plot_spacer() +
  wrap_elements(grid::textGrob("B17-B13", vjust = 4, rot = 0, gp = grid::
gpar(fontsize = 16))) +
  B17_B16_GAM + theme(axis.title.x = element_blank(), axis.text.x.bott-
om = element_blank(), axis.title.y = element_text(size = 20)) +
  B16_B15_GAM + theme(axis.title.y = element_blank(), axis.text.y.left =
element_blank(), axis.title.x = element_blank(), axis.text.x.bottom = el-
ement_blank()) +
  B15_Xs_GAM + theme(axis.title.y = element_blank(), axis.text.y.left =
element_blank(), axis.title.x = element_blank(), axis.text.x.bottom = el-
ement_blank()) +
  Xs_B14_GAM + theme(axis.title.y = element_blank(), axis.text.y.left =
element_blank(), axis.title.x = element_blank(), axis.text.x.bottom = el-
ement_blank()) +
  B14_B13_GAM + theme(axis.title.y = element_blank(), axis.text.y.left =
element_blank(), axis.title.x = element_blank(), axis.text.x.bottom = el-
ement_blank()) + plot_spacer() +
  B17_B13_GAM + theme(axis.title.y = element_blank(), axis.text.y.left =
element_blank(), axis.title.x = element_blank(), axis.text.x.bottom = el-
ement_blank()) +
  B17_B16_Compensation_graph + theme(axis.title.x = element_blank(), axi-
s.title.y = element_text(size = 20), axis.text.x.bottom = element_blank(
)) +
  B16_B15_Compensation_graph + theme(axis.title.y = element_blank(), axi-
s.text.y.left = element_blank(), axis.title.x = element_blank(), axis.te-
xt.x.bottom = element_blank()) +
  B15_Xs_Compensation_graph + theme(axis.title.y = element_blank(), axis-
.text.y.left = element_blank(), axis.title.x = element_blank(), axis.te-
xt.x.bottom = element_blank()) +
  Xs_B14_Compensation_graph + theme(axis.title.y = element_blank(), axis-
.text.y.left = element_blank(), axis.title.x = element_blank(), axis.te-
xt.x.bottom = element_blank()) +
  B14_B13_Compensation_graph + theme(axis.title.y = element_blank(), axi-
s.text.y.left = element_blank(), axis.title.x = element_blank(), axis.te-
xt.x.bottom = element_blank()) + plot_spacer() +
  B17_B13_Compensation_graph + theme(axis.title.y = element_blank(), axi-
s.text.y.left = element_blank(), axis.title.x = element_blank(), axis.te-
xt.x.bottom = element_blank()) +
  B17_B16_Mi + theme(axis.title.x = element_blank(), axis.text.x.bottom =
element_blank(), axis.title.y = element_text(size = 20)) +
  B16_B15_Mi + theme(axis.title.y = element_blank(), axis.text.y.left =
element_blank(), axis.title.x = element_blank(), axis.text.x.bottom = el-
ement_blank())

```

```

element_blank() +
  B15_Xs_Mi + theme(axis.title.y = element_blank(), axis.text.y.left = element_blank(), axis.title.x = element_blank(), axis.text.x.bottom = element_blank()) +
  Xs_B14_Mi + theme(axis.title.y = element_blank(), axis.text.y.left = element_blank(), axis.title.x = element_blank(), axis.text.x.bottom = element_blank()) +
  B14_B13_Mi + theme(axis.title.y = element_blank(), axis.text.y.left = element_blank(), axis.title.x = element_blank(), axis.text.x.bottom = element_blank()) + plot_spacer() +
  B17_B13_Mi + theme(axis.title.y = element_blank(), axis.text.y.left = element_blank(), axis.title.x = element_blank(), axis.text.x.bottom = element_blank()) +
  B17_B16_Ri + theme(axis.title.x = element_blank(), axis.title.y = element_text(size = 20)) +
  B16_B15_Ri + theme(axis.title.y = element_blank(), axis.text.y.left = element_blank(), axis.title.x = element_blank()) +
  B15_Xs_Ri + theme(axis.title.y = element_blank(), axis.text.y.left = element_blank(), axis.title.x = element_blank()) +
  Xs_B14_Ri + theme(axis.title.y = element_blank(), axis.text.y.left = element_blank(), axis.title.x = element_blank()) +
  B14_B13_Ri + theme(axis.title.y = element_blank(), axis.text.y.left = element_blank(), axis.title.x = element_blank()) + plot_spacer() +
  B17_B13_Ri + theme(axis.title.y = element_blank(), axis.text.y.left = element_blank(), axis.title.x = element_blank()) +
  plot_layout(guides = "collect", ncol = 7, widths = c(1,1,1,1,1,0.3,1))

GAM_BPc_plot & theme(axis.text.x = element_text(size = 16),
                      axis.text.y = element_text(size = 16))

ggsave(
  "2018_BPc_GAMs_Compensations.tiff",
  plot = last_plot(),
  device = tiff,
  scale = 2,
  width = 22,
  height = 16,
  units = c("cm"),
  dpi = 300
)

# Figure 3: Taxonomy graphs ####

B17_B16_Contributions$species <- gsub("_", " ", B17_B16_Contributions$species)

top_B17_B16_Contributions <- B17_B16_Contributions %>%
  group_by(species, Nsp_active) %>%
  summarise(mean_contribution = mean(species_contribution, na.rm = T))

top20_B17_B16_Contributions <- top_B17_B16_Contributions %>%
  group_by(species) %>%
  summarise(Nsp_active = Nsp_active,
            mean_contribution = mean_contribution,
            species_mean_contribution = mean(mean_contribution),

```

```

    species_starting_contribution = mean(mean_contribution[Nsp_active == 52]),
    species_final_contribution = mean(mean_contribution[Nsp_active == 17]))}

# select only top 20 species based off species mean contribution at the
# starting richness
top20_B17_B16_Contributions <- top20_B17_B16_Contributions %>%
  arrange(-species_starting_contribution) %>%
  group_by(Nsp_active) %>%
  slice(1:20)

rm(top_B17_B16_Contributions)

B16_B15_Contributions$species <- gsub("_", " ", B16_B15_Contributions$species)

top_B16_B15_Contributions <- B16_B15_Contributions %>%
  group_by(species, Nsp_active) %>%
  summarise(mean_contribution = mean(species_contribution, na.rm = T))

top20_B16_B15_Contributions <- top_B16_B15_Contributions %>%
  group_by(species) %>%
  summarise(Nsp_active = Nsp_active,
            mean_contribution = mean_contribution,
            species_mean_contribution = mean(mean_contribution),
            species_starting_contribution = mean(mean_contribution[Nsp_active == 42]),
            species_final_contribution = mean(mean_contribution[Nsp_active == 15]))}

# select only top 20 species based off species mean contribution at the
# starting richness
top20_B16_B15_Contributions <- top20_B16_B15_Contributions %>%
  arrange(-species_starting_contribution) %>%
  group_by(Nsp_active) %>%
  slice(1:20)

rm(top_B16_B15_Contributions)

B15_Xs_Contributions$species <- gsub("_", " ", B15_Xs_Contributions$species)

top_B15_Xs_Contributions <- B15_Xs_Contributions %>%
  group_by(species, Nsp_active) %>%
  summarise(mean_contribution = mean(species_contribution, na.rm = T))

top20_B15_Xs_Contributions <- top_B15_Xs_Contributions %>%
  group_by(species) %>%
  summarise(Nsp_active = Nsp_active,
            mean_contribution = mean_contribution,
            species_mean_contribution = mean(mean_contribution),
            species_starting_contribution = mean(mean_contribution[Nsp_active == 40])),
```

```

    species_final_contribution = mean(mean_contribution[Nsp_active == 16])))

# select only top 20 species based off species mean contribution at the
# starting richness
top20_B15_Xs_Contributions <- top20_B15_Xs_Contributions %>%
  arrange(-species_starting_contribution) %>%
  group_by(Nsp_active) %>%
  slice(1:20)

rm(top_B15_Xs_Contributions)

Xs_B14_Contributions$species <- gsub("_", " ", Xs_B14_Contributions$species)

top_Xs_B14_Contributions <- Xs_B14_Contributions %>%
  group_by(species, Nsp_active) %>%
  summarise(mean_contribution = mean(species_contribution, na.rm = T))

top20_Xs_B14_Contributions <- top_Xs_B14_Contributions %>%
  group_by(species) %>%
  summarise(Nsp_active = Nsp_active,
            mean_contribution = mean_contribution,
            species_mean_contribution = mean(mean_contribution),
            species_starting_contribution = mean(mean_contribution[Nsp_active == 41]),
            species_final_contribution = mean(mean_contribution[Nsp_active == 10])))

# select only top 20 species based off species mean contribution at the
# starting richness
top20_Xs_B14_Contributions <- top20_Xs_B14_Contributions %>%
  arrange(-species_starting_contribution) %>%
  group_by(Nsp_active) %>%
  slice(1:20)

rm(top_Xs_B14_Contributions)

B14_B13_Contributions$species <- gsub("_", " ", B14_B13_Contributions$species)

top_B14_B13_Contributions <- B14_B13_Contributions %>%
  group_by(species, Nsp_active) %>%
  summarise(mean_contribution = mean(species_contribution, na.rm = T))

top20_B14_B13_Contributions <- top_B14_B13_Contributions %>%
  group_by(species) %>%
  summarise(Nsp_active = Nsp_active,
            mean_contribution = mean_contribution,
            species_mean_contribution = mean(mean_contribution),
            species_starting_contribution = mean(mean_contribution[Nsp_active == 27]),
            species_final_contribution = mean(mean_contribution[Nsp_active == 11]))

```

```

# select only top 20 species based off species mean contribution at the
starting richness
top20_B14_B13_Contributions <- top20_B14_B13_Contributions %>%
  arrange(-species_starting_contribution) %>%
  group_by(Nsp_active) %>%
  slice(1:20)

rm(top_B14_B13_Contributions)

B17_B13_Contributions$species <- gsub("_", " ", B17_B13_Contributions$sp
ecies)

top_B17_B13_Contributions <- B17_B13_Contributions %>%
  group_by(species, Nsp_active) %>%
  summarise(mean_contribution = mean(species_contribution, na.rm = T))

top20_B17_B13_Contributions <- top_B17_B13_Contributions %>%
  group_by(species) %>%
  summarise(Nsp_active = Nsp_active,
            mean_contribution = mean_contribution,
            species_mean_contribution = mean(mean_contribution),
            species_starting_contribution = mean(mean_contribution[Nsp_a
ctive == 52]),
            species_final_contribution = mean(mean_contribution[Nsp_acti
ve == 11])))

# select only top 20 species based off species mean contribution at the
starting richness
top20_B17_B13_Contributions <- top20_B17_B13_Contributions %>%
  arrange(-species_starting_contribution) %>%
  group_by(Nsp_active) %>%
  slice(1:20)

rm(top_B17_B13_Contributions)

B17_B16_Taxon_graph <- ggplot(top20_B17_B16_Contributions, aes(x = Nsp_ac
tive, y = reorder(species, species_starting_contribution), fill = mean_co
ntribution)) + geom_tile() +
  coord_cartesian(xlim = c(0,70)) +
  geom_vline(xintercept = 17, col = "red", linetype = "dashed", size =1.
1) +
  geom_vline(xintercept = 52, col = "green", size = 1.1) +
  scale_fill_gradient(low = "azure", high = "#648FFF", limits = c(0,20))
+ # need to replace all taxon graphs with this
# guides(y.sec = guide_axis_label_trans(~paste(rev(top20_B17_B16_Func_
Groups$Combined)))) +
  theme_classic() +
  theme(legend.position="right", axis.text.y = element_text(face = "ital
ic")) +
  labs(x = "Species richness", y = "B17-B16",
       fill = "Contribution to BPc (%)")

B16_B15_Taxon_graph <- ggplot(top20_B16_B15_Contributions, aes(x = Nsp_a

```

```

ctive, y = reorder(species, species_starting_contribution), fill = mean_c
ontribution)) + geom_tile() +
  coord_cartesian(xlim = c(0,70)) +
  geom_vline(xintercept = 15, col = "red", linetype = "dashed", size =1.
1) +
  geom_vline(xintercept = 42, col = "green", size = 1.1) +
  scale_fill_gradient(low = "azure", high = "#648FFF", limits = c(0,20))
+
  # guides(y.sec = guide_axis_label_trans(~paste(rev(top20_B16_B15_Func_
Groups$Combined)))) +
  theme_classic() +
  theme(legend.position="right", axis.text.y = element_text(face = "ital
ic")) +
  labs(x = "Species richness", y = "B16-B15",
    fill = "Contribution to BPc (%)")

B15_Xs_Taxon_graph <- ggplot(top20_B15_Xs_Contributions, aes(x = Nsp_act
ive, y = reorder(species, species_starting_contribution), fill = mean_con
tribution)) + geom_tile() +
  coord_cartesian(xlim = c(0,70)) +
  geom_vline(xintercept = 16, col = "red", linetype = "dashed", size =1.
1) +
  geom_vline(xintercept = 40, col = "green", size = 1.1) +
  scale_fill_gradient(low = "azure", high = "#648FFF", limits = c(0,20))
+
  # guides(y.sec = guide_axis_label_trans(~paste(rev(top20_B15_Xs_Func_G
roups$Combined)))) +
  theme_classic() +
  theme(legend.position="right", axis.text.y = element_text(face = "ital
ic")) +
  labs(x = "Species richness", y = "B15-Xs",
    fill = "Contribution to BPc (%)")

Xs_B14_Taxon_graph <- ggplot(top20_Xs_B14_Contributions, aes(x = Nsp_act
ive, y = reorder(species, species_starting_contribution), fill = mean_con
tribution)) + geom_tile() +
  coord_cartesian(xlim = c(0,70)) +
  geom_vline(xintercept = 10, col = "red", linetype = "dashed", size =1.
1) +
  geom_vline(xintercept = 41, col = "green", size = 1.1) +
  scale_fill_gradient(low = "azure", high = "#648FFF", limits = c(0,20))
+
  # guides(y.sec = guide_axis_label_trans(~paste(rev(top20_Xs_B14_Func_G
roups$Combined)))) +
  theme_classic() +
  theme(legend.position="right", axis.text.y = element_text(face = "ital
ic")) +
  labs(x = "Species richness", y = "Xs-B14",
    fill = "Contribution to BPc (%)")

B14_B13_Taxon_graph <- ggplot(top20_B14_B13_Contributions, aes(x = Nsp_a
ctive, y = reorder(species, species_starting_contribution), fill = mean_c
ontribution)) + geom_tile() +
  coord_cartesian(xlim = c(0,70)) +
  geom_vline(xintercept = 11, col = "red", linetype = "dashed", size =1.
1) +

```

```

geom_vline(xintercept = 27, col = "green", size = 1.1) +
  scale_fill_gradient(low = "azure", high = "#648FFF", limits = c(0,20))
+
  # guides(y.sec = guide_axis_label_trans(~paste(rev(top20_B14_B13_Func_
Groups$Combined)))) +
  theme_classic() +
  theme(legend.position="right", axis.text.y = element_text(face = "ital
ic")) +
  labs(x = "Species richness", y = "B14-B13",
       fill = "Contribution to BPc (%)")

B17_B13_Taxon_graph <- ggplot(top20_B17_B13_Contributions, aes(x = Nsp_a
ctive, y = reorder(species,species_starting_contribution), fill = mean_c
ontribution)) + geom_tile() +
  coord_cartesian(xlim = c(0,70)) +
  geom_vline(xintercept = 11, col = "red", linetype = "dashed", size =1.
1) +
  geom_vline(xintercept = 52, col = "green", size = 1.1) +
  scale_fill_gradient(low = "azure", high = "#648FFF", limits = c(0,20))
+
  # guides(y.sec = guide_axis_label_trans(~paste(rev(top20_B17_B13_Func_
Groups$Combined)))) +
  theme_classic() +
  theme(legend.position="right", axis.text.y = element_text(face = "ital
ic")) +
  labs(x = "Species richness", y = "B17-B13",
       fill = "Contribution to BPc (%)")

  Taxon_plots <- wrap_elements(grid::textGrob("B17-B16", vjust = 8, ro
t = 0, gp = grid::gpar(fontsize = 24))) + wrap_elements(grid::textGrob(
"B16-B15", vjust = 8, rot = 0, gp = grid::gpar(fontsize = 24))) +
  wrap_elements(grid::textGrob("B15-Xs", vjust = 8, rot = 0, gp = grid::
gpar(fontsize = 24))) +
  wrap_elements(grid::textGrob("Xs-B14", vjust = 8, rot = 0, gp = grid::
gpar(fontsize = 24))) +
  wrap_elements(grid::textGrob("B14-B13", vjust = 8, rot = 0, gp = grid:
:gpar(fontsize = 24))) +
  plot_spacer() +
  wrap_elements(grid::textGrob("B17-B13", vjust = 8, rot = 0, gp = grid:
:gpar(fontsize = 24))) +
    B17_B16_Taxon_graph + theme(axis.title = element_blank()) +
  B16_B15_Taxon_graph + theme(axis.title = element_blank()) +
  B15_Xs_Taxon_graph + theme(axis.title = element_blank()) +
  Xs_B14_Taxon_graph + theme(axis.title = element_blank()) +
  B14_B13_Taxon_graph + theme(axis.title = element_blank()) +
  plot_spacer() +
  B17_B13_Taxon_graph + theme(axis.title = element_blank()) +
  plot_layout(ncol = 7, guides = "collect", widths = c(1,1,1,1,1,0.5,1
))

Taxon_plots & theme(axis.text.x = element_text(size = 24),
                     axis.text.y = element_text(size = 12),
                     legend.key.size = unit(1,"cm"),
                     legend.title = element_text(size = 20),
                     legend.text = element_text(size = 12))

```

```

ggsave(
  "2018_Taxonomy_reorganisation.tiff",
  plot = last_plot(),
  device = tiff,
  scale = 2,
  width = 50,
  height = 12,
  units = c("cm"),
  dpi = 300
)

# Figure 4: Climate vulnerability ~ Scenario #####
plot1 <- B17_B16_BPc %>%
  filter(!is.na(Nsp_active)) %>%
  group_by(Simulation, Nsp, Nsp_active) %>%
  summarise(Alive_Vulnerability = Alive_Vulnerability,
            AllExtSpExtProb = mean(c(ExtSpExtProb, CoExtSpExtProb, CoExtSp2ExtProb), na.rm=T)) %>%
  filter(!is.nan(AllExtSpExtProb)) %>%
  ggplot(., aes(x=Nsp_active, y=log(Alive_Vulnerability)))+
  geom_point(colour="grey", alpha=0.1, size = 1)+
  geom_point(aes(y=log(AllExtSpExtProb)), alpha=0.05, col = "purple", size = 1) +
  geom_smooth(size= 4, method = lm, se = TRUE, aes(y = log(AllExtSpExtProb)), x= Nsp_active, col = "darkorchid4") +
  geom_smooth(size= 4, method = lm, se = TRUE, aes(y = log(Alive_Vulnerability)), x= Nsp_active, col = "grey42") +
  # ggpubr::stat_cor(npcy = 0.95, npcx = 0.05,
  #                   aes(Nsp_active, log(AllExtSpExtProb), label = paste(..r.Label.., ..rr.Label.., ..p.Label.., sep = "~~~")),
  #                   geom = "Label_npc", size = 3, col = "purple", label.y.npc = "top", label.x.npc = "left") +
  # ggpubr::stat_cor(npcy = 0.9, npcx = 0.05,
  #                   aes(Nsp_active, log(Alive_Vulnerability), label = paste(..r.Label.., ..rr.Label.., ..p.Label.., sep = "~~~")),
  #                   geom = "Label_npc", size = 3, col = "grey42", label.y.npc = "top", label.x.npc = "left") +
  geom_vline(xintercept = 17, col = "red", linetype = "dashed", size = 0.8) +
  geom_vline(xintercept = 52, col = "green", size = 0.8) +
  geom_text(size = 12, x = 65, y = -6.1, label = "a") +
  scale_y_continuous(name = expression(low %<-% "Climate change pressure (log)" %->% high), limits = c(-6.5,-4)) +
  scale_x_continuous(limits = c(0,70)) +
  theme_classic()+
  theme(legend.position="right") +
  labs(y = "Vulnerability",
       x = "Species Richness") +
  plot_layout(tag_level = 'new')

plot2 <- B17_B16_BPc %>%
  filter(!is.na(Nsp_active)) %>%
  group_by(Simulation, Nsp, Nsp_active) %>%
  summarise(Alive_Vulnerability = Alive_Vulnerability,
            Extinction_Vulnerability = ExtSpExtProb,
            CoExtinction_Vulnerability = mean(c(CoExtSpExtProb, CoExtSp2E

```

```

xtProb), na.rm=T)) %>%
  filter(!is.na(Extinction_Vulnerability)) %>%
  ggplot(., aes(x=Nsp_active,y=log(Alive_Vulnerability)))+
  geom_point(colour="grey",alpha=0.05, size = 1)+
  geom_point(aes(y=log(Extinction_Vulnerability)), alpha=0.05, colour =
"blue", size = 1) +
  geom_point(aes(y=log(CoExtinction_Vulnerability)), alpha=0.05, colour
= "yellow2", size = 1) +
  geom_smooth(size= 4,method = lm, se = TRUE, aes(y =log(Extinction_Vulnerability), x= Nsp_active), col = "blue") +
  geom_smooth(size= 4,method = lm, se = TRUE, aes(y =log(Alive_Vulnerability), x= Nsp_active), col = "grey42") +
  geom_smooth(size= 4,method = lm, se = TRUE, aes(y =log(CoExtinction_Vulnerability), x= Nsp_active), col = "yellow3") +
  # ggpubr::stat_cor(npcy = 0.95, npcx = 0.05,
  #                   aes(Nsp_active, log(Extinction_Vulnerability), label
L = paste(..r.Label.., ..rr.Label.., ..p.Label.., sep = "~~~")),
  #                   geom = "label_npc", size = 3, col = "blue", label.y.
  npc = "top", label.x.npc = "Left") +
  # ggpubr::stat_cor(npcy = 9, npcx = 0.05,
  #                   aes(Nsp_active, log(CoExtinction_Vulnerability),
  label = paste(..r.Label.., ..rr.Label.., ..p.Label.., sep = "~~~")),
  #                   geom = "label_npc", size = 3, col = "yellow2", label
.y.npc = "top", label.x.npc = "Left") +
  geom_vline(xintercept = 17, col = "red", linetype = "dashed", size = 0
.8) +
  geom_vline(xintercept = 52, col = "green", size = 0.8) +
  geom_text(size = 12,x = 65, y = -6.1, label = "g") +
  scale_y_continuous(name = expression(low %<-% "Climate change pressure
(log)" %->% high), limits = c(-6.5,-4)) +
  scale_x_continuous(limits = c(0,70)) +
  theme_classic()+
  theme(legend.position="right") +
  labs(x = "Species Richness") + plot_layout(tag_level = 'new')

plot3 <- B16_B15_BPc %>%
  filter(!is.na(Nsp_active)) %>%
  group_by(Simulation, Nsp, Nsp_active) %>%
  summarise(Alive_Vulnerability = Alive_Vulnerability,
            AllExtSpExtProb = mean(c(ExtSpExtProb,CoExtSpExtProb,CoExtSp
2ExtProb), na.rm=T)) %>%
  ggplot(.,aes(x=Nsp_active,y=log(Alive_Vulnerability)))+
  geom_point(colour="grey",alpha=0.05, size = 1) +
  geom_point(aes(y=log(AllExtSpExtProb)), alpha=0.05, col = "purple", si
ze = 1) +
  geom_smooth(size= 4,method = lm, se = TRUE, aes(y =log(AllExtSpExtProb
)), x= Nsp_active), col = "darkorchid4") +
  geom_smooth(size= 4,method = lm, se = TRUE, aes(y =log(Alive_Vulnerabi
lity), x= Nsp_active), col = "grey42") +
  # ggpubr::stat_cor(npcy = 0.95, npcx = 0.05,
  #                   aes(Nsp_active, log(AllExtSpExtProb), label = paste
(..r.Label.., ..rr.Label.., ..p.Label.., sep = "~~~")),
  #                   geom = "label_npc", size = 3, col = "purple", label.
y.npc = "top", label.x.npc = "Left") +
  # ggpubr::stat_cor(npcy = 0.9, npcx = 0.05,
  #                   aes(Nsp_active, log(Alive_Vulnerability), label =

```

```

paste(..r.Label.., ..rr.Label.., ..p.Label.., sep = "~~~")),
  #                                     geom = "Label_npc", size = 3, col ="grey42", label.
y.npc = "top", label.x.npc = "Left") +
  geom_vline(xintercept = 15, col = "red", linetype = "dashed", size = 0
.8) +
  geom_vline(xintercept = 42, col = "green", size = 0.8) +
  geom_text(size = 12,x = 65, y = -6.1, label = "b") +
  scale_y_continuous(name = expression(low %<-% "Climate change pressure
(log)" %->% high), limits = c(-6.5,-4)) +
  scale_x_continuous(limits = c(0,70)) +
  theme_classic()+
  theme(legend.position="right") +
  labs(y = "Vulnerability",
       x = "Species Richness") + plot_layout(tag_level = 'new')

plot4 <- B16_B15_BPc %>%
  filter(!is.na(Nsp_active)) %>%
  group_by(Simulation, Nsp, Nsp_active) %>%
  summarise(Alive_Vulnerability = Alive_Vulnerability,
            Extinction_Vulnerability = ExtSpExtProb,
            CoExtinction_Vulnerability = mean(c(CoExtSpExtProb,CoExtSp2E
xtProb), na.rm=T)) %>%
  ggplot(., aes(x=Nsp_active,y=log(Alive_Vulnerability)))+
  geom_point(colour="grey",alpha=0.05, size = 1)+
  geom_point(aes(y=log(Extinction_Vulnerability)), alpha=0.05, colour =
"blue", size = 1) +
  geom_point(aes(y=log(CoExtinction_Vulnerability)), alpha=0.05, colour
= "yellow2", size = 1) +
  geom_smooth(size= 4,method = lm, se = TRUE, aes(y =log(Extinction_Vuln
erability), x= Nsp_active), col = "blue") +
  geom_smooth(size= 4,method = lm, se = TRUE, aes(y =log(Alive_Vulnerabi
lity), x= Nsp_active), col = "grey42") +
  geom_smooth(size= 4,method = lm, se = TRUE, aes(y =log(CoExtinction_Vu
lnerability), x= Nsp_active), col = "yellow3") +
  # ggpubr::stat_cor(npcy = 0.95, npcx = 0.05,
  #                   aes(Nsp_active, log(Extinction_Vulnerability), label
L = paste(..r.Label.., ..rr.Label.., ..p.Label.., sep = "~~~")),
  #                                     geom = "Label_npc", size = 3, col ="blue", label.y.
npc = "top", label.x.npc = "left") +
  #   ggpubr::stat_cor(npcy = 0.9, npcx = 0.05,
  #                   aes(Nsp_active, log(CoExtinction_Vulnerability),
  Label = paste(..r.Label.., ..rr.Label.., ..p.Label.., sep = "~~~")),
  #                                     geom = "Label_npc", size = 3, col ="yellow2", label
.y.npc = "top", Label.x.npc = "left") +
  geom_vline(xintercept = 15, col = "red", linetype = "dashed", size = 0
.8) +
  geom_vline(xintercept = 42, col = "green", size = 0.8) +
  geom_text(size = 12,x = 65, y = -6.1, label = "h") +
  scale_y_continuous(name = expression(low %<-% "Climate change pressure
(log)" %->% high), limits = c(-6.5,-4)) +
  scale_x_continuous(limits = c(0,70)) +
  theme_classic()+
  theme(legend.position="right") +
  labs(x = "Species Richness") + plot_layout(tag_level = 'new')

plot5 <- B15_Xs_BPc %>%

```

```

filter(!is.na(Nsp_active)) %>%
  group_by(Simulation, Nsp, Nsp_active) %>%
  summarise(Alive_Vulnerability = Alive_Vulnerability,
            AllExtSpExtProb = mean(c(ExtSpExtProb, CoExtSpExtProb), na.rm
= T)) %>%
  ggplot(., aes(x=Nsp_active, y=log(Alive_Vulnerability)))+
  geom_point(colour="grey", alpha=0.05, size = 1)+
  geom_point(aes(y=log(AllExtSpExtProb)), alpha=0.05, col = "purple", si
ze = 1) +
  geom_smooth(size= 4, method = lm, se = TRUE, aes(y =log(AllExtSpExtProb
), x= Nsp_active), col = "darkorchid4") +
  geom_smooth(size= 4, method = lm, se = TRUE, aes(y =log(Alive_Vulnerabi
lity), x= Nsp_active), col = "grey42") +
  # ggpubr::stat_cor(npcy = 0.95, npcx = 0.05,
  #                   aes(Nsp_active, log(AllExtSpExtProb), Label = paste
(..r.Label.., ..rr.Label.., ..p.Label.., sep = "~~~")),
  #                   geom = "label_npc", size = 3, col = "purple", Label.
y.npc = "top", Label.x.npc = "left") +
  # ggpubr::stat_cor(npcy = 0.9, npcx = 0.05,
  #                   aes(Nsp_active, log(Alive_Vulnerability), Label =
paste(..r.Label.., ..rr.Label.., ..p.Label.., sep = "~~~")),
  #                   geom = "label_npc", size = 3, col = "grey42", Label.
y.npc = "top", Label.x.npc = "left") +
  geom_vline(xintercept = 16, col = "red", linetype = "dashed", size = 0
.8) +
  geom_vline(xintercept = 40, col = "green", size = 0.8) +
  geom_text(size = 12, x = 65, y = -6.1, label = "c") +
  scale_y_continuous(name = expression(low %<-% "Climate change pressure
(log)" %->% high), limits = c(-6.5,-4)) +
  scale_x_continuous(limits = c(0,70)) +
  theme_classic()+
  theme(legend.position="right") +
  labs(y = "Vulnerability",
       x = "Species Richness") + plot_layout(tag_level = 'new')

plot6 <- B15_Xs_BPc %>%
  filter(!is.na(Nsp_active)) %>%
  ggplot(., aes(x=Nsp_active, y=log(Alive_Vulnerability)))+
  geom_point(colour="grey", alpha=0.05)+
  geom_point(aes(y=log(ExtSpExtProb)), alpha=0.05, colour = "blue", size
= 1) +
  geom_point(aes(y=log(CoExtSpExtProb)), alpha=0.05, colour = "yellow2",
size = 1) +
  geom_smooth(size= 4, method = lm, se = TRUE, aes(y =log(ExtSpExtProb),
x= Nsp_active), col = "blue") +
  geom_smooth(size= 4, method = lm, se = TRUE, aes(y =log(Alive_Vulnerabi
lity), x= Nsp_active), col = "grey40") +
  geom_smooth(size= 4, method = lm, se = TRUE, aes(y =log(CoExtSpExtProb)
, x= Nsp_active), col = "yellow3") +
  # ggpubr::stat_cor(npcy = 0.95, npcx = 0.05,
  #                   aes(Nsp_active, log(ExtSpExtProb), Label = paste(..r.
Label.., ..rr.Label.., ..p.Label.., sep = "~~~")),
  #                   geom = "label_npc", size = 3, col = "blue", Label.y.
npc = "top", Label.x.npc = "left") +
  # ggpubr::stat_cor(npcy = 0.9, npcx = 0.05,
  #                   aes(Nsp_active, log(CoExtSpExtProb), Label = past

```

```

e(..r.Label.., ..rr.Label.., ..p.Label.., sep = "~~~")),
  #                     geom = "Label_npc", size = 3, col ="yellow2", Label
.y.npc = "top", Label.x.npc = "Left") +
  geom_vline(xintercept = 16, col = "red", linetype = "dashed", size = 0
.8) +
  geom_vline(xintercept = 40, col = "green", size = 0.8) +
  geom_text(size = 12, x = 65, y = -6.1, label = "i") +
  scale_y_continuous(name = expression(low %<-% "Climate change pressure
(log)" %->% high), limits = c(-6.5,-4)) +
  scale_x_continuous(limits = c(0,70)) +
  theme_classic()+
  theme(legend.position="right") +
  labs(x = "Species Richness") + plot_layout(tag_level = 'new')

plot7 <- Xs_B14_BPc %>%
  filter(!is.na(Nsp_active)) %>%
  group_by(Simulation, Nsp, Nsp_active) %>%
  summarise(Alive_Vulnerability = Alive_Vulnerability,
            AllExtSpExtProb = mean(c(ExtSpExtProb,CoExtSpExtProb), na.rm
=TRUE)) %>%
  ggplot(.,aes(x=Nsp_active,y=log(Alive_Vulnerability)))+
  geom_point(colour="grey",alpha=0.05, size = 1)+
  geom_point(aes(y=log(AllExtSpExtProb)), alpha=0.05, col = "purple", si
ze = 1) +
  geom_smooth(size= 4,method = lm, se = TRUE, aes(y =log(AllExtSpExtProb
), x= Nsp_active), col = "darkorchid4") +
  geom_smooth(size= 4,method = lm, se = TRUE, aes(y =log(Alive_Vulnerabi
lity), x= Nsp_active), col = "grey42") +
  # ggpubar::stat_cor(npcy = 0.95, npcx = 0.05,
  #                     aes(Nsp_active, log(AllExtSpExtProb), label = paste
(..r.Label.., ..rr.Label.., ..p.Label.., sep = "~~~")),
  #                     geom = "Label_npc", size = 3, col ="purple", Label
.y.npc = "top", label.x.npc = "Left") +
  # ggpubar::stat_cor(npcy = 0.9, npcx = 0.05,
  #                     aes(Nsp_active, log(Alive_Vulnerability), label =
paste(..r.Label.., ..rr.Label.., ..p.Label.., sep = "~~~")),
  #                     geom = "Label_npc", size = 3, col ="grey42", Label
.y.npc = "top", label.x.npc = "Left") +
  geom_vline(xintercept = 10, col = "red", linetype = "dashed", size = 0
.8) +
  geom_vline(xintercept = 41, col = "green", size = 0.8) +
  geom_text(size = 12, x = 65, y = -6.1, label = "d") +
  scale_y_continuous(name = expression(low %<-% "Climate change pressure
(log)" %->% high), limits = c(-6.5,-4)) +
  scale_x_continuous(limits = c(0,70)) +
  theme_classic()+
  theme(legend.position="right") +
  labs(y = "Vulnerability",
       x = "Species Richness") + plot_layout(tag_level = 'new')

plot8 <- Xs_B14_BPc %>%
  filter(!is.na(Nsp_active)) %>%
  ggplot(., aes(x=Nsp_active,y=log(Alive_Vulnerability)))+
  geom_point(colour="grey",alpha=0.05, size = 1)+
  geom_point(aes(y=log(ExtSpExtProb)), alpha=0.05, color = "blue", size

```

```

= 1) +
  geom_point(aes(y=log(CoExtSpExtProb)), alpha=0.05, colour = "yellow2",
size = 1) +
  geom_smooth(size= 4,method = lm, se = TRUE, aes(y =log(ExtSpExtProb),
x= Nsp_active), col = "blue") +
  geom_smooth(size= 4,method = lm, se = TRUE, aes(y =log(Alive_Vulnerabi
lity), x= Nsp_active), col = "grey40") +
  geom_smooth(size= 4,method = lm, se = TRUE, aes(y =log(CoExtSpExtProb)
, x= Nsp_active), col = "yellow3") +
  # ggpubr::stat_cor(npcy = 0.95, npcx = 0.05,
  #                   aes(Nsp_active, log(ExtSpExtProb), Label = paste(..r.
  r.Label.., ..rr.Label.., ..p.Label.., sep = "~~~")),
  #                   geom = "label_npc", size = 3, col ="blue", Label.y.
  npc = "top", Label.x.npc = "Left") +
  # ggpubr::stat_cor(npcy = 0.9, npcx = 0.05,
  #                   aes(Nsp_active, log(CoExtSpExtProb), Label = past
e(..r.Label.., ..rr.Label.., ..p.Label.., sep = "~~~")),
  #                   geom = "label_npc", size = 3, col ="yellow2", Label
.y.npc = "top", Label.x.npc = "Left") +
  geom_vline(xintercept = 10, col = "red", linetype = "dashed", size = 0
.8) +
  geom_vline(xintercept = 41, col = "green", size = 0.8) +
  geom_text(size = 12, x = 65, y = -6.1, label = "j") +
  scale_y_continuous(name = expression(low %<-% "Climate change pressure
(log)" %->% high), limits = c(-6.5,-4)) +
  scale_x_continuous(limits = c(0,70)) +
  theme_classic()+
  theme(legend.position="right") +
  labs(x = "Species Richness") + plot_layout(tag_level = 'new')

plot9 <- B14_B13_BPc %>%
  filter(!is.na(Nsp_active)) %>%
  group_by(Simulation, Nsp, Nsp_active) %>%
  summarise(Alive_Vulnerability = Alive_Vulnerability,
            AllExtSpExtProb = mean(c(ExtSpExtProb,CoExtSpExtProb), na.rm
= T)) %>%
  ggplot(.,aes(x=Nsp_active,y=log(Alive_Vulnerability)))+
  geom_point(colour="grey",alpha=0.05, size = 1) +
  geom_point(aes(y=log(AllExtSpExtProb)), alpha=0.05, col = "purple", si
ze = 1) +
  geom_smooth(size= 4,method = lm, se = TRUE, aes(y =log(AllExtSpExtProb)
, x= Nsp_active), col = "darkorchid4") +
  geom_smooth(size= 4,method = lm, se = TRUE, aes(y =log(Alive_Vulnerabi
lity), x= Nsp_active), col = "grey42") +
  # ggpubr::stat_cor(npcy = 0.95, npcx = 0.05,
  #                   aes(Nsp_active, log(AllExtSpExtProb), Label = paste
(..r.Label.., ..rr.Label.., ..p.Label.., sep = "~~~")),
  #                   geom = "label_npc", size = 3, col ="purple", Label.
  y.npc = "top", Label.x.npc = "Left") +
  # ggpubr::stat_cor(npcy = 0.9, npcx = 0.05,
  #                   aes(Nsp_active, log(Alive_Vulnerability), Label =
  paste(..r.Label.., ..rr.Label.., ..p.Label.., sep = "~~~")),
  #                   geom = "label_npc", size = 3, col ="grey42", Label.
  y.npc = "top", Label.x.npc = "Left") +
  geom_vline(xintercept = 11, col = "red", linetype = "dashed", size = 0
.8) +

```

```

geom_vline(xintercept = 27, col = "green", size = 0.8) +
geom_text(size = 12, x = 65, y = -6.1, label = "e") +
scale_y_continuous(name = expression(low %<-% "Climate change pressure
(log)" %->% high), limits = c(-6.5,-4)) +
scale_x_continuous(limits = c(0,70)) +
theme_classic()+
theme(legend.position="right") +
labs(y = "Vulnerability",
x = "Species Richness") + plot_layout(tag_level = 'new')

plot10 <- B14_B13_BPc %>%
  filter(!is.na(Nsp_active)) %>%
  ggplot(., aes(x=Nsp_active,y=log(Alive_Vulnerability)))+
  geom_point(colour="grey",alpha=0.05, size = 1)+
  geom_point(aes(y=log(ExtSpExtProb)), alpha=0.05, color = "blue", size
= 1) +
  geom_point(aes(y=log(CoExtSpExtProb)), alpha=0.05, colour = "yellow2",
size = 1) +
  geom_smooth(size= 4,method = lm, se = TRUE, aes(y =log(ExtSpExtProb),
x= Nsp_active), col = "blue") +
  geom_smooth(size= 4,method = lm, se = TRUE, aes(y =log(Alive_Vulnerabi
lity), x= Nsp_active), col = "grey40") +
  geom_smooth(size= 4,method = lm, se = TRUE, aes(y =log(CoExtSpExtProb)
, x= Nsp_active), col = "yellow3") +
  # ggpubr::stat_cor(npcy = 0.95, npcx = 0.05,
  #                   aes(Nsp_active, log(ExtSpExtProb), Label = paste(..r.Label.., ..rr.Label.., ..p.Label.., sep = "~~~")),
  #                   geom = "label_npc", size = 3, col ="blue", Label.y.
  npc = "top", Label.x.npc = "left") +
  # ggpubr::stat_cor(npcy = 0.9, npcx = 0.05,
  #                   aes(Nsp_active, log(CoExtSpExtProb), Label = past
e(..r.Label.., ..rr.Label.., ..p.Label.., sep = "~~~")),
  #                   geom = "label_npc", size = 3, col ="yellow2", Label
.y.npc = "top", Label.x.npc = "left") +
  geom_vline(xintercept = 11, col = "red", linetype = "dashed", size = 0
.8) +
  geom_vline(xintercept = 27, col = "green", size = 0.8) +
  geom_text(size = 12,x = 65, y = -6.1, label = "k") +
  scale_y_continuous(name = expression(low %<-% "Climate change pressure
(log)" %->% high), limits = c(-6.5,-4)) +
  scale_x_continuous(limits = c(0,70)) +
  theme_classic()+
  theme(legend.position="right") +
  labs(x = "Species Richness") + plot_layout(tag_level = 'new')

plot11 <- B17_B13_BPc %>%
  filter(!is.na(Nsp_active)) %>%
  group_by(Simulation, Nsp, Nsp_active) %>%
  summarise(Alive_Vulnerability = Alive_Vulnerability,
  AllExtSpExtProb = mean(c(ExtSpExtProb,CoExtSpExtProb), na.rm
=TRUE)) %>%
  ggplot(.,aes(x=Nsp_active,y=log(Alive_Vulnerability)))+
  geom_point(colour="grey",alpha=0.05, size = 1)+
  geom_point(aes(y=log(AllExtSpExtProb)), alpha=0.05, col = "purple", si
ze = 1) +
  geom_smooth(size= 4,method = lm, se = TRUE, aes(y =log(AllExtSpExtProb)
, x= Nsp_active), col = "blue") +
  geom_text(size = 12,x = 65, y = -6.1, label = "k") +
  scale_y_continuous(name = expression(low %<-% "Climate change pressure
(log)" %->% high), limits = c(-6.5,-4)) +
  scale_x_continuous(limits = c(0,70)) +
  theme_classic()+
  theme(legend.position="right") +
  labs(x = "Species Richness") + plot_layout(tag_level = 'new')

```

```

), x= Nsp_active), col = "darkorchid4") +
  geom_smooth(size= 4,method = lm, se = TRUE, aes(y =log(Alive_Vulnerability), x= Nsp_active), col = "grey42") +
  # ggpubr::stat_cor(npcy = 0.95, npcx = 0.05,
  #                   aes(Nsp_active, log(ALLExtSpExtProb), label = paste(..r.Label.., ..rr.Label.., ..p.Label.., sep = "~~~")),
  #                   geom = "label_npc", size = 3, col = "purple", label.y.npc = "top", label.x.npc = "left") +
  # ggpubr::stat_cor(npcy = 0.9, npcx = 0.05,
  #                   aes(Nsp_active, log(Alive_Vulnerability), label = paste(..r.Label.., ..rr.Label.., ..p.Label.., sep = "~~~")),
  #                   geom = "label_npc", size = 3, col = "grey42", label.y.npc = "top", label.x.npc = "left") +
  geom_vline(xintercept = 11, col = "red", linetype = "dashed", size = 0.8) +
  geom_vline(xintercept = 52, col = "green", size = 0.8) +
  geom_text(size = 12, x = 65, y = -6.1, label = "f") +
  scale_y_continuous(name = expression(low %<-% "Climate change pressure (log)" %->% high), limits = c(-6.5,-4)) +
  scale_x_continuous(limits = c(0,70)) +
  theme_classic()+
  theme(legend.position="right") +
  labs(y = "Vulnerability",
       x = "Species Richness") + plot_layout(tag_level = 'new')

plot12 <- B17_B13_BPc %>%
  filter(!is.na(Nsp_active)) %>%
  ggplot(., aes(x=Nsp_active,y=log(Alive_Vulnerability)))+
  geom_point(colour="grey",alpha=0.05, size = 1)+
  geom_point(aes(y=log(ExtSpExtProb)), alpha=0.01, color = "blue", size = 1) +
  geom_point(aes(y=log(CoExtSpExtProb)), alpha =0.01, colour = "yellow2",
             size = 1) +
  geom_smooth(size= 4,method = lm, se = TRUE, aes(y =log(ExtSpExtProb),
  x= Nsp_active), col = "blue") +
  geom_smooth(size= 4,method = lm, se = TRUE, aes(y =log(Alive_Vulnerability), x= Nsp_active), col = "grey40") +
  geom_smooth(size= 4,method = lm, se = TRUE, aes(y =log(CoExtSpExtProb),
  x= Nsp_active), col = "yellow3") +
  # ggpubr::stat_cor(npcy = 0.95, npcx = 0.05,
  #                   aes(Nsp_active, log(ExtSpExtProb), label = paste(..r.Label.., ..rr.Label.., ..p.Label.., sep = "~~~")),
  #                   geom = "label_npc", size = 3, col = "blue", label.y.npc = "top", label.x.npc = "left") +
  # ggpubr::stat_cor(npcy = 0.9, npcx = 0.05,
  #                   aes(Nsp_active, log(CoExtSpExtProb), label = paste(..r.Label.., ..rr.Label.., ..p.Label.., sep = "~~~")),
  #                   geom = "label_npc", size = 3, col = "yellow2", label.y.npc = "top", label.x.npc = "left") +
  geom_vline(xintercept = 11, col = "red", linetype = "dashed", size = 0.8) +
  geom_vline(xintercept = 52, col = "green", size = 0.8) +
  geom_text(size = 12, x = 65, y = -6.1, label = "l") +
  scale_y_continuous(name = expression(low %<-% "Climate change pressure (log)" %->% high), limits = c(-6.5,-4)) +
  scale_x_continuous(limits = c(0,70)) +

```

```

theme_classic()+
  theme(legend.position="right") +
  labs(x = "Species Richness")

Vulnerability_plots <- wrap_elements(grid::textGrob("B17-B16", vjust = 6
, rot = 0, gp = grid::gpar(fontsize = 16))) +
  wrap_elements(grid::textGrob("B16-B15", vjust = 6, rot = 0, gp = grid::gpar(fontsize = 16))) +
  wrap_elements(grid::textGrob("B15-Xs", vjust = 6, rot = 0, gp = grid::gpar(fontsize = 16))) +
  wrap_elements(grid::textGrob("Xs-B14", vjust = 6, rot = 0, gp = grid::gpar(fontsize = 16))) +
  wrap_elements(grid::textGrob("B14-B13", vjust = 6, rot = 0, gp = grid::gpar(fontsize = 16))) +
  plot_spacer() +
  wrap_elements(grid::textGrob("B17-B13", vjust = 6, rot = 0, gp = grid::gpar(fontsize = 16))) +
  (plot1 + theme(axis.title.x = element_blank(), axis.text.x = element_blank(), axis.title.y = element_blank(), axis.text.y = element_text(size = 16))) +
  (plot3 + theme(axis.title.x = element_blank(), axis.text.x = element_blank(), axis.title.y = element_blank(), axis.text.y = element_blank())) +
  (plot5 + theme(axis.title.x = element_blank(), axis.text.x = element_blank(), axis.title.y = element_blank(), axis.text.y = element_blank())) +
  (plot7 + theme(axis.title.x = element_blank(), axis.text.x = element_blank(), axis.title.y = element_blank(), axis.text.y = element_blank())) +
  (plot9 + theme(axis.title.x = element_blank(), axis.text.x = element_blank(), axis.title.y = element_blank(), axis.text.y = element_blank())) +
  plot_spacer() +
  (plot11 + theme(axis.title.x = element_blank(), axis.text.x = element_blank(), axis.title.y = element_blank(), axis.text.y = element_text(size = 16))) +
  (plot2 + theme(axis.title.x = element_blank(), axis.title.y = element_blank(), axis.text.x = element_text(size = 16),
                 axis.text.y = element_text(size = 16))) +
  (plot4 + theme(axis.title.x = element_blank(), axis.title.y = element_blank(), axis.text.y = element_blank(), axis.text.x = element_text(size = 16))) +
  (plot6 + theme(axis.title.x = element_blank(), axis.title.y = element_blank(), axis.text.y = element_blank(), axis.text.x = element_text(size = 16))) +
  (plot8 + theme(axis.title.x = element_blank(), axis.title.y = element_blank(), axis.text.y = element_blank(), axis.text.x = element_text(size = 16))) +
  (plot10 & theme(axis.title.x = element_blank(), axis.title.y = element_blank(), axis.text.y = element_blank(), axis.text.x = element_text(size = 16))) +
  plot_spacer() +
  (plot12 & theme(axis.title.x = element_blank(), axis.title.y = element_blank(), axis.text.x = element_text(size = 16),
                 axis.text.y = element_text(size = 16))) +
  plot_layout(ncol = 7, nrow = 3, widths = c(1,1,1,1,1,0.3,1))

```

## Appendix E

```
# Vulnerability_plots <- Vulnerability_plots & theme(axis.title.y = element_blank(),
#                                                 axis.title.x = element_blank(),
#                                                 axis.text.x = element_text(size = 6),
#                                                 axis.text.y = element_text(size = 6))

ggsave(
  "2018_vulnerability_superplot.tiff",
  plot = Vulnerability_plots,
  device = tiff,
  scale = 2,
  width = 24,
  height = 10,
  units = c("cm"),
  dpi = 300
)
```

## Glossary of Terms

**Anthropocene** ..... the proposed geologic time period in which human activities have had a dominant impact on Earth's systems.

**Arctic** ..... the region surrounding the North Pole with proposed boundaries delineated by the AMAP

**Benthos** ..... the community of organisms that live on, in, or near the bottom of a water body

**Biodiversity** ..... the extent of genetic, taxonomic, and ecological diversity over a specific spatial and temporal scale

**Biodiversity-ecosystem function (BEF)** ..... the relationship between the biodiversity within an ecosystem and the resulting functioning or performance of that ecosystem, encompassing the understanding that the composition, richness, and functional traits of species contribute to its stability, productivity, nutrient cycling, and other ecological processes

**Biological trait** ..... a morpho-physio-phenological characteristic of an individual organism which contributes to the overall fitness of the individual. Examples include body size, growth rate, feeding rate, biomass

**Biomineralisation** ..... the process by which mineral crystals are deposited in the matrix of living organisms, often to harden or stiffen existing tissues

**Carbon sequestration** ..... the process of capture and long-term storage of atmospheric carbon

**Coral paleoclimatology** ..... the use of geochemical records from the skeletons of fossil or modern corals to reconstruct tropical climate variability during the time the coral lived

**Denitrification** ..... the microbial reduction of  $\text{NO}_3^-$  to  $\text{N}_2\text{O}$ , and of  $\text{N}_2\text{O}$  to  $\text{N}_2$

**Diversity** ..... the variation within a specific genetic, taxonomic or ecological group across a predefined spatial and temporal scale

**Early warning signal** ..... (*indicator*) statistical characteristic that allow prediction of a regime shift

**Ecological resilience** ..... capacity of an ecosystem to absorb and adapt to disturbances while maintaining its essential structure and function

**Ecosystem engineer** ..... organism or structure produced by organisms that alter substrate, flow regime, geochemical setting, food supply, or predation pressure for associated organisms

**Ecosystem function** ..... a change in energy and matter over time and space through biological activity, that sustain one or multiple ecosystem services. Examples include productivity, decomposition, nutrient cycling, carbon sequestration

**Ecosystem process** ..... the biological, chemical, and physical activities or interactions that occur within an ecosystem, influencing the flow of energy and matter (see '*ecosystem function*').

**Ecosystem service** ..... a benefit that humans obtain from ecosystems

**Ectotherm** ..... (*ectothermic*) an organism unable to regulate body temperatures independently from the ambient state

**Effect trait** ..... a biological trait that via their expression, influences ecosystem processes

**Epifauna** ..... benthic fauna that live on the sediment surface or hard substrates found on the seafloor

**Extinction** ..... a decline in an organism's population to the point that it no longer exists

**Fauna** ..... animal organism

**Functional diversity** ..... diversity based on species ecological traits rather than taxonomy

**Functional group** ..... organisms with similar trophic, morphological, physiological, behavioural, biochemical, or environmental responses

**Functional redundancy** ..... species or aspects of the ecological system that perform similar roles

**Functional trait** ..... see '*effect trait*'

**Genotype** ..... the complete genetic makeup of an individual organism that consists of the inherited set of genes that it carries within its DNA

**Infauna** ..... benthic fauna that live within the sediment matrix

**Inter-specific trait variability** ..... (*variation*) the difference or similarities in the values of biological traits between different species that result from the development and adaptation of species to environmental change

**Intra-specific trait variability** (*variation*) the difference or similarities in the values of biological traits within one species that result from the development and adaptation of organisms to environmental change

**Large Marine Ecosystem (LME)** extensive regions of ocean space ( $\geq 200,000 \text{ km}^2$ ) that are defined based on ecological criteria, including bathymetry, hydrography, productivity, and the interconnectedness of populations. Arctic LMEs are set out by the PAME working group

**Macrofauna** .....animal organisms over 1mm in size

**Macrozoobenthos** .....the invertebrate community living in or on the sediment or hard substrates and retained on a 1 mm mesh sieve. Examples include crustaceans, polychaetes, bivalves

**Megafauna** .....animal organisms over 1cm in size, but is typically used only to describe marine mammals and large fish

**Meiofauna** .....animal organisms from 0.06 to 1mm in size. Examples include nematodes, foraminiferans, gastrotiches, harpacticoids, or ostracodes

**Microfauna** .....animal organisms smaller than 0.06 mm. Examples include bacteria, ciliates, and flagellates.

**Mineralisation** .....the process of degrading organic material

**Multifunctionality** .....the potential for individual organisms to contribute to more than one ecosystem function

**Niche partitioning** .....(*shifting*) the process by which natural selection drives competing species into different patterns of resource use or different niches

**Patch** .....a spatial aggregation of resources

**Phenotype** .....the observable physical and behavioural traits of an organism that are a result of the interaction between its genotype and the environment

**Phenotypic plasticity** .....the ability of individual genotypes to produce different phenotypes when exposed to different environmental conditions

**Polynya** .....ice-free sea surrounded by sea ice

**Regime shift** .....ecosystem threshold is crossed due to due to a sudden change in feedbacks

## Glossary of Terms

**Resistance**.....capacity of ecology to remain unchanged in the face of disturbance

**Response trait** .....a biological trait that determines how an organism reacts to a disturbance or a change in abiotic or biotic processes in its environment

**Upwelling** .....wind-driven and/or topographic-induced motion of dense, cooler, and usually nutrient-rich water toward the ocean surface

## List of References

Abdalla, M. and Abdalla, M. 'The Grey Hoodie Project: Big Tobacco, Big Tech, and the Threat on Academic Integrity', *Proceedings of the 2021 AAAI/ACM Conference on AI, Ethics, and Society*, 287-297.

Adkins, J. F., Boyle, E. A., Curry, W. B. and Lutringer, A. (2003) 'Stable isotopes in deep-sea corals and a new mechanism for "vital effects"', *Geochimica et Cosmochimica Acta*, 67(6), pp. 1129-1143.

Adkins, J. F., Cheng, H., Boyle, E. A., Druffel, E. R. M. and Edwards, R. L. (1998) 'Deep-Sea coral evidence for rapid change in ventilation of the deep north atlantic 15,400 years Ago', *Science*, 280(5364), pp. 725-8.

Alava, J. J., Cisneros-Montemayor, A. M., Sumaila, U. R. and Cheung, W. W. L. (2018) 'Projected amplification of food web bioaccumulation of MeHg and PCBs under climate change in the Northeastern Pacific', *Scientific Reports*, 8(1), pp. 13460.

Albert, C. H., Thuiller, W., Yoccoz, N. G., Soudant, A., Boucher, F., Saccone, P. and Lavorel, S. (2010) 'Intraspecific functional variability: extent, structure and sources of variation', *Journal of Ecology*, 98(3), pp. 604-613.

Alexander, J. M., Chalmandrier, L., Lenoir, J., Burgess, T. I., Essl, F., Haider, S., Kueffer, C., McDougall, K., Milbau, A., Nunez, M. A., Pauchard, A., Rabitsch, W., Rew, L. J., Sanders, N. J. and Pellissier, L. (2018) 'Lags in the response of mountain plant communities to climate change', *Global Change Biology*, 24(2), pp. 563-579.

Alexander, J. M., Diez, J. M. and Levine, J. M. (2015) 'Novel competitors shape species' responses to climate change', *Nature*, 525(7570), pp. 515-8.

Alibert, C., Kinsley, L., Fallon, S. J., McCulloch, M. T., Berkelmans, R. and McAllister, F. (2003) 'Source of trace element variability in Great Barrier Reef corals affected by the Burdekin flood plumes', *Geochimica Et Cosmochimica Acta*, 67(2), pp. 231-246.

Alibert, C. and McCulloch, M. T. (1997) 'Strontium/calcium ratios in modern *Porites* corals from the Great Barrier Reef as a proxy for sea surface temperature: Calibration of the thermometer and monitoring of ENSO', *Paleoceanography*, 12(3), pp. 345-363.

Allan, B. M., Nimmo, D. G., Ierodiaconou, D., VanDerWal, J., Koh, L. P. and Ritchie, E. G. (2018) 'Futurecasting ecological research: the rise of technoeontology', *Ecosphere*, 9(5).

Allison, N. and Finch, A. A. (2004) 'High-resolution Sr/Ca records in modern *Porites lobata* corals: Effects of skeletal extension rate and architecture', *Geochemistry Geophysics Geosystems*, 5.

Alpert, A. E., Cohen, A. L., Oppo, D. W., DeCarlo, T. M., Gove, J. M. and Young, C. W. (2016) 'Comparison of equatorial Pacific sea surface temperature variability and trends with Sr/Ca records from multiple corals', *Paleoceanography*, 31(2), pp. 252-265.

Alvarez, J., Yumashev, D. and Whiteman, G. (2020) 'A framework for assessing the economic impacts of Arctic change', *Ambio*, 49(2), pp. 407-418.

Ambrose, W. G. and Renaud, P. E. (1995) 'Benthic Response to Water Column Productivity Patterns - Evidence for Benthic-Pelagic Coupling in the Northeast Water Polynya', *Journal of Geophysical Research-Oceans*, 100(C3), pp. 4411-4421.

## List of References

Anagnostou, E., Huang, K. F., You, C. F., Sikes, E. L. and Sherrell, R. M. (2012) 'Evaluation of boron isotope ratio as a pH proxy in the deep sea coral *Desmophyllum dianthus*: Evidence of physiological pH adjustment', *Earth and Planetary Science Letters*, 349, pp. 251-260.

Anagnostou, E., Sherrell, R. M., Gagnon, A., LaVigne, M., Field, M. P. and McDonough, W. F. (2011) 'Seawater nutrient and carbonate ion concentrations recorded as P/Ca, Ba/Ca, and U/Ca in the deep-sea coral *Desmophyllum dianthus*', *Geochimica Et Cosmochimica Acta*, 75(9), pp. 2529-2543.

Andrade, M., De Marchi, L., Soares, A., Rocha, R. J. M., Figueira, E. and Freitas, R. (2019) 'Are the effects induced by increased temperature enhanced in *Mytilus galloprovincialis* submitted to air exposure?', *Science of the Total Environment*, 647, pp. 431-440.

Andrews, A. H., Stone, R. P., Lundstrom, C. C. and DeVogelaere, A. P. (2009) 'Growth rate and age determination of bamboo corals from the northeastern Pacific Ocean using refined 210Pb dating', *Marine Ecology Progress Series*, 397, pp. 173-185.

Anisimova, N. A., Jørgensen, L. L., Lyubin, P. A. and Manushin, I. E. (2010) *Mapping and monitoring of benthos in the Barents Sea and Svalbard waters: Results from the joint Russian - Norwegian benthic programme 2006-2008.*: IMR-PINRO.

Applebaum, S. L., Pan, T. C., Hedgecock, D. and Manahan, D. T. (2014) 'Separating the nature and nurture of the allocation of energy in response to global change', *Integrative and Comparative Biology*, 54(2), pp. 284-95.

Aranha, R., Edinger, E., Layne, G. and Piercy, G. (2014) 'Growth rate variation and potential paleoceanographic proxies in *Primnoa pacifica*: Insights from high-resolution trace element microanalysis', *Deep-Sea Research Part II-Topical Studies in Oceanography*, 99, pp. 213-226.

Arctic-Council (2004) *Arctic Human Development Report*: Arctic Council. Available at: <https://oaarchive.arctic-council.org>.

Arese Lucini, F., Morone, F., Tomassone, M. S. and Makse, H. A. (2020) 'Diversity increases the stability of ecosystems', *PLoS One*, 15(4), pp. e0228692.

Arnberg, M., Calosi, P., Spicer, J. I., Tandberg, A. H. S., Nilsen, M., Westerlund, S. and Bechmann, R. K. (2012) 'Elevated temperature elicits greater effects than decreased pH on the development, feeding and metabolism of northern shrimp (*Pandalus borealis*) larvae', *Marine Biology*, 160(8), pp. 2037-2048.

Arrigo, K. R., van Dijken, G. L., Cameron, M. A., van der Grint, J., Wedding, L. M., Hazen, L., Leape, J., Leonard, G., Merkl, A., Micheli, F., Mills, M. M., Monismith, S., Ouellette, N. T., Zivian, A., Levi, M. and Bailey, R. M. (2020) 'Synergistic interactions among growing stressors increase risk to an Arctic ecosystem', *Nature Communications*, 11(1), pp. 6255.

Ashton, G. V., Morley, S. A., Barnes, D. K. A., Clark, M. S. and Peck, L. S. (2017) 'Warming by 1 degrees C Drives Species and Assemblage Level Responses in Antarctica's Marine Shallows', *Current Biology*, 27(17), pp. 2698-2705 e3.

Asnicar, D., Novoa-Abelleira, A., Minichino, R., Badocco, D., Pastore, P., Finos, L., Munari, M. and Marin, M. G. (2021) 'When site matters: Metabolic and behavioural responses of adult sea urchins from different environments during long-term exposure to seawater acidification', *Marine Environmental Research*, 169, pp. 105372.

Auger, M., Morrow, R., Kestenare, E., Sallee, J. B. and Cowley, R. (2021) 'Southern Ocean in-situ temperature trends over 25 years emerge from interannual variability', *Nature Communications*, 12(1), pp. 514.

Aune, M., Aschan, M. M., Greenacre, M., Dolgov, A. V., Fossheim, M. and Primicerio, R. (2018) 'Functional roles and redundancy of demersal Barents Sea fish: Ecological implications of environmental change', *PLoS One*, 13(11), pp. e0207451.

Azetsu-Scott, K., Clarke, A., Falkner, K., Hamilton, J., Jones, E. P., Lee, C., Petrie, B., Prinsenberg, S., Starr, M. and Yeats, P. (2010) 'Calcium carbonate saturation states in the waters of the Canadian Arctic Archipelago and the Labrador Sea', *Journal of Geophysical Research-Oceans*, 115(C11).

Azetsu-Scott, K., Petrie, B., Yeats, P. and Lee, C. (2012) 'Composition and fluxes of freshwater through Davis Strait using multiple chemical tracers', *Journal of Geophysical Research-Oceans*, 117(C12), pp. n/a-n/a.

Bailey, R. G. (1998) *Ecoregions*. Springer New York, NY.

Bailey, R. M. and van der Grient, J. M. A. (2020) 'OSIRIS: A model for integrating the effects of multiple stressors on marine ecosystems', *Journal of Theoretical Biology*, 493, pp. 110211.

Baker, D. J., Hartley, A. J., Butchart, S. H. and Willis, S. G. (2016) 'Choice of baseline climate data impacts projected species' responses to climate change', *Global Change Biology*, 22(7), pp. 2392-404.

Balvanera, P., Pfisterer, A. B., Buchmann, N., He, J. S., Nakashizuka, T., Raffaelli, D. and Schmid, B. (2006) 'Quantifying the evidence for biodiversity effects on ecosystem functioning and services', *Ecology Letters*, 9(10), pp. 1146-56.

Barner, A. K., Chan, F., Hettinger, A., Hacker, S. D., Marshall, K. and Menge, B. A. (2018) 'Generality in multispecies responses to ocean acidification revealed through multiple hypothesis testing', *Global Change Biology*, 24(10), pp. 4464-4477.

Barnes, D. K. A., Andrade, L., Braun, J., Broad, E., Brunner, L., Downes, P., Dixon, J., Ensor, N., Evans, J., Faust, J., Godbold, J., Henley, S., Jones, R., May, R., McAfee, C., Mesher, T., Murdoch, I., Owen, R., Reed, A., Rühl, S., Sales de Freitas, F., Stevenson, M., Venables, E., Vincent, S., Walkinshaw, C., Williams, T., Wood, C., Zaencker, B. and Zindorf, M. (2019) *Changing Arctic Ocean Seafloor JR18006 Cruise Report*.

Barnes, D. K. A., Ashton, G. V., Morley, S. A. and Peck, L. S. (2021) '1 degrees C warming increases spatial competition frequency and complexity in Antarctic marine macrofauna', *Commun Biol*, 4(1), pp. 208.

Barnes, D. K. A., Fleming, A., Sands, C. J., Quartino, M. L. and Dereibus, D. (2018) 'Icebergs, sea ice, blue carbon and Antarctic climate feedbacks', *Philosophical Transactions of the Royal Society A*, 376(2122).

Barnes, E. A. and Screen, J. A. (2015) 'The impact of Arctic warming on the midlatitude jet-stream: Can it? Has it? Will it?', *WIREs Climate Change*, 6(3), pp. 277-286.

Barnosky, A. D., Matzke, N., Tomiya, S., Wogan, G. O., Swartz, B., Quental, T. B., Marshall, C., McGuire, J. L., Lindsey, E. L., Maguire, K. C., Mersey, B. and Ferrer, E. A. (2011) 'Has the Earth's sixth mass extinction already arrived?', *Nature*, 471(7336), pp. 51-7.

Barton, B. I., Lenn, Y. D. and Lique, C. (2018) 'Observed Atlantification of the Barents Sea Causes the Polar Front to Limit the Expansion of Winter Sea Ice', *Journal of Physical Oceanography*, 48(8), pp. 1849-1866.

Baskett, M. L., Fabina, N. S. and Gross, K. (2014) 'Response diversity can increase ecological resilience to disturbance in coral reefs', *The American Naturalist*, 184(2), pp. E16-31.

## List of References

Battaglia, G. and Joos, F. (2018) 'Hazards of decreasing marine oxygen: the near-term and millennial-scale benefits of meeting the Paris climate targets', *Earth System Dynamics*, 9(2), pp. 797-816.

Bayer, F. M. (1956) *Octocorallia*.

Bayne, B. L., Bayne, B. L., Programme, I. B. and Press, C. U. (1976) *Marine Mussels: Their Ecology and Physiology*. Cambridge University Press.

Bayne, B. L., Brown, D. A., Burns, K., Dixon, D. R., Ivanovici, A., Linvingstone, D. R., Lowe, D. M., Moore, M. N., Stebbing, A. R. D. and Widdows, J. (1985) *The Effects of Stress and Pollution on Marine Animals*. Praeger.

Ben-Shachar, M., Lüdecke, D. and Makowski, D. (2020) 'effectsize: Estimation of Effect Size Indices and Standardized Parameters', *Journal of Open Source Software*, 5(56).

Bennett, E. M., Cramer, W., Begossi, A., Cundill, G., Diaz, S., Egoh, B. N., Geijzendorffer, I. R., Krug, C. B., Lavorel, S., Lazos, E., Lebel, L., Martin-Lopéz, B., Meyfroidt, P., Mooney, H. A., Nel, J. L., Pascual, U., Payet, K., Harguindeguy, N. P., Peterson, G. D., Prieur-Richard, A. H. N., Reyers, B., Roebeling, P., Seppelt, R., Solan, M., Tschakert, P., Tscharntke, T., Turner, B. L., Verburg, P. H., Viglizzo, E. F., White, P. C. L. and Woodward, G. (2015) 'Linking biodiversity, ecosystem services, and human well-being: three challenges for designing research for sustainability', *Current Opinion in Environmental Sustainability*, 14, pp. 76-85.

Bennett, S., Duarte, C. M., Marba, N. and Wernberg, T. (2019) 'Integrating within-species variation in thermal physiology into climate change ecology', *Philosophical Transactions of the Royal Society B: Biological Sciences*, 374(1778), pp. 20180550.

Benton, M. J. and Twitchett, R. J. (2003) 'How to kill (almost) all life: the end-Permian extinction event', *Trends in Ecology & Evolution*, 18(7), pp. 358-365.

Berezina, N. A., Maximov, A. A. and Vladimirova, O. M. (2019) 'Influence of benthic invertebrates on phosphorus flux at the sediment-water interface in the easternmost Baltic Sea', *Marine Ecology Progress Series*, 608, pp. 33-43.

Berge, J., Daase, M., Renaud, P. E., Ambrose, W. G., Jr., Darnis, G., Last, K. S., Leu, E., Cohen, J. H., Johnsen, G., Moline, M. A., Cottier, F., Varpe, O., Shunatova, N., Balazy, P., Morata, N., Massabuau, J. C., Falk-Petersen, S., Kosobokova, K., Hoppe, C. J., Weslawski, J. M., Kuklinski, P., Legezynska, J., Nikishina, D., Cusa, M., Kedra, M., Włodarska-Kowalcuk, M., Vogedes, D., Camus, L., Tran, D., Michaud, E., Gabrielsen, T. M., Granovitch, A., Gonchar, A., Krapp, R. and Callesen, T. A. (2015) 'Unexpected Levels of Biological Activity during the Polar Night Offer New Perspectives on a Warming Arctic', *Current Biology*, 25(19), pp. 2555-61.

Berge, J. A., Bjerkeng, B., Pettersen, O., Schaanning, M. T. and Oxnevad, S. (2006) 'Effects of increased sea water concentrations of CO<sub>2</sub> on growth of the bivalve *Mytilus edulis* L', *Chemosphere*, 62(4), pp. 681-7.

Bernhardt, J. R. and Leslie, H. M. (2013) 'Resilience to climate change in coastal marine ecosystems', *Annual Review of Marine Science*, 5, pp. 371-92.

Bestion, E., Teyssier, A., Richard, M., Clobert, J. and Cote, J. (2015) 'Live Fast, Die Young: Experimental Evidence of Population Extinction Risk due to Climate Change', *PLoS Biology*, 13(10), pp. e1002281.

Biggs, C. R., Yeager, L. A., Bolser, D. G., Bonsell, C., Dichiera, A. M., Hou, Z., Keyser, S. R., Khursigara, A. J., Lu, K., Muth, A. F., Negrete, B. and Erisman, B. E. (2020) 'Does functional

redundancy affect ecological stability and resilience? A review and meta-analysis', *Ecosphere*, 11(7).

Biles, C. L., Solan, M., Isaksson, I., Paterson, D. M., Emes, C. and Raffaelli, D. G. (2003) 'Flow modifies the effect of biodiversity on ecosystem functioning: an in situ study of estuarine sediments', *Journal of Experimental Marine Biology and Ecology*, 285, pp. 165-177.

Bimler, M. D., Stouffer, D. B., Lai, H. R. and Mayfield, M. M. (2018) 'Accurate predictions of coexistence in natural systems require the inclusion of facilitative interactions and environmental dependency', *Journal of Ecology*, 106(5), pp. 1839-1852.

Birch, J. R., Fissel, D. B., Lemon, D. D., Cornford, A. B., Herlinveaux, R. H., Lake, R. A. and Smiley, B. D. (1983) *ARCTIC DATA COMPILATION AND APPRAISAL VOLUME 5. Baffin Bay: Physical Oceanography - Temperature, Salinity, Currents and Water Levels*, Sidney, B. C.: Institute of Ocean Sciences Department of Fisheries and Oceans.

Bishop, D. W., Brown Jr, F. A., Jahn, T. L., Prosser, C. L. and Wulff, V. J. (1950) *Comparative Animal Physiology*.

Blois, J. L., Zarnetske, P. L., Fitzpatrick, M. C. and Finnegan, S. (2013) 'Climate change and the past, present, and future of biotic interactions', *Science*, 341(6145), pp. 499-504.

Blott, S. J. and Pye, K. (2001) 'GRADISTAT: A grain size distribution and statistics package for the analysis of unconsolidated sediments', *Earth Surface Processes and Landforms*, 26(11), pp. 1237-1248.

Bluhm, B. A., Gradinger, R. and Hopcroft, R. R. (2011) 'Editorial - Arctic Ocean Diversity: synthesis', *Marine Biodiversity*, 41(1), pp. 1-4.

Boetius, A., Albrecht, S., Bakker, K., Bienhold, C., Felden, J., Fernandez-Mendez, M., Hendricks, S., Katlein, C., Lalande, C., Krumpen, T., Nicolaus, M., Peek, I., Rabe, B., Rogacheva, A., Rybakova, E., Somavilla, R., Wenzhofer, F. and Party, R. V. P. A.-S. S. (2013) 'Export of algal biomass from the melting Arctic sea ice', *Science*, 339(6126), pp. 1430-2.

Bolnick, D. I., Amarasekare, P., Araujo, M. S., Burger, R., Levine, J. M., Novak, M., Rudolf, V. H., Schreiber, S. J., Urban, M. C. and Vasseur, D. A. (2011) 'Why intraspecific trait variation matters in community ecology', *Trends Ecology and Evolution*, 26(4), pp. 183-92.

Bolnick, D. I., Svanback, R., Fordyce, J. A., Yang, L. H., Davis, J. M., Hulsey, C. D. and Forister, M. L. (2003) 'The ecology of individuals: incidence and implications of individual specialization', *The American Naturalist*, 161(1), pp. 1-28.

Bonamour, S., Chevin, L. M., Charmantier, A. and Teplitsky, C. (2019) 'Phenotypic plasticity in response to climate change: the importance of cue variation', *Philosophical Transactions of the Royal Society B: Biological Sciences*, 374(1768), pp. 20180178.

Borer, E. T., Harpole, W. S., Adler, P. B., Lind, E. M., Orrock, J. L., Seabloom, E. W. and Smith, M. D. (2014) 'Finding generality in ecology: a model for globally distributed experiments', *Methods in Ecology and Evolution*, 5(1), pp. 65-+.

Boudreau, B. P. and Jørgensen, B. B. (2001) *The benthic boundary layer: transport processes and biogeochemistry*.: Oxford University Press.

Boyd, P. W., Cornwall, C. E., Davison, A., Doney, S. C., Fourquez, M., Hurd, C. L., Lima, I. D. and McMinn, A. (2016) 'Biological responses to environmental heterogeneity under future ocean conditions', *Global Change Biology*, 22(8), pp. 2633-50.

## List of References

Boyles, J. G. and Storm, J. J. (2007) 'The perils of picky eating: dietary breadth is related to extinction risk in insectivorous bats', *PLoS One*, 2(7), pp. e672.

Bracken, M. E., Friberg, S. E., Gonzalez-Dorantes, C. A. and Williams, S. L. (2008) 'Functional consequences of realistic biodiversity changes in a marine ecosystem', *Proceedings of the National Academy of Sciences of the United States of America*, 105(3), pp. 924-8.

Bremner, J., Rogers, S. I. and Frid, C. L. J. (2006) 'Methods for describing ecological functioning of marine benthic assemblages using biological traits analysis (BTA)', *Ecological Indicators*, 6(3), pp. 609-622.

Brockington, S. and Peck, L. S. (2001) 'Seasonality of respiration and ammonium excretion in the Antarctic echinoid *Sterechinus neumayeri*', *Marine Ecology Progress Series*, 219, pp. 159-168.

Brodie, J. F., Aslan, C. E., Rogers, H. S., Redford, K. H., Maron, J. L., Bronstein, J. L. and Groves, C. R. (2014) 'Secondary extinctions of biodiversity', *Trends Ecology and Evolution*, 29(12), pp. 664-72.

Brook, B. W., Sodhi, N. S. and Bradshaw, C. J. (2008) 'Synergies among extinction drivers under global change', *Trends Ecology and Evolution*, 23(8), pp. 453-60.

Brousseau, L., Bonal, D., Cigna, J. and Scotti, I. (2013) 'Highly local environmental variability promotes intrapopulation divergence of quantitative traits: an example from tropical rain forest trees', *Annals of Botany*, 112(6), pp. 1169-79.

Buch, E., Madsen, M. S., She, J., Stendel, M., Leth, O. K., Fjæraa, A. M. and Rattenborg, M. (2019) *Arctic In Situ Data Availability*: European Environment Agency.

Buchholz, R., Banusiewicz, J. D., Burgess, S., Crocker-Buta, S., Eveland, L. and Fuller, L. (2019) 'Behavioural research priorities for the study of animal response to climate change', *Animal Behaviour*, 150, pp. 127-137.

Buchi, L. and Vuilleumier, S. (2014) 'Coexistence of specialist and generalist species is shaped by dispersal and environmental factors', *The American Naturalist*, 183(5), pp. 612-24.

Buckley, L. B., Waaser, S. A., MacLean, H. J. and Fox, R. (2011) 'Does including physiology improve species distribution model predictions of responses to recent climate change?', *Ecology*, 92(12), pp. 2214-21.

Bulling, M. T., Hicks, N., Murray, L., Paterson, D. M., Raffaelli, D., White, P. C. and Solan, M. (2010) 'Marine biodiversity-ecosystem functions under uncertain environmental futures', *Philosophical Transactions of the Royal Society B: Biological Sciences*, 365(1549), pp. 2107-16.

Bulling, M. T., Solan, M., Dyson, K. E., Hernandez-Milian, G., Luque, P., Pierce, G. J., Raffaelli, D., Paterson, D. M. and White, P. C. (2008) 'Species effects on ecosystem processes are modified by faunal responses to habitat composition', *Oecologia*, 158(3), pp. 511-20.

Burgass, M. J., Milner-Gulland, E. J., Stewart Lowndes, J. S., O'Hara, C., Afflerbach, J. C. and Halpern, B. S. (2018) 'A pan-Arctic assessment of the status of marine social-ecological systems', *Regional Environmental Change*, 19(1), pp. 293-308.

Burkepile, D. E. and Hay, M. E. (2007) 'Predator release of the gastropod *Cyphoma gibbosum* increases predation on gorgonian corals', *Oecologia*, 154(1), pp. 167-73.

Burrows, M. T., Schoeman, D. S., Buckley, L. B., Moore, P., Poloczanska, E. S., Brander, K. M., Brown, C., Bruno, J. F., Duarte, C. M., Halpern, B. S., Holding, J., Kappel, C. V., Kiessling, W., O'Connor, M. I., Pandolfi, J. M., Parmesan, C., Schwing, F. B., Sydeman, W. J. and Richardson, A. J.

(2011) 'The pace of shifting climate in marine and terrestrial ecosystems', *Science*, 334(6056), pp. 652-5.

Bushnell, P. G., Steffensen, J. F., Schurmann, H. and Jones, D. R. (1994) 'Exercise metabolism in two species of cod in arctic waters', *Polar Biology*, 14, pp. 43-48.

Byrne, M. (2012) 'Global change ecotoxicology: Identification of early life history bottlenecks in marine invertebrates, variable species responses and variable experimental approaches', *Marine Environmental Research*, 76, pp. 3-15.

Byrne, M., Foo, S. A., Ross, P. M. and Putnam, H. M. (2020) 'Limitations of cross- and multigenerational plasticity for marine invertebrates faced with global climate change', *Global Change Biology*, 26(1), pp. 80-102.

Byrne, M. and Przeslawski, R. (2013) 'Multistressor impacts of warming and acidification of the ocean on marine invertebrates' life histories', *Integrative and Comparative Biology*, 53(4), pp. 582-96.

CAFF (2013) *Arctic Biodiversity Assessment. Status and trends in Arctic biodiversity.*, Akureyri: Conservation of Arctic Flora and Fauna.

Cahill, A. E., Aiello-Lammens, M. E., Fisher-Reid, M. C., Hua, X., Karanewsky, C. J., Ryu, H. Y., Sbeglia, G. C., Spagnolo, F., Waldron, J. B., Warsi, O. and Wiens, J. J. (2013) 'How does climate change cause extinction?', *Proceedings of the Royal Society B: Biological Sciences*, 280(1750), pp. 20121890.

Cahyarini, S. Y., Pfeiffer, M. and Dullo, W. C. (2009) 'Improving SST reconstructions from coral Sr/Ca records: multiple corals from Tahiti (French Polynesia)', *International Journal of Earth Sciences*, 98(1), pp. 31-40.

Cahyarini, S. Y., Pfeiffer, M., Timm, O., Dullo, W. C. and Schonberg, D. G. (2008) 'Reconstructing seawater delta O-18 from paired coral delta O-18 and Sr/Ca ratios: Methods, error analysis and problems, with examples from Tahiti (French Polynesia) and Timor (Indonesia)', *Geochimica Et Cosmochimica Acta*, 72(12), pp. 2841-2853.

Calder-Potts, R. N., Spicer, J. I., Calosi, P., Findlay, H. S., Queiros, A. M. and Widdicombe, S. (2018) 'Density-dependent responses of the brittlestar *Amphiura filiformis* to moderate hypoxia and consequences for nutrient fluxes', *Marine Ecology Progress Series*, 594, pp. 175-191.

Callaghan, T. V., Johansson, M., Key, J., Prowse, T., Ananicheva, M. and Klepikov, A. (2011) 'Feedbacks and Interactions: From the Arctic Cryosphere to the Climate System', *Ambio*, 40(S1), pp. 75-86.

Callendar, G. S. (1938) 'The artificial production of carbon dioxide and its influence on temperature', *Quarterly Journal of the Royal Meteorological Society*, 64(275), pp. 223-240.

Calosi, P., Bilton, D. T. and Spicer, J. I. (2008) 'Thermal tolerance, acclimatory capacity and vulnerability to global climate change', *Biology Letters*, 4(1), pp. 99-102.

Calosi, P., Melatunyan, S., Turner, L. M., Artioli, Y., Davidson, R. L., Byrne, J. J., Viant, M. R., Widdicombe, S. and Rundle, S. D. (2017) 'Regional adaptation defines sensitivity to future ocean acidification', *Nature Communications*, 8, pp. 13994.

Cardinale, B. J., Duffy, J. E., Gonzalez, A., Hooper, D. U., Perrings, C., Venail, P., Narwani, A., Mace, G. M., Tilman, D., Wardle, D. A., Kinzig, A. P., Daily, G. C., Loreau, M., Grace, J. B., Larigauderie, A., Srivastava, D. S. and Naeem, S. (2012) 'Biodiversity loss and its impact on humanity', *Nature*, 486(7401), pp. 59-67.

## List of References

Cardinale, B. J., Srivastava, D. S., Duffy, J. E., Wright, J. P., Downing, A. L., Sankaran, M. and Jouseau, C. (2006) 'Effects of biodiversity on the functioning of trophic groups and ecosystems', *Nature*, 443(7114), pp. 989-92.

Carey, N., Dupont, S., Lundve, B. and Sigwart, J. D. (2014) 'One size fits all: stability of metabolic scaling under warming and ocean acidification in echinoderms', *Marine Biology*, 161(9), pp. 2131-2142.

Carpenter, S. R. (1996) 'Microcosm Experiments have Limited Relevance for Community and Ecosystem Ecology', *Ecology*, 77(3), pp. 677-680.

Carroll, M. L. and Ambrose, W. G. (2012) 'Benthic infaunal community variability on the northern Svalbard shelf', *Polar Biology*, 35(8), pp. 1259-1272.

Carroll, M. L., Denisenko, S. G., Renaud, P. E. and Ambrose, W. G. (2008) 'Benthic infauna of the seasonally ice-covered western Barents Sea: Patterns and relationships to environmental forcing', *Deep-Sea Research Part II-Topical Studies in Oceanography*, 55(20-21), pp. 2340-2351.

Case, D. H., Robinson, L. F., Auro, M. E. and Gagnon, A. C. (2010) 'Environmental and biological controls on Mg and Li in deep-sea scleractinian corals', *Earth and Planetary Science Letters*, 300(3-4), pp. 215-225.

Cassidy, C. (2020) *The effect of environmental variation on species functional traits*. Doctor of Philosophy, University of Southampton.

Cassidy, C., Grange, L. J., Garcia, C., Bolam, S. G. and Godbold, J. A. (2020) 'Species interactions and environmental context affect intraspecific behavioural trait variation and ecosystem function', *Proceedings of the Royal Society B: Biological Sciences*, 287(1919), pp. 20192143.

Castorani, M. C. N. and Hovel, K. A. (2005) 'Invasive prey indirectly increase predation on their native competitors', *Ecology*, 96(7), pp. 1911-1922.

Catford, J. A., Bode, M. and Tilman, D. (2018) 'Introduced species that overcome life history tradeoffs can cause native extinctions', *Nature Communications*, 9(1), pp. 2131.

Chaabane, S., Correa, M. L., Ziveri, P., Trotter, J., Kallel, N., Douville, E., McCulloch, M., Taviani, M., Linares, C. and Montagna, P. (2019) 'Elemental systematics of the calcitic skeleton of *Corallium rubrum* and implications for the Mg/Ca temperature proxy', *Chemical Geology*, 524, pp. 237-258.

Chaine, A. S. and Clobert, J. (2012) 'Dispersal', in *Behavioural Responses to a Changing World: Mechanisms and Consequences* [Online]. Version. Available at: <https://doi.org/10.1093/acprof:osobl/9780199602568.003.0005> (Accessed: 5/23/2023).

Chapelle, G., Peck, L. S. and Clarke, A. (1994) 'Effects of Feeding and Starvation on the Metabolic-Rate of the Necrophagous Antarctic Amphipod *Waldeckia-Obesa* (Chevreux, 1905)', *Journal of Experimental Marine Biology and Ecology*, 183(1), pp. 63-76.

Chen, T., Cobb, K. M., Roff, G., Zhao, J., Yang, H., Hu, M. and Zhao, K. (2018) 'Coral-Derived Western Pacific Tropical Sea Surface Temperatures During the Last Millennium', *Geophysical Research Letters*, 45(8), pp. 3542-3549.

Chevin, L. M., Lande, R. and Mace, G. M. (2010) 'Adaptation, plasticity, and extinction in a changing environment: towards a predictive theory', *PLoS Biology*, 8(4), pp. e1000357.

Chow, T. J. and Goldberg, E. D. (1960) 'On the marine geochemistry of barium', *Geochimica et Cosmochimica Acta*, 20, pp. 192-198.

Chown, S. L., Gaston, K. J. and Fox, C. (2015) 'Macrophysiology – progress and prospects', *Functional Ecology*, 30(3), pp. 330-344.

Christiansen, J. S., Sparboe, M., Saether, B. S. and Siikavuopio, S. I. (2015) 'Thermal behaviour and the prospect spread of an invasive benthic top predator onto the Euro-Arctic shelves', *Diversity and Distributions*, 21(9), pp. 1004-1013.

Cianciaruso, M. V., Batalha, M. A., Gaston, K. J. and Petchey, O. L. (2009) 'Including intraspecific variability in functional diversity', *Ecology*, 90(1), pp. 81-9.

Clare, D. S., Spencer, M., Robinson, L. A. and Frid, C. L. (2016) 'Species-Specific Effects on Ecosystem Functioning Can Be Altered by Interspecific Interactions', *PLoS One*, 11(11), pp. e0165739.

Clark, J. S., Bell, D. M., Hersh, M. H., Kwit, M. C., Moran, E., Salk, C., Stine, A., Valle, D. and Zhu, K. (2011) 'Individual-scale variation, species-scale differences: inference needed to understand diversity', *Ecology Letters*, 14(12), pp. 1273-87.

Clark, M. S., Sommer, U., Sihra, J. K., Thorne, M. A., Morley, S. A., King, M., Viant, M. R. and Peck, L. S. (2017) 'Biodiversity in marine invertebrate responses to acute warming revealed by a comparative multi-omics approach', *Global Change Biology*, 23(1), pp. 318-330.

Clark, T. D., Sandblom, E. and Jutfelt, F. (2013) 'Aerobic scope measurements of fishes in an era of climate change: respirometry, relevance and recommendations', *Journal of Experimental Biology*, 216(Pt 15), pp. 2771-82.

Clarke, A. (1993) 'Temperature and Extinction in the Sea: A Physiologist's View', *Paleobiology*, 19(4), pp. 499-518.

Clarke, A., Aronson, R. B., Crame, J. A., Gil, J. M. and Blake, D. B. (2004) 'Evolution and diversity of the benthic fauna of the Southern Ocean continental shelf', *Antarctic Science*, 16(4), pp. 559-568.

Clarke, H., D'Olivo, J. P., Conde, M., Evans, R. D. and McCulloch, M. T. (2019) 'Coral Records of Variable Stress Impacts and Possible Acclimatization to Recent Marine Heat Wave Events on the Northwest Shelf of Australia', *Paleoceanography and Paleoceanography*, 34(11), pp. 1672-1688.

Clements, J. C., Bishop, M. M. and Hunt, H. L. (2017) 'Elevated temperature has adverse effects on GABA-mediated avoidance behaviour to sediment acidification in a wide-ranging marine bivalve', *Marine Biology*, 164(3).

Clements, J. C. and Hunt, H. L. (2014) 'Influence of sediment acidification and water flow on sediment acceptance and dispersal of juvenile soft-shell clams (*Mya arenaria* L.)', *Journal of Experimental Marine Biology and Ecology*, 453, pp. 62-69.

Clements, J. C., Woodard, K. D. and Hunt, H. L. (2016) 'Porewater acidification alters the burrowing behavior and post-settlement dispersal of juvenile soft-shell clams (*Mya arenaria*)', *Journal of Experimental Marine Biology and Ecology*, 477, pp. 103-111.

Cobb, G. W. (1998) *Introduction to Design and Analysis of Experiments. Textbooks in Mathematical Sciences* 1 edn.: Key College Emeryville, CA, p. 795.

Cochrane, S. K. J., Denisenko, S. G., Renaud, P. E., Emblow, C. S., Ambrose, W. G., Ellingsen, I. H. and Skarohamar, J. (2009) 'Benthic macrofauna and productivity regimes in the Barents Sea - Ecological implications in a changing Arctic', *Journal of Sea Research*, 61(4), pp. 222-233.

Cochrane, S. K. J., Pearson, T. H., Greenacre, M., Costelloe, J., Ellingsen, I. H., Dahle, S. and Gulliksen, B. (2012) 'Benthic fauna and functional traits along a Polar Front transect in the Barents

## List of References

Sea - Advancing tools for ecosystem-scale assessments', *Journal of Marine Systems*, 94, pp. 204-217.

Cohen, A. L., Layne, G. D., Hart, S. R. and Lobel, P. S. (2001) 'Kinetic control of skeletal Sr/Ca in a symbiotic coral: Implications for the paleotemperature proxy', *Paleoceanography*, 16(1), pp. 20-26.

Collins, C. L., Burnett, N. P., Ramsey, M. J., Wagner, K. and Zippay, M. L. (2020) 'Physiological responses to heat stress in an invasive mussel *Mytilus galloprovincialis* depend on tidal habitat', *Marine Environmental Research*, 154, pp. 104849.

Constable, A. J., Harper, S., Dawson, J., Holsman, K., Mustonen, T., Piepenburg, D. and Rost, B. (2022) 'Cross-Chapter Paper 6: Polar Regions.', in Pörtner, H.-O., Roberts, D.C., Tignor, M., Poloczanska, E.S., Mintenbeck, K., Alegría, A., Craig, M., Langsdorf, S., Löschke, S., Möller, V., Okem, A. and Rama, B. (eds.) *Climate Change 2022: Impacts, Adaptation, and Vulnerability.*.: Cambridge University Press.

Convey, P. and Peck, L. S. (2019) 'Antarctic environmental change and biological responses', *Science Advances*, 5(11), pp. eaaz0888.

Coppola, F., Tavares, D. S., Henriques, B., Monteiro, R., Trindade, T., Soares, A., Figueira, E., Polese, G., Pereira, E. and Freitas, R. (2019) 'Remediation of arsenic from contaminated seawater using manganese spinel ferrite nanoparticles: Ecotoxicological evaluation in *Mytilus galloprovincialis*', *Environmental Research*, 175, pp. 200-212.

Cornwall, C. E., Hepburn, C. D., McGraw, C. M., Currie, K. I., Pilditch, C. A., Hunter, K. A., Boyd, P. W. and Hurd, C. L. (2013) 'Diurnal fluctuations in seawater pH influence the response of a calcifying macroalga to ocean acidification', *Proceedings of the Royal Society B: Biological Sciences*, 280(1772), pp. 20132201.

Costa, S., Coppola, F., Petti, C., Intorre, L., Meucci, V., Soares, A., Sole, M. and Freitas, R. (2020) 'Biochemical and physiological responses of two clam species to Triclosan combined with climate change scenario', *Science of the Total Environment*, 724, pp. 138143.

Cross, E. L., Peck, L. S. and Harper, E. M. (2015) 'Ocean acidification does not impact shell growth or repair of the Antarctic brachiopod *Liothyrella uva* (Broderip, 1833)', *Journal of Experimental Marine Biology and Ecology*, 462, pp. 29-35.

Csapo, H. K., Grabowski, M. and Weslawski, J. M. (2021) 'Coming home - Boreal ecosystem claims Atlantic sector of the Arctic', *Science of the Total Environment*, 771, pp. 144817.

Culter, A. (1991) 'Nested Faunas and Extinction in Frameneted Habitats', *Conservation Biology*, 5(4), pp. 496-505.

Cummings, V., Hewitt, J., Van Rooyen, A., Currie, K., Beard, S., Thrush, S., Norkko, J., Barr, N., Heath, P., Halliday, N. J., Sedcole, R., Gomez, A., McGraw, C. and Metcalf, V. (2011) 'Ocean acidification at high latitudes: potential effects on functioning of the Antarctic bivalve *Laternula elliptica*', *PLoS One*, 6(1), pp. e16069.

Cuny-Guirriec, K., Douville, E., Reynaud, S., Allemand, D., Bordier, L., Canesi, M., Mazzoli, C., Taviani, M., Canese, S., McCulloch, M., Trotter, J., Rico-Esenaro, S. D., Sanchez-Cabeza, J. A., Ruiz-Fernandez, A. C., Carricart-Ganivet, J. P., Scott, P. M., Sadekov, A. and Montagna, P. (2019) 'Coral Li/Mg thermometry: Caveats and constraints', *Chemical Geology*, 523, pp. 162-178.

Dale, S. (2001) 'Female-biased dispersal, low female recruitment, unpaired males, and the extinction of small and isolated bird populations', *Oikos*, 92(2), pp. 344-356.

Dalpadado, P., Arrigo, K. R., van Dijken, G. L., Skjoldal, H. R., Bagoien, E., Dolgov, A. V., Prokophchuk, I. P. and Sperfeld, E. (2020) 'Climate effects on temporal and spatial dynamics of phytoplankton and zooplankton in the Barents Sea', *Progress in Oceanography*, 185.

Danovaro, R., Corinaldesi, C., Dell'Anno, A. and Snelgrove, P. V. R. (2017) 'The deep-sea under global change', *Current Biology*, 27(11), pp. R461-R465.

Darnell, M. Z., Yeghissian, T. G. and Lane, Z. M. (2020) 'Balancing risk and reward: mating opportunity influences thermal refuge use in fiddler crabs', *Animal Behaviour*, 169, pp. 51-56.

Davenport, J. (1997) 'The feeding mechanism of *Yoldia* (= *Aequiyoldia*) *eightsi* (Courthouy)', *Proceedings of the Royal Society B: Biological Sciences*, 232(1269), pp. 431-442.

Davey, C. M., Chamberlain, D. E., Newson, S. E., Noble, D. G. and Johnston, A. (2012) 'Rise of the generalists: evidence for climate driven homogenization in avian communities', *Global Ecology and Biogeography*, 21(5), pp. 568-578.

Davis, M. A. (2003) 'Biotic Globalization: Does Competition from Introduced Species Threaten Biodiversity?', *Bioscience*, 53(5), pp. 481-489.

Davis, M. B. and Shaw, R. G. (2001) 'Range shifts and adaptive responses to Quaternary climate change', *Science*, 292(5517), pp. 673-9.

De Marchi, L., Neto, V., Pretti, C., Chiellini, F., Morelli, A., Soares, A., Figueira, E. and Freitas, R. (2018) 'Does the exposure to salinity variations and water dispersible carbon nanotubes induce oxidative stress in *Hediste diversicolor*?', *Marine Environmental Research*, 141, pp. 186-195.

de Smit, J. C., Brückner, M. Z. M., Mesdag, K. I., Kleinhans, M. G. and Bouma, T. J. (2021) 'Key Bioturbator Species Within Benthic Communities Determine Sediment Resuspension Thresholds', *Frontiers in Marine Science*, 8.

Deb, J. C. and Bailey, S. A. (2023) 'Arctic marine ecosystems face increasing climate stress', *Environmental Reviews*.

DeCarlo, T. M., Gaetani, G. A., Cohen, A. L., Foster, G. L., Alpert, A. E. and Stewart, J. A. (2016) 'Coral Sr-U thermometry', *Paleoceanography*, 31(6), pp. 626-638.

DeCarlo, T. M., Gaetani, G. A., Holcomb, M. and Cohen, A. L. (2015) 'Experimental determination of factors controlling U/Ca of aragonite precipitated from seawater: Implications for interpreting coral skeleton', *Geochimica Et Cosmochimica Acta*, 162, pp. 151-165.

Degen, R. and Faulwetter, S. (2019) 'The Arctic Traits Database - a repository of Arctic benthic invertebrate traits', *Earth System Science Data*, 11(1), pp. 301-322.

DeLong, K. L., Flannery, J. A., Maupin, C. R., Poore, R. Z. and Quinn, T. M. (2011) 'A coral Sr/Ca calibration and replication study of two massive corals from the Gulf of Mexico', *Palaeogeography Palaeoclimatology Palaeoecology*, 307(1-4), pp. 117-128.

DeLong, K. L., Quinn, T. M. and Taylor, F. W. (2007) 'Reconstructing twentieth-century sea surface temperature variability in the southwest Pacific: A replication study using multiple coral Sr/Ca records from New Caledonia', *Paleoceanography*, 22(4), pp. n/a-n/a.

Delorme, N. J., Biessy, L., South, P. M., Zamora, L. N., Ragg, N. L. C. and Burritt, D. J. (2020) 'Stress-on-stress responses of a marine mussel, *Perna canaliculus*: food limitation reduces the ability to cope with heat stress in juveniles', *Marine Ecology Progress Series*, 644, pp. 105-117.

## List of References

Des Roches, S., Post, D. M., Turley, N. E., Bailey, J. K., Hendry, A. P., Kinnison, M. T., Schweitzer, J. A. and Palkovacs, E. P. (2018) 'The ecological importance of intraspecific variation', *Nature Ecology and Evolution*, 2(1), pp. 57-64.

di Prisco, G., Convey, P., Gutt, J., Cowan, D., Conlan, K. and Verde, C. (2012) 'Understanding and protecting the world's biodiversity: the role and legacy of the SCAR programme "Evolution and Biodiversity in the Antarctic"', *Marine Genomics*, 8, pp. 3-8.

Dickinson, G. H., Matoo, O. B., Tourek, R. T., Sokolova, I. M. and Beniash, E. (2013) 'Environmental salinity modulates the effects of elevated CO<sub>2</sub> levels on juvenile hard-shell clams, *Mercenaria mercenaria*', *Journal of Experimental Biology*, 216(Pt 14), pp. 2607-18.

Dickson, A. G. (1990) 'Thermodynamics of the Dissociation of Boric-Acid in Synthetic Seawater from 273.15-K to 318.15-K', *Deep-Sea Research Part I-Oceanographic Research Papers*, 37(5), pp. 755-766.

Dickson, A. G. and Millero, F. J. (1987) 'A Comparison of the Equilibrium-Constants for the Dissociation of Carbonic-Acid in Seawater Media', *Deep-Sea Research Part I-Oceanographic Research Papers*, 34(10), pp. 1733-1743.

Dillon, M. E., Wang, G. and Huey, R. B. (2010) 'Global metabolic impacts of recent climate warming', *Nature*, 467(7316), pp. 704-6.

Dingemanse, N. J. and Wolf, M. (2013) 'Between-individual differences in behavioural plasticity within populations: causes and consequences', *Animal Behaviour*, 85(5), pp. 1031-1039.

Dolbeth, M., Crespo, D., Leston, S. and Solan, M. (2019) 'Realistic scenarios of environmental disturbance lead to functionally important changes in benthic species-environment interactions', *Marine Environmental Research*, 150, pp. 104770.

Doney, S. C., Ruckelshaus, M., Duffy, J. E., Barry, J. P., Chan, F., English, C. A., Galindo, H. M., Grebmeier, J. M., Hollowed, A. B., Knowlton, N., Polovina, J., Rabalais, N. N., Sydeman, W. J. and Talley, L. D. (2012) 'Climate change impacts on marine ecosystems', *Annual Review of Marine Science*, 4, pp. 11-37.

Duffy, J. E. (2003) 'Biodiversity loss, trophic skew and ecosystem functioning', *Ecology Letters*, 6(8), pp. 680-687.

Duffy, J. E. (2009) 'Why biodiversity is important to the functioning of real-world ecosystems', *Frontiers in Ecology and the Environment*, 7(8), pp. 437-444.

Dunn, R. R., Harris, N. C., Colwell, R. K., Koh, L. P. and Sodhi, N. S. (2009) 'The sixth mass coextinction: are most endangered species parasites and mutualists?', *Proceedings of the Royal Society B: Biological Sciences*, 276(1670), pp. 3037-45.

Edwards, M. and Richardson, A. J. (2004) 'Impact of climate change on marine pelagic phenology and trophic mismatch', *Nature*, 430(7002), pp. 881-4.

Ellingsen, K. E., Yoccoz, N. G., Tveraa, T., Frank, K. T., Johannessen, E., Anderson, M. J., Dolgov, A. V. and Shackell, N. L. (2020) 'The rise of a marine generalist predator and the fall of beta diversity', *Global Change Biology*, 26(5), pp. 2897-2907.

Ellis, E. C., Antill, E. C. and Kreft, H. (2012) 'All is not loss: plant biodiversity in the anthropocene', *PLoS One*, 7(1), pp. e30535.

Emmerson, M. C., Solan, M., Emes, C., Paterson, D. M. and Raffaelli, D. (2001) 'Consistent patterns and the idiosyncratic effects of biodiversity in marine ecosystems', *Nature*, 411(6833), pp. 73-7.

Epskamp, S., Cramer, A. O. J., Waldorp, L. J., Schmittmann, V. D. and Borsboom, D. (2012) 'qgraph: Network Visualizations of Relationships in Psychometric Data', *Journal of Statistical Software*, 48(4), pp. 1-18.

Ericson, J. A., Ho, M. A., Miskelly, A., King, C. K., Virtue, P., Tilbrook, B. and Byrne, M. (2011) 'Combined effects of two ocean change stressors, warming and acidification, on fertilization and early development of the Antarctic echinoid *Sterechinus neumayeri*', *Polar Biology*, 35(7), pp. 1027-1034.

Evans, M. R. (2012) 'Modelling ecological systems in a changing world', *Philosophical Transactions of the Royal Society B: Biological Sciences*, 367(1586), pp. 181-90.

Farmer, J. R., Honisch, B., Robinson, L. F. and Hill, T. M. (2015) 'Effects of seawater-pH and biomineralization on the boron isotopic composition of deep-sea bamboo corals', *Geochimica Et Cosmochimica Acta*, 155, pp. 86-106.

Farmer, J. R., Robinson, L. F. and Honisch, B. (2015) 'Growth rate determinations from radiocarbon in bamboo corals (genus *Keratoisis*)', *Deep-Sea Research Part I-Oceanographic Research Papers*, 105, pp. 26-40.

Fauchald, P., Arneberg, P., Debernard, J. B., Lind, S., Olsen, E. and Hausner, V. H. (2021) 'Poleward shifts in marine fisheries under Arctic warming', *Environmental Research Letters*, 16(7).

Faulwetter, S., Markantonatou, V., Pavloudi, C., Papageorgiou, N., Keklikoglou, K., Chatzinikolaou, E., Pafilis, E., Chatzigeorgiou, G., Vasileiadou, K., Dailianis, T., Fanini, L., Koulouri, P. and Arvanitidis, C. (2014) 'Polytraits: A database on biological traits of marine polychaetes', *Biodiversity Data Journal*, (2), pp. e1024.

Faust, J. C., Stevenson, M. A., Abbott, G. D., Knies, J., Tessin, A., Mannion, I., Ford, A., Hilton, R., Peakall, J. and Marz, C. (2020) 'Does Arctic warming reduce preservation of organic matter in Barents Sea sediments?', *Philosophical Transactions of the Royal Society A*, 378(2181), pp. 20190364.

Fedewa, E. J., Jackson, T. M., Richar, J. I., Gardner, J. L. and Litzow, M. A. (2020) 'Recent shifts in northern Bering Sea snow crab (*Chionoecetes opilio*) size structure and the potential role of climate-mediated range contraction', *Deep-Sea Research Part II-Topical Studies in Oceanography*, 181.

Feely, R. A., Doney, S. C. and Cooley, S. R. (2009) 'Ocean Acidification: Present Conditions and Future Changes in a High-CO<sub>2</sub> World', *Oceanography*, 22(4), pp. 36-47.

Feely, R. A., Sabine, C. L., Lee, K., Millero, F. J., Lamb, M. F., Greeley, D., Bullister, J. L., Key, R. M., Peng, T. H., Kozyr, A., Ono, T. and Wong, C. S. (2002) 'In situ calcium carbonate dissolution in the Pacific Ocean', *Global Biogeochemical Cycles*, 16(4), pp. 91-1-91-12.

Ferguson, N., White, C. R. and Marshall, D. J. (2013) 'Competition in benthic marine invertebrates: the unrecognized role of exploitative competition for oxygen', *Ecology*, 94(1), pp. 126-35.

Ferrari, M. C. O., Dixson, D. L., Munday, P. L., McCormick, M. I., Meekan, M. G., Sih, A. and Chivers, D. P. (2011) 'Intrageneric variation in antipredator responses of coral reef fishes affected by ocean acidification: implications for climate change projections on marine communities', *Global Change Biology*, 17(9), pp. 2980-2986.

Ferrier-Pagès, C., Boisson, F., Allemand, D. and Tambutté, E. (2002) 'Kinetics of strontium uptake in the scleractinian coral *Stylophora pistillata*', *Marine Ecology Progress Series*, 245, pp. 93-100.

## List of References

Fetzer, I., Johst, K., Schawe, R., Banitz, T., Harms, H. and Chatzinotas, A. (2015) 'The extent of functional redundancy changes as species' roles shift in different environments', *Proceedings of the National Academy of Sciences of the United States of America*, 112(48), pp. 14888-93.

Figuerola, B., Hancock, A. M., Bax, N., Cummings, V. J., Downey, R., Griffiths, H. J., Smith, J. and Stark, J. S. (2021) 'A Review and Meta-Analysis of Potential Impacts of Ocean Acidification on Marine Calcifiers From the Southern Ocean', *Frontiers in Marine Science*, 8.

Findlay, H. S., Burrows, M. T., Kendall, M. A., Spicer, J. I. and Widdicombe, S. (2010) 'Can ocean acidification affect population dynamics of the barnacle *Semibalanus balanoides* at its southern range edge?', *Ecology*, 91(10), pp. 2931-40.

Flöter, S. (2019) *The potential of bamboo corals to record environmental conditions in their calcitic skeletons*. PhD, Christian-Albrechts-Universität zu Kiel.

Flöter, S., Fietzke, J., Gutjahr, M., Farmer, J., Hönisch, B., Nehrke, G. and Eisenhauer, A. (2019) 'The influence of skeletal micro-structures on potential proxy records in a bamboo coral', *Geochimica et Cosmochimica Acta*, 248, pp. 43-60.

Flöter, S., Fietzke, J., Gutjahr, M., Nehrke, G. and Eisenhauer, A. (2022) 'Incorporation of Na and S in bamboo coral skeletons', *Chemical Geology*, 597.

Folk, R. L. (1974) *Petrology of Rocks*. 1st edn.

Foo, S. A. and Byrne, M. (2017) 'Marine gametes in a changing ocean: Impacts of climate change stressors on fecundity and the egg', *Marine Environmental Research*, 128, pp. 12-24.

Forbis Jr, R. and Hayhoe, K. (2018) 'Does Arctic governance hold the key to achieving climate policy targets?', *Environmental Research Letters*, 13(2).

Form, A. U. and Riebesell, U. (2012) 'Acclimation to ocean acidification during long-term CO<sub>2</sub> exposure in the cold-water coral *Lophelia pertusa*', *Global Change Biology*, 18(3), pp. 843-853.

Forsman, A. and Wennersten, L. (2016) 'Inter-individual variation promotes ecological success of populations and species: evidence from experimental and comparative studies', *Ecography*, 39(7), pp. 630-648.

Frainer, A., Primicerio, R., Dolgov, A., Fossheim, M., Johannessen, E., Lind, S. and Aschan, M. (2021) 'Increased functional diversity warns of ecological transition in the Arctic', *Proceedings of the Royal Society B: Biological Sciences*, 288(1948), pp. 20210054.

Frainer, A., Primicerio, R., Kortsch, S., Aune, M., Dolgov, A. V., Fossheim, M. and Aschan, M. M. (2017) 'Climate-driven changes in functional biogeography of Arctic marine fish communities', *Proceedings of the National Academy of Sciences of the United States of America*, 114(46), pp. 12202-12207.

Frank, N., Paterne, M., Ayliffe, L., van Weering, T., Henriet, J.-P. and Blamart, D. (2004) 'Eastern North Atlantic deep-sea corals: tracing upper intermediate water Δ<sup>14</sup>C during the Holocene', *Earth and Planetary Science Letters*, 219(3-4), pp. 297-309.

Fraser, M. W., Kendrick, G. A., Statton, J., Hovey, R. K., Zavala-Perez, A. and Walker, D. I. (2014) 'Extreme climate events lower resilience of foundation seagrass at edge of biogeographical range', *Journal of Ecology*, 102(6), pp. 1528-1536.

Frederiksen, M. (2017) 'Synthesis: Status and trends of Arctic marine biodiversity and monitoring', *CAFF State of the Arctic Marine Biodiversity Report*. Akureyri, Iceland: Conservation of Arctic Flora and Fauna International Secretariat, pp. 175-195.

Freitas, R., Coppola, F., Costa, S., Pretti, C., Intorre, L., Meucci, V., Soares, A. and Sole, M. (2019) 'The influence of temperature on the effects induced by Triclosan and Diclofenac in mussels', *Science of the Total Environment*, 663, pp. 992-999.

Freitas, R., Coppola, F., Henriques, B., Wrona, F., Figueira, E., Pereira, E. and Soares, A. (2017a) 'Does pre-exposure to warming conditions increase *Mytilus galloprovincialis* tolerance to Hg contamination?', *Comp Biochem Physiol C Toxicol Pharmacol*, 203, pp. 1-11.

Freitas, R., De Marchi, L., Bastos, M., Moreira, A., Velez, C., Chiesa, S., Wrona, F. J., Figueira, E. and Soares, A. M. V. M. (2017b) 'Effects of seawater acidification and salinity alterations on metabolic, osmoregulation and oxidative stress markers in *Mytilus galloprovincialis*', *Ecological Indicators*, 79, pp. 54-62.

Freitas, R., Pires, A., Moreira, A., Wrona, F. J., Figueira, E. and Soares, A. M. (2016) 'Biochemical alterations induced in *Hediste diversicolor* under seawater acidification conditions', *Marine Environmental Research*, 117, pp. 75-84.

Frenkel, M. M., LaVigne, M., Miller, H. R., Hill, T. M., McNichol, A. and Gaylord, M. L. (2017) 'Quantifying bamboo coral growth rate nonlinearity with the radiocarbon bomb spike: A new model for paleoceanographic chronology development', *Deep-Sea Research Part I-Oceanographic Research Papers*, 125, pp. 26-39.

Frid, C. L. J. and Caswell, B. A. (2015) 'Is long-term ecological functioning stable: The case of the marine benthos?', *Journal of Sea Research*, 98, pp. 15-23.

Fritschie, K. J. and Olden, J. D. (2016) 'Disentangling the influences of mean body size and size structure on ecosystem functioning: an example of nutrient recycling by a non-native crayfish', *Ecology and Evolution*, 6(1), pp. 159-69.

Fritz, S. A., Schnitzler, J., Eronen, J. T., Hof, C., Bohning-Gaese, K. and Graham, C. H. (2013) 'Diversity in time and space: wanted dead and alive', *Trends Ecology and Evolution*, 28(9), pp. 509-16.

Frolova, E. A., Lyubina, O. S., Dikaeva, D. R., Akhmetchina, O. Y. and Frolov, A. A. (2007) 'Effect of climatic changes on the zoobenthos of the Barents Sea (on the example of several abundant species)', *Doklady Biological Sciences*, 416, pp. 349-51.

Fujiwara, A., Hirawake, T., Suzuki, K., Eisner, L., Imai, I., Nishino, S., Kikuchi, T. and Saitoh, S. I. (2016) 'Influence of timing of sea ice retreat on phytoplankton size during marginal ice zone bloom period on the Chukchi and Bering shelves', *Biogeosciences*, 13(1), pp. 115-131.

Fukami, T. and Wardle, D. A. (2005) 'Long-term ecological dynamics: reciprocal insights from natural and anthropogenic gradients', *Proceedings of the Royal Society B: Biological Sciences*, 272(1577), pp. 2105-15.

Furukawa, Y. (2005) 'Biogeochemical consequences of infaunal activities', in Kristensen, E., Haese, R.R. and Kostka, J.E. (eds.) *Interactions Between Macro- and Microorganisms in Marine Sediments Coastal and Estuarine Studies*, pp. 159-177.

Gaetani, G. A., Cohen, A. L., Wang, Z. R. and Crusius, J. (2011) 'Rayleigh-based, multi-element coral thermometry: A biomineralization approach to developing climate proxies', *Geochimica Et Cosmochimica Acta*, 75(7), pp. 1920-1932.

## List of References

Gagan, M. K., Chivas, A. R. and Isdale, P. J. (1994) 'High-Resolution Isotopic Records from Corals Using Ocean Temperature and Mass-Spawning Chronometers', *Earth and Planetary Science Letters*, 121(3-4), pp. 549-558.

Gagan, M. K., Chivas, A. R. and Isdale, P. J. (1996) 'Timing coral-based climatic histories using  $^{13}\text{C}$  enrichments driven by synchronized spawning', *Geology*, 24(11), pp. 1009-1012.

Gagnon, A. C., Adkins, J. F., Fernandez, D. P. and Robinson, L. F. (2007) 'Sr/Ca and Mg/Ca vital effects correlated with skeletal architecture in a scleractinian deep-sea coral and the role of Rayleigh fractionation', *Earth and Planetary Science Letters*, 261(1-2), pp. 280-295.

Gaitan-Espitia, J. D., Bacigalupe, L. D., Opitz, T., Lagos, N. A., Osores, S. and Lardies, M. A. (2017) 'Exploring physiological plasticity and local thermal adaptation in an intertidal crab along a latitudinal cline', *Journal of Thermal Biology*, 68(Pt A), pp. 14-20.

Gammal, J., Hewitt, J., Norkko, J., Norkko, A. and Thrush, S. (2020) 'Does the use of biological traits predict a smooth landscape of ecosystem functioning?', *Ecology and Evolution*, 10(19), pp. 10395-10407.

Garcia, C., Solan, M., Bolam, S. G., Sivyer, D., Parker, R. and Godbold, J. A. (2021) 'Exploration of multiple post-extinction compensatory scenarios improves the likelihood of determining the most realistic ecosystem future', *Environmental Research Communications*, 3(4).

García Molinos, J., Halpern, Benjamin S., Schoeman, David S., Brown, Christopher J., Kiessling, W., Moore, Pippa J., Pandolfi, John M., Poloczanska, Elvira S., Richardson, Anthony J. and Burrows, Michael T. (2015) 'Climate velocity and the future global redistribution of marine biodiversity', *Nature Climate Change*, 6(1), pp. 83-88.

Gardner, W. S., Briones, E. E., Kaegi, E. C. and Rowe, G. T. (1993) 'Ammonium Excretion by Benthic Invertebrates and Sediment-Water Nitrogen Flux in the Gulf-of-Mexico near the Mississippi River Outflow', *Estuaries*, 16(4), pp. 799-808.

Garnier, S., Ross, N., Rudis, R., Camargo, A. P., Sciaiani, M. and Scherer, C. (2021) 'viridis - Colorblind-Friendly Color Maps for R'.

Gaston, K. J. and Fuller, R. A. (2009) 'The sizes of species' geographic ranges', *Journal of Applied Ecology*, 46(1), pp. 1-9.

Gattuso, J.-P. and Hansson, L. (2011) *Ocean Acidification*

Gazeau, F., Parker, L. M., Comeau, S., Gattuso, J. P., O'Connor, W. A., Martin, S., Portner, H. O. and Ross, P. M. (2013) 'Impacts of ocean acidification on marine shelled molluscs', *Marine Biology*, 160(8), pp. 2207-2245.

Geoffroy, M., Algar, C., Archambault, P., Cote, D., Edinger, E., Hubert, C., Laing, R., Limoges, A., Mercier, A., Neves, B. r. d. M., Normandeau, A., Robert, K., Sherwood, O., Snelgrove, P., Hayes, V. W. and Zedel1, L. (2021) *Leg 2 - Labrador Sea, Davis Strait and Baffin Bay*: Amundsen Science.

GEOTRACES-Intermediate-Data-Product-Group (2021) 'The GEOTRACES Intermediate Data Product 2021 (IDP2021)'. Available at: <https://www.geotrades.org/geotrades- intermediate-data-product-2021/>.

Geyman, B. M., Ptacek, J. L., LaVigne, M. and Horner, T. J. (2019) 'Barium in deep-sea bamboo corals: Phase associations, barium stable isotopes, & prospects for paleoceanography', *Earth and Planetary Science Letters*, 525.

Ghalambor, C. K., Hoke, K. L., Ruell, E. W., Fischer, E. K., Reznick, D. N. and Hughes, K. A. (2015) 'Non-adaptive plasticity potentiates rapid adaptive evolution of gene expression in nature', *Nature*, 525(7569), pp. 372-5.

Ghalambor, C. K., McKay, J. K., Carroll, S. P. and Reznick, D. N. (2007) 'Adaptive versus non-adaptive phenotypic plasticity and the potential for contemporary adaptation in new environments', *Functional Ecology*, 21(3), pp. 394-407.

Gianguzza, P., Visconti, G., Gianguzza, F., Vizzini, S., Sara, G. and Dupont, S. (2014) 'Temperature modulates the response of the thermophilous sea urchin *Arbacia lixula* early life stages to CO<sub>2</sub>-driven acidification', *Marine Environmental Research*, 93, pp. 70-7.

Gibbin, E. M., Massamba N'Siala, G., Chakravarti, L. J., Jarrold, M. D. and Calosi, P. (2017) 'The evolution of phenotypic plasticity under global change', *Scientific Reports*, 7(1), pp. 17253.

Gilbert, A. L. and Miles, D. B. (2019) 'Antagonistic Responses of Exposure to Sublethal Temperatures: Adaptive Phenotypic Plasticity Coincides with a Reduction in Organismal Performance', *The American Naturalist*, 194(3), pp. 344-355.

Glazier, D. S. (2005) 'Beyond the '3/4-power law': variation in the intra- and interspecific scaling of metabolic rate in animals', *Biological reviews of the Cambridge Philosophical Society*, 80(4), pp. 611-62.

Godbolt, J. A., Bulling, M. T. and Solan, M. (2011) 'Habitat structure mediates biodiversity effects on ecosystem properties', *Proceedings of the Royal Society B: Biological Sciences*, 278(1717), pp. 2510-8.

Godbolt, J. A., Hale, R., Wood, C. L. and Solan, M. (2017) 'Vulnerability of macronutrients to the concurrent effects of enhanced temperature and atmospheric pCO<sub>2</sub> in representative shelf sea sediment habitats', *Biogeochemistry*, 135(1), pp. 89-102.

Godbolt, J. A., Rosenberg, R. and Solan, M. (2009) 'Species-specific traits rather than resource partitioning mediate diversity effects on resource use', *PLoS One*, 4(10), pp. e7423.

Godbolt, J. A. and Solan, M. (2013) 'Long-term effects of warming and ocean acidification are modified by seasonal variation in species responses and environmental conditions', *Philosophical Transactions of the Royal Society B: Biological Sciences*, 368(1627), pp. 20130186.

Gonneea, M. E., Cohen, A. L., DeCarlo, T. M. and Charette, M. A. (2017) 'Relationship between water and aragonite barium concentrations in aquaria reared juvenile corals', *Geochimica Et Cosmochimica Acta*, 209, pp. 123-134.

Gonzalez, A., Germain, R. M., Srivastava, D. S., Filotas, E., Dee, L. E., Gravel, D., Thompson, P. L., Isbell, F., Wang, S., Kefi, S., Montoya, J., Zelnik, Y. R. and Loreau, M. (2020) 'Scaling-up biodiversity-ecosystem functioning research', *Ecology Letters*, 23(4), pp. 757-776.

Gonzalez, A. and Loreau, M. (2009) 'The Causes and Consequences of Compensatory Dynamics in Ecological Communities', *Annual Review of Ecology Evolution and Systematics*, 40(1), pp. 393-414.

Goodwin, M., Halvorsen, K. T., Jiao, L., Knausgård, K. M., Martin, A. H., Moyano, M., Oomen, R. A., Rasmussen, J. H., Sørdsalen, T. K., Thorbjørnsen, S. H. and Demer, D. (2022) 'Unlocking the potential of deep learning for marine ecology: overview, applications, and outlook', *ICES Journal of Marine Science*, 79(2), pp. 319-336.

Gradinger, R. (1997) 'Climate change and biological oceanography of the Arctic Ocean', *Philosophical Transactions of the Royal Society of London. Series A: Physical and Engineering Sciences*, 352(1699), pp. 277-286.

## List of References

Graham, M. H. and Edwards, M. S. (2001) 'Statistical significance versus fit: estimating the importance of individual factors in ecological analysis of variance', *Oikos*, 93(3), pp. 505-513.

Grebmeier, J. M. (2012) 'Shifting patterns of life in the Pacific Arctic and sub-Arctic seas', *Annual Review of Marine Science*, 4, pp. 63-78.

Grebmeier, J. M. and Barry, J. P. (2007) 'Chapter 11 Benthic Processes in Polynyas', *Polynyas: Windows to the World Elsevier Oceanography Series*, pp. 363-390.

Grebmeier, J. M., Bluhm, B. A., Cooper, L. W., Denisenko, S. G., Iken, K., Kedra, M. and Serratos, C. (2015) 'Time-Series Benthic Community Composition and Biomass and Associated Environmental Characteristics in the Chukchi Sea During the RUSALCA 2004-2012 Program', *Oceanography*, 28(3), pp. 116-133.

Grebmeier, J. M., Cooper, L. W., Feder, H. M. and Sirenko, B. I. (2006a) 'Ecosystem dynamics of the Pacific-influenced Northern Bering and Chukchi Seas in the Amerasian Arctic', *Progress in Oceanography*, 71(2-4), pp. 331-361.

Grebmeier, J. M., Frey, K. E., Cooper, L. W. and Kedra, M. (2018) 'Trends in Benthic Macrofaunal Populations, Seasonal Sea Ice Persistence, and Bottom Water Temperatures in the Bering Strait Region', *Oceanography*, 31(2), pp. 136-151.

Grebmeier, J. M., Overland, J. E., Moore, S. E., Farley, E. V., Carmack, E. C., Cooper, L. W., Frey, K. E., Helle, J. H., McLaughlin, F. A. and McNutt, S. L. (2006b) 'A major ecosystem shift in the northern Bering Sea', *Science*, 311(5766), pp. 1461-4.

Green, D. S., Christie, H., Pratt, N., Boots, B., Godbold, J. A., Solan, M. and Hauton, C. (2017) 'Competitive interactions moderate the effects of elevated temperature and atmospheric CO<sub>2</sub> on the health and functioning of oysters', *Marine Ecology Progress Series*, 582, pp. 93-103.

Griffith, G. P., Hop, H., Vihtakari, M., Wold, A., Kalhagen, K. and Gabrielsen, G. W. (2019) 'Ecological resilience of Arctic marine food webs to climate change', *Nature Climate Change*, 9(11), pp. 868-+.

Griffiths, J. R., Kadin, M., Nascimento, F. J. A., Tamelander, T., Tornroos, A., Bonaglia, S., Bonsdorff, E., Bruchert, V., Gardmark, A., Jarnstrom, M., Kotta, J., Lindegren, M., Nordstrom, M. C., Norkko, A., Olsson, J., Weigel, B., Zydelis, R., Blenckner, T., Niiranen, S. and Winder, M. (2017) 'The importance of benthic-pelagic coupling for marine ecosystem functioning in a changing world', *Global Change Biology*, 23(6), pp. 2179-2196.

Gross, K. and Cardinale, B. J. (2005) 'The functional consequences of random vs. ordered species extinctions', *Ecology Letters*, 8(4), pp. 409-418.

Gross, K. and Cardinale, B. J. (2007) 'Does species richness drive community production or vice versa? Reconciling historical and contemporary paradigms in competitive communities', *The American Naturalist*, 170(2), pp. 207-220.

Gulliksen, B., Hop, H. and Nilsen, M. (2009) 'Benthic life.', in Sakshaug, E., Johnsen, G.H. and Kovacs, K.M. (eds.) *Ecosystem Barents Sea*: Tapir Academic Press, pp. 339-372.

Gunderson, A. R., Armstrong, E. J. and Stillman, J. H. (2016) 'Multiple Stressors in a Changing World: The Need for an Improved Perspective on Physiological Responses to the Dynamic Marine Environment', *Annual Review of Marine Science*, 8, pp. 357-78.

Gunn, R. L., Hartley, I. R., Algar, A. C., Niemelä, P. T. and Keith, S. A. (2021) 'Understanding behavioural responses to human-induced rapid environmental change: a meta-analysis', *Oikos*, 2022(4).

Guscelli, E., Spicer, J. I. and Calosi, P. (2019) 'The importance of inter-individual variation in predicting species' responses to global change drivers', *Ecology and Evolution*, 9(8), pp. 4327-4339.

Gutt, J., Bertler, N., Bracegirdle, T. J., Buschmann, A., Comiso, J., Hosie, G., Isla, E., Schloss, I. R., Smith, C. R., Tournadre, J. and Xavier, J. C. (2015) 'The Southern Ocean ecosystem under multiple climate change stresses--an integrated circumpolar assessment', *Global Change Biology*, 21(4), pp. 1434-53.

Hale, R., Mavrogordato, M. N., Tolhurst, T. J. and Solan, M. (2014) 'Characterizations of how species mediate ecosystem properties require more comprehensive functional effect descriptors', *Scientific Reports*, 4, pp. 6463.

Hamilton, C. D., Kovacs, K. M. and Lydersen, C. (2018) 'Individual variability in diving, movement and activity patterns of adult bearded seals in Svalbard, Norway', *Scientific Reports*, 8(1), pp. 16988.

Hannah, L. J. (2012) *Saving a Million Species Extinction Risk from Climate Change*. United States of America: Island Press.

Hansen, A. S., Nielsen, T. G., Levinsen, H., Madsen, S. D., Thingstad, T. F. and Hansen, B. W. (2003) 'Impact of changing ice cover on pelagic productivity and food web structure in Disko Bay, West Greenland: a dynamic model approach', *Deep-Sea Research Part I-Oceanographic Research Papers*, 50(1), pp. 171-187.

Hansen, B. B., Pedersen, A. O., Peeters, B., Le Moullec, M., Albon, S. D., Herfindal, I., Saether, B. E., Grotan, V. and Aanes, R. (2019) 'Spatial heterogeneity in climate change effects decouples the long-term dynamics of wild reindeer populations in the high Arctic', *Global Change Biology*, 25(11), pp. 3656-3668.

Hansen, M. L. S., Piepenburg, D., Pantiukhin, D. and Kraan, C. (2020) 'Unraveling the effects of environmental drivers and spatial structure on benthic species distribution patterns in Eurasian-Arctic seas (Barents, Kara and Laptev Seas)', *Polar Biology*, 43(11), pp. 1693-1705.

Harley, C. D. (2011) 'Climate change, keystone predation, and biodiversity loss', *Science*, 334(6059), pp. 1124-7.

Hart, S. R., Cohen, A. L. and Ramsay, P. 'Microscale analysis of Sr/Ca and Ba/Ca in *Porites*', *Proceedings of the 8th International Coral Reef Symposium*, 1707-1712.

Harvey, E., Seguin, A., Nozais, C., Archambault, P. and Gravel, D. (2013) 'Identity effects dominate the impacts of multiple species extinctions on the functioning of complex food webs', *Ecology*, 94(1), pp. 169-79.

Hathorne, E. C., Felis, T., Suzuki, A., Kawahata, H. and Cabioch, G. (2013) 'Lithium in the aragonite skeletons of massive *Porites* corals: A new tool to reconstruct tropical sea surface temperatures', *Paleoceanography*, 28(1), pp. 143-152.

Heide-Jørgensen, M. P., Laidre, K. L., Logsdon, M. L. and Nielsen, T. G. (2007) 'Springtime coupling between chlorophyll a, sea ice and sea surface temperature in Disko Bay, West Greenland', *Progress in Oceanography*, 73(1), pp. 79-95.

Heikoop, J. M., Hickmott, D. D., Risk, M. J., Shearer, C. K. and Atudorei, V. (2002) 'Potential climate signals from the deep-sea gorgonian coral *Primnoa resedaeformis*', *Hydrobiologia*, 471(1), pp. 117-124.

## List of References

Heino, M. (1998) 'Noise colour, synchrony and extinctions in spatially structured populations', *Oikos*, 83(2), pp. 368-375.

Hendry, K. R., Pyle, K. M., Barney Butler, G., Cooper, A., Fransson, A., Chierici, M., Leng, M. J., Meyer, A. and Dodd, P. A. (2018) 'Spatiotemporal Variability of Barium in Arctic Sea-Ice and Seawater', *Journal of Geophysical Research: Oceans*, 123(5), pp. 3507-3522.

Henn, J. J., Buzzard, V., Enquist, B. J., Halbritter, A. H., Klanderud, K., Maitner, B. S., Michaletz, S. T., Potsch, C., Seltzer, L., Telford, R. J., Yang, Y., Zhang, L. and Vandvik, V. (2018) 'Intraspecific Trait Variation and Phenotypic Plasticity Mediate Alpine Plant Species Response to Climate Change', *Frontiers in Plant Science*, 9, pp. 1548.

Heuer, R. M. and Grosell, M. (2014) 'Physiological impacts of elevated carbon dioxide and ocean acidification on fish', *American Journal of Physiology-Regulatory, Integrative and Comparative Physiology*, 307(9), pp. R1061-84.

Hevia, V., Martin-Lopéz, B., Palomo, S., Garcia-Llorente, M., de Bello, F. and Gonzalez, J. A. (2017) 'Trait-based approaches to analyze links between the drivers of change and ecosystem services: Synthesizing existing evidence and future challenges', *Ecology and Evolution*, 7(3), pp. 831-844.

Hewitt, J. E., Ellis, J. I. and Thrush, S. F. (2016) 'Multiple stressors, nonlinear effects and the implications of climate change impacts on marine coastal ecosystems', *Global Change Biology*, 22(8), pp. 2665-75.

Hicks, N., Bulling, M. T., Solan, M., Raffaelli, D., White, P. C. and Paterson, D. M. (2011) 'Impact of biodiversity-climate futures on primary production and metabolism in a model benthic estuarine system', *BMC Ecology*, 11(7), pp. 7.

Highsmith, R. C. and Coyle, K. O. (1990) 'High Productivity of Northern Bering Sea Benthic Amphipods', *Nature*, 344(6269), pp. 862-864.

Hijmans, R. (2022) *terra: Spatial Data Analysis*. Available at: <https://CRAN.R-project.org/package=terra>.

Hill, T. M., LaVigne, M., Spero, H. J., Guilderson, T., Gaylord, B. and Clague, D. (2012) 'Variations in seawater Sr/Ca recorded in deep-sea bamboo corals', *Paleoceanography*, 27(3), pp. n/a-n/a.

Hill, T. M., Spero, H. J., Guilderson, T., LaVigne, M., Clague, D., Macalello, S. and Jang, N. (2011) 'Temperature and vital effect controls on bamboo coral (Isididae) isotope geochemistry: A test of the "lines method"', *Geochemistry, Geophysics, Geosystems*, 12(4), pp. n/a-n/a.

Hirst, A. G. and Forster, J. (2013) 'When growth models are not universal: evidence from marine invertebrates', *Proceedings of the Royal Society B: Biological Sciences*, 280(1768), pp. 20131546.

Schindelin, J., Arganda-Carreras, I., Frise, E., Kaynig, V., Longair, M., Pietzsch, T., Preibisch, S., Rueden, C., Saalfeld, S., Schmid, B., Tinevez, J. Y., White, D. J., Hartenstein, V., Eliceiri, K., Tomancak, P. and Cardona, A. (2020) *LinkedView: A Fiji/ImageJ Plugin for Visualisation and Annotation of Correlative Images*.

Hochachka, P. W. and Somero, G. N. (2002) *Biochemical Adaptation Mechanism and Process in Physiological Evolution*.

Hoegh-Guldberg, O., Jacob, D. and Taylor, M. (2018) 'Impacts of 1.5°C global warming on natural and human systems'.

Hoffmann, A. A. and Sgro, C. M. (2011) 'Climate change and evolutionary adaptation', *Nature*, 470(7335), pp. 479-85.

Hollander, J. and Butlin, R. K. (2010) 'The adaptive value of phenotypic plasticity in two ecotypes of a marine gastropod', *BMC Evol Biol*, 10, pp. 333.

Hooper, D. U., Chapin, F. S., Ewel, J. J., Hector, A., Inchausti, P., Lavorel, S., Lawton, J. H., Lodge, D. M., Loreau, M., Naeem, S., Schmid, B., Setala, H., Symstad, A. J., Vandermeer, J. and Wardle, D. A. (2005) 'Effects of biodiversity on ecosystem functioning: A consensus of current knowledge', *Ecological Monographs*, 75(1), pp. 3-35.

Hoover, S. E. R. and Tylianakis, J. M. (2012) 'Species interactions', in Candolin, U. and Wong, B.B.M. (eds.) *Behavioural Responses to a Changing World*. Oxford: Oxford University Press, pp. 129-142.

Hu, M., Chen, T. G. and Zhang, W. (2018) 'Inter-species and inter-colony differences of Sr/Ca-SST calibration in *Porites lobata*.', *Journal of Tropical Oceanography*, 27(6), pp. 74-84.

Huey, R. B., Berrigan, D., Gilchrist, G. W. and Herron, J. C. (1999) 'Testing the Adaptive Significance of Acclimation: A Strong Inference Approach', *American Zoologist*, 39.

Hughes, L. (2012) 'Climate Change Impacts on Species Interactions: Assessing the Threat of Cascading Extinctions', in Hannah, L. (ed.) *Saving a Million Species*: Island Press, pp. 337-359.

Hughes, T. P., Bellwood, D. R., Folke, C., Steneck, R. S. and Wilson, J. (2005) 'New paradigms for supporting the resilience of marine ecosystems', *Trends Ecology and Evolution*, 20(7), pp. 380-6.

Hull, P. M., Darroch, S. A. and Erwin, D. H. (2015) 'Rarity in mass extinctions and the future of ecosystems', *Nature*, 528(7582), pp. 345-51.

Hutchison, C., Guichard, F., Legagneux, P., Gauthier, G., Bety, J., Berteaux, D., Fauteux, D. and Gravel, D. (2020) 'Seasonal food webs with migrations: multi-season models reveal indirect species interactions in the Canadian Arctic tundra', *Philosophical Transactions of the Royal Society A*, 378(2181), pp. 20190354.

Ingvaldsen, R. B., Assmann, K. M., Primicerio, R., Fossheim, M., Polyakov, I. V. and Dolgov, A. V. (2021) 'Physical manifestations and ecological implications of Arctic Atlantification', *Nature Reviews Earth & Environment*, 2(12), pp. 874-889.

IPCC (2018) 'Summary for Policymakers', in Masson-Delmotte, V., Zhai, P., Pörtner, H.-O., Roberts, D., Skea, J., Shukla, P.R., Pirani, A., Moufouma-Okia, W., Péan, C., Pidcock, R., Connors, S., Matthews, J.B.R., Chen, Y., Zhou, X., Gomis, M.I., Lonnoy, E., Maycock, T., Tignor, M. and Waterfield, T. (eds.) *Global Warming of 1.5°C. An IPCC Special Report on the impacts of global warming of 1.5°C above pre-industrial levels and related global greenhouse gas emission pathways, in the context of strengthening the global response to the threat of climate change, sustainable development, and efforts to eradicate poverty*.

IPCC (2021) 'Summary for Policymakers', *Climate Change 2021: The Physical Science Basis. Contribution of Working Group I to the Sixth Assessment Report of the Intergovernmental Panel on Climate Change*.

IPCC (2023) *AR6 Synthesis Report: Climate Change 2023*: International Panel on Climate Change.

Isbell, F., Cowles, J., Dee, L. E., Loreau, M., Reich, P. B., Gonzalez, A., Hector, A. and Schmid, B. (2018) 'Quantifying effects of biodiversity on ecosystem functioning across times and places', *Ecology Letters*, 21(6), pp. 763-778.

Isotalo, T., Rotenbiller, L. and Candolin, U. (2022) 'The importance of considering the duration of extreme temperatures when investigating responses to climate change', *Global Change Biology*, 28(22), pp. 6577-6585.

## List of References

Iswarya, K. (2014) 'Security Issues Associated with Big Data in Cloud Computing', *SSRG International Journal of Computer Science and Engineering*, 1(8), pp. 1-8.

Janzen, D. H. (1967) 'Why Mountain Passes are Higher in the Tropics', *The American Naturalist*, 101(919), pp. 233-249.

Jay, C. V., Fischbach, A. S. and Kochnev, A. A. (2012) 'Walrus areas of use in the Chukchi Sea during sparse sea ice cover', *Marine Ecology Progress Series*, 468, pp. 1-13.

Ježkova, T., Olah-Hemmings, V. and Riddle, B. R. (2011) 'Niche shifting in response to warming climate after the last glacial maximum: inference from genetic data and niche assessments in the chisel-toothed kangaroo rat (*Dipodomys microps*)', *Global Change Biology*, 17(11), pp. 3486-3502.

Jochum, K. P., Weis, U., Stoll, B., Kuzmin, D., Yang, Q. C., Raczek, I., Jacob, D. E., Stracke, A., Birbaum, K., Frick, D. A., Gunther, D. and Enzweiler, J. (2011) 'Determination of Reference Values for NIST SRM 610-617 Glasses Following ISO Guidelines', *Geostandards and Geoanalytical Research*, 35(4), pp. 397-429.

Johannes, R. E. and Wiebe, W. J. (1970) 'Method for Determination of Coral Tissue Biomass and Composition', *Limnology and Oceanography*, 15(5), pp. 822-8.

Jones, B. R., Kelley, A. L. and Mincks, S. L. (2021) 'Changes to benthic community structure may impact organic matter consumption on Pacific Arctic shelves', *Conservation Physiology*, 9(1), pp. coab007.

Jones, C. G., Lawton, J. H. and Shachak, M. (1994) 'Organisms as Ecosystem Engineers', *Oikos*, 69(3), pp. 373-386.

Jones, M. C. and Cheung, W. W. L. (2018) 'Using fuzzy logic to determine the vulnerability of marine species to climate change', *Global Change Biology*, 24(2), pp. e719-e731.

Jonsson, M. and Malmqvist, B. (2003) 'Mechanisms behind positive diversity effects on ecosystem functioning: testing the facilitation and interference hypotheses', *Oecologia*, 134(4), pp. 554-9.

Jørgensen, L. L., Ljubin, P., Skjoldal, H. R., Ingvaldsen, R. B., Anisimova, N. and Manushin, I. (2015) 'Distribution of benthic megafauna in the Barents Sea: baseline for an ecosystem approach to management', *ICES Journal of Marine Science*, 72(2), pp. 595-613.

Jørgensen, L. L., Primicerio, R., Ingvaldsen, R. B., Fossheim, M., Strelkova, N., Thangstad, T. H., Manushin, I. and Zakharov, D. (2019) 'Impact of multiple stressors on sea bed fauna in a warming Arctic', *Marine Ecology Progress Series*, 608, pp. 1-12.

Josefson, A. B. and Mokievsky, V. O. (2012) 'Marine Invertebrates', *Arctic Biodiversity Assessment: Conservation of Arctic Flora and Fauna*, pp. 277-309.

Joshi, J., Schmid, B., Caldeira, M. C., Dimitrakopoulos, P. G., Good, J., Harris, R., Hector, A., Huss-Danell, K., Jumpponen, A., Minns, A., Mulder, C. P. H., Pereira, J. S., Prinz, A., Scherer-Lorenzen, M., Siamantziouras, A. S. D., Terry, A. C., Troumbis, A. Y. and Lawton, J. H. (2001) 'Local adaptation enhances performance of common plant species', *Ecology Letters*, 4(6), pp. 536-544.

Juul-Pedersen, T., Nielsen, T. G., Michel, C., Moller, E. F., Tiselius, P., Thor, P., Olesen, M., Selander, E. and Gooding, S. (2006) 'Sedimentation following the spring bloom in Disko Bay, West Greenland, with special emphasis on the role of copepods', *Marine Ecology Progress Series*, 314, pp. 239-255.

Kahru, M., Brotas, V., Manzano-Sarabia, M. and Mitchell, B. G. (2011) 'Are phytoplankton blooms occurring earlier in the Arctic?', *Global Change Biology*, 17(4), pp. 1733-1739.

Kaiser, B. A., Fernandez, L. M. and Vestergaard, N. (2016) 'The future of the marine Arctic: environmental and resource economic development issues', *The Polar Journal*, 6(1), pp. 152-168.

Kawaguchi, S., Ishida, A., King, R., Raymond, B., Waller, N., Constable, A., Nicol, S., Wakita, M. and Ishimatsu, A. (2013) 'Risk maps for Antarctic krill under projected Southern Ocean acidification', *Nature Climate Change*, 3(9), pp. 843-847.

Kawakubo, Y., Yokoyama, Y., Suzuki, A., Okai, T., Alibert, C., Kinsley, L. and Eggins, S. (2014) 'Precise determination of Sr/Ca by laser ablation ICP-MS compared to ICP-AES and application to multi-century temperate corals', *Geochemical Journal*, 48(2), pp. 145-152.

Kearney, M., Shine, R. and Porter, W. P. (2009) 'The potential for behavioral thermoregulation to buffer "cold-blooded" animals against climate warming', *Proceedings of the National Academy of Sciences of the United States of America*, 106(10), pp. 3835-40.

Kędra, M., Moritz, C., Choy, E. S., David, C., Degen, R., Duerksen, S., Ellingsen, I., Górska, B., Grebmeier, J. M., Kirievskaya, D., van Oevelen, D., Piwoz, K., Samuelsen, A. and Węsławski, J. M. (2015) 'Status and trends in the structure of Arctic benthic food webs', *Polar Research*, 34(1).

Keith, D. A., Akcakaya, H. R., Thuiller, W., Midgley, G. F., Pearson, R. G., Phillips, S. J., Regan, H. M., Araujo, M. B. and Rebelo, T. G. (2008) 'Predicting extinction risks under climate change: coupling stochastic population models with dynamic bioclimatic habitat models', *Biology Letters*, 4(5), pp. 560-3.

Kershaw, J., Stewart, J. A., Strawson, I., Ferreira, M. L. D., Robinson, L. F., Hendry, K. R., Samperiz, A., Burke, A., Rae, J. W. B., Day, R. D., Etnoyer, P. J., Williams, B. and Haussermann, V. (2023) 'Ba/Ca of stylasterid coral skeletons records dissolved seawater barium concentrations', *Chemical Geology*, 622.

Kimball, J. B., Dunbar, R. B. and Guilderson, T. P. (2014) 'Oxygen and carbon isotope fractionation in calcitic deep-sea corals: Implications for paleotemperature reconstruction', *Chemical Geology*, 381, pp. 223-233.

Kimura, F., Matsuno, K., Abe, Y. and Yamaguchi, A. (2022) 'Effects of Early Sea-Ice Reduction on Zooplankton and Copepod Population Structure in the Northern Bering Sea During the Summers of 2017 and 2018', *Frontiers in Marine Science*, 9.

Kiørboe, T. and Hirst, A. G. (2014) 'Shifts in mass scaling of respiration, feeding, and growth rates across life-form transitions in marine pelagic organisms', *The American Naturalist*, 183(4), pp. E118-30.

Klausmeier, C. A., Litchman, E., Daufresne, T. and Levin, S. A. (2004) 'Optimal nitrogen-to-phosphorus stoichiometry of phytoplankton', *Nature*, 429(6988), pp. 171-4.

Knell, R. J. and Thackeray, S. J. (2016) 'Volitinism and resilience to climate-induced phenological mismatch', *Climatic Change*, 137(3-4), pp. 525-539.

Koh, L. P., Dunn, R. R., Sodhi, N. S., Colwell, R. K., Proctor, H. C. and Smith, V. S. (2004) 'Species coextinctions and the biodiversity crisis', *Science*, 305(5690), pp. 1632-4.

Kohnemann, S. H. E., Heinemann, G., Bromwich, D. H. and Gutjahr, O. (2017) 'Extreme Warming in the Kara Sea and Barents Sea during the Winter Period 2000-16', *Journal of Climate*, 30(22), pp. 8913-8927.

Kordas, R. L., Harley, C. D. G. and O'Connor, M. I. (2011) 'Community ecology in a warming world: The influence of temperature on interspecific interactions in marine systems', *Journal of Experimental Marine Biology and Ecology*, 400(1-2), pp. 218-226.

## List of References

Kortsch, S., Primicerio, R., Aschan, M., Lind, S., Dolgov, A. V. and Planque, B. (2018) 'Food-web structure varies along environmental gradients in a high-latitude marine ecosystem', *Ecography*, 42(2), pp. 295-308.

Kortsch, S., Primicerio, R., Fossheim, M., Dolgov, A. V. and Aschan, M. (2015) 'Climate change alters the structure of arctic marine food webs due to poleward shifts of boreal generalists', *Proceedings of the Royal Society B: Biological Sciences*, 282(1814), pp. 31-39.

Kotov, S. and Pälike, H. (2018) *QAnalySeries – a cross-platform time series tuning and analysis tool*.

Kovats, R. S., Woolhouse, M. E. J., Dye, C., Campbell-Lendrum, D. H., McMichel, A. J., Woodward, A. and Cox, J. S. H. (2001) 'Early effects of climate change: do they include changes in vector-borne disease?', *Philosophical Transactions of the Royal Society of London. Series B: Biological Sciences*, 356(1411), pp. 1057-1068.

Kroeker, K. J., Kordas, R. L., Crim, R., Hendriks, I. E., Ramajo, L., Singh, G. S., Duarte, C. M. and Gattuso, J. P. (2013) 'Impacts of ocean acidification on marine organisms: quantifying sensitivities and interaction with warming', *Global Change Biology*, 19(6), pp. 1884-96.

Kroeker, K. J., Kordas, R. L., Crim, R. N. and Singh, G. G. (2010) 'Meta-analysis reveals negative yet variable effects of ocean acidification on marine organisms', *Ecology Letters*, 13(11), pp. 1419-34.

Kroeker, K. J., Micheli, F., Gambi, M. C. and Martz, T. R. (2011) 'Divergent ecosystem responses within a benthic marine community to ocean acidification', *Proceedings of the National Academy of Sciences of the United States of America*, 108(35), pp. 14515-20.

Kröger, S., Parker, R., Cripps, G. and Williamson, P. (2018) *Shelf Seas: The Engine of Productivity, Policy Report on NERC-Defra Shelf Sea Biogeochemistry programme*. Lowesloft: Cefas.

Laidre, K. L., Atkinson, S., Regehr, E. V., Stern, H. L., Born, E. W., Wiig, O., Lunn, N. J. and Dyck, M. (2020) 'Interrelated ecological impacts of climate change on an apex predator', *Ecology Applications*, 30(4), pp. e02071.

Langer, J. A. F., Meunier, C. L., Ecker, U., Horn, H. G., Schwenk, K. and Boersma, M. (2019) 'Acclimation and adaptation of the coastal calanoid copepod *Acartia tonsa* to ocean acidification: a long-term laboratory investigation', *Marine Ecology Progress Series*, 619, pp. 35-51.

Lam-Gordillo, O., Baring, R. and Dittmann, S. (2020) 'Ecosystem functioning and functional approaches on marine macrobenthic fauna: A research synthesis towards a global consensus', *Ecological Indicators*, 115.

Lapeyrolerie, M., Chapman, M. S., Norman, K. E. A. and Boettiger, C. (2022) 'Deep reinforcement learning for conservation decisions', *Methods in Ecology and Evolution*, 13(11), pp. 2649-2662.

Larsen, J. N., Anisimov, O. A., Constable, A., Hollowed, A. B., Maynard, N., Prestrud, P., Prowse, T. D. and Stone, J. M. R. (2014) 'Polar Regions', in Barros, V.R., Field, C.B., Dokken, D.J., Mastrandrea, M.D., Mach, K.J., Bilir, T.E., Chatterjee, M., Ebi, K.L., Estrada, Y.O., Genova, R.C., Girma, B., Kissel, E.S., Levy, A.N., MacCracken, S., Mastrandrea, P.R. and White, L.L. (eds.) *Climate Change 2014: Impacts, Adaptation, and Vulnerability. Part B: Regional Aspects. Contribution of Working Group II to the Fifth Assessment Report of the Intergovernmental Panel on Climate Change*. Cambridge, United Kingdom. New York, USA: Cambridge University Press, pp. 1567-1612.

Lau, S. C. Y., Grange, L. J., Peck, L. S. and Reed, A. J. (2018) 'The reproductive ecology of the Antarctic bivalve *Aequiyoeldia eightsii* (Protobranchia: Sareptidae) follows neither Antarctic nor taxonomic patterns', *Polar Biology*, 41(9), pp. 1693-1706.

Laubenstein, T. D., Rummer, J. L., McCormick, M. I. and Munday, P. L. (2019) 'A negative correlation between behavioural and physiological performance under ocean acidification and warming', *Scientific Reports*, 9(1), pp. 4265.

Laverock, B., Kitidis, V., Tait, K., Gilbert, J. A., Osborn, A. M. and Widdicombe, S. (2013) 'Bioturbation determines the response of benthic ammonia-oxidizing microorganisms to ocean acidification', *Philosophical Transactions of the Royal Society B: Biological Sciences*, 368(1627), pp. 20120441.

LaVigne, M., Grottoli, A. G., Palardy, J. E. and Sherrell, R. M. (2016) 'Multi-colony calibrations of coral Ba/Ca with a contemporaneous in situ seawater barium record', *Geochimica Et Cosmochimica Acta*, 179, pp. 203-216.

LaVigne, M., Hill, T. M., Spero, H. J. and Guilderson, T. P. (2011) 'Bamboo coral Ba/Ca: Calibration of a new deep ocean refractory nutrient proxy', *Earth and Planetary Science Letters*, 312(3-4), pp. 506-515.

Lawler, J. J. (2009) 'Climate change adaptation strategies for resource management and conservation planning', *Annals of the New York Academy of Sciences*, 1162, pp. 79-98.

Lawton, J. H. (1994) 'What Do Species Do in Ecosystems?', *Oikos*, 71(3), pp. 367-374.

Lawton, J. H. (1996) 'Patterns in ecology', *Oikos*, 75(2), pp. 145-147.

Lazareth, C. E., Soares-Pereira, C., Douville, E., Brahmi, C., Dissard, D., Le Corne, F., Thil, F., Gonzalez-Roubaud, C., Caquineau, S. and Cabioch, G. (2016) 'Intra-skeletal calcite in a live-collected *Porites* sp.: Impact on environmental proxies and potential formation process', *Geochimica Et Cosmochimica Acta*, 176, pp. 279-294.

Le Borgne, R. (1986) 'The release of soluble end products of metabolism', in Corner, E.D.S. and O'Hara, S.C.M. (eds.) *The Biological Chemistry of Marine Copepods*, pp. 109-164.

Leadley, P., Pereira, H. M., Alkemade, R., Fernandez-Manjarrés, J. F., Proença, V., Scharlemann, J. P. W. and Walpole, M. J. (2010) *Biodiversity Scenarios: Projections of 21st century change in biodiversity and associated ecosystem services.* Secretariat of the Convention on Biological Diversity, Montreal.

Lee, C. M., Curry, B. and Petrie, B. (2011) 'Volume, Freshwater, and Heat Fluxes through Davis Strait, 2004-05\*', *Journal of Physical Oceanography*, 41(3), pp. 429-436.

Legendre, P. (2018) *lmodel2: Model II Regression*. Available at: <https://CRAN.R-project.org/package=lmodel2>.

Leu, E., Soreide, J. E., Hessen, D. O., Falk-Petersen, S. and Berge, J. (2011) 'Consequences of changing sea-ice cover for primary and secondary producers in the European Arctic shelf seas: Timing, quantity, and quality', *Progress in Oceanography*, 90(1-4), pp. 18-32.

Levin, L. A. and Le Bris, N. (2015) 'The deep ocean under climate change', *Science*, 350(6262), pp. 766-8.

Li, Y., Han, T., Bi, K., Liang, K., Chen, J., Lu, J., He, C. and Lu, Z. (2020) 'The 3D Reconstruction of Pocillopora Colony Sheds Light on the Growth Pattern of This Reef-Building Coral', *iScience*, 23(6), pp. 101069.

Lighton, J. R. B. (2008) *Measuring metabolic rates: a manual for scientists*. Oxford University Press.

## List of References

Link, H., Piepenburg, D. and Archambault, P. (2013) 'Are hotspots always hotspots? The relationship between diversity, resource and ecosystem functions in the Arctic', *PLoS One*, 8(9), pp. e74077.

Linsley, B. K., Wellington, G. M., Schrag, D. P., Ren, L., Salinger, M. J. and Tudhope, A. W. (2004) 'Geochemical evidence from corals for changes in the amplitude and spatial pattern of South Pacific interdecadal climate variability over the last 300 years', *Climate Dynamics*, 22(1), pp. 1-11.

Lischka, S. and Riebesell, U. (2012) 'Synergistic effects of ocean acidification and warming on overwintering pteropods in the Arctic', *Global Change Biology*, 18(12), pp. 3517-3528.

Liu, K., Lin, H. S., He, X. B., Huang, Y. Q., Li, Z., Lin, J. H., Mou, J. F., Zhang, S. Y., Lin, L. S., Wang, J. J. and Sun, J. (2019a) 'Functional trait composition and diversity patterns of marine macrobenthos across the Arctic Bering Sea', *Ecological Indicators*, 102, pp. 673-685.

Liu, W., Fedorov, A. and Sevellec, F. (2019b) 'The Mechanisms of the Atlantic Meridional Overturning Circulation Slowdown Induced by Arctic Sea Ice Decline', *Journal of Climate*, 32(4), pp. 977-996.

Loarie, S. R., Duffy, P. B., Hamilton, H., Asner, G. P., Field, C. B. and Ackerly, D. D. (2009) 'The velocity of climate change', *Nature*, 462(7276), pp. 1052-5.

Loeng, H. (1991) 'Features of the Physical Oceanographic Conditions of the Barents Sea', *Polar Research*, 10(1), pp. 5-18.

Lopéz Correa, M., Sherwood, O., Montagna, P., Rüggeberg, A., Roak, B., Edinger, E. and McCulloch, M. (2011) 'Geochemical Records in Canadian Bamboo Corals, Potentials and Pitfalls', *Geophysical Research Letters*, 13.

Lord, J. and Whitlatch, R. (2015) 'Predicting competitive shifts and responses to climate change based on latitudinal distributions of species assemblages', *Ecology*, 96(5), pp. 1264-74.

Lurgi, M., Lopéz, B. C. and Montoya, J. M. (2012) 'Novel communities from climate change', *Philosophical Transactions of the Royal Society B: Biological Sciences*, 367(1605), pp. 2913-22.

Lutringer, A., Blamart, D., Frank, N. and Labeyrie, L. (2005) 'Paleotemperatures from deep-sea corals: scale effects', in Freiwald, A. and Roberts, J.M. (eds.) *Cold-Water Corals and Ecosystems*. Berlin, Heidelberg: Springer Berlin Heidelberg, pp. 1081-1096.

Ma, G., Bai, C. M., Wang, X. J., Majeed, M. Z. and Ma, C. S. (2018) 'Behavioural thermoregulation alters microhabitat utilization and demographic rates in ectothermic invertebrates', *Animal Behaviour*, 142, pp. 49-57.

Magozzi, S. and Calosi, P. (2015) 'Integrating metabolic performance, thermal tolerance, and plasticity enables for more accurate predictions on species vulnerability to acute and chronic effects of global warming', *Global Change Biology*, 21(1), pp. 181-94.

Maire, O., Merchant, J. N., Bulling, M., Teal, L. R., Gremare, A., Duchene, J. C. and Solan, M. (2010) 'Indirect effects of non-lethal predation on bivalve activity and sediment reworking', *Journal of Experimental Marine Biology and Ecology*, 395(1-2), pp. 30-36.

Mallory, M. L., Gilchrist, H. G., Janssen, M., Major, H. L., Merkel, F., Provencher, J. F. and Strom, H. (2018) 'Financial costs of conducting science in the Arctic: examples from seabird research', *Arctic Science*, 4(4), pp. 624-633.

Mankoff, K. D., Solgaard, A., Colgan, W., Ahlstrom, A. P., Khan, S. A. and Fausto, R. S. (2020) 'Greenland Ice Sheet solid ice discharge from 1986 through March 2020', *Earth System Science Data*, 12(2), pp. 1367-1383.

Manno, C., Morata, N. and Primicerio, R. (2012) 'Limacina retroversa's response to combined effects of ocean acidification and sea water freshening', *Estuarine Coastal and Shelf Science*, 113, pp. 163-171.

Mardones, M. L., Thatje, S., Fenberg, P. B. and Hauton, C. (2022) 'The short and long-term implications of warming and increased sea water pCO<sub>2</sub> on the physiological response of a temperate neogastropod species', *Marine Biology*, 169(1).

Markle, T. M. and Kozak, K. H. (2018) 'Low acclimation capacity of narrow-ranging thermal specialists exposes susceptibility to global climate change', *Ecology and Evolution*, 8(9), pp. 4644-4656.

MarLIN (2006) *BIOTIC - Biological Traits Information Catalogue*. Network., M.L.I.

Marshall, D. J. (2008) 'Transgenerational plasticity in the sea: context-dependent maternal effects across the life history', *Ecology*, 89(2), pp. 418-27.

Marshall, J. F. and McCulloch, M. T. (2002) 'An assessment of the Sr/Ca ratio in shallow water hermatypic corals as a proxy for sea surface temperature', *Geochimica Et Cosmochimica Acta*, 66(18), pp. 3263-3280.

Marz, C., Freitas, F. S., Faust, J. C., Godbold, J. A., Henley, S. F., Tessin, A. C., Abbott, G. D., Airs, R., Arndt, S., Barnes, D. K. A., Grange, L. J., Gray, N. D., Head, I. M., Hendry, K. R., Hilton, R. G., Reed, A. J., Ruhl, S., Solan, M., Souster, T. A., Stevenson, M. A., Tait, K., Ward, J. and Widdicombe, S. (2022) 'Biogeochemical consequences of a changing Arctic shelf seafloor ecosystem', *Ambio*, 51(2), pp. 370-382.

Matoo, O. B., Ivanina, A. V., Ullstad, C., Beniash, E. and Sokolova, I. M. (2013) 'Interactive effects of elevated temperature and CO<sub>2</sub> levels on metabolism and oxidative stress in two common marine bivalves (*Crassostrea virginica* and *Mercenaria mercenaria*)', *Comp Biochem Physiol A Mol Integr Physiol*, 164(4), pp. 545-53.

Mauro, A. A., Shah, A. A., Martin, P. R. and Ghalambor, C. K. (2022) 'An Integrative Perspective On the Mechanistic Basis of Context- Dependent Species Interactions', *Integrative and Comparative Biology*, 62(2), pp. 164-178.

McEntire, K. D., Gage, M., Grawne, R., Hadfield, M. G., Hulshof, C., Johnson, M. A., Levesque, D. L., Segura, J. and Pinter-Wollman, N. (2022) 'Understanding Drivers of Variation and Predicting Variability Across Levels of Biological Organization', *Integrative and Comparative Biology*, 61(6), pp. 2119-2131.

McGill, B. J., Dornelas, M., Gotelli, N. J. and Magurran, A. E. (2015) 'Fifteen forms of biodiversity trend in the Anthropocene', *Trends Ecology and Evolution*, 30(2), pp. 104-13.

McGill, B. J., Enquist, B. J., Weiher, E. and Westoby, M. (2006) 'Rebuilding community ecology from functional traits', *Trends Ecology and Evolution*, 21(4), pp. 178-85.

McIlroy, D. and Logan, G. A. (1999) 'The impact of bioturbation on infaunal ecology and evolution during the Proterozoic-Cambrian transition', *Palaios*, 14(1), pp. 58-72.

McIntyre, P. B., Jones, L. E., Flecker, A. S. and Vanni, M. J. (2007) 'Fish extinctions alter nutrient recycling in tropical freshwaters', *Proceedings of the National Academy of Sciences of the United States of America*, 104(11), pp. 4461-6.

## List of References

McKinney, M. L. (1997) 'EXTINCTION VULNERABILITY AND SELECTIVITY: Combining Ecological and Paleontological Views', *Annual Review Ecology and Systematics*: Annual Reviews, pp. 495-516.

McKinney, M. L. and Lockwood, J. L. (1999) 'Biotic homogenization: a few winners replacing many losers in the next mass extinction', *Trends Ecology and Evolution*, 14(11), pp. 450-453.

McLean, M., Auber, A., Graham, N. A. J., Houk, P., Villeger, S., Violle, C., Thuiller, W., Wilson, S. K. and Mouillot, D. (2019) 'Trait structure and redundancy determine sensitivity to disturbance in marine fish communities', *Global Change Biology*, 25(10), pp. 3424-3437.

McLean, N., Lawson, C. R., Leech, D. I. and van de Pol, M. (2016) 'Predicting when climate-driven phenotypic change affects population dynamics', *Ecology Letters*, 19(6), pp. 595-608.

Mehrbach, C., Culberson, C. H., Hawley, J. E. and Pytkowicz, R. M. (1973) 'Measurement of the Apparent Dissociation Constants of Carbonic Acid in Seawater At Atmospheric Pressure', *Limnology and Oceanography*, 18(6), pp. 897-907.

Melatunan, S., Calosi, P., Rundle, S. D., Moody, A. J. and Widdicombe, S. (2011) 'Exposure to elevated temperature and  $\text{Pco}_2$  reduces respiration rate and energy status in the periwinkle *Littorina littorea*', *Physiological and Biochemical Zoology: Ecological and Evolutionary Approaches* 84(6), pp. 583-94.

Melillo, J. M., Frey, S. D., DeAngelis, K. M., Werner, W. J., Bernard, M. J., Bowles, F. P., Pold, G., Knorr, M. A. and Grandy, A. S. (2017) 'Long-term pattern and magnitude of soil carbon feedback to the climate system in a warming world', *Science*, 358(6359), pp. 101-105.

Memmott, J., Waser, N. M. and Price, M. V. (2004) 'Tolerance of pollination networks to species extinctions', *Proceedings of the Royal Society B: Biological Sciences*, 271(1557), pp. 2605-11.

Mendes, J. M. and Woodley, J. D. (2002) 'Timing of reproduction in *Montastraea annularis*: relationship to environmental variables', *Marine Ecology Progress Series*, 227, pp. 241-251.

Mercier, A. and Hamel, J. F. (2011) 'Contrasting reproductive strategies in three deep-sea octocorals from eastern Canada: *Primnoa resedaeformis*, *Keratoisis ornata*, and *Anthomastus grandiflorus*', *Coral Reefs*, 30(2), pp. 337-350.

Meredith, M., Sommerkorn, M., Cassotta, S., Derksen, C., Ekyakin, A., Hollowed, A., Kofinas, G., Mackintosh, A., Melbourne-Thomas, J., Muelbert, M. M. G., Ottersen, G., Pritchard, H. and Schuur, E. A. G. (2022) 'Polar Regions', in Pörtner, H.-O., Roberts, D.C., MassonDelmotte, V., Zhai, P., Tignor, M., Poloczanska, E., Mintenbeck, K., Alegría, A., Nicolai, M., Okem, A., Petzold, J., Rama, B. and M., W.N. (eds.) *The Ocean and Cryosphere in a Changing Climate*. Cambridge, UK and New York, NY, USA: Cambridge University Press, pp. 203-320.

Mermilliod-Blondin, F., Lefour, C., Lalouette, L., Renault, D., Malard, F., Simon, L. and Douady, C. J. (2013) 'Thermal tolerance breadths among groundwater crustaceans living in a thermally constant environment', *Journal of Experimental Biology*, 216(Pt 9), pp. 1683-94.

Meyer, S. T., Ebeling, A., Eisenhauer, N., Hertzog, L., Hillebrand, H., Milcu, A., Pompe, S., Abbas, M., Bessler, H., Buchmann, N., De Luca, E., Engels, C., Fischer, M., Gleixner, G., Hudewenz, A., Klein, A. M., de Kroon, H., Leimer, S., Loranger, H., Mommer, L., Oelmann, Y., Ravenek, J. M., Roscher, C., Rottstock, T., Scherber, C., Scherer-Lorenzen, M., Scheu, S., Schmid, B., Schulze, E. D., Staudler, A., Strecker, T., Temperton, V., Tscharntke, T., Vogel, A., Voigt, W., Weigelt, A., Wilcke, W. and Weisser, W. W. (2016) 'Effects of biodiversity strengthen over time as ecosystem functioning declines at low and increases at high biodiversity', *Ecosphere*, 7(12).

Meysman, F. J., Middelburg, J. J. and Heip, C. H. (2006) 'Bioturbation: a fresh look at Darwin's last idea', *Trends Ecology and Evolution*, 21(12), pp. 688-95.

Michalsen, K., Dalpadado, P., Eriksen, E., Gjosaeter, H., Ingvaldsen, R. B., Johannessen, E., Jorgensen, L. L., Knutsen, T., Prozorkevich, D. and Skern-Mauritzen, M. (2013) 'Marine living resources of the Barents Sea - Ecosystem understanding and monitoring in a climate change perspective', *Marine Biology Research*, 9(9), pp. 932-947.

Michaud, E., Desrosiers, G., Mermilliod-Blondin, F., Sundby, B. and Stora, G. (2005) 'The functional group approach to bioturbation: The effects of biodiffusers and gallery-diffusers of the *Macoma balthica* community on sediment oxygen uptake', *Journal of Experimental Marine Biology and Ecology*, 326(1), pp. 77-88.

Mills, B. R. (2022) *MetBrewer Color Palettes Inspired by Works at the Metropolitan Museum of Art*.

Montagna, P., McCulloch, M., Douville, E., Lopéz Correa, M., Trotter, J., Rodolfo-Metalpa, R., Dissard, D., Ferrier-Pages, C., Frank, N., Freiwald, A., Goldstein, S., Mazzoli, C., Reynaud, S., Ruggeberg, A., Russo, S. and Taviani, M. (2014) 'Li/Mg systematics in scleractinian corals: Calibration of the thermometer', *Geochimica Et Cosmochimica Acta*, 132, pp. 288-310.

Montagna, P., McCulloch, M., Taviani, M., Remia, A. and Rouse, G. (2005) 'High-resolution trace and minor element compositions in deep-water scleractinian corals (*Desmophyllum dianthus*) from the Mediterranean Sea and the Great Australian Bight', in Freiwald, A. and Robert, J.M. (eds.) *Cold-Water Corals and Ecosystems*, pp. 1109-1126.

Montoya, J. M. and Raffaelli, D. (2010) 'Climate change, biotic interactions and ecosystem services', *Philosophical Transactions of the Royal Society B: Biological Sciences*, 365(1549), pp. 2013-8.

Moore, S. E. and Stabeno, P. J. (2015) 'Synthesis of Arctic Research (SOAR) in marine ecosystems of the Pacific Arctic Preface', *Progress in Oceanography*, 136, pp. 1-11.

Moreira, A., Figueira, E., Mestre, N. C., Schrama, D., Soares, A., Freitas, R. and Bebianno, M. J. (2018) 'Impacts of the combined exposure to seawater acidification and arsenic on the proteome of *Crassostrea angulata* and *Crassostrea gigas*', *Aquatic Toxicology*, 203, pp. 117-129.

Morley, S. A., Barnes, D. K. A. and Dunn, M. J. (2019) 'Predicting Which Species Succeed in Climate-Forced Polar Seas', *Frontiers in Marine Science*, 5.

Morley, S. A., Martin, S. M., Day, R. W., Ericson, J., Lai, C. H., Lamare, M., Tan, K. S., Thorne, M. A. and Peck, L. S. (2012) 'Thermal reaction norms and the scale of temperature variation: latitudinal vulnerability of intertidal nacellid limpets to climate change', *PLoS One*, 7(12), pp. e52818.

Moss, D. K., Ivany, L. C., Judd, E. J., Cummings, P. W., Bearden, C. E., Kim, W. J., Artruc, E. G. and Driscoll, J. R. (2016) 'Lifespan, growth rate, and body size across latitude in marine Bivalvia, with implications for Phanerozoic evolution', *Proceedings of the Royal Society B: Biological Sciences*, 283(1836).

Mulder, C. P., Uliassi, D. D. and Doak, D. F. (2001) 'Physical stress and diversity-productivity relationships: the role of positive interactions', *Proceedings of the National Academy of Sciences of the United States of America*, 98(12), pp. 6704-8.

Munday, P. L., Warner, R. R., Monro, K., Pandolfi, J. M. and Marshall, D. J. (2013) 'Predicting evolutionary responses to climate change in the sea', *Ecology Letters*, 16(12), pp. 1488-500.

Munguia, P., Backwell, P. R. Y. and Darnell, M. Z. (2017) 'Thermal constraints on microhabitat selection and mating opportunities', *Animal Behaviour*, 123, pp. 259-265.

## List of References

Murphy, E. J., Cavanagh, R. D., Drinkwater, K. F., Grant, S. M., Heymans, J. J., Hofmann, E. E., Hunt, G. L., Jr. and Johnston, N. M. (2016) 'Understanding the structure and functioning of polar pelagic ecosystems to predict the impacts of change', *Proceedings of the Royal Society B: Biological Sciences*, 283(1844).

Murray, F., Douglas, A. and Solan, M. (2014) 'Species that share traits do not necessarily form distinct and universally applicable functional effect groups', *Marine Ecology Progress Series*, 516, pp. 23-34.

Murray, F., Widdicombe, S., McNeill, C. L. and Douglas, A. (2017) 'Assessing the consequences of environmental impacts: variation in species responses has unpredictable functional effects', *Marine Ecology Progress Series*, 583, pp. 35-47.

Murray, F., Widdicombe, S., McNeill, C. L. and Solan, M. (2013) 'Consequences of a simulated rapid ocean acidification event for benthic ecosystem processes and functions', *Marine Pollution Bulletin*, 73(2), pp. 435-42.

Mykra, H. and Heino, J. (2017) 'Decreased habitat specialization in macroinvertebrate assemblages in anthropogenically disturbed streams', *Ecological Complexity*, 31, pp. 181-188.

Naeem, S. (2006) 'Expanding scales in biodiversity-based research: challenges and solutions for marine systems', *Marine Ecology Progress Series*, 311, pp. 273-283.

Naeem, S. (2008) 'Advancing realism in biodiversity research', *Trends Ecology and Evolution*, 23(8), pp. 414-6.

Naeem, S. and Wright, J. P. (2003) 'Disentangling biodiversity effects on ecosystem functioning: deriving solutions to a seemingly insurmountable problem', *Ecology Letters*, 6(6), pp. 567-579.

Nagelkerken, I. and Munday, P. L. (2016) 'Animal behaviour shapes the ecological effects of ocean acidification and warming: moving from individual to community-level responses', *Global Change Biology*, 22(3), pp. 974-89.

Nagelkerken, I., Russell, B. D., Gillanders, B. M. and Connell, S. D. (2015) 'Ocean acidification alters fish populations indirectly through habitat modification', *Nature Climate Change*, 6(1), pp. 89-93.

Nardi, A., Mincarelli, L. F., Benedetti, M., Fattorini, D., d'Errico, G. and Regoli, F. (2017) 'Indirect effects of climate changes on cadmium bioavailability and biological effects in the Mediterranean mussel *Mytilus galloprovincialis*', *Chemosphere*, 169, pp. 493-502.

Neves, B. d. M., Edinger, E., Hillaire-Marcel, C., Saucier, E. H., France, S. C., Treble, M. A. and Wareham, V. E. (2014) 'Deep-water bamboo coral forests in a muddy Arctic environment', *Marine Biodiversity*, 45(4), pp. 867-871.

Nielsen, T. G. and Hansen, B. (1995) 'Plankton Community Structure and Carbon Cycling on the Western Coast of Greenland during and after the Sedimentation of a Diatom Bloom', *Marine Ecology Progress Series*, 125(1-3), pp. 239-257.

Nielsen, T. G. and Hansen, B. W. (1999) 'Plankton community structure and carbon cycling on the western coast of Greenland during the stratified summer situation. I. Hydrography, phytoplankton and bacterioplankton', *Aquatic Microbial Ecology*, 16(3), pp. 205-216.

Noé, S. U. and Dullo, W. C. (2006) 'Skeletal morphogenesis and growth mode of modern and fossil deep-water isidid gorgonians (Octocorallia) in the West Pacific (New Zealand and Sea of Okhotsk)', *Coral Reefs*, 25(3), pp. 303-320.

Noé, S. U., Lembke-Jene, L. and Dullo, W. C. (2007) 'Varying growth rates in bamboo corals: sclerochronology and radiocarbon dating of a mid-Holocene deep-water gorgonian skeleton (*Keratoisis* sp.: Octocorallia) from Chatham Rise (New Zealand)', *Facies*, 54(2), pp. 151-166.

Norin, T. and Metcalfe, N. B. (2019) 'Ecological and evolutionary consequences of metabolic rate plasticity in response to environmental change', *Philosophical Transactions of the Royal Society B: Biological Sciences*, 374(1768), pp. 20180180.

Norling, K., Rosenberg, R., Hulth, S., Gremare, A. and Bonsdorff, E. (2007) 'Importance of functional biodiversity and species-specific traits of benthic fauna for ecosystem functions in marine sediment', *Marine Ecology Progress Series*, 332, pp. 11-23.

Nozaki, Y. (1997) 'A Fresh Look at Element Distribution in the North Pacific', *EOS American Geophysical Union*, 78.

Nusbaumer, J., Alexander, P. M., LeGrande, A. N. and Tedesco, M. (2019) 'Spatial Shift of Greenland Moisture Sources Related to Enhanced Arctic Warming', *Geophysical Research Letters*, 46(24), pp. 14723-14731.

Ó Cofaigh, C., Hogan, K. A., Jennings, A. E., Callard, S. L., Dowdeswell, J. A., Noormets, R. and Evans, J. (2018) 'The role of meltwater in high-latitude trough-mouth fan development: The Disko Trough-Mouth Fan, West Greenland', *Marine Geology*, 402, pp. 17-32.

O'Connor, N. E. and Donohue, I. (2013) 'Environmental context determines multi-trophic effects of consumer species loss', *Global Change Biology*, 19(2), pp. 431-40.

O'Garra, T. (2017) 'Economic value of ecosystem services, minerals and oil in a melting Arctic: A preliminary assessment', *Ecosystem Services*, 24, pp. 180-186.

Olsen, J. (2020) 'Adaptive capacity of Arctic communities in the context of climate change and shipping growth: A review of Russian and Western literature', *Polar Record*, 56.

Onarheim, I. H. and Teigen, S. H. (2018) *Statistical position of the oceanic polar front in the Barents Sea: EquinorMAD-RE2018-016*.

Orlova, E. L., Dolgov, A. V., Renaud, P. E., Greenacre, M., Halsband, C. and Ivshin, V. A. (2015) 'Climatic and ecological drivers of euphausiid community structure vary spatially in the Barents Sea: relationships from a long time series (1952â€“2009)', *Frontiers in Marine Science*, 1(JAN).

Ouellette, D., Desrosiers, G., Gagne, J. P., Gilbert, F., Poggiale, J. C., Blier, P. U. and Stora, G. (2004) 'Effects of temperature on in vitro sediment reworking processes by a gallery biodiffusor, the polychaete *Neanthes virens*', *Marine Ecology Progress Series*, 266, pp. 185-193.

Overland, J., Francis, J. A., Hall, R., Hanna, E., Kim, S.-J. and Vihma, T. (2015) 'The Melting Arctic and Midlatitude Weather Patterns: Are They Connected?\*', *Journal of Climate*, 28(20), pp. 7917-7932.

Overland, J. E. (2016) 'A difficult Arctic science issue: Midlatitude weather linkages', *Polar Science*, 10(3), pp. 210-216.

Overpeck, J., Whitlock, C. and Huntley, B. (2003) 'Terrestrial Biosphere Dynamics in the Climate System: Past and Future', in Alverson, K.D., Pedersen, T.F. and Bradley, R.S. (eds.) *Paleoclimate, Global Change and the Future Global Change — The IGBP Series*. Berlin, Heidelberg: Springer Berlin Heidelberg, pp. 81-103.

## List of References

Oziel, L., Neukermans, G., Ardyna, M., Lancelot, C., Tison, J. L., Wassmann, P., Sirven, J., Ruiz-Pino, D. and Gascard, J. C. (2017) 'Role for Atlantic inflows and sea ice loss on shifting phytoplankton blooms in the Barents Sea', *Journal of Geophysical Research-Oceans*, 122(6), pp. 5121-5139.

Oziel, L., Sirven, J. and Gascard, J. C. (2016) 'The Barents Sea frontal zones and water masses variability (1980-2011)', *Ocean Science*, 12(1), pp. 169-184.

Padilla-Gamino, J. L., Kelly, M. W., Evans, T. G. and Hofmann, G. E. (2013) 'Temperature and CO<sub>2</sub> additively regulate physiology, morphology and genomic responses of larval sea urchins, *Strongylocentrotus purpuratus*', *Proceedings of the Royal Society B: Biological Sciences*, 280(1759), pp. 20130155.

Pages-Escola, M., Hereu, B., Garrabou, J., Montero-Serra, I., Gori, A., Gomez-Gras, D., Figuerola, B. and Linares, C. (2018) 'Divergent responses to warming of two common co-occurring Mediterranean bryozoans', *Scientific Reports*, 8(1), pp. 17455.

Palkovacs, E. P. and Dalton, C. M. (2012) 'Ecosystem consequences of behavioural plasticity and contemporary evolution', in Candolin, U. and Wong, B.B.M. (eds.) *Behavioural Responses to a Changing World Mechanisms and Consequences*. 1st ed. Oxford, United Kingdom: Oxford University Press, pp. 175-189.

Pan, Q., Tian, D., Naeem, S., Auerswald, K., Elser, J. J., Bai, Y., Huang, J., Wang, Q., Wang, H., Wu, J. and Han, X. (2016) 'Effects of functional diversity loss on ecosystem functions are influenced by compensation', *Ecology*, 97(9), pp. 2293-2302.

Parker, L. M., Ross, P. M., O'Connor, W. A., Portner, H. O., Scanes, E. and Wright, J. M. (2013) 'Predicting the response of molluscs to the impact of ocean acidification', *Biology (Basel)*, 2(2), pp. 651-92.

Parmesan, C. and Yohe, G. (2003) 'A globally coherent fingerprint of climate change impacts across natural systems', *Nature*, 421(6918), pp. 37-42.

Pasotti, F., Manini, E., Giovannelli, D., Wölfl, A. C., Monien, D., Verleyen, E., Braeckman, U., Abele, D. and Vanreusel, A. (2014) 'Antarctic shallow water benthos in an area of recent rapid glacier retreat', *Marine Ecology*, 36(3), pp. 716-733.

Pearson, T. (2001) 'Functional group ecology in soft-sediment marine benthos: the role of bioturbation', in Gibson, R.N., Barnes, M. and Atkinson, R.J.A. (eds.) *Oceanography and Marine Biology An Annual Review*. London: Taylor & Francis, pp. 233-268.

Peck, L. S. (2005) 'Prospects for survival in the Southern Ocean: vulnerability of benthic species to temperature change', *Antarctic Science*, 17(4), pp. 497-507.

Peck, L. S. (2011) 'Organisms and responses to environmental change', *Marine Genomics*, 4(4), pp. 237-43.

Peck, L. S., Morley, S. A., Richard, J. and Clark, M. S. (2014) 'Acclimation and thermal tolerance in Antarctic marine ectotherms', *Journal of Experimental Biology*, 217(Pt 1), pp. 16-22.

Peck, L. S., Webb, K. E. and Bailey, D. M. (2004) 'Extreme sensitivity of biological function to temperature in Antarctic marine species', *Functional Ecology*, 18(5), pp. 625-630.

Pedersen, T. L. (2022) *patchwork: The Composer of PLots*. Available at: <https://CRAN.R-project.org/package=patchwork>.

Pedruski, M. T. and Arnott, S. E. (2011) 'The effects of habitat connectivity and regional heterogeneity on artificial pond metacommunities', *Oecologia*, 166(1), pp. 221-8.

Pelletier, M. C., Ebersole, J., Mulvaney, K., Rashleigh, B., Gutierrez, M. N., Chintala, M., Kuhn, A., Molina, M., Bagley, M. and Lane, C. (2020) 'Resilience of aquatic systems: Review and management implications', *Aquatic Science*, 82(2), pp. 1-44.

Pereira, H. M., Leadley, P. W., Proenca, V., Alkemade, R., Scharlemann, J. P., Fernandez-Manjarres, J. F., Araujo, M. B., Balvanera, P., Biggs, R., Cheung, W. W., Chini, L., Cooper, H. D., Gilman, E. L., Guenette, S., Hurt, G. C., Huntington, H. P., Mace, G. M., Oberdorff, T., Revenga, C., Rodrigues, P., Scholes, R. J., Sumaila, U. R. and Walpole, M. (2010) 'Scenarios for global biodiversity in the 21st century', *Science*, 330(6010), pp. 1496-501.

Petchey, O. L., Eklof, A., Borrrell, C. and Ebenman, B. (2008) 'Trophically unique species are vulnerable to cascading extinction', *The American Naturalist*, 171(5), pp. 568-79.

Petchey, O. L., McPhearson, P. T., Casey, T. M. and Morin, P. J. (1999) 'Environmental warming alters food-web structure and ecosystem function', *Nature*, 402(6757), pp. 69-72.

Petchey, O. L., Morin, P. J., Hulot, F. D., Loreau, M., McGrady-Steed, J. and Naeem, S. (2002) 'Contributions of aquatic model systems to our understanding of biodiversity and ecosystem functioning.', in Kinzig, A.P., Pacala, S.W. and Tilman, D. (eds.) *The Functional Consequences of Biodiversity*. Princeton: Princeton University Press, pp. 127-138.

Peterson, G. H. and Curtis, M. A. (1980) 'Differences in energy flow through major components of subarctic, temperate and tropical marine shelf ecosystems', *Dana*, 1, pp. 53-64.

Pfeiffer, M., Reuning, L., Zinke, J., Garbe-Schoenberg, D., Leupold, M. and Dullo, W. C. (2019) '20th Century delta O-18 Seawater and Salinity Variations Reconstructed From Paired delta O-18 and Sr/Ca Measurements of a La Reunion Coral', *Paleoceanography and Paleoceanography*, 34(12), pp. 2183-2200.

Pichler, M., Boreux, V., Klein, A. M., Schleuning, M., Hartig, F. and Carvalheiro, L. (2019) 'Machine learning algorithms to infer trait-matching and predict species interactions in ecological networks', *Methods in Ecology and Evolution*, 11(2), pp. 281-293.

Pichler, M. and Hartig, F. (2023) 'Machine learning and deep learning—A review for ecologists', *Methods in Ecology and Evolution*, 14(4), pp. 994-1016.

Pickart, R. S., Spall, M. A., Ribergaard, M. H., Moore, G. W. and Milliff, R. F. (2003) 'Deep convection in the Irminger Sea forced by the Greenland tip jet', *Nature*, 424(6945), pp. 152-6.

Pickart, R. S., Torres, D. J. and Clarke, R. A. (2002) 'Hydrography of the Labrador Sea during active convection', *Journal of Physical Oceanography*, 32(2), pp. 428-457.

Piepenburg, D., Archambault, P., Ambrose, W. G., Blanchard, A. L., Bluhm, B. A., Carroll, M. L., Conlan, K. E., Cusson, M., Feder, H. M., Grebmeier, J. M., Jewett, S. C., Lévesque, M., Petryashev, V. V., Sejr, M. K., Sirenko, B. I. and Włodarska-Kowalcuk, M. (2010) 'Towards a pan-Arctic inventory of the species diversity of the macro- and megabenthic fauna of the Arctic shelf seas', *Marine Biodiversity*, 41(1), pp. 51-70.

Piepenburg, D., Blackburn, T. H., Vondorrien, C. F., Gutt, J., Hall, P. O. J., Hulth, S., Kendall, M. A., Opalinski, K. W., Rachor, E. and Schmid, M. K. (1995) 'Partitioning of Benthic Community Respiration in the Arctic (Northwestern Barents Sea)', *Marine Ecology Progress Series*, 118(1-3), pp. 199-213.

Pierrejean, M., Grant, C., Neves, B. D., Chaillou, G., Edinger, E., Blanchet, F. G., Maps, F., Nozais, C. and Archambault, P. (2020) 'Influence of Deep-Water Corals and Sponge Gardens on Infaunal Community Composition and Ecosystem Functioning in the Eastern Canadian Arctic', *Frontiers in Marine Science*, 7.

## List of References

Pigliucci, M. (2001) *Phenotypic Plasticity: Beyond Nature and Nurture*. Johns Hopkins University Press.

Pimm, S. L., Jones, H. L. and Diamond, J. (1988) 'On the Risk of Extinction', *The American Naturalist*, 132(6), pp. 757-785.

Pinheiro, J., Bates, D. and R\_Core\_Team (2022) 'nlme: Linear and Nonlinear Mixed Effects Models'.

Pinheiro, J. and Bates, D. M. (2000) *Mixed-Effects Models in S and S-PLUS. Statistics and Computing* 1 edn. New York, NY: Springer.

Pinheiro, J. C. and Bates, D. M. (2000) *Mixed-Effects Models in S and S-PLUS. Statistics and Computing*: Springer, p. 528.

Pistevos, J. C. A., Calosi, P., Widdicombe, S. and Bishop, J. D. D. (2011) 'Will variation among genetic individuals influence species responses to global climate change?', *Oikos*, 120(5), pp. 675-689.

Pold, G., Baillargeon, N., Lepe, A., Rastetter, E. B. and Sistla, S. A. (2021) 'Warming effects on arctic tundra biogeochemistry are limited but habitat-dependent: a meta-analysis', *Ecosphere*, 12(10).

Poloczanska, E. S., Brown, C. J., Sydeman, W. J., Kiessling, W., Schoeman, D. S., Moore, P. J., Brander, K., Bruno, J. F., Buckley, L. B., Burrows, M. T., Duarte, C. M., Halpern, B. S., Holding, J., Kappel, C. V., O'Connor, M. I., Pandolfi, J. M., Parmesan, C., Schwing, F., Thompson, S. A. and Richardson, A. J. (2013) 'Global imprint of climate change on marine life', *Nature Climate Change*, 3(10), pp. 919-925.

Poloczanska, E. S., Burrows, M. T., Brown, C. J., Molinos, J. G., Halpern, B. S., Hoegh-Guldberg, O., Kappel, C. V., Moore, P. J., Richardson, A. J., Schoeman, D. S. and Sydeman, W. J. (2016) 'Responses of Marine Organisms to Climate Change across Oceans', *Frontiers in Marine Science*, 3.

Polyakov, I. V., Walsh, J. E. and Kwok, R. (2012) 'Recent Changes of Arctic Multiyear Sea Ice Coverage and the Likely Causes', *Bulletin of the American Meteorological Society*, 93(2), pp. 145-151.

Pörtner, H.-O. (2008) 'Ecosystem effects of ocean acidification in times of ocean warming: a physiologist's view', *Marine Ecology Progress Series*, 373, pp. 203-217.

Pörtner, H.-O. (2012) 'Integrating climate-related stressor effects on marine organisms: unifying principles linking molecule to ecosystem-level changes', *Marine Ecology Progress Series*, 470, pp. 273-290.

Pörtner, H.-O. (2021) 'Climate impacts on organisms, ecosystems and human societies: integrating OCLTT into a wider context', *Journal of Experimental Biology*, 224(Pt Suppl 1).

Pörtner, H.-O., Bock, C. and Mark, F. C. (2017) 'Oxygen- and capacity-limited thermal tolerance: bridging ecology and physiology', *Journal of Experimental Biology*, 220(Pt 15), pp. 2685-2696.

Pörtner, H.-O. and Farrell, A. P. (2008) 'Ecology. Physiology and climate change', *Science*, 322(5902), pp. 690-2.

Pörtner, H.-O. and Knust, R. (2007) 'Climate change affects marine fishes through the oxygen limitation of thermal tolerance', *Science*, 315(5808), pp. 95-7.

Pörtner, H.-O. and Peck, M. A. (2010) 'Climate change effects on fishes and fisheries: towards a cause-and-effect understanding', *Journal of Fish Biology*, 77(8), pp. 1745-79.

Post, E., Alley, R. B., Christensen, T. R., Macias-Fauria, M., Forbes, B. C., Gooseff, M. N., Iler, A., Kerby, J. T., Laidre, K. L., Mann, M. E., Olofsson, J., Stroeve, J. C., Ulmer, F., Virginia, R. A. and Wang, M. (2019) 'The polar regions in a 2 degrees C warmer world', *Science Advances*, 5(12), pp. eaaw9883.

Pounds, J. A., Fogden, M. P. L. and Campbell, J. H. (1999) 'Biological response to climate change on a tropical mountain', *Nature*, 398(6728), pp. 611-615.

Przeslawski, R., Byrne, M. and Mellin, C. (2015) 'A review and meta-analysis of the effects of multiple abiotic stressors on marine embryos and larvae', *Global Change Biology*, 21(6), pp. 2122-40.

Przeslawski, R., Zhu, Q. and Aller, R. (2009) 'Effects of abiotic stressors on infaunal burrowing and associated sediment characteristics', *Marine Ecology Progress Series*, 392, pp. 33-42.

Pucko, C., Beckage, B., Perkins, T. and Keeton, W. S. (2011) 'Species shifts in response to climate change: Individual or shared responses?', *Journal of the Torrey Botanical Society*, 138(2), pp. 156-176.

Purvis, A., Gittleman, J. L., Cowlishaw, G. and Mace, G. M. (2000) 'Predicting extinction risk in declining species', *Proceedings of the Royal Society B: Biological Sciences*, 267(1456), pp. 1947-52.

Pyšek, P., Blackburn, T. M., García-Berthou, E., Perglová, I. and Rabitsch, W. (2017) 'Displacement and Local Extinction of Native and Endemic Species', *Impact of Biological Invasions on Ecosystem Services*, pp. 157-175.

Queirós, A. M., Fernandes, J. A., Faulwetter, S., Nunes, J., Rastrick, S. P., Mieszkowska, N., Artioli, Y., Yool, A., Calosi, P., Arvanitidis, C., Findlay, H. S., Barange, M., Cheung, W. W. and Widdicombe, S. (2015) 'Scaling up experimental ocean acidification and warming research: from individuals to the ecosystem', *Global Change Biology*, 21(1), pp. 130-43.

Quentin, L. B., Ross, R. M. and Uchio, K. (1980) 'Metabolic Characteristics of Midwater Zooplankton - Ammonia Excretion, O-N Ratios, and the Effect of Starvation', *Marine Biology*, 59(4), pp. 201-209.

Quinn, T. M. and Sampson, D. E. (2002) 'A multiproxy approach to reconstructing sea surface conditions using coral skeleton geochemistry', *Paleoceanography*, 17(4).

R Core Team (2020) *R: A language and environment for statistical computing*.

R Core Team (2022) *R: A language and environment for statistical computing*. Available at: <https://www.R-project.org/>.

Raffaelli, D., Emmerson, M., Solan, M., Biles, C. and Paterson, D. (2003) 'Biodiversity and ecosystem processes in shallow coastal waters: an experimental approach', *Journal of Sea Research*, 49(2), pp. 133-141.

Raffaelli, D. and Moller, H. (1999) 'Manipulative Field Experiments in Animal Ecology: Do they Promise More than they Can Deliver?', *Advances in Ecological Research Volume 30 Advances in Ecological Research*, pp. 299-338.

Raffaelli, D., Solan, M. and Webb, T. J. (2005) 'Do marine and terrestrial ecologists do it differently?', *Marine Ecology Progress Series*, 304, pp. 271-307.

Rantanen, M., Karpechko, A. Y., Lipponen, A., Nordling, K., Hyvarinen, O., Ruosteenoja, K., Vihma, T. and Laaksonen, A. (2022) 'The Arctic has warmed nearly four times faster than the globe since 1979', *Communications Earth & Environment*, 3(1).

## List of References

Ratcliffe, S., Wirth, C., Jucker, T., van der Plas, F., Scherer-Lorenzen, M., Verheyen, K., Allan, E., Benavides, R., Bruelheide, H., Ohse, B., Paquette, A., Ampoorter, E., Bastias, C. C., Bauhus, J., Bonal, D., Bouriaud, O., Bussotti, F., Carnol, M., Castagneyrol, B., Checko, E., Dawud, S. M., Wandeler, H., Domisch, T., Finer, L., Fischer, M., Fotelli, M., Gessler, A., Granier, A., Grossiord, C., Guyot, V., Haase, J., Hattenschwiler, S., Jactel, H., Jaroszewicz, B., Joly, F. X., Kambach, S., Kolb, S., Koricheva, J., Liebersgesell, M., Milligan, H., Muller, S., Muys, B., Nguyen, D., Nock, C., Pollastrini, M., Purschke, O., Radoglou, K., Raulund-Rasmussen, K., Roger, F., Ruiz-Benito, P., Seidl, R., Selvi, F., Seiferling, I., Stenlid, J., Valladares, F., Vesterdal, L. and Baeten, L. (2017) 'Biodiversity and ecosystem functioning relations in European forests depend on environmental context', *Ecology Letters*, 20(11), pp. 1414-1426.

Reed, A. J., Godbold, J. A., Grange, L. J., Solan, M. and Webb, T. (2020) 'Growth of marine ectotherms is regionally constrained and asymmetric with latitude', *Global Ecology and Biogeography*, 30(3), pp. 578-589.

Reed, A. J., Godbold, J. A., Solan, M. and Grange, L. J. (2021) 'Invariant Gametogenic Response of Dominant Infaunal Bivalves From the Arctic Under Ambient and Near-Future Climate Change Conditions', *Frontiers in Marine Science*, 8.

Renaud, P. E., Sejr, M. K., Bluhm, B. A., Sirenko, B. and Ellingsen, I. H. (2015) 'The future of Arctic benthos: Expansion, invasion, and biodiversity', *Progress in Oceanography*, 139, pp. 244-257.

Renaud, P. E., Wallhead, P., Kotta, J., Włodarska-Kowalczuk, M., Bellerby, R. G. J., Rätsep, M., Slagstad, D. and Kukliński, P. (2019) 'Arctic Sensitivity? Suitable Habitat for Benthic Taxa Is Surprisingly Robust to Climate Change', *Frontiers in Marine Science*, 6(September), pp. 1-14.

Renes, S. E., Sjostedt, J., Fetzer, I. and Langenheder, S. (2020) 'Disturbance history can increase functional stability in the face of both repeated disturbances of the same type and novel disturbances', *Scientific Reports*, 10(1), pp. 11333.

Reynolds, R. W., Rayner, N. A., Smith, T. M., Stokes, D. C. and Wang, W. Q. (2002) 'An improved in situ and satellite SST analysis for climate', *Journal of Climate*, 15(13), pp. 1609-1625.

Ricciardi, A. and Rasmussen, J. B. (1999) 'Extinction rates of North American freshwater fauna', *Conservation Biology*, 13(5), pp. 1220-1222.

Richard, J., Morley, S. A., Deloffre, J. and Peck, L. S. (2012a) 'Thermal acclimation capacity for four Arctic marine benthic species', *Journal of Experimental Marine Biology and Ecology*, 424, pp. 38-43.

Richard, J., Morley, S. A., Thorne, M. A. and Peck, L. S. (2012b) 'Estimating long-term survival temperatures at the assemblage level in the marine environment: towards macrophysiology', *PLoS One*, 7(4), pp. e34655.

Ries, J. B., Cohen, A. L. and McCorkle, D. C. (2009) 'Marine calcifiers exhibit mixed responses to CO<sub>2</sub>-induced ocean acidification', *Geology*, 37(12), pp. 1131-1134.

Roark, E. B., Guilderson, T. P., Flood-Page, S., Dunbar, R. B., Ingram, B. L., Fallon, S. J. and McCulloch, M. (2005) 'Radiocarbon-based ages and growth rates of bamboo corals from the Gulf of Alaska', *Geophysical Research Letters*, 32(4).

Robbins, L. L., Hansen, M. E., Kleypas, J. A. and Meylan, S. C. (2010) *CO2calc: A user-friendly carbon calculator for Windows, Mac OS X, and iOS (iPhone)* U.S. Geological Survey.

Robinson, L. F., Adkins, J. F., Frank, N., Gagnon, A. C., Prouty, N. G., Brendan Roark, E. and de Flierdt, T. v. (2014) 'The geochemistry of deep-sea coral skeletons: A review of vital effects and

applications for palaeoceanography', *Deep-Sea Research Part II: Topical Studies in Oceanography*, 99, pp. 184-198.

Robinson, L. F., Adkins, J. F., Keigwin, L. D., Southon, J., Fernandez, D. P., Wang, S. L. and Scheirer, D. S. (2005) 'Radiocarbon variability in the western North Atlantic during the last deglaciation', *Science*, 310(5753), pp. 1469-73.

Rogers, A. D. (2015) 'Environmental Change in the Deep Ocean', *Annual Review of Environment and Resources*, Vol 40, 40(1), pp. 1-38.

Rohatgi, A. (2022) *WebPlotDigitizer* (Version 4.6). Available at: <http://arohatgi.info/WebPlotDigitizer>.

Ross, C. L., DeCarlo, T. M. and McCulloch, M. T. (2019) 'Calibration of Sr/Ca, Li/Mg and Sr-U Paleothermometry in Branching and Foliose Corals', *Paleoceanography and Paleoclimatology*, 34(8), pp. 1271-1291.

Ross, P. M., Parker, L. and Byrne, M. (2016) 'Transgenerational responses of molluscs and echinoderms to changing ocean conditions', *Ices Journal of Marine Science*, 73(3), pp. 537-549.

Ruckelshaus, M., Doney, S. C., Galindo, H. M., Barry, J. P., Chan, F., Duffy, J. E., English, C. A., Gaines, S. D., Grebmeier, J. M., Hollowed, A. B., Knowlton, N., Polovina, J., Rabalais, N. N., Sydeman, W. J. and Talley, L. D. (2013) 'Securing ocean benefits for society in the face of climate change', *Marine Policy*, 40, pp. 154-159.

Rysgaard, S. and Nielsen, T. G. (2006) 'Carbon cycling in a high-arctic marine ecosystem - Young Sound, NE Greenland', *Progress in Oceanography*, 71(2-4), pp. 426-445.

Sæther, B. E. and Engen, S. (2015) 'The concept of fitness in fluctuating environments', *Trends Ecology and Evolution*, 30(5), pp. 273-81.

Salo, T. and Gustafsson, C. (2016) 'The Effect of Genetic Diversity on Ecosystem Functioning in Vegetated Coastal Ecosystems', *Ecosystems*, 19(8), pp. 1429-1444.

Sanders, D., Kehoe, R. and van Veen, F. J. (2015) 'Experimental Evidence for the Population-Dynamic Mechanisms Underlying Extinction Cascades of Carnivores', *Current Biology*, 25(23), pp. 3106-9.

Sanders, D., Thebault, E., Kehoe, R. and Frank van Veen, F. J. (2018) 'Trophic redundancy reduces vulnerability to extinction cascades', *Proceedings of the National Academy of Sciences of the United States of America*, 115(10), pp. 2419-2424.

Savva, I., Bennett, S., Roca, G., Jorda, G. and Marba, N. (2018) 'Thermal tolerance of Mediterranean marine macrophytes: Vulnerability to global warming', *Ecology and Evolution*, 8(23), pp. 12032-12043.

Sax, D. F., Gaines, S. D. and Brown, J. H. (2002) 'Species invasions exceed extinctions on islands worldwide: a comparative study of plants and birds', *The American Naturalist*, 160(6), pp. 766-83.

Schaum, E., Rost, B., Millar, A. J. and Collins, S. (2012) 'Variation in plastic responses of a globally distributed picoplankton species to ocean acidification', *Nature Climate Change*, 3(3), pp. 298-302.

Schiffers, K., Teal, L. R., Travis, J. M. and Solan, M. (2011) 'An open source simulation model for soil and sediment bioturbation', *PLoS One*, 6(12), pp. e28028.

## List of References

Schlegel, P., Havenhand, J. N., Gillings, M. R. and Williamson, J. E. (2012) 'Individual variability in reproductive success determines winners and losers under ocean acidification: a case study with sea urchins', *PLoS One*, 7(12), pp. e53118.

Schloerke, B., Cook, D., Larmarange, J., Briatte, F., Marbach, M., Thoen, E., Elberg, A. and Crowley, J. (2021) *GGally: Extension to 'ggplot2'*. Available at: <https://CRAN.R-project.org/package=GGally>.

Schloss, C. A., Nunez, T. A. and Lawler, J. J. (2012) 'Dispersal will limit ability of mammals to track climate change in the Western Hemisphere', *Proceedings of the National Academy of Sciences of the United States of America*, 109(22), pp. 8606-11.

Schmid, B., Balvanera, P., Cardinale, B. J., Godbold, J., Pfisterer, A. B., Raffaelli, D., Solan, M. and Srivastava, D. S. (2009) 'Consequences of species loss for ecosystem functioning: meta-analyses of data from biodiversity experiments', *Biodiversity, Ecosystem Functioning, and Human Wellbeing*, pp. 14-29.

Schmid, B. and Hector, A. (2004) 'The value of biodiversity experiments', *Basic and Applied Ecology*, 5(6), pp. 535-542.

Schmidt-Nielsen, K. (1990) *Animal Physiology Adaption and Environment*. 4 edn.

Schmidt-Nielsen, K. (2012) *How Animals Work*.

Schmidt-Traub, G. (2021) 'National climate and biodiversity strategies are hamstrung by a lack of maps', *Nature Ecology and Evolution*, 5(10), pp. 1325-1327.

Schurmann, H. and Steffensen, J. F. (1992) 'Lethal Oxygen Levels at Different Temperatures and the Preferred Temperature during Hypoxia of the Atlantic Cod, *Gadus-Morhua L*', *Journal of Fish Biology*, 41(6), pp. 927-934.

Screen, J. A. (2014) 'Arctic amplification decreases temperature variance in northern mid- to high-latitudes', *Nature Climate Change*, 4(7), pp. 577-582.

Screen, J. A., Bracegirdle, T. J. and Simmonds, I. (2018) 'Polar Climate Change as Manifest in Atmospheric Circulation', *Current Climate Change Reports*, 4(4), pp. 383-395.

Seguin, A., Harvey, E., Archambault, P., Nozais, C. and Gravel, D. (2014) 'Body size as a predictor of species loss effect on ecosystem functioning', *Scientific Reports*, 4, pp. 4616.

Seibel, B. A., Maas, A. E. and Dierssen, H. M. (2012) 'Energetic plasticity underlies a variable response to ocean acidification in the pteropod, *Limacina helicina antarctica*', *PLoS One*, 7(4), pp. e30464.

Sellman, S., Saterberg, T. and Ebenman, B. (2016) 'Pattern of functional extinctions in ecological networks with a variety of interaction types', *Theoretical Ecology*, 9(1), pp. 83-94.

Serreze, M. C. and Barry, R. G. (2011) 'Processes and impacts of Arctic amplification: A research synthesis', *Global and Planetary Change*, 77(1-2), pp. 85-96.

Sharma, P., Patel, I. K., Singh, A. T., Meloth, T. and Ravindra, R. (2020) 'Glacier Response to Climate in Arctic and Himalaya During Last Seventeen Years: A Case Study of Svalbard, Arctic and Chandra Basin, Himalaya', *Climate Change and the White World*, pp. 139-156.

Sheaves, M., Mattone, C., Connolly, R., Hernandez, S., Nagelkerken, I., Murray, N., Ronan, M., Waltham, N. J. and Bradley, M. (2021) 'Ecological Constraint Mapping: Understanding Outcome-Limiting Bottlenecks for Improved Environmental Decision-Making in Marine and Coastal Environments', *Frontiers in Marine Science*, 8.

Shepley, A., Falzon, G., Meek, P. and Kwan, P. (2021) 'Automated location invariant animal detection in camera trap images using publicly available data sources', *Ecology and Evolution*, 11(9), pp. 4494-4506.

Sherwood, O. A. and Edinger, E. N. (2009) 'Ages and growth rates of some deep-sea gorgonian and antipatharian corals of Newfoundland and Labrador', *Canadian Journal of Fisheries and Aquatic Sciences*, 66(1), pp. 142-152.

Sherwood, O. A., Edinger, E. N., Guilderson, T. P., Ghaleb, B., Risk, M. J. and Scott, D. B. (2008) 'Late Holocene radiocarbon variability in Northwest Atlantic slope waters', *Earth and Planetary Science Letters*, 275(1-2), pp. 146-153.

Sherwood, O. A., Heikoop, J. M., Scott, D. B., Risk, M. J., Guilderson, T. P. and McKinney, R. A. (2005a) 'Stable isotopic composition of deep-sea gorgonian corals *Primnoa* spp.: a new archive of surface processes', *Marine Ecology Progress Series*, 301, pp. 135-148.

Sherwood, O. A., Heikoop, J. M., Sinclair, D. J., Scott, D. B., Risk, M. J., Shearer, C. and Azetsu-Scott, K. (2005b) 'Skeletal Mg/Ca in *Primnoa* resedaeformis: relationship to temperature?', in Freiwald, A. and Roberts, J.M. (eds.) *Cold-Water Corals and Ecosystems*. Berlin, Heidelberg: Springer Berlin Heidelberg, pp. 1061-1079.

Sherwood, O. A., Lehmann, M. F., Schubert, C. J., Scott, D. B. and McCarthy, M. D. (2011) 'Nutrient regime shift in the western North Atlantic indicated by compound-specific delta15N of deep-sea gorgonian corals', *Proceedings of the National Academy of Sciences of the United States of America*, 108(3), pp. 1011-5.

Sherwood, O. A. and Risk, M. J. (2007) 'Chapter Twelve Deep-Sea Corals: New Insights to Paleoceanography', *Proxies in Late Cenozoic Paleoceanography Developments in Marine Geology*, pp. 491-522.

Shirai, K., Kusakabe, M., Nakai, S., Ishii, T., Watanabe, T., Hiyagon, H. and Sano, Y. (2005) 'Deep-sea coral geochemistry: Implication for the vital effect', *Chemical Geology*, 224(4), pp. 212-222.

Siefert, A. (2012) 'Incorporating intraspecific variation in tests of trait-based community assembly', *Oecologia*, 170(3), pp. 767-75.

Sinclair, D. and McCulloch, M. (2004) 'Corals record low mobile barium concentrations in the Burdekin River during the 1974 flood: evidence for limited Ba supply to rivers?', *Palaeogeography, Palaeoclimatology, Palaeoecology*, 214(1-2), pp. 155-174.

Sinclair, D. J., Williams, B., Allard, G., Ghaleb, B., Fallon, S., Ross, S. W. and Risk, M. (2011) 'Reproducibility of trace element profiles in a specimen of the deep-water bamboo coral *Keratoisis* sp.', *Geochimica Et Cosmochimica Acta*, 75(18), pp. 5101-5121.

Sinclair, D. J., Williams, B. and Risk, M. (2006) 'A biological origin for climate signals in corals—Trace element "vital effects" are ubiquitous in Scleractinian coral skeletons', *Geophysical Research Letters*, 33(17).

Sirenko, B. I. (2001) *List of Species of Free-living Invertebrates of Eurasian Arctic Seas and Adjacent Deep Waters. Exploration of the Fauna of the Seas* (59 vols). Russian Academy of Sciences Zoological Institute.

Sivel, E., Planque, B., Lindstrøm, U. and Yoccoz, N. G. (2022) 'Combined effects of temperature and fishing mortality on the Barents Sea ecosystem stability', *Fisheries Oceanography*, 32(1), pp. 106-120.

## List of References

Skjoldal, H. R., Eriksen, E. and Gjosæter, H. (2022) 'Size-fractioned zooplankton biomass in the Barents Sea: Spatial patterns and temporal variations during three decades of warming and strong fluctuations of the capelin stock (1989-2020)', *Progress in Oceanography*, 206.

Slattery, M. and McClintock, J. B. (1995) 'Population structure and feeding deterrence in three shallow-water antarctic soft corals', *Marine Biology*, pp. 461-470.

Smalås, A., Strøm, J. F., Amundsen, P. A., Dieckmann, U., Primicerio, R. and Heino, J. (2019) 'Climate warming is predicted to enhance the negative effects of harvesting on high-latitude lake fish', *Journal of Applied Ecology*, 57(2), pp. 270-282.

Small, D. P., Calosi, P., Boothroyd, D., Widdicombe, S. and Spicer, J. I. (2015) 'Stage-Specific Changes in Physiological and Life-History Responses to Elevated Temperature and Pco<sub>2</sub> during the Larval Development of the European Lobster *Homarus gammarus* (L.)', *Physiological and Biochemical Zoology: Ecological and Evolutionary Approaches* 88(5), pp. 494-507.

Smith, G. C., Allard, R., Babin, M., Bertino, L., Chevallier, M., Corlett, G., Crout, J., Davidson, F., Delille, B., Gille, S. T., Hebert, D., Hyder, P., Intrieri, J., Lagunas, J., Larnicol, G., Kaminski, T., Kater, B., Kauker, F., Marec, C., Mazloff, M., Metzger, E. J., Mordy, C., O'Carroll, A., Olsen, S. M., Phelps, M., Posey, P., Prandi, P., Rehm, E., Reid, P., Rigor, I., Sandven, S., Shupe, M., Swart, S., Smedstad, O. M., Solomon, A., Storto, A., Thibaut, P., Toole, J., Wood, K., Xie, J., Yang, Q. and Group, W. P. S. (2019) 'Polar Ocean Observations: A Critical Gap in the Observing System and Its Effect on Environmental Predictions From Hours to a Season', *Frontiers in Marine Science*, 6.

Smith, J. E., Schwarcz, H. P., Risk, M. J., McConaughey, T. A. and Keller, N. (2000) 'Paleotemperatures from deep-sea corals: Overcoming "vital effects"', *Palaios*, 15(1), pp. 25-32.

Snelgrove, P. V., Thrush, S. F., Wall, D. H. and Norkko, A. (2014) 'Real world biodiversity-ecosystem functioning: a seafloor perspective', *Trends Ecology and Evolution*, 29(7), pp. 398-405.

Snelgrove, P. V. R., Soetaert, K., Solan, M., Thrush, S., Wei, C. L., Danovaro, R., Fulweiler, R. W., Kitazato, H., Ingole, B., Norkko, A., Parkes, R. J. and Volkenborn, N. (2018) 'Global Carbon Cycling on a Heterogeneous Seafloor', *Trends Ecology and Evolution*, 33(2), pp. 96-105.

Solan, M., Archambault, P., Renaud, P. E. and Marz, C. (2020a) 'The changing Arctic Ocean: consequences for biological communities, biogeochemical processes and ecosystem functioning', *Philosophical Transactions of the Royal Society A*, 378(2181), pp. 20200266.

Solan, M., Aspden, R. J. and Paterson, D. M. (2012) *Marine Biodiversity & Ecosystem Functioning*.

Solan, M., Bennett, E. M., Mumby, P. J., Leyland, J. and Godbold, J. A. (2020b) 'Benthic-based contributions to climate change mitigation and adaptation', *Philosophical Transactions of the Royal Society B: Biological Sciences*, 375(1794), pp. 20190107.

Solan, M., Cardinale, B. J., Downing, A. L., Engelhardt, K. A., Ruesink, J. L. and Srivastava, D. S. (2004a) 'Extinction and ecosystem function in the marine benthos', *Science*, 306(5699), pp. 1177-80.

Solan, M., Ward, E. R., White, E. L., Hibberd, E. E., Cassidy, C., Schuster, J. M., Hale, R. and Godbold, J. A. (2019) 'Worldwide measurements of bioturbation intensity, ventilation rate, and the mixing depth of marine sediments', *Scientific Data*, 6(1), pp. 58.

Solan, M., Ward, E. R., Wood, C. L., Reed, A. J., Grange, L. J. and Godbold, J. A. (2020c) 'Climate-driven benthic invertebrate activity and biogeochemical functioning across the Barents Sea polar front', *Philosophical Transactions of the Royal Society A*, 378(2181), pp. 20190365.

Solan, M. and Whiteley, N. M. (2016) *Stressors in the marine environment: Physiological and ecological responses societal implications*.

Solan, M. and Wigham, B. D. (2005) 'Biogenic particle reworking and bacterial-invertebrate interactions in marine sediments', *Interactions Between Macro- and Microorganisms in Marine Sediments Coastal and Estuarine Studies*, pp. 105-124.

Solan, M., Wigham, B. D., Hudson, I. R., Kennedy, R., Coulon, C. H., Norling, K., Nilsson, H. C. and Rosenberg, R. (2004b) 'In situ quantification of bioturbation using time-lapse fluorescent sediment profile imaging (f-SPI), luminophore tracers and model simulation', *Marine Ecology Progress Series*, 271, pp. 1-12.

Soltwedel, T., Bauerfeind, E., Bergmann, M., Bracher, A., Budaeva, N., Busch, K., Cherkasheva, A., Fahl, K., Grzelak, K., Hasemann, C., Jacob, M., Kraft, A., Lalande, C., Metfies, K., Nothig, E. M., Meyer, K., Queric, N. V., Schewe, I., Włodarska-Kowalcuk, M. and Klages, M. (2016) 'Natural variability or anthropogenically-induced variation? Insights from 15 years of multidisciplinary observations at the arctic marine LTER site HAUSGARTEN', *Ecological Indicators*, 65, pp. 89-102.

Somero, G. N. (2010) 'The physiology of climate change: how potentials for acclimatization and genetic adaptation will determine 'winners' and 'losers'', *Journal of Experimental Biology*, 213(6), pp. 912-20.

Song, H. J., Lee, J. H., Kim, G. W., Ahn, S. H., Joo, H. M., Jeong, J. Y., Yang, E. J., Kang, S. H. and Lee, S. H. (2016) 'In-situ measured primary productivity of ice algae in Arctic sea ice floes using a new incubation method', *Ocean Science Journal*, 51(3), pp. 387-396.

Spalding, M. D., Fox, H. E., Halpern, B. S., McManus, M. A., Molnar, J., Allen, G. R., Davidson, N., Jorge, Z. A., Lombana, A. L., Lourie, S. A., Martin, K. D., McManus, E., Molnar, J., Recchia, C. A. and Robertson, J. (2007) 'Marine ecoregions of the world: A bioregionalization of coastal and shelf areas', *Bioscience*, 57(7), pp. 573-583.

Spiess, A.-N. and Neumeyer, N. (2010) 'An evaluation of R2 as an inadequate measure for nonlinear models in pharmacological and biochemical research: a Monte Carlo approach', *BMC Pharmacology*, 10(6).

Spooner, P. T., Robinson, L. F., Hemsing, F., Morris, P. and Stewart, J. A. (2018) 'Extended calibration of cold-water coral Ba/Ca using multiple genera and co-located measurements of dissolved barium concentration', *Chemical Geology*, 499, pp. 100-110.

Srivastava, D. S. (2002) 'The role of conservation in expanding biodiversity research', *Oikos*, 98(2), pp. 351-360.

Standish, C. D., Chalk, T. B., Babilia, T. L., Milton, J. A., Palmer, M. R. and Foster, G. L. (2019) 'The effect of matrix interferences on in situ boron isotope analysis by laser ablation multi-collector inductively coupled plasma mass spectrometry', *Rapid Commun Mass Spectrom*, 33(10), pp. 959-968.

Steiner, N. S., Bowman, J., Campbell, K., Chierici, M., Eronen-Rasimus, E., Falardeau, M., Flores, H., Fransson, A., Herr, H., Insley, S. J., Kauko, H. M., Lannuzel, D., Loseto, L., Lynnes, A., Majewski, A., Meiners, K. M., Miller, L. A., Michel, L. N., Moreau, S., Nacke, M., Nomura, D., Tedesco, L., van Franeker, J. A., van Leeuwe, M. A. and Wongpan, P. (2021) 'Climate change impacts on sea-ice ecosystems and associated ecosystem services', *Elementa-Science of the Anthropocene*, 9(1).

Stevens, G. C. (1989) 'The Latitudinal Gradient in Geographical Range - How So Many Species Coexist in the Tropics', *The American Naturalist*, 133(2), pp. 240-256.

## List of References

Stewart, J. A., Anagnostou, E. and Foster, G. L. (2016) 'An improved boron isotope pH proxy calibration for the deep-sea coral *Desmophyllum dianthus* through sub-sampling of fibrous aragonite', *Chemical Geology*, 447, pp. 148-160.

Stewart, J. A., Robinson, L. F., Day, R. D., Strawson, I., Burke, A., Rae, J. W. B., Spooner, P. T., Samperiz, A., Etnoyer, P. J., Williams, B., Paytan, A., Leng, M. J., Haussermann, V., Wickes, L. N., Bratt, R. and Pryer, H. (2020) 'Refining trace metal temperature proxies in cold-water scleractinian and stylasterid corals', *Earth and Planetary Science Letters*, 545.

Stillman, J. H. (2003) 'Acclimation capacity underlies susceptibility to climate change', *Science*, 301(5629), pp. 65.

Stralberg, D., Matsuoka, S. M., Hamann, A., Bayne, E. M., Solymos, P., Schmiegelow, F. K., Wang, X., Cumming, S. G. and Song, S. J. (2015) 'Projecting boreal bird responses to climate change: the signal exceeds the noise', *Ecology Applications*, 25(1), pp. 52-69.

Stratmann, T., van Oevelen, D., Martinez Arbizu, P., Wei, C. L., Liao, J. X., Cusson, M., Scrosati, R. A., Archambault, P., Snelgrove, P. V. R., Ramey-Balci, P. A., Burd, B. J., Kenchington, E., Gilkinson, K., Belley, R. and Soetaert, K. (2020) 'The BenBioDen database, a global database for meio-, macro- and megabenthic biomass and densities', *Scientific Data*, 7(1), pp. 206.

Strona, G. (2015) 'Past, present and future of host-parasite co-extinctions', *International Journal for Parasitology: Parasites and Wildlife*, 4(3), pp. 431-41.

Strona, G. and Bradshaw, C. J. A. (2018) 'Co-extinctions annihilate planetary life during extreme environmental change', *Scientific Reports*, 8(1), pp. 16724.

Strona, G. and Bradshaw, C. J. A. (2022) 'Coextinctions dominate future vertebrate losses from climate and land use change', *Science Advances*, 8(50), pp. eabn4345.

Sunday, J. M., Bates, A. E. and Dulvy, N. K. (2011) 'Global analysis of thermal tolerance and latitude in ectotherms', *Proceedings of the Royal Society B: Biological Sciences*, 278(1713), pp. 1823-30.

Sundin, J., Amcoff, M., Mateos-Gonzalez, F., Raby, G. D. and Clark, T. D. (2019) 'Long-term acclimation to near-future ocean acidification has negligible effects on energetic attributes in a juvenile coral reef fish', *Oecologia*, 190(3), pp. 689-702.

Svenning, J.-C., Eiserhardt, W. L., Normand, S., Ordonez, A. and Sandel, B. (2015) 'The Influence of Paleoclimate on Present-Day Patterns in Biodiversity and Ecosystems', *Annual Review of Ecology, Evolution, and Systematics*, 46(1), pp. 551-572.

Swanson, D. K. (2021) 'Permafrost thaw-related slope failures in Alaska's Arctic National Parks, c. 1980–2019', *Permafrost and Periglacial Processes*, 32(3), pp. 392-406.

Sweetman, A. K., Thurber, A. R., Smith, C. R., Levin, L. A., Mora, C., Wei, C. L., Gooday, A. J., Jones, D. O. B., Rex, M., Yasuhara, M., Ingels, J., Ruhl, H. A., Frieder, C. A., Danovaro, R., Wurzberg, L., Baco, A., Grupe, B. M., Pasulka, A., Meyer, K. S., Dunlop, K. M., Henry, L. A. and Roberts, J. M. (2017) 'Major impacts of climate change on deep-sea benthic ecosystems', *Elementa-Science of the Anthropocene*, 5, pp. 1-23.

Tait, K., Laverock, B., Shaw, J., Somerfield, P. J. and Widdicombe, S. (2013) 'Minor impact of ocean acidification to the composition of the active microbial community in an Arctic sediment', *Environ Microbiol Rep*, 5(6), pp. 851-60.

Tanzil, J. T. I., Goodkin, N. F., Sin, T. M., Chen, M. L., Fabbro, G. N., Boyle, E. A., Lee, A. C. and Toh, K. B. (2019) 'Multi-colony coral skeletal Ba/Ca from Singapore's turbid urban reefs: Relationship

with contemporaneous in-situ seawater parameters', *Geochimica Et Cosmochimica Acta*, 250, pp. 191-208.

Telesca, L., Peck, L. S., Sanders, T., Thyrring, J., Sejr, M. K. and Harper, E. M. (2019) 'Biomineralization plasticity and environmental heterogeneity predict geographical resilience patterns of foundation species to future change', *Global Change Biology*, 25(12), pp. 4179-4193.

Terblanche, J. S. and Hoffmann, A. A. (2020) 'Validating measurements of acclimation for climate change adaptation', *Current Opinion in Insect Science*, 41, pp. 7-16.

Terhaar, J., Kwiatkowski, L. and Bopp, L. (2020) 'Emergent constraint on Arctic Ocean acidification in the twenty-first century', *Nature*, 582(7812), pp. 379-383.

Thébault, E., Huber, V. and Loreau, M. (2007) 'Cascading extinctions and ecosystem functioning: contrasting effects of diversity depending on food web structure', *Oikos*, 116(1), pp. 163-173.

Thomas, C. D., Cameron, A., Green, R. E., Bakkenes, M., Beaumont, L. J., Collingham, Y. C., Erasmus, B. F., De Siqueira, M. F., Grainger, A., Hannah, L., Hughes, L., Huntley, B., Van Jaarsveld, A. S., Midgley, G. F., Miles, L., Ortega-Huerta, M. A., Peterson, A. T., Phillips, O. L. and Williams, S. E. (2004) 'Extinction risk from climate change', *Nature*, 427(6970), pp. 145-8.

Thomas, D. N. (2021) *Arctic Ecology*.

Thomas, H., Mucci, A., Mears, C., Charette, M. A. and Dehairs, F. (2021) 'Inorganic Carbon, Ra, Ba and,  $\delta^{18}\text{O}$  tracer distribution in the Canadian Arctic Archipelago from the 2015 Canadian GEOTRACES expedition'. Available at: <https://doi.org/10.1594/PANGAEA.929298> (Accessed).

Thomsen, M. S., Garcia, C., Bolam, S. G., Parker, R., Godbold, J. A. and Solan, M. (2017) 'Consequences of biodiversity loss diverge from expectation due to post-extinction compensatory responses', *Scientific Reports*, 7, pp. 43695.

Thomsen, M. S., Godbold, J. A., Garcia, C., Bolam, S. G., Parker, R. and Solan, M. (2019) 'Compensatory responses can alter the form of the biodiversity-function relation curve', *Proceedings of the Royal Society B: Biological Sciences*, 286(1901), pp. 20190287.

Thresher, R., Rintoul, S. R., Koslow, J. A., Weidman, C., Adkins, J. and Proctor, C. (2004) 'Oceanic evidence of climate change in southern Australia over the last three centuries', *Geophysical Research Letters*, 31(7), pp. n/a-n/a.

Thresher, R. E. (2009) 'Environmental and compositional correlates of growth rate in deep-water bamboo corals (Gorgonacea; Isididae)', *Marine Ecology Progress Series*, 397, pp. 187-196.

Thresher, R. E., Fallon, S. J. and Townsend, A. T. (2016a) 'A "core-top" screen for trace element proxies of environmental conditions and growth rates in the calcite skeletons of bamboo corals (Isididae)', *Geochimica et Cosmochimica Acta*, 193, pp. 75-99.

Thresher, R. E. and Neil, H. (2016b) 'Scale dependence of environmental and physiological correlates of delta O-18 and delta C-13 in the magnesium calcite skeletons of bamboo corals (Gorgonacea; Isididae)', *Geochimica Et Cosmochimica Acta*, 187, pp. 260-278.

Thresher, R. E., Wilson, N. C., MacRae, C. M. and Neil, H. (2010) 'Temperature effects on the calcite skeletal composition of deep-water gorgonians (Isididae)', *Geochimica Et Cosmochimica Acta*, 74(16), pp. 4655-4670.

Tilman, D., Knops, J., Wedin, D. and Reich, P. (2002) 'Plant diversity and composition: effects on productivity and nutrient dynamics of experimental grasslands.', in Loreau, M., Naeem, S. and

## List of References

Inchausti, P. (eds.) *Biodiversity and Ecosystem Functioning. Synthesis and Perspectives*. Oxford: Oxford University Press, pp. 21-35.

Tilman, D., Lehman, C. L. and Thomson, K. T. (1997) 'Plant diversity and ecosystem productivity: theoretical considerations', *Proceedings of the National Academy of Sciences of the United States of America*, 94(5), pp. 1857-61.

Tracey, D. M., Neil, H., Marriott, P., Andrews, A. H., Cailliet, G. M. and Sanchez, J. A. (2007) 'Age and growth of two genera of deep-sea bamboo corals (family Isididae) in New Zealand waters', *Bulletin of Marine Science*, 81(3), pp. 393-408.

Tracy, C. R. and George, T. L. (1992) 'On the Determinants of Extinction', *The American Naturalist*, 139(1), pp. 102-122.

Truchy, A., Angeler, D. G., Sponseller, R. A., Johnson, R. K. and McKie, B. G. (2015) 'Linking Biodiversity, Ecosystem Functioning and Services, and Ecological Resilience', *Ecosystem Services - From Biodiversity to Society, Part 1 Advances in Ecological Research*, pp. 55-96.

Tuomainen, U. and Candolin, U. (2011) 'Behavioural responses to human-induced environmental change', *Biological reviews of the Cambridge Philosophical Society*, 86(3), pp. 640-57.

Urban, M. C. (2015) 'Climate change. Accelerating extinction risk from climate change', *Science*, 348(6234), pp. 571-3.

Uthicke, S., Ebert, T., Liddy, M., Johansson, C., Fabricius, K. E. and Lamare, M. (2016) 'Echinometra sea urchins acclimatized to elevated pCO<sub>2</sub> at volcanic vents outperform those under present-day pCO<sub>2</sub> conditions', *Global Change Biology*, 22(7), pp. 2451-61.

Valdovinos, F. S., Ramos-Jiliberto, R., Garay-Narvaez, L., Urbani, P. and Dunne, J. A. (2010) 'Consequences of adaptive behaviour for the structure and dynamics of food webs', *Ecology Letters*, 13(12), pp. 1546-59.

Valiente-Banuet, A., Aizen, M. A., Alcántara, J. M., Arroyo, J., Cocucci, A., Galetti, M., García, M. B., García, D., Gómez, J. M., Jordano, P., Medel, R., Navarro, L., Obeso, J. R., Oviedo, R., Ramírez, N., Rey, P. J., Traveset, A., Verdú, M., Zamora, R. and Johnson, M. (2014) 'Beyond species loss: the extinction of ecological interactions in a changing world', *Functional Ecology*, 29(3), pp. 299-307.

Valladares, F., Matesanz, S., Guilhaumon, F., Araujo, M. B., Balaguer, L., Benito-Garzon, M., Cornwell, W., Gianoli, E., van Kleunen, M., Naya, D. E., Nicotra, A. B., Poorter, H. and Zavala, M. A. (2014) 'The effects of phenotypic plasticity and local adaptation on forecasts of species range shifts under climate change', *Ecology Letters*, 17(11), pp. 1351-64.

Van Colen, C., Ong, E. Z., Briffa, M., Wethey, D. S., Abatih, E., Moens, T. and Woodin, S. A. (2020) 'Clam feeding plasticity reduces herbivore vulnerability to ocean warming and acidification', *Nature Climate Change*, 10(2), pp. 162-166.

Van Gaever, S., Raes, M., Pasotti, F. and Vanreusel, A. (2010) 'Spatial scale and habitat-dependent diversity patterns in nematode communities in three seepage related sites along the Norwegian Sea margin', *Marine Ecology*, 31(1), pp. 66-77.

Vaughan, D. G., Marshall, G. J., Connolley, W. M., Parkinson, C., Mulvaney, R., Hodgson, D. A., King, J. C., Pudsey, C. J. and Turner, J. T. (2003) 'Recent Rapid Regional Climate Warming of the Antarctic Peninsula', *Climatic Change*, 60, pp. 243-274.

Vetrov, A. A. and Romankevich, E. A. (2004) *Carbon Cycle in the Russian Arctic Seas*. 1 edn. Berlin: Springer Berlin, Heidelberg.

Vetter, V. M. S., Kreyling, J., Dengler, J., Apostolova, I., Arfin-Khan, M. A. S., Berauer, B. J., Berwaers, S., De Boeck, H. J., Nijs, I., Schuchardt, M. A., Sopotlieva, D., von Gillhausen, P., Wilfahrt, P. A., Zimmermann, M. and Jentsch, A. (2020) 'Invader presence disrupts the stabilizing effect of species richness in plant community recovery after drought', *Global Change Biology*, 26(6), pp. 3539-3551.

Vibe, C. (1967) *Arctic Animals in Relation to Climate Fluctuations: The Danish Zoogeographical Investigations in Greenland*. C. A. Reitzel.

Vieira, M. C., Cianciaruso, M. V. and Almeida-Neto, M. (2013) 'Plant-pollinator coextinctions and the loss of plant functional and phylogenetic diversity', *PLoS One*, 8(11), pp. e81242.

Vink, S. and Atkinson, M. J. (1985) 'High Dissolved C-P Excretion Ratios for Large Benthic Marine-Invertebrates', *Marine Ecology Progress Series*, 21(1-2), pp. 191-195.

Vogt, G. (2019) 'A compilation of longevity data in decapod crustaceans', *Nauplius*, 27.

von Dassow, P., John, U., Ogata, H., Probert, I., Bendif el, M., Kegel, J. U., Audic, S., Wincker, P., Da Silva, C., Claverie, J. M., Doney, S., Glover, D. M., Flores, D. M., Herrera, Y., Lescot, M., Garet-Delmas, M. J. and de Vargas, C. (2015) 'Life-cycle modification in open oceans accounts for genome variability in a cosmopolitan phytoplankton', *The ISME Journal*, 9(6), pp. 1365-77.

Walther, G. R., Post, E., Convey, P., Menzel, A., Parmesan, C., Beebee, T. J., Fromentin, J. M., Hoegh-Guldberg, O. and Bairlein, F. (2002) 'Ecological responses to recent climate change', *Nature*, 416(6879), pp. 389-95.

Wang, Q., Wekerle, C., Wang, X. Z., Danilov, S., Koldunov, N., Sein, D., Sidorenko, D., von Appen, W. J. and Jung, T. (2020) 'Intensification of the Atlantic Water Supply to the Arctic Ocean Through Fram Strait Induced by Arctic Sea Ice Decline', *Geophysical Research Letters*, 47(3).

Wangensteen, O. S., Dupont, S., Casties, I., Turon, X. and Palacin, C. (2013) 'Some like it hot: Temperature and pH modulate larval development and settlement of the sea urchin *Arbacia lixula*', *Journal of Experimental Marine Biology and Ecology*, 449, pp. 304-311.

Ward, N. D., Bianchi, T. S., Medeiros, P. M., Seidel, M., Richey, J. E., Keil, R. G. and Sawakuchi, H. O. (2017) 'Where Carbon Goes When Water Flows: Carbon Cycling across the Aquatic Continuum', *Frontiers in Marine Science*, 4.

Wardle, D. A. and Zackrisson, O. (2005) 'Effects of species and functional group loss on island ecosystem properties', *Nature*, 435(7043), pp. 806-10.

Wassmann, P., Duarte, C. M., Agusti, S. and Sejr, M. K. (2011) 'Footprints of climate change in the Arctic marine ecosystem', *Global Change Biology*, 17(2), pp. 1235-1249.

Wassmann, P. and Reigstad, M. (2011) 'Future Arctic Ocean Seasonal Ice Zones and Implications for Pelagic-Benthic Coupling', *Oceanography*, 24(3), pp. 220-231.

Watling, L., Saucier, E. H. and France, S. C. (2022) 'Towards a revision of the bamboo corals (Octocorallia): Part 4, delineating the family Keratoisididae', *Zootaxa*, 5093(3), pp. 337-375.

Weinbauer, M. G., Brandstatter, F. and Velimirov, B. (2000) 'On the potential use of magnesium and strontium concentrations as ecological indicators in the calcite skeleton of the red coral *Corallium rubrum*', *Marine Biology*, 137, pp. 801-809.

Weinbauer, M. G. and Velimirov, B. (1995) 'Morphological Variations in the Mediterranean-Sea Fan Eunicella-Cavolini (Coelenterata, Gorgonacea) in Relation to Exposure, Colony Size and Colony Region', *Bulletin of Marine Science*, 56(1), pp. 283-295.

## List of References

Weiskopf, S. R., Rubenstein, M. A., Crozier, L. G., Gaichas, S., Griffis, R., Halofsky, J. E., Hyde, K. J. W., Morelli, T. L., Morisette, J. T., Munoz, R. C., Pershing, A. J., Peterson, D. L., Poudel, R., Staudinger, M. D., Sutton-Grier, A. E., Thompson, L., Vose, J., Weltzin, J. F. and Whyte, K. P. (2020) 'Climate change effects on biodiversity, ecosystems, ecosystem services, and natural resource management in the United States', *Science of the Total Environment*, 733, pp. 137782.

Welter, S., Brunner, K., Hofstraat, J. W. and De Cola, L. (2003) 'Electroluminescent device with reversible switching between red and green emission', *Nature*, 421(6918), pp. 54-7.

Wernberg, T., Russell, B. D., Moore, P. J., Ling, S. D., Smale, D. A., Campbell, A., Coleman, M. A., Steinberg, P. D., Kendrick, G. A. and Connell, S. D. (2011) 'Impacts of climate change in a global hotspot for temperate marine biodiversity and ocean warming', *Journal of Experimental Marine Biology and Ecology*, 400(1-2), pp. 7-16.

Wernberg, T., Smale, D. A. and Thomsen, M. S. (2012) 'A decade of climate change experiments on marine organisms: procedures, patterns and problems', *Global Change Biology*, 18(5), pp. 1491-1498.

West, B. T., Welch, K. B. and Galecki, A. T. (2014a) *Linear Mixed Models A Practical Guide Using Statistical Software*. 2nd edn.: Taylor & Francis Group.

West, B. T., Welch, K. B. and Galecki, A. T. (2014b) *Linear Mixed Models: A Practical Guide Using Statistical Software*. New York: Chapman and Hall/CRC.

Weydmann, A., Soreide, J. E., Kwasniewski, S. and Widdicombe, S. (2012) 'Influence of CO<sub>2</sub>-induced acidification on the reproduction of a key Arctic copepod *Calanus glacialis*', *Journal of Experimental Marine Biology and Ecology*, 428, pp. 39-42.

Whitehouse, G. A., Aydin, K., Essington, T. E. and Hunt, G. L. (2014) 'A trophic mass balance model of the eastern Chukchi Sea with comparisons to other high-latitude systems', *Polar Biology*, 37(7), pp. 911-939.

Whiteley, N. M. (2011) 'Physiological and ecological responses of crustaceans to ocean acidification', *Marine Ecology Progress Series*, 430, pp. 257-271.

Wickham, H., Averick, M., Bryan, J., Chang, W., McGowan, L., François, R., Grolemund, G., Hayes, A., Henry, L., Hester, J., Kuhn, M., Pedersen, T., Miller, E., Bache, S., Müller, K., Ooms, J., Robinson, D., Seidel, D., Spinu, V., Takahashi, K., Vaughan, D., Wilke, C., Woo, K. and Yutani, H. (2019) 'Welcome to the Tidyverse', *Journal of Open Source Software*, 4(43).

Williams, A., Althaus, F., Dunstan, P. K., Poore, G. C. B., Bax, N. J., Kloser, R. J. and McEnnulty, F. R. (2010) 'Scales of habitat heterogeneity and megabenthos biodiversity on an extensive Australian continental margin (100-1100 m depths)', *Marine Ecology-an Evolutionary Perspective*, 31(1), pp. 222-236.

Williams, S. E., Shoo, L. P., Isaac, J. L., Hoffmann, A. A. and Langham, G. (2008) 'Towards an integrated framework for assessing the vulnerability of species to climate change', *PLoS Biology*, 6(12), pp. 2621-6.

Wilson, M. W., Ridlon, A. D., Gaynor, K. M., Gaines, S. D., Stier, A. C. and Halpern, B. S. (2020) 'Ecological impacts of human-induced animal behaviour change', *Ecology Letters*, 23(10), pp. 1522-1536.

Winfree, R., Fox, J. W., Williams, N. M., Reilly, J. R. and Cariveau, D. P. (2015) 'Abundance of common species, not species richness, drives delivery of a real-world ecosystem service', *Ecology Letters*, 18(7), pp. 626-35.

Wisz, M. S., Pottier, J., Kissling, W. D., Pellissier, L., Lenoir, J., Damgaard, C. F., Dormann, C. F., Forchhammer, M. C., Grytnes, J. A., Guisan, A., Heikkinen, R. K., Høye, T. T., Kuhn, I., Luoto, M., Maiorano, L., Nilsson, M. C., Normand, S., Ockinger, E., Schmidt, N. M., Termansen, M., Timmermann, A., Wardle, D. A., Aastrup, P. and Svenning, J. C. (2013) 'The role of biotic interactions in shaping distributions and realised assemblages of species: implications for species distribution modelling', *Biological reviews of the Cambridge Philosophical Society*, 88(1), pp. 15-30.

Wernberg, T., Smale, D. A. and Thomsen, M. S. (2012) 'A decade of climate change experiments on marine organisms: procedures, patterns and problems', *Global Change Biology*, 18(5), pp. 1491-1498.

Wittmann, A. C. and Portner, H. O. (2013) 'Sensitivities of extant animal taxa to ocean acidification', *Nature Climate Change*, 3(11), pp. 995-1001.

Wohlgemuth, D., Solan, M. and Godbold, J. A. (2016) 'Specific arrangements of species dominance can be more influential than evenness in maintaining ecosystem process and function', *Scientific Reports*, 6, pp. 39325.

Wohlgemuth, D., Solan, M. and Godbold, J. A. (2017) 'Species contributions to ecosystem process and function can be population dependent and modified by biotic and abiotic setting', *Proceedings of the Royal Society B: Biological Sciences*, 284(1855).

Wolgemuth, K. and Broecker, W. S. (1970) 'Barium in Sea Water', *Earth and Planetary Science Letters*, 8(5), pp. 372-.

Wong, B. B. M. and Candolin, U. (2014) 'Behavioral responses to changing environments', *Behavioral Ecology*, 26(3), pp. 665-673.

Wood, H. L., Spicer, J. I., Kendall, M. A., Lowe, D. M. and Widdicombe, S. (2011) 'Ocean warming and acidification; implications for the Arctic brittlestar *Ophiocoma sericeum*', *Polar Biology*, 34(7), pp. 1033-1044.

Wood, H. L., Spicer, J. I. and Widdicombe, S. (2008) 'Ocean acidification may increase calcification rates, but at a cost', *Proceedings of the Royal Society B: Biological Sciences*, 275(1644), pp. 1767-73.

Wood, S. N. (2011) 'Fast stable restricted maximum likelihood and marginal likelihood estimation of semiparametric generalized linear models', *Journal of the Royal Statistical Society Series B-Statistical Methodology*, 73(1), pp. 3-36.

Wood, S. N. (2017) *Generalized Additive Models An Introduction With R*. 2nd edn.: CRC Press.

Woodin, S. A., Volkenborn, N., Pilditch, C. A., Lohrer, A. M., Wethey, D. S., Hewitt, J. E. and Thrush, S. F. (2016) 'Same pattern, different mechanism: Locking onto the role of key species in seafloor ecosystem process', *Scientific Reports*, 6, pp. 26678.

Woods, H. A., Dillon, M. E. and Pincebourde, S. (2015) 'The roles of microclimatic diversity and of behavior in mediating the responses of ectotherms to climate change', *Journal of Thermal Biology*, 54, pp. 86-97.

Woodward, G., Perkins, D. M. and Brown, L. E. (2010) 'Climate change and freshwater ecosystems: impacts across multiple levels of organization', *Philosophical Transactions of the Royal Society B: Biological Sciences*, 365(1549), pp. 2093-106.

## List of References

Woodworth-Jefcoats, P. A., Polovina, J. J. and Drazen, J. C. (2017) 'Climate change is projected to reduce carrying capacity and redistribute species richness in North Pacific pelagic marine ecosystems', *Global Change Biology*, 23(3), pp. 1000-1008.

Worm, B., Barbier, E. B., Beaumont, N., Duffy, J. E., Folke, C., Halpern, B. S., Jackson, J. B., Lotze, H. K., Micheli, F., Palumbi, S. R., Sala, E., Selkoe, K. A., Stachowicz, J. J. and Watson, R. (2006) 'Impacts of biodiversity loss on ocean ecosystem services', *Science*, 314(5800), pp. 787-90.

Wright, J. P., Ames, G. M. and Mitchell, R. M. (2016) 'The more things change, the more they stay the same? When is trait variability important for stability of ecosystem function in a changing environment', *Philosophical Transactions of the Royal Society B: Biological Sciences*, 371(1694).

Yachi, S. and Loreau, M. (1999) 'Biodiversity and ecosystem productivity in a fluctuating environment: the insurance hypothesis', *Proceedings of the National Academy of Sciences of the United States of America*, 96(4), pp. 1463-8.

Yamamoto-Kawai, M., McLaughlin, F. A., Carmack, E. C., Nishino, S. and Shimada, K. (2009) 'Aragonite undersaturation in the Arctic Ocean: effects of ocean acidification and sea ice melt', *Science*, 326(5956), pp. 1098-100.

Yan, C. A., He, F. L., He, J. X. and Zhang, Z. B. (2022) 'The relationship between local and regional extinction rates depends on species distribution patterns', *Ecography*, 2022(2).

Yang, C., Xu, Y. and Nebert, D. (2013) 'Redefining the possibility of digital Earth and geosciences with spatial cloud computing', *International Journal of Digital Earth*, 6(4), pp. 297-312.

Yusuf, B. (2022) *The world's first digital twin of a polar research ship, powered by navvis*: NavVis GmbH. Available at: <https://www.navvis.com/blog/worlds-first-digital-twin-research-ship-powered-navvis> (Accessed: 08 April 2023).

Zajac, R. N., Whitlatch, R. B. and Thrush, S. F. (1998) 'Recolonization and succession in soft-sediment infaunal communities: the spatial scale of controlling factors', *Hydrobiologia*, 375-76, pp. 227-240.

Zenkevitch, L. (1963) *Biology of the Seas of the U.S.S.R.* London: George Allen & Unwin Ltd.

Zhou, X., Gu, X. and Smaill, S. J. (2023) 'Rethinking experiments that explore multiple global change factors', *Trends Ecology and Evolution*, 38(5), pp. 399-401.

Zhou, Z., Bouma, T. J., Fivash, G. S., Ysebaert, T., van, I. L., van Dalen, J., van Dam, B. and Walles, B. (2022) 'Thermal stress affects bioturbators' burrowing behavior: A mesocosm experiment on common cockles (*Cerastoderma edule*)', *Science of the Total Environment*, 824, pp. 153621.

Zscheischler, J., Westra, S., van den Hurk, B. J. J. M., Seneviratne, S. I., Ward, P. J., Pitman, A., AghaKouchak, A., Bresch, D. N., Leonard, M., Wahl, T. and Zhang, X. (2018) 'Future climate risk from compound events', *Nature Climate Change*, 8(6), pp. 469-477.

Zuur, A. F., Ieno, E. N. and Elphick, C. S. (2010) 'A protocol for data exploration to avoid common statistical problems', *Methods in Ecology and Evolution*, 1(1), pp. 3-14.

Zuur, A. F., Ieno, E. N., Walker, N. J., Saveliev, A. A. and Smith, G. M. (2009) 'Mixed Effects Modelling for Nested Data', in Zuur, A.F., Ieno, E.N., Walker, N., Saveliev, A.A. and Smith, G.M. (eds.) *Mixed effects models and extensions in ecology with R Statistics for Biology and Health*. New York, NY: Springer New York, pp. 101-142.

Zweng, M. M. and Munchow, A. (2006) 'Warming and freshening of Baffin Bay, 1916-2003', *Journal of Geophysical Research-Oceans*, 111(C7).